THE UNIVERSITY
of EDINBURGH

Analysis and Applications of Dynamic Density Functional Theory

R. D. Mills–Williams

Doctor of Philosophy
University of Edinburgh
2020

Declaration

I declare that this thesis was composed by myself and that the work contained therein is my own, except where explicitly stated otherwise in the text, and that this work has not been submitted for any other degree or professional qualification except as specified.

(*R. D. Mills–Williams, April 2020*)

Lay Summary

A common picture of liquids and gases is that they are comprised of molecules. Then, the molecules are made up of atoms. Further, the atoms are made up of electrons, protons, and neutrons. Most of the time, we do not need to consider this granular nature of matter, and, to all intents and purposes, everyday liquids and gases are 'continuous'. However there are many natural phenomena which cannot be accurately described by continuous thinking alone, such as: the exact profile of wine at the liquid-glass-air interface, the shape of freezing raindrops and the structure of liquid crystals.

Equally, there are interesting multiscale phenomena in nature, in which discrete elements interact with one another, and, when squinting one's eyes, appear to behave continuously, such as: the flocking of birds, the effervescent paths of ant armies over forest floors, and the dynamics of colloidal fluids. In modelling any of these situations we can see that there is an advantage to considering the systems as 'continuous'. Naturally, if the individual particles in the systems are so numerous, keeping track of all of them means one would need a lot of computer power. Furthermore, to observe very fast changes in the dynamics of such systems requires very fine snapshots in time, leading to slow computer simulations, given the speed limits of current processors. On the other hand, if one were to average over the behaviour of the individuals, both temporally by considering longer snapshots, and spatially by coarsening over the individuals' position and velocity data, it is conceivable that we might throw away the particular information which gave rise to the interesting phenomenon in the first place.

In this thesis we consider a continuous way of thinking of fluids describing multiscale phenomena, without losing the interesting effects.

Abstract

Classical fluid mechanics and, in particular, the general compressible Navier-Stokes-Fourier equations, have long been of great use in the prediction and understanding of the flow of fluids in various scenarios. While the classical theory is well established in increasingly rigorous mathematical frameworks, the atomistic properties and microscopic processes of fluids must be considered by other means. A central problem in fluid mechanics concerns capturing microscopic effects in meso/macroscopic continuum models. With more attention given to the non-Newtonian properties of many naturally occurring fluid flows, resolving the gaps between the atomistic viewpoint and the continuum approach of Navier-Stokes-Fourier is a rich and open field.

This thesis centres on the modelling, analysis and computation of one continuum method designed to resolve the highly multiscale nature of non-equilibrium fluid flow on the particle scale: Dynamic Density Functional Theory (DDFT). A generalised version of DDFT is derived from first principles to include: driven flow, inertia and hydrodynamic interactions (HI) and it is observed that the equations reproduce known dynamics in heuristic overdamped and inviscid limits.

Also included are rigorous, analytical derivations of the short-range lubrication forces on particles at low Reynolds number, with accompanying asymptotic theory, uniformly valid in the entire regime of particle distances and size ranges, which were previously unknown. As well as demonstrating an improvement on known classical results, these calculations were determined necessary to comply with the continuous nature of the integro-differential equations for DDFT. The numerical implementation of the driven, inertial equations with short range HI for a range of colloidal systems in confining geometries is also included by developing the pseudo-spectral collocation scheme 2DChebClass [67].

A further area of interest for non-equilibrium fluids is mathematical well–posedness. This thesis provides, for the first time, the existence and uniqueness of weak solutions to an overdamped DDFT with HI, as well as a rigorous investigation of its equilibrium behaviour.

Acknowledgements

It is my pleasant duty to thank Dr. Ben Goddard and Dr. Jin Sun for their unstinting guidance and support throughout my PhD. The breadth of Ben's mathematical and computational talents are quite astonishing, and, having worked with him, I can safely say that any integral that he cannot do 'by parts' is not worth considering with. Equally, Jin's knowledge of fluid mechanics and computational engineering has always left me impressed, and I am very grateful for all the stimulating discussions we have had together. Furthermore, I am pleased to thank Prof. Grigorios Pavliotis for his continual advice and encouragement over the course of my PhD.

I'd like to thank Jim Morrice and Lesley Wilson for their support over my PhD years, having known me my entire life; putting me up when I first moved to Auld Reekie; keeping me and Emma well plied with food, wine and whisky; and for imparting on us their wise Leither philosophy. I'd also like to thank Calum, Joe, Isla, and Mark. You'll never know the extent to which the weekend adventures, East and West, has helped produce this thesis. Calum, thank you for your dear friendship; as my fellow mechanical fettler, and as an accomplished academic in your own right, I have enjoyed many stimulating scientific conversations with you. Not to mention the Skotebi boys. And of course, James and Kayne, the North Berwick Riders.

I cannot thank enough the institution of *Womtopia*, and all those who inhabit it. Diolch yn fawr. A echo of fiddles, concertinas and choir music lingers in the wood and stone, having provided a hospital haven, in a time of convalescence, for the final chapter of this thesis which I completed 'one–handed'.

I want to thank Mum, Dad, and Sam for their support in getting me here, each in their own ways. Mum for raising me right in Reading, Dad for providing wonder in Wales, and Sam for keeping me laughing and connected to reality. Lastly, I would like to thank Emma Brierley for her love, patience and magic.

Publications & Presentations

Contributions to the literature related to this thesis:

[68] B. D. Goddard, R. D. Mills-Williams, and G. A. Pavliotis. Well-posedness and equilibrium behaviour of overdamped dynamic density functional theory. *arXiv preprint arXiv:2002.11663*, 2020.

[69] B. D. Goddard, R. D. Mills-Williams, and J. Sun. The singular hydrodynamic interactions between two spheres in Stokes flow. *arXiv preprint arXiv:1809.05459*, 2020.

This work has been presented at the following conferences:

2017 British Applied Mathematics Colloquium, Surrey, UK "Dynamical Density Functional Theory with a Short Range Hydrodynamic Interaction".

2018 71st Annual Meeting of the APS Division of Fluid Dynamics, Atlanta Georgia, USA "Exact Solutions, Asymptotics and Numerics for Unequal Spheres in in Viscous Fluid".

2019 Hewitt-Reese Spring School on Modelling Multiphase Flows, Glasgow, UK "An Introduction to Dynamic Density Functional Theory".

2019 British Applied Mathematics Colloquium, Bath, UK "Dynamic Density Functional Theory: Well–Posedness, Global Asymptotic Stability".

For my family

Contents

List of Figures

List of Tables

Nomenclature

Lower Case Greek

α	Mass diffusivity
α, η_1, η_2	Spherical bipolar radial ordinate
β	$(k_B\mathrm{T})^{-1}$
β	Sphere radii ratio r_2/r_1
$\beta_i^{(\kappa_2)}$, $\theta_i^{(\kappa_2)}$	Expansion coefficients used in Theorem 7.6.10
β_n^{-1}	Eigenvalues of $\mathscr{R}$ from Definition 7.6.4
γ	Friction coefficient, Stokes unit
γ	Euler–Mascheroni constant
$\gamma_k^{(\kappa_2)}$	Eigenvalues of $\mathscr{A}_{\kappa_2}$ defined in (7.6.17)
γ_n	$\coth\alpha\coth(n+\frac{1}{2})\alpha$
δ_n, ϕ_n, ψ_n	Expansion coefficients used in Theorem 7.4.3
ϵ	Small nondimensional parameter
ε	Small perturbation from X_ϕ
ζ_i^a	Gaussian white noise process
(η,ξ,θ)	Spherical bipolar coordinates
κ_1	Nondimensional external potential strength
κ_2	Nondimensional two body potential strength
$\kappa_{2\sharp}$	Point of critical stability defined in (7.6.22)
λ	Separation constant in Chapters 3 and 4
λ	Scalar value of $\mathbb{C}$ used in Lemma 7.4.2
$\lambda(\kappa_2)$	Eigenvalue of $\mathscr{L}_1$ used in Theorem 7.6.10
λ_i	Eigenvalues of $\boldsymbol{R}$ in Chapter 5
μ	Probability measure
μ	Dynamic viscosity
μ_c	Chemical potential
μ_i	Eigenvalues of $\boldsymbol{D}$ defined in (7.2.6)
$\mu_{\max}$, $\mu_{\min}$	Largest and smallest eigenvalues of $\boldsymbol{D}$ respectively
ρ	Constant fluid density
ϱ	Non-constant colloid density
ϱ_0	Initial colloid density
ϱ_n	n-particle configuration space distribution function, for $n \geq 2$
ϱ_∞	Unique equilibrium density
σ	Sphere diameter
σ_H	Hydrodynamic diameter
τ	Characteristic time scale
ϕ	Volume fraction
ϕ_g	Gauss packing fraction $\frac{\pi}{3\sqrt{2}}$
ϕ_n	Eigenvalues of $\mathbf{1}+\mathscr{Z}_1^\varrho-\lambda\mathscr{Z}_2^\varrho$ used in Theorem 7.4.3
χ	Compact stream function
χ_ϵ	Convex approximation to $\lvert\cdot\rvert$ in Definition 7.9.1
ψ, ψ_1, ψ_2	Stream functions in Chapter 3

Upper Case Greek

$\boldsymbol{\Gamma}$	$3N \times 3N$ friction tensor, equivalently $\boldsymbol{R}$
$\tilde{\boldsymbol{\Gamma}}_{ij}$	Nondimensional 3×3 friction tensor
$\boldsymbol{\Gamma}_{ij}$	3×3 block matrices of $\boldsymbol{\Gamma}$
Θ	Step function in FMT excess free energy density
Ξ	Grand partition function
Π, Π_1	Nonlinear and linear boundary operators respectively, (7.2.3), (7.6.15)
$\Delta(n)$	Solution coefficient in (3.6.3)
Ω	Mermin energy functional in Chapter 2
	Fluid domain in Chapters 3, 4

Lower Case Roman

$\mathbf{a}$	Flux
a_n, b_n, c_n, d_n	Squeeze summation coefficients in (3.7.5)–(3.7.6)
$a(\cdot)$, $b(\cdot)$	Squeezing and shearing scalar resistance functions resp.
c	Spherical bipolar focal length
c_{ls}	Log–Sobolev constant
c_{pw}	Poincaré–Wirtinger constant
d	Centre to centre distance
d_1, d_2	Centre distance to O, sphere 1 and 2 resp.
$d_{\min}$	Minimal centre to centre distance
$\mathbf{e}_i$	Eigenvectors of $\boldsymbol{D}$ defined in (7.2.6)
$f(\mathbf{r}, \mathbf{p}, t)$	Phase space density
f_m, g_m	Summation terms in [90]
$g(\mathbf{r}, \mathbf{r}', [\varrho])$	Two body correlation function
h	Planck constant in Chapter 2
	Dimensional surface distance in Chapters 3, 4
$\mathfrak{h}$	Metrical coefficient for spherical bipolar coordinates
k_B	Boltzmann constant
m	Mass of colloidal particle
$\mathbf{n}$	Unit normal vector into fluid domain
$\mathbf{n}_{ij}$, $(\hat{\mathbf{n}}_{ij})$	Intersphere (and normalised) distance vector
p	Fluid pressure
$\mathbf{p}_i$	Momentum vector of particle i
$\mathbf{r}$	Position vector
r	$\lvert\mathbf{r}\rvert$
r_1, r_2	Radii of sphere 1 and 2 resp.
$\mathbf{r}_i$, $\mathbf{v}_i$	Individual sphere position and velocity vectors resp.
$\mathbf{r}^N$, $\mathbf{v}^N$	$3N$ sphere momentum and position vectors resp.
r_{ij}	$\lvert\mathbf{r}_j - \mathbf{r}_i\rvert$
t	Time
u_n	Eigenfunctions of $\mathscr{R}$ from Definition 7.6.4
$\mathbf{u}$	Velocity of Stokes fluid
$\mathbf{v}$	Mean hard sphere fluid velocity
$v_k^{(\kappa_2)}$	Eigenfunctions of $\mathscr{A}_{\kappa_2}$ defined in (7.6.17)
$w^{(\kappa_2)}$	Eigenfunction of $\mathscr{L}_1$ used in Theorem 7.6.10
$\mathbf{w}_n$	Eigenfunctions of $\mathbf{1} + \mathscr{Z}_1^{\varrho} - \lambda\mathscr{Z}_2^{\varrho}$ used in Theorem 7.4.3
$\mathfrak{x}$	$\cos\xi$
(x, y, z)	Cartesian coordinates
(z, r, θ)	Cylindrical polar coordinates

Upper Case Roman

$\mathbf{1}$	3×3 identity matrix
$\mathbf{1} + \mathscr{Z}_1^{\varrho}$	Local operator on acting on $\mathbf{a}$ defined in (7.4.2a)
A	Characteristic flux scale
$\boldsymbol{A}([\mathbf{a}], t)$	Advection tensor defined in (7.2.4)
A_{ij}^X, X_{ij}^A ,Y_{ij}^A	Jeffrey & Onishi scalar functions
A_n–H_n	Shear summation coefficients in (4.6.1)–(4.6.2)
$\mathscr{A}_{\varrho}$	The operator $(\mathbf{1} + \mathscr{Z}_1^{\varrho})^{-1}\mathscr{Z}_2^{\varrho}$
$\mathscr{A}_{\kappa_2}$	Differential operator defined in (7.6.16a)
$\boldsymbol{B}$	$(mk_B\mathrm{T}\boldsymbol{\Gamma})^{1/2}$
$\mathscr{B}$	Nonlocal operator (7.6.16b)
$C(T)$	Constant dependent on the final time T
$\boldsymbol{D}(\mathbf{r}, [\varrho], t)$	Diffusion tensor defined in (7.1.4)
F	Nonlinear map defined in (7.5.6)
$\boldsymbol{F}$	Non-dissipative force
$\boldsymbol{F}^{\mathrm{diss}}$	Dissipative force
$\mathscr{F}$	Free energy functional defined in (7.1.6)
Fr	Froude number
F_x	Shearing force
F_z	Squeezing force
$\mathscr{F}$	Free energy functional used in Chapter 7
$\mathscr{F}_{ex}$	Excess free energy
$\mathscr{F}_H$	Total Helmholtz free energy defined in (2.1.4)
$\mathscr{F}_{in}$	Intrinsic Helmholtz free energy defined in (2.1.2)
$\mathscr{F}_{\mathbf{u}}$	Augmented Helmholtz free energy in Chapter 2
$\mathscr{H}$	Relative entropy functional defined in (7.6.4)
L	Characteristic length scale
$\mathscr{L}_1$	Linearised nonlocal differential operator defined in (7.6.13)
$\boldsymbol{M}$	Mass matrix
N	Number of particles or spheres
Pe	Péclet number
P_n	Legendre polynomial of degree n
Q_n	$P_{n+1} - P_{n-1}$
$\boldsymbol{R}$	Resistance matrix, equivalently $\boldsymbol{\Gamma}$
Re	Reynolds number
$\mathscr{R}$	Nonlocal operator from Definition 7.6.4
S_N	N–sphere configuration state space
T	Temperature
T	Final time
$\mathscr{T}$	Nonlocal operator defined in (7.8.4)
U	Characteristic velocity scale in Chapters 2, 3, 4
	Spatial domain in Chapter 7
U_T	Space-time cylinder $U \times [0, T]$ in Chapter 7
V	Volume
V	Potential energy
V_1, V_2, V_n	External, two body and n-body potentials respectively
W, X, Y, Z	Auxiliary functions in (4.2.4a)–(4.2.4d)
$\mathscr{X}_{\varrho}$	Inverse operator $(\mathbf{1} + \mathscr{Z}_1^{\varrho} + \mathscr{Z}_2^{\varrho})^{-1}$ used in Theorem 7.4.5
$\boldsymbol{Z}_1$, $\boldsymbol{Z}_2$	Diagonal and off-diagonal matrices
Z	Normalisation constant
$\boldsymbol{Z}_1(\mathbf{r}_1, \mathbf{r}_2)$	Diagonal two body HI tensor
$\boldsymbol{Z}_2(\mathbf{r}_1, \mathbf{r}_2)$	Off-diagonal two body HI tensor
$\mathscr{Z}_2^{\varrho}$	Nonlocal operator acting on $\mathbf{a}$ defined in (7.4.2b)

Notation From Jeffrey & Onishi [92]

r	d
a_1, a_2	r_1, r_2
λ	r_2/r_1
ξ	$\frac{d-r_1-r_2}{\frac{1}{2}(r_1+r_2)}$
s	$\frac{d-r_1-r_2}{\frac{1}{2}(r_1+r_2)}+2$

Abbreviations, Sets & Mathematical Operations

DFT	Density Functional Theory
DDFT	Dynamic(al) Density Functional Theory
FMT	Fundamental Measure Theory
GMS	Goddard, Mills, Sun (label for present work of Chapters 3, 4)
HI(s)	Hydrodynamic Interaction(s)
MD	Molecular Dynamics
ODE	Ordinary Differential Equation
PDE	Partial Differential Equation
SD	Stokesian Dynamics
SDE	Stochastic Differential Equation
$L^2(U, \varrho^{-1})$	Weighted $L^2(U)$ space
$P_{ac}(U)$	Space of absolutely continuous probability densities supported on U
$P_{ac}^+(U)$	$P_{ac}(U)$ restricted to strictly positive functions
Tr	Trace operator
$\top$	Transpose
$\partial_{\mathbf{n}}$	Directional derivative in $\mathbf{n}$
$\top$	Transpose
∇	Gradient
$\nabla\times$	Curl
$\nabla\cdot$	Divergence
∇^2	Laplacian
$u \star v$	Convolution of two functions $\int_U \mathrm{d}\mathbf{r}\, u(\mathbf{r}-\mathbf{r}')v(\mathbf{r}')$
$\mathbf{u} \otimes \mathbf{v}$	Outer product / dyadic of two vectors $\mathbf{u}\mathbf{v}^\top$

Chapter 1

Introduction

Motivation

In this thesis we consider three topics:

1. **Dynamic Density Functional Theory (DDFT)**: A 3D coupled system of nonlinear, nonlocal, integro-partial differential equations (PDEs) describing the statistical mechanical evolution of a large assembly of interacting particles subject to thermal noise, hydrodynamic interactions, and external currents, which form a wider class of equations governing the flow of nonequilibrium inhomogeneous fluids.

2. **Hydrodynamic Interactions in Colloidal Fluids**: A derivation and analysis of analytical solutions to Stokes equations for the singular interaction of a two–sphere system immersed in viscous fluid, including a presentation of the currently attainable asymptotic theory.

3. **Well-Posedness and Equilibrium Behaviour of Overdamped DDFT**: The first establishment of the existence and uniqueness of weak solutions to overdamped DDFT with hydrodynamic interactions, which constitute nonlinear, nonlocal, integro PDEs for the spatially varying number density, as well as an analysis of equilibrium states including bifurcation theory for confined systems.

These three topics combine in such a way to model complex multiscale fluid flows. Such fluids often display different flow patterns and equilibrium states, compared to classical ones (air, water, honey etc.), because they have multiscale properties. In particular, the complex fluid may have a dispersed solid or liquid phase within a liquid or gas solvent, meaning it has multiple *spatial* scales. An example is shown in Figure 1.1a showing drawing ink, which is composed of solid pigment particles dispersed in a liquid carrier medium. Alternatively, Figure 1.1b shows mechanical grease, which is an emulsification of soap in oil. In each case the combined solid–liquid or liquid–liquid medium is known as a colloidal fluid, and the equilibrium and thermodynamic quantities such as the number density distributions, surface tensions and bulk viscosities may differ substantially from classical fluids.

Multiscale properties of fluids may also manifest in dynamical behaviour. For example, Figure 1.1c shows a silicone polymeric fluid, which, due to the complex intermolecular interactions of the long polymer chains, behaves as a viscous liquid on long time scales but as an elastic solid over a short time scales, giving rise to a nonlinear stress–strain relationship of the bulk fluid. Furthermore, Figure 1.1d shows a murmuration, which is an example of an active atomistic fluid. A minimal description of the murmuration is that the starlings move more or less in the same direction as their nearest neighbours, remain close together, and do not collide. Such individual dynamical properties may be compared with the equilibrium microscopic properties of nematic liquid crystals, whose repulsive molecules arrange themselves in parallel orientations [130].

Additionally, a fluid may possess fast processes on microscopic scales, such as the smaller molecules of the dispersion medium being subject to thermal agitation, which is not felt by the

(a) Drawing ink is a colloid of solid pigment particles dispersed in liquid.

(b) Grease is a liquid-liquid colloid with soap emulsified in oil.

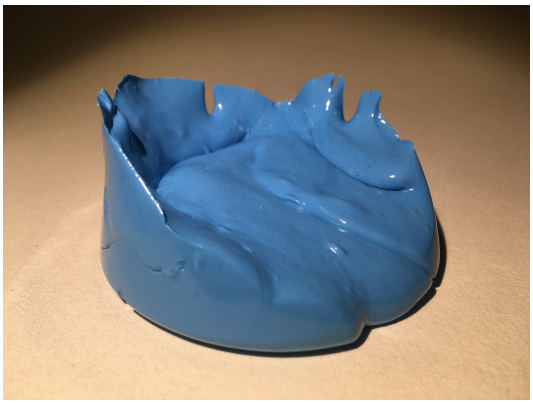

(c) A shear thickening visco-elastic fluid, 'therapy putty', used in medical applications.

(d) A mumuration of starlings. [Source: Rasmussen, Wikimedia]

Figure 1.1: Examples of complex multiscale fluids.

larger and heavier colloidal molecules making up the bulk. This means it has multiple *temporal* scales. For example, a typical collision timescale for water molecules is $10^{-15}s$, whereas a typical relaxation time of the colloidal particle momenta due to friction with the dispersion medium is $10^{-7}s$ [61]. Such a large difference in the magnitude of these collision times leads to a time scale separation in the dynamics of the particles making up the colloidal fluid.

1.1 Colloids

In the atomistic description, a fluid can be composed of particles of typical size covering the range of mist, fine dust and particulate matter in smoke all the way down to the diameter of the atoms which make up the molecules, at which point, one must introduce quantum effects. This definition of a particle, depending on the perspective of the reader, may not be remarkable until one observes that it directly corresponds to the size range of a cricket ball up to the diameter of the earth (see [75, Figure 1-1.1]). This reveals the highly multiscale nature of fluids, and, given this covering of orders of magnitude, one is confronted with the inherent dimensionality and therefore computational challenges involved in the theory of fluids. Despite the apparent difficulty this poses, significant theoretical advances were made in the 19th century, when the first continuum models of fluids were introduced. Additionally the theory of viscous fluids is very established, and is applicable to larger molecules and polymers immersed in a bulk of much smaller particles.

The fluids under investigation in this thesis, colloidal fluids, are composed of particles (typical size 10nm–10μm) suspended in a solvent of much smaller and lighter particles (around $1nm$ in size) [42]. The average number density of the colloids therefore has spatial variation.

Equilibrium Properties

When the solvent liquid is at rest, and in the presence of an external field, the colloids will move to minimise the free energy of the system, to find the most favourable configuration at equilibrium. In general, the most favourable configuration will change depending on the shape of the individual colloids. In bounded systems with a bath (dispersion medium) at constant temperature, the free energy is the Helmholtz free energy $\mathscr{F}_H$, to be discussed in Sections 1.6 and 2.1, and is the central thermodynamic quantity in density functional theories. It is the energy which the density minimises at equilibrium.

As an example of the kind of equilibrium states, consider container of solution of colloids with larger (diameters greater than 10μm) particles. The larger particles settle to the bottom under gravity. The colloidal particles are subjected to Brownian motion and at equilibrium the upwards flux of the colloids (due to the Brownian motion), from an area of high concentration to low concentration, will balance with gravity. The larger colloidal particles are still subject to Brownian motion, but gravity is the dominating force for them, owing to their greater mass, and hence they sink to the bottom of the container.

Dynamical Properties

The hydrodynamic interactions described in this thesis are dynamical properties, that is, only existing for the colloidal particles with finite relative velocities with respect to the velocity of the dispersion fluid. Obtaining knowledge on the motions of the colloids interacting with each other will inform us of the evolution of the suspension as a whole. Equally, the evolution of the suspension will determine the forces on the particles, and thus the relationship between the microscopic and macroscopic dynamics is interconnected. One can see this in the case of the Rotne–Prager [154], the so called long range HI, in which the motion of a individual colloid induces motion on the other colloid giving rise to collective motion.

Another manifestation of scale separation occurs between the bath particles (the solvent) and the colloidal particles (the active system). The bath and the colloids are at the same temperature but since the bath particles are much lighter, and so small that they are more readily agitated by heat, they move faster, and bombard the larger colloidal particles with microscopic momentum exchanges to cause Brownian motion of the colloid. This leads to a temporal scale separation for the entire system.

A property of the system will be the diffusion constant $D = k_B\mathrm{T}/\gamma$, where k_B is Boltzmann's constant, T is temperature, and γ is the friction coefficient or Stokes drag. This relationship between D and γ provides a measure of the propensity of colloids to diffuse and goes back to Einstein [48]. The greater the friction of the bath on the colloids the smaller the diffusion, conversely the higher the temperature, the greater the diffusion. Thermodynamically, this phenomenon is described by the fluctuation dissipation relation: the root mean square fluctuation in energy of the colloidal particles is proportional to the heat capacity of the bulk [77, 142]. This describes, roughly speaking, the mechanism to dissipate kinetic energy to heat energy is bath friction, and vice versa: the Brownian motion of the bath particles transforms microscopic heat energy to kinetic energy [100].

Modelling Challenges

For simple colloid shapes (spheres and ellipsoids) dispersed in an unbounded flow there are many analytical solution techniques to determine the mobility and resistance of a given colloid as a function of geometric constants (radius, centre distances etc) and special functions. Complex geometries, the presence of walls, corners etc, many be dealt with by convergent numerical methods.

However, complex particle shapes abound: flakes, grains, ribbons as well as asymmetric shapes. For example in studying lyotropic materials (the generation of a liquid crystal upon the addition of a solvent), the isotropic-nematic transitions and stability of the macroscopic crystals require accurate knowledge of hydrodynamics of the individual grains. Such problems require large computational resources. Accounting for the shape of the individual elements, deforming under local fluid stress, is a very computationally challenging problem. Additionally, taking

into account the three-dimensional flow of such systems adds to complexity of the numerical solution.

Due to the fundamental limitations imposed on the integration time of a single processor, relying on unparallelised numerical methods to integrate a set of fluid equations is unsustainable from a computational point of view. Parallelised computer architectures are an answer, where they can be used, and have provided many orders of magnitude in speedups for molecular dynamics simulation. Numerical schemes for computational fluid dynamics, i.e. (1.2.2b)-(1.2.2a) only for nearest neighbour interactions could be implemented in parallel computer architectures. In Section 1.5 we discuss, by climbing scales, different ways in which one can model molecular systems.

In practical applications, the evolution of the fluid structures may help or hinder many real world flows. In hydraulics, passive components such as venturi, orifices and nozzles may subject the fluid to large pressure gradients over relatively small spatial distances [11]. In these regions the interruption in continuity of liquid oil due to multiscale effects modifies the flow, and the dynamic interaction between liquid and solid boundaries is changed. In terms of the hydraulic application, the flow paths may altered such as to lessen the force applicable to solid boundaries causing a decrease in power output, head and efficiency.

1.2 Classical Fluid Mechanics

Navier-Stokes Equations

In 1821 the first of two memoirs by Claude-Louis Navier was published on the theoretical flow of an incompressible fluid taking into account molecular and body forces [123]. The equations governing the evolution of the fluid velocity $\mathbf{u}$ and pressure p are given by

$$\partial_t \mathbf{u} + (\mathbf{u} \cdot \nabla)\, \mathbf{u} = -\frac{1}{\rho}\nabla p + \nu \Delta \mathbf{u} + \mathbf{f}, \tag{1.2.1a}$$

$$\nabla \cdot \mathbf{u} = 0. \tag{1.2.1b}$$

where $\nu = \mu/\rho$ is the kinematic viscosity of the fluid, ρ is the constant density of the fluid and $\mathbf{f}$ is a body force. Before (1.2.1a)–(1.2.1b), the theory of fluid flows was limited to perfect fluids which exert no frictional force on the solid surfaces past which they move [50] (ommiting pressure forces acting purely in the normal direction). The effects of molecular forces, or viscosity, were identified as the main reason for the discrepancies found between theory and experiment. Navier did not understand the notion of shear stress in a fluid, but he correctly modified Euler's inviscid equations to take into account the forces between the molecules [3]. This advancement was substantial because after all, a fluid is composed of molecules, and the notion of fluid viscosity was finally starting to be developed. Since then, the compressible Navier-Stokes (1.2.1a)–(1.2.1b) have rigorously been shown to be the first order correction to the Euler equations (with zero viscosity), by taking a hydrodynamic limit of the Boltzmann equation for small Knudsen number, a nondimensional measure of the mean-free path length of a typical molecule in the fluid, see for example [71, Sec 5.2].

Validity and Considerations

For many purposes, continuum models of fluid flow such as (1.2.1a)–(1.2.1b) are insufficient for an accurate mathematical model and prediction of flow at length scales comparable to the size of the particles constituting the fluid [42]. A consideration of the atomistic nature of fluids is important at this scale, in particular there are various microscopic and chemical properties of liquids and gases, as well as hydrodynamical particle mechanics which are relevant.

An application of the Navier-Stokes equations at this scale is known to lead to unphysical results. This may be seen in a wide variety of settings, but particularly: the classical moving contact line problem in droplet (de)wetting leading to a non-integrable stress at the trijunction [86] and an incorrect prediction of the motion of Crookes radiometer for flow in a partial vacuum [160]. Similarly, the restriction to continuum based formalisms in condensed matter type systems leads to inconsistent results, such as the incorrect prediction of the cusp singularities

in the freezing of liquid drops[161], [2]. The first and last of these examples cite sensitivity to conditions at solid, liquid and vapour interfaces, where there are large densities differences and the dynamics of interfacial phenomena are complex. The second example conveys the incorrect predictions Navier-Stokes-Fourier for low density gases.

Additionally, either by design or not, fluids are often multiphase in many industrial applications. For example, in hydraulic applications the forces that tend to hold the liquid oil particles together and stop the formation of any phase differences are external pressure and intermolecular forces. However the oil may also be entrained with non-condensable substances, nucleation agents, emulsifiers and various colloids and, we can imagine that in a fluid system possessing complicated geometries, temperature, pressure and velocity variations, it must be the case that non-trivial interior fluid structures may evolve such as cavitation and vortex structure [99].

Stokes Equations

The slow flow incompressible equations, Stokes equations, were proposed by George Gabriel Stokes in 1845 for flows with dominating internal friction over inertial effects. Stokes equations may be applicable to slowly moving liquids and viscous non-rarefied gases and are given by [163]

$$\nabla^2 \mathbf{u} - \frac{1}{\mu}\nabla p = 0, \tag{1.2.2a}$$

$$\nabla \cdot \mathbf{u} = 0, \tag{1.2.2b}$$

where μ is the dynamic viscosity of the fluid measured in [kg m^{-1} s^{-1}]. From equations (1.2.2a)–(1.2.2b), one may calculate the drag force F_z on a single spherical particle moving through a viscous fluid, such as steel ball falling through honey, to be

$$F_z = 6\pi\mu U a, \tag{1.2.3}$$

where U is the velocity of the steel ball and a is its radius. It is the viscous resistance of the fluid which decreases the acceleration of the ball until a terminal velocity is reached. So long as the ball is small enough, or the motion is slow enough, the force is proportional to the instantaneous velocity of the ball, as seen in (1.2.3).

This law, Stokes law, is very good when one is concerned with suspensions of particles sufficiently disperse that they do not mutually disturb the velocity fields local the their neighbours. However, the particles in most instances will not be disperse. Obtaining a description for the motion of an assemblage of many particles that disturb the velocity fields of their neighbours in a bounded domain would be very desirable for many applications and is a starting point for the work in this thesis.

1.3 Direct Numerical Solution Of Colloids In Stokes Flow

Stokes equations (1.2.2b)–(1.2.2a) are second order linear PDEs for the fluid velocity and pressure for which analytical solutions for given geometries and boundary conditions are generally unknown. The numerical solution of (1.2.2b)–(1.2.2a) may in general be computationally expensive. Discretising a general fluid domain with N finite elements (nodes) results in large linear systems which are usually solved with Gaussian elimination, requiring $O(\mathrm{N}^3)$ floating point operations. If one would like to mesh a fluid domain consisting of many hard spheres with narrow interstitial regions, where pressures are expexted to become very large, then N will also become very large. What is more, as the system of spheres becomes more dense, many remeshings will have to be made, in order to accurately capture the known normal and tangential singularities for the inter-sphere HI, $\sim \epsilon^{-1}$ and $\log \epsilon^{-1}$ respectively. Hence a full finite element method quickly becomes impractical. One way to overcome the computational cost is to use a Boundary Integral Method (BIM) to resolve the fluid flow in the interstitial region between the particles [83].

Boundary Integral Methods

Often, the boundaries of the fluid domain do not fit into a curvilinear coordinate system and hence there is no way in which closed form analytical expressions for the velocity and pressure may be derived. By using a BIM, the fluid disturbance far away from the particle surface can be described by using a multipole expansion, and the moments of the expansion are solved numerically for successive coefficients. For simple particle shapes, the basis functions forming the solution are distributions of singularities in the particle interior which dictate the boundary shape of the particle. For more complicated particle shapes the singularities are brought near to the boundary of the particle shape giving the name Boundary Integral Method.

These methods reduce the complexity of corresponding numerical methods (finite difference or finite element on the full 3D equations) by one spatial dimension. In particular, a 3D PDE is transformed to a set of 2D integral equations for a set of Stokes singularities distributed along the surface of the particle boundary (or indeed the boundary of the fluid domain if it include some bounding surfaces). In particular, the integral equations take the form [98, Section 14.4]

$$\begin{aligned}
\mathbf{u}(\mathbf{y}) = &-\frac{1}{8\pi\mu}\oint_S \mathrm{d}S(\boldsymbol{\xi})\,\mathscr{G}(\mathbf{y}-\boldsymbol{\xi})\cdot(\sigma(\xi;\mathbf{u})\cdot\mathbf{n}(\boldsymbol{\xi})) \\
&-\oint_S \mathrm{d}S(\boldsymbol{\xi})\;(\mathbf{n}(\boldsymbol{\xi})\cdot\boldsymbol{\Sigma}(\mathbf{y},\boldsymbol{\xi})))\cdot\mathbf{u}(\boldsymbol{\xi}) \quad \text{for } \mathbf{y}\in Q \qquad (1.3.1)\\
p(\mathbf{y}) = &-\frac{1}{8\pi\mu}\oint_S \mathrm{d}S(\boldsymbol{\xi})\,\mathscr{P}(\mathbf{y}-\boldsymbol{\xi})\cdot(\sigma(\xi;\mathbf{u})\cdot\mathbf{n}(\boldsymbol{\xi})) \\
&-\frac{1}{4\pi}\oint_S \mathrm{d}S(\boldsymbol{\xi})\;(\mathbf{n}(\boldsymbol{\xi})\cdot\nabla_{\mathbf{y}}\mathscr{P}(\mathbf{y},\boldsymbol{\xi})))\cdot\mathbf{u}(\boldsymbol{\xi}) \quad \text{for } \mathbf{y}\in Q
\end{aligned}$$

where Q is the fluid domain, $\mathbf{n}(\boldsymbol{\xi})$ is the unit vector pointing into Q and $\boldsymbol{\xi}$ parametrises the surface of the particle. Furthermore, $\mathscr{G}$ is the Oseen tensor, $\mathscr{P}$ is the pressure field of the Oseen tensor, σ is the stress tensor, Σ is the stress field or Oseen-Burgers tensor such that $8\pi\mu\Sigma_{ijk} = -\mathscr{P}_j\delta_{jk} + \mu\left(\mathscr{G}_{ij,k} + \mathscr{G}_{kj,i}\right)$, each given by the relations

$$\begin{aligned}
\mathscr{G} &= \frac{1}{r}\left(\mathbf{1} + \frac{\mathbf{r}\otimes\mathbf{r}}{r^2}\right), \qquad (1.3.2)\\
\mathscr{P} &= -2\mu\nabla(r^{-1}),\\
\sigma &= -p\mathbf{1} + 2\mu\boldsymbol{e},\\
\boldsymbol{e} &= \frac{1}{2}\left(\nabla\mathbf{u} + \nabla\mathbf{u}^{\top}\right)
\end{aligned}$$

and $\mathbf{r}$ is a position vector with $r = |\mathbf{r}|$. The rate of strain tensor, $\boldsymbol{e}$, is independent of $\nabla\cdot\mathbf{u}$ because the fluid is assumed to be incompressible. The first integral in (1.3.1) is known as the single layer potential, since it corresponds to a single layer of charges distributed over the surface of an electrical conductor, by analogy with electric potential theory [165]. Conversely, the second integral is known as the double layer potential, corresponding to a surface distribution of electric dipoles, here a double layer of Stokeslets.

Computational Cost

There are computational advantages in using BIMs: first, the method reduces the computational effort required for discretisation of the fluid domain by the dimensionality reduction and second, in time independent problems, no grid remeshing is required at each time step. However the asymptotic behaviour of the Stokes singularities emanating from the boundary of the particles decay algebraically, propagating in all directions. Therefore a BIM tends to give rise to dense systems (c.f. finite element methods for full the 3D Stokes equations) with N–body interactions which does not lend itself well to parallelisation.

1.4 Microhydrodynamics Of Hard Spheres

Hydrodynamic interactions (HI) between bodies immersed in viscous fluid have been shown to be important in modelling many complex fluid phenomena in physics, biology and engineering. For example, in suspensions of cornstarch and other solid particles of micron sizes at high solid volume fractions, the interplay between HI and particle contacts gives rise to a sudden increase in viscosity with increasing shear stress [54, 107]. HI also affects complex fluid behaviour at many length scales. At the small scale, the flow properties of suspended particles in emulsions and gels have historically determined their physical and chemical classification. In hemodynamics, blood is a suspension of platelets, white cells and high fractions of red cells in plasma, where fluidity and stability may be significantly altered during disease processes [49].

On larger scales, the formation of topographical features under sea water is due to turbidity currents, where both inertial effects and slow motion of the suspensions are important [12]. In terms of numerical modelling, such as dynamical density functional theory formalisms for two dimensional colloidal flow, the inclusion of HI is enough to alter the dynamics of the density even when solving for dilute particle collections [61]. The relevance and applicability of HI are therefore well established in many fluid flow problems in science and engineering. Many physical models for the flow of particles accounting for such phenomena have largely varying spatial scales which makes their computation challenging. Generally speaking, a numerical model that accurately predicts complex fluid phenomena requires the full knowledge of the HI between the suspended particles.

In Stokesian dynamics (SD), the quasi-static motion of a suspension of N rigid spherical particles at low Reynolds number is given by [13]

$$\boldsymbol{F}^{\text{diss}}(\mathbf{r}^N, \mathbf{v}^N) + \boldsymbol{F} = \boldsymbol{M}\frac{\mathrm{d}\mathbf{v}^N}{\mathrm{d}t}, \tag{1.4.1}$$

where $\boldsymbol{M}$ is a mass matrix, $\boldsymbol{F}^{\text{diss}}$ is the dissipative force due to the HI of the particles mediated by the solvent fluid, $\mathbf{r}^N = [\mathbf{r}_1, \cdots \mathbf{r}_N]^\top$ is a vector of $6N$ particle position coordinates and $v^N = [\mathbf{v}_1, \cdots \mathbf{v}_N]^\top = \mathrm{d}\mathbf{r}^N/\mathrm{d}t$. The vector $\boldsymbol{F}$ accounts for conservative and non-conservative applied forces for example: the force due to gravity and the frictional force applied to the particle surfaces at contact, respectively. By nondimensionalising (1.4.1) with an appropriately defined Reynolds number Re, the dissipative forces are taken as linear in the velocity of the particles, and after setting $Re = 0$, equation (1.4.1) reads

$$-\boldsymbol{R}(\mathbf{r}^N)\mathbf{v}^N + \boldsymbol{F} = 0, \tag{1.4.2}$$

where $\boldsymbol{R}$ is the resistance matrix for the conformation of particles with position vector $\mathbf{r}^N$. As is standard in the theory, $\boldsymbol{R}$ is independent of the properties of the solvent fluid, as well as the magnitudes and directions of the particle velocities. Rather, $\boldsymbol{R}$ depends only on the particle separations and sizes. Note also that by adding a noise term to (1.4.2), correlated to the thermal fluctuations of the solvent fluid according to the generalised fluctuation-dissipation theorem [142], one may obtain the dynamics of Brownian motion.

In theory $\boldsymbol{R}$ has a large bandwidth, owing to N- body interactions. As in SD, in order to solve for the particle velocities, one must invert a dense matrix in $O(N^3)$ operations which will be computationally expensive. Approximations to $\boldsymbol{R}$ may be made in order to reduce the computational cost for SD simulations. For example, Ball and Melrose [13] showed that $\boldsymbol{R}$ is made sparse by approximating the full N-body interactions to a two-body formalism of long range forces, with elements decaying as $1/r_{ij}$, where $r_{ij} = |\mathbf{r}_i - \mathbf{r}_j|$ is the distance between the centres of sphere i and j (c.f. Rotne-Prager [154]). Such an approximation of $\boldsymbol{R}$ is valid for non-dense systems, and, in this dilute regime, the hydrodynamic force due to lubrication is dominated by the long range mobility force.

Conversely, in the highly concentrated regime the lubrication forces will dominate the elements of $\boldsymbol{R}$. This may be justified by expanding $\boldsymbol{R}$ in moments including the one, two, three, $\cdots$, n- body interactions. One finds that the pairwise lubrication forces dominate the expansion and higher order effects found using far-field expansions such as the method of reflections will fade in comparison due to the divergent scalar functions of the lubrication forces [19].

The hydrodynamics of well-separated particles has been implemented in DDFT formalisms, [146], [62], [66], and tested against Brownian dynamics therein. The HIs in this regime of particle separation were first developed by Oseen [98], and later Rotne and Prager [154]. The formalism is based on the Green's function solution to the Stokes flow problem for a sufficiently well separated particle, that is

$$\begin{aligned} \nabla^2 \mathbf{u} - \frac{1}{\mu}\nabla p &= \mathbf{f}(\mathbf{r}), \\ \nabla \cdot \mathbf{u} &= 0, \end{aligned}$$

where $\mathbf{f}(\mathbf{r})$ is some force applied to the particle at position $\mathbf{r}$. To solve with a Green's function approach, we let $\mathbf{f}$ be a point force at the origin and by Fourier analysis or similar [98], the Green's function or *Oseen tensor* is given by

$$\mathscr{G}_{ij}(\mathbf{r}) = \frac{1}{r}\delta_{ij} + \frac{1}{r^3} r_i r_j \tag{1.4.4}$$

where r is the distance from the origin and r_i is the i^{th} component of the position vector $\mathbf{r}$. The Green's function is given in tensor form in (1.3.2) and presented in component form in (1.4.4). From the Oseen tensor the fundamental solution pair may be constructed

$$\mathbf{u}(\mathbf{r}) = \mathbf{f} \cdot \frac{\mathscr{G}}{8\pi\mu}, \quad p = \mathbf{f} \cdot \frac{\mathscr{P}}{8\pi\mu} \tag{1.4.5}$$

where $\mathscr{P}$ is the pressure field of the Oseen tensor given by

$$\mathscr{P}_j = 2\mu \frac{r_i}{r^3} + \mathscr{P}_j^{\infty}$$

for $\mathscr{P}_j^{\infty}$ an ambient (constant) pressure. The solution $\mathbf{u}(\mathbf{r})$ in (1.4.5) is known as the Stokeslet, or point force solution. The limiting assumption for the Stokeslet is that the sphere has been treated as point-like. For finite-sized spheres or disks, this assumption will lead to non-physical velocity and pressure fields. Not least, constructing a diffusion tensor from the Oseen tensor in (1.4.4) does not result in a strictly positive tensor at all particle separations. In particular, at small particle separations the smallest positive eigenvalue passes through zero leading to a non-invertible friction tensor, violating the positivity of the rate of mechanical energy dissipation. This also leads to issues when performing stochastic dynamics where one must take the square root of the diffusion tensor, which is only possible if the tensor is positive-definite.

For finite sized spheres, one may use a multipole expansion to approximate the integral of the Oseen tensor, along with a force distribution, over a sphere's surface. For a sphere of radius a at $\mathbf{r}_j$, to leading order the fluid velocity under the Stokes flow for a force $\mathbf{f}_j$ applied to the sphere is

$$\mathbf{u}(\mathbf{r}) = \left(1 + \frac{a^2}{6}\nabla^2_{\mathbf{r}_j}\right) \mathbf{f} \cdot \frac{\mathscr{G}(\mathbf{r} - \mathbf{r}_j)}{8\pi\mu}.$$

For a second sphere at $\mathbf{r}_i$ moving at velocity $\mathbf{v}_i$, Faxen's law states the force $\mathbf{f}_i$ felt by sphere i is proportional the the difference between $\mathbf{v}_i$ and the ambient velocity $\mathbf{v}^{\infty}$ (at $\mathbf{r}_i$), generated by the motions of the other spheres. Therefore one has

$$\mathbf{v}_i = \frac{1}{6\pi\mu a}\mathbf{f}_i + \left(1 + \frac{a^2}{6}\nabla^2_{\mathbf{r}_i}\right) \mathbf{v}^{\infty}(\mathbf{r}_i). \tag{1.4.6}$$

Now we note that in this two–body formalism one has that $\mathbf{v}^{\infty}$ is simply the sum over all

leading order fluid velocities local to each sphere (not including self interaction)

$$\mathbf{v}^{\infty}(\mathbf{r}_i) = \sum_{j\neq i}\left(1+\frac{a^2}{6}\nabla^2_{\mathbf{r}_j}\right)\mathbf{f}\cdot\frac{\mathscr{G}(\mathbf{r}_i-\mathbf{r}_j)}{8\pi\mu}. \tag{1.4.7}$$

Therefore, by combining (1.4.6) and (1.4.7) we obtain

$$\mathbf{v}_i = \frac{1}{6\pi\mu a}\mathbf{f}_i + \sum_{j\neq i}\left(1+\frac{a^2}{6}\nabla^2_{\mathbf{r}_i}\right)\left(1+\frac{a^2}{6}\nabla^2_{\mathbf{r}_j}\right)\mathbf{f}\cdot\frac{\mathscr{G}(\mathbf{r}_i-\mathbf{r}_j)}{8\pi\mu} \quad := \sum_j \boldsymbol{D}(\mathbf{r}_i,\mathbf{r}_j)\mathbf{f}_j + O\left(\frac{a}{r^4}\right)$$

where in the last line we have defined the diffusion tensor $\boldsymbol{D}$. It may shown, by Taylor expansion that, for two spheres centred at $\mathbf{r}_i$ and $\mathbf{r}_j$

$$\boldsymbol{D}(\mathbf{r}_i,\mathbf{r}_j) = \frac{1}{8\pi\mu}\left(\frac{1}{r}\mathbf{1}+\frac{\mathbf{r}\otimes\mathbf{r}}{r^3}+\frac{2a^2}{r^2}\left[\frac{1}{3r}\mathbf{1}-\frac{\mathbf{r}\otimes\mathbf{r}}{r^3}\right]\right)$$

where $\mathbf{r}=\mathbf{r}_i-\mathbf{r}_j$ and $r=|\mathbf{r}|$. For $i=j$ one has $\boldsymbol{D}=\mathbf{1}/(6\pi\mu a)$ which is classical result of the mobility of a single particle. Also, $\boldsymbol{D}$ is positive definite for all particle separations such that $r>2a$, which exactly corresponds to the case of non-overlapping hard spheres of radius a.

Short Range Forces

The Model for the Resistance Matrix $\boldsymbol{R}$

For the analysis in this thesis, we are interested in highly concentrated systems. We specify the three approximations we make in our construction of $\boldsymbol{R}$.

A1 The HI are **lubrication dominated**, that is, the divergent interactions between close surfaces dominate the elements of $\boldsymbol{R}$ in the highly concentrated regime.

A2 The HI are **strongly coupled** and we neglect n-body HI for $n>2$.

A3 The HI are **frame-invariant**; the justification being that the solvent fluid (over large enough distances) comoves with the particles.

Assumption **A3** says that for a steady solvent velocity $\mathbf{u}$ of a Stokes fluid in a domain Ω one has

$$\frac{1}{|\Omega|}\int_{\Omega}\mathrm{d}\mathbf{r}\,\mathbf{u}(\mathbf{r}) = \frac{1}{N}\sum_{i=1}^{N}\mathbf{v}_i,$$

where $|\Omega|$ is the size of the fluid domain. Such an assumption is not valid for sedimentation problems, where the solvent velocity $\mathbf{u}=0$ in Ω and the sphere velocities are collinear and non-zero. Non-frame-invariant simulations of Brownian motion in shear flow show shear induced ordering at low volume fractions, deviating from experimental observations [51]. We may however relax **A3** by rewriting the resistance matrix, as we will in Chapter 6.

With Assumptions **A1**, **A2**, **A3** we now present our model for the resistance matrix $\boldsymbol{R}$. For a finite Reynolds number, and in components, the force balance in (1.4.1), in the absence of external and contact forces, is given by an equation for the velocity $\mathbf{v}_i$ of the i^{th} particle

$$Re\,\dot{\mathbf{v}}_i = -\sum_{j=1}^{N} a(\mathbf{n}_{ij})(\mathbf{v}_i-\mathbf{v}_j)\cdot\hat{n}_{ij}\otimes\hat{n}_{ij} + b(\mathbf{n}_{ij})(\mathbf{v}_i-\mathbf{v}_j)\cdot(\mathbb{I}-\hat{n}_{ij}\otimes\hat{n}_{ij}) \tag{1.4.8}$$

for $1\leq i\leq N$, where $\mathbf{n}_{ij}$ ($\hat{n}_{ij}$) is the (normalised) vector pointing between the centre of sphere j to i, and $\mathbb{I}$ is the identity tensor.

Here $a(\mathbf{n}_{ij})$ and $b(\mathbf{n}_{ij})$ are the normal and tangential components of the hydrodynamic interaction respectively as functions of $\mathbf{n}_{ij}$. A crucial observation is that in the diffuse system limit, both $a(\cdot)$ and $b(\cdot)$ should decay to unity so that Stokes law is recovered: the total force

on particle i is proportional to its velocity with proportionality constant Stokes unit $-\gamma$. In terms of the spectral properties of $\boldsymbol{R}$, this means the eigenvalues must be degenerate in the dilute sphere limit, and the general solution to (1.4.8) (after setting $Re = 1$) becomes

$$\mathbf{v}_i(t) = e^{-\gamma t} \sum_{j=1}^{N} c_j \mathbf{e}_j$$

for $\{e_j\}_{j=1}^{N}$ a basis of R^{3N} and c_j constants dependent on the initial velocity data.

Additionally, if $\mathbf{v}_i = \mathbf{v}_j = \mathbf{c}$ for all i, j then the total HI force on each particle is zero in the reference frame co-moving at velocity $\mathbf{c}$. This is equivalent to saying that $\boldsymbol{R}$ has a zero eigenvalue associated with the translation of the entire system of particles at some uniform velocity, or that the interaction model is Galilean invariant.

We may expand the summation in (1.4.8) and collect together terms multiplying $\mathbf{v}_i$ to define the resistance matrix $\boldsymbol{R}$ in block form, here determined by diagonal and off-diagonal submatrices and $\boldsymbol{Z}_1$, $\boldsymbol{Z}_2$ respectively. We have

$$\boldsymbol{R} = \begin{pmatrix} \sum_{l\neq 1} \boldsymbol{Z}_1(\mathbf{r}_1, \mathbf{r}_l) & \boldsymbol{Z}_2(\mathbf{r}_1, \mathbf{r}_2) & \cdots & \boldsymbol{Z}_2(\mathbf{r}_1, \mathbf{r}_N) \\ \boldsymbol{Z}_2(\mathbf{r}_2, \mathbf{r}_1) & \sum_{l\neq 2} \boldsymbol{Z}_1(\mathbf{r}_2, \mathbf{r}_l) & \cdots & \vdots \\ \vdots & \vdots & \ddots & \vdots \\ \boldsymbol{Z}_2(\mathbf{r}_N, \mathbf{r}_1) & \cdots & \cdots & \sum_{l\neq N} \boldsymbol{Z}_1(\mathbf{r}_N, \mathbf{r}_l) \end{pmatrix}, \tag{1.4.9}$$

where the block matrices $\boldsymbol{Z}_1$ and $\boldsymbol{Z}_2$ are defined as

$$\boldsymbol{Z}_1(\mathbf{r}_i, \mathbf{r}_l) = -a(r_{il}) \frac{\mathbf{r}_i \otimes \mathbf{r}_l}{r_{il}^2} - b(r_{il}) \left(\mathbf{1} - \frac{\mathbf{r}_i \otimes \mathbf{r}_l}{r_{il}^2} \right)$$

$$\boldsymbol{Z}_2(\mathbf{r}_i, \mathbf{r}_j) = a(r_{ij}) \frac{\mathbf{r}_i \otimes \mathbf{r}_j}{r_{ij}^2} + b(r_{ij}) \left(\mathbf{1} - \frac{\mathbf{r}_i \otimes \mathbf{r}_j}{r_{ij}^2} \right)$$

and where $r_{ij} = |\mathbf{r}_i - \mathbf{r}_j|$ and $a(\cdot)$, $b(\cdot)$ are the scalar resistance functions corresponding to the divergent squeezing and shearing lubrication interactions of the close surfaces at high concentrations respectively. We note that the block-wise notation of (1.4.9) with summations on the diagonal is standard notation in statistical mechanical models of suspensions such as dynamic density functional theories (DDFTs), see [61], [62]. Note that the rows of $\boldsymbol{R}$ sum to zero, which implies that whenever $\mathbf{v}^N = c_0 \mathbf{e}_i$ for some constant vector $c_0 \in \mathbb{R}$, and e_i a basis vector of $\mathbb{R}^{3N}$, then $\mathbf{v}^N \in \ker \boldsymbol{R}$ and the interaction is Galilean invariant.

With the model for the resistance matrix $\boldsymbol{R}$ defined we now discuss the model for the scalar resistance functions which make up the elements of $\boldsymbol{R}$.

The Model for the Scalar Resistance Functions $a(\cdot)$ and $b(\cdot)$

For short range HI current models use asymptotic formulae for $a(\cdot)$ and $b(\cdot)$, for example the expressions found in Kim & Karrila [98], valid in a 'close' region of particle separation, combined with an arbitrary outer cut-off. It would be preferable to have a formula for both $a(\cdot)$ and $b(\cdot)$ valid at all particle distances so that arbitrary cut-offs are avoided. This property is particularly desirable in continuum formalisms, where the HI appear as convolution integrals with a separate additive Stokes term. The convergence of such integrals requires knowledge of the behaviour and decay of the scalar resistance functions over the entire support of the hard sphere number density for accurate numerical solutions. As such, this thesis provides a derivation and analysis of both resistance functions $a(\cdot)$ and $b(\cdot)$ valid at all particle separations. The analytical $b(\cdot)$ for two spheres of unequal radii is not considered in the main text, because we found that in this case, the boundary equations which need to be solved for the final set of series coefficients are an intractable system of coupled recurrence equations requiring dedicated computer algebra.

We determine $a(\cdot)$ and the corresponding stream function at all particle separations, which, to our knowledge, has not been previously obtained. We restrict the calculations to two non-rotating spheres with opposite velocities. By the linearity of Stokes equations however, the

angular component of the stream function for two approaching spheres rotating asymmetrically may be linearly superimposed.

To compare to existing results, we provide in the following section a history of slow viscous flow problems for two spheres.

History of Slow Viscous Flow Problems for Two Spheres

The singular HIs for each of the scalar resistance functions $a(\cdot)$ and $b(\cdot)$ which are computed in this paper take the general form of infinite series. These are not the same solutions to problems for two spheres in bipolar coordinates previously considered, e.g., Stimson and Jeffery [162], Goldman et al. [70]. It is the boundary condition choice, entire regime of validity, and singular nature of the HI that distinguishes this from previous works, described as follows.

The classical work concerning exact solutions for two spheres with equal velocities in viscous flow was presented by Stimson and Jeffery [162] for two *drafting* spheres. Similarly, Goldman et al. [70] consider two spheres *settling side by side* for a single mode of tangential interaction. Our derivations use the same formalisms but with opposite velocities, leading to the ϵ^{-1} and $\log \epsilon^{-1}$ singularities respectively. In that paper [162], there are two errata: firstly, for the first equation of their section 4, the factor inside the square bracket $-(1-\mu^2)$ should be $(1-\mu^2)$ (where $\mu = \cos\xi$ in their notation, we use $\mathfrak{x} = \cos\xi$, see Nomenclature), secondly their equation (37) for λ, a nondimensional force, is defined as half the correct value as noted in Happel and Brenner [75]. While on the subject of errata, we refer the reader to Townsend [169] for a discussion and derivation of corrections to the scalar resistance functions computed in Jeffrey and Onishi [92].

Not long after the result of Stimson and Jeffery [162], Faxén [55] gave a value of the hydrodynamic force on the two drafting spheres at contact. Both results have since been validated by Bart [14], who experimentally measured the force on two equal spheres settling under gravity in viscous fluid and showed good agreement with the theoretical value. Later work by Maude [117], adapting Stimson and Jeffery [162], calculated the finite-size effects of a falling-sphere viscometer. Hence the chosen bipolar formalism for exact solutions has good experimental validation as a method to compute flow around two spheres.

The subsequent history of the mathematical treatment of viscous flow around two spheres can be divided into two classes: exact and approximate. In the exact class, notable results are obtained by employing bipolar coordinates to solve for the fluid velocity and hydrodynamic force. Boundary condition cases include those due to O'Neill [128], considering the parallel motion of a sphere to a plane wall; O'Neill and Majumdar [129] treating the rolling and translating motion parallel to a stationary sphere in viscous fluid; Goldman et al. [70] studying the motion of two spheres settling under gravity; and finally Cox and Brenner [37] treating the motion of a sphere normal to a plane wall and considering the asymptotic limits at small separations. The asymptotic methods presented in this paper are analogous to those in Cox and Brenner [37], also similar to a treatment by Hansford [74], but therein the work is based on the constants determined by Brenner [23]. The asymptotics in the present work go beyond the statement that the $O(1)$ term cannot be obtained by asymptotic analysis (see Kim and Karrila [98], chapter 7).

There have also been more recent studies and applications of the solutions arising from the bipolar coordinate system, e.g., by Papavassiliou and Alexander [132] which concerns the motion of a sphere in viscous flow near a convex shell. For completeness, the study of droplets should be mentioned: Wacholder and Weihs [173] considered the exact solution to Stokes equations both inside and outside spherical droplets with equal settling velocities, and Haber et al. [73] generalised the former to two spherical droplets of different viscosities. Both of these studies concern a non-singular hydrodynamic interaction between droplets, which is different to the present boundary condition choice.

In the approximate class lie techniques such as the method of reflections (a series solution best suited for widely separated spheres [98]) and lubrication theory (solving Stokes equations directly by a perturbation expansion). Notable publications are, e.g., by Jeffrey [90] on which a popular reference for the singular hydrodynamic force between two collinear spheres in viscous fluid Kim and Karrila [98] is based. The derivation by perturbation methods in the latter, apart from algebraic errors not affecting the final result, is not valid as the sphere separation increases.

This means arbitrary truncations must be used for numerical implementation [170]. The choice of location of the cut-off and convergence of the truncated expressions remains mysterious. A fundamental assumption shared by these formalisms is the choice of scaling ratio between the cylindrical coordinates $z/r \sim \epsilon^{1/2}$ defining a singular perturbation problem, which has not been justified until the analysis in the present work. In particular we show this scaling is correct by expanding the bipolar coordinate system and infinite series around the singular contact point.

An alternative approach is the multipole method. To do this for our chosen sphere configuration, one would compute the velocity and pressure fields using the method of reflections around the two sphere centres, separated by a distance R. Using the addition theorems for spherical harmonics, the pressure and velocity are written as linear combinations of Lamb's solutions to Stokes equations. However, this results in an infinite set of series coefficients for the velocity and pressure, which are obtained only in the form of another series in R^{-1}, the coefficients of which satisfy known but non-analytical recurrence relations [98]. The method is by no means explicit, only obtaining Taylor series representations of the velocity and pressure fields and requires unavoidable computer algebra. What is more, to compute the hydrodynamic force on two spheres to a given accuracy will require ever more expansion terms as R decreases, making the method computationally unfavourable in the near-contact limit.

In this paper we give the first quantitative comparison, for this particular two-sphere interaction, between the present solution obtained by spherical bipolar methods and the one obtained by the multipole methods[92]. As a result, we are able to highlight the analytical and practical strengths of the present work by implementing both the novel and existing results in a numerical example for colloidal flow.

1.5 Beyond Direct Numerical Solution Of Colloids In Stokes Flow

Molecular Dynamics

One way to understand the evolution of a many body systems such as colloids, is to sample the statistical ensembles which generate realisations of all possible states of the macroscopic system, given a set of fixed thermodynamic conditions. For a general fluid comprising larger molecules which are composed of atoms held together by chemical bonds, in order to understand the overall properties of the entire system of molecules, one may simulate the motion, deformation and interaction of the molecules and use this data to compute bulk thermodynamic variables.

Due to the large number of molecules present, and the forces of interaction between them, the evolution of a typical molecular system displays chaotic behaviour and sensitivity to initial conditions. Nevertheless, molecular dynamics methods have demonstrated their ability to estimate bulk variables and averaged dynamics consistent with continuum methods where appropriate as well as retrieving high resolution microscopic dynamics which is typically eluded by continuum methods.

The limitation of molecular dynamics simulations is scale. The fact that there are 2×10^{25} hydrogen and oxygen atoms in a glass of water means the initial positions and momenta of each of the atoms must be stored in 1.2×10^{26} blocks of memory [105]. Hence the simulation of familiarly sized quantities soon becomes computationally intractable. The speed and capacity of modern high performance computing architectures therefore limits many simulations to the cubic nanometer scale, however if the interactions between the molecules are sufficiently weak, for example, considering only the rapid decay of short range forces, many millions of atoms may be simulated. The prevalence of such weakly interacting systems in nature however is uncommon, as many organic molecules possess electrostatic interactions in their atoms which decay over long range. This restricts the time step size in many numerical schemes, because the time taken for a given snapshot of the system to change due to one interaction is so short.

Molecular Scale: Hamiltonian Systems

Systems in which the total energy is conserved may be best described by Hamiltonian dynamics. The equations of motion for a collection of N molecules with mass m_i are written for some

smoothly varying interaction potential

$$\dot{\mathbf{r}}_i = \nabla_{\mathbf{p}_i} H, \tag{1.5.1a}$$
$$\dot{\mathbf{p}}_i = -\nabla_{\mathbf{r}_i} H \tag{1.5.1b}$$

where $H = \frac{1}{2}\mathbf{p} \cdot \boldsymbol{M}^{-1}\mathbf{p} + V(\mathbf{r})$ and $\boldsymbol{M} = \text{diag}(m_i)$ is the mass matrix. The set of all positions and momenta such that the energy, or Hamiltonian, is finite is the known as the phase space.

The existence and uniqueness of solutions (phase points) relies on the fact that with the energy constraint $H(\mathbf{x}) = E$, if the potential energy is bounded below, then a phase point $\mathbf{p}$ remains bounded for all time. As for the positions, one has $V_0 \leq V(\mathbf{r}) \leq E$ hence if the level sets $V(\mathbf{r}) = s$ are uniformly bounded $s \in [V_0, E]$, $\mathbf{r}$ must remain confined to a compact set in the phase space. In other words $\mathbf{r}$ cannot discontinuously jump between level surfaces. A more complete derivation of the existence and uniqueness is given in [105]. The uniform boundedness in the potential energy also implies that V must confine the phase trajectories. For systems without confining potentials, existence and uniqueness of the phase points will rely on either periodic or no flux boundary conditions to ensure that trajectories are confined to compact sets of the phase space.

Typical trajectories of the ordinary differential equations (1.5.1a)-(1.5.1b) will show sensitivity in initial conditions. The individual paths of the hard spheres will have a complicated dependence on the motion of all the other spheres in the system since the path is dictated by the momentum exchange at collision. Since typical collision times are very fast (the speed of sound in water is 1.5×10^3 m/s at room temperature), in a short time the dynamics of the system will be quickly memoryless of its initial data.

Hard Sphere Systems

One of the first molecular models considered was the hard sphere model, where molecules are taken as spheres which collide with each other elastically when they meet. Such models are known as 'event driven' where time is marched up until the next collision event where two molecules' velocities are updated. The interactions are non smooth, or infinite at short range since the velocity of each sphere is only modified at contact. Smoothly varying hard core exclusion and attraction is more difficult to model with event driven dynamics, since the definition for next contact time is ambiguous. For purely hard sphere collisions one may use a constrained Hamiltonian framework, namely

$$H = \frac{1}{2}\mathbf{p} \cdot \boldsymbol{M}^{-1}\mathbf{p} + V(\mathbf{r}), \tag{1.5.2a}$$
$$\|\mathbf{r}_i - \mathbf{r}_j\| \geq \frac{\sigma_i + \sigma_j}{2},$$

for $1 \leq i \neq j \leq N$ and σ_i is the diameter of sphere i. The first term in (1.5.2a) defines the total energy of the hard sphere system, where as the inequality imposes hard sphere exclusion. At collision the exchange of momentum and kinetic energy is elastic hence the model requires an infinite potential energy for overlapping spheres and zero otherwise. Hence, the Hamiltonian for the hard sphere system may be consolidated into

$$H_{hs} = \frac{1}{2}\mathbf{p} \cdot \boldsymbol{M}^{-1}\mathbf{p} + V(\mathbf{r}) + V_\infty$$

where

$$V_\infty = \begin{cases} \infty & \text{for} \quad \|\mathbf{r}_i - \mathbf{r}_j\| \leq \frac{\sigma_i + \sigma_j}{2}, \\ 0 & \text{otherwise.} \end{cases}$$

Hard sphere attraction may also be accounted for, as a proxy for electrostatic interactions, e.g., a Hydrogen electric dipole, in a perturbative manner with inclusion of a Lennard Jones type potential added in linear combination to V_∞. The DFT counterpart to such systems is discussed in Section 1.6.

An implementation of the Hamiltonian H_{hs} would not in general involve computing V_∞ because of the numerical instability in using an infinitely valued characteristic function. Instead the system of hard spheres is evolved by H until the first overlap between two spheres is detected, upon which the dynamics is reverted to the latest time step before the collision and velocities of the two spheres is updated according to the conservation of momentum. The system is evolved by composing a flow map consisting of a collision operator with a choice of numerical schemes. The schemes are based on collision detection during the time step, at the end of the time step or approximation the time to the next collision [118], [84] [56]. The speedups in using multiple cores to handle subgroups of the system are computationally appetising, and the Hamiltonian system must be split in order to do this. This method may be particularly useful if there are parts of the computational domain in which it is known that few collisions will happen, so that resources may be devoted to stiffer regions with high collision frequency.

Primitive splitting involves defining a ballistic Hamiltonian $H_b = \frac{1}{2}\mathbf{p}\cdot\boldsymbol{M}^{-1}\mathbf{p} + V_\infty$ to evolve the spheres with intermittent exposure to the potential energy. Such schemes, depending on the implementation, can be shown to force the energy to become unbounded in finite time. However, for a finite number of collisions, the numerical error of such splitting algorithms are typically $O(h)$ where h is the step size [84].

Molecular Scale: Stochastic Systems

We now make the connection between the Newtonian dynamics discussed in the previous sections to Stochastic systems. For two macroscopic systems in contact, one larger than the other, the sum of the energy of the heat bath (the larger system) and the energy of the active system (the smaller system) will be conserved, hence in principle one may use a Hamiltonian framework to compute trajectories of all the molecules of the ensemble. However it would be very computationally demanding to compute the trajectories of the bath since they are so numerous. Additionally, if overlooking the bath, constant energy dynamics (such as the hard sphere dynamics) can not sample the Canonical distribution, since the Microcanonical Ensemble (characterised by constant energy) cannot access volumes of the phase space different to that as prescribed by the initial data $H(\mathbf{x}_0) = E_0$. Hence, in general, one needs a different method to sample the dynamics of the underlying macroscopic system.

A dynamical representation of the underlying Canonical Ensemble characterised by constant temperature is thermostated MD. One way of generating dynamical trajectories is by sampling the paths of the Langevin dynamics

$$\frac{\mathrm{d}\mathbf{r}_i}{\mathrm{d}t} = \frac{1}{m}\mathbf{p_i}, \tag{1.5.3a}$$

$$\frac{\mathrm{d}\mathbf{p}_i}{\mathrm{d}t} = -\nabla_{\mathbf{r}_i} V(\mathbf{r}) - \gamma\mathbf{p}_i + \sqrt{\gamma m k_B \mathrm{T}}\mathbf{f}_i \tag{1.5.3b}$$

where $\mathbf{f}_i(t) = (\zeta_i^x(t), \zeta_i^y(t), \zeta_i^z(t))^\top$ is a Gaussian white noise term with mean $\langle \xi_i^a(t)\rangle = 0$ and autocorrelation $\langle \xi_i^a(t), \xi_j^b(t)\rangle = 2\delta_{ij}\delta^{ab}\delta(t-t')$. Here the energy exchange with the heat bath is provided by the friction coefficient and random bombardments from the bath particles. The Hamiltonian of the active system (colloidal particles) may fluctate but the temperature is controlled through the noise term. The Langevin equations (1.5.3a)-(1.5.3b) may be rigorously determined to be the correct dynamics for the system, by considering a single heavy particle coupled to a finite number smaller particles acting as oscillators with which momentum and kinetic energy may be transferred. At sufficiently high frequencies, the oscillations manifest as a Wiener process, with the mean effect of retarding the heavy particle by a magnitude proportional to its momentum with small random perturbations owing to heat energy of the bath [57].

Many generalisations of this molecular model may be made, in particular, for a solid phase dispersed in a liquid medium such as hard sphere colloids, one may consider the additional effects due to the hydrodynamic interactions (HI) between the molecules of the active system mediated by the bulk. This generalisation augments the friction term $-\gamma\mathbf{p}_i$ to the action of a friction tensor on the momentum vector, and the noise term becomes proportional the square root of this tensor, as dictated by the generalised fluctuation dissipation theorem. In particular,

for HI between the colloids, the Langevin equation becomes

$$\begin{aligned}\frac{\mathrm{d}\mathbf{r}_i}{\mathrm{d}t} =& \frac{1}{m}\mathbf{p}_i \\ \frac{\mathrm{d}\mathbf{p}_i}{\mathrm{d}t} =& -\nabla_{\mathbf{r}_i} V(\mathbf{r}^N, t) - \sum_{j=1}^{N} \mathbf{\Gamma}_{ij}(\mathbf{r}^N)\mathbf{p}_j + \sum_{j=1}^{N} \boldsymbol{B}_{ij}(\mathbf{r}^N)\mathbf{f}_j(t)\end{aligned}$$

where m is the particle mass, $\mathbf{r}^N = (\mathbf{r}_1, \cdots, \mathbf{r}_N)^\top$, $\mathbf{p}^N = (\mathbf{p}_1, \cdots, \mathbf{p}_N)^\top$, $\boldsymbol{B} = (mk_{\mathrm{B}}\mathrm{T}\mathbf{\Gamma})^{1/2}$, V is a potential, k_{B}, T, γ are Boltzmann's constant, temperature and friction coefficient respectively. These Langevin dynamics, including HI, constitute the central dynamical system considered in Chapter 2. In order to compute trajectories of the Langevin dynamics however, one needs construct the friction tensor $\mathbf{\Gamma}$ with formulae for the HI between the colloidal particles, which we will derive in Chapters 3 and 4.

1.6 Density Functional Theory

Density Functional Theory (DFT) was first developed in the 1960s for quantum mechanical systems as a method to calculate electron densities in the presence an external potential [81]. It is motivated by the computational scaling solving the Schrödinger equation in Slater determinants [60]. DFT replaces the wave function with an electron density which is a function of three spatial variables, independently of the number of electrons. In their seminal paper [81], Hohenberg and Kohn developed DFT and proved that the ground state wavefunction is a unique functional of the density, and equally all other statistics, including the energy, flux etc are functionals of the density.

At the centre of DFT is the surprising result that the N body probability density for the full phase space $\varrho^{(N)}$ is a functional of the one body probability density $\varrho(\mathbf{r})$, dependent only on a single particle position and momentum variable. This may be established by the fact that, for a fixed interparticle interaction kernel, a system at a given temperature T and chemical potential μ_c^i (for each of the constituent particles' species), there is an invertible mapping between the external potential and the one-body density profiles $\{\varrho_i\}$. Then, since $\varrho^{(N)}$ is determined by the external field V_{ex}, there is a one to one map may be may between ϱ and $\varrho^{(N)}$. DFT has become a very popular method in quantum mechanics to compute the ground states of various electronic equilibrium systems [16].

DFT For Classical Fluids

Since Hohenberg and Kohn [81], DFT has been extended to classical fluid systems with non-constant number density [53], [46], and has been shown to be an accurate approach in modelling microscopic structure in many condensed matter systems: in soft matter [93], atomic systems [152], polyatomic systems [31], multiphase systems in the presence of hard geometries [133] not to mention the classical moving contact line problem for droplet spreading [158].

The Hohenberg-Kohn-Mermin theorem establishes an intrinsic Helmholtz energy functional that is independent of the external potential. Then, functional derivatives of the Helmholtz energy lead to multibody correlation functions that allow the determination of both the structure and thermodynamic properties of the equilibrium fluid [179]. Such properties include accurate surface tension calculations at the liquid–vapour interface[53], and surface tension and density profiles of the interface between the demixed fluid phases of a binary mixture [8]. Additionally there have been many fruitful applications of DFT in the theory of phase transitions [159], crystal growth [131], not to mention invertible mapping for density profiles with non zero momentum distributions in off-equilibrium problems [115], [30].

For classical DFTs one requires reliable approximations for the excess Helmholtz energy functional to account for intermolecular interactions. One strategy which is commonly used to do this is to seek a direct approximation of the free-energy functional by a local- density ansatz depending on the phenomenology one wishes to to include (for example, hard spheres [148], disks [149] or rods [140]). Such examples account for the hard core exclusion of the particles.

To account for attractive forces, contributions to the intrinsic free energy density are treated in a perturbative manner [182], [167].

DFT has made many complicated systems in fluid mechanics, biology and soft matter including large spatial and temporal scale separations computationally tractable, where a direct application of the Schrödinger equation would be impractical. Thermodynamic properties, such as fixed temperature, chemical potential and volume, are incorporated into the formulation of DFT instead of being indirectly computed from the mechanical evolution of the particles in molecular dynamics. What is more, DFT provides an effective way to predict mesoscopic/-macroscopic variables intrinsic to continuum models of fluid flow (for example the Navier-Stokes equations), where the overlap is rigorously known to be valid. To do this one must construct the Helmholtz free energy which we now discuss.

The basic DFT formalism for classical fluids states that there is a unique intrinsic free energy $\mathscr{F}_{in}$, which is a functional of the density profile $\varrho(\mathbf{r})$ and not the external potential. In other words the grand potential energy Ω is written as

$$\Omega[\varrho] = \mathscr{F}_{in}[\varrho] + \int \mathrm{d}\mathbf{r}\varrho(\mathbf{r})(V(\mathbf{r}) - \mu_c) \tag{1.6.1}$$

and is minimised by the Grand Canonical equilibrium density distribution for the system in presence of external potential $V(\mathbf{r})$ and in contact with a reservoir of particles at chemical potential μ_c. The equilibrium density is obtained by a solution to the Euler Lagrange equation

$$\frac{\delta\Omega}{\delta\varrho}[\varrho] = 0$$

which is a drastic simplification, compared to the direct evaluation of the grand partition function to compute the equilibrium density ϱ

$$\varrho(\mathbf{r}) = \Big\langle \sum_{i=1}^{N} \delta(\mathbf{r} - \mathbf{r}_i) \Big\rangle \equiv \frac{1}{\Xi} \sum_{N\geq 0} \frac{e^{\frac{\mu_c N}{k_B \mathrm{T}}}}{(N-1)!h^{3N}} \int \prod_{i=1}^{N} \mathrm{d}\mathbf{r}_i e^{-\frac{V_N}{k_B \mathrm{T}}} \delta(\mathbf{r} - \mathbf{r}_i)$$

where $\mathbf{r}_i$ are the particle centres, Ξ is the normalisation constant and $V_N = V_N(\mathbf{r}_1, \cdots \mathbf{r}_N)$ is the total potential energy of the particles including molecular interactions and external potential energy and h is the thermal wavelength (Planck constant).

Free Energy

The free energy may be split in the ideal gas contribution plus an excess free energy, $\mathscr{F}_{ex}[\varrho]$ to be discussed. In hard core systems for example, $\mathscr{F}_{ex}$ takes into account the entropy reduction arising from the exclusion of the hard sphere cores. One may write

$$\mathscr{F}[\varrho] = \mathscr{F}_{id}[\varrho] + \mathscr{F}_{ex}[\varrho]$$

where $\mathscr{F}_{id}[\varrho] = \beta^{-1} \int \mathrm{d}\mathbf{r}\, \varrho(\log \Lambda^3 \varrho - 1)$, $\beta = (k_B \mathrm{T})^{-1}$, and Λ^3 is the de Broglie wavelength. The free energy $\mathscr{F}_{id}$ is the intrinsic free energy of a non-interacting ideal gas. We have, therefore,

$$\mathscr{F}_{in}[\varrho] = \int \mathrm{d}\mathbf{r}\ [\Phi_{id}(\varrho(\mathbf{r})) + \Phi_{ex}([\varrho]; \mathbf{r})]$$

for $\Phi_{id}(\varrho(\mathbf{r})) = \beta^{-1}\varrho(\log \Lambda^3 \varrho - 1)$ where as the excess free energy density $\Phi_{ex}([\varrho]; \mathbf{r})$ is a function of $\mathbf{r}$ and a functional of ϱ. Since there is more than one way to separate the total free energy excess of the system in terms of local contributions, there may be more than one choice of Φ giving rise to the same $\mathscr{F}_{ex}[\varrho]$. More complicated systems may be considered too, for example (1.6.1) may be summed over all particle species or segments of a polymeric chain with segment specific external potentials. At any rate $\mathscr{F}_{ex}[\varrho]$ is not always known and must either be posed or computed from microscopic dynamics.

Density Expansion Methods

An expression of the excess free energy at low densities $\varrho(\mathbf{r}) \to 0$ may be obtained for a general system interacting via pairwise potentials $V_{in}(|\mathbf{r}_i - \mathbf{r}_j|)$. We let $V_{in}(|\mathbf{r} - \mathbf{r}'|) = \infty$ for $|\mathbf{r} - \mathbf{r}'| < \sigma$ and zero otherwise. Furthermore, by introducing the pair distribution function $g(\mathbf{r}_1, \mathbf{r}_2)$ such that

$$g(\mathbf{r}_1, \mathbf{r}_2) = \frac{\varrho^{(N)}(\mathbf{r}_1, \mathbf{r}_2)}{\varrho(\mathbf{r}_1)\varrho(\mathbf{r}_2))} = \frac{N(N-1)}{\varrho(\mathbf{r}_1)\varrho(\mathbf{r}_2))} \frac{1}{\Xi} \int \mathrm{d}\mathbf{r}^{N-2}\, e^{-\beta V(\mathbf{r}^N)},$$

where $V = V_{in} + V_{ex}$ is the total potential energy, one expands the excess free energy term, $\mathscr{F}_{ex}[\varrho] = \mathrm{Tr} f_0 V_{in}$, in (2.1.2) in a Taylor series to obtain the so called virial expansion

$$\begin{aligned}\beta\mathscr{F}_{ex}[\varrho] = -\frac{1}{2}\int \mathrm{d}\mathbf{r}_1\, \varrho(\mathbf{r}_1) \int \mathrm{d}\mathbf{r}_2\, \varrho(\mathbf{r}_2) f(r_{12}) \\ - \frac{1}{6}\int \mathrm{d}\mathbf{r}_1\, \varrho(\mathbf{r}_1) \int \mathrm{d}\mathbf{r}_2\, \varrho(\mathbf{r}_2) \int \mathrm{d}\mathbf{r}_3\, \varrho(\mathbf{r}_3) f(r_{12}) f(r_{23}) f(r_{31}) + \cdots\end{aligned}$$

where $r_{ij} = |\mathbf{r}_i - \mathbf{r}_j|$ and f is the Mayer function $f(r_{ij}) = \exp(-\beta V_{in}(r_{ij})) - 1$. For hard sphere systems, the Mayer function masks the volume of the computational domain which is not accessible for a given hard sphere [151]. For multiple hard core species, by functional differentiation, the leading order term of the excess free energy, relative to the ideal gas, is given by the pair exclusion at low densities thus

$$\beta \frac{\delta \mathscr{F}_{ex}}{\delta \varrho_i}[\varrho_i] \longrightarrow \sum_{j=1}^{\nu} \int \mathrm{d}\mathbf{r}' \varrho_j(\mathbf{r}') \Theta\left(|\mathbf{r} - \mathbf{r}'| - \tfrac{1}{2}(\sigma_i + \sigma_j)\right)$$

as $\varrho_j \to 0$, where σ_i is the diameter of species i, and Θ is a step function such that $\Theta(x > 0) = 0$ and $\Theta(x \leq 0) = 1$. It then remains to obtain a closed form expression for Θ in terms of a functional of the density of hard core species i, which has been obtained explicitly in the case of a few cases, e.g., hard rods, discs and spheres.

Other Fluid Models

Polymeric Fluids

Other density expansion methods have been used in van der Waals theory of capillarity [155] and phase transitions in binary fluids [25]. The central idea in these methods is to expand the Helmholtz energy functional Taylor expansion around a differential density profile $\Delta\phi_i$ corresponding to an equilibrium density for the binary fluid. One poses a Helmholtz energy $\mathscr{F}_{ex}[\varrho]$ of the form

$$\beta\mathscr{F}_{ex}[\varrho] = \int \mathrm{d}\mathbf{r}\, f[\phi_i^0(\mathbf{r})] + \frac{1}{2}\sum_{i,j} \int \mathrm{d}\mathbf{r}' \int \mathrm{d}\mathbf{r}\, \Upsilon_{ij}(\mathbf{r} - \mathbf{r}') \Delta\phi_i(\mathbf{r}) \Delta\phi_j(\mathbf{r}') + \cdots,$$

where ϕ_i^0 is the volume fraction of phase i, $f[\phi_i]$ is the Helmholtz energy density of a single phase system with volume fraction ϕ_i, $\Delta\phi_i = \phi_i - \bar{\phi}_i$ is the differential volume fraction. $\bar{\phi}_i$ is the local average volume fraction and Υ is known as the vertex function which, for polymeric systems, encodes correlations between different segments from the same chain and from different chains. Such density expansions are used for polymeric fluids [31] and the Ramakrishnan-Yussouff theory of freezing [143]. There are numerous ways to define the Helmholtz energy density $f[\phi_i]$, $\bar{\phi}_i$ and Υ_{ij} which may or may not give rise to phase transitions [40].

Anisotropic Fluids

For systems with a non-constant number density of rigid asymmetric molecules one may specify the density profile ϱ, as a function of centre of mass $\mathbf{r}$ and orientation ω in order to study isotropic-nematic phase transitions. The Helmholtz energy functional as proposed by Onsager

[130] is given by

$$\beta\mathscr{F}_{ex}[\varrho] = \sum_i \int \mathrm{d}\mathbf{r} \int \mathrm{d}\omega\, \varrho_i(\mathbf{r},\omega)[\log 4\pi\varrho_i(\mathbf{r},\omega) - 1] \\ - \frac{1}{2}\sum_{i,j}\int \mathrm{d}\mathbf{r}\int \mathrm{d}\omega \int \mathrm{d}\mathbf{r}'\int \mathrm{d}\omega'\, f_{ij}(\mathbf{r}-\mathbf{r}',\omega,\omega') + \cdots$$

where f_{ij} is the Mayer function, dependent on the pair potential between the molecules as a two body approximation, this time with angular dependence. The expression for $\mathscr{F}_{ex}[\varrho]$ here was first proposed as Helmholtz energy giving rise to density profiles in lyotropic liquid crystals (a liquid crystal formed by adding a solvent e.g. soapy water). Other applications include platelets in blood and more general rod fluids [76].

Mean Field Approximations

In the mean field approximation (MFA), one considers only very soft molecular potentials and the particles may be assumed to be fully uncorrelated so that the excess free energy is given by, for a single species,

$$\mathscr{F}_{ex}[\varrho] = \frac{1}{2}\int \mathrm{d}\mathbf{r}\varrho V_2 \star \varrho$$

where V_2 is a two body molecular interaction and $\star$ denotes the convolution operation. From the rules of functional calculus one obtains

$$\frac{\delta\mathscr{F}_{ex}}{\delta\varrho}[\varrho] = V_2 \star \varrho$$

which may be taken as the potential created on a particle at $\mathbf{r}$ by virtue of the distribution of the particles in the system as a whole, on average. The MFA is a good approximation for soft interactions, as for those found between dissolved polymer chains. For hard particles, to avoid overlap, V_2 must be infinite inside the core. Often such systems are treated with a mixture of MFA and hard core exclusion, the former accounting for attractive forces between molecules and is known as the generalized van der Waals approximation.

Hard Core Systems

One of the most successful density functional formalisms for inhomogeneous systems with hard cores is Fundamental Measure Theory (FMT). Developed first through weighted density approximations, FMT has many applications for polydisperse systems, liquid crystals and many interfacial phenomena. In classical fluid mechanics it is common to observe fine structure, such as layering at wall interfaces, attributed to molecular packing. Hence accurate free energy computations of hard spheres are required to determine a reliable Helmholtz free energy for confined systems. The exact free energy computation for hard rods, presented by Percus in 1976 [140], established a reliable test case for DFT as well as insight into how to extend to 2D hard disks and 3D hard spheres. The first step to establishing FMT was through Weighted Density Approximations (WDAs) in the 1980s before the appearance of FMT in 1990s.

1D Hard Rods

One of the few density functional formalisms for the exact intrinsic free energy calculation of for a system of particles is 1 dimensional hard rods, as presented by Percus in 1976 [140]. The excess free energy density is given by

$$\Phi_{ex}([\varrho];x) = -\frac{\varrho(x+\sigma/2)+\varrho(x-\sigma/2)}{2}\log\left[1-\int_{-\sigma/2}^{\sigma/2}\mathrm{d}x'\,\varrho(x+x')\right] \tag{1.6.2}$$

where the integral inside the logarithm represents the probability that the point x is covered by one of the hard rods and σ is the rod length. The Euler-Lagrange equation, (1.6), for a system using the excess free energy of 1D hard rods in a confining potential V in thermal contact with a bath at chemical potential μ_c is given by

$$\log \varrho(x) + \beta \frac{\delta \mathscr{F}_{ex}}{\delta \varrho}[\varrho] + \beta V(x) - \beta \mu_c = 0. \tag{1.6.3}$$

Note that by definition of the excess free energy density (1.6.2) the functional derivative in (1.6.3) produces an integral equation for $\varrho(x)$ and the density profile therefore cannot be solved independently for each x. The Euler-Lagrange equation therefore becomes a non-local problem for the equilibrium density.

Fundamental Measure Theory

Fundamental Measure Theory (FMT) was first introduced in 1989 by Rosenfeld [148] and was considered to be big step in free energy computations of hard core systems, which up until that time had seen mostly unsuccessful attempts to generalise Percus excess free energy density to higher dimensions. The monodisperse case is neater to present. The central idea is to include the packing fraction as an essential non-local measure of the free energy contributed by the hard sphere. For mass $m = 1$ spheres the dimensionless packing fraction $\eta = \pi \varrho \sigma^3/6$ is the ratio of the volume occupied by the hard sphere to the total system volume.

The natural extension to hard sphere systems is the local packing fraction, as a function of the spatial variable $\mathbf{r}$

$$\eta(\mathbf{r}) = \int \mathrm{d}\mathbf{r}' \, \varrho(\mathbf{r} + \mathbf{r}') \Theta\left(\frac{\sigma}{2} - |\mathbf{r}'|\right)$$

where Θ is the Heaviside function, which represents the probability that $\mathbf{r}$ is inside a hard sphere core for random configurations over the conical ensemble. The main idea of FMT is that it is the shape of a single molecule (sphere), rather that the excluded volume between the molecules, which describes the non-local dependence of the excess free energy density $\Phi_{ex}([\varrho]; \mathbf{r})$. In particular $\Phi_{ex}([\varrho]; \mathbf{r})$ is represented as a function of the local packing fraction and weighted densities, each convolutions in the density profile within the range of the hard sphere radius.

The excess free energy density in (1.6.2) may be written in terms of a (surface) weighted density $n(\mathbf{r})$ as $\Phi_{ex}([\varrho]; x) = -n(x) \log[1 - \eta(x)]$ where n is given by $n(\mathbf{r}) = \int \mathrm{d}\mathbf{r}' \, \varrho(\mathbf{r} + \mathbf{r}') w(\mathbf{r}')$ and w is the normalized molecular surface weight function, $w(\mathbf{r}) = \frac{\delta(|\mathbf{r}| - \sigma/2)}{s_d}$ for s_D the molecular surface in d dimensions. In this way one sees how the free energy density of 1D hard rods is a special case of the present formalism. The leap that Rosenfeld made was noticing that the Mayer function $f(r_{ij})$ for a mixture (multiple species with diameters σ_i) of hard spheres may be decomposed into

$$-f(r_{ij}) = \omega_3^i \otimes \omega_0^j + \omega_0^i \otimes \omega_3^j + \omega_2^i \otimes \omega_1^j + \omega_1^i \otimes \omega_2^j - \boldsymbol{\omega}_2^i \otimes \boldsymbol{\omega}_1^j - \boldsymbol{\omega}_1^i \otimes \boldsymbol{\omega}_2^j$$

where

$$\omega_3^i(\mathbf{r}) = \Theta\left(\frac{\sigma_i}{2} - r\right), \tag{1.6.4a}$$

$$\omega_2^i(\mathbf{r}) = \delta\left(\frac{\sigma_i}{2} - r\right), \tag{1.6.4b}$$

$$\boldsymbol{\omega}_2^i(\mathbf{r}) = \frac{\mathbf{r}}{r} \delta\left(\frac{\sigma_i}{2} - r\right), \tag{1.6.4c}$$

and $\omega_1^i = \omega_2^i/(2\pi\sigma_i)$, $\omega_0^i(\mathbf{r}) = \omega_2^i(\mathbf{r})/(\pi\sigma_i^2)$ and $\omega_1^i(\mathbf{r}) = \omega_2^i(\mathbf{r})/(2\pi\sigma_i)$. The operation $\otimes$ is known as the 3 dimensional convolution, defined by

$$\omega_i^\alpha \otimes \omega_j^\beta(\mathbf{r} = \mathbf{r}_i - \mathbf{r}_j) = \int \mathrm{d}\mathbf{r}' \, \omega_i^\alpha(\mathbf{r}' - \mathbf{r}_i) \omega_j^\beta(\mathbf{r}' - \mathbf{r}_j). \tag{1.6.5}$$

For the convolution between the vector fields ω_i^α the scalar product is implied in the integral

of (1.6.5). By definition, integration over the weight functions ω_α^i gives: the volume ($\alpha = 3$), surface area ($\alpha = 2$), mean radius of curvature ($\alpha = 1$) and Euler characteristic ($\alpha = 0$) for species i, giving rise to the name FMT. Rosenfeld's decomposition decomposition of the Mayer function is not unique, in particular Kierlik & Rosinberg [97] proposed another decomposition without vector weight functions although substitute this difficulty with a decomposition in terms of derivatives of the Dirac delta function.

In Rosenfeld's original presentation, the vector fields $\boldsymbol{\omega}_i^\alpha$ are needed to obtain a jump discontinuity expressed as a convolution for the hard spherical shell. Natural dimensional weighted densities that represent either surface or volume-averaged densities come about from the ω_i^α

$$n_\alpha(\mathbf{r}) = \sum_{i=1}^{\nu} \int \mathrm{d}\mathbf{r}' \varrho_i(\mathbf{r}') \omega_i^\alpha(\mathbf{r} - \mathbf{r}') \tag{1.6.6}$$

where ν is the number of distinct hard core species. With this definition, Rosenfeld suggests the excess free energy density

$$\mathscr{F}_{ex}[\varrho_i] = \int \mathrm{d}\mathbf{r}' \, \Phi_{ex}([n_\alpha(\mathbf{r}')])$$

where

$$\Phi_{ex} = f_1(n_3)n_0 + f_2(n_3)n_1 n_2 + f_3(n_3)\mathbf{n}_1 \cdot \mathbf{n}_2 + f_4(n_3)n_2^3 + f_5(n_3)n_2 \mathbf{n}_2 \cdot \mathbf{n}_2$$

which is argued by dimensional analysis as the correct form, for some functions f_i to be determined. In simulations the single component hard sphere model has been shown from simulations that the model undergoes a first order freezing transition, which is a purely entropy driven transition.

Lennard–Jones Fluid

For DFT for a fluid in which the particles interact via a pair potential which has both a sharply repulsive component and a longer ranged attractive component, e.g. the noble gases, and their mixtures, one may begin by approximating the free energy functional by a hard sphere system combined with a meanfield theory

$$\mathscr{F}_{ex}[\{\varrho_i\}] = \mathscr{F}_{ex}^{hs}[\{\varrho_i\}] + \frac{1}{2} \sum_{i,j} \int \mathrm{d}\mathbf{r} \int \mathrm{d}\mathbf{r}' \, \varrho_i(\mathbf{r}) \varrho_j(\mathbf{r}') \phi_{ij}^{att}(\mathbf{r} - \mathbf{r}')$$

where $\mathscr{F}_{ex}^{hs}[\{\varrho\}]$ is the excess free energy functional obtained from a hard sphere mixture of multiple species, e.g., FMT and $\phi_{ij}^{att}(\mathbf{r} - \mathbf{r}')$ is an attractive pair potential between species i and j.

1.7 Organisation Of The Thesis

This thesis is organised as follows. In Chapter 2 we outline the statistical mechanical framework of atomistic fluids and derive, from first principles, a novel DDFT to include inertia, HI and external currents. In Chapter 3 we consider analytical solutions to Stokes equations in order to compute the normal mode of the singular HI, $a(\cdot)$. In Chapter 4 we consider analytical solutions to Stokes equations in order to compute the tangential mode of the singular HI, $b(\cdot)$, as far as equal spheres. In Chapter 5 we use the results of Chapters 3 and 4 to establish positivity of the resistance matrix $\boldsymbol{R}$ using the present theory, GMS, for some simple particle configurations, and compare to the spectral behaviour when assembling $\boldsymbol{R}$ with existing formalisms, particularly Kim & Karrila and Jeffrey & Onishi. In Chapter 6 we consider numerical solutions to DDFT by using pseudospectral methods to discretise the density, including short range HI according to the three formalisms: GMS, Kim & Karrila, and Jeffrey & Onishi. In particular we consider a few dynamical scenarios, including colloidal flow in a potential, colloids in an oscillating trap, and flow in an infinite slit (to include confinement effects with rigid boundaries). In Chapter 7 we present the well-posedness of overdamped DDFT with two body HI including, convergence to equilibrium and bifurcation theory for confined densities. In Chapter 8 we make our concluding remarks regarding the results of the previous chapters, as well as discussing open problems. Finally in the Appendix A we provide additional details for calculations undertaking in previous chapters including: Appendix A.1, the asymptotic theory applicable to Chapter 3; Appendix B.1, recurrence relations for unequal spheres for the tangential interaction in Chapter 4; and Appendix C, which provides more detail on the pseudospectral collocation schemes used to compute the solutions to the PDEs in Chapter 6.

Chapter 2

Dynamic Density Functional Theory

In this chapter we derive the DDFT for classical fluids driven by a steady external current. The derivations extend the PDEs found in previous formalisms [112], [7], [146], [61], [62], to a wider class of systems, namely driven colloids with inertia and hydrodynamic interactions. We present the essential elements required to determine an inertial case DDFT with an applied external flow and hydrodynamic interactions. In Section 2.1 we present the statistical mechanical framework for the classical atomistic fluids. In Section 2.2 we discuss the history and recent advances in DDFT. In Section 2.3 we present the Langevin dynamics for the system, define the main modelling assumptions and show that the stochastic equations reduce to those found in overdamped formalisms. In Section 2.4 we derive the Fokker-Planck equation associated to the Langevin dynamics. In Section 2.5 we derive, from first principles, the DDFT for the driven system. In Section 2.6 we present the equations of motion in compact form, along with the assumed boundary conditions. In Section 2.7 we take heuristic limits of the derived equations, showing agreement with previously studied DDFTs (for example, in the overdamped limit $\gamma \to \infty$, [21], [145], [144]). Finally in Section 2.8 we determine a Bernoulli principle for the new equations.

2.1 Statistical Mechanics Of Classical Fluids

In this thesis the convergence to steady state of hydrodynamic quantities of a liquid, such as the density and flux, as well as the dynamical dependence on short range hydrodynamic interactions and external currents, is investigated. In order to formalise the steady states of systems, we present the grand canonical density defining the equilibrium probability density for the grand canonical ensemble of a full macroscopic system with $6N$ degrees of freedom to describe position and momentum of the N particles in 3D dimensional space. For an open system at temperature T, chemical potential μ_c and volume V, the equilibrium probability density f_0 characterising the Grand Canonical ensemble defining is given by

$$f_0 := \Xi^{-1} e^{-\beta(H-\mu_c N)}$$

where H is the Hamiltonian for N particles, here assumed to include inter-particle potential energy and $\beta = 1/k_B\mathrm{T}$. The operator Ξ is the grand partition function and is given by

$$\Xi = \mathrm{Tr}\, e^{-\beta(H_N-\mu_c N)}$$

where the classical trace operator, Tr, is defined as

$$\mathrm{Tr} := \sum_{N=0}^{\infty} \tfrac{1}{h^{3N}N!} \int \mathrm{d}\mathbf{r}^N\, \mathrm{d}\mathbf{p}^N$$

where h is Planck's constant, included for historical and quantum mechanical reasons, to nondimensionalise the resulting integral in terms of the kinetic energy of an electron ganied or lost after accelerating across a voltage in a vacuum. One sees that Ξ, the Partition function, is a normalisation factor. The Mermin functional [121] given by

$$\Omega[f] := \operatorname{Tr} f(H_N - \mu_c N + \beta^{-1} \log f).$$

is minimised by f_0 and, in particular at f_0 we have

$$\Omega[f_0] = -\beta^{-1} \log \Xi =: \Omega$$

where Ω is now defined as the Grand Potential. It is elementary to see that

$$\Omega[f] = \Omega[f_0] + \beta^{-1}(\operatorname{Tr} f \log f - \operatorname{Tr} f \log f_0). \tag{2.1.1}$$

Hence as long as $f \neq f_0$ then Gibbs' inequality holds $\operatorname{Tr} f \log f - \operatorname{Tr} f \log f_0 > 0$, and therefore by (2.1.1), $\Omega[f] > \Omega[f_0]$ meaning f_0 is the global minimiser of Ω.

Now restricting to Hamiltonians of the form

$$H = Q + V_{in} + V_{ex}$$

where $Q = \sum_{i=1}^{N} \mathbf{p}_i^2/2m$ denotes total kinetic energy of the particles, $V_{in} = V_{in}(\mathbf{r}_1, \mathbf{r}_2, \cdots, \mathbf{r}_N)$ denotes all two-body interparticle potentials and higher, and $V_{ex} = \sum_{i=1}^{N} V_1(\mathbf{r}_i)$. denotes all one body potentials.

Definition 2.1.1. *The equilibrium density $\rho_0(\mathbf{r})$ for a system is given by $\rho_0(\mathbf{r}) = \langle \hat{\rho}(\mathbf{r}) \rangle$ where*

$$\hat{\rho}(\mathbf{r}) = \sum_{i=1}^{N} \delta(\mathbf{r} - \mathbf{r}_i)$$

is the empirical density operator, and the configuration average of any operator $\mathscr{L}$ is defined

$$\langle \mathscr{L} \rangle := \operatorname{Tr} f_0 \mathscr{L}.$$

Note that since f_0 is a function of V_{ex} then ρ_0 is a functional of V_{ex}. The Hohenberg, Kohn and Mermin theorem also holds, that for a given V_{in}, the external potential energy V_{ex} is uniquely determined by ρ_0 (that is knowing the density means one can in principle identify which external field constructed it). Then, we know that V_{ex} determines f_0 and therefore f_0 is a functional of ρ_0.

Definition 2.1.2. *The intrinsic Helmholtz free energy is given by*

$$\mathscr{F}_{in}[\rho] = \operatorname{Tr} f(Q + V_{in} + \beta^{-1} \log f), \tag{2.1.2}$$

for any probability density with $\operatorname{Tr} f = 1$.

It then follows that for each V_{in}, $\mathscr{F}_{in}[\varrho]$ is a unique functional of ρ, and similarly for external potentials. It is this powerful result that will let us develop the DDFT in Section 2.5. The next key energy functional is total free energy functional.

Definition 2.1.3. *The free energy of the system at temperature* T*, chemical potential μ_c inside a fixed volume* V *is defined as*

$$\Omega_{V_{ex}}[\rho] = \int \mathrm{d}\mathbf{r}\, \rho(\mathbf{r}) V_{ex}(\mathbf{r}) + \mathscr{F}_{in}[\rho] - \mu_c \int \mathrm{d}\mathbf{r}\, \rho(\mathbf{r}).$$

When $\rho = \rho_0$, $\Omega_{V_{ex}}[\rho_0] = \Omega[\rho_0]$ the grand potential and this is the minimum functional value and the density ϱ_0 minimises $\Omega_{V_{ex}}$ over all densities that can be associated with V_{ex}. We note that the value of the chemical potential μ_c determines the number of particles in the fixed

volume V. Since ϱ_0 is a minimiser, we must also have, from calculus of variations

$$\frac{\delta \Omega_{V_{ex}}}{\delta \varrho}[\varrho_0] = 0. \tag{2.1.3}$$

We now define the total Helmholtz free energy.

Definition 2.1.4. *The total Helmholtz free energy at temperature* T*, inside a fixed volume* $\mathscr{V}$*, is defined as*

$$\mathscr{F}_H[\varrho] = \int \mathrm{d}\mathbf{r}\, V_{ex}(\mathbf{r})\varrho(\mathbf{r}) + \mathscr{F}_{in}[\varrho]. \tag{2.1.4}$$

We see that, for an isothermal process, $-\delta\mathscr{F}_H[\varrho]$ *is the maximum amount of useful work that may be extracted from the system during an infinitesimal process. When there is no work being done, a spontaneous process (such as the free expansion of gas into a vacuum) can only ever decrease the Helmholtz free energy, and the steady states* (T, ϱ, N) *coincide with a minimum of* $\mathscr{F}_H[\varrho]$*. For a more detailed explanation and review of the thermodynamics, see Plischke and Bergersen [142].*

By the minimisation equation (2.1.3) we obtain, at equilibrium

$$V_{ex}(\mathbf{r}) + \mu_{in}[\varrho_0; \mathbf{r}] = \mu_c \tag{2.1.5}$$

where the intrinsic chemical potential is defined to be

$$\mu_{in}[\varrho_0; \mathbf{r}] := \frac{\delta \mathscr{F}_{in}}{\delta \varrho}[\varrho_0].$$

Equation (2.1.5) is an equation for the equilibrium density ϱ_0, given one has reliable knowledge of $\mu_{in}[\varrho_0; \mathbf{r}]$. Now that we have defined the relevant free energy functionals we continue to the next chapter in which we derive, from first principles, a DDFT to include driven background flows including inertia and HI.

2.2 Dynamic Density Functional Theory

The time dependent DFT was introduced by Marconi and Tarazona [112], Chan and Finken [30] to classical fluids by extending the equilibrium DFT to nonequilibrium systems. Therein nonequilibrium, refers to out of equilibrium systems in the presence of time-dependent fields. To obtain the time dependent DFT for classical fluids, Chan and Finken used the ideas of Runge and Gross [156], who developed a time dependent DFT for quantum mechanical systems by constructing an invertible mapping between the wave function and the one-body density $\varrho(\mathbf{r}_1, t)$ by using the time dependent potential as an intermediary $\Psi(\mathbf{r}_1, \cdot, \mathbf{r}_N, t) \leftrightarrow V(\mathbf{r}_1, t) \leftrightarrow \varrho(\mathbf{r}_1, t)$. Alternative derivations include Archer [6], showing that when isothermal compressibility is small, the DDFT generates the correct value for the speed of sound in a dense liquid and can be used to describe glass transition.

Recent advances for DDFTs have allowed modelling out of equilibrium classical fluids with the inclusion of inertia [7, 114], multiple species [5, 64, 106, 153], hydrodynamic interactions (HI) [61, 62, 144, 146], background flows [145], temperature gradients [4, 177], hard spheres [147, 150, 152, 164], confined geometries [66, 181], arbitrary shaped particles [175], and active microswimmers [80, 120].

For equilibrium fluids, there is a rigorous mathematical framework proving the existence of non-trivial fluid densities, different from those found by classical fluid dynamical formalisms, by taking into account both many body effects and external force fields. This is commonly known as (classical) density functional theory (DFT) [121]. It is able to predict effects driven by the microscale, e.g., the non-smooth droplet profiles which are formed at the gas-liquid-solid trijunction in contact line problems [15] and the coexistence of multiple fluid films at critical values of chemical potential energy in droplet spreading [141]. It has been used to resolve the paradox of stress and pressure singularities normally found in classical moving contact line

problems [157]. What is more, DFT agrees well with molecular dynamics simulations; see, e.g., [108] and references therein. These advancements motivate more mathematical analysis, in particular, on the well-posedness of the underlying equations being used.

As a non-equilibrium extension to DFT for classical fluids, dynamic DFT (DDFT) has been applied to a wide range of problems: polymeric solutions [139], spinodal decomposition [9], phase separation [5], granular dynamics [111, 113], nucleation [172], liquid crystals [176], and evaporating films [10]. Recently, a stochastic version of DDFT has been derived [109], which allows the study of energy barrier crossings, such as in nucleation. A crucial point is that the computational complexity of DDFT is (essentially) constant in the number of particles, which allows the treatment of macroscopically large systems, whilst retaining microscopic information. Furthermore, due to the universality of the underlying nonlinear, nonlocal partial differential equations, DDFT may be considered as a generalisation of a wider class of such models used in the continuum modelling of many natural phenomena consisting of complex, many body, multi-agent interparticle effects including: pattern formation [26], the murmurations of birds, cell proliferation, the self organising of morphogenetic and bacterial species [27, 28], nonlocal reaction-diffusion equations [1] and even consensus modelling in opinion dynamics[33]. Many of these applications are often described as systems of interacting (Brownian) particles and, in the case of hard particle viscous suspensions, bath-mediated HI effects may be included.

The HI are forces on the colloids mediated by the bath flow, generated by the motion of the colloidal particles, or more generally polymeric molecules. This in turn produces a non-trivial particle–fluid–particle hydrodynamic phenomenon, the inclusion of which has been shown to have substantial effects on the physics of many systems; for example, they have been found to be the underlying mechanism for the increased viscosity of suspensions compared to a pure bath [47], the blurring of laning that arises in driven flow [180], the migration of molecules away from a wall [79], and are particularly complex in confined systems [75, 102], and for active particles and microswimmers, which result in additional HI [85].

Mathematically, these effects can be described through the hydrodynamic fields ϱ and $\mathbf{v}$, the one-body density and one-body velocity fields, respectively. These fields, inherent to a continuum description of a collection of particles, are derived by considering successive moments (density, velocity, heat flux, ...) of the underlying kinetic system [72]. In particular, for systems of interacting Newtonian particles, when the momenta are non-negligible, the evolution of the phase space density $f(\mathbf{r}^N, \mathbf{p}^N, t)$ for a system of N colloids determining the probability of finding the system in the state $(\mathbf{r}^N, \mathbf{p}^N)$ is described by the N-body Fokker-Planck equation and the dynamics of the hydrodynamic fields are defined by obtaining closed equations for $\{\varrho, \varrho\mathbf{v}\} := \int \mathrm{d}\mathbf{r}^{N-1}\,\mathrm{d}\mathbf{p}^N\,\{1, \mathbf{p}/m\} f(\mathbf{r}^N, \mathbf{p}^N, t)$, where m is the particle mass. Here, $\mathbf{r}^N$ and $\mathbf{p}^N$ denote the $3N$-dimensional position and momentum vectors of all N particles.

The inclusion of HI leads to a much richer hierachy of fluid equations compared to systems without HI; compare e.g. [62] and [7]. In particular, in [62], by integration over all but one particle position, the one-body Fokker-Planck equation may be obtained. If, in addition, two-body HI and interparticle interactions are assumed and the inertia of the colloids is considered small, a high friction limit $\gamma \to \infty$ may be taken [63]. The result is that the velocity distribution converges to a Maxwellian, and one can eliminate the momentum variable through an adiabatic elimination process that is based on multiscale analysis [135]. The final one-body Smoluchowski equation for ϱ is a novel, nonlinear, nonlocal PDE shown to be independent of the unknown kinetic pressure term $\int \mathrm{d}\mathbf{r}\,\mathrm{d}\mathbf{p}\, m^{-2}\mathbf{p}\otimes\mathbf{p} f(\mathbf{r}, \mathbf{p}, t)$, which normally persists at $\gamma = O(1)$ (see[63], Theorem 4.1).

2.3 Langevin Dynamics

For this work we present numerical solutions to the underdamped partial differential equation (PDE) associated to the system of interacting stochastic differential equations (SDEs) on $\mathbb{R}^{6N}$, which govern the positions and momenta $\mathbf{r}_i$, $\mathbf{p}_i$ of $i = 1, \cdots N$ hard spherically symmetric colloidal particles with HI in the presence of a flowing, background field $\mathbf{u}$ of many more and

much smaller particles, of the following form

$$\frac{\mathrm{d}\mathbf{r}_i}{\mathrm{d}t} = \frac{1}{m}\mathbf{p}_i, \tag{2.3.1a}$$

$$\frac{\mathrm{d}\mathbf{p}_i}{\mathrm{d}t} = -\nabla_{\mathbf{r}_i} V(\mathbf{r}^N, t) - \sum_{j=1}^{N} \boldsymbol{\Gamma}_{ij}(\mathbf{r}^N)(\mathbf{p}_j - m\mathbf{u}(\mathbf{r}_j)) + \sum_{j=1}^{N} \boldsymbol{B}_{ij}(\mathbf{r}^N)\mathbf{f}_j(t) \tag{2.3.1b}$$

where m is the particle mass, $\mathbf{r}^N = (\mathbf{r}_1, \cdots, \mathbf{r}_N)$, $\mathbf{p}^N = (\mathbf{p}_1, \cdots, \mathbf{p}_N)$, $\boldsymbol{B} = (mk_{\mathrm{B}}\mathrm{T}\boldsymbol{\Gamma})^{1/2}$, V is a potential, k_{B}, T, γ are Boltzmann's constant, temperature and friction coefficient respectively and $\mathbf{f}_i(t) = (\zeta_i^x(t), \zeta_i^y(t), \zeta_i^z(t))^\top$ is a Gaussian white noise term with $\langle \zeta_i^a(t) \rangle = 0$ and $\langle \zeta_i^a(t), \zeta_j^b(t) \rangle = 2\delta_{ij}\delta^{ab}\delta(t - t')$. A background flow is imposed by the term $\mathbf{u}(\mathbf{r}_j)$, which is assumed incompressible and curl-free at each $\mathbf{r} \in \mathbb{R}^3$. In general we assume that $\mathbf{u}$ is not the gradient of some potential. In general the friction tensor $\boldsymbol{\Gamma}$ comprises N^2 positive definite 3×3 resistance matrices $\boldsymbol{\Gamma}_{ij}$, and describes interchange of momenta caused by fluid flows in the bath owing to the motion of the individual colloids. We make the following assumptions on the friction tensor and the potential.

Assumptions A

- The friction tensor positive definite and is written with Stokes drag separated out

$$\boldsymbol{\Gamma}_{ij} = \gamma\mathbf{1} + \gamma\tilde{\boldsymbol{\Gamma}}_{ij} \tag{A1}$$

  where γ is the friction coefficient with units $[s^{-1}]$ and for $d = 3$ dimensions, the friction tensor $\tilde{\boldsymbol{\Gamma}}_{ij}$ comprises N^2 positive definite 3×3 resistance matrices $\boldsymbol{\Gamma}_{ij}$ for the colloidal particles.

- The potential is decomposed into confining and interparticle contributions

$$V(\mathbf{r}^N, t) = \sum_{i=1}^{N} V_1(\mathbf{r}_i, t) + \sum_{n=2}^{N} \frac{1}{n!} \sum_{i_1 \neq \cdots \neq i_n = 1} V_n(\mathbf{r}_{i_1}, \cdots \mathbf{r}_{i_n}) \tag{A2}$$

  where we have assume the interparticle potentials have no explicit time dependence.

The Langevin dynamics requires computing the square root of $\boldsymbol{\Gamma}$ with complexity $O(N^3)$ floating point operations or, with more sophisticated algorithms, no better than $O(N^{2.38})$ [35]. This means the Langevin system (2.3.1a)-(2.3.1b) for systems with more than a few thousand particles are computationally intractable for most modern machines. This motivates the need for another description of the motion of particles, for example the Fokker-Planck equation. As we will see however, the corresponding Fokker-Planck equation for (2.3.1a)-(2.3.1b) is a high-dimensional PDE and, as such, one would normally be solved by Monte Carlo methods in the SDE formalism. One way to overcome the computational limitation is to ignore the HI by setting $\boldsymbol{\Gamma} = \gamma\mathbf{1}$. Whilst this reduces the computational complexity of the Langevin dynamics it neglects the HI, which will alter considerably the dynamical path to equilibrium. This motivates reduced order models such as DDFT. The novelty of the work here is the steady state of the system of colloids is characterised by the steadily flowing solvent. Such systems have only been considered before in the overdamped regime [21, 144, 145] but here we include the effects of inertia and HI.

Overdamped Limit

It will be observed that by heuristic arguments, Brownian dynamics may be reproduced by assuming that the average acceleration of the colloids is zero:

$$0 = -\nabla_{\mathbf{r}^N} V(\mathbf{r}^N, t) - \boldsymbol{\Gamma}(\mathbf{r}^N)(\mathbf{p}^N - m\mathbf{u}^N) + \boldsymbol{B}(\mathbf{r}^N)\mathbf{f}(t), \tag{2.3.2}$$

implying

$$\frac{\mathrm{d}\mathbf{r}^N}{\mathrm{d}t} = \mathbf{u}^N - \tfrac{\boldsymbol{D}(\mathbf{r}^N)}{mk_BT}\nabla_{\mathbf{r}^N}V(\mathbf{r}^N,t) + \sqrt{\boldsymbol{D}(\mathbf{r}^N)}\mathbf{f}$$

where $\mathbf{u}^N = [\mathbf{u}(\mathbf{r}_1),\cdots,\mathbf{u}(\mathbf{r}_N)]^\top$ and $\mathbf{f}$ is the vector of Brownian motions $\mathbf{f}_i$. The term $\boldsymbol{D}$ is the diffusion tensor given by the Einstein relation $\boldsymbol{D} = k_B\mathrm{T}\boldsymbol{\Gamma}^{-1}$. It will be seen that $\boldsymbol{D}$ must be positive definite for the Brownian dynamics (2.3.2) to be well posed. The dynamics (2.3.2) should be compared with DDFTs for overdamped colloids in an external flow [145], [144], in particular we show consistency with their Langevin equations upon setting $\boldsymbol{D} = \mathbf{1}$. The overdamped limit may be performed more rigorously with perturbation methods and Fredholm theory applied to the Fokker-Planck equation associated to (2.3.1a)-(2.3.1b) (see [63]).

2.4 The Fokker–Planck Equation

We begin by deriving the Fokker-Planck equation for the driven Langevin dynamics (2.3.1a)-(2.3.1b)

Theorem 2.4.1. *The Fokker-Planck equation for the $N-$body probability function associated with the Langevin dynamics of* (2.3.1a)-(2.3.1b) *is*

$$\begin{aligned}\partial_t f^{(N)} = &-\tfrac{1}{m}\sum_{k=1}^N \mathbf{p}_k\cdot\nabla_{\mathbf{r}_k} f^{(N)} + \sum_{k=1}^N \nabla_{\mathbf{p}_k}\cdot\left(\nabla_{\mathbf{r}_k}V(\mathbf{r}^N,t) + \sum_{j=1}^N \boldsymbol{\Gamma}_{kj}(\mathbf{r}^N)(\mathbf{p}_j - m\mathbf{u}(\mathbf{r}_j))\right) f^{(N)}\\ &+ m\,k_B\mathrm{T}\sum_{k,j=1}^N \boldsymbol{\Gamma}_{kj} : \nabla_{\mathbf{p}_k}\nabla_{\mathbf{p}_l} f^{(N)} \end{aligned} \tag{2.4.1}$$

where $f^{(N)} = f^{(N)}(\mathbf{r}^N,\mathbf{p}^N,t)$. We equip (2.4.1) *with homogeneous boundary conditions*

$$f^{(N)}\to 0, \quad \nabla_{\mathbf{r}_n} f^{(N)},\, \nabla_{\mathbf{p}_n} f^{(N)} \to \mathbf{0}$$

for each $n = 1,\cdots,N$ as both $|\mathbf{r}^N|$, $|\mathbf{p}^N|\to\infty$. Alternatively, for confined systems the boundary condition is imposed on, for example, the walls of the box containing the colloids.

Proof. Let $f^{(N)}(\mathbf{z}^N,\mathbf{q}^N,t+\delta t|\mathbf{y}^N,\mathbf{u}^N,s)$ be the probability that particles find themselves with positions $\mathbf{z}^N$ and momenta $\mathbf{q}^N$ at time $t+\delta t$ given they previously had positions $\mathbf{y}^N$ and momenta $\mathbf{u}^N$ at time s for $t>s$, $\delta t>0$. Then by the partition theorem

$$\begin{aligned} &f^{(N)}(\mathbf{z}^N,\mathbf{q}^N,t+\delta t|\mathbf{y}^N,\mathbf{u}^N,s)\\ &\quad = \iint \mathrm{d}\mathbf{r}^N\mathrm{d}\mathbf{p}^N f^{(N)}(\mathbf{z}^N,\mathbf{q}^N,t+\delta t|\mathbf{r}^N,\mathbf{p}^N,t) f^{(N)}(\mathbf{r}^N,\mathbf{p}^N,t|\mathbf{y}^N,\mathbf{u}^N,s). \end{aligned} \tag{2.4.2}$$

Now let $\varphi\in C_0^\infty(\mathbb{R}^{6N})$ be a smooth compactly supported test function. By multiplying (2.4.2) by $\varphi(\mathbf{z}^N,\mathbf{q}^N)$ and integrating $\mathrm{d}\mathbf{z}^N\,\mathrm{d}\mathbf{q}^N$, substituting the dummy variables $\mathbf{z}^N$ for $\mathbf{r}^N$ and $\mathbf{q}^N$ for $\mathbf{p}^N$ on the left hand side and interchanging the order of integration on the right hand side, one has

$$\begin{aligned} &\iint \mathrm{d}\mathbf{r}^N\,\mathrm{d}\mathbf{p}^N\,\varphi(\mathbf{r}^N,\mathbf{p}^N) f^{(N)}(\mathbf{r}^N,\mathbf{p}^N,t+\delta t|\mathbf{y}^N,\mathbf{u}^N,s)\\ &= \iint \mathrm{d}\mathbf{r}^N\,\mathrm{d}\mathbf{p}^N \iint \mathrm{d}\mathbf{z}^N\,\mathrm{d}\mathbf{q}^N \varphi(\mathbf{z}^N,\mathbf{q}^N) f^{(N)}(\mathbf{z}^N,\mathbf{q}^N,t+\delta t|\mathbf{r}^N,\mathbf{p}^N,t) f^N(\mathbf{r}^N,\mathbf{p}^N,t|\mathbf{y}^N,\mathbf{u}^N,s). \end{aligned} \tag{2.4.3}$$

Now by Taylor expanding (2.4.3) in both N position and N momentum directions $\mathbf{z}_i = \mathbf{r}_i$ and

$\mathbf{q}_i = \mathbf{p}_i$, $1 \leq i \leq N$ one has

$$\begin{aligned}
&\iint \mathrm{d}\mathbf{r}^N\,\mathrm{d}\mathbf{p}^N\,\varphi(\mathbf{r}^N,\mathbf{p}^N) f^N(\mathbf{r}^N,\mathbf{p}^N,t+\delta t|\mathbf{y}^N,\mathbf{u}^N,s)\\
&= \iint \mathrm{d}\mathbf{r}^N\,\mathrm{d}\mathbf{p}^N \iint \mathrm{d}\mathbf{z}^N\,\mathrm{d}\mathbf{q}^N f^N(\mathbf{z}^N,\mathbf{q}^N,t+\delta t|\mathbf{r}^N,\mathbf{p}^N,t)\Big[\varphi(\mathbf{r}^N,\mathbf{p}^N)\\
&\quad+\sum_{k=1}^N(\mathbf{q}_k-\mathbf{p}_k)\cdot\nabla_{\mathbf{p}_k}\varphi(\mathbf{r}^N,\mathbf{p}^N)+\frac{1}{2}\sum_{k,l=1}^N(\mathbf{q}_k-\mathbf{p}_k)\otimes(\mathbf{q}_k-\mathbf{p}_k):\nabla_{\mathbf{p}_k}\nabla_{\mathbf{p}_l}\varphi(\mathbf{r}^N,\mathbf{p}^N)\\
&\quad+\sum_{k=1}^N(\mathbf{z}_k-\mathbf{r}_k)\cdot\nabla_{\mathbf{r}_k}\varphi(\mathbf{r}^N,\mathbf{p}^N)+\frac{1}{2}\sum_{k,l=1}^N(\mathbf{z}_k-\mathbf{r}_k)\otimes(\mathbf{z}_k-\mathbf{r}_k):\nabla_{\mathbf{r}_k}\nabla_{\mathbf{r}_l}\varphi(\mathbf{r}^N,\mathbf{p}^N)\\
&\quad+\sum_{k=1}^N o(||\mathbf{z}_k-\mathbf{r}_k||^2)+\sum_{k=1}^N o((\mathbf{q}_k-\mathbf{p}_k)\cdot(\mathbf{z}_k-\mathbf{r}_k))+\sum_{k=1}^N o(||\mathbf{q}_k-\mathbf{p}_k||^2)\Big]\\
&\quad\times f^{(N)}(\mathbf{r}^N,\mathbf{p}^N,t|\mathbf{y}^N,\mathbf{u}^N,s).
\end{aligned}\tag{2.4.4}$$

where $\otimes$ is the dyadic product and : is the matrix inner product. We now refer to (2.3.1a)-(2.3.1b) as an an integration formula. For the remaining terms in (2.4.4) we identify moments $\mathbb{E}(\mathbf{r}_k^n)$, $\mathbb{E}(\mathbf{p}_k^n)$ for $n \in \mathbb{N}$ of the underlying Langevin dynamics. In other words, we recast (2.3.1a)-(2.3.1b) into the computational definition, for $1 \leq i \leq N$

$$\begin{aligned}
\mathrm{d}\mathbf{r}_i &= \delta t\tfrac{\mathbf{p}_i}{m},\\
\mathrm{d}\mathbf{p}_i &= \left[-\nabla_{\mathbf{r}_i}V(\mathbf{r}^N,t)-\sum_{j=1}^N\mathbf{\Gamma}_{ij}(\mathbf{r}^N)(\mathbf{p}_j-m\mathbf{u}(\mathbf{r}_j))+\sum_{j=1}^N A_{ij}(\mathbf{r}^N)\,\mathrm{d}\mathbf{W}_j(t)\right]\delta t
\end{aligned}$$

where $\mathrm{d}\mathbf{W}_j(t) \sim_{\text{iid}} [\mathscr{N}(0,\delta t^{-1}),\,\mathscr{N}(0,\delta t^{-1}),\,\mathscr{N}(0,\delta t^{-1})]^\top$ and $\mathrm{d}\mathbf{x} := \mathbf{x}(t+\delta t)-\mathbf{x}(t)$ to compute sucessive spatial and momentum moments. Note this Wiener process has variance δt^{-1} so that the diffusion term in the Langevin equation scales correctly with time. By inspection we see that the first term in (2.4.4) is the probability density $f^{(N)}(\mathbf{z}^N,\mathbf{q}^N,t+\delta t|\mathbf{r}^N,\mathbf{p}^N,t)$ integrated over its entire support and is therefore equal to unity. Letting $\mathbb{E}(\cdot)$ denote the expected value, one has the following identity for the first momentum moment

$$\begin{aligned}
&\iint \mathrm{d}\mathbf{z}^N\,\mathrm{d}\mathbf{q}^N\sum_{k=1}^N(\mathbf{q}_k-\mathbf{p}_k)f^{(N)}(\mathbf{z}^N,\mathbf{q}^N,t+\delta t|\mathbf{r}^N,\mathbf{p}^N,t)\\
&\quad=\sum_{k=1}^N\mathbb{E}(\mathbf{q}_k(t+\delta t)-\mathbf{p}_k|\mathbf{q}_k(t)=\mathbf{p}_k)\\
&\quad=\sum_{k=1}^N\mathbb{E}\left[-\nabla_{\mathbf{r}_k}V(\mathbf{r}^N,t)-\sum_{j=1}^N\mathbf{\Gamma}_{kj}(\mathbf{r}^N)(\mathbf{p}_j-m\mathbf{u}(\mathbf{r}_j))+\sum_{j=1}^N A_{kj}(\mathbf{r}^N)\,\mathrm{d}\mathbf{W}_j(t)\right]\delta t\\
&\quad=-\delta t\nabla_{\mathbf{r}_k}V(\mathbf{r}^N,t)-\delta t\sum_{j=1}^N\mathbf{\Gamma}_{kj}(\mathbf{r}^N)(\mathbf{p}_j-m\mathbf{u}(\mathbf{r}_j))
\end{aligned}\tag{2.4.5}$$

where we have used $\mathbb{E}(d\mathbf{W}_j) = 0$. Similarly for the first moment of space we obtain

$$\begin{aligned}
&\iint \mathrm{d}\mathbf{z}^N \, \mathrm{d}\mathbf{q}^N \sum_{k=1}^{N} (\mathbf{z}_k - \mathbf{r}_k) f^{(N)}(\mathbf{z}^N, \mathbf{q}^N, t + \delta t | \mathbf{r}^N, \mathbf{p}^N, t) \\
&\quad = \sum_{k=1}^{N} \mathbb{E}(\mathbf{z}_k(t + \delta t) - \mathbf{r}_k | \mathbf{z}_k(t) = \mathbf{r}_k) \\
&\quad = \tfrac{\delta t}{m} \sum_{k=1}^{N} \mathbf{p}_k. \qquad (2.4.6)
\end{aligned}$$

For the second momentum moment we use the fact that $\mathbb{E}(\mathrm{d}\mathbf{W}_j^2) = \delta t^{-1}$ to obtain

$$\begin{aligned}
&\iint \mathrm{d}\mathbf{z}^N \, \mathrm{d}\mathbf{q}^N \sum_{k=1}^{N} (\mathbf{q}_k - \mathbf{p}_k) \otimes (\mathbf{q}_k - \mathbf{p}_k) f^{(N)}(\mathbf{z}^N, \mathbf{q}^N, t + \delta t | \mathbf{r}^N, \mathbf{p}^N, t) \\
&\quad = \sum_{k=1}^{N} \mathbb{E}((\mathbf{q}_k(t + \delta t) - \mathbf{p}_k) \otimes (\mathbf{q}_k(t + \delta t) - \mathbf{p}_k) | \mathbf{q}_k(t) = \mathbf{p}_k) \\
&\quad = m \, k_{\mathrm{B}} \mathrm{T} \sum_{j=1}^{N} \mathbf{\Gamma}_{kj} \, \delta t + o(\delta t), \qquad (2.4.7)
\end{aligned}$$

where we have used the generalised fluctuation-dissipation relation $\boldsymbol{B}_{ij}(\mathbf{r}) = \sqrt{m k_B \mathrm{T} \mathbf{\Gamma}_{ij}(\mathbf{r})}$. For the second position moment one has

$$\begin{aligned}
&\iint \mathrm{d}\mathbf{z}^N \, \mathrm{d}\mathbf{q}^N \sum_{k=1}^{N} (\mathbf{z}_k - \mathbf{r}_k) \otimes (\mathbf{z}_k - \mathbf{r}_k) f^{(N)}(\mathbf{z}^N, \mathbf{q}^N, t + \delta t | \mathbf{r}^N, \mathbf{p}^N, t) \\
&\quad = \sum_{k=1}^{N} \mathbb{E}((\mathbf{z}_k(t + \delta t) - \mathbf{r}_k) \otimes (\mathbf{z}_k(t + \delta t) - \mathbf{r}_k) | \mathbf{z}_k(t) = \mathbf{r}_k) = o(\delta t). \qquad (2.4.8)
\end{aligned}$$

Using the identities (2.4.5), (2.4.6), (2.4.7), (2.4.8) and substituting into (2.4.4) one obtains

$$\begin{aligned}
&\iint \mathrm{d}\mathbf{r}^N \, \mathrm{d}\mathbf{p}^N \, \varphi(\mathbf{r}^N, \mathbf{p}^N) f^{(N)}(\mathbf{r}^N, \mathbf{p}^N, t + \delta t | \mathbf{y}^N, \mathbf{u}^N, s) \\
&= \iint \mathrm{d}\mathbf{r}^N \, \mathrm{d}\mathbf{p}^N \Big[\varphi(\mathbf{r}^N, \mathbf{p}^N) \\
&\quad + \delta t \sum_{k=1}^{N} \left(-\nabla_{\mathbf{r}_k} V(\mathbf{r}^N, t) - \sum_{j=1}^{N} \mathbf{\Gamma}_{kj}(\mathbf{r}^N)(\mathbf{p}_j - m\mathbf{u}(\mathbf{r}_j)) \right) \cdot \nabla_{\mathbf{p}_k} \varphi(\mathbf{r}^N, \mathbf{p}^N) \\
&\quad + \delta t \, m k_{\mathrm{B}} \mathrm{T} \sum_{k,j=1}^{N} \mathbf{\Gamma}_{kj} : \nabla_{\mathbf{p}_k} \nabla_{\mathbf{p}_l} \varphi(\mathbf{r}^N, \mathbf{p}^N) + \tfrac{\delta t}{m} \sum_{k=1}^{N} \mathbf{p}_k \cdot \nabla_{\mathbf{r}_k} \varphi(\mathbf{r}^N, \mathbf{p}^N) \Big] \\
&\quad \times f^{(N)}(\mathbf{r}^N, \mathbf{p}^N, t | \mathbf{y}^N, \mathbf{u}^N, s) + o(\delta t).
\end{aligned}$$

Now rearranging to one integral and integrating by parts and using the assumed boundary

conditions one obtains

$$
\begin{aligned}
0 = &\iint \mathrm{d}\mathbf{r}^N\,\mathrm{d}\mathbf{p}^N\,\varphi(\mathbf{r}^N,\mathbf{p}^N) f^{(N)}(\mathbf{r}^N,\mathbf{p}^N,t+\delta t|\mathbf{y}^N,\mathbf{u}^N,s)\\
&-\iint \mathrm{d}\mathbf{r}^N\,\mathrm{d}\mathbf{p}^N\,\varphi(\mathbf{r}^N,\mathbf{p}^N)\Big[f^{(N)}(\mathbf{r}^N,\mathbf{p}^N,t|\mathbf{y}^N,\mathbf{u}^N,s)\\
&+\delta t\sum_{k=1}^{N}\nabla_{\mathbf{p}_k}\cdot\left(-\nabla_{\mathbf{r}_k}V(\mathbf{r}^N,t)-\sum_{j=1}^{N}\mathbf{\Gamma}_{kj}(\mathbf{r}^N)(\mathbf{p}_j-m\mathbf{u}(\mathbf{r}_j))\right) f^{(N)}(\mathbf{r}^N,\mathbf{p}^N,t|\mathbf{y}^N,\mathbf{u}^N,s)\\
&-m\,k_{\mathrm{B}}\mathrm{T}\,\delta t\sum_{k,j=1}^{N}\mathbf{\Gamma}_{kj}:\nabla_{\mathbf{p}_k}\nabla_{\mathbf{p}_l}f^{(N)}(\mathbf{r}^N,\mathbf{p}^N,t|\mathbf{y}^N,\mathbf{u}^N,s)\\
&+\tfrac{\delta t}{m}\sum_{k=1}^{N}\mathbf{p}_k\cdot\nabla_{\mathbf{r}_k}f^{(N)}(\mathbf{r}^N,\mathbf{p}^N,t|\mathbf{y}^N,\mathbf{u}^N,s)\Big]+o(\delta t).
\end{aligned}
$$

Now since the function φ is an arbitrary smooth test function we must have

$$
\begin{aligned}
0 = &\,\delta t^{-1}(f^{(N)}(\mathbf{r}^N,\mathbf{p}^N,t+\delta t|\mathbf{y}^N,\mathbf{u}^N,s)-f^{(N)}(\mathbf{r}^N,\mathbf{p}^N,t|\mathbf{y}^N,\mathbf{u}^N,s))\\
&+\sum_{k=1}^{N}\nabla_{\mathbf{p}_k}\cdot\left(-\nabla_{\mathbf{r}_k}V(\mathbf{r}^N,t)-\sum_{j=1}^{N}\mathbf{\Gamma}_{kj}(\mathbf{r}^N)(\mathbf{p}_j-m\mathbf{u}(\mathbf{r}_j))\right) f^{(N)}(\mathbf{r}^N,\mathbf{p}^N,t|\mathbf{y}^N,\mathbf{u}^N,s)\\
&-m\,k_{\mathrm{B}}\mathrm{T}\sum_{k,j=1}^{N}\mathbf{\Gamma}_{kj}:\nabla_{\mathbf{p}_k}\nabla_{\mathbf{p}_l}f^{(N)}(\mathbf{r}^N,\mathbf{p}^N,t|\mathbf{y}^N,\mathbf{u}^N,s)\\
&+\tfrac{1}{m}\sum_{k=1}^{N}\mathbf{p}_k\cdot\nabla_{\mathbf{r}_k}f^{(N)}(\mathbf{r}^N,\mathbf{p}^N,t|\mathbf{y}^N,\mathbf{u}^N,s)+o(1).
\end{aligned}
$$

Now formally taking the limit $\delta t\to 0$ we obtain the required result. Typically one substitutes the conditioned states for an initial configuration distribution at time $s=0$, $\mathbf{y}^N=\mathbf{r}_0^N$, $\mathbf{u}^N=\mathbf{p}_0^N$. □

We conclude this section with the following remarks on the Fokker-Planck equation (2.4.1).

Remark 2.4.2. *The Fokker-Planck equation* (2.4.1) *is a high dimensional PDE. A naive discretisation of M points in the $6N$ position and momenta components results in a total of M^{6N} discretisation points, that is an exponential increase in the number of computational points as a function of the total number of particles where M is fixed. This is known as the curse of dimensionality. In practise, to solve* (2.4.1) *one would sample the Langevin dynamics* (2.3.1a)-(2.3.1b) *via Monte Carlo methods.*

To determine a reduced model, and overcome this intrinsic computational complexity, additional integrations are performed to obtain evolution equations for local and bulk quantities such as density, velocity, stress, temperature and flux, each of which are characterised by particular moments of the stochastic process associated to flow of the probability function $f^{(n)}$. This technique is known as coarse graining, is more rigorously defined as an iterative projection of the invariant manifold on which the one-body distribution evolves, to the plane of macroscopic hydrodynamic fields (ρ, $\mathbf{v}$, σ...) which parametrise $f^{(1)}$ [72].

2.5 DDFT In A Steady External Flow

The associated Fokker-Planck equation to the SDE (2.3.1a)-(2.3.1b) is given by Theorem 2.4.1 which we provide for convenience

$$\begin{aligned}
&\partial_t f^{(N)}(\mathbf{r}^N,\mathbf{p}^N,t)+\sum_{i=1}^{N}\tfrac{\mathbf{p}_i}{m}\cdot\nabla_{\mathbf{r}_i}f^{(N)}(\mathbf{r}^N,\mathbf{p}^N,t)\\
&-\sum_{i=1}^{N}\nabla_{\mathbf{r}_i}V(\mathbf{r}^N,t)\cdot\nabla_{\mathbf{p}_i}f^{(N)}(\mathbf{r}^N,\mathbf{p}^N,t)\\
&=\sum_{i,j=1}^{N}\nabla_{\mathbf{p}_i}\cdot\Big[\mathbf{\Gamma}_{ij}(\mathbf{r}^N)(\mathbf{p}_j-m\mathbf{u}(\mathbf{r}_j)+mk_{\mathrm{B}}\mathrm{T}\nabla_{\mathbf{p}_j})f^{(N)}(\mathbf{r}^N,\mathbf{p}^N,t)\Big] \qquad (2.5.1)
\end{aligned}$$

where $f^{(N)}(\mathbf{r}^N,\mathbf{p}^N,t)$ is the probability of finding each particle j at position $\mathbf{r}_j$ with momentum $\mathbf{p}_j$ at time t referred to as the $N-$body density. Equation (2.4.1) remains a high dimensional PDE, indeed the number of discretisation points increases exponentially in N. To continue we integrate (2.5.1) and derive equations for its moments, giving an infinite hierarchy to be truncated with moment closure. We begin by providing the definitions of the reduced phase space functions.

Definition 2.5.1 (Reduced Phase Space Functions)**.** *Let $f^{(N)}$ be a solution to the Fokker-Planck equation* (2.5.1)*. Then we make the following definitions*

1. *The reduced phase space densities $f^{(n)}$ are defined by*

$$f^{(n)}(\mathbf{r}^n,\mathbf{p}^n,t):=\frac{N!}{(N-n)!}\int \mathrm{d}\mathbf{r}^{N-n}\,\mathrm{d}\mathbf{p}^{N-n}\,f^{(N)}(\mathbf{r}^N,\mathbf{p}^N,t). \qquad (2.5.2)$$

2. *The reduced configuration densities $\varrho^{(n)}$ are defined by*

$$\varrho^{(n)}(\mathbf{r}^n,t):=\int \mathrm{d}\mathbf{p}^n\,f^{(n)}(\mathbf{r}^n,\mathbf{p}^n,t) \qquad (2.5.3)$$

   where $\varrho^{(1)}\equiv\varrho$.

3. *The probability current is defined by*

$$\mathbf{j}(\mathbf{r}_1,t):=\int \mathrm{d}\mathbf{p}_1\,\tfrac{\mathbf{p}_1}{m}f^{(1)}(\mathbf{r}_1,\mathbf{p}_1,t). \qquad (2.5.4)$$

The first result of this section is to obtain a continuity equation for the one body density in the presence of an external flow. Unsurprisingly the continuity equation is the same as the ones found in the absence of external flows, which is a consequence of writing the Langevin dynamics in an inertial frame of reference by the transformation $\mathbf{p}^N_{\mathrm{old}}\to\mathbf{p}^N-m\mathbf{u}^N$ where $\mathbf{p}^N_{\mathrm{old}}$ is the momentum vector of the system (2.3.1a)-(2.3.1b) when $\mathbf{u}^N\equiv\mathbf{0}$.

Lemma 2.5.2. *The one body density $\varrho(\mathbf{r}_1,t)$ defined by* (2.5.3)*, satisfies the continuity equation*

$$\partial_t\varrho(\mathbf{r}_1,t)+\nabla_{\mathbf{r}_1}\cdot\mathbf{j}(\mathbf{r}_1,t)=0 \qquad (2.5.5)$$

where $\mathbf{j}(\mathbf{r}_1,t)$ is defined by (2.5.4)*.*

Proof. Integrating (2.5.1) over all but on particle position $\mathbf{r}_1$, using the definitions (2.5.2), (2.5.3) and (2.5.4) along with the boundary conditions $f^N=0$ and $\nabla_{\mathbf{p}_i}f^N=\nabla_{\mathbf{r}_i}f^N=\mathbf{0}$ as both $|\mathbf{r}_i|$ and $|\mathbf{p}_i|\to\infty$ for each $1\le i\le N$ yields the result. □

We now begin the moment closure of (2.5.1) by obtaining an evolution equation for the probability current $\mathbf{j}$.

Lemma 2.5.3. *The probability current* $\mathbf{j}$ *given by* (2.5.4) *evolves according to*

$$\begin{aligned}
&\partial_t \mathbf{j}(\mathbf{r}_1,t) + \nabla_{\mathbf{r}_1} \cdot \int \mathrm{d}\mathbf{p}_1 \, \tfrac{\mathbf{p}_1}{m} \otimes \tfrac{\mathbf{p}_1}{m} f^{(1)}(\mathbf{r}_1,\mathbf{p}_1,t) \\
&\quad + \frac{1}{m}\varrho(\mathbf{r}_1,t)\nabla_{\mathbf{r}_1} V_1(\mathbf{r}_1,t) + \frac{1}{m}\sum_{n=2}^{N} \int \mathrm{d}\mathbf{r}^{n-1} \nabla_{\mathbf{r}_1} V_n(\mathbf{r}^n) \varrho^{(n)}(\mathbf{r}^n,t) \\
&\quad + \gamma(\mathbf{j}(\mathbf{r}_1,t) - \varrho(\mathbf{r}_1,t)\mathbf{u}(\mathbf{r}_1)) \\
&\quad + \frac{\gamma N}{m}\sum_{j=1}^{N} \int \mathrm{d}\mathbf{r}^{N-1} \, \mathrm{d}\mathbf{p}^N \, \tilde{\mathbf{\Gamma}}_{1j}(\mathbf{r}^N)(\mathbf{p}_j - m\mathbf{u}_1) f^{(N)}(\mathbf{r}^N,\mathbf{p}^N,t) \\
&\quad = 0
\end{aligned} \tag{2.5.6}$$

where $\varrho(\mathbf{r}_1,t)$ *is defined by* (2.5.3).

Proof. Multiplying (2.5.1) by $N\mathbf{p_1}/m$ and integrating over all but one particle position $\mathbf{r}_1$ we obtain the following identities. First, for the time derivative of $f^{(N)}$

$$\int \mathrm{d}\mathbf{r}^{N-1} \, \mathrm{d}\mathbf{p}^N \, \frac{N}{m}\mathbf{p}_1 \partial_t f^{(N)}(\mathbf{r}^N,\mathbf{p}^N,t) = \partial_t \mathbf{j}(\mathbf{r}_1,t). \tag{2.5.7}$$

Second, for the advective derivative of $f^{(N)}$

$$\int \mathrm{d}\mathbf{r}^{N-1} \, \mathrm{d}\mathbf{p}^N \, \frac{N}{m}\mathbf{p}_1 \times \sum_{i=1}^{N} \tfrac{\mathbf{p}_i}{m} \cdot \nabla_{\mathbf{r}_i} f^{(N)}(\mathbf{r}^N,\mathbf{p}^N,t) = \nabla_{\mathbf{r}_1} \cdot \int \mathrm{d}\mathbf{p}_1 \, \frac{\mathbf{p}_1}{m} \otimes \frac{\mathbf{p}_1}{m} f^{(1)}(\mathbf{r}_1,\mathbf{p}_1,t)$$

where we have used the boundary conditions $f^N = \nabla_{\mathbf{p}_i} f^N = 0$ as $|\mathbf{r}_i|$ and $|\mathbf{p}_i| \to \infty$ for each $1 \le i \le N$. Third, by assumption (A2), the potential energy term may be divided into two parts

$$\begin{aligned}
&\int \mathrm{d}\mathbf{r}^{N-1} \, \mathrm{d}\mathbf{p}^N \, \frac{N}{m}\mathbf{p}_1 \times \sum_{i=1}^{N} \nabla_{\mathbf{r}_i} V(\mathbf{r}^N,t) \cdot \nabla_{\mathbf{p}_i} f^{(N)}(\mathbf{r}^N,\mathbf{p}^N,t) \\
&\quad = \int \mathrm{d}\mathbf{r}^{N-1} \, \mathrm{d}\mathbf{p}^N \, \frac{N}{m}\mathbf{p}_1 \times \sum_{i=1}^{N} \nabla_{\mathbf{r}_i} \left(\sum_{j=1}^{N} V_1(\mathbf{r}_j,t) + \sum_{n=2}^{N} \frac{1}{n!} \sum_{j_1 \neq j_n = 1} V_n(\mathbf{r}_{j_1},\cdots,\mathbf{r}_{j_n}) \right) \\
&\quad = -\frac{1}{m}\varrho(\mathbf{r}_1,t)\nabla_{\mathbf{r}_1} V_1(\mathbf{r}_1,t) - \frac{1}{m}\sum_{n=2}^{N} \int \mathrm{d}\mathbf{r}^{n-1} \nabla_{\mathbf{r}_1} V_n(\mathbf{r}^n) \varrho^{(n)}(\mathbf{r}^n,t)
\end{aligned}$$

where we have integrated by parts in the $\mathbf{p}_1$ variable and used the definitions(2.5.3). Fourthly, for the friction term, we use the assumption (A1) to obtain

$$\begin{aligned}
&\int \mathrm{d}\mathbf{r}^{N-1} \, \mathrm{d}\mathbf{p}^N \, \frac{N}{m}\mathbf{p}_1 \times \sum_{i,j=1}^{N} \nabla_{\mathbf{p}_i} \cdot \Big(\mathbf{\Gamma}_{ij}(\mathbf{r}^N)(\mathbf{p}_j - m\mathbf{u}(\mathbf{r}_j)) f^{(N)}(\mathbf{r}^N,\mathbf{p}^N,t) \Big) \\
&\quad = -\int \mathrm{d}\mathbf{r}^{N-1} \, \mathrm{d}\mathbf{p}^N \, \frac{N}{m} \sum_{j=1}^{N} \nabla_{\mathbf{p}_i} \cdot \Big(\mathbf{\Gamma}_{ij}(\mathbf{r}^N)(\mathbf{p}_j - m\mathbf{u}(\mathbf{r}_j)) f^{(N)}(\mathbf{r}^N,\mathbf{p}^N,t) \Big) \\
&\quad = -\gamma(\mathbf{j}(\mathbf{r}_1,t) - \varrho(\mathbf{r}_1,t)\mathbf{u}(\mathbf{r}_1)) - \frac{\gamma N}{m}\sum_{j=1}^{N} \int \mathrm{d}\mathbf{r}^{N-1} \, \mathrm{d}\mathbf{p}^N \, \tilde{\mathbf{\Gamma}}_{1j}(\mathbf{r}^N)(\mathbf{p}_j - m\mathbf{u}_1) f^{(N)}(\mathbf{r}^N,\mathbf{p}^N,t)
\end{aligned}$$

where we expand $\mathbf{\Gamma}_{ij}$ using (A1), integrated by parts in the $\mathbf{p}_1$ variable and used the definitions

(2.5.3), (2.5.4). Lastly, we observe that

$$\int \mathrm{d}\mathbf{r}^{N-1}\,\mathrm{d}\mathbf{p}^N\,\frac{N}{m}\mathbf{p}_1 \times \sum_{i,j=1}^{N} mk_{\mathrm{B}}\mathrm{T}\nabla_{\mathbf{p}_i}\cdot\nabla_{\mathbf{p}_j} f^{(N)}(\mathbf{r}^N,\mathbf{p}^N,t)$$
$$= -Nk_{\mathrm{B}}\mathrm{T}\int \mathrm{d}\mathbf{r}^{N-1}\,\mathrm{d}\mathbf{p}^N \sum_{j=1}^{N}\nabla_{\mathbf{p}_j} f^{(N)}(\mathbf{r}^N,\mathbf{p}^N,t) = \mathbf{0} \tag{2.5.8}$$

where we have used the boundary condition $f^N = 0$ as $|\mathbf{p}_i| \to \infty$ for each $1 \le i \le N$. By combining (2.5.7)-(2.5.8) we obtain the required result. □

To close the system of equations (2.5.5), (2.5.6), equations are needed for the kinetic pressure term $\frac{\mathbf{p}_1}{m}\otimes\frac{\mathbf{p}_1}{m}f^{(1)}(\mathbf{r}_1,\mathbf{p}_1,t)$, the reduced configuration densities $\varrho^{(n)}$ and HI term. This will be done in the usual way, for the $\varrho^{(n)}(\mathbf{r},t)$ we assume that higher order densities ($n \ge 2$) are enslaved to ϱ and equilibrate on a faster timescale. For the kinetic pressure term we will use an approximation which states that the momentum of each colloids is follows a Maxwell-Boltzmann distribution centred at the background flow. For the HI term we will assume the existence of a correlation function relating the one body phase densities to the pair density.

Assumption B

- The Adiabatic Assumption

  For $n \ge 2$, the $\varrho^{(n)}(\mathbf{r}^{(n)},t)$ are enslaved to $\varrho(\mathbf{r},t)$ and equilibrate on a timescale smaller than $\sim o\left(\gamma^{-1}\right)$. (B1)

The assumption (B1) amounts to that the n–body densities in the true non-equilibrium system are well approximated by the n–body densities in the corresponding equilibrium system with the same density. We now use the define the augmented Helmholtz free energy functional to take into account the kinetic energy of the colloids in the solvent.

Definition 2.5.4 (Free Energy Functional For the Driven System)**.** *We define $\mathscr{F}_{\mathbf{u}} : C(\mathbb{R}) \to \mathbb{R}$ such that*

$$\mathscr{F}_{\mathbf{u}}[\varrho] = k_B\mathrm{T}\int \mathrm{d}\mathbf{r}_1\,\varrho(\log(\Lambda^3\varrho)-1) + \int \mathrm{d}\mathbf{r}_1\,\varrho V_1(\mathbf{r}_1,t) + \mathscr{F}_{ex}[\varrho] + \tfrac{1}{2}m\int \mathrm{d}\mathbf{r}\,\varrho|\mathbf{u}|^2 \tag{2.5.9}$$

where Λ is the de Broglie wavelength (which in general is superfluous) and $\mathscr{F}_{ex}[\varrho]$ is the excess over ideal gas term. By definition we have the following identity

$$\mathscr{F}_{\mathbf{u}}[\varrho] = \mathscr{F}_H[\varrho] + \tfrac{1}{2}m\int \mathrm{d}\mathbf{r}\,\varrho|\mathbf{u}|^2$$

where $\mathscr{F}_H$ is the Helmholtz free energy functional defined in (2.1.4)*.*

Note that we do not assume $\mathbf{u}$ is a potential flow, however such a condition is sufficient to satisfy the irrotationality assumption, which we will later relax. We make an additional assumption on the interparticle forces

Assumptions C

- The background flow is incompressible and irrotational

$$\nabla_{\mathbf{r}}\cdot\mathbf{u} = 0, \tag{C1}$$
$$\nabla_{\mathbf{r}}\times\mathbf{u} = 0. \tag{C2}$$

The following result establishes the Maxwell Boltzmann distribution for the steady system.

Proposition 2.5.5 (Maxwell Boltzmann Distribution)**.** *Let assumptions* (A1) *hold. At steady state the the one particle distribution function takes the Maxwell—Boltzmann form*

$$f^{(1)}(\mathbf{r},\mathbf{p}) = \frac{\varrho(\mathbf{r})}{(2\pi m k_B \mathrm{T})^{3/2}} e^{-\frac{|\mathbf{p}-m\mathbf{u}|^2}{2mk_B\mathrm{T}}}.$$

Proof. To establish the result we study the kinetic equation for the N–body density in nondimensional units

$$\partial_t f^{(N)}(\mathbf{r}^N,\mathbf{p}^N,t) + \frac{1}{\epsilon}\sum_{i=1}^N \frac{\mathbf{p}_i}{m}\cdot\nabla_{\mathbf{r}_i} f^{(N)}(\mathbf{r}^N,\mathbf{p}^N,t) - \frac{1}{\epsilon}\sum_{i=1}^N \nabla_{\mathbf{r}_i} V(\mathbf{r}^N,t)\cdot\nabla_{\mathbf{p}_i} f^{(N)}(\mathbf{r}^N,\mathbf{p}^N,t)$$
$$= \frac{1}{\epsilon^2}\sum_{i,j=1}^N \nabla_{\mathbf{p}_i}\cdot\Big[\mathbf{\Gamma}_{ij}(\mathbf{r}^N)(\mathbf{p}_j - m\mathbf{u}(\mathbf{r}_j) + \nabla_{\mathbf{p}_j}) f^{(N)}(\mathbf{r}^N,\mathbf{p}^N,t)\Big] \tag{2.5.10}$$

which may be obtained by rescaling the Fokker-Planck equation (2.5.1) and $\epsilon = \sqrt{k_B\mathrm{T}/m}\gamma^{-1}$. We note that $\sqrt{k_B\mathrm{T}/m}$ is the average thermal equilibrium speed of a particle at temperature T, whilst γ^{-1} is approximately the time required for the velocity distribution of the colloids to equilibrate. Therefore, the steady momentum distribution is determined in the limit $\gamma^{-1}\to 0$. Note that ϵ has units of length, and therefore a characteristic length scale must be introduced to make it nondimensional. This length scale is problem dependent and could be, for example: the mean free path length of a typical colloidal particle, the length over which the external potential varies, or in confined systems, the dimension of the bounding domain.

We now expand f^N in powers of ϵ as a Hilbert expansion

$$f^N(\mathbf{r}^N,\mathbf{p}^N) = \sum_{n=0}^\infty \epsilon^n f_n^N(\mathbf{r}^N,\mathbf{p}^N). \tag{2.5.11}$$

Due to the singular nature of (2.5.10), we do not expect such a regular perturbation expansion to converge uniformly. The expansion should be valid only for times $t \gg \epsilon$ and not for shorter times and we expect there to be a boundary layer in time of size $O(\epsilon)$. Since we are interested in times much larger than ϵ, interest lies in only the leading order term. We also assume that such an expansion then converges, in particular, that the f_n^N are sufficiently well behaved in $\mathbf{r}^N$ and $\mathbf{p}^N$.

We substitute (2.5.11) in (2.5.10), and write for ease of notation $\hat{\mathbf{p}}_j := \mathbf{p}_j - m\mathbf{u}(\mathbf{r}_j)$. By collecting powers of ϵ we obtain a hierarchy of equations to be solved sequentially. At the leading of ϵ we obtain

$$\sum_{i,j=1}^N \nabla_{\mathbf{p}_i}\cdot\big[\mathbf{\Gamma}_{ij}(\mathbf{r}^N)(\hat{\mathbf{p}}_j + \nabla_{\mathbf{p}_j}) f_0^N(\mathbf{r}^N,\mathbf{p}^N,t)\big] = 0. \tag{2.5.12}$$

We now determine the form of solutions to this equations, consisting of functions of the form $f_0^N = \phi^N(\mathbf{r}^N,t)\prod_{i=1}^N \exp\left(-\frac{|\hat{\mathbf{p}}_i|^2}{2}\right)$ for some ϕ^N dependent only on the spatial coordinates $\mathbf{r}^N$. To do this, we instead suppose that $\phi^N = \phi^N(\mathbf{r}^N,\mathbf{p}^N,t)$ and observe that

$$(\hat{\mathbf{p}}_j + \nabla_{\mathbf{p}_j})\left[\phi^N(\mathbf{r}^N,\mathbf{p}^N,t)\prod_{i=1}^N \exp\left(-\tfrac{|\hat{\mathbf{p}}_i|^2}{2}\right)\right] = \nabla_{\mathbf{p}_j}\phi^N(\mathbf{r}^N,\mathbf{p}^N)\prod_{i=1}^N \exp\left(-\tfrac{|\hat{\mathbf{p}}_i|^2}{2}\right). \tag{2.5.13}$$

Hence, by inserting (2.5.13) into (2.5.12) we obtain

$$\sum_{i,j=1}^N \nabla_{\mathbf{p}_i}\cdot\left[\mathbf{\Gamma}_{ij}(\mathbf{r}^N)\nabla_{\mathbf{p}_j}\phi^N(\mathbf{r}^N,\mathbf{p}^N,t)\prod_{i=1}^N \exp\left(-\tfrac{|\hat{\mathbf{p}}_i|^2}{2}\right)\right] = 0.$$

By multiplying this equation by $-\log\phi^N$ and integrating we obtain

$$0 = -\int \mathrm{d}\mathbf{r}^N\,\mathrm{d}\mathbf{p}^N\,\log\phi^N(\mathbf{r}^N,\mathbf{p}^N,t)\sum_{i,j=1}^N \nabla_{\mathbf{p}_i}\cdot\left[\mathbf{\Gamma}_{ij}(\mathbf{r}^N)\nabla_{\mathbf{p}_j}\phi^N(\mathbf{r}^N,\mathbf{p}^N,t)\prod_{i=1}^N \exp\left(-\tfrac{|\hat{\mathbf{p}}_i|^2}{2}\right)\right].$$

Now, by interchanging the order of integration and summation and integrating by parts we obtain

$$0 = \sum_{i,j=1}^N \int \mathrm{d}\mathbf{r}^N\,\mathrm{d}\mathbf{p}^N\,\frac{\nabla_{\mathbf{p}_j}\phi^N(\mathbf{r}^N,\mathbf{p}^N,t)}{\phi^N(\mathbf{r}^N,\mathbf{p}^N,t)}\cdot\left[\mathbf{\Gamma}_{ij}(\mathbf{r}^N)\nabla_{\mathbf{p}_j}\phi^N(\mathbf{r}^N,\mathbf{p}^N,t)\prod_{i=1}^N \exp\left(-\tfrac{|\hat{\mathbf{p}}_i|^2}{2}\right)\right].$$

Now by the positive definiteness of $\mathbf{\Gamma}$ we have that there exists $\delta > 0$ such that

$$0 \geq \delta\sum_{i,j=1}^N \int \mathrm{d}\mathbf{r}^N\,\mathrm{d}\mathbf{p}^N\,\frac{|\nabla_{\mathbf{p}_j}\phi^N(\mathbf{r}^N,\mathbf{p}^N,t)|^2}{\phi^N(\mathbf{r}^N,\mathbf{p}^N,t)}\prod_{i=1}^N \exp\left(-\tfrac{|\hat{\mathbf{p}}_i|^2}{2}\right). \tag{2.5.14}$$

Since δ and the integrand in (2.5.14) are positive we must have

$$\int \mathrm{d}\mathbf{r}^N\,\mathrm{d}\mathbf{p}^N\,\frac{|\nabla_{\mathbf{p}_j}\phi^N(\mathbf{r}^N,\mathbf{p}^N,t)|^2}{\phi^N(\mathbf{r}^N,\mathbf{p}^N,t)}\prod_{i=1}^N \exp\left(-\tfrac{|\hat{\mathbf{p}}_i|^2}{2}\right) = 0,$$

and in particular

$$\frac{\nabla_{\mathbf{p}_j}\phi^N(\mathbf{r}^N,\mathbf{p}^N,t)|^2}{\phi^N(\mathbf{r}^N,\mathbf{p}^N,t)} = 0$$

for almost every $\mathbf{r}^N,\mathbf{p}^N$ in the phase space. Hence we have that $\phi^N = C\phi^N(\mathbf{r}^N,t)$ where C is a normalisation constant. Hence the proposition is proved. □

We now obtain the following steady sum rule for steady states of the system governed by (2.5.5), (2.5.6).

Lemma 2.5.6 (Steady Sum Rule)**.** *Given the adiabatic assumption* (B1)*, the system* (2.5.5), (2.5.6) *obeys the steady sum rule*

$$\varrho(\mathbf{r}_1)\nabla_{\mathbf{r}_1}\tfrac{\delta\mathscr{F}_{ex}}{\delta\varrho}[\varrho] = \sum_{n=2}^N \int \mathrm{d}\mathbf{r}^{N-1}\nabla_{\mathbf{r}_1}V_n(\mathbf{r}^n)\varrho^{(n)}(\mathbf{r}^n).$$

Proof. At steady flow, the one body phase space function is a Maxwell-–Boltzmann distribution centred at the solvent velocity

$$f^{(1)}(\mathbf{r}_1,\mathbf{p}) := \tfrac{\varrho(\mathbf{r}_1)}{(2\pi m k_B\mathrm{T})^{3/2}}\exp\left(-\tfrac{|\mathbf{p}-m\mathbf{u}(\mathbf{r}_1)|^2}{2mk_B\mathrm{T}}\right). \tag{2.5.15}$$

With this we see that as the momentum distribution equilibrates, the kinetic pressure term may be calculated by

$$\nabla_{\mathbf{r}_1}\cdot\int \mathrm{d}\mathbf{p}_1\,\tfrac{\mathbf{p}_1}{m}\otimes\tfrac{\mathbf{p}_1}{m}f^{(1)}(\mathbf{r}_1,\mathbf{p}_1) = \tfrac{k_B\mathrm{T}}{m}\nabla_{\mathbf{r}_1}\varrho(\mathbf{r}_1,t) + \nabla_{\mathbf{r}_1}\cdot\left[\varrho(\mathbf{r}_1,t)\mathbf{u}(\mathbf{r}_1)\otimes\mathbf{u}(\mathbf{r}_1)\right]. \tag{2.5.16}$$

Note that in steady state the density is being advected by $\mathbf{u}$, hence the equilibrium density in the inertial frame of reference is characterised by its material derivative being zero, that is $\mathrm{D}/(\mathrm{D}t)\varrho = 0$. All in all, and in steady state, using equations (2.5.15), (2.5.16), equation (2.5.6)

becomes

$$\partial_t \varrho(\mathbf{r}_1,t)\mathbf{u}(\mathbf{r}_1) + \tfrac{k_B\mathrm{T}}{m}\nabla_{\mathbf{r}_1}\varrho(\mathbf{r}_1,t) + \nabla_{\mathbf{r}_1}\cdot[\varrho(\mathbf{r}_1,t)\mathbf{u}(\mathbf{r}_1)\otimes\mathbf{u}(\mathbf{r}_1)] + \frac{1}{m}\varrho(\mathbf{r}_1,t)\nabla_{\mathbf{r}_1}V_1(\mathbf{r}_1,t) + \frac{1}{m}\sum_{n=2}^{N}\int \mathrm{d}\mathbf{r}^{n-1}\nabla_{\mathbf{r}_1}V_n(\mathbf{r}^n)\varrho^{(n)}(\mathbf{r}^n,t) = 0. \tag{2.5.17}$$

We observe the equality

$$\begin{aligned}\partial_t \varrho(\mathbf{r}_1,t)\mathbf{u}(\mathbf{r}_1) + \nabla_{\mathbf{r}_1}\cdot[\varrho(\mathbf{r}_1,t)\mathbf{u}(\mathbf{r}_1)\otimes\mathbf{u}(\mathbf{r}_1)] &= \partial_t\varrho\mathbf{u}(\mathbf{r}_1) + \mathbf{u}(\mathbf{r}_1)\nabla_{\mathbf{r}_1}\cdot(\varrho u) + \varrho(\mathbf{u}\cdot\nabla_{\mathbf{r}_1})\mathbf{u}\\ &= \mathbf{u}\left[\tfrac{\mathrm{D}\varrho}{\mathrm{D}t} + \varrho\nabla_{\mathbf{r}_1}\cdot\mathbf{u}\right] + \varrho(\mathbf{u}\cdot\nabla_{\mathbf{r}_1})\mathbf{u} = \varrho(\mathbf{u}\cdot\nabla_{\mathbf{r}_1})\mathbf{u}\end{aligned}$$

where we have used $\mathrm{D}\varrho/(\mathrm{D}t) = 0$ in steady state along with the incompressibility condition (C1). Therefore, we find equation (2.5.17) becomes

$$\varrho(\mathbf{u}\cdot\nabla_{\mathbf{r}_1})\mathbf{u} + \tfrac{k_B\mathrm{T}}{m}\nabla_{\mathbf{r}_1}\varrho(\mathbf{r}_1,t) + \frac{1}{m}\varrho(\mathbf{r}_1,t)\nabla_{\mathbf{r}_1}V_1(\mathbf{r}_1,t) + \frac{1}{m}\sum_{n=2}^{N}\int \mathrm{d}\mathbf{r}^{n-1}\nabla_{\mathbf{r}_1}V_n(\mathbf{r}^n)\varrho^{(n)}(\mathbf{r}^n,t) = 0. \tag{2.5.18}$$

Now by computing the gradient of the functional derivative of $\mathscr{F}_{\mathbf{u}}$ with respect to ϱ, the Euler-Lagrange equation for the equilibrium density is

$$0 = \frac{1}{m}\varrho\nabla_{\mathbf{r}_1}\frac{\delta\mathscr{F}_{\mathbf{u}}[\varrho]}{\delta\varrho} = \frac{k_B\mathrm{T}}{m}\nabla_{\mathbf{r}_1}\varrho + \frac{1}{m}\varrho\nabla_{\mathbf{r}_1}V_1 + \frac{1}{m}\varrho\nabla_{\mathbf{r}_1}\frac{\delta\mathscr{F}_{\mathrm{ex}}[\varrho]}{\delta\varrho} + \varrho(\mathbf{u}\cdot\nabla_{\mathbf{r}_1})\mathbf{u} \tag{2.5.19}$$

where we have used the vector identity

$$\nabla\left(\frac{1}{2}|\mathbf{u}|^2\right) = (\mathbf{u}\cdot\nabla)\mathbf{u} + \mathbf{u}\times(\nabla\times\mathbf{u}) = (\mathbf{u}\cdot\nabla)\mathbf{u}$$

since $\mathbf{u}$ is assumed to be irrotational by (C2). By subtracting (2.5.18) from (2.5.19) one obtains the steady sum rule

$$\varrho(\mathbf{r}_1)\nabla_{\mathbf{r}_1}\tfrac{\delta\mathscr{F}_{\mathrm{ex}}}{\delta\varrho}[\varrho] = \sum_{n=2}^{\mathrm{N}}\int \mathrm{d}\mathbf{r}^{N-1}\nabla_{\mathbf{r}_1}V_n(\mathbf{r}^n)\varrho^{(n)}(\mathbf{r}^n) \tag{2.5.20}$$

and the lemma is proved. □

Adiabatic Approximation

We now determine closed equations for the dynamics of the density $\varrho(\mathbf{r},t)$. It is assumed that the dynamic $\varrho^{(n)}(\mathbf{r}^n,t)$ as defined by (2.5.3) are well approximated by their counterpart n- body densities for an equilibrium fluid, i.e. that (2.5.20) holds out of steady state. This permits the particle interaction term involving the reduced phase space densities $\varrho^{(n)}(\mathbf{r}^n,t)$ appearing in (2.5.6) to be substituted with an expression of the free energy $\mathscr{F}_{\mathbf{u}}$. Using the definition of $\mathscr{F}_{\mathbf{u}}$ along with equations (2.5.6) and (2.5.20) gives

$$\partial_t\mathbf{j}(\mathbf{r}_1,t) + \boldsymbol{A}(\mathbf{r}_1,t) + \mathbf{u}(\mathbf{r}_1)(\mathbf{u}(\mathbf{r}_1)\cdot\nabla_{\mathbf{r}_1}\varrho(\mathbf{r}_1,t)) + \frac{1}{m}\varrho(\mathbf{r}_1,t)\nabla_{\mathbf{r}_1}\frac{\delta\mathscr{F}_{\mathbf{u}}[\varrho]}{\delta\varrho} + \gamma(\mathbf{j}(\mathbf{r}_1,t) - \varrho(\mathbf{r}_1,t)\mathbf{u}(\mathbf{r}_1)) + \frac{\gamma N}{m}\sum_{j=1}^{N}\int \mathrm{d}\mathbf{r}^{N-1}\,\mathrm{d}\mathbf{p}^N\,\tilde{\mathbf{\Gamma}}_{1j}(\mathbf{r}^N)(\mathbf{p}_j - m\mathbf{u}(\mathbf{r}_1))f^{(N)}(\mathbf{r}^N,\mathbf{p}^N,t) = 0 \tag{2.5.21}$$

where

$$\boldsymbol{A}(\mathbf{r}_1,t)=\nabla_{\mathbf{r}_1}\cdot\int \mathrm{d}\mathbf{p}_1\,\left(\tfrac{\mathbf{p}_1}{m}\otimes\tfrac{\mathbf{p}_1}{m}-\tfrac{k_B\mathrm{T}}{m}\mathbf{1}-\mathbf{u}\otimes\mathbf{u}\right)f^{(1)}(\mathbf{r}_1,\mathbf{p}_1,t).$$

Note that at equilibrium $\boldsymbol{A}$ is zero at steady state and the left hand side of (2.5.21) reduces to the Euler-Lagrange equation

$$\frac{1}{m}\varrho(\mathbf{r}_1,t)\nabla_{\mathbf{r}_1}\frac{\delta\mathscr{F}_{\mathbf{u}}[\varrho]}{\delta\varrho}=\frac{1}{m}\varrho(\mathbf{r}_1,t)\nabla_{\mathbf{r}_1}\frac{\delta\mathscr{F}[\varrho]}{\delta\varrho}+(\mathbf{u}\cdot\nabla)\mathbf{u}=0$$

where $\mathscr{F}_H$ is the usual Helmholtz free energy functional and we have used $\mathrm{D}\varrho/(\mathrm{D}t)=0$ in steady state. We now assume that the momenta of each colloid is distributed according to the Maxwell- Boltzmann distribution centred at the local velocity flow $\mathbf{v}(\mathbf{r}_1,t)$. It will be seen, in the following sections, that $\mathbf{v}(\mathbf{r}_1,t)\to\mathbf{u}(\mathbf{r}_1)$ as $t\to\infty$ which agrees with the natural principle that the colloids suspended in the background fluid are passively advected, and in the absence of external forces their velocity equals the local velocity of the surrounding fluid. We write

$$f^{(1)}(\mathbf{r}_1,\mathbf{p},t)=f^{(1)}_{\mathrm{neq}}(\mathbf{r}_1,\mathbf{p},t)+f^{(1)}_{\mathrm{le}}(\mathbf{r}_1,\mathbf{p},t)$$

where

$$f^{(1)}_{\mathrm{le}}(\mathbf{r}_1,\mathbf{p},t)=\tfrac{\varrho(\mathbf{r}_1,t)}{(2\pi mk_B\mathrm{T})^{3/2}}\exp\left(-\tfrac{|\mathbf{p}-m\mathbf{v}(\mathbf{r}_1,t)|^2}{2mk_B\mathrm{T}}\right).$$

and the first few moments of this distribution are

$$\int \mathrm{d}\mathbf{p}_1\, f^{(1)}_{\mathrm{le}}(\mathbf{r}_1,\mathbf{p},t)=\varrho(\mathbf{r}_1,t), \tag{2.5.22}$$

$$\int \mathrm{d}\mathbf{p}_1\,\mathbf{p}_1 f^{(1)}_{\mathrm{le}}(\mathbf{r}_1,\mathbf{p},t)=m\varrho(\mathbf{r}_1,t)\mathbf{v}(\mathbf{r}_1,t),$$

$$\int \mathrm{d}\mathbf{p}_1\,|\mathbf{p}_1-m\mathbf{v}(\mathbf{r}_1,t)|^2 f^{(1)}_{\mathrm{le}}(\mathbf{r}_1,\mathbf{p},t)$$

$$=mk_B\mathrm{T}\varrho(\mathbf{r}_1,t). \tag{2.5.23}$$

Next we impose the natural integral restrictions on $f^{(1)}_{\mathrm{neq}}$, since f^1_{le} determines the correct first three moments (2.5.22)-(2.5.23)

$$\int \mathrm{d}\mathbf{p}_1\, f^{(1)}_{\mathrm{neq}}(\mathbf{r}_1,\mathbf{p},t)=0,$$

$$\int \mathrm{d}\mathbf{p}_1\,\mathbf{p}_1 f^{(1)}_{\mathrm{neq}}(\mathbf{r}_1,\mathbf{p},t)=0,$$

$$\int \mathrm{d}\mathbf{p}_1\,|\mathbf{p}_1-m\mathbf{v}(\mathbf{r}_1,t)|^2 f^{(1)}_{\mathrm{neq}}(\mathbf{r}_1,\mathbf{p},t)=0. \tag{2.5.24}$$

By equations (2.5.22)-(2.5.24) we may compute $\mathbf{A}(\mathbf{r}_1,t)$ explicitly

$$\begin{aligned}\boldsymbol{A}(\mathbf{r}_1,t)&=\nabla_{\mathbf{r}_1}\cdot\int \mathrm{d}\mathbf{p}_1\,\left(\tfrac{\mathbf{p}_1\otimes\mathbf{p}_1}{m^2}-\tfrac{k_B\mathrm{T}}{m}\mathbf{1}-\mathbf{u}\otimes\mathbf{u}\right)\left[f^{(1)}_{\mathrm{le}}(\mathbf{r}_1,\mathbf{p}_1,t)+f^{(1)}_{\mathrm{neq}}(\mathbf{r}_1,\mathbf{p}_1,t)\right]\\
&=\nabla_{\mathbf{r}_1}\cdot\int \mathrm{d}\mathbf{p}_1\,\left(\tfrac{\mathbf{p}_1\otimes\mathbf{p}_1}{m^2}-\tfrac{k_B\mathrm{T}}{m}\mathbf{1}-\mathbf{u}\otimes\mathbf{u}\right)\tfrac{\varrho(\mathbf{r}_1,t)}{(2\pi mk_B\mathrm{T})^{3/2}}\exp\left(-\tfrac{|\mathbf{p}-m\mathbf{v}(\mathbf{r}_1,t)|^2}{2mk_B\mathrm{T}}\right)\\
&\quad+\nabla_{\mathbf{r}_1}\cdot\int \mathrm{d}\mathbf{p}_1\,\tfrac{\mathbf{p}_1\otimes\mathbf{p}_1}{m^2}f^{(1)}_{\mathrm{neq}}(\mathbf{r}_1,\mathbf{p}_1,t)\\
&=\nabla_{\mathbf{r}_1}\cdot[\varrho(\mathbf{r}_1,t)\mathbf{v}(\mathbf{r}_1,t)\otimes\mathbf{v}(\mathbf{r}_1,t))]-\nabla_{\mathbf{r}_1}\cdot[\varrho(\mathbf{r}_1,t)\mathbf{u}(\mathbf{r}_1,t)\otimes\mathbf{u}(\mathbf{r}_1,t))]\\
&\quad+\nabla_{\mathbf{r}_1}\cdot\int \mathrm{d}\mathbf{p}_1\,\tfrac{\mathbf{p}_1\otimes\mathbf{p}_1}{m^2}f^{(1)}_{\mathrm{neq}}(\mathbf{r}_1,\mathbf{p}_1,t).\end{aligned} \tag{2.5.25}$$

We insert the expression for $\mathbf{A}(\mathbf{r}_1, t)$ in (2.5.25) into (2.5.21) to obtain

$$\begin{aligned}
&\partial_t \left[\varrho(\mathbf{r}_1,t)\mathbf{v}(\mathbf{r}_1,t)\right] + \nabla_{\mathbf{r}_1}\cdot\left[\varrho(\mathbf{r}_1,t)\mathbf{v}(\mathbf{r}_1,t)\otimes\mathbf{v}(\mathbf{r}_1,t)\right] \\
&\quad + \nabla_{\mathbf{r}_1}\cdot\int \mathrm{d}\mathbf{p}_1\, \tfrac{\mathbf{p}_1\otimes\mathbf{p}_1}{m^2} f^{(1)}_{\mathrm{neq}}(\mathbf{r}_1,\mathbf{p}_1,t) \\
&\quad + \frac{1}{m}\varrho(\mathbf{r}_1,t)\nabla_{\mathbf{r}_1}\tfrac{\delta\mathscr{F}[\varrho]}{\delta\varrho} + \gamma\varrho(\mathbf{r}_1,t)(\mathbf{v}(\mathbf{r}_1,t)-\mathbf{u}(\mathbf{r}_1)) \\
&\quad + \frac{\gamma N}{m}\sum_{j=1}^{N}\int \mathrm{d}\mathbf{r}^{N-1}\,\mathrm{d}\mathbf{p}^N\,\tilde{\mathbf{\Gamma}}_{1j}(\mathbf{r}^N)(\mathbf{p}_j - m\mathbf{u}(\mathbf{r}_j))f^{(N)}(\mathbf{r}^N,\mathbf{p}^N,t) = 0
\end{aligned} \tag{2.5.26}$$

where we have now reintroduced the usual Helmholtz free energy functional $\mathscr{F}_{\mathbf{u}}$ to consolidate the number of terms. We neglect the f_{neq} term, since it may be shown to be small, at least in the overdamped limit $\gamma \to \infty$, by use of adiabatic elimination process that is based on multiscale analysis [63]. It now remains to simplify the HI term in equation (2.5.26), for this we require additional assumptions on the form of the HI, particularly that the interactions are two body and the two particle distribution function $f^{(2)}$ is expressed in terms of a pairwise correlation function.

Assumptions D

- The HI are assumed to be two body

$$\tilde{\mathbf{\Gamma}}_{ij}(\mathbf{r}^N) = \delta_{ij}\sum_{l\neq i}\boldsymbol{Z}_1(\mathbf{r}_i,\mathbf{r}_l) + (1-\delta_{ij})\boldsymbol{Z}_2(\mathbf{r}_i,\mathbf{r}_j). \tag{D1}$$

  where $\boldsymbol{Z}_1$, $\boldsymbol{Z}_2$ are the diagonal and off diagonal blocks respectively of the translational component of the grand resistance matrix $\boldsymbol{R}$ originating in the classical theory of low Reynolds' number hydrodynamics between suspended particles [92], [75].

- The Kirkwood approximation is used

$$f^{(2)}(\mathbf{r}_1,\mathbf{r}_2,\mathbf{p}_1,\mathbf{p}_2,t) = f^{(1)}(\mathbf{r}_1,\mathbf{p}_1,t)f^{(1)}(\mathbf{r}_2,\mathbf{p}_2,t)g(\mathbf{r}_1,\mathbf{r}_2,[\varrho]) \tag{D2}$$

  where $g(\mathbf{r}_1,\mathbf{r}_2,[\varrho])$ is the two body correlation function.

The two body assumption (D1) is reasonable for many scenarios, particularly, one finds that the pairwise lubrication forces dominate in concentrated systems [19]. The Kirkwood assumption is a standard one for the closure of BBGKY type hierarchies and requires a form correlation function g, which ultimately must be estimated from the microscopic dynamics. There are however good candidates, such as for a hard sphere fluid: $g(|\mathbf{r}-\mathbf{r}'|) = 0$ for $|\mathbf{r}-\mathbf{r}'| < \sigma$ where σ is a sphere diameter, and $g = 1$ otherwise, which has been shown to be accurate where comparison with the results of Brownian dynamics simulations has been made.

With the assumptions (D1), (2.5) we may simplify the HI summation in equation (2.5.26). We obtain

$$\begin{aligned}
&\frac{\gamma N}{m}\sum_{j=1}^{N}\int \mathrm{d}\mathbf{r}^{N-1}\,\mathrm{d}\mathbf{p}^N\,\tilde{\mathbf{\Gamma}}_{1j}(\mathbf{r}^N)(\mathbf{p}_j - m\mathbf{u}(\mathbf{r}_j))f^{(N)}(\mathbf{r}^N,\mathbf{p}^N,t) \\
&= \frac{\gamma N}{m}\sum_{j=1}^{N}\int \mathrm{d}\mathbf{r}^{N-1}\,\mathrm{d}\mathbf{p}^N\,\left[\delta_{1j}\sum_{l\neq 1}\boldsymbol{Z}_1(\mathbf{r}_1,\mathbf{r}_l) + (1-\delta_{1j})\boldsymbol{Z}_2(\mathbf{r}_i,\mathbf{r}_j)\right] \\
&\quad \times (\mathbf{p}_j - m\mathbf{u}(\mathbf{r}_j))f^{(N)}(\mathbf{r}^N,\mathbf{p}^N,t) \\
&= \gamma\varrho(\mathbf{r}_1,t)\int \mathrm{d}\mathbf{r}_2\,\left[\boldsymbol{Z}_1(\mathbf{r}_1,\mathbf{r}_2)(\mathbf{v}(\mathbf{r}_1,t)-\mathbf{u}(\mathbf{r}_1)) + \boldsymbol{Z}_2(\mathbf{r}_1,\mathbf{r}_2)(\mathbf{v}(\mathbf{r}_2,t)-\mathbf{u}(\mathbf{r}_2))\right] \\
&\quad \times \varrho(\mathbf{r}_2,t)g(\mathbf{r}_1,\mathbf{r}_2,[\varrho])
\end{aligned}$$

where we have used the Enskog approximation (2.5) and the definition of the reduced phase space density (2.5.3).

2.6 Equations Of Motion

We summarise the equations of motion for inertial, driven DDFT including HI given by the coupled pair of nonlinear nonlocal PDEs for the one body density $\varrho(\mathbf{r}_1,t)$ and velocity $\mathbf{v}(\mathbf{r}_1,t)$

$$\begin{cases} \partial_t\varrho(\mathbf{r}_1,t)+\nabla_{\mathbf{r}_1}\cdot(\varrho(\mathbf{r}_1,t)\mathbf{v}(\mathbf{r}_1,t))=0, \\ \partial_t\mathbf{v}(\mathbf{r}_1,t)+(\mathbf{v}(\mathbf{r}_1,t)\cdot\nabla_{\mathbf{r}_1})\mathbf{v}(\mathbf{r}_1,t)+\frac{1}{m}\nabla_{\mathbf{r}_1}\frac{\delta\mathscr{F}_{\mathbf{u}}[\varrho]}{\delta\varrho}(\mathbf{r}_1,t)+\gamma\mathbf{w}(\mathbf{r}_1,t) \\ \quad+\gamma\int\mathrm{d}\mathbf{r}_2\,[\boldsymbol{Z}_1(\mathbf{r}_1,\mathbf{r}_2)\mathbf{w}(\mathbf{r}_1,t)+\boldsymbol{Z}_2(\mathbf{r}_1,\mathbf{r}_2)\mathbf{w}(\mathbf{r}_2,t)]\times\varrho(\mathbf{r}_2,t)g(\mathbf{r}_1,\mathbf{r}_2,[\varrho])=0, \end{cases} \tag{2.6.1}$$

subject to the steady flow condition

$$\tfrac{1}{m}\nabla_{\mathbf{r}_1}\frac{\delta\mathscr{F}_{\mathbf{u}}[\varrho]}{\delta\varrho}(\mathbf{r}_1)=0\quad\text{as}\quad t\to\infty. \tag{2.6.2}$$

where $\mathbf{w}(\mathbf{r}_1,t)=\mathbf{v}(\mathbf{r}_1,t)-\mathbf{u}(\mathbf{r}_1)$. The system (2.6.1) governs the conservation of mass and momentum respectively of the colloidal system coupled to the background flow.

Boundary Conditions

When the physical domain is the whole real space we impose both $\varrho(\mathbf{r}_1,t)$, $\mathbf{v}(\mathbf{r}_1,t)\to 0$ as $|\mathbf{r}_1|\to\infty$. This will be ensured, for example, by letting the confining potential V_1 grow at least linearly at infinity. For bounded domains, for example a confining channel, we impose

$$\mathbf{v}(\mathbf{r}_1,t)\cdot\mathbf{n}\big|_{\text{wall}}=0$$

where $\mathbf{n}$ is the unit normal vector pointing out of the fluid domain from the channel wall. For the channel ends at $\pm\infty$, both $\varrho(\mathbf{r}_1,t)$, $\mathbf{v}(\mathbf{r}_1,t)$ vanish. Observe that $\mathbf{v}\to\mathbf{u}$ as $t\to\infty$. Note that upon substituting $\mathbf{u}=0$ one recovers previously studied DDFT [62] including inertia and HI.

2.7 Heuristic Limits

In this section we consider formal limits of the equations of motion. We begin with the overdamped limit $\gamma\to\infty$.

Overdamped Limit

After the solvent has been flowing for a sufficiently long time, the average acceleration of the colloids should equal the local acceleration of the bath and no average acceleration in the reference frame moving with $\mathbf{u}$ should take place. By enforcing the average acceleration of the colloidal system equal to the bath's material acceleration, that is $\mathrm{D}\mathbf{v}/(\mathrm{D}t)=\mathrm{D}\mathbf{u}/(\mathrm{D}t)$, the momentum equation in (2.6.1) becomes

$$\begin{aligned}&\tfrac{1}{m}\nabla_{\mathbf{r}_1}\frac{\delta\mathscr{F}_{\mathbf{u}}[\varrho]}{\delta\varrho}(\mathbf{r}_1,t)+\gamma(\mathbf{v}(\mathbf{r}_1,t)-\mathbf{u}(\mathbf{r}_1))+\gamma\int\mathrm{d}\mathbf{r}_2\,[\boldsymbol{Z}_1(\mathbf{r}_1,\mathbf{r}_2)(\mathbf{v}(\mathbf{r}_1,t)-\mathbf{u}(\mathbf{r}_1))\\&\quad+\boldsymbol{Z}_2(\mathbf{r}_1,\mathbf{r}_2)(\mathbf{v}(\mathbf{r}_2,t)-\mathbf{u}(\mathbf{r}_2))]\times\varrho(\mathbf{r}_2,t)g(\mathbf{r}_1,\mathbf{r}_2,[\varrho])=0.\end{aligned}$$

Now assuming that inter particle HI are weak that is $\boldsymbol{Z}_2\approx 0$ we obtain

$$\tfrac{1}{m}\nabla_{\mathbf{r}_1}\frac{\delta\mathscr{F}_{\mathbf{u}}[\varrho]}{\delta\varrho}(\mathbf{r}_1,t)+\gamma\boldsymbol{D}^{-1}(\mathbf{r}_1,[\varrho],t)(\mathbf{v}(\mathbf{r}_1,t)-\mathbf{u}(\mathbf{r}_1))=0. \tag{2.7.1}$$

where $\boldsymbol{D}$ is the diffusion tensor, known rigorously to be positive definite and therefore invertible and is given by

$$\boldsymbol{D}(\mathbf{r}_1,[\varrho],t) := \left[\mathbf{1} + \int \mathrm{d}\mathbf{r}_2\, \boldsymbol{Z}_1(\mathbf{r}_1,\mathbf{r}_2)\varrho(\mathbf{r}_2,t)g(\mathbf{r}_1,\mathbf{r}_2,[\varrho])\right]^{-1}.$$

Now by adding zero to the conservation of mass equation:

$$\partial_t \varrho + \nabla_{\mathbf{r}_1}\cdot(\varrho(\mathbf{v}-\mathbf{u}) + \varrho\mathbf{u}) = 0, \tag{2.7.2}$$

by combining (2.7.1) and (2.7.2) we obtain

$$\partial_t\varrho(\mathbf{r}_1,t) + \nabla_{\mathbf{r}_1}\cdot(\varrho(\mathbf{r}_1,t)\mathbf{u}(\mathbf{r}_1,t)) = \frac{1}{m\gamma}\nabla_{\mathbf{r}_1}\cdot\left(\varrho(\mathbf{r}_1,t)\boldsymbol{D}(\mathbf{r}_1,[\varrho])\nabla_{\mathbf{r}_1}\frac{\delta\mathscr{F}_{\mathbf{u}}[\varrho]}{\delta\varrho}\right) \tag{2.7.3}$$

which may be compared with the DDFT in equation [27] of [145]. Equation (2.7.3) is the Smoluchowski equation, differing to the one found in [145] and other formalisms starting from Brownian dynamics, by the definition of the free energy functional since $\mathscr{F}_{\mathbf{u}}$ includes the kinetic energy of the density in the solvent. We may however show that this contribution is small as $\gamma\to\infty$, in particular by expanding out the right hand side, (2.7.3) becomes

$$\begin{aligned}&\partial_t\varrho(\mathbf{r}_1,t) + \nabla_{\mathbf{r}_1}\cdot(\varrho(\mathbf{r}_1,t)\mathbf{u}(\mathbf{r}_1,t))\\ &\quad= \frac{1}{m\gamma}\nabla_{\mathbf{r}_1}\cdot\left(\varrho(\mathbf{r}_1,t)\boldsymbol{D}(\mathbf{r}_1,[\varrho])\nabla_{\mathbf{r}_1}\frac{\delta\mathscr{F}_H[\varrho]}{\delta\varrho}\right) + \frac{1}{m\gamma}\nabla_{\mathbf{r}_1}\cdot\left[m\left(\mathbf{u}\cdot\nabla_{\mathbf{r}_1}\right)\mathbf{u}\right]\end{aligned}$$

Now by nondimensionalising

$$\mathbf{r}_1 \sim L\tilde{\mathbf{r}}_1,\quad t\sim\tau\tilde{t},\quad \varrho\sim\tfrac{1}{L^3}\tilde{\varrho},\quad \mathbf{u}\sim U\tilde{\mathbf{u}},\quad \mathscr{F}_H\sim k_B\mathrm{T}\tilde{\mathscr{F}}_H,\quad U=\tfrac{L}{\tau}$$

we obtain (after dropping circumflexes)

$$\begin{aligned}&\partial_t\varrho(\mathbf{r}_1,t) + \nabla_{\mathbf{r}_1}\cdot(\varrho(\mathbf{r}_1,t)\mathbf{u}(\mathbf{r}_1,t))\\ &\quad= \frac{k_B\mathrm{T}\tau}{m\gamma L^2}\nabla_{\mathbf{r}_1}\cdot\left(\varrho(\mathbf{r}_1,t)\boldsymbol{D}(\mathbf{r}_1,[\varrho])\nabla_{\mathbf{r}_1}\frac{\delta\mathscr{F}_H[\varrho]}{\delta\varrho}\right) + \frac{\tau U^2}{m\gamma L^2}\nabla_{\mathbf{r}_1}\cdot\left[m\left(\mathbf{u}\cdot\nabla_{\mathbf{r}_1}\right)\mathbf{u}\right]\end{aligned} \tag{2.7.4}$$

Now using the friction coefficient defined by $\gamma = 6\pi\mu r m^{-1}$ where μ is the dynamic viscosity of the solvent and r is a typical colloid radius we observe that

$$\begin{aligned}\frac{\tau U^2}{m\gamma L^2}\nabla_{\mathbf{r}_1}\cdot(m(\mathbf{u}\cdot\nabla_{\mathbf{r}_1}\mathbf{u})) &= \frac{\tau U^2}{6\pi\mu r L^2}\nabla_{\mathbf{r}_1}\cdot(m(\mathbf{u}\cdot\nabla_{\mathbf{r}_1}\mathbf{u}))\\ &= \frac{U\Phi L}{6\pi\mu}\nabla_{\mathbf{r}_1}\cdot((\mathbf{u}\cdot\nabla_{\mathbf{r}_1}\mathbf{u})) = \frac{Re}{6\pi}\nabla_{\mathbf{r}_1}\cdot\left[(\mathbf{u}\cdot\nabla_{\mathbf{r}_1})\,\mathbf{u}\right]\end{aligned}$$

where Re is Reynolds number and we have defined the characteristic density scale $\Phi = m/(L^2 r)$. All in all the dimensionless Smoluchowski equation (2.7.4) becomes

$$\partial_t\varrho(\mathbf{r}_1,t) + \nabla_{\mathbf{r}_1}\cdot(\varrho(\mathbf{r}_1,t)\mathbf{u}(\mathbf{r}_1,t)) = Fr^{-1}\nabla_{\mathbf{r}_1}\cdot\left(\varrho(\mathbf{r}_1,t)\boldsymbol{D}(\mathbf{r}_1,[\varrho])\nabla_{\mathbf{r}_1}\frac{\delta\mathscr{F}_H[\varrho]}{\delta\varrho}\right) + O(Re)$$

as $\gamma\to\infty$ where we have defined the Froude number

$$Fr = \frac{m\gamma^2L^2}{k_B\mathrm{T}},$$

kept $Fr = O(1)$, and used the viscous time scale $\tau = \gamma^{-1}$. Hence we have recovered the known driven overdamped DDFT up to errors of order $O(Re)$ which are small and ever vanishing as $\gamma\to\infty$ (equivalently $\mu\to\infty$).

Inviscid Limit

Taking the inviscid limit $\gamma \to 0$ of equations (2.6.1), we obtain Euler idealised equations

$$\begin{cases} \partial_t \varrho(\mathbf{r}_1,t) + \nabla_{\mathbf{r}_1} \cdot (\varrho(\mathbf{r}_1,t)\mathbf{v}(\mathbf{r}_1,t)) = 0, \\ \partial_t \mathbf{v}(\mathbf{r}_1,t) + (\mathbf{v}(\mathbf{r}_1,t)\cdot\nabla_{\mathbf{r}_1})\mathbf{v}(\mathbf{r}_1,t) + \frac{1}{m}\nabla_{\mathbf{r}_1}\frac{\delta \mathscr{F}_{\mathbf{u}}[\varrho]}{\delta \varrho}(\mathbf{r}_1,t) = 0, \end{cases} \tag{2.7.5}$$

subject to the steady flow condition

$$\tfrac{1}{m}\nabla_{\mathbf{r}_1}\frac{\delta \mathscr{F}_{\mathbf{u}}[\varrho]}{\delta \varrho}(\mathbf{r}_1) = 0 \quad \text{as} \quad t \to \infty.$$

While the inviscid limit taken here formally correct, the assumptions used to determine the DDFT (2.6.1), particularly the local to steady flow approximation on the Maxwell-Boltzmann distribution rely on the friction of the bath to provide viscous resistance to the colloids. It is therefore unclear whether equations (2.7.5) would give good agreement to molecular dynamics simulations for inviscid colloidal flow. This should be compared with, for example, the classical singular perturbation problem for high Reynolds flows on the classical Navier-Stokes equations. We note that equations (2.7.5) agree with those found in [7] after setting $\mathbf{u} = 0$.

2.8 Bernoulli's Principle For The Density

We now relax the assumption that the solvent velocity $\mathbf{u}$ is irrotational to determine a Bernoulli principle for the colloid flow. Recall that for an incompressible fluid with constant density ρ, the total head is constant along the streamlines of steady flow

$$\frac{p}{\rho} + \frac{1}{2}|\mathbf{u}|^2 + \chi = c_0$$

where p is the pressure and χ is an external field and $c_0 \in \mathbb{R}$. We will derive an analogous result for the advected density ϱ solving (2.6.1).

The derivation of the following DDFT is much the same as in Section 2.5 however the Euler-Lagrange equation now contains the rotational contribution from the flowing solvent, in particular by using the definition of $\mathscr{F}_{\mathbf{u}}$ in (2.5.9), equation (2.5.19) now becomes

$$\begin{aligned} 0 &= \frac{1}{m}\varrho\nabla_{\mathbf{r}_1}\frac{\delta \mathscr{F}_{\mathbf{u}}[\varrho]}{\delta \varrho} \\ &= \frac{k_B\mathrm{T}}{m}\nabla_{\mathbf{r}_1}\varrho + \frac{1}{m}\varrho\nabla_{\mathbf{r}_1}V_1 + \frac{1}{m}\varrho\nabla_{\mathbf{r}_1}\frac{\delta \mathscr{F}_{\mathrm{ex}}[\varrho]}{\delta \varrho} + (\mathbf{u}\cdot\nabla)\mathbf{u} + \mathbf{u}\times\nabla_{\mathbf{r}_1}\times\mathbf{u}. \end{aligned}$$

It will be seen that despite the relaxation to permit rotational solvents the steady sum rule still holds along curves that are tangent to $\mathbf{u}$, in particular the Euler-Lagrange equation for the steady density along streamlines of the flowing solvent is

$$\begin{aligned} 0 &= \frac{1}{m}\mathbf{u}\cdot\varrho\nabla_{\mathbf{r}_1}\frac{\delta \mathscr{F}_{\mathbf{u}}[\varrho]}{\delta \varrho} \\ &= \frac{k_B\mathrm{T}}{m}\mathbf{u}\cdot\nabla_{\mathbf{r}_1}\varrho + \frac{1}{m}\varrho\mathbf{u}\cdot\nabla_{\mathbf{r}_1}V_1 + \frac{1}{m}\varrho\mathbf{u}\cdot\nabla_{\mathbf{r}_1}\frac{\delta \mathscr{F}_{\mathrm{ex}}[\varrho]}{\delta \varrho} + \mathbf{u}\cdot((\mathbf{u}\cdot\nabla)\mathbf{u}) \end{aligned} \tag{2.8.1}$$

where we have used the fact that $\mathbf{u}\cdot(\mathbf{u}\times\nabla_{\mathbf{r}_1}\times\mathbf{u}) \equiv 0$ since it is a triple scalar product with two repeated entries. By taking the inner product of equation (2.5.18) with $\mathbf{u}$ and subtracting equation (2.8.1) we obtain the streamwise steady sum rule

$$\varrho(\mathbf{r}_1)\mathbf{u}\cdot\nabla_{\mathbf{r}_1}\tfrac{\delta \mathscr{F}_{\mathrm{ex}}}{\delta \varrho}[\varrho] = \mathbf{u}\cdot\sum_{n=2}^{\mathrm{N}}\int \mathrm{d}\mathbf{r}^{N-1}\nabla_{\mathbf{r}_1}V_n(\mathbf{r}^n)\varrho^{(n)}(\mathbf{r}^n).$$

The derivation of the DDFT follows the same procedure from equation (2.5.21) onwards, but now performing all calculations along the streamlines of $\mathbf{u}$. All in all the dynamical momentum equation is preserved when projected onto $\mathbf{u}$ and reads:

$$\begin{aligned}\mathbf{u}\cdot\Big\{&\partial_t\mathbf{v}(\mathbf{r}_1,t)+(\mathbf{v}(\mathbf{r}_1,t)\cdot\nabla_{\mathbf{r}_1})\mathbf{v}(\mathbf{r}_1,t)+\tfrac{1}{m}\nabla_{\mathbf{r}_1}\frac{\delta\mathscr{F}_H[\varrho]}{\delta\varrho}(\mathbf{r}_1,t)\\&+\gamma(\mathbf{v}(\mathbf{r}_1,t)-\mathbf{u}(\mathbf{r}_1))+\gamma\int\mathrm{d}\mathbf{r}_2\,[\boldsymbol{Z}_1(\mathbf{r}_1,\mathbf{r}_2)(\mathbf{v}(\mathbf{r}_1,t)-\mathbf{u}(\mathbf{r}_1))\\&+\boldsymbol{Z}_2(\mathbf{r}_1,\mathbf{r}_2)(\mathbf{v}(\mathbf{r}_2,t)-\mathbf{u}(\mathbf{r}_2))]\times\varrho(\mathbf{r}_2,t)g(\mathbf{r}_1,\mathbf{r}_2,[\varrho])\Big\}=0,\end{aligned}\tag{2.8.2}$$

which converges to, at steady state

$$\mathbf{u}\cdot\Big\{\tfrac{1}{m}\nabla_{\mathbf{r}_1}\frac{\delta\mathscr{F}_H[\varrho]}{\delta\varrho}(\mathbf{r}_1)+(\mathbf{u}\cdot\nabla)\mathbf{u}\Big\}=0\quad\text{ as }\quad t\to\infty.$$

We now examine the steady equation in (2.8.2). First by writing $(\mathbf{u}\cdot\nabla)\mathbf{u}=\nabla_{\mathbf{r}_1}\left(\frac{1}{2}|\mathbf{u}|^2\right)+(\nabla\times\mathbf{u})\times\mathbf{u}$ and expanding out the free energy term we obtain

$$\mathbf{u}\cdot\Big\{\frac{k_B\mathrm{T}}{m}\frac{\nabla_{\mathbf{r}_1}\varrho}{\varrho}+\frac{1}{m}\nabla_{\mathbf{r}_1}V_1+\frac{1}{m}\nabla_{\mathbf{r}_1}\frac{\delta\mathscr{F}_{\mathrm{ex}}[\varrho]}{\delta\varrho}+\nabla_{\mathbf{r}_1}\left(\tfrac{1}{2}|\mathbf{u}|^2\right)+(\nabla\times\mathbf{u})\times\mathbf{u}\Big\}=0.$$

Now by carrying through the inner product and once again using the fact that $(\nabla\times\mathbf{u})\times\mathbf{u}$ is perpendicular to $\mathbf{u}$ we obtain

$$\mathbf{u}\cdot\Big\{\nabla_{\mathbf{r}_1}\left(\tfrac{1}{2}|\mathbf{u}|^2\right)+\frac{1}{m}\nabla_{\mathbf{r}_1}V_1+\frac{1}{m}\nabla_{\mathbf{r}_1}\frac{\delta\mathscr{F}_{\mathrm{ex}}[\varrho]}{\delta\varrho}\Big\}=-\frac{k_B\mathrm{T}}{m}\mathbf{u}\cdot\frac{\nabla_{\mathbf{r}_1}\varrho}{\varrho}.\tag{2.8.3}$$

Now along a streamline of $\mathbf{u}$, and since $\mathbf{u}$ is incompressible, the conservation of mass gives $\mathbf{u}\cdot\nabla_{\mathbf{r}_1}\varrho=0$ therefore (2.8.3) becomes

$$\mathbf{u}\cdot\nabla_{\mathbf{r}_1}\Big\{\tfrac{1}{2}|\mathbf{u}|^2+\frac{1}{m}V_1+\frac{1}{m}\frac{\delta\mathscr{F}_{\mathrm{ex}}[\varrho]}{\delta\varrho}\Big\}=0$$

and we determine the Bernoulli principle that the total head

$$\tfrac{1}{2}|\mathbf{u}|^2+\frac{1}{m}V_1+\frac{1}{m}\frac{\delta\mathscr{F}_{\mathrm{ex}}[\varrho]}{\delta\varrho}=c_0$$

remains constant along a streamline of $\mathbf{u}$, for some fixed $c_0\in(-\infty,\infty)$. The first term is the dynamic pressure of the density, the second is analogous to the hydraulic head of the density confined to an external field and the third is the static pressure of the inhomogeneous mixture.

Chapter 3

Microhydrodynamics 1: Spheres Converging Along Their Line Of Centres

3.1 Introduction

For the normal component of the HI, we study exact solutions for the slow viscous flow of an infinite liquid caused by two rigid spheres approaching each either along their line of centres, valid at all separations. This goes beyond the applicable range of existing solutions for singular hydrodynamic interactions (HIs) which, for practical applications, are limited to the near-contact or far field region of the flow. By use of a bipolar coordinate system, we derive the stream function for the flow as $Re \to 0$, and a formula for the singular (squeeze) force between the spheres as an infinite series. We also obtain, in Appendix A.1, the asymptotic behaviour of the forces as the nondimensional separation between the spheres goes to zero and infinity, rigorously confirming and improving upon known results relevant to a widely accepted lubrication theory. Additionally, in Appendix A.2, we recover the force on a sphere moving perpendicularly to a plane as a special case. All results hold for retreating spheres, consistent with the reversibility of Stokes flow.

In this chapter we also give the first quantitative comparison, for this particular two-sphere interaction, between the present solution obtained by spherical bipolar methods and the ones obtained by the perturbative and multipole methods [98], [92]. As a result, we are able to highlight the analytical and practical strengths of the present work.

3.2 Organisation Of The Chapter

This chapter presents the rigorous derivation of the singular scalar resistance function $a(\cdot)$, valid for all non-contacting particle separations. We relegate the asymptotic analysis of $a(\cdot)$ to Appendix A.1 in which we derive rigorous small and large argument, as well as showing agreement with the perpendicular motion of a sphere and plane. In Section 3.3 we provide the definition of the bipolar coordinate system. Following this, in Section 3.4 we present the steady flow equations and in Section 3.4.1 we transform them into spherical bipolar coordinates. Section 3.5 defines the Stokes equations for the normal interaction, Section 3.6 details the derivation of the stream functions and in Section 3.7 we calculate the scalar resistance function, $a(\cdot)$, as an infinite series. Finally, in Section 3.8, we compare our results for $a(\cdot)$ to the widely used expressions determined by the method of multipole expansions.

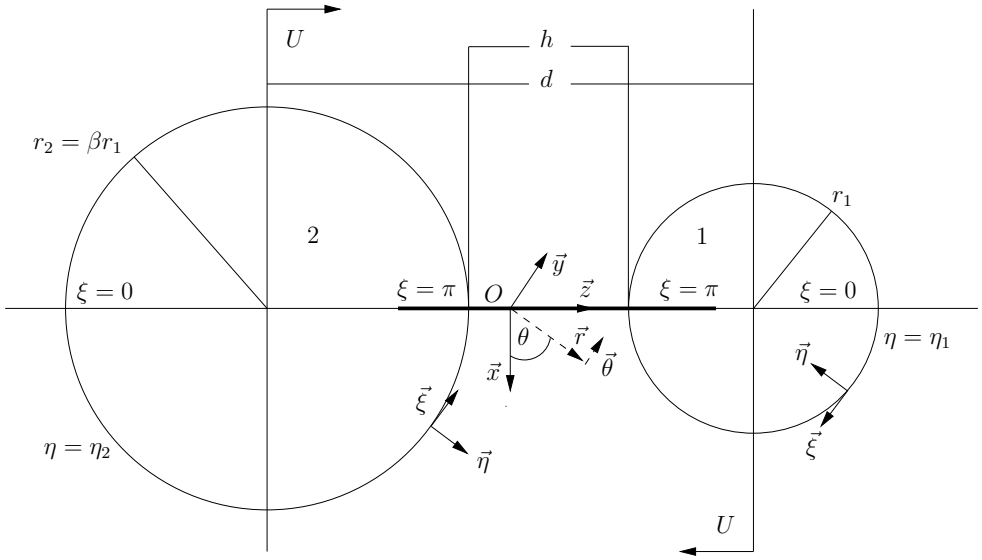

Figure 3.1: Schematic of two unequal spheres of radii r_1, r_2 converging along their line of centres in viscous fluid. Included in the diagram are the cylindrical and bipolar unit vectors, the dimensional gap distance h, and centre to centre distance d. Note that η_1 and η_2 are implicit functions of r_1, r_2 and d.

3.3 Spherical Bipolar Coordinates

The spherical bipolar coordinate system is a convenient setting in which to apply the boundary conditions on both spheres. The coordinate transformation from cylindrical coordinates $\mathfrak{r} = (r,\, z,\, \theta)$ to spherical bipolar coordinates $\mathfrak{q} = (\eta,\, \xi,\, \theta)$ is

$$z + ir = ic \cot \tfrac{1}{2}(\xi + i\eta) \tag{3.3.1}$$

where θ remains unchanged and $i = \sqrt{-1}$. The parameter $c > 0$ is a geometrical constant determining the foci of the two spheres, which, for equal spheres, in the x–z plane are at $(-c, 0)$ and $(c, 0)$. Note that c is not chosen but is a function of the sphere centre distance d. Every point in $(r,\, z)$ space is represented uniquely in (η, ξ) space, so long as $\xi \in [0, \pi]$, $-\infty < \eta < \infty$, $\theta \in [0, 2\pi)$. Expanding the cotangent and equating real and imaginary parts one obtains

$$z = z(\eta, \xi) = c\frac{\sinh \eta}{\cosh \eta - \cos \xi}, \quad r = r(\eta, \xi) = c\frac{\sin \xi}{\cosh \eta - \cos \xi}. \tag{3.3.2}$$

The foci of the spheres drawn by the set of Cartesian coordinates (z, r) are at $(-c, 0)$ and $(c, 0)$. Finally, the constant c is superfluous and the derived quantities of drag and stress do not depend on it.

There is a one to one correspondence between $\mathfrak{r}$ and $\mathfrak{q}$ except at the limiting points $\eta = \pm\infty$ where ξ is multivalued. Geometrically this occurs when the spheres are vanishingly small. As such, these points indicate the limit direction in which to obtain classical Stokes drag. The surfaces $\eta =$ constant are non-intersecting coaxial spheres with centres at the cartesian coordinates $(r, z) = (0,\, c \coth \eta)$ and radii $c|\operatorname{csch} \eta|$. Denoting the centre distance from sphere i to the origin O by d_i and its radius by r_i, we identify the bipolar ordinates defining sphere 1 and 2 as

$$\cosh \eta_1 := \tfrac{d_1}{r_1}, \qquad \cosh \eta_2 := \tfrac{d_2}{r_2}.$$

Note that $\eta_1 > 0$ and $\eta_2 < 0$. The geometry is summarised in Figure 3.1, and we refer the reader to [75, Appendix A-19] for more details on curvilinear coordinate system. In Figure 3.1, ξ varies between 0 and π by moving the axis pair $(\overrightarrow{\eta},\, \overrightarrow{\xi})$ along a circle (not shown) curvilinear to $\eta = \eta_1$ in the lower half plane. The foci are found at either end of the bold line

segment, along which $\xi = \pi$ and off this line segment, along the $\overrightarrow{z}$ axis, one has $\xi = 0$. Other interesting works in the area of coordinate geometry that discuss spherical bipolar coordinates in depth include Jeffery [87], Moon and Spencer [122]. For readers unfamiliar with spherical bipolar coordinates, the coordinate geometry is a highly practical coordinate system for many problems in fluid mechanics, and, in particular, has received increasing attention in recent years; such as in Gilbert and Giacomin [59] for canonical solutions to classical heat, mass and momentum transport problems where Cartesian and polar coordinate systems are deficient; additionally Papavassiliou and Alexander [132] have used the bipolar coordinates for modelling the HI between swimming microscopic organisms.

3.4 Steady Flow Equations

Consider the steady incompressible Navier-Stokes equations governing the evolution of the fluid velocity $\mathbf{u}$ and pressure p in an unbounded domain Ω outside of the spheres:

$$Re\,(\mathbf{u}\cdot\nabla)\,\mathbf{u} = -\nabla p + \nabla^2\mathbf{u}, \tag{3.4.1a}$$

$$\nabla\cdot\mathbf{u} = 0 \tag{3.4.1b}$$

where $Re = \rho UL/\mu$ for U a characteristic velocity, L a characteristic length, ρ the fluid density and μ the dynamic viscosity. Here ρ and μ are assumed to be constant.

3.4.1 Transformation Of The Steady Flow Equations

We begin this section by determining the relationship between the Laplacian in Cartesian coordinates to the Laplacian in spherical bipolar coordinates.

Lemma 3.4.1. *Let $f : \mathbb{C} \to \mathbb{C}$ be differentiable at the point $\omega = \xi + i\eta$ in some open subset of $\mathbb{C}$. Then for a conjugate coordinate system of revolution defined by*

$$z + ir = f(\xi + i\eta), \tag{3.4.2}$$

the second order partial derivatives are related by

$$\partial_z^2 + \partial_r^2 = \mathfrak{h}^{-2}\left[\partial_\xi^2 + \partial_\eta^2\right]$$

where $\mathfrak{h} = \mathfrak{h}_\eta = \mathfrak{h}_\xi$ is the metrical coefficient defined by the transformation (3.4.2).

Proof. By the chain rule applied to f one sees

$$\partial_\xi f = \partial_\xi z\partial_z f + \partial_\xi r\partial_r f,$$
$$\partial_\eta f = \partial_\eta z\partial_z f + \partial_\eta r\partial_r f$$

which we may invert for expressions for $\partial_z f, \partial_r f$

$$\begin{bmatrix}\partial_z f\\ \partial_r f\end{bmatrix} = \frac{1}{(\partial_\xi z\partial_\eta r - \partial_\xi r\partial_\eta z)}\begin{bmatrix}\partial_\eta r & -\partial_\xi r\\ -\partial_\eta z & \partial_\xi z\end{bmatrix}\begin{bmatrix}\partial_\xi f\\ \partial_\eta f\end{bmatrix}.$$

By definition and differentiability of f, z and r satisfy the Cauchy-Riemann equations, $\partial_\xi z = \partial_\eta r, \partial_\eta z = -\partial_\xi r$ and therefore we may write the metrical coefficient of the transformations $\mathfrak{h}$ such that $\mathfrak{h}_\eta = \mathfrak{h}_\xi = \mathfrak{h}$ where

$$\mathfrak{h}^{-2} = (\partial_\eta r)^2 + (\partial_\eta z)^2 = (\partial_\xi r)^2 + (\partial_\xi z)^2.$$

With $\mathfrak{h}$ the second order partial derivatives may be written

$$\partial_z^2 f = \mathfrak{h}^{-2}\left[(\partial_\eta r\partial_\xi - \partial_\xi r\partial_\eta)\left(\mathfrak{h}^{-2}\left[\partial_\eta r\partial_\xi f - \partial_\xi r\partial_\eta f\right]\right)\right], \tag{3.4.3}$$

$$\partial_r^2 f = \mathfrak{h}^{-2}\left[(\partial_\xi z\partial_\eta - \partial_\eta z\partial_\xi)\left(\mathfrak{h}^{-2}\left[\partial_\xi z\partial_\eta f - \partial_\eta z\partial_\xi f\right]\right)\right] \tag{3.4.4}$$

and upon expanding and adding together (3.4.3), (3.4.4) one obtains

$$\begin{aligned}\partial_z^2 f + \partial_r^2 f &= \mathfrak{h}^{-2}\left[\partial_\xi^2 + \partial_\eta^2\right] f \\ &\quad + \partial_\xi f\left[-2\mathfrak{h}^{-4}\partial_\xi \mathfrak{h} + 2\mathfrak{h}^{-4}(\partial_\xi z \partial_{\xi\eta}^2 r + \partial_\eta z \partial_{\eta\eta}^2 r)\right] \\ &\quad + \partial_\eta f\left[-2\mathfrak{h}^{-4}\partial_\eta \mathfrak{h} + 2\mathfrak{h}^{-4}(\partial_\eta r \partial_{\xi\eta}^2 z + \partial_\eta z \partial_{\eta\eta}^2 z)\right] \\ &= \mathfrak{h}^{-2}\left[\partial_\xi^2 + \partial_\eta^2\right] f.\end{aligned}$$

where in the last line we have observed that the terms in the parentheses in the above equality are identically zero by direct computation of the partial derivatives $\partial_\xi \mathfrak{h}$, $\partial_\eta \mathfrak{h}$. □

Now that we have the form of the Laplacian we may construct the full operator L_k.

Definition 3.4.2. *The family of axisymmetric potential operators L_k is defined as*

$$L_k := \partial_z^2 + \partial_r^2 + \frac{k}{r}\partial_r.$$

Lemma 3.4.3. *The family of axisymmetric potential operators L_k transformed into spherical bipolar coordinates read*

$$L_k = r^{-k}\mathfrak{h}^{-2}\left[\partial_\xi\left(r^k \partial_\xi\right) + \partial_\eta\left(r^k \partial_\eta\right)\right].$$

Proof. By the proof of Lemma 3.4.1 we have

$$\partial_r = \mathfrak{h}^{-2}\left[\partial_\xi r + \partial_\eta r\right]$$

and thus by combining the result of Lemma 3.4.1, along with Definition 3.4.1, we have

$$\begin{aligned}\partial_z^2 + \partial_r^2 + kr^{-1}\partial_r &= \mathfrak{h}^{-2}\left[\partial_\xi^2 + \partial_\eta^2\right] + kr^{-1}\mathfrak{h}^{-2}\left[\partial_\xi r + \partial_\eta r\right] \\ &= r^{-k}\mathfrak{h}^{-2}\left[r^{-k}(\partial_\xi^2 + \partial_\eta^2) + kr^{k-1}(\partial_\xi r + \partial_\eta r)\right] \\ &= r^{-k}\mathfrak{h}^{-2}\left[\partial_\xi\left(r^k \partial_\xi\right) + \partial_\eta\left(r^k \partial_\eta\right)\right]\end{aligned}$$

where in the last line we have used the product rule. □

We now give expressions for the metrical coefficients in spherical bipolar coordinates which will be useful for future calculations.

Lemma 3.4.4. *The metrical coefficients $\mathfrak{h}_\xi$, $\mathfrak{h}_\eta$ are given by*

$$\mathfrak{h}_k^2 = \mathfrak{h}^2 = \frac{c^2}{(\cosh\eta - \cos\xi)^2} \qquad \text{for } k = \xi, \eta.$$

Proof. Since r, z satisfy the Cauchy-Riemann equations we have

$$\partial_\xi z = \partial_\eta r, \quad \partial_\eta z = -\partial_\xi r,$$

thus by squaring and adding these equations

$$\mathfrak{h}_\xi^2 = (\partial_\xi z)^2 + (\partial_\xi r)^2 = (\partial_\eta z)^2 + (\partial_\xi r)^2 = \mathfrak{h}_\eta^2.$$

For a general transformation $f : (q_1, q_2) \mapsto (r_1, r_2)$ in Lemma 3.4.1 the metrical coefficient is defined as in Happel and Brenner [75]

$$\mathfrak{h}_k^{-2} = (\partial_{q_k} r)^2 + (\partial_{q_k} z)^2 \qquad \text{for } k = 1, 2.$$

Thus by (3.3.2) and direct calculation we find

$$\mathfrak{h}_\xi^{-2} = \mathfrak{h}_\eta^{-2} = \frac{c^2}{(\cosh\eta - \cos\xi)^2}$$

and the Lemma is proved. □

With Lemmas 3.4.1-3.4.4 we convert the Stokes problem (3.4.1a)-(3.4.1b) to spherical bipolar coordinates with the following result.

Lemma 3.4.5. *The full stream function formulation of the Navier-Stokes equations in Spherical Bipolar coordinates is given by*

$$L_{-1}^2\psi = Re\,\mathfrak{h}^2 r\left[\partial_\eta\psi\partial_\xi\left(r^{-2}L^{-1}\psi\right) - \partial_\xi\psi\partial_\eta\left(r^{-2}L^{-1}\psi\right)\right]. \tag{3.4.5}$$

Proof. We identify $\mathbf{e}_z$ as an axis of symmetry, and pose flow of the form $\mathbf{u} = [u_r,\, u_z,\, 0]^\top$. Now suppose we existence of a stream function ψ such that

$$u_r = -r^{-1}\partial_z\psi, \qquad u_z = r^{-1}\partial_r\psi.$$

Note that in cylindrical coordinates this definition of ψ means can be written as a curl

$$\mathbf{u} = -\frac{1}{r}\begin{vmatrix}\mathbf{e}_r & \mathbf{e}_z & r\,\mathbf{e}_\theta\\ \partial_r & \partial_z & \partial_\theta\\ 0 & 0 & \psi\end{vmatrix} = -\mathrm{curl}\left(\frac{\psi}{r}\mathbf{e}_\theta\right) \tag{3.4.6}$$

where in (3.4.6) we have identified the definition of the curl with respect to cylindrical coordinates. The incompressibility condition (3.4.1b) is satisfied since the curl is divergence free, or by direct calculation, in cylindrical coordinates

$$\nabla\cdot\mathbf{u} = \frac{1}{r}\left[-\partial_r\left(r\,r^{-1}\partial_z\psi\right) + \partial_z\left(r\,r^{-1}\partial_r\psi\right)\right] = 0.$$

The vorticity $\boldsymbol{\omega}$ is defined as $\boldsymbol{\omega} := \nabla\times\mathbf{u} = \omega\,\hat{\mathbf{e}}_\theta$, or equivalently $\boldsymbol{\omega} = \mathrm{curl}^2\left(\frac{\psi}{r}\right)$. Thus one obtains an explicit expression for ω in terms of ψ

$$\boldsymbol{\omega} = \mathrm{curl}\,\mathbf{u} = r^{-1}L_{-1}\psi\,\hat{\mathbf{e}}_\theta$$

where L_{-1} is the differential operator given by $L_{-1} = \partial_z^2 + \partial_r^2 - r^{-1}\partial_r$. Now taking successive curls of $\boldsymbol{\omega}$ we obtain

$$\begin{aligned}\nabla\times\boldsymbol{\omega} &= r^{-1}\partial_z L_{-1}\psi\mathbf{e}_r - r^{-1}\partial_r L_{-1}\psi\mathbf{e}_z\\ \nabla\times\nabla\times\boldsymbol{\omega} &= -r^{-1}L_{-1}^2\psi\mathbf{e}_\theta.\end{aligned}$$

We also have the vector calculus identity $(\mathbf{u}\cdot\nabla)\,\mathbf{u} = \frac{1}{2}|\mathbf{u}|^2 - \mathbf{u}\times\nabla\times\mathbf{u}$, which, after taking the curl and using the definition of $\boldsymbol{\omega}$, we determine that $\nabla\times[(\mathbf{u}\cdot\nabla)\,\mathbf{u}] = -\nabla\times[\mathbf{u}\times\boldsymbol{\omega}]$ where we have used that the curl of a gradient is zero. Equation (3.4.1a) therefore becomes

$$Re\,\nabla\times[\mathbf{u}\times\boldsymbol{\omega}] = \mathrm{curl}^3\mathbf{u}, \tag{3.4.7}$$

where we have used that $\nabla^2\mathbf{u} = \nabla(\nabla\cdot\mathbf{u}) - \nabla\times\nabla\times\mathbf{u}$. In cylindrical coordinates the right hand side of (3.4.7) becomes $-r^{-1}L_{-1}^2\psi\mathbf{e}_\theta$, and after computing the internal cross product of the left hand side we obtain $Re\,\nabla\times\left[r^{-2}L_{-1}\psi\nabla\psi\right] = -r^{-1}L_{-1}^2\psi\mathbf{e}_\theta$. Now expanding the left hand side, once again using the fact that the curl of a gradient is zero we obtain

$$Re\,\left[\partial_r\psi\partial_z\left(r^{-2}L_{-1}\psi\right) - \partial_z\psi\partial_r\left(r^{-2}L_{-1}\psi\right)\right] = -r^{-1}L_{-1}^2\psi.$$

After rearranging this equation, and using the conversion $\nabla\psi = \mathfrak{h}\partial_\eta\psi\,\mathbf{e}_\eta + \mathfrak{h}\partial_\xi\psi\,\mathbf{e}_\xi$, the lemma is proved. □

3.5 Stokes Equations

For axisymmetric flow the assumed existence of a stream function ψ permits (3.4.1a), (3.4.1b) to be recast into a single PDE

$$\tfrac{1}{Re\, r} L_{-1}^2 \psi = \partial_z \psi \, \partial_r (\tfrac{1}{r^2} L_{-1} \psi) - \partial_r \psi \, \partial_z (\tfrac{1}{r^2} L_{-1} \psi).$$

The differential operator L_{-1} is a member of the class of axisymmetric potential operators $L_k := \partial_z^2 + \partial_r^2 + k r^{-1} \partial_r$ for $k \in (-\infty, \infty)$, with $k = -1$. By Lemma 3.4.5 we have that $L_k = r^{-k} \mathfrak{h}^{-2} [\partial_\xi (r^k \partial_\xi) + \partial_\eta (r^k \partial_\eta)]$ where $\mathfrak{h}$ is the metrical coefficient arising from the transformation between coordinate systems, defined by $\mathfrak{h}^2 = (\partial_\xi z)^2 + (\partial_\xi r)^2 = (\partial_\eta r)^2 + (\partial_\eta z)^2 = c^2/(\cosh \eta - \cos \xi)^2$. After setting $Re = 0$ the first approximation to the flow around the two spheres yields the biharmonic equation subject to two no slip and two no flux conditions

$$\left[\tfrac{r}{\mathfrak{h}^2} \left(\partial_\xi \left(r^{-1} \partial_\xi \right) + \partial_\eta \left(r^{-1} \partial_\eta \right) \right) \right]^2 \psi = 0, \qquad \text{in } \Omega \tag{3.5.1}$$

$$\psi \pm \tfrac{U r^2}{2} = 0, \quad \partial_n \left(\psi \pm \tfrac{U r^2}{2} \right) = 0, \tag{3.5.2}$$

where the signs are taken according to the choice of sphere and the direction of their velocities. By rescaling the spatial coordinates and the stream function one may use (3.4.5) to compute higher order corrections to the velocity field for small Re, by taking into account contributions proportional the square of the velocity of the spheres, (see for example [24] for the classical single sphere at infinity). For this work we restrict to motions of spheres linear in their velocity.

3.6 Solution In Spherical Bipolar Coordinates

Here we write the stream function in spherical bipolar coordinates. To solve the PDE (3.5.1) it will be seen that is sufficient to write

$$\psi = \psi_1 + z \, \psi_2 \tag{3.6.1}$$

where $L_{-1} \psi_i = 0$ for both $i = 1, 2$. The extent to which the ansatz (3.6.1) is complete, that is includes the appropriate set of basis functions which will satisfy the problem in hand ((3.5.1), (3.5.2)), is not formally treated here. At any rate it may be heuristically justified by reference to [137] wherein the appropriate combination of axisymmetric potential functions is chosen accordingly such that the optimal combination as a solution for a specific problem will dependent on the geometry of the boundary on which the boundary and far field conditions must be satisfied. A combination suitable for one problem may be completely intractable for another.

We calculate an explicit form for ψ with the following lemma.

Lemma 3.6.1. *Let $\mathfrak{x} = \cos \xi$ and $P_n(\mathfrak{x})$ be the n^{th} Legendre polynomial of the first kind.*

i There is a solution to $L_{-1} \psi_1 = 0$ of the form

$$\psi_1(\xi, \eta) = \sum_{n=1}^{\infty} \left[a_n \cosh(n + \tfrac{1}{2}) \eta + b_n \sinh(n + \tfrac{1}{2}) \eta \right] \frac{Q_n(\mathfrak{x})}{\sqrt{\cosh \eta - \mathfrak{x}}} \tag{3.6.2}$$

where $Q_n(\mathfrak{x}) := P_{n+1}(\mathfrak{x}) - P_{n-1}(\mathfrak{x})$.

ii The Q_n satisfy the ODE

$$(1 - \mathfrak{x}^2) \frac{\mathrm{d}^2 Q_n}{\mathrm{d}\mathfrak{x}^2} + n(n+1) Q_n(\mathfrak{x}) = 0. \tag{3.6.3}$$

iii The Q_n satisfy the recurrence relation

$$\mathfrak{x} \, Q_n(\mathfrak{x}) = \frac{n+2}{2n+3} Q_{n+1}(\mathfrak{x}) + \frac{n-1}{2n-1} Q_{n-1}(\mathfrak{x}). \tag{3.6.4}$$

Proof. By referring to [75] and using techniques therein we make an ansatz in the form of a separation solution

$$\psi_1 = r^{1/2} f(\xi) g(\eta)$$

and after inserting into $L_{-1}\psi_1 = 0$ we find the functions f and g must satisfy

$$-\frac{3fg}{4\sin^2\xi} + f''g + g''f = 0.$$

Equivalently we have the system of ODEs

$$\begin{aligned} f'' + \left(\lambda^2 - \frac{3}{4\sin^2\xi}\right) f = 0, \\ g'' - \lambda^2 g = 0, \end{aligned}$$

where λ^2 is a separation constant. The η equation is trivially solved with a linear combination of hyperbolic trigonometric functions. For the ξ equation we make the ansatz $f = (\bar{\xi}^2 - 1)^{1/4}\bar{f}$ to yield

$$\left(1 - \bar{\xi}^2\right)\bar{f}'' - 2\bar{\xi}\bar{f}' + \left(\lambda^2 - \frac{1}{4} - \frac{1}{1-\bar{\xi}^2}\right)\bar{f} = 0$$

which we recognise as the associated Legendre equation with $m = 1$ and $\lambda = n + \frac{1}{2}$ for n a non-negative integer. Thus

$$\bar{f} = P_n^1(\bar{\xi})$$

where $P_n^1(\mathfrak{x})$ is the associated Legendre function at order n with $m = 1$. By using the definition of $P_n^1(\mathfrak{x})$

$$P_n^1(\mathfrak{x}) = -(1-\mathfrak{x}^2)^{1/2}\frac{\mathrm{d}P_n}{\mathrm{d}\mathfrak{x}},$$

along with Bonnet's first recursion formula

$$\frac{\mathfrak{x}^2 - 1}{n}\frac{\mathrm{d}P_n}{\mathrm{d}\mathfrak{x}} = \mathfrak{x}\, P_n(\mathfrak{x}) - P_{n-1}(\mathfrak{x}),$$

and the principle of linear superposition we have

$$\psi_1(\xi,\eta) = \sum_{n=1}^{\infty}\left[a_n \cosh(n+\tfrac{1}{2})\eta + b_n \sinh(n+\tfrac{1}{2})\eta\right]\frac{\mathfrak{x}P_n(\mathfrak{x}) - P_{n-1}(\mathfrak{x})}{\sqrt{\cosh\eta - \mathfrak{x}}} \tag{3.6.5}$$

where a_n, b_n are arbitrary constants and a similar expression exists for ψ_2. We remark that the sums are to be taken starting $n = 1, 2, ..$ because of the appearance of P_{n-1}. We continue manipulating the Legendre Polynomials to seek a simplified expression for ψ_1. By using Bonnet's second recurrence formula

$$(n+1)P_{n+1}(\mathfrak{x}) = (2n+1)xP_n(\mathfrak{x}) - nP_{n-1}(\mathfrak{x}),$$

substituted into (3.6.5) we have a simplified expression for ψ_1 namely (3.6.2). Since P_{n+1}, P_{n-1} are Legendre polynomials it is elementary to see that their difference, the Q_n, satisfy the ODE (3.6.3) by subtracting Legendre's equation at order $n-1$ from Legendre's equation at $n+1$ and using the product rule. Upon applying Bonnet's second recurrence formula to both P_{n+1} and P_{n-1} we see the Q_n satisfy the recursion relation (3.6.4). □

3.6.1 Constructing The Stream Function

We compute a compact form of the stream function with the following lemma.

Lemma 3.6.2. *The stream function ψ maybe written in the compact form*

$$\psi(\xi,\eta) = (\cosh\eta - \mathfrak{x})^{-3/2}\,\chi(\xi,\eta) \tag{3.6.6}$$

with

$$\chi(\xi,\eta) := \sum_{n=1}^{\infty} Q_n(\mathfrak{x}) R_n(\eta)$$

where

$$R_n(\eta) = a_n \cosh(n+\tfrac{3}{2})\eta + b_n \sinh(n+\tfrac{3}{2})\eta + c_n \cosh(n-\tfrac{1}{2})\eta + d_n \sinh(n-\tfrac{1}{2})\eta$$

and the a_n, b_n, c_n and d_n are arbitrary constants.

Proof. As stated in [162] for the queuing spheres case, to find a solution of the PDE (3.5.1) it is sufficient to write

$$\psi = \psi_1 + z\,\psi_2$$

where $L_{-1}\psi_i = 0$ for $i = 1, 2$. Using the results of section 3.6 we construct ψ as

$$\begin{aligned}\psi = \psi_1 + z\,\psi_2 = (\cosh\eta - \mathfrak{x})^{-3/2} \\ \times \sum_{n=1}^{\infty} \big[\big\{ a_n \cosh(n+\tfrac{1}{2})\eta \; + b_n \sinh(n+\tfrac{1}{2})\eta \big\} (\cosh\eta - \mathfrak{x}) \\ + \big\{ c_n \cosh(n+\tfrac{1}{2})\eta + d_n \sinh(n+\tfrac{1}{2})\eta \big\} \sinh\eta \big]\, Q_n(\mathfrak{x}).\end{aligned} \tag{3.6.7}$$

We use of the fact that the constants a_n, b_n, c_n and d_n remain arbitrary before boundary conditions are applied, therefore they may be trivially redefined upon absorption of any multiplying constants. First notice that with compound angle formulae the terms without the factor $\mathfrak{x}$ in (3.6.7) may be written in arbitrary weights of the hyperbolic functions $\cosh(n+\frac{3}{2})\eta$, $\cosh(n-\frac{1}{2})\eta$, $\sinh(n+\frac{3}{2})\eta$ and $\sinh(n-\frac{1}{2})\eta$. This yields

$$\begin{aligned}\psi = (\cosh\eta - \mathfrak{x})^{-3/2} \\ \times \sum_{n=1}^{\infty} \big[\big\{ a_n \cosh(n+\tfrac{3}{2})\eta \; + b_n \sinh(n+\tfrac{3}{2})\eta + c_n \cosh(n-\tfrac{1}{2})\eta + d_n \sinh(n-\tfrac{1}{2})\eta \big\} \\ + \big\{ e_n \cosh(n+\tfrac{1}{2})\eta + f_n \sinh(n+\tfrac{1}{2})\eta \big\} \cos\xi \big]\, Q_n(\mathfrak{x})\end{aligned} \tag{3.6.8}$$

where e_n and f_n are arbitrary. For the term with the factor of $\mathfrak{x}$ we use the recurrence relation (3.6.4) to remove all $\mathfrak{x}$ dependence within the summand. In particular the recurrence relation reads

$$\begin{aligned}\big\{ e_n \cosh(n+\tfrac{1}{2})\eta + f_n \sinh(n+\tfrac{1}{2})\eta \big\} \cos\xi\, Q_n(\mathfrak{x}) \\ = e_n \left(\frac{n-1}{2n-1}\right) \cosh(n+\tfrac{1}{2})\eta\, Q_{n-1}(\mathfrak{x}) + f_n \left(\frac{n-1}{2n-1}\right) \sinh(n+\tfrac{1}{2})\eta\, Q_{n-1}(\mathfrak{x}) \\ + e_n \left(\frac{n+2}{2n+3}\right) \cosh(n+\tfrac{1}{2})\eta\, Q_{n+1}(\mathfrak{x}) + f_n \left(\frac{n+2}{2n+3}\right) \sinh(n+\tfrac{1}{2})\eta\, Q_{n+1}(\mathfrak{x}).\end{aligned}$$

With this expanded form the summation is freely shifted so that $\cosh(n+\frac{1}{2})$ is written as an arbitrary sum of $\cosh(n+\frac{3}{2})$ and $\cosh(n-\frac{1}{2})$ translating e_n to e_{n-1} etc. This produces a common factor of $Q_n(\mathfrak{x})$ inside summation (3.6.8) and we obtain the separated expansion form (3.6.6). □

3.6.2 Boundary Conditions

The stream function (3.6.6) is the most convenient form in the present coordinate system to apply boundary conditions. We impose no-flux and no-slip boundary conditions, typical for fluid problems of viscous type, although we remark that other constitutive conditions may be applied such as varying slip conditions depending on the physical system being studied, making the present solution method generalisable and thus demonstrating the utility of the change in coordinate system. The boundary conditions in (3.5.2) are combined with the expressions for r and z in (3.3.2) and (3.6.6) to become

$$\begin{aligned}
\frac{\chi(\xi,\eta_1)}{(\cosh\eta_1-\mathfrak{x})^{3/2}}+\frac{c^2U\sin^2\xi}{2(\cosh\eta_1-\mathfrak{x})}&=0,\\
\partial_\eta\left[\frac{\chi(\xi,\eta)}{(\cosh\eta-\mathfrak{x})^{3/2}}+\frac{c^2U\sin^2\xi}{2(\cosh\eta-\mathfrak{x})}\right]_{\eta_1}&=0,\\
\frac{\chi(\xi,\eta_2)}{(\cosh\eta_2-\mathfrak{x})^{3/2}}-\frac{c^2U\sin^2\xi}{2(\cosh\eta_2-\mathfrak{x})}&=0,\\
\partial_\eta\left[\frac{\chi(\xi,\eta)}{(\cosh\eta-\mathfrak{x})^{3/2}}-\frac{c^2U\sin^2\xi}{2(\cosh\eta-\mathfrak{x})}\right]_{\eta_2}&=0
\end{aligned}$$

where U is the characteristic velocity scale and $\eta_1>0$, $\eta_2<0$ correspond to the spheres 1 and 2 respectively. Simplifying these expressions we obtain on sphere 1

$$\begin{aligned}
\chi(\xi,\eta_1)&=-\frac{c^2U\sin^2\xi}{2(\cosh\eta_1-\mathfrak{x})^{1/2}},\\
\partial_\eta\chi(\xi,\eta_1)&=-\frac{c^2U\sin^2\xi\sinh\eta_1}{4(\cosh\eta_1\cos\xi)^{3/2}},
\end{aligned}\tag{3.6.9}$$

and

$$\begin{aligned}
\chi(\xi,\eta_2)&=\frac{c^2U\sin^2\xi}{2(\cosh\eta_2-\mathfrak{x})^{1/2}},\\
\partial_\eta\chi(\xi,\eta_2)&=\frac{c^2U\sin^2\xi\sinh\eta_2}{4(\cosh\eta_2\cos\xi)^{3/2}}.
\end{aligned}\tag{3.6.10}$$

on sphere 2. We proceed to find a_n, b_n, c_n and d_n by using orthogonality of the basis functions P_n. By definition of the Q_n in lemma 3.6.1 we have

$$\chi(\xi,\eta)=\sum_{n=1}^{\infty}R_n(\eta)\left[P_{n+1}(\mathfrak{x})-P_{n-1}(\mathfrak{x})\right]$$

so that as long as $\xi\neq0,\pi$, we have the following equation implicitly determining the unknown constants

$$\chi(\xi,\eta)P_m(\mathfrak{x})\sin\xi=\sum_{n=1}^{\infty}R_n(\eta)P_{n+1}(\mathfrak{x})P_m(\mathfrak{x})\sin\xi-\sum_{n=1}^{\infty}R_n(\eta)P_{n-1}(\mathfrak{x})P_m(\mathfrak{x})\sin\xi.\tag{3.6.11}$$

By differentiating equation (3.6.11) with respect to η (where appropriate) and integrating over the domain $\xi\in[0,\pi]$, interchanging the order of summation and integration one may obtain explicit expressions for the constants a_n,b_n,c_n,d_n. More explicitly the four equations determining the four unknowns are given by sequentially substituting equations (3.6.9), (3.6.10) into

equation (3.6.11). In other words

$$-\frac{c^2U\sin^2\xi}{2(\cosh\eta_1-\mathfrak{x})^{1/2}}P_m(\mathfrak{x})\sin\xi=\sum_{n=1}^{\infty}R_n(\eta_1)Q_n(\mathfrak{x})P_m(\mathfrak{x})\sin\xi, \tag{3.6.12a}$$

$$-\frac{c^2U\sin^2\xi\sinh\eta_1}{4(\cosh\eta_1\cos\xi)^{3/2}}P_m(\mathfrak{x})\sin\xi=\sum_{n=1}^{\infty}R_n'(\eta_1)Q_n(\mathfrak{x})P_m(\mathfrak{x})\sin\xi, \tag{3.6.12b}$$

$$\frac{c^2U\sin^2\xi}{2(\cosh\eta_2-\mathfrak{x})^{1/2}}P_m(\mathfrak{x})\sin\xi=\sum_{n=1}^{\infty}R_n(\eta_2)Q_n(\mathfrak{x})P_m(\mathfrak{x})\sin\xi, \tag{3.6.12c}$$

$$\frac{c^2U\sin^2\xi\sinh\eta_2}{4(\cosh\eta_1\cos\xi)^{3/2}}P_m(\mathfrak{x})\sin\xi=\sum_{n=1}^{\infty}R_n'(\eta_2)Q_n(\mathfrak{x})P_m(\mathfrak{x})\sin\xi, \tag{3.6.12d}$$

where $'$ denotes differentiation with respect to η. We provide the following lemma which permits us to commute a summation and integral sign.

Lemma 3.6.3. *For each η when integrating equations* (3.6.12a)-(3.6.12d) *over $\xi\in[0,\pi]$, the order of summation and integration may be interchanged.*

Proof. Define $f_n:[0,\pi]\to\mathbb{R}$ by

$$f_n(\xi):=\alpha_n(\eta)Q_n(\cos\xi)P_m(\cos\xi)\sin\xi.$$

where α_n is an arbitrary function of η. Let $\langle .\,,.\rangle$ define the usual inner product for real functions on the closed interval $[-1,1]$. Then we see that

$$\begin{aligned}\sum_{n=1}^{N}\int_0^{\pi}f_n(\xi)\,\mathrm{d}\xi&=\sum_{n=1}^{N}\alpha_n(\eta)\,\langle P_{n-1}-P_n,P_m\rangle\\&=\sum_{n=1}^{N}\frac{2\delta_{m\,n-1}\alpha_{n-1}(\eta)}{2n-1}-\frac{2\delta_{m\,n}\alpha_n(\eta)}{2n+1}\le\sum_{n=1}^{N}\frac{2\delta_{m\,n-1}\alpha_{n-1}(\eta)}{2n-1}<\frac{\alpha_m(\eta)}{m}\end{aligned}$$

where we have used the orthogonality condition $\langle P_l,\,P_k\rangle=\frac{2\delta_{l\,k}}{2k+1}$. Thus the $\sum_{n=1}^{N}f_n$ is bounded by and integrable function and we may write

$$\int_0^{\pi}\sum_{n=1}^{\infty}f_n\,\mathrm{d}\xi=\int_0^{\pi}\lim_{N\to\infty}\sum_{n=1}^{N}f_n\,\mathrm{d}\xi=\lim_{N\to\infty}\sum_{n=1}^{N}\int_0^{\pi}f_n\,\mathrm{d}\xi=\sum_{n=1}^{\infty}\int_0^{\pi}f_n\,\mathrm{d}\xi.$$

Therefore by taking $\alpha_n(\eta)=R_n(\eta)$, $R_n'(\eta)$ the lemma is proved. □

We use Lemma 3.6.3 to swap the sum and integral signs once the boundary conditions (3.6.12a)-(3.6.12d) have been integrated over $\xi\in[0,\pi]$. We will use the standard technique of orthogonal transformation. The Legendre functions are orthogonal with unit weighting in the sense

$$\int_{-1}^{1}P_m(\mathfrak{x})P_n(\mathfrak{x})\,\mathrm{d}\mathfrak{x}=\frac{2}{2m+1}\delta_{nm} \tag{3.6.13}$$

where δ_{nm} is the Kronecker delta tensor. We will use iteratively the identity (3.6.13) and provide the useful identity

$$\int_{-1}^{1}P_m(\mathfrak{x})Q_k(\mathfrak{x})\,\mathrm{d}\mathfrak{x}=\frac{2}{2k+3}\delta_{m\,k+1}-\frac{2}{2k-1}\delta_{m\,k-1}. \tag{3.6.14}$$

We will also use the following lemma.

Lemma 3.6.4. *For every* $\mathfrak{x} \in [-1,1]$ *and* $n \in \mathbb{N}$ *the* P_n *and* Q_n *satisfy*

$$(2n+1)(1-\mathfrak{x}^2)P_n(\mathfrak{x}) = \frac{n(n-1)}{2n-1}Q_{n-1}(\mathfrak{x}) - \frac{(n+1)(n+2)}{2n+3}Q_{n+1}(\mathfrak{x}), \tag{3.6.15}$$

$$\frac{2n+1}{n+1}(1-\mathfrak{x})^2\frac{\mathrm{d}}{\mathrm{d}\mathfrak{x}}P_n(\mathfrak{x}) = -n\,Q_n(\mathfrak{x}). \tag{3.6.16}$$

Proof. First consider equation (3.6.15). By definition we have

$$Q_n(\mathfrak{x}) = P_{n+1}(\mathfrak{x}) - P_{n-1}(\mathfrak{x}).$$

Bonnet's second recursion formula is

$$(n+1)P_{n+1}(\mathfrak{x}) = (2n+1)xP_n(\mathfrak{x}) - nP_{n-1}(\mathfrak{x}), \tag{3.6.17}$$

and by multiplying through by $\mathfrak{x}$ and subtracting $(2n+1)P_n(\mathfrak{x})$ from both sides we find

$$(2n+1)(1-\mathfrak{x}^2)P_n(\mathfrak{x}) = (2n+1)P_n(\mathfrak{x}) - nxP_{n-1}(\mathfrak{x}) - (n+1)xP_{n+1}(\mathfrak{x})$$

and by using (3.6.17) again we find

$$\begin{aligned}
&(2n+1)(1-\mathfrak{x}^2)P_n(\mathfrak{x}) \\
&= (2n+1)P_n(\mathfrak{x}) - \frac{n+1}{2n+3}\left[(n+2)P_{n+2}(\mathfrak{x}) + (n+1)P_n(\mathfrak{x})\right] - \frac{n}{2n-1}\left[nP_n(\mathfrak{x}) + (n-1)P_{n-2}(\mathfrak{x})\right] \\
&= \frac{(n+1)(n+2)}{(2n+3)}P_{n-2}(\mathfrak{x}) - 2\frac{(2n+1)(n^2+n-1)}{(2n-1)(2n+3)}P_n(\mathfrak{x}) + \frac{n(n+1)}{(2n-1)}P_{n-2}(\mathfrak{x}).
\end{aligned}$$

Then by writing $n^2+n-1 = (n+1)(n+2)-(2n+3)$ and collecting like P_n's the result follows. Now consider (3.6.16). Bonnet's first recursion formula is

$$\frac{\mathfrak{x}^2-1}{n}\frac{\mathrm{d}}{\mathrm{d}\mathfrak{x}}P_n(\mathfrak{x}) = \mathfrak{x}P_n(\mathfrak{x}) - P_{n-1}(\mathfrak{x})$$

which may be combined with (3.6.17) to yield the result. □

Finally to ease notation we will rescale the stream function with natural dimensions by writing $\psi \sim Uc^2/2\,\psi'$, now dropping primes.

No Slip

Lemma 3.6.3 permits us to commute the order of the integrals and summations of the equations of the boundary conditions. Considering first the no slip conditions (3.6.12a), (3.6.12c), we integrate both sides with respect to ξ and apply lemma 3.6.3 to obtain

$$\begin{aligned}
-\int_{-\pi}^{0}\frac{\sin^3\xi P_m(\cos\xi)}{(\cosh\eta_1-\cos\xi)^{1/2}}\,\mathrm{d}\xi &= -\int_{-1}^{1}\frac{(1-\mathfrak{x}^2)P_m(\mathfrak{x})}{(\cosh\eta_1-\mathfrak{x})^{1/2}}\,\mathrm{d}\mathfrak{x} \\
&= \frac{2}{2m-1}R_{m-1}(\eta_1) - \frac{2}{2m+3}R_{m+1}(\eta_1). \qquad (3.6.18)\\
\int_{-\pi}^{0}\frac{\sin^3\xi P_m(\cos\xi)}{(\cosh\eta_2-\cos\xi)^{1/2}}\,\mathrm{d}\xi &= \int_{-1}^{1}\frac{(1-\mathfrak{x}^2)P_m(\mathfrak{x})}{(\cosh\eta_2-\mathfrak{x})^{1/2}}\,\mathrm{d}\mathfrak{x} \\
&= \frac{2}{2m-1}R_{m-1}(\eta_2) - \frac{2}{2m+3}R_{m+1}(\eta_2).
\end{aligned}$$

Where we have used the substitution $\mathfrak{x} = \cos\xi$ on the left hand integrals and used (3.6.13) to evaluate the right hand integrals. The left hand integral may be evaluated explicitly. Consider

the factor $(\cosh\eta - \mathfrak{x})^{-1/2}$ as a Newtonian potential[1], it may be written

$$\frac{1}{(\cosh\eta-\mathfrak{x})^{1/2}} = \frac{1}{\sqrt{\zeta^2+\zeta'^2-2\zeta\zeta'\mathfrak{x}}} = \frac{1}{\zeta}\sum_{k=0}^{\infty}\left(\frac{\zeta'}{\zeta}\right)^k P_k(\mathfrak{x}) \tag{3.6.19}$$

where $\zeta' = \zeta^{-1}/2$ and $\zeta = e^{\pm\eta/2}/\sqrt{2}$ and the sign is taken according to the sign of η so that the exponential takes negative argument. Since P_m is a polynomial so is $(1-\mathfrak{x}^2)P_m(\mathfrak{x})$, therefore we may expand it into a linear combination of Legendre polynomials, in particular we have (3.6.15). The motivation is to remove powers of $\mathfrak{x}$ to obtain an equation containing only inner products of Legendre polynomials so that (3.6.13) may be used. Using the expression (3.6.15) with (3.6.18), (3.6.18) and (3.6.19) we commute integration and summation to find that the first relation the unknown constants satisfy for sphere 1 is given by

$$\begin{aligned}
&\sqrt{2}\int_{-1}^{1}(1-\mathfrak{x})^2 P_m(\mathfrak{x})\frac{1}{\zeta}\sum_{k=0}^{\infty}\left(\frac{\zeta'}{\zeta}\right)^k P_k(\mathfrak{x})\mathrm{d}\mathfrak{x}\\
&\quad=\sqrt{2}\int_{-1}^{1}P_m(\mathfrak{x})\sum_{k=0}^{\infty}\frac{k(k+1)e^{-(k+1/2)\eta_1}}{2k+1}\left[\frac{(k+2)Q_{k+1}(\mathfrak{x})}{k(2k+3)}-\frac{(k-1)Q_{k-1}(\mathfrak{x})}{(k+1)(2k-1)}\right]\mathrm{d}\mathfrak{x}.
\end{aligned}$$

Commuting the sum and integral we obtain

$$\begin{aligned}
&=\sqrt{2}\sum_{k=0}^{\infty}\frac{k(k+1)e^{-(k+1/2)\eta_1}}{2k+1}\\
&\quad\times\left\{\tfrac{(k+2)}{k(2k+3)}\left[\tfrac{2}{2k+5}\delta_{m\,k+2}-\tfrac{2}{2k+1}\delta_{m\,k}\right]-\tfrac{(k-1)}{(k+1)(2k-1)}\left[\tfrac{2}{2k+1}\delta_{m\,k}-\tfrac{2}{2k-3}\delta_{m\,k-2}\right]\right\}\\
&=\tfrac{2}{2m-1}R_{m-1}(\eta_1)-\tfrac{2}{2m+3}R_{m+1}(\eta_1)
\end{aligned}$$

where we have used (3.6.14). Distributing the sum we find

$$\begin{aligned}
&=\sqrt{2}\sum_{k'=2}^{\infty}\frac{k'e^{-(k'-1/2)\eta_1}}{2k'-1}\frac{(k'+1)}{(2k'+1)}\left[\frac{2}{2k'+3}\delta_{m\,k'+1}-\frac{2}{2k'-1}\delta_{m\,k'-1}\right]\\
&\quad-\sqrt{2}\sum_{k'=-1}^{\infty}\frac{(k'+1)e^{-(k'+3/2)\eta_1}}{2k'+3}\frac{k'}{(2k'+1)}\left[\frac{2}{2k'+3}\delta_{m\,k'+1}-\frac{2}{2k'-1}\delta_{m\,k'-1}\right]\\
&=\frac{2}{2m-1}R_{m-1}(\eta_1)-\frac{2}{2m+3}R_{m+1}(\eta_1)
\end{aligned}$$

where we have made the substitutions $k = k'-1$ and $k = k'+1$ for the former and latter sums respectively. We therefore find

$$=2\sqrt{2}\frac{m(m+1)}{2m+1}\left[\frac{e^{-(m-1/2)\eta_1}}{2m-1}-\frac{e^{-(m+3/2)\eta_1}}{2m+3}\right]=\frac{2}{2m-1}R_{m-1}(\eta_1)-\frac{2}{2m+3}R_{m+1}(\eta_1).$$

Via a similar argument for sphere 2 we obtain

$$-2\sqrt{2}\frac{m(m+1)}{2m+1}\left[\frac{e^{-(m-1/2)\eta_2}}{2m-1}-\frac{e^{-(m+3/2)\eta_2}}{2m+3}\right]=\frac{2}{2m-1}R_{m-1}(\eta_2)-\frac{2}{2m+3}R_{m+1}(\eta_2). \tag{3.6.20}$$

recalling that $\eta_2 < 0$ so the exponential functions in (3.6.20) decay with m.

[1]Historically speaking one might regard this by definition, as in 1782 Adrien-Marie Legendre introduced his polynomials as coefficients in a series expansion of the function $|\mathfrak{x}-\mathfrak{x}'|^{-1/2}$.

No Flux

Continuing to the no flux conditions (3.6.12b), (3.6.12d) similar methods are applied with the use of an additional integration formula. Consider sphere 1 whose no flux condition is

$$-\frac{1}{2}\int_{-\pi}^{0}\frac{\sin^3\xi\sinh\eta_1 P_m(\cos\xi)}{(\cosh\eta_1-\cos\xi)^{3/2}}\,\mathrm{d}\xi=\frac{\sinh\eta_1}{2}\int_{-1}^{1}\frac{(1-\mathfrak{x}^2)P_m(\mathfrak{x})}{(\cosh\eta_1-\mathfrak{x})^{3/2}}\,\mathrm{d}\mathfrak{x}$$
$$=\frac{2}{2m-1}r'_{m-1}(\eta_1)-\frac{2}{2m+3}r'_{m+1}(\eta_1) \tag{3.6.21}$$

The left hand side of equation (3.6.21) is problematic because the factor $(\cosh\eta_1-\mathfrak{x})^{-3/2}$ is not a Newtonian potential like the no-slip case. We may however write the integrand as a total derivative

$$\frac{\sinh\eta_1}{2}\int_{-1}^{1}P_m(\mathfrak{x})(1-\mathfrak{x}^2)\frac{\mathrm{d}}{\mathrm{d}\mathfrak{x}}(\cosh\eta_1-\mathfrak{x})^{-1/2}\,\mathrm{d}\mathfrak{x}$$
$$=\sqrt{2}\frac{\sinh\eta_1}{2}\int_{-1}^{1}P_m(\mathfrak{x})(1-\mathfrak{x}^2)\frac{\mathrm{d}}{\mathrm{d}\mathfrak{x}}\sum_{k=0}^{\infty}e^{-(k+1/2)\eta_1}P_k(\mathfrak{x})\,\mathrm{d}\mathfrak{x}$$
$$=\frac{2}{2m-1}r'_{m-1}(\eta_1)-\frac{2}{2m+3}r'_{m+1}(\eta_1).$$

Note that the summand converges uniformly to zero as long as $\eta_1>0$ where $e^{-(k+1/2)\eta_1}P_k(\mathfrak{x})$ decays exponentially as $k\to\infty$. We may therefore pass the derivative through the infinite summation and use lemma 3.6.3 to commute the order of integration and summation to obtain

$$-\sqrt{2}\frac{\sinh\eta_1}{2}\sum_{k=0}^{\infty}\frac{k(k+1)e^{-(k+1/2)\eta_1}}{2k+1}\int_{-1}^{1}P_m(\mathfrak{x})Q_k(\mathfrak{x})\,\mathrm{d}\mathfrak{x}$$
$$=-\frac{1}{\sqrt{2}}\sum_{k=0}^{\infty}\frac{k(k+1)}{2k+1}\left[e^{-(k-1/2)\eta_1}-e^{-(k+3/2)\eta_1}\right]\int_{-1}^{1}P_m(\mathfrak{x})Q_k(\mathfrak{x})\,\mathrm{d}\mathfrak{x}$$
$$=\frac{2}{2m-1}r'_{m-1}(\eta_1)-\frac{2}{2m+3}r'_{m+1}(\eta_1).$$

where we have used the integration formula (3.6.16).

3.6.3 Linear System

The constants a_n, b_n, c_n and d_n are determined by inverting the linear system of equations

$$M_n\mathbf{a}_n:=\begin{bmatrix}m_n^{11}&m_n^{12}&m_n^{13}&m_n^{14}\\m_n^{21}&m_n^{22}&m_n^{23}&m_n^{24}\\m_n^{31}&m_n^{32}&m_n^{33}&m_n^{34}\\m_n^{41}&m_n^{42}&m_n^{43}&m_n^{44}\end{bmatrix}\mathbf{a}_n=\mathbf{G}_n$$

with $\mathbf{a}=(a_n,b_n,c_n,d_n)$, the no slip components

$$m_n^{11}=\cosh(n+\tfrac{3}{2})\eta_1,\quad m_n^{21}=\cosh(n+\tfrac{3}{2})\eta_2,$$
$$m_n^{12}=\sinh(n+\tfrac{3}{2})\eta_1,\quad m_n^{22}=\sinh(n+\tfrac{3}{2})\eta_2,$$
$$m_n^{13}=\cosh(n-\tfrac{1}{2})\eta_1,\quad m_n^{23}=\cosh(n-\tfrac{1}{2})\eta_2,$$
$$m_n^{14}=\sinh(n-\tfrac{1}{2})\eta_1,\quad m_n^{24}=\sinh(n-\tfrac{1}{2})\eta_2,$$

the no flux components

$$
\begin{aligned}
m_n^{31} &= (n+\tfrac{3}{2})\sinh(n+\tfrac{3}{2})\eta_1, \quad m_n^{41} = (n+\tfrac{3}{2})\sinh(n+\tfrac{3}{2})\eta_2,\\
m_n^{32} &= (n+\tfrac{3}{2})\cosh(n+\tfrac{3}{2})\eta_1, \quad m_n^{42} = (n+\tfrac{3}{2})\cosh(n+\tfrac{3}{2})\eta_2,\\
m_n^{33} &= (n-\tfrac{1}{2})\sinh(n-\tfrac{1}{2})\eta_1, \quad m_n^{43} = (n-\tfrac{1}{2})\sinh(n-\tfrac{1}{2})\eta_2,\\
m_n^{34} &= (n-\tfrac{1}{2})\cosh(n-\tfrac{1}{2})\eta_1, \quad m_n^{44} = (n-\tfrac{1}{2})\cosh(n-\tfrac{1}{2})\eta_2
\end{aligned}
$$

and

$$
\mathbf{G}_n = \begin{bmatrix}
-\frac{\sqrt{2}n(n+1)}{2n+1}\left[\frac{e^{-(n-1/2)\eta_1}}{2n-1} - \frac{e^{-(n+3/2)\eta_1}}{2n+3}\right]\\
\frac{\sqrt{2}n(n+1)}{2n+1}\left[\frac{e^{(n-1/2)\eta_2}}{2n-1} - \frac{e^{(n+3/2)\eta_2}}{2n+3}\right]\\
\frac{n(n+1)}{\sqrt{2}(2n+1)}\left[e^{-(n-1/2)\eta_1} - e^{-(n+3/2)\eta_1}\right]\\
\frac{n(n+1)}{\sqrt{2}(2n+1)}\left[e^{(n-1/2)\eta_2} - e^{(n+3/2)\eta_2}\right]
\end{bmatrix}.
$$

Making the definitions

$$
c(n) := \frac{\sqrt{2}n(n+1)}{(2n+1)(2n-1)(2n+3)},
$$

and

$$
\Delta := 4\sinh^2(n+\tfrac{1}{2})(\eta_1-\eta_2) - (2n+1)^2\sinh^2(\eta_1-\eta_2),
$$

we determine the unknowns a_n, b_n, c_n, d_n where, our parentheses sparing convention will not be confused in the following sense

$$
\tfrac{\sinh}{\cosh}(w+x)(y+z) \equiv \tfrac{\sinh}{\cosh}[(w+x)(y+z)] \quad \forall\, w,x,y,z.
$$

One finds

$$
\begin{aligned}
\Delta\, a_n = {} & c(n)(2n+3)\left[(2n+1)(n-\tfrac{1}{2})(\cosh 2\eta_1 - \cosh 2\eta_2)\right.\\
& -2\left((2n-1)\sinh(n+\tfrac{1}{2})(\eta_1-\eta_2)\sinh(n+\tfrac{1}{2})(\eta_1+\eta_2)\right.\\
& \left.\left.-(2n+1)\sinh(n+\tfrac{3}{2})(\eta_1-\eta_2)\sinh(n-\tfrac{1}{2})(\eta_1+\eta_2)\right)\right],\\
\Delta\, b_n = {} & -c(n)(2n+3)\left[(2n+1)(n-\tfrac{1}{2})(\sinh 2\eta_2 - \sinh 2\eta_1)\right.\\
& -2\left((2n-1)\sinh(n+\tfrac{1}{2})(\eta_1-\eta_2)\cosh(n+\tfrac{1}{2})(\eta_1+\eta_2)\right.\\
& -(2n+1)\sinh(n+\tfrac{3}{2})(\eta_1-\eta_2)\cosh(n-\tfrac{1}{2})(\eta_1+\eta_2)\Big)\\
& +4\cdot\exp\left\{-(\eta_1-\eta_2)(n+\tfrac{1}{2})\right\}\sinh(n+\tfrac{1}{2})(\eta_1-\eta_2)\\
& \left.+(2n+1)^2\exp\{\eta_1-\eta_2\}\sinh(\eta_1-\eta_2)\right],\\
\Delta\, c_n = {} & -c(n)(2n-1)\left[(2n+1)(n+\tfrac{3}{2})(\cosh 2\eta_1 - \cosh 2\eta_2)\right.\\
& +2\left((2n+3)\sinh(n+\tfrac{1}{2})(\eta_1-\eta_2)\sinh(n+\tfrac{1}{2})(\eta_1+\eta_2)\right.\\
& \left.\left.+(2n+1)\sinh(n+\tfrac{3}{2})(\eta_1+\eta_2)\sinh(n-\tfrac{1}{2})(\eta_2-\eta_1)\right)\right],\\
\Delta\, d_n = {} & c(n)(2n-1)\left[(2n+1)(n+\tfrac{3}{2})(\sinh 2\eta_1 - \sinh 2\eta_2)\right.\\
& +2\left((2n+3)\sinh(n+\tfrac{1}{2})(\eta_1-\eta_2)\cosh(n+\tfrac{1}{2})(\eta_1+\eta_2)\right.\\
& +(2n+1)\cosh(n+\tfrac{3}{2})(\eta_1+\eta_2)\sinh(n-\tfrac{1}{2})(\eta_2-\eta_1)\Big)\\
& +4\cdot\exp\left\{-(\eta_1-\eta_2)(n+\tfrac{1}{2})\right\}\sinh(n+\tfrac{1}{2})(\eta_1-\eta_2)\\
& \left.-(2n+1)^2\exp\{-(\eta_1-\eta_2)\}\sinh(\eta_1-\eta_2)\right].
\end{aligned}
$$

These coefficients are distinct from those found by Stimson and Jeffery [162] because of the present choice in boundary conditions. Note that the method here is generalisable in the boundary conditions, demonstrating the utility of the coordinate system. A corollary of the

result is that the calculations are valid for retreating spheres, since the change in boundary conditions is equivalent to the permutation of two rows of M, which amounts to a change in the sign of $\det M$ and thus a global sign change on a_n, b_n, c_n, d_n. This can also be seen as a consequence of the reversibility of Stokes flow.

3.7 The Force Experienced By The Spheres

Happel and Brenner [75] give an exact expression for the force on a sphere given in terms of the stream function in cylindrical coordinates

$$F_z = \mu\pi \int_S r^3 \, \partial_{\mathbf{n}} \left(\frac{L_{-1}\psi}{r^2} \right) \mathrm{d}s \tag{3.7.1}$$

where μ is dynamic viscosity, S is a meridian line of the sphere and $\mathrm{d}s$ is an infinitesimal arc length measured in radians. Thus we require an explicit expression for L_{-1}, applied to ψ, in bipolar coordinates.

Lemma 3.7.1. *In bipolar coordinates the integrand of* (3.7.1) *before applying the normal derivative takes the form*

$$\begin{aligned}\left[\frac{L_{-1}\psi}{r^2} \right]_n = \frac{(\cosh\eta - \mathfrak{x})^{5/2}}{c^4(1-\mathfrak{x}^2)} \Big[& Q_n(\mathfrak{x}) \left(R_n''(\eta) - \tfrac{2\sinh\eta}{\cosh\eta - \mathfrak{x}} R_n'(\eta) \right. \\ & \left. + \tfrac{3}{4} \tfrac{3\mathfrak{x} + \cosh\eta}{\cosh\eta - \mathfrak{x}} R_n(\eta) \right) + (1-\mathfrak{x}^2) R_n(\eta) \left(Q_n''(\mathfrak{x}) + \tfrac{2}{\cosh\eta - \mathfrak{x}} Q_n'(\mathfrak{x}) \right) \Big].\end{aligned} \tag{3.7.2}$$

Proof. We work with the representation of the result L_{-1} as found in Lemma 3.4.3. We choose the latter setting $k = -1$ therein. With this form we take (3.6.6) and apply $r^{-2}L_{-1}$, assuming the summand decays sufficiently fast for uniform convergence to permit the commutation of the summation sign and two derivatives in ξ and η. With this it is not too hard to obtain the term wise expression of the integrand

$$\begin{aligned}\left[\frac{L_{-1}\psi}{r^2} \right]_n = -\Big[& (\cot\xi - \cosh\eta \, \csc\xi)^2 (4Q_n(\cos\xi)(2\sinh\eta \, R_n(\eta) \\ & + (\cos\xi - \cosh\eta) R_n''(\eta)) + R_n(\eta)(-3(3\cos\xi + \cosh\eta) Q_n(\cos\xi) \\ & + 4(\cosh\eta \, \cot\xi - \csc\xi + 3\sin\xi) \tfrac{\mathrm{d}}{\mathrm{d}\xi} Q_n(\cos\xi) \\ & + 4(\cos\xi - \cosh\eta) \tfrac{\mathrm{d}^2}{\mathrm{d}\xi^2} Q_n(\cos\xi)) \Big] / \left(4\, c^4 \sqrt{\cosh\eta - \cos\xi} \right)\end{aligned} \tag{3.7.3}$$

By writing $\mathfrak{x} = \cos\xi$ and performing the ξ derivatives explicitly

$$\begin{aligned}\tfrac{\mathrm{d}}{\mathrm{d}\xi} Q_n(\cos\xi) &= -\sin\xi \, Q_n'(\mathfrak{x}), \\ \tfrac{\mathrm{d}^2}{\mathrm{d}\xi^2} Q_n(\cos\xi) &= -\mathfrak{x} \, Q_n'(\mathfrak{x}) + (1-\mathfrak{x}^2) Q_n''(\mathfrak{x}).\end{aligned}$$

and rearranging one recovers (3.7.3) thus lemma is proved. □

We now use the expression for the integrand in Lemma 3.7.1 to compute the force. First we identify an integral which will be useful for the following calculations.

Lemma 3.7.2. *Fix $\eta \in (-\infty, \infty)$. For each $n \in \mathrm{N}$, Q_n as in Lemma 3.6.1 one has*

$$\int_{-1}^{1} \frac{\mathrm{d}\mathfrak{x} \, Q_n(\mathfrak{x})}{(\cosh\eta - \mathfrak{x})^{1/2}} = 2\sqrt{2} \left[\frac{e^{\mp\left(n+\frac{3}{2}\right)\eta}}{2n+3} - \frac{e^{\mp\left(n-\frac{1}{2}\right)\eta}}{2n-1} \right]$$

where the signs are chosen according to satisfaction of boundary conditions and to obtain uniform convergence upon infinite summation where required.

Proof. By using the expansion form of the quotient integrand, (3.6.19) we have by direct calculation

$$\int_{-1}^{1}\frac{\mathrm{d}\mathfrak{x}\,Q_n(\mathfrak{x})}{(\cosh\eta-\mathfrak{x})^{1/2}}=\sqrt{2}\int_{-1}^{1}\mathrm{d}\mathfrak{x}\,Q_n(\mathfrak{x})\sum_{k=0}^{\infty}e^{\mp(k+\frac{1}{2})}P_k(\mathfrak{x})=\sqrt{2}\sum_{k=0}^{\infty}e^{\mp(k+\frac{1}{2})}\int_{-1}^{1}\mathrm{d}\mathfrak{x}\,Q_n(\mathfrak{x})P_k(\mathfrak{x})$$
$$=2\sqrt{2}\left[\frac{e^{\mp\left(n+\frac{3}{2}\right)\eta}}{2n+3}-\frac{e^{\mp\left(n-\frac{1}{2}\right)\eta}}{2n-1}\right]$$

where we have used uniform convergence from the exponentially decaying summand to interchange the integrand and summation signs and in the last line we have used the identity (3.6.14). □

Definition 3.7.3. *Let $n\in\mathbb{N}$ and define*

$$w_n(\eta):=2\sqrt{2}\left[\frac{e^{\mp\left(n+\frac{3}{2}\right)\eta}}{2n+3}-\frac{e^{\mp\left(n-\frac{1}{2}\right)\eta}}{2n-1}\right].$$

Lemma 3.7.4. *The infinitesimal line element of the integral* (3.7.1) *has the explicit form*

$$r^3\mathrm{d}s=-c^4\frac{(1-\mathfrak{x}^2)\,\mathrm{d}\mathfrak{x}}{(\cosh\eta-\mathfrak{x})^4}.$$

Proof. By referring to appendicies of [75] the line element along an arbitrary curve for a general curvilinear orthogonal coordinate system $\mathbf{q}$ transformed from orthogonal coordinates $\mathbf{r}$ is given by

$$\mathrm{d}s^2=\mathfrak{h}_\eta^2\mathrm{d}q_1^2+\mathfrak{h}_\xi^2\mathrm{d}q_2^2+\mathfrak{h}_3^2\mathrm{d}q_3^2$$

where $\mathfrak{h}_\eta$, $\mathfrak{h}_\xi$, $\mathfrak{h}_3$ are the metrical coefficients corresponding to the transformation from $\mathbf{r}$ to $\mathbf{q}$ space, and the $\mathfrak{h}_i$ are defined as the reciprocal of the definition in [75]. Note that by Lemma 3.4.4 $\mathfrak{h}_\eta=\mathfrak{h}_\xi$ and $\mathfrak{h}_\theta=1$ is the metrical coefficient corresponding to the unchanged polar angle θ. Note too that in (3.7.1) the radius of the bipolar circle is held constant, thus $\mathrm{d}q_1=\mathrm{d}\eta=0$. Note also that along a meridian line of a sphere $\mathrm{d}\theta=0$, thus the only contribution to the line integral is $\mathrm{d}\xi$. Therefore after combining these facts, using the expression (3.3.2) and substituting $\mathfrak{x}=\cos\xi$ on obtains

$$r^3\mathrm{d}s=-\frac{c^3\sin^3\xi}{(\cosh\eta-\cos\xi)^3}\cdot\frac{c}{\cosh\eta-\cos\xi}\cdot\frac{\mathrm{d}\mathfrak{x}}{\sin\xi}.$$

Upon writing $\sin^2\xi=1-\mathfrak{x}^2$ the lemma is proved. □

Remark 3.7.5. *The length of a half equator may be calculated by choosing a stream function φ such that $\partial_{\mathbf{n}}r^{-2}L_{-1}\varphi=r^{-3}$. Take the formula* (3.7.1) *with φ defined such, then*

$$\int_S r^3\partial_{\mathbf{n}}\left[\tfrac{L_{-1}\varphi}{r^2}\right]\mathrm{d}s=-c\int_0^\pi\tfrac{\mathrm{d}\xi}{\cosh\eta-\cos\xi}=\frac{2c\,\mathrm{arctanh}\left[\frac{(\cosh\eta+1)\tan\frac{\xi}{2}}{\sqrt{1-\cosh^2\eta}}\right]}{\sqrt{1-\cosh^2\eta}}\Bigg|_0^\pi=\tfrac{c\pi}{\sinh\eta}=\pi r_1.$$

Lemma 3.7.6. *In spherical bipolar coordinates the normal derivative is given by*

$$\partial_n=\mathfrak{h}^{-1}\partial_\eta.$$

Proof. By definition the normal derivative is $\mathbf{n}\cdot\nabla_{\mathbf{q}}$. Now by referring to [75] the gradient operator is given by

$$\nabla_{\mathbf{q}}=\mathfrak{h}^{-1}\mathbf{i}_\eta\partial_\eta+\mathfrak{h}^{-1}\mathbf{i}_\xi\partial_\xi+\mathfrak{h}_\theta^{-1}\mathbf{i}_\theta\partial_\theta$$

thus by orthogonality of the basis $\{\mathbf{i}_\eta, \mathbf{i}_\xi, \mathbf{i}_\theta\}$ to $\mathbf{n}$ parallel $\mathbf{i}_\eta$ by direct computation we have

$$\partial_n = \mathbf{n} \cdot [\mathfrak{h}^{-1}\mathbf{i}_\eta \partial_\eta + \mathfrak{h}^{-1}\mathbf{i}_\xi \partial_\xi + \mathfrak{h}_\theta^{-1}\mathbf{i}_\theta \partial_\theta] = \mathfrak{h}^{-1}\partial_\eta$$

where we have used $\mathbf{i}_\eta = \mathbf{n}$. □

Remark 3.7.7. *The first few derivatives of $w_n(\eta)$ are*

$$\begin{aligned}
\frac{\mathrm{d}w_n}{\mathrm{d}\eta} &= -\tfrac{\sinh\eta}{2}\int_{-1}^{1} \tfrac{\mathrm{d}\mathfrak{x}\, Q_n(\mathfrak{x})}{(\cosh\eta-\mathfrak{x})^{3/2}}, \\
\frac{\mathrm{d}^2w_n}{\mathrm{d}\eta^2} &= \tfrac{3\,\sinh^2\eta}{4}\int_{-1}^{1} \tfrac{\mathrm{d}\mathfrak{x}\, Q_n(\mathfrak{x})}{(\cosh\eta-\mathfrak{x})^{5/2}} - \tfrac{\cosh\eta}{2}\int_{-1}^{1} \tfrac{\mathrm{d}\mathfrak{x}\, Q_n(\mathfrak{x})}{(\cosh\eta-\mathfrak{x})^{3/2}}, \\
\frac{\mathrm{d}^3w_n}{\mathrm{d}\eta^3} &= -\tfrac{\sinh\eta}{2}\int_{-1}^{1} \tfrac{\mathrm{d}\mathfrak{x}\, Q_n(\mathfrak{x})}{(\cosh\eta-\mathfrak{x})^{3/2}} + \tfrac{9\,\sinh\eta\,\cosh\eta}{4}\int_{-1}^{1} \tfrac{\mathrm{d}\mathfrak{x}\, Q_n(\mathfrak{x})}{(\cosh\eta-\mathfrak{x})^{5/2}} - \tfrac{15\,\sinh^3\eta}{8}\int_{-1}^{1} \tfrac{\mathrm{d}\mathfrak{x}\, Q_n(\mathfrak{x})}{(\cosh\eta-\mathfrak{x})^{7/2}}.
\end{aligned}$$

Lemma 3.7.8. *The force experienced by either sphere can be written in the form*

$$F_z = \sum_{n=1}^{\infty} s^{(1)}(n) + s^{(2)}(n) + s^{(3)}(n) + s^{(4)}(n)$$

where the $s^{(i)}(n)$ are a linear combination of the derivatives of $w_n(\eta)$.

Proof. First consider the integral representation of $w_n(\eta)$

$$w_n(\eta) = \int_{-1}^{1} \frac{\mathrm{d}\mathfrak{x}\, Q_n(\mathfrak{x})}{(\cosh\eta - \mathfrak{x})^{1/2}}.$$

Starting with the result of lemma 3.7.1 we differentiate (3.7.2) with respect to η (again assuming uniform convergence of the implicit infinite summation), which is the directional derivative parallel to the outward normal unit $\mathbf{n}$. Performing the differentiation term-wise we write the right hand side in terms of $w_n(\eta)$ and its derivatives. We will define intermediate integrals $\mathscr{G}_j$, $j = 1, 2, 3, 4, 5$ before collecting like powers of $\cosh\eta - \mathfrak{x}$. Firstly observe that

$$\begin{aligned}
&\mathfrak{h}^{-1}\partial_\eta\left[\frac{(\cosh\eta-\mathfrak{x})^{5/2}}{c^4(1-\mathfrak{x}^2)}Q_n(\mathfrak{x})R_n''(\eta)\right] \\
&\quad= \tfrac{Q_n(\mathfrak{x})}{c^5(1-\mathfrak{x}^2)}\left[\tfrac{5}{2}R_n''(\eta)\sinh\eta\,(\cosh\eta-\mathfrak{x})^{5/2} + R_n^{(3)}(\eta)(\cosh\eta-\mathfrak{x})^{7/2}\right].
\end{aligned}$$

Multiplying by $r^3\mathrm{d}s$, the form as in Lemma 3.7.4, and integrating over $[-1, 1]$ one has

$$\mathscr{G}_1 := -c^{-1}\int_{-1}^{1} \mathrm{d}\mathfrak{x}\, Q_n(\mathfrak{x})\left[\tfrac{5}{2}\tfrac{R_n''(\eta)\sinh\eta}{(\cosh\eta-\mathfrak{x})^{3/2}} + \tfrac{R_n^{(3)}(\eta)}{(\cosh\eta-\mathfrak{x})^{1/2}}\right].$$

Secondly one has

$$\begin{aligned}
&\mathfrak{h}^{-1}\partial_\eta\left[-\tfrac{2(\cosh\eta-\mathfrak{x})^{3/2}}{c^4(1-\mathfrak{x}^2)}\sinh\eta\, Q_n(\mathfrak{x})R_n'(\eta)\right] \\
&= -\tfrac{2\,Q_n(\mathfrak{x})}{c^5(1-\mathfrak{x}^2)}\Big[R_n''(\eta)\sinh\eta\,(\cosh\eta-\mathfrak{x})^{5/2} \\
&\qquad + R_n'(\eta)\left(\cosh\eta\,(\cosh\eta-\mathfrak{x})^{5/2} + \tfrac{3}{2}\sinh^2\eta\,(\cosh\eta-\mathfrak{x})^{3/2}\right)\Big].
\end{aligned}$$

Multiplying this expression by $r^3\mathrm{d}s$ and integrating over $[-1, 1]$ one has

$$\mathscr{G}_2 := c^{-1}\int_{-1}^{1} \mathrm{d}\mathfrak{x}\, 2\, Q_n(\mathfrak{x})\left[\tfrac{R_n''(\eta)\sinh\eta}{(\cosh\eta-\mathfrak{x})^{3/2}} + \tfrac{R_n'(\eta)\,\cosh\eta}{(\cosh\eta-\mathfrak{x})^{3/2}} + \tfrac{3\sinh^2\eta\, R_n'(\eta)}{2(\cosh\eta-\mathfrak{x})^{5/2}}\right].$$

Thirdly we compute

$$\mathfrak{h}^{-1}\partial_\eta\left[\tfrac{3}{4}\tfrac{(\cosh\eta-\mathfrak{x})^{5/2}}{c^4(1-\mathfrak{x}^2)}\tfrac{\cosh\eta+3x}{\cosh\eta-\mathfrak{x}}Q_n(\mathfrak{x})R_n(\eta)\right]$$

by writing $\cosh\eta=-3\cosh\eta+4\cosh\eta$ to control the form of the individual terms. In particular one obtains

$$\begin{aligned}&\mathfrak{h}^{-1}\partial_\eta\left[\tfrac{3}{4}\tfrac{(\cosh\eta-\mathfrak{x})^{5/2}}{c^4(1-\mathfrak{x}^2)}\tfrac{\cosh\eta+3x}{\cosh\eta-\mathfrak{x}}Q_n(\mathfrak{x})R_n(\eta)\right]\\&=\tfrac{3\,Q_n(\mathfrak{x})}{4c^5(1-\mathfrak{x}^2)}\left[\tfrac{5}{2}\left(\cosh\eta-\mathfrak{x}\right)^{5/2}(\tfrac{4\cosh\eta}{\cosh\eta-\mathfrak{x}}-3)R_n(\eta)\sinh\eta\right.\\&\quad+(\cosh\eta-\mathfrak{x})^{7/2}(\tfrac{4\sinh\eta}{\cosh\eta-\mathfrak{x}}-\tfrac{4\sinh\eta\cosh\eta}{(\cosh\eta-\mathfrak{x})^2})R_n(\eta)\\&\quad\left.+(\cosh\eta-\mathfrak{x})^{7/2}(\tfrac{4\cosh\eta}{\cosh\eta-\mathfrak{x}}-3)R_n'(\eta)\right]\end{aligned}$$

Multiplying this expression by $r^3\mathrm{d}s$ and integrating over $[-1,\,1]$ one has

$$\begin{aligned}\mathscr{G}_3:=-c^{-1}\int_{-1}^{1}\mathrm{d}\mathfrak{x}\,&\tfrac{3\,Q_n(\mathfrak{x})}{4(\cosh\eta-\mathfrak{x})^4}\left[\tfrac{5}{2}\left(\cosh\eta-\mathfrak{x}\right)^{5/2}(\tfrac{4\cosh\eta}{\cosh\eta-\mathfrak{x}}-3)R_n(\eta)\sinh\eta\right.\\&+(\cosh\eta-\mathfrak{x})^{7/2}(\tfrac{4\sinh\eta}{\cosh\eta-\mathfrak{x}}-\tfrac{4\sinh\eta\cosh\eta}{(\cosh\eta-\mathfrak{x})^2})R_n(\eta)\\&\left.+(\cosh\eta-\mathfrak{x})^{7/2}(\tfrac{4\cosh\eta}{\cosh\eta-\mathfrak{x}}-3)R_n'(\eta)\right].\end{aligned}$$

equivalently

$$\mathscr{G}_3=-c^{-1}\int_{-1}^{1}\mathrm{d}\mathfrak{x}\,\tfrac{3}{4}Q_n(\mathfrak{x})\left[\tfrac{6\,\sinh\eta\,\cosh\eta\,R_n(\eta)}{(\cosh\eta-\mathfrak{x})^{5/2}}-\tfrac{7\,\sinh\eta\,R_n(\eta)}{2(\cosh\eta-\mathfrak{x})^{3/2}}+\tfrac{4\cosh\eta\,R_n'(\eta)}{(\cosh\eta-\mathfrak{x})^{3/2}}-\tfrac{3\,R_n'(\eta)}{(\cosh\eta-\mathfrak{x})^{1/2}}\right].$$

Fourthly we compute

$$\mathfrak{h}^{-1}\partial_\eta\left[\tfrac{(\cosh\eta-\mathfrak{x})^{5/2}}{(1-\mathfrak{x}^2)}\tfrac{(1-\mathfrak{x}^2)}{c^4}Q_n''(\mathfrak{x})R_n(\eta)\right].$$

Using the ODE (3.6.3) as an integration formula for $Q_n''(\mathfrak{x})$ one obtains

$$\begin{aligned}&\mathfrak{h}^{-1}\partial_\eta\left[\tfrac{(\cosh\eta-\mathfrak{x})^{5/2}}{(1-\mathfrak{x}^2)}\tfrac{(1-\mathfrak{x}^2)}{c^4}Q_n''(\mathfrak{x})R_n(\eta)\right]\\&\quad=-\tfrac{n(n+1)Q_n(\mathfrak{x})}{c^5(1-\mathfrak{x}^2)}\left[\tfrac{5}{2}(\cosh\eta-\mathfrak{x})^{5/2}\sinh\eta\,R_n(\eta)+(\cosh\eta-\mathfrak{x})^{7/2}R_n'(\eta)\right].\end{aligned}$$

Multiplying this expression by $r^3\mathrm{d}s$ and integrating over $[-1,\,1]$ one has

$$\mathscr{G}_4:=c^{-1}\int_{-1}^{1}\mathrm{d}\mathfrak{x}\,n(n+1)Q_n(\mathfrak{x})\left[\tfrac{5\,\sinh\eta\,R_n(\eta)}{2(\cosh\eta-\mathfrak{x})^{3/2}}+\tfrac{R_n'(\eta)}{(\cosh\eta-\mathfrak{x})^{1/2}}\right].$$

Fifthly we compute

$$\mathfrak{h}^{-1}\partial_\eta\left[\tfrac{2(\cosh\eta-\mathfrak{x})^{3/2}}{c^4}Q_n'(\mathfrak{x})R_n(\eta)\right].$$

The derivative of $Q_n'(\mathfrak{x})$ will be removed by integration by parts, computing the normal derivative first one has

$$\begin{aligned}&\mathfrak{h}^{-1}\partial_\eta\left[\tfrac{2(\cosh\eta-\mathfrak{x})^{3/2}}{c^4}Q_n'(\mathfrak{x})R_n(\eta)\right]\\&\quad=\tfrac{2Q_n'(\mathfrak{x})}{c^5}\left[\tfrac{3}{2}(\cosh\eta-\mathfrak{x})^{3/2}\sinh\eta\,R_n(\eta)+(\cosh\eta-\mathfrak{x})^{5/2}R_n'(\eta)\right].\end{aligned}$$

Now multiplying by $r^3\mathrm{d}s$ in the form of Lemma 3.7.4 and integrating over $[-1,\,1]$ one has the

expression

$$-c^{-1}\int_{-1}^{1}\mathrm{d}\mathfrak{x}\,\tfrac{2(1-\mathfrak{x}^2)Q_n'(\mathfrak{x})}{(\cosh\eta-\mathfrak{x})^4}\left[\tfrac{3}{2}(\cosh\eta-\mathfrak{x})^{3/2}\sinh\eta\,R_n(\eta)+(\cosh\eta-\mathfrak{x})^{5/2}R_n'(\eta)\right].$$

Now integrating by parts one obtains

$$\begin{aligned}
&-c^{-1}\int_{-1}^{1}\mathrm{d}\mathfrak{x}\,\tfrac{2(1-\mathfrak{x}^2)Q_n'(\mathfrak{x})}{(\cosh\eta-\mathfrak{x})^4}\left[\tfrac{3}{2}(\cosh\eta-\mathfrak{x})^{3/2}\sinh\eta\,R_n(\eta)+(\cosh\eta-\mathfrak{x})^{5/2}R_n'(\eta)\right]\\
&\quad=c^{-1}\int_{-1}^{1}\mathrm{d}\mathfrak{x}\,(1-\mathfrak{x}^2)Q_n(\mathfrak{x})\left[\tfrac{15\,\sinh\eta\,R_n(\eta)}{2(\cosh\eta-\mathfrak{x})^{7/2}}+\tfrac{3\,R_n'(\eta)}{(\cosh\eta-\mathfrak{x})^{5/2}}\right]\\
&\quad-c^{-1}\int_{-1}^{1}\mathrm{d}\mathfrak{x}\,\mathfrak{x}\,Q_n(\mathfrak{x})\left[\tfrac{6\,\sinh\eta\,R_n(\eta)}{(\cosh\eta-\mathfrak{x})^{5/2}}+\tfrac{4\,R_n'(\eta)}{(\cosh\eta-\mathfrak{x})^{3/2}}\right]
\end{aligned}\tag{3.7.4}$$

The integrals on the right hand side of (3.7.4) are not all yet proportional to $w_n(\eta)$ or its derivatives due to the powers of $\mathfrak{x}$ present in the integrand. To proceed we use the recurrence relation (3.6.4) and an elementary corollary, namely

$$(1-\mathfrak{x}^2)\,Q_n(\mathfrak{x})=-\tfrac{(n+2)(n+3)}{(2n+3)(2n+5)}Q_{n+2}(\mathfrak{x})+\tfrac{2n\,(n+1)}{(2n-1)(2n+3)}Q_n(\mathfrak{x})-\tfrac{(n-1)(n-2)}{(2n-1)(2n-3)}Q_{n-2}(\mathfrak{x})$$

so that the final integral is given by

$$\begin{aligned}
\mathscr{G}_5:=c^{-1}&\int_{-1}^{1}\mathrm{d}\mathfrak{x}\,\left[-\tfrac{(n+2)(n+3)}{(2n+3)(2n+5)}Q_{n+2}(\mathfrak{x})+\tfrac{2n\,(n+1)}{(2n-1)(2n+3)}Q_n(\mathfrak{x})-\tfrac{(n-1)(n-2)}{(2n-1)(2n-3)}Q_{n-2}(\mathfrak{x})\right]\\
&\times\left[\tfrac{15\,\sinh\eta\,R_n(\eta)}{2(\cosh\eta-\mathfrak{x})^{7/2}}+\tfrac{3\,R_n'(\eta)}{(\cosh\eta-\mathfrak{x})^{5/2}}\right]\\
-c^{-1}&\int_{-1}^{1}\mathrm{d}\mathfrak{x}\,\left[\tfrac{n+2}{2n+3}Q_{n+1}(\mathfrak{x})+\tfrac{n-1}{2n-1}Q_{n-1}(\mathfrak{x})\right]\left[\tfrac{6\,\sinh\eta\,R_n(\eta)}{(\cosh\eta-\mathfrak{x})^{5/2}}+\tfrac{4\,R_n'(\eta)}{(\cosh\eta-\mathfrak{x})^{3/2}}\right].
\end{aligned}$$

Collecting like powers of $\cosh\eta-\mathfrak{x}$ in the integrands of the $\mathscr{G}_j$ we may define the four following $s^{(i)}$, $i=1,2,3,4$

$$s^{(1)}:=\int_{-1}^{1}\mathrm{d}\mathfrak{x}\,\tfrac{Q_n(\mathfrak{x})}{(\cosh\eta-\mathfrak{x})^{1/2}}\left[-R_n^{(3)}(\eta)+\tfrac{9}{4}R_n'(\eta)+n(n+1)R_n'(\eta)\right],$$

$$\begin{aligned}
s^{(2)}:=&\int_{-1}^{1}\mathrm{d}\mathfrak{x}\,\tfrac{Q_n(\mathfrak{x})}{(\cosh\eta-\mathfrak{x})^{3/2}}\left[-\tfrac{1}{2}R_n''(\eta)\,\sinh\eta-\cosh\eta\,R_n'(\eta)\right.\\
&\left.+\tfrac{21}{8}\sinh\eta\,R_n(\eta)+\tfrac{5}{2}n(n+1)\sinh\eta\,R_n(\eta)\right]\\
&-\int_{-1}^{1}\mathrm{d}\mathfrak{x}\,\left[\tfrac{n+2}{2n+3}Q_{n+1}(\mathfrak{x})+\tfrac{n-1}{2n-1}Q_{n-1}(\mathfrak{x})\right]\tfrac{4\,R_n'(\eta)}{(\cosh\eta-\mathfrak{x})^{3/2}},
\end{aligned}$$

$$\begin{aligned}
s^{(3)}:=&\int_{-1}^{1}\mathrm{d}\mathfrak{x}\tfrac{Q_n(\mathfrak{x})}{(\cosh\eta-\mathfrak{x})^{5/2}}\left[3\sinh^2\eta\,R_n'(\eta)-\tfrac{9}{2}\sinh\eta\,\cosh\eta\,R_n(\eta)\right]\\
&-\int_{-1}^{1}\mathrm{d}\mathfrak{x}\,\left[\tfrac{n+2}{2n+3}Q_{n+1}(\mathfrak{x})+\tfrac{n-1}{2n-1}Q_{n-1}(\mathfrak{x})\right]\tfrac{6\,\sinh\eta\,R_n(\eta)}{(\cosh\eta-\mathfrak{x})^{5/2}}\\
&+\int_{-1}^{1}\mathrm{d}\mathfrak{x}\,\left[-\tfrac{(n+2)(n+3)}{(2n+3)(2n+5)}Q_{n+2}(\mathfrak{x})+\tfrac{2n\,(n+1)}{(2n-1)(2n+3)}Q_n(\mathfrak{x})\right.\\
&\left.-\tfrac{(n-1)(n-2)}{(2n-1)(2n-3)}Q_{n-2}(\mathfrak{x})\right]\tfrac{3\,R_n'(\eta)}{(\cosh\eta-\mathfrak{x})^{5/2}},
\end{aligned}$$

$$s^{(4)} := \int_{-1}^{1} \mathrm{d}\mathfrak{x} \left[-\tfrac{(n+2)(n+3)}{(2n+3)(2n+5)} Q_{n+2}(\mathfrak{x}) + \tfrac{2n\,(n+1)}{(2n-1)(2n+3)} Q_n(\mathfrak{x}) \right.$$
$$\left. -\tfrac{(n-1)(n-2)}{(2n-1)(2n-3)} Q_{n-2}(\mathfrak{x}) \right] \tfrac{15 \sinh\eta\, R_n(\eta)}{2(\cosh\eta - \mathfrak{x})^{7/2}}.$$

By inspection one sees each of the $\mathscr{F}_i$ may be written as linear combinations of high order derivatives of $w_n(\eta)$. □

Lemma 3.7.9. *Let $p \in \mathbb{N}$ then there exists explicit expressions for the integral*

$$\mathscr{I}^n_{p\,2} := \int_{-1}^{1} \frac{\mathrm{d}\mathfrak{x}\, Q_n(\mathfrak{x})}{(\cosh\eta - \mathfrak{x})^{p+1/2}}$$

in terms of linear combinations of the derivatives of $w_n(\eta)$. In particular for the first few p one has

$$\mathscr{I}^n_{3\,2} = -2\,\mathrm{csch}\,\eta\, w_n'(\eta),$$

$$\mathscr{I}^n_{5\,2} = \tfrac{4\,\mathrm{csch}^2\,\eta}{3} \left[w_n''(\eta) + \tfrac{\cosh\eta}{2} \mathscr{I}^n_{3\,2} \right],$$

$$\mathscr{I}^n_{7\,2} = -\tfrac{8\,\mathrm{csch}^3\,\eta}{15} \left[w_n^{(3)}(\eta) - \tfrac{9\,\cosh\eta\,\sinh\eta}{4} \mathscr{I}^n_{5\,2} + \tfrac{\sinh\eta}{2} \mathscr{I}^n_{3\,2} \right]$$

Proof. By Remark 3.7.7 one may obtain the explicit expressions. □

Theorem 3.7.10. *The force experienced by either sphere in dimensional form is given by*

$$F_z^1 = \sqrt{2} c\pi\mu U \sum_{n=1}^{\infty} (2n+1)(a_n + b_n + c_n + d_n), \tag{3.7.5}$$

$$F_z^2 = -\sqrt{2} c\pi\mu U \sum_{n=1}^{\infty} (2n+1)(-a_n + b_n - c_n + d_n). \tag{3.7.6}$$

Proof. By substituting the formulae in Lemma 3.7.9 into Lemma 3.7.8 and rearranging we are done.

□

Note that nowhere in the calculation is any information on the a_n, b_n, c_n, d_n required. In particular, alternative boundary condition choices amount to a different linear system to be solved and a redefinition of these series coefficients. For practical applications the series (3.7.5), (3.7.6) must be truncated at some order $n = N_* < \infty$, but since we know the behaviour of the functions a_n, b_n, c_n, d_n by (3.6.3), particularly they decay exponentially in n for each fixed η_1 and η_2, the truncation will produce only exponentially small errors.

3.8 Comparison With Existing Methods

In this section we compare our expression for $a(\cdot)$ to the results obtained using multipole and perturbative methods. We make use of computer code which computes expansion coefficients for the multipole method available online [88]. We show that our results are significantly more accurate and efficient to compute, and cannot be reproduced by the multipole expansion programme. It is widely accepted that for two sphere problems, when tractable, spherical bipolar coordinates will yield the most accurate method to calculate the force. We refer the reader to previous publications making reference to this, which instead use multipole and lubrication methods to carry out the calculations [91, 92, 98]. Whilst such spherical bipolar methods have been used in previous studies of hydrodynamic interactions, we can find no reference to their use in the singular problem studied here.

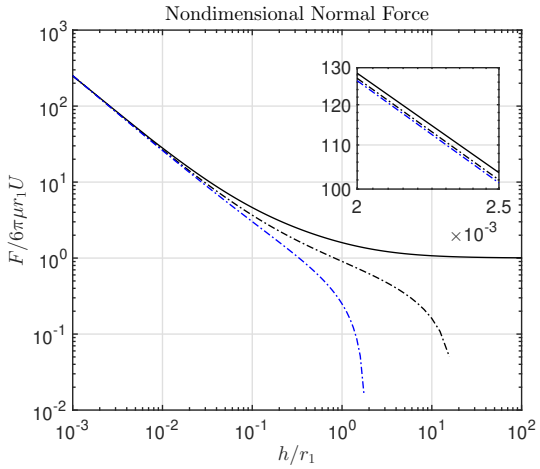

(a) A comparison of the force for equal spheres $r_1 = r_2$. F_z^1 (**solid-black**), F_z^e (**black-dot-dashed**), $F_{z,l}$ (blue-dot-dashed). Inset: magnified view of each solution as $h/r_1 \to 0$.

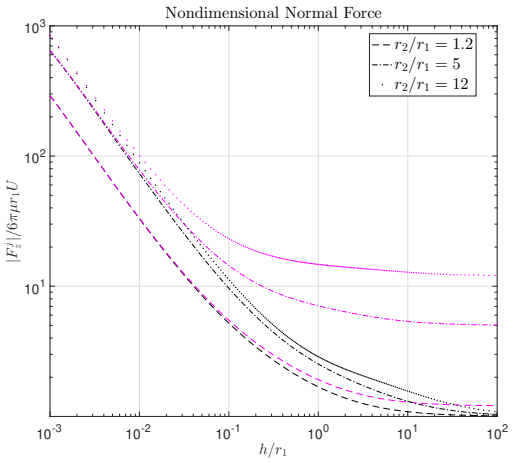

(b) The hydrodynamic force on sphere 1 (**black**) and sphere 2 (magenta) for three different radii ratios r_2/r_1 using the present theory and formulas (3.7.5), (3.7.6).

Figure 3.2: Plots of the present theory and the lubrication results for the squeezing force.

We do this because we have identified the absence of any analytical calculations reducing corresponding expressions available in spherical bipolar coordinates to asymptotic expansions for the force in the separation distance. Previous such 'asymptotic' results, such as those in Kim and Karilla [98], are, in fact, not asymptotic and contain divergent terms both as the spheres approach (which is physically reasonable), and as the spheres become widely-separated (which is completely unphysical). This introduces a need for artificial cutoffs, or matching procedures.

Up until now there has been no ratification of the expressions for the widely used resistance functions X_{11}^A, X_{22}^A, for the force on sphere 1 and 2 respectively, as defined in [92] against spherical bipolar coordinates. There is simply (unquantified) wisdom concerning the inefficiency of the computation of the X_{11}^A, X_{22}^A as the separation distance tends to zero [91]. Pertaining to this, we provide the numerical comparison and identify the short comings in using the series representations of X_{11}^A, X_{22}^A for practical applications.

3.8.1 Inner Region Lubrication Theory

In this section we present a comparison between the exact (3.7.5),(3.7.6) (valid for all separation and sphere sizes), and asymptotic formulae (A.1.9)–(A.1.10) (valid for all sphere sizes) determined by the present work and the existing lubrication theory [98]. In Table 3.1 and Figure 3.3 we compare F_z^i ((3.7.5),(3.7.6)), F_z^e (A.1.10), and $F_{z,l}$ by defining the 'lubrication theory' formula

$$F_{z,l} := \tfrac{2\beta^2\epsilon^{-1}}{(1+\beta)^2} + \tfrac{2\beta(1+7\beta+\beta^2)}{5(1+\beta)^3}\log\epsilon^{-1}. \tag{3.8.1}$$

We have truncated this expression to $\log(\cdot)$, omitting terms equal to and higher than $\epsilon\log\epsilon$ because those higher order terms are based on the expansion of a stream function at $r = \infty$ without proper control on the convergence of the force integral used to compute $F_{z,l}$. The exact force, as given by (3.7.5), as well as an interpolant produces a hydrodynamic force varying smoothly between the small and large argument limits, as seen in Figure 3.2a for two equal spheres. In Figure 3.2b we plot the functions (3.7.5), (3.7.6) for different radii ratios.

The force calculated from the asymptotic formula (A.1.10) deviates from the exact solution and becomes unphysical at large separation, as expected. However, from Figure 3.2a (with inset), we observe that our asymptotic formula F_z^e agrees more closely with the exact formula F_z^1 than $F_{z,l}$. In particular F_z^e is barely visible on top of the black curve. This is true even for distances up to one radius, r_1, whilst $F_{z,l}$ agrees with F_z^1 only for distances less than one tenth of r_1.

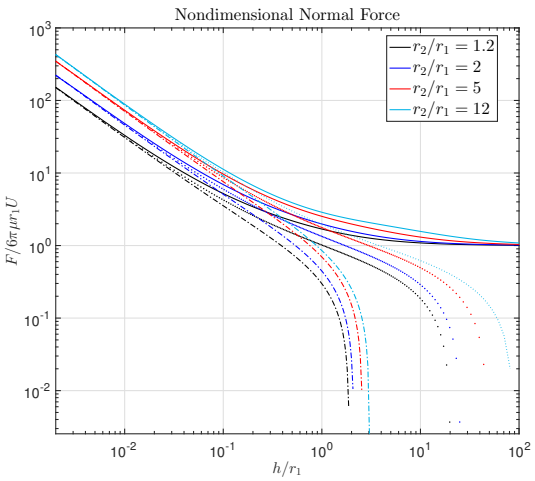

(a) The force on sphere 1 for different radii ratios $r_2/r_1 \geq 1$. Exact F_z^1 (solid), $F_{z,l}$ (dot-dashed) and F_z^e (dot).

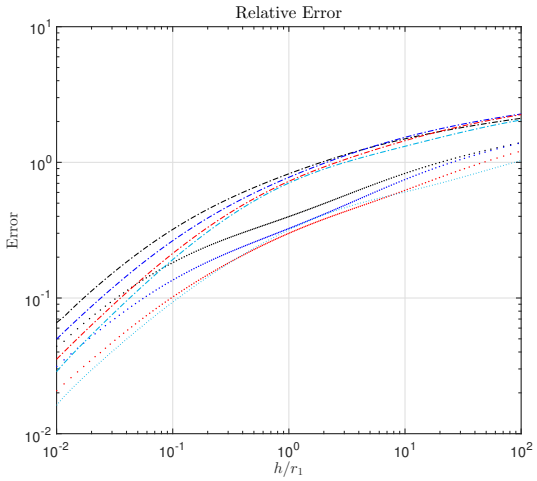

(b) The relative error to the exact force for each the two asymptotic formulae, $F_{z,l}$ (dot-dashed) and F_z^e (dot). Colours as in (a).

Figure 3.3: A comparison of force formulae with varying radii ratios. For exact unequal spheres (A.1.1) was solved numerically to obtain corresponding η_1, η_2 ordinates before summing the functionals (3.7.5), (3.7.6) and truncating the infinite series to within machine precision.

Table 3.1: Comparison of exact and approximate nondimensional forces with $r_2/r_1 = 5$.

h	$\frac{\text{Centre Distance}}{\text{Diameter}}$		$F_z^1 \cdot 10^4$	$-F_z^2 \cdot 10^3$	$F_z^* \cdot 10^4$	$F_{z,l} \cdot 10^4$
	sphere 1	sphere 2			sphere 1	sphere 1
0.0001	3.0000	0.6000	1.3896	2.7801	1.3896	1.3894
0.0212	3.0106	0.6021	0.0069	0.0148	0.0069	0.0068
0.1008	3.0504	0.6101	0.0017	0.0043	0.0017	0.0015
0.3217	3.1609	0.6322	0.0007	0.0023	0.0007	0.0005
1.1291	3.5646	0.7129	0.0003	0.0016	0.0003	0.0001
9.9660	7.9830	1.5966	0.0002	0.0011	0.00004	-0.0001
∞	∞	∞	0.0001	0.0010	-	-

We also demonstrate the applicability of the exact and asymptotic formulae to unequal spheres of various size ratios in Figure 3.2b, 3.3a and 3.3b. In each of these figures $h = d - r_1 - r_2$ is dimensional. We remark that in Figure 3.2b we plot the magnitude of the force on either sphere for different radii ratios and note that, by the definitions (3.3), as $d_1 + d_2 \to r_1 + r_2$ and hence as $h \to 0$, the forces are equal and opposite as we would expect by Newton's third law. That is, once the forces F_z^j are scaled by the same Stokes constant, they collapse onto each other for all $r_2/r_1 > 0$. This may be seen more rigorously by repeating the analysis of Section A.1 on sphere 2; one finds $F_z^2/(6\pi\mu U r_2) \sim -4\beta^2/(1+\beta)^3\alpha^{-2}$. The force magnitude, however, increases as the radii ratio increases; see Figures 3.2b, 3.3a. The relative error for the present asymptotic formula in Figure 3.3b using (A.1.9) improves monotonically as r_2/r_1 becomes larger. This was observed to hold for even larger ratios (not shown for clarity).

3.8.2 The Multipole Expansion Functions

In this section we examine the behaviour of the multipole scalar resistance functions X_{ij}^A as defined in Jeffrey and Onishi [92]. Local to this section only we define some notation to be consistent with Jeffrey and Onishi [92]: a_1, a_2 are the radii of spheres 1 and 2 respectively, λ is the sphere radii ratio, s is a nondimensional separation parameter, ξ is s shifted by two, and h

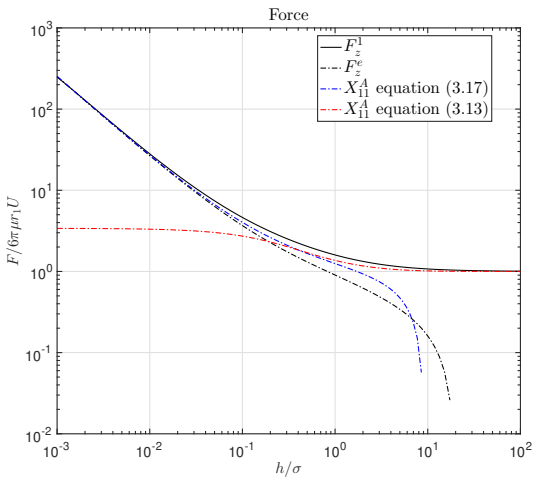

(a) The force on sphere 1 comparing various formalisms with $r_2/r_1 = 1$. Key: spherical bipolar coordinates (**black-solid**), asymptotic expansion F_z^e obtained by spherical bipolar coordinates (**black-dot-dashed**), X_{11}^A (red-dot-dashed) as computed using provided 300 terms in Jeffrey [88] for the equation (3.13) in Jeffrey and Onishi [92], the expansion of X_{11}^A including the order 1 term A_{11}^X equation (3.17) of Jeffrey and Onishi [92] (blue-dot-dashed).

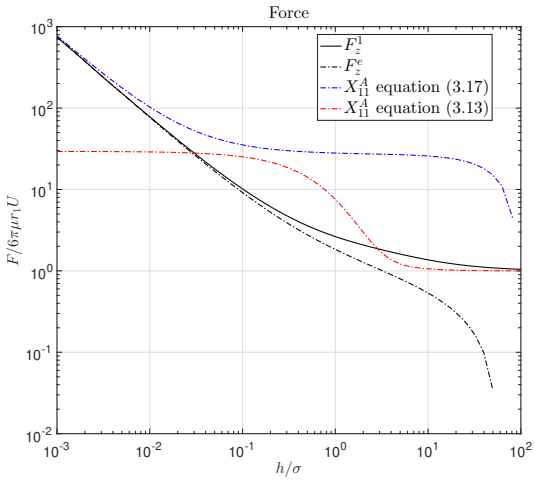

(b) The force on unequal spheres for $r_2/r_1 = 2\pi$: spherical bipolar coordinates (**black-solid**), asymptotic expansion F_z^e obtained by spherical bipolar coordinates (**black-dashed -dot**), X_{ij}^A as computed using 15 terms in the equation (3.13) of Jeffrey and Onishi [92] (red-dot-dashed), the expansion of X_{11}^A including the order 1 term A_{11}^X equation (3.17) of Jeffrey and Onishi [92] (blue-dot-dashed).

Figure 3.4: A comparison of the normal component of the HI as obtained by the present theory and multipole methods.

is the dimensional sphere surface separation. The following hold

$$\lambda = \frac{a_2}{a_1}, \quad s - 2 = 2\frac{h/a_1}{1+\lambda}, \quad \xi = s - 2.$$

The existing programs consist of Fortran code for the resistance functions X_{11}^A (and X_{22}^A) as defined in Jeffrey and Onishi [92], provided by D. J. Jeffrey [88]. The functions X_{11}^A and X_{22}^A are expressions for the force normal to the sphere surfaces due to sphere 1 and sphere 2, respectively. We now demonstrate that our corresponding functions F_z^1 and F_z^2 are more accurate than X_{11}^A and X_{22}^A in computing the force both for arbitrary sphere size ratios and for arbitrary sphere separations. See Figures 3.4a and 3.4b.

For Figure 3.4a we computed both the X_{11}^A by using equation (3.13) of Jeffrey and Onishi [92] and via the asymptotic form (3.17) of Jeffrey and Onishi [92] using the first 300 terms f_m as provided by the code [89] and compared to the results obtained by spherical bipolar coordinates. Indeed Figure 3.4a shows a substantial difference in the singular behaviour between the spherical bipolar and multipole formalisms, particularly in the small argument region where many summand terms are required for an accurate representation of X_{11}^A. The largest shortcoming of the multipole method is that the coefficients of summand of X_{11}^A, denoted $f_k(\lambda)$, are not all known for all λ and require large computing resources [88, 91]. When computing more $f_m(\lambda)$ the authors found the solution of recurrence relation (3.9) Jeffrey and Onishi [92] increasingly difficult for both m, $\lambda \to \infty$. For the expanded version of X_{11}^A given by eq (3.17) of Jeffrey and Onishi [92] the behaviour can be understood by closely looking at the formula for the order 1 term A_{11}^X (3.17)

$$A_{11}^X = 1 - \tfrac{1}{4}g_1 + \sum_{\substack{m=2 \\ m \text{ even}}}^{\infty} [2^{-m}(1+\lambda)^{-m} f_m(\lambda) - g_1 - 2m^{-1}g_2 + 4m^{-1}m_1^{-1}g_3]$$

where $g_1(\lambda)$, $g_2(\lambda)$, $g_3(\lambda)$, $m_1(m)$ are all known. We see that this series has a divergent term, namely $-2m^{-1}g_2$. Using this formula for A_{11}^X and the expansion as $\xi \to 0$ one has

$$X_{11}^A = g_1(\lambda)\xi^{-1} + g_2(\lambda)\log\xi^{-1} + A_{11}^X(\lambda) + g_3(\lambda)\xi\log\xi^{-1} \quad \text{as } \xi \to 0,$$

which we compare to the expansion F_z^e (A.1.10) as well as the formula F_z^1 valid for arbitrary separations.

It is apparent from Figure 3.4b (using the first 15 terms as provided by Jeffrey [88]) that when using the infinite series formula for X_{11}^A to compute the force for a larger aspect ratio $r_2/r_1 = 2\pi$ we see a considerable disagreement with the calculations obtained in spherical bipolar coordinates. The X_{11}^A may perform better in the near field when more f_m are known, but computing these coefficients is inefficient for practical applications, and more so for larger aspect ratios $\lambda \to \infty$, as we found when calculating more than 15 f_m for the purposes of this work. We are confident in the calculation of X_{11}^A used to produce Figures 3.4a-3.4b because we were able to reproduce the tabulated values of $A_{11}^X(1)$ as listed in section 3.3 in Jeffrey and Onishi [92]. Meanwhile the spherical bipolar formalism gives an explicit formula for all summand terms and provides the correct decay structure both as the centre distance decreases and increases. We therefore contend that the results obtained using spherical bipolar coordinates are more efficient, accurate and cannot already be produced with existing methods.

Chapter 4

Microhydrodynamics 2: Spheres Converging Perpendicular To Their Line Of Centres

In this chapter we solve Stokes equations in spherical bipolar coordinates with the view to calculate the tangential component of the short range hydrodynamic interaction. We study exact solutions for the slow viscous flow of an infinite liquid caused by two rigid spheres moving parallel to their line of centres, valid at all separations. As in the case of the normal component of the interaction, this goes beyond the applicable range of existing solutions for singular HI which, for practical applications, are limited to the near-contact or far field region of the flow.

For this tangential component of the HI, by use of a bipolar coordinate system, we obtain the corresponding infinite series expression of the (shear) singular force between the spheres. However, due to the reduction in the symmetry of the system, principally because the flow is no longer isotropic, there is a limit to the amount of analytical progress which can be made. In particular, it is not possible to obtain asymptotic formulae on the local profile of the tangential force, due to the deficiency in the number of analytical expressions for expansion coefficients for the velocity field. The complete set of coefficients constructing the velocity field are found to satisfy depend on a single three term recurrence relation which must be solved numerically.

4.1 Organisation Of The Chapter

This chapter presents the rigorous derivation and asymptotic analysis of the singular HI $b(\cdot)$ valid for all non-contacting particle separations. In Section 4.2 we state boundary value problem to be solved and decompose Stokes equations into a coupled set of simpler PDEs. In Section 4.3 we transform the PDEs to spherical bipolar variables and solve each of them sequentially. In Section 4.4 we transform the boundary conditions into spherical bipolar coordinates. In Appendix B.1 we provide the recurrence relations determining series coefficients for general unequal spheres. In Section 4.5 we determine simpler three term recurrence relation for the equal sphere sub case. Finally in Section 4.6 we calculate the force as an infinite series in the solutions of the recurrence relations found in the previous sections.

4.2 Stokes Equations

When the fluid velocity between the spheres can not be expressed as the curl of a scalar field we instead consider the uncurled incompressible Navier-Stokes equations for laminar flow, (by setting $Re = 0$

$$\mu^{-1}\nabla p = \nabla^2 \mathbf{u},$$
$$\nabla \cdot \mathbf{u} = 0.$$

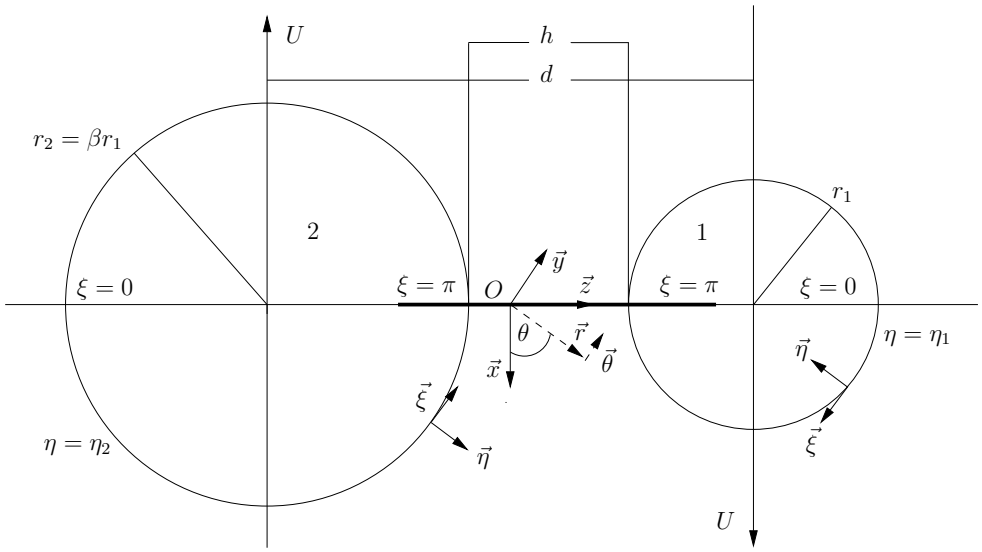

Figure 4.1: Schematic of two unequal spheres of radii r_1, r_2 converging perpendicular to their line of centres in viscous fluid. Included in the diagram are the cylindrical and bipolar unit vectors, the dimensional gap distance h, and centre to centre distance d. Note that η_1 and η_2 are implicit functions of r_1, r_2 and d.

The appropriate boundary conditions will be seen to be

$$\begin{aligned} \mathbf{u} &= U\hat{\mathbf{e}}_x \qquad \text{on sphere 1,} \\ \mathbf{u} &= -U\hat{\mathbf{e}}_x \quad \text{on sphere 2} \end{aligned}$$

along with the far field condition $\mathbf{u} \to \mathbf{0}$ as $|\mathbf{x}| \to \infty$. In circular cylindrical coordinates the equations governing fluid pressure and the three velocity fields read

$$\mu^{-1}\partial_r p = \left(\nabla^2 - \frac{1}{r^2}\right) u_r - \frac{2}{r^2}\partial_\theta u_\theta, \tag{4.2.1a}$$

$$\mu^{-1} r^{-1}\partial_\theta p = \left(\nabla^2 - \frac{1}{r^2}\right) u_\theta + \frac{2}{r^2}\partial_\theta u_r, \tag{4.2.1b}$$

$$\mu^{-1}\partial_z p = \nabla^2 u_z \tag{4.2.1c}$$

where it is emphasised that ∇^2 is now expressed in cylindrical coordinates

$$\nabla^2 = \partial_r^2 + r^{-1}\partial_r + r^{-2}\partial_\theta^2 + \partial_z^2.$$

The incompressibility condition becomes

$$\partial_r u_r + r^{-1}u_r + r^{-1}\partial_\theta u_\theta + \partial_z u_z = 0 \tag{4.2.2}$$

and the boundary conditions are

$$u_r = U\cos\theta, \quad u_\theta = -U\sin\theta, \quad u_z = 0, \quad \text{on sphere 1} \tag{4.2.3a}$$

$$u_r = -U\cos\theta, \quad u_\theta = U\sin\theta, \quad u_z = 0. \quad \text{on sphere 2.} \tag{4.2.3b}$$

Our interest is in solving momentum equations (4.2.1a)–(4.2.1c), along with the incompressibility assumption (4.2.2), subject to the no flux and no slip boundary conditions (4.2.3a), (4.2.3b) in spherical bipolar coordinates. The coordinate system is the same as the one considered in Chapter 3 for the normal HI mode, and we provide for convenience a schematic of the spherical bipolar geometry with appropriate velocities for the tangential HI mode in Figure 4.1. We now seek to convert our equations to spherical bipolar coordinates. Firstly we recast the

cylindrical equations (4.2.1a)–(4.2.1c) and incompressibility condition (4.2.2) into a simpler set of coupled boundary value PDEs in terms of the axisymmetric potential operators L_1.

4.2.1 Projection Onto Legendre Functions

By the careful choice of three auxiliary functions $(X(r,z), Y(r,z), Z(r,z))$, the governing equations (4.2.1a), (4.2.1b), (4.2.1c) can be written in terms of a known differential operator. Firstly consider the decomposition

$$c\,p = 2\mu U W(r,z)\cos\theta, \tag{4.2.4a}$$
$$c\,u_r = U\left[rW(r,z) + c\left(X(r,z)+Y(r,z)\right)\right]\cos\theta, \tag{4.2.4b}$$
$$c\,u_\theta = U\left[X(r,z) - Y(r,z)\right]\sin\theta, \tag{4.2.4c}$$
$$c\,u_z = U\left[zW(r,z) + 2cZ(r,z)\right]\cos\theta \tag{4.2.4d}$$

where $c > 0$ is the same geometrical constant as in Chapter 3, U is an arbitrary velocity scale and μ is the fluid viscosity. By substituting these relations into the velocity equations and incompressibility condition we obtain the following equations

$$\partial_r W = \left(\partial_r^2 + r^{-1}\partial_r - 2r^{-2} + \partial_z^2\right)\frac{c}{2}\left(X+Y\right) + \left(\partial_r^2 + r^{-1}\partial_r - 2r^{-2} + \partial_z^2\right)\frac{rW}{2} - \frac{c\left(X-Y\right)}{r^2}, \tag{4.2.5a}$$
$$0 = \left(\partial_r^2 + r^{-1}\partial_r - 2r^{-2} + \partial_z^2\right)\frac{c}{2}\left(X-Y\right) - \frac{c\left(X+Y\right)}{r^2}, \tag{4.2.5b}$$
$$\partial_z W = \left(\partial_r^2 + r^{-1}\partial_r - r^{-2} + \partial_z^2\right)zW + 2c\left(\partial_r^2 + r^{-1}\partial_r - r^{-2} + \partial_z^2\right)Z, \tag{4.2.5c}$$
$$0 = 3W + r\partial_r W + z\partial_z W + c\partial_r Y + c\partial_r X + 2cr^{-1}X + 2c\partial_z Z. \tag{4.2.5d}$$

By adding (4.2.5a) to equation (4.2.5b), subtracting (4.2.5b) from equation (4.2.5a) and along with (4.2.5c) and (4.2.5d) we have the solvability conditions in terms of the differential operator L_1

$$L_1 W = \frac{W}{r^2}, \tag{4.2.6a}$$
$$L_1 X = \frac{4X}{r^2}, \tag{4.2.6b}$$
$$L_1 Y = 0, \tag{4.2.6c}$$
$$L_1 Z = \frac{Z}{r^2}, \tag{4.2.6d}$$
$$0 = 3W + r\partial_r W + z\partial_z W + c\partial_r Y + c\partial_r X + 2cr^{-1}X + 2c\partial_z Z \tag{4.2.6e}$$

where

$$L_1 = \partial_z^2 + \partial_r^2 + r^{-1}\partial_r.$$

Recall that L_1 is a particular case of the differential operator L_k given by

$$L_k = \partial_z^2 + \partial_r^2 + k\,r^{-1}\partial_r$$

which is a closely studied operator in axially symmetric potential theory by those such as Weinstein[174] and Payne [136] and in particular [137] wherein explicit solutions for Stokes flow around classes of axially symmetric bodies are considered. Solutions to equations such as

$$L_k\omega(r,z) = 0$$

are referred to as axially symmetric potential functions, and by formulating the translating sphere problem in terms of the operator L_k we may exploit the properties of solutions to such equations. Notably the homogeneous problem $L_1\omega = 0$ in spherical bipolar coordinates has a

solution expressable in a complete basis of Legendre polynomials.

4.3 Conversion To Spherical Bipolar Coordinates

By making the transformation (3.3.1) the generalised operator L_k is given in bipolar spherical coordinates as

$$L_k = r^{-k}\mathfrak{h}^2\left\{\partial_\xi\left(r^k\partial_\xi\right) + \partial_\eta\left(r^k\partial_\eta\right)\right\}.$$

4.3.1 Equation For Y

We would like to solve the simplest PDE of the system (4.2.6a)-(4.2.6e) namely equation (4.2.6c). We write $\hat{Y}(\xi,\eta) = Y(r(\xi,\eta), z(\xi,\eta))$ and as in [75] we make the ansatz (taking $k=1$)

$$\hat{Y}(\xi,\eta) = r^{-1/2}f(\xi)g(\eta)$$

then it will be seen that $\hat{Y}$ is a solution to $L_1\hat{Y}$ provided

$$\frac{fg}{4h^2r^2} + f''g + g''f = 0. \tag{4.3.1}$$

Moreover the PDE (4.3.1) is solvable via a separation solution in f and g provided $\mathfrak{h}^{-2}r^{-2}$ is partitionable in functions of ξ and η, more explicitly we require

$$\frac{1}{\mathfrak{h}^2r^2} = P(\xi) + Q(\eta)$$

for some P and Q functions solely of ξ and η respectively. Indeed this is the case, in particular in spherical bipolar coordinates one observes the metrical coefficient $\mathfrak{h}$ is such that

$$\frac{1}{\mathfrak{h}^2r^2} = \csc^{-2}\xi.$$

Thus we take $P(\xi) = \csc^{-2}\xi$ and $Q(\eta) \equiv 0$. By writing equation (4.3.1) with functions of ξ on one side and functions of η on the other, we conclude that both sides vary independently in ξ and η and must therefore equal a separation constant $-\lambda^2$. It is necessary to take the separation constant negative in order to satisfy the boundary conditions. In summary we must solve the system of ODEs

$$f'' + \left(\lambda^2 - \frac{1}{4\sin^2\xi}\right)f = 0, \tag{4.3.2}$$

$$g'' - \lambda^2 g = 0. \tag{4.3.3}$$

The ODE (4.3.3) is elementary, being solved by an arbitrary linear combination of hyperbolic trigonometric functions

$$g(\eta) = A\cosh\lambda\eta + B\sinh\lambda\eta.$$

For the ODE (4.3.2) we make the transformation $\bar{\xi} = \cos\xi$ rendering it

$$\left(1-\bar{\xi}^2\right)f'' - \bar{\xi}f' + \left(\lambda^2 - \frac{1}{4\left(1-\bar{\xi}^2\right)}\right)f = 0.$$

We make a further ansatz $f = \left(\bar{\xi}^2-1\right)^{1/4}\bar{f}$ to obtain an equation for $\bar{f}$

$$\left(1-\bar{\xi}^2\right)\bar{f}'' - 2\bar{\xi}\bar{f}' + \left(\lambda^2 - \frac{1}{4}\right)\bar{f} = 0.$$

Now upon writing $n(n+1) = \lambda^2 - \frac{1}{4}$ we find that

$$\lambda = n + \tfrac{1}{2} \quad \text{for} \quad n = 0, 1, 2, ...$$

and $\bar{f} = P_n$ is the Legendre polynomial of order n. Using the principle of linear superposition we have the general solution to (4.2.6c)

$$\hat{Y}(\xi, \eta) = \sqrt{\cosh\eta - \cos\xi} \sum_{n=0}^{\infty} \left[D_n \cosh(n + \tfrac{1}{2})\eta + E_n \sinh(n + \tfrac{1}{2})\eta \right] P_n(\cos\xi).$$

4.3.2 Equation For W And Z

To solve equation (4.2.6a) (equivalently (4.2.6d)) we use an analogous separation method that was used for (4.2.6c) in section 4.3.1. We write $\hat{W}(\xi, \eta) = W(r(\xi, \eta), z(\xi, \eta))$ and upon choosing the ansatz

$$\hat{W}(\xi, \eta) = r^{-1/2} f(\xi) g(\eta)$$

where f and g are not necessarily the same functions found in Sections 3.6, 4.3.1 we find we must solve

$$-\frac{3fg}{4\sin\xi^2} + f''v + v''f = 0.$$

Equivalently we have the system of ODEs

$$f'' + \left(\lambda^2 - \frac{3}{4\sin^2\xi} \right) f = 0,$$
$$g'' - \lambda^2 g = 0.$$

where λ^2 is the separation constant (not necessarily the same as in section 4.3.1). We make the ansatz $f = (\bar{\xi}^2 - 1)^{1/4} \bar{f}$ to yield

$$\left(1 - \bar{\xi}^2\right) \bar{f}'' - 2\bar{\xi}\bar{f}' + \left(\lambda^2 - \frac{1}{4} - \frac{1}{1 - \bar{\xi}^2} \right) \bar{f} = 0$$

which we recognise as the associated Legendre equation with $m = 1$ and $\lambda = n + \frac{1}{2}$. Thus

$$\bar{f} = P_n^{(1)}(\bar{\xi})$$

where $P_n^{(1)}(\mathfrak{x})$ is the associated Legendre function with $m = 1$. Upon using the standard relation

$$P_n^{(1)}(\mathfrak{x}) = (-1)^m (1 - \mathfrak{x}^2)^{m/2} \frac{\mathrm{d}^m}{\mathrm{d}\mathfrak{x}^m} P_n(\mathfrak{x}) \tag{4.3.4}$$

along with the principle of linear superposition we have

$$\hat{W}(\xi, \eta) = \sin\xi \sqrt{\cosh\eta - \cos\xi} \sum_{n=1}^{\infty} \left[B_n \cosh(n + \tfrac{1}{2})\eta \; + C_n \sinh(n + \tfrac{1}{2})\eta \right] P_n'(\cos\xi),$$
$$\hat{Z}(\xi, \eta) = \sin\xi \sqrt{\cosh\eta - \cos\xi} \sum_{n=1}^{\infty} \left[A_n \cosh(n + \tfrac{1}{2})\eta \; + H_n \sinh(n + \tfrac{1}{2})\eta \right] P_n'(\cos\xi).$$

We remark that the sums are to be taken starting $n = 1, 2, ..$ because solutions to the associated Legendre equation are nonzero and nonsingular when $0 \leq m = 1 \leq n$.

4.3.3 Equation For X

To solve equation (4.2.6b) we write $\hat{X}(\xi,\eta) = X(r(\xi,\eta), z(\xi,\eta))$ and make the usual separation ansatz. The separated ξ dependent ODE becomes

$$\left(1-\bar{\xi}^2\right)\bar{f}'' - 2\bar{\xi}\bar{f}' + \left(\lambda^2 - \frac{1}{4} - \frac{4}{1-\bar{\xi}^2}\right)\bar{f} = 0$$

which we recognise as the associated Legendre equation with $m = 2$ and $\lambda = n + \frac{1}{2}$. Thus after using (4.3.4) with $m = 2$ we have the general solution for $\hat{X}$

$$\hat{X}(\xi,\eta) = \sin^2\xi\sqrt{\cosh\eta - \cos\xi}\sum_{n=2}^{\infty}\left[F_n\cosh(n+\tfrac{1}{2})\eta + G_n\sinh(n+\tfrac{1}{2})\eta\right]P_n''(\cos\xi)$$

noting the sums are to be taken starting $n = 2, 3, ..$ because solutions to the associated Legendre equation are nonzero and nonsingular when $0 \le m = 2 \le n$.

All that remains is to apply the boundary conditions (4.2.3a)-(4.2.3b) transformed into spherical-bipolar coordinates to the appropriately combined general solutions $\hat{W}$, $\hat{X}$, $\hat{Y}$, $\hat{Z}$.

4.4 Boundary Conditions

The boundary conditions (4.2.3a), (4.2.3b) are transformed into the corresponding conditions on the auxiliary fields $W(r,z), X(r,z), Y(r,z), Z(r,z)$. By the expressions for u_r, u_θ, u_z (4.2.4b), (4.2.4c), (4.2.4d) respectively we obtain on sphere 1

$$\frac{1}{c}r^{(1)}W_1 + X_1 + Y_1 = 1, \tag{4.4.1}$$

$$X_1 - Y_1 = -1, \tag{4.4.2}$$

$$z^{(1)}W_1 + 2cZ_1 = 0, \tag{4.4.3}$$

and on sphere 2

$$\frac{1}{c}r^{(2)}W_2 + X_2 + Y_2 = -1, \tag{4.4.4}$$

$$X_2 - Y_2 = 1, \tag{4.4.5}$$

$$z^{(2)}W_2 + 2cZ_2 = 0, \tag{4.4.6}$$

where

$$z^{(1)} = c\frac{\sinh\eta_1}{\cosh\eta_1 - \cos\xi}, \qquad r^{(1)} = c\frac{\sin\xi}{\cosh\eta_1 - \cos\xi},$$
$$z^{(2)} = c\frac{\sinh\eta_2}{\cosh\eta_2 - \cos\xi}, \quad r^{(2)} = c\frac{\sin\xi}{\cosh\eta_2 - \cos\xi}.$$

In the singular case, when two spheres are converging perpendicular to there line of centres we do not expect the fluid pressure to remain bounded. Since we expect a divergent pressure field for small separations along the z axis, equivalently $\cos\xi = \pm 1$, the general solution to (4.2.6a)–(4.2.6e) is found by setting $H_n = 0$ for every n. The six boundary conditions along with the incompressibility condition (4.2.6e) form seven equations for the seven unknowns A_n–G_n.

4.5 Recurrence Relations For Equal Spheres

We now obtain the unknown constants for the case of equal spheres. A set of recurrence relations for the unequal sphere case are presented in Appendix B.1 but are not solved due to algebraic complexity in the relations, which may be overcome with computer algebra. As such we set $\eta_1 = -\eta_2 = \alpha > 0$. In the equal sphere cases, the cylindrical polar (r, z) and spherical bipolar

(η, ξ, θ) coordinates in the right and left hand planes are related by

$$z^{(1)} = c\frac{\sinh\alpha}{\cosh\alpha - \cos\xi}, \qquad r^{(1)} = c\frac{\sin\xi}{\cosh\alpha - \cos\xi},$$
$$z^{(2)} = -c\frac{\sinh\alpha}{\cosh\alpha - \cos\xi}, \quad r^{(2)} = c\frac{\sin\xi}{\cosh\alpha - \cos\xi},$$

where $\alpha \in (0, \infty)$ is the spherical bipolar coordinate which draws a sphere of radius $r_1 = c|\operatorname{csch}\alpha|$ in the right and left hand planes. Additionally, α and is a proxy for the sphere centre distance where $\cosh\alpha = d/r_1$ where d is the centre distance of the spheres.

We now determine A_n–G_n. We once again let $\mathfrak{x} = \cos\xi$, and, by subtracting (4.4.6) from (4.4.3) we find

$$B_n = 0$$

for every n. Similarly by adding together (4.4.1), (4.4.4), similarly (4.4.2) to (4.4.5) we find

$$D_n = F_n = 0$$

for every n. Note that these zero conditions are the complement of the of the zero conditions found in [70]. Using the Bonnet recursion formula

$$(n+1)P_{n+1}(\mathfrak{x}) = (2n+1)\mathfrak{x}P_n(\mathfrak{x}) - nP_{n-1}(\mathfrak{x})$$

along with the integration formula

$$(2n+1)P_n(\mathfrak{x}) = P'_{n+1}(\mathfrak{x}) - P'_{n-1}(\mathfrak{x})$$

one can derive

$$\mathfrak{x}P'_n(\mathfrak{x}) = \frac{n+1}{2n+1}P'_{n-1}(\mathfrak{x}) + \frac{n}{2n+1}P'_{n+1}(\mathfrak{x}). \tag{4.5.1}$$

By adding (4.4.3) to (4.4.6) we find

$$\sinh\alpha\sum_{n=1}^{\infty} C_n \sinh(n+\tfrac{1}{2})\alpha P'_n(\mathfrak{x}) + 2\cosh\alpha\sum_{n=1}^{\infty}\cosh(n+\tfrac{1}{2})\alpha P'_n(\mathfrak{x})$$
$$- 2\sum_{n=1}^{\infty} A_n\cosh(n+\tfrac{1}{2})\alpha\left[\frac{n+1}{2n+1}P'_{n-1}(\mathfrak{x}) + \frac{n}{2n+1}P'_{n-1}(\mathfrak{x})\right] = 0$$

and we obtain a relation for C_n in terms of A_n

$$C_n = 2A_{n+1}\frac{n+1}{2n+3}[\gamma_n + 1] - 2\gamma_n A_n + 2A_{n-1}\frac{n-1}{2n-1}[\gamma_n - 1]$$

where $\gamma_n = \coth\alpha\coth(n+\frac{1}{2})\alpha$ and we have used (4.5.1). Note the definition of γ_n is different to that in [70]. By subtracting (4.4.4) from (4.4.1) and subtracting (4.4.5) from (4.4.2) and finally adding (4.4.6) to (4.4.3) we obtain

$$\frac{\sin\xi}{\cosh\alpha - \mathfrak{x}}[W_1 - W_2] + X_1 - X_2 + Y_1 - Y_2 = 1, \tag{4.5.2}$$
$$X_1 - X_2 - [Y_1 - Y_2] = -1, \tag{4.5.3}$$
$$\frac{\sinh\alpha}{\cosh\alpha - \mathfrak{x}}[W_1 - W_2] + 2[Z_1 + Z_2] = 0.$$

Adding together (4.5.2) and (4.5.3) we find

$$\sum_{n=2}^{\infty} G_n \sinh(n+\tfrac{1}{2})\alpha P_n''(\mathfrak{x}) = \operatorname{csch}\alpha \sum_{n=1}^{\infty} A_n \cosh(n+\tfrac{1}{2})\alpha P_n'(\mathfrak{x})$$

and using the integration formula

$$(2n+1)P_n'(\mathfrak{x}) = P_{n+1}''(\mathfrak{x}) - P_{n-1}''(\mathfrak{x})$$

we obtain a relation for G_n in terms of A_n

$$G_n = \frac{A_{n-1}}{2n-1}\left[\gamma_n - 1\right] - \frac{A_{n+1}}{2n+3}\left[\gamma_n + 1\right].$$

Finally by subtracting (4.5.3) from (4.5.2) we obtain

$$\begin{aligned} 2 = &-\frac{\sin^2\xi}{\sinh\alpha}(\cosh\alpha - \mathfrak{x})^{1/2} \sum_{n=1}^{\infty} A_n \cosh(n+\tfrac{1}{2})\alpha P_n'(\mathfrak{x}) \\ &+ (\cosh\alpha - \mathfrak{x})^{1/2} \sum_{n=1}^{\infty} E_n \sinh(n+\tfrac{1}{2})\alpha P_n(\mathfrak{x}) \end{aligned}$$

and upon using the generating function $(\cosh\alpha - \mathfrak{x})^{-1/2} = \sum_{n=0}^{\infty} s_n P_n(\mathfrak{x})$ where

$$s_n = \sqrt{2}e^{-(n+\frac{1}{2})\alpha}$$

along with the identity

$$(1-\mathfrak{x}^2)P_n'(\mathfrak{x}) = \frac{n(n+1)}{(2n+1)}\left[P_{n-1}(\mathfrak{x}) - P_{n+1}(\mathfrak{x})\right]$$

we obtain a relation for E_n in terms of A_n

$$E_n = 2\sqrt{2}e^{-(n+\frac{1}{2})\alpha}\operatorname{csch}(n+\tfrac{1}{2})\alpha + A_{n+1}\frac{(n+1)(n+2)}{2n+3}\left[\gamma_n+1\right] - A_{n-1}\frac{n(n-1)}{2n-1}\left[\gamma_n - 1\right].$$

We have now obtained six equations involving the seven unknowns A_n–G_n. The only condition thus far unused is the incompressibility condition (4.2.6e), which we will use to identify A_n. Since the incompressibility condition (4.2.6e) is invariant in the choice of boundary conditions we may use the relation (3.56) [37] with our redefined constants. The incompressibility condition (4.2.6e) transformed to spherical bipolar coordinates evaluated on the surface of the sphere $\eta = \alpha$ may be written in the form

$$\mathbf{q}_n(\alpha)\cdot\left[A_{n-1}, A_n, A_{n+1}\right]^{\top} = p_n(\alpha),$$

where

$$\begin{aligned} \mathbf{q}_n(\alpha) := \Big[&(n-1)(\gamma_{n-1}-1) - \tfrac{(n-1)(2n-3)}{2n-1}(\gamma_n - 1), \\ &- \tfrac{n(2n-1)}{2n+1}(\gamma_{n-1}+1) + (2n+1) - 5\gamma_n + \tfrac{(n+1)(2n+3)}{2n+1}(\gamma_{n+1}-1), \\ &\qquad \tfrac{(n+2)(2n+5)}{2n+3}(\gamma_n+1) - (n+2)(\gamma_{n+1}+1)\Big]. \end{aligned}$$

and the right hand side vector may be obtained in a similar way, with the exception that sech's are substituted for csch's.

$$p_n(\alpha) := -\sqrt{2}e^{-(n+1/2)\alpha}\left[e^{\alpha}\operatorname{csch}(n-\tfrac{1}{2})\alpha - 2\operatorname{csch}(n+\tfrac{1}{2})\alpha + e^{\alpha}\operatorname{csch}(n+\tfrac{3}{2})\alpha\right] \qquad (4.5.4)$$

Both equations (4.5) and (4.5.4) were checked with computer algebra.

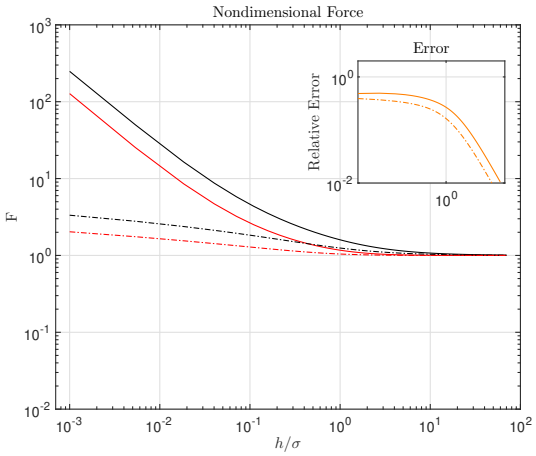

(a) A plot of the normal and tangential components of the force using the formulae valid for arbitrary separation of Jeffrey & Onishi [92] and the present theory **GMS**. The inset shows the relative error between the two formalisms as a function of the sphere distance. The correct far-field behaviour is obtained by Jeffrey & Onishi but the formulae fail in the boundary layer $h/\sigma \sim \epsilon^{1/2}$.

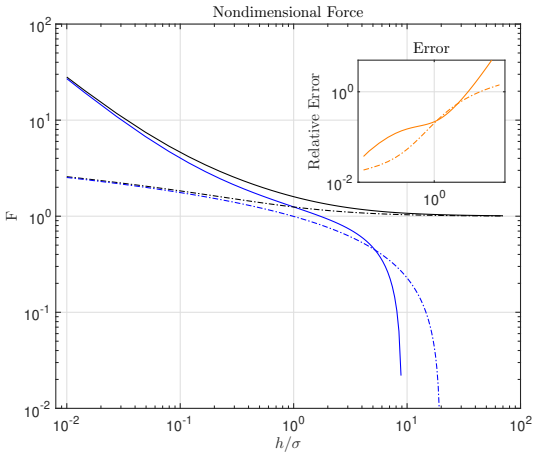

(b) A plot of the normal and tangential components of the force using the formulae valid for the inner region of Kim & Karrila [98] and the present theory **GMS**. The inset shows the relative error between the two formalisms as a function of the sphere distance. Using the inner region formulae of Kim & Karrila, the correct singular behaviour is obtained but the far-field is not valid.

Figure 4.2: A comparison of the normal (solid) and tangential (dashed) forces and the (inset, relative error) between the present work **GMS** and (a) multipole methods of Jeffrey & Onishi and (b) perturbative methods of Kim & Karrila.

4.6 The Force Experienced By The Spheres

There is an exact expression for the force on either sphere for the spherical bipolar coordinate system, first obtained by O'Neil [128] in general form and applied to the case of a single sphere moving parallel to a plane wall. We may use the expression for a two sphere problem, albeit with different summation coefficients owing to the present choice of boundary conditions. We have for equally sized spheres, in dimensional form,

$$F_x^1 = -\sqrt{2}\pi\mu U c \sum_{n=1}^{\infty} E_n + n(n+1)C_n \quad \text{on sphere 1} \tag{4.6.1}$$

$$F_x^2 = \sqrt{2}\pi\mu U c \sum_{n=1}^{\infty} E_n + n(n+1)C_n \quad \text{on sphere 2.} \tag{4.6.2}$$

These expressions may be nondimensionalised with the characteristic drag scale $6\pi\mu U r_1$, recalling that $r_1 = c|\operatorname{csch}\alpha|$. We compute the force as given by the summations (4.6.1), (4.6.2) by solving the three term recurrence relation (4.5) with the boundary condition $A_N = 0$ for a large N for each η. Recall that $d_1/r_1 = \cosh\eta$ where d_1 and r_1 are the centre distance to the origin and radius of the equal spheres respectively. Therefore η acts as a proxy for the sphere distance in spherical bipolar coordinates. The numerical procedure for A_n amounts to solving a tridiagonal linear system with right hand side of (4.5). After A_n has been computed for some set $n \in \{1, \cdots, N\}$ we compute C_n by using (4.5) and E_n by using (4.5).

Once the C_n, E_n are computed for a fixed η, the infinite summations (4.6.1), (4.6.2) may be made (which is now truncated to a partial sum of N terms). This numerical procedure relies on the fact that C_N and E_N (and therefore A_N) decay sufficiently quickly in N for each η. We expect the errors made in this truncation to be exponentially small, c.f. the discussion after Theorem 3.7.

In Figure 4.2 we plot the scalar resistance functions (3.7.5), (4.6.1) to observe their relative magnitude, for varying sphere centre distances, along with $F_{x,l}$ and $F_{z,l}$, formulae (9.24) and (9.33) as found in Kim and Karrila [98, Chapter 9]. For **GMS** the centre distance parameter η is not given in terms of analytical functions for a given centre distance d and radii r_1. As in the normal interaction in Chapter 3, we compute η for each d and r_1 by solving the coupled set of nonlinear equations (A.1.1). As seen in Figure 4.2a, the force as computed with multipole methods Jeffrey & Onishi [92] fails to capture the correct singular behaviour. The inset shows the relative error between the two formalisms (**GMS** and Jeffrey & Onishi) as a function of the sphere distance. Also, as seen in Figure 4.2b, the force as computed with the lubrication theory methods of Kim & Karrila fail to capture the correct far field behaviour. The inset shows the relative error between the two formalisms of **GMS** and Kim & Karrila as a function of the sphere distance.

Chapter 5

Positivity of R

In this chapter we show that the present theory preserves positive definiteness of the grand resistance matrix, which is highly desirable for stochastic simulations of colloidal flow. Conversely we show that the grand resistance matrix as constructed from solutions to Stokes equations obtained by inner region expansions of multipole solutions may become non-positive definite at large enough particle separations.

The Resistance Matrix R

The positivity of the resistance matrix is an important property for many computational applications of the HI including Monte Carlo simulations of stochastic particle dynamics. In particular, for Langevin dynamics of colloids, one must compute $\boldsymbol{R}^{1/2}$, which is defined by the diagonalisation

$$\boldsymbol{R}^{1/2} = \boldsymbol{S}\Lambda^{1/2}\boldsymbol{S}^{-1},$$

where Λ is a diagonal matrix consisting of the eigenvalues of $\boldsymbol{R}$ and $\boldsymbol{S}$ is a unitary matrix consisting of columns of orthonormal eigenvectors of $\boldsymbol{R}$. Such a diagonalisation is ensured to exists when $\boldsymbol{R}$ is symmetric and real. Mathematically speaking, the positivity of $\boldsymbol{R}$ ensures the existence and uniqueness of $\boldsymbol{R}^{1/2}$. Meanwhile, in the sampling of such Langevin trajectories, the positivity is related to the fact that for a particle undergoing friction in a thermostated bath, the rate of mechanical energy dissipation should be positive. A non-positive definite resistance matrix would allow the non-physical situation that a given particle may gain kinetic energy under drag.

In this section we demonstrate that our construction of $\boldsymbol{R}$, using scalar resistance functions determined in spherical bipolar coordinates, conserves positivity as a function of sphere separation for the selected sphere set-ups considered, whereas, the alternative constructions given by assembling $\boldsymbol{R}$ with entries originating from perturbation (Kim & Karrila) or multipole methods (Jeffrey & Onishi), in general do not. For each formalism we obtain numerically the eigenvalues of $\boldsymbol{R}$ such that

$$\boldsymbol{R}\mathbf{e}_i = \lambda_i \mathbf{e}_i$$

for $i = 1, \cdots, 3N$ where λ_i are smooth functions of the intersphere distance for sequence of particle numbers, $N = 2, 3, \cdots$. We use MATLAB's built in function `eig`, which is a robust eigenvalue solver based on QZ iteration for symmetric matrices. The function `eig` uses a Cholesky decomposition when $\boldsymbol{R}$ is positive definite, however for the present work, the definiteness of the resistance matrices for each of the different scalar function assemblies is not known *a priori*, and in particular, one may suspect $\boldsymbol{R}$ may not be positive for some of particle separations (c.f. Oseen tensor[154] as an approximation to the mobility tensor $\boldsymbol{R}^{-1}$) depending on the model used to construct it.

We compute the eigenvalues of $\boldsymbol{R}$ for a) a two sphere system and b) a three sphere system, the schematic for both systems are depicted in Figure 5.1 and Figure 5.2. For both cases we

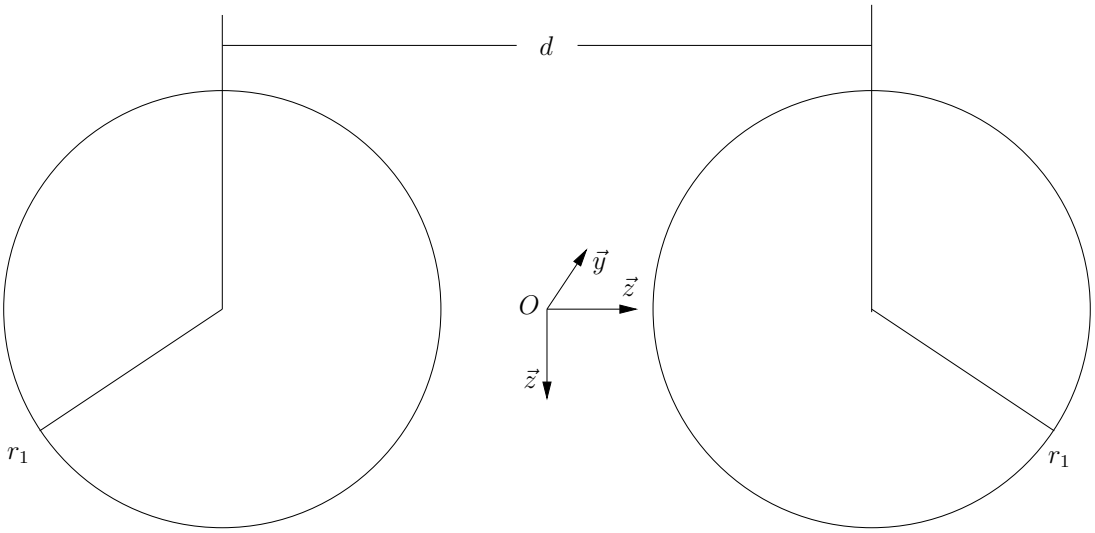

Figure 5.1: Schematic of the two sphere system where d is varied between $\sigma < d < \infty$.

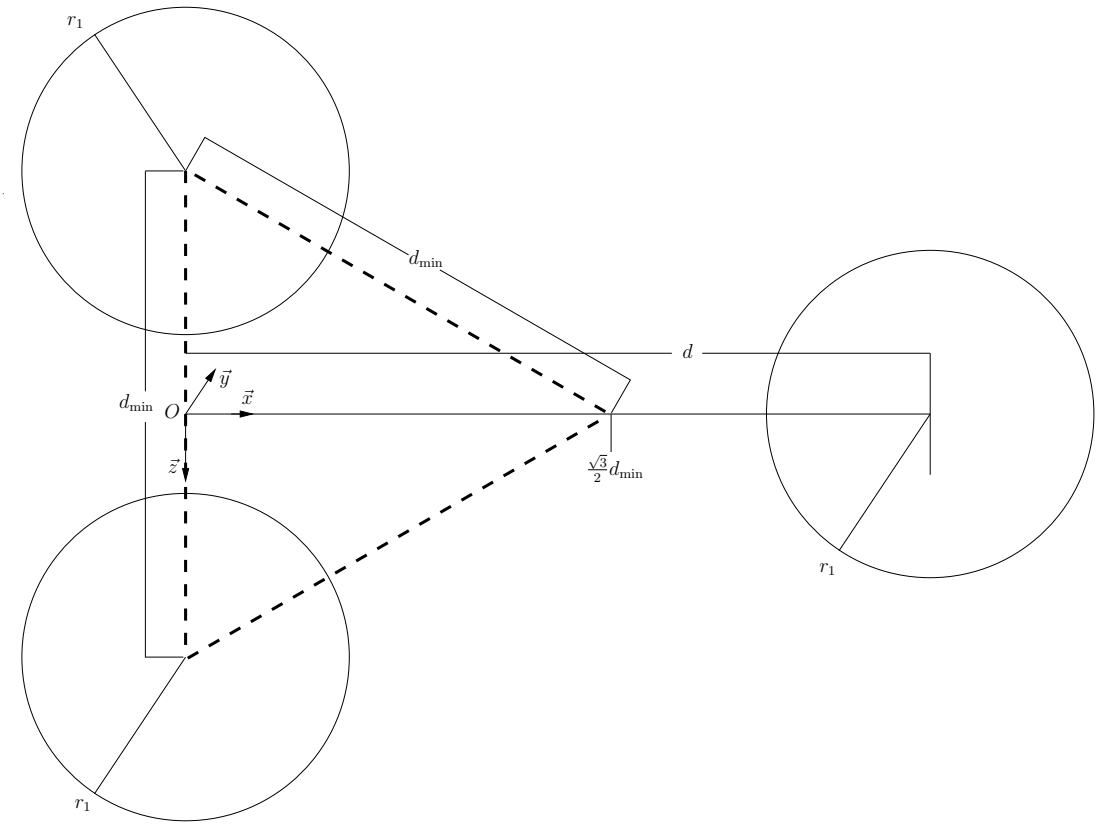

Figure 5.2: Schematic of the three sphere system where two spheres are held fixed, and the centre of a third free sphere at $x = d$ is varied between for $\frac{\sqrt{3}}{2}d_{\min} < d < \infty$ while $d_{\min}$ is held fixed.

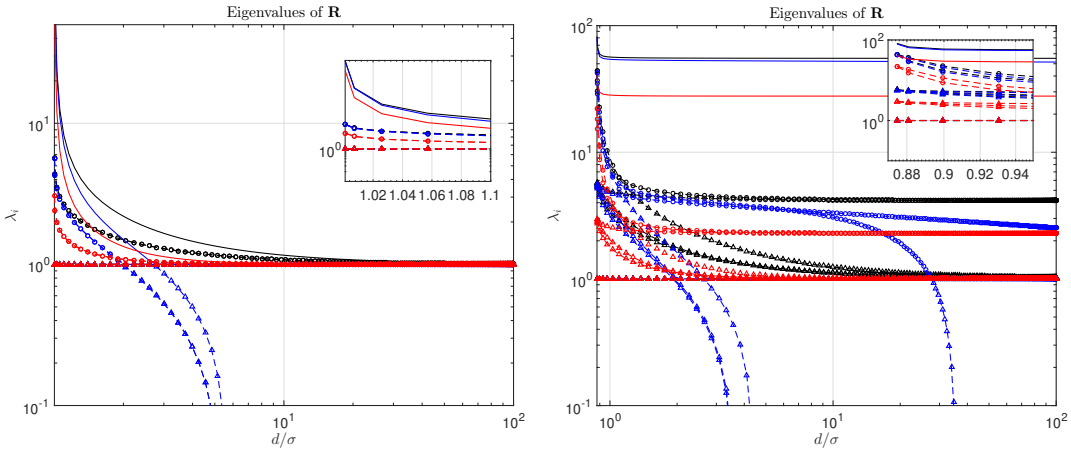

(a) Eigenvalues of $\boldsymbol{R}$ for the two sphere system in Figure 5.1.

(b) Eigenvalues of $\boldsymbol{R}$ for the three sphere system in Figure 5.2.

Figure 5.3: Eigenvalues of $\boldsymbol{R}$ as a function of the centre distance d for a) a two sphere system and b) a three sphere system. Key: **GMS** (F_z), Kim & Karrila (equiv. X_A^{11} (3.17) and Y_A^{11} (4.15)) and Jeffrey & Onishi (equiv. X_A^{11} (3.20) and Y_A^{11} (4.19)). Symbols indicate multiplicity of the eigenvalues: solid = 1, circles = 2, triangles = 3. The insets show the failure of Jeffrey & Onishi to capture the correct eigenvalues in the singular limit.

fix $\sigma = 1$.

Two Sphere System

We refer the reader to Figure 5.1 for the following discussion. For the two sphere system, the eigenvalues $\{\lambda_i\}_{i=1}^{6}$ are computed for d varied between $\sigma < d < \infty$ by using **GMS** (present work, formulae (3.7.5),(3.7.6) and (4.6.1),(4.6.2)), Kim & Karrila [98] and Jeffrey & Onishi [92] and are presented in Figure 5.3a. In this case the eigenvalues correspond to 6 modes: 1 squeezing interaction, 2 shearing interactions, and 3 co-translating interactions, each of multiplicity 1, 2, and 3, respectively, owing to the repeated ways in which shearing and squeezing may occur in 3D. This may be seen by considering the centre to centre axis of two spheres in 3D space: first, along which is the squeezing interaction; second, normal and binormal to the axis are two shearing interactions; and third, colinear, normal and binormal to the axis are 3 translating interactions for a fixed intersphere distance. Hence, in Figure 5.3a, repeated eigenvalues are plotted on top of each other, and, in particular the repeated eigenvalues corresponding translation of **GMS** and Jeffrey & Onishi (black and red triangles) are indistinguishable.

We observe that the asymptotic behaviour of the Kim & Karrila eigenvalues agree with the **GMS** eigenvalues as $d/\sigma \to 1$ (as we expect since the inner region theories agree) but diverge in the far field (as we expect as the lubrication approximation breaks down). Both the **GMS** and Jeffrey & Onishi eigenvalues remain positive for all $d/\sigma > 1$, in particular both sets of eigenvalue converge to unity as $d/\sigma \to \infty$, which corresponds to the intrinsic Stokes drag at infinity included in both formalisms. However we know by Figure 3.2a that Jeffrey & Onishi does not provide the correct singular behaviour in the limit $d/\sigma \to 1$, and in particular we observe the eigenvalues are mismatched to both **GMS** and Kim & Karrila in the inner regime.

Three Sphere System

We refer the reader to Figure 5.2 which is a schematic for the three sphere configuration. We consider three spheres confined to the plane $y = 0$, where two of the spheres are held fixed. The pairwise sphere axes form an equilateral triangle when the third free sphere is moved to the minimum mutual separation $d = d_{\min}$. For the eigenvalues $\{\lambda_i\}_{i=1}^{9}$ we move the location of a third sphere away from the former fixed pair by varying d such that $\frac{\sqrt{3}}{2} d_{\min} < d < \infty$ and compute the eigenvalues of $\boldsymbol{R}$ as a function of d.

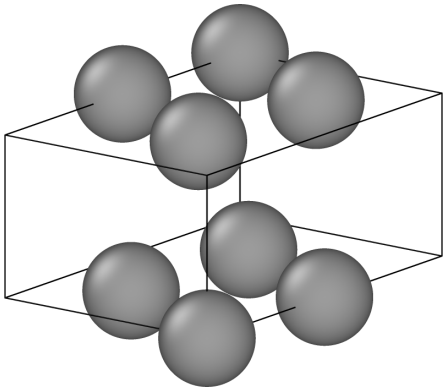

(a) Configuration of $N = 8$ spheres in a regular arrangement with $d_{\min} = 2$ corresponding to a packing fraction of $\phi = 0.370$, or about 50% of maximum packing.

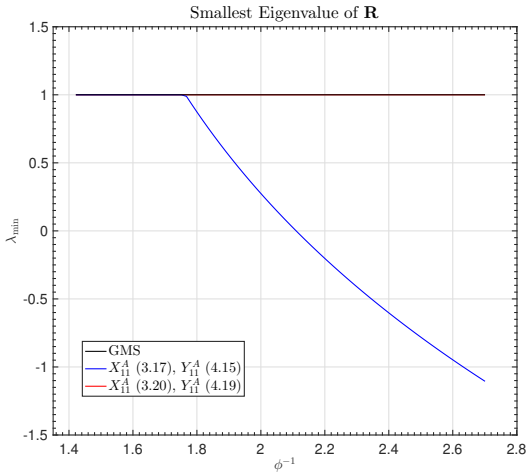

(b) A plot of the smallest eigenvalue of $\boldsymbol{R}$ for the $N = 8$ sphere configuration in Figure 5.4a. The **GMS** and Jeffrey & Onishi curves are indistinguishable where as the Kim & Karrila curve starts to diverges at a volume fraction around $\phi = 57\%$.

Figure 5.4: a) A regular configuration of $N = 8$ spheres of diameter $\sigma = 1$ with nearest neighbour centre to centre distance $d_{\min}$ and b) The smallest eigenvalue of $\boldsymbol{R}$ with configuration as in a) with varying volume fraction.

In Figure 5.3b we plot the eigenvalues and preserve the labelling **GMS**, Kim & Karrila and Jeffrey & Onishi. As in the two sphere case, we obtain repeated curves owing to the multiplicity of the eigenvalues. In Figure 5.3b we report a similar property in the eigenvalue distribution, that the **GMS** are uniformly positive, and, the eigenvalues corresponding to the pairwise interactions between the third free and the two fixed spheres converge to unity for large as $d \to \infty$. Kim & Karrila do not preserve positivity for the three sphere system, in particular, we see that the eigenvalues diverge, and in particular, in a smaller regime of d than in the two sphere system. Jeffrey & Onishi preserves positivity however, as in the two sphere system, Jeffrey & Onishi does not provide the correct singular behaviour in the limit $d/\sigma \to 1$.

The emergence of multiple constant eigenvalues as $d \to \infty$ corresponds to convergence to the isolated pair system as the third free sphere is sufficiently separated. There is a particular disagreement in the eigenvalues of **GMS** and Jeffrey & Onishi (solid black and red) for the singular interactions. Additionally, the resistance matrix for the three-body system in Figure 5.3b is obtained by superposition of the two-body system, and the difference we observe in spectral behaviour of $\boldsymbol{R}$, particularly between **GMS** and Jeffrey & Onishi, is most likely a consequence of the inefficient computation of the singular terms by Jeffrey & Onishi. This leads us to believe that the present theory, **GMS**, will lead to significant differences in SD simulations of large colloidal systems, compared to the existing theory, where two–body HIs are a common assumption.

Larger Systems

In assembling the resistance matrix for an arbitrary monodisperse system, the main parameters are the inter-sphere distances and the number of spheres. As the number of spheres increases so does the dimension of the resistance matrix. The inter-sphere distances dictate how the eigenvalues are distributed. Positivity may not necessarily be obtained for an arbitrary system. However, we may obtain some formal results about the spectral properties of $\boldsymbol{R}$ by examining a few regular systems. We let S_N denote the set of all possible states of the system of N spheres in a confining box. Additionally we let $X_\phi \in S_N$ denote the regular sphere packing at some volume fraction $\phi \in (0, \phi_g)$ for $\phi_g = \frac{\pi}{3\sqrt{2}}$ Gauss' constant such that for each sphere in S_N,

the centre to centre distance of each nearest neighbour is $d_{\min}$. X_ϕ is a natural configuration to consider because it represents the lowest entropy state of the system at the hydrodynamic diameter $d_{\min}$. Therefore if the spectrum of $\boldsymbol{R}(X_\phi)$ may be controlled, i.e., bounded from below, one expects to be able to control $\boldsymbol{R}(X_\phi + \varepsilon)$, where $\varepsilon \in S_N$ represents a perturbation from X_ϕ.

We may investigate the spectral properties of $\boldsymbol{R}$ for larger systems by computing the eigenvalues of $\boldsymbol{R}(X_\phi)$ as a function of $\phi \in (0, \phi_g)$ using the different scalar resistance functions. Note that $\phi = \phi_g$ corresponds to contact and is the singular limit of $\boldsymbol{R}$, which cannot be evaluated. Since for each N, $\boldsymbol{R}$ has $3N$ eigenvalues, in order to examine positive definiteness we need only compute the smallest eigenvalue $\lambda_{\min}$ for each formalism. Figure 5.4a shows a unit cell of S_8 which may be repeated to produce hexagonal close packing at a hydrodynamic diameter of $d_{\min} = 2$ for spheres of diameter $\sigma = 1$. The hydrodynamic diameter $d_{\min}$ and the volume fraction are related by $\phi = \pi/(3\sqrt{2})(\sigma/d_{\min})$ hence as $d_{\min}$ increases ϕ decreases and vice versa. In Figure 5.4b we plot the smallest eigenvalue of each formalism **GMS**, Kim & Karrila and Jeffrey & Onishi verses ϕ^{-1} for S_8 (so that large ϕ^{-1} correspond to dilute S_8). We report that both **GMS** and Jeffrey & Onishi preserve positivity and that the smallest eigenvalue of Kim & Karrila starts to diverge at volume fractions around $\phi = 57\%$.

Plotting the smallest eigenvalue as a function of ϕ gives a rough estimate for the volume fraction at which the Lubrication theory of Kim & Karrila becomes invalid. The theory becomes invalid for volume fractions smaller than 57% because the singular eigenvalues of Kim & Karrila begin to deviate from the exact eigenvalues of **GMS** at much smaller ϕ (not shown). We present only the smallest eigenvalues to forgo plotting 24 eigenvalues on a single axes. Additionally, the authors stopped computing the spectra of $\boldsymbol{R}$ for each **GMS**, Kim & Karrila and Jeffrey & Onishi at $N = 8$, since, beyond this sphere number, the computation time for computing the eigenvalues for regular configurations of S_N outstrips gains in insight of the positivity of $\boldsymbol{R}$.

We expect the positivity to be preserved by **GMS** for each S_N since the boundary layer in the inner region of the resistance functions occurs only for nearest neighbours in the configuration, and the squeezing and shearing forces quickly decay to unity for centre distances of order of a sphere diameter. Additionally, the property that the rate of mechanical energy dissipation should be positive is essentially a consequence of the fact that the total solvent fluid velocity may be partitioned into the velocity fields created by the motions of the individual spheres (see Section 8–5 *Generalized treatment of multiparticle systems* Happel and Brenner [75]), which is intrinsic to the spherical bipolar formalism. This cannot be said to hold rigorously for the asymptotic formalisms (Kim & Karrila, multipole methods) since the velocity fields as found by those methods are valid only in local flow regimes (for example near to or far from sphere surfaces). The advantage of **GMS**, therefore, over the formulae provided by multipole methods of Jeffrey & Onishi, is to more efficiently obtain the correct singular behaviour in the close sphere surface flow regime.

Chapter 6

Numerical Applications

In this chapter we demonstrate substantial differences in numerical simulations of colloidal dynamics when using the present theory of microhydrodynamics compared with existing multipole and perturbation methods, within DDFT.

6.1 Computation Of Convolutions

Computations of the density ϱ and the FMT weight functions χ are performed in real space, without using the convolution theorem (C.0.1). Typically, in FMT, the weight functions χ are narrow, with small supports (around the size of a particle diameter) whereas the density varies slowly in large parts of the physical domain. The density profiles ϱ themselves may usually be represented very accurately with few collocation points over the entire domain. However computing the convolutions for the weighted densities on a coarse grid can be inaccurate due to the typical nondifferentiability of the weight functions χ. This may be observed for test convolution of a Gaussian function for a 1D infinite spectral line [127, Section 3.3 - Figure 2] when translating the convolution operator over collocation points.

To get around this, the convolutions are rewritten as

$$n \star \chi(y) = \int_{\mathscr{I}(y)} \mathrm{d}\hat{y}\, \chi(-\hat{y}) n_y(\hat{y})$$

where $n_y(\hat{y}) = n(y + \hat{y})$ and $\hat{y} \in \mathscr{I}(y)$ is the intersection between the support of the weight functionχ and the shifted density n_y, centred at y. Since we expect the density profile to vary slowly at far field, the convolutions will be dominated by the behaviour of the weight functions χ and hence one can now discretise the intersection $\mathscr{I}(y)$ centred at a collocation point $y = y_n$ and concentrate collocation points in $\mathscr{I}(y)$ where they are most needed. The procedure for computation of convolutions is summarised as follows

For each y_n

1. Discretise $\mathscr{I}(y_n)$ with M collocation points $\hat{y}_m$ and compute integration weights $\hat{w}_m$ for this sub domain.
2. Evaluate $\chi_m = \chi(-\hat{y}_m)$ for the discretisation points of $\mathscr{I}(y_n)$.
3. Compute the interpolation operator $\boldsymbol{IP}_n$ (parametrised by y_n) for the subdomain $\mathscr{I}(y_n)$, using the $\hat{y}_n$.
4. Set $(\boldsymbol{C}_\chi)_n = \hat{w}_n \,\mathrm{diag}(\chi_m)\boldsymbol{IP}_n$, where $\hat{w}_n$ are the integration weights for the subdomain.

This algorithm is also used in computing the convolutions arising from the HI tensors $\boldsymbol{Z}_1$, $\boldsymbol{Z}_2$ for the dynamics. The complexity of the algorithm is $O(MN^2)$ floating point operations for N collocation points in the original domain and M collocation points for each subdomain centred on y_n, much higher than the typical complexity when performing the convolution via the convolution theorem in Fourier space, taking $(O(N \log N))$ floating point operations. However the construction of $(\boldsymbol{C}_\chi)_n$ may be parallelised and need only be computed once and saved for

a given geometry choice. Also, a direct comparison of numerical procedures by means of their complexity is meaningful only if computation times become a hindrance, in particular this is normally when the number of discretisation points for both procedures is large, or when the results are of the same accuracy. It has been shown that the real-space convolution procedure, leads to a higher accuracy while employing a considerably lower number of discretisation points [127].

Partial Confinement of Hard Spheres

The numerical solutions we present are for 2D fluids, that is the spheres are 3D in 3D space but are restricted to 2D planes. By the curse of dimensionality a full 3D fluid systems are computationally expensive. The restriction to a 2D (hard sphere) fluid is however not so limiting, since the situation is physically interesting, and, numerically speaking, the excellent computational performance of spectral representations of the density can be demonstrated.

Physically there two ways in which confined 2D systems may arise. First, both the bulk and colloidal particles are confined to 2D. In this instance it is known that the transport coefficients in 2D are not well defined, and, the restriction of Stokes equations to two dimensions can lead to well known inconsistencies, for unbounded fluids, such as Stokes' paradox. Second, the colloidal particles could be confined to a 2D plane but the bulk particles are unrestricted to move out of plane. This situation is known as partial confinement and may be applicable for confinement of the colloids in an electric potential, or, the confinement due to external forces such as optical tweezers. We assume the colloids are confined to a plane, where the HI modes are well defined in this instance, and the analytical solutions to Stokes equations in Chapters 3, 4 will be applicable.

6.2 Assembling The HI Operators

The HI matrices must now be assembled. We will present the general construction of the friction tensor, also known as the grand resistance matrix denoted $\boldsymbol{R}$ in classical microhydrodynamics [13] and denoted $\boldsymbol{\Gamma}$ in DDFT literature [61], before identifying the tensor for the two body interactions. For the Langevin dynamics, (2.3.1a)–(2.3.1b), recall that the friction tensor is written as

$$\boldsymbol{\Gamma}_{ij} = \gamma\delta_{ij}\mathbf{1} + \gamma\tilde{\boldsymbol{\Gamma}}_{ij} \tag{6.2.1}$$

where

$$\tilde{\boldsymbol{\Gamma}}_{ij} = \delta_{ij}\sum_{i\neq l}\boldsymbol{Z}_1(\mathbf{r}_i,\mathbf{r}_l) + (1-\delta_{ij})\boldsymbol{Z}_2(\mathbf{r}_i,\mathbf{r}_j).$$

The block structure of $\boldsymbol{\Gamma}_{ij}$ for N colloids is given by

$$\boldsymbol{\Gamma} = \begin{pmatrix} \sum_{l\neq 1}\boldsymbol{Z}_1(\mathbf{r}_1,\mathbf{r}_l) & \boldsymbol{Z}_2(\mathbf{r}_1,\mathbf{r}_2) & \cdots & \boldsymbol{Z}_2(\mathbf{r}_1,\mathbf{r}_N) \\ \boldsymbol{Z}_2(\mathbf{r}_2,\mathbf{r}_1) & \sum_{l\neq 2}\boldsymbol{Z}_1(\mathbf{r}_2,\mathbf{r}_l) & \cdots & \vdots \\ \vdots & \vdots & \ddots & \vdots \\ \boldsymbol{Z}_2(\mathbf{r}_N,\mathbf{r}_1) & \cdots & \cdots & \sum_{l\neq N}\boldsymbol{Z}_1(\mathbf{r}_N,\mathbf{r}_l) \end{pmatrix}.$$

The block matrices $\boldsymbol{Z}_1$ and $\boldsymbol{Z}_2$ are defined as

$$\boldsymbol{Z}_1(\mathbf{r}_i,\mathbf{r}_l) = -a(r_{il})\frac{\mathbf{r}_i\otimes\mathbf{r}_l}{r_{il}^2} - b(r_{il})\left(\mathbf{1} - \frac{\mathbf{r}_i\otimes\mathbf{r}_l}{r_{il}^2}\right)$$
$$\boldsymbol{Z}_2(\mathbf{r}_i,\mathbf{r}_j) = a(r_{ij})\frac{\mathbf{r}_i\otimes\mathbf{r}_j}{r_{ij}^2} + b(r_{ij})\left(\mathbf{1} - \frac{\mathbf{r}_i\otimes\mathbf{r}_j}{r_{ij}^2}\right)$$

where $r_{ij} = |\mathbf{r}_i - \mathbf{r}_j|$ and $a(\cdot)$, $b(\cdot)$ are place holder scalar resistance functions, which will be populated according to the formalism being considered. In equation (6.2.1), the first tensor

takes into account Stokes drag on the ith particle and the second determines the HI between particle i and particle j.

6.2.1 Consolidation Of The Scalar Resistance Functions

The scalar resistance functions we use for $a(\cdot)$ and $b(\cdot)$ to build the diagonal and off-diagonal block matrices $\boldsymbol{Z}_1$, $\boldsymbol{Z}_2$ are given by the following:

For the $a(\cdot)$

- F_z^1, F_z^2 (3.7.5), (3.7.6) as found in Chapter 3
- $F_{z,l}$ (9.33) as found in Kim and Karrila [98, Chapter 9].
- X_{11}^A (3.20) as found in Jeffrey and Onishi [92, Section 3 and 4].

For the $b(\cdot)$

- F_x^1, F_x^2 (4.6.1), (4.6.2) as found in Chapter 4.
- $F_{x,l}$ (9.24) as found in Kim and Karrila [98, Chapter 9].
- Y_{11}^A (4.19) as found in Jeffrey and Onishi [92, Section 3 and 4].

Key To Numerical Solutions :

The key to our numerical solutions are as follows

- **GMS** denotes solutions using the functions (3.7.5), (3.7.6) and (4.6.1), (4.6.2).
- Kim & Karrila denotes solutions using the functions, $F_{z,l}$ and $F_{x,l}$.
- Jeffrey & Onishi denotes solutions using the functions, X_{11}^A and Y_{11}^A.
- Zero HI denotes solutions using the functions $a(\cdot) = b(\cdot) = 0$ for all r_{ij}.

For **GMS**, when computing the HI tensors for spheres of equal sizes, we use the scalar resistance function (3.7.5) with appropriate sign, since the force on two spheres will be equal and opposite for two converging spheres. We will consider numerical solutions to non-driven systems to demonstrate the substantial differences in dynamics which arise when implementing the HI as derived in this work. Solutions for driven systems, as in numerical experiments for the DDFT derived in Chapter 2 have been implemented but are not shown here.

6.3 Numerical Experiments

In this section we present numerical applications of the HI formalism of Chapters 3, 4 for three systems. A fully formed, in depth numerical study of solutions to DDFTs with these extensions will be considered in a separate publication. The aim of this section is to elucidate to the reader the differences which may be observed between the present and existing HI formalisms in computational settings.

6.3.1 Colloids In An External Potential

We consider the probability distribution $\varrho(\mathbf{r}, t)$ for the positions of a large collection of hard spherical particles immersed in a background bath of many more, much smaller and much lighter bath particles treated essentially as a continuum. The larger particles cause fluid flows in the bath, in turn causing forces on all other particles. These forces are considered to be the short range HI mediated by the bath and are prescribed by the resistance tensor $\boldsymbol{R}$. For the following discussion we assume **A1**–**A3**.

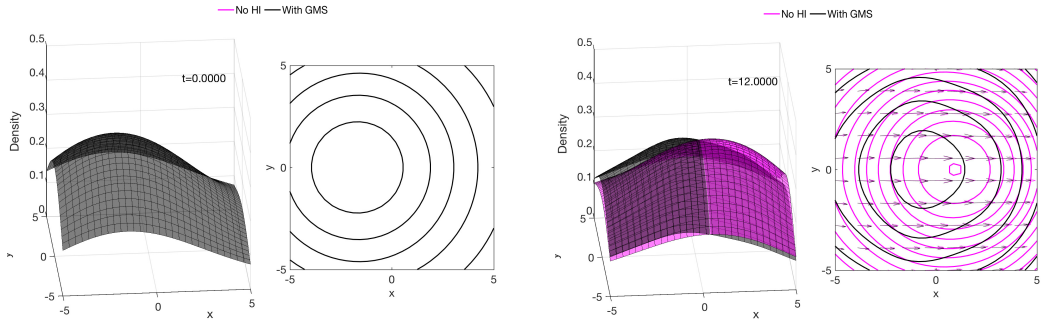

(a) $t = 0.00$ (b) $t = 12.00$

Figure 6.1: Numerical solution of the DDFT (6.3.1)–(6.3.2) including the present theory (**GMS**) compared to a reference solution with (Zero HI). The left hand panels show the density of colloids, $\varrho(\mathbf{r}, t)$, trapped inside a confining poential on the 2D plane. The right hand panels show the level curves of the density and the bulk velocity of the colloidal system (given by the arrows). Figure 6.1a shows the initial density and velocity meanwhile Figure 6.1b shows the evolved density under a translation the confining potential over a period of $t = 12$ time units.

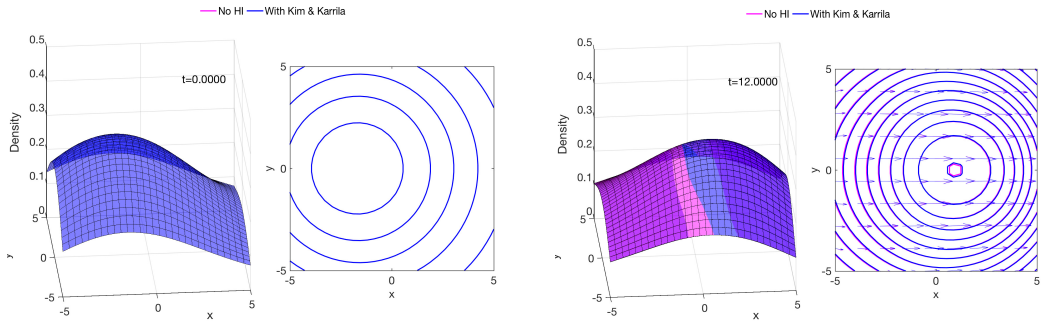

(a) $t = 0.00$ (b) $t = 12.00$

Figure 6.2: Numerical solution of the DDFT (6.3.1)–(6.3.2) including the existing theory (Kim & Karrila) compared to a reference solution with (Zero HI). The left and right hand pannels are as described in Figure 6.1 with same initial density and velocity, that is, Figures 6.1a and 6.2a would be indistinguishable if plotted on top of each other. After the same time period the density and velocity are substantially different to 6.1b owing to the underestimate in the lubrication effect by the truncation inherent in the series F_z.

In the DDFT setting it is commonplace to separate out the column space of $\boldsymbol{R}$ corresponding to isolated spheres diffusing at infinity. In particular we write $\boldsymbol{R}_{ij} = \boldsymbol{\Gamma}_{ij} = \gamma\mathbf{1} + \gamma\tilde{\boldsymbol{\Gamma}}_{ij}$ where γ is the friction coefficient (Stokes constant) and $\tilde{\boldsymbol{\Gamma}}_{ij}$ are the nondimensional two body HI tensors. The first tensor takes into account Stokes drag on the ith particle and the second determines the HI between particle i and particle j. The inertial DDFTs are nonlinear, nonlocal, integro-partial differential equations in 3D for the one-body density $\varrho(\mathbf{r}, t)$ and one-body velocity $\mathbf{v}(\mathbf{r}, t)$ describing conservation of mass and momentum of a fluid with non-constant number density, as discussed in Chapter 2. In particular, we consider the numerical solution of

$$\partial_t \varrho(\mathbf{r}_1, t) + \nabla_{\mathbf{r}_1} \cdot (\varrho(\mathbf{r}_1, t)\mathbf{v}(\mathbf{r}_1, t)) = 0, \tag{6.3.1}$$

$$\begin{aligned}\partial_t \mathbf{v}(\mathbf{r}_1, t) + (\mathbf{v}(\mathbf{r}_1, t) \cdot \nabla_{\mathbf{r}_1})\mathbf{v}(\mathbf{r}_1, t) + \tfrac{1}{m}\nabla_{\mathbf{r}_1} \frac{\delta \mathscr{F}_H[\varrho]}{\delta \varrho}(\mathbf{r}_1, t) \\ + \gamma\mathbf{v}(\mathbf{r}_1, t) + \gamma \int \mathrm{d}\mathbf{r}_2 \, [\boldsymbol{Z}_1(\mathbf{r}_1, \mathbf{r}_2)\mathbf{v}(\mathbf{r}_1, t)) + \boldsymbol{Z}_2(\mathbf{r}_1, \mathbf{r}_2)\mathbf{v}(\mathbf{r}_2, t))] \, \varrho(\mathbf{r}_2, t) g(\mathbf{r}_1, \mathbf{r}_2, [\varrho]) = 0.\end{aligned} \tag{6.3.2}$$

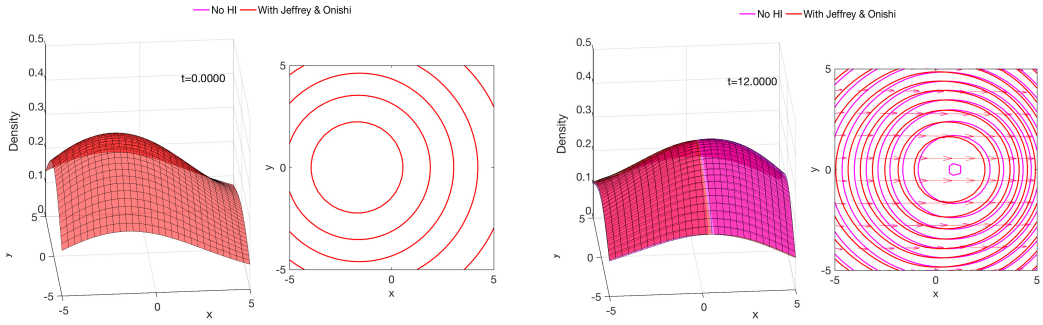

(a) $t = 0.00$ (b) $t = 12.00$

Figure 6.3: Numerical solution of the DDFT (6.3.1)–(6.3.2) including the existing theory (Jeffrey & Onishi) compared to a reference solution without HI (magenta). The left and right hand pannels are as described in Figure 6.1 with same initial density and velocity, that is, Figures 6.1a, 6.2a, and 6.3a would be indistinguishable if plotted on top of each other. After the same time period the density and velocity are substantially different to 6.1b owing to the underestimate in the lubrication effect in the inner region by the multipole functions X_{11}^A, Y_{11}^A.

For the system of PDEs (6.3.1)–(6.3.2) there are 5 required inputs: 1) Initial density and velocity data, 2) Free energy functional $\mathscr{F}_H$, 3) Friction coefficient γ, 4) Pairwise HI tensors $\boldsymbol{Z}_j$, 5) Correlation function $g(\mathbf{r}_1, \mathbf{r}_2, [\varrho])$. The initial data are found by solving an equilibrium DFT problem, which amounts to solving the nonlinear functional equation $(\delta\mathscr{F}_H)/(\delta\varrho)[\varrho] = \mu_c$ where μ_c is the chemical potential of the hard sphere species. The free energy functional $\mathscr{F}_H[\varrho]$ is modelled with fundamental measure theory (FMT), which provides the functional form of the free energy density taking account of the entropy reduction produced by hard sphere exclusion (see Rosenfeld [148] or Roth [151]). Additionally, in $\mathscr{F}_H$, one may include external potentials such as gravity as well as interparticle potentials, for electrostatic interactions. The friction coefficient γ may be varied as a proxy for the solvent viscosity. The pairwise resistance tensors take into account the HI, which we will construct using the resistance functions of the present work, as well as the existing perturbative and multipole counterparts. The correlation function is not known exactly and must ultimately be obtained from the microscopic dynamics, but for a hard sphere fluid may be approximated by $g(|\mathbf{r} - \mathbf{r}'|) = 0$ for $|\mathbf{r} - \mathbf{r}'| < \sigma$ (denoting exclusion) and unity otherwise. Such an approximation has been shown to give good agreement with comparative stochastic simulations of the underlying Langevin dynamics Goddard et al. [61],Goddard et al. [62], Goddard et al. [65].

We solve (6.3.1)–(6.3.2) with the pseudospectral collocation scheme 2DChebClass [67]. A detailed analysis of the numerical method, including the basic quadrature technique of the convolutions of the HI matrices, is found in Nold et al. [127]. We present three solutions: one labelled **GMS** to denote $\boldsymbol{Z}_1$, $\boldsymbol{Z}_2$ constructed with the scalar resistance function (3.7.5) obtained by present work (Figure 6.1), one labelled Kim & Karrila (Figure 6.2) which uses the well known, widely used expression (3.8.1) to construct $\boldsymbol{Z}_1$, $\boldsymbol{Z}_2$, and one labelled Jeffrey & Onishi (Figure 6.3) which uses the scalar functions X_{ij}^A, Y_{ij}^A. A reference solution in both cases with Zero HI $\boldsymbol{Z}_1 = \boldsymbol{Z}_2 = 0$ is also shown. For the solution using Kim & Karrila, a necessary outer cuttoff was chosen at 2 sphere diameters which is accepted in the community as standard [170]. For **GMS** and Jeffrey & Onishi no outer cut off is required.

We consider flow in a time dependent potential. We take $\gamma = 2$, with 50 colloids, but many more may be included since the dimensionality of DDFT is independent of the number of colloids. The HI terms as constructed by **GMS**, Kim & Karrila, and Jeffrey & Onishi all retard the flow of the colloid particles in comparison with DDFTs with Zero HI, which is what we expect from the standard descriptions of the effects of lubrication forces. This is in contrast to overdamped DDFT equations including long-range forces, for HI terms corresponding to two-body $\boldsymbol{R}^{-1}$, which essentially enhance collective motion Goddard et al. [66].

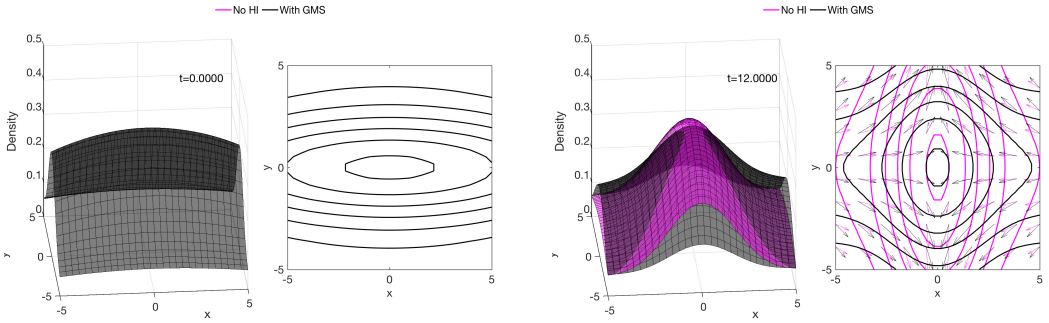

(a) **GMS** $t = 0$.

(b) **GMS** $t = 12$.

Figure 6.4: $N = 50$ particles evolving: with **GMS** and without HI trapped in a oscillating potential.

To drive the flow, we use an external potential of the form

$$V_{ex} = V_0 + V_{mov}$$

where V_0 is a weak quadratic background potential and V_{mov}, is a Gaussian potential well with

$$V_{mov} = \exp\left(-\frac{(y_1 - y_{1a})^2}{2\sigma_1^2} - \frac{(y_2 - y_{2a})^2}{2\sigma_2^2}\right) \tag{6.3.3}$$

such that y_{1a} varies, to move the potential in the physical y_1 direction.

Figures 6.1, 6.2, and 6.3 show a substantial difference in the evolution of the density ϱ (and flux) of the suspension, in particular between **GMS** and both Kim & Karrila and Jeffrey & Onishi, which appear to underestimate the effect of the lubrication force on the overall dynamics of the density. We observe that **GMS** shows the onset of extrusion in the density contours not visible using existing theory.

6.3.2 Colloids In An Oscillating Trap

The second example we present is a colloidal flow in a 2D planar geometry subject to an oscillating external potential.

The assumption in the continuum description of colloidal dispersions that the HI are limited to two body is particularly compatible with the HI formalism **GMS**, because the solution to Stokes equations have been determined analytically and are uniformly valid in sphere separation. Therefore the property that the total ambient fluid velocity may be partitioned into the velocity fields created by the motions of the individual spheres (see Section 8–5 [75]), each of which require exact solutions to Stokes equations for two-body sphere motion in order to construct a well-posed positive definite grand resistance matrix $\boldsymbol{R}$, is provided by the solutions presented in this thesis theory. This cannot be said to hold rigorously for the asymptotic formalisms (Kim & Karrila, Jeffrey & Onishi) since the velocity fields as found by those methods are valid only in local flow regimes (for example near to or far from sphere surfaces).

Once again, we numerically solve the inertial DDFT (2.6.1) with two body short range HI and present the three solutions: one labelled **GMS**, Kim & Karrila, and Jeffrey & Onishi. A reference solution in both cases with Zero HI $\boldsymbol{Z}_1 = \boldsymbol{Z}_2 = 0$ is also shown. For the solution using Kim & Karrila, the necessary outer cuttoff was chosen at 2 sphere diameters. Additionally, we once again take $\gamma = 2$, with 50 colloids. To drive the flow, we use an external potential of the form

$$V_{ex} = V_0 + V_{osc}$$

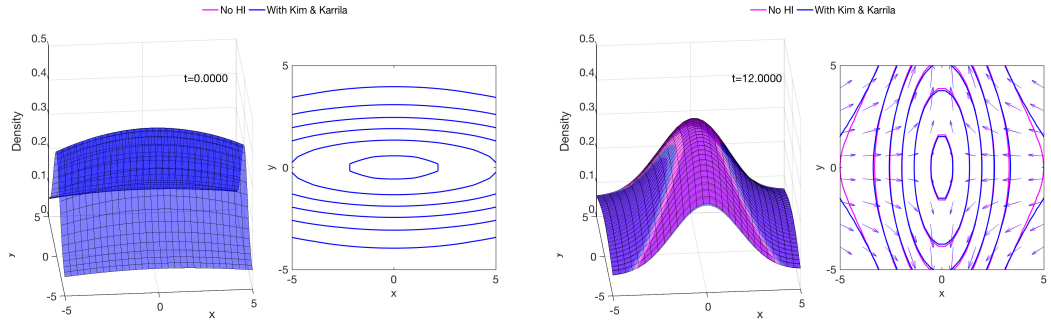

(a) Kim & Karrila $t = 0$. (b) Kim & Karrila $t = 12$.

Figure 6.5: $N = 50$ particles evolving with: Kim & Karrila and without HI trapped in a oscillating potential.

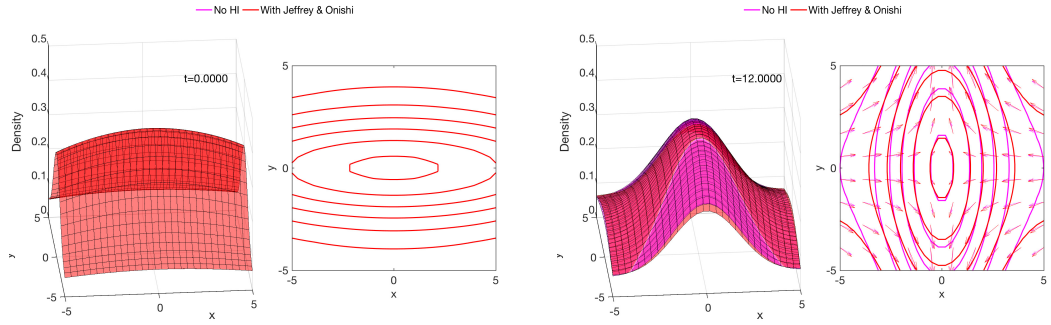

(a) Jeffrey & Onishi $t = 0$. (b) Jeffrey & Onishi $t = 12$.

Figure 6.6: $N = 50$ particles evolving with: Jeffrey & Onishi and without HI trapped in a oscillating potential.

where V_0 is a weak quadratic background potential and V_{osc}, is a Gaussian potential well with

$$V_{osc} = \exp\left(-\frac{(y_1 - y_{1a})^2}{2\sigma_1^2} - \frac{(y_2 - y_{2a})^2}{2\sigma_2^2}\right)$$

such that σ_1 and σ_2 vary periodically to stretch the potential in the physical y_1, y_2 directions.

In Figures 6.4, 6.5, and 6.6 in which we present the oscillating system on the whole real space demonstrates substantial difference between the HI derived in this thesis, resulting in a large difference in the path to equilibrium between the three formalisms. In particular, both Kim & Karrila, and Jeffrey & Onishi appear to drastically underestimate the lubrication effect on the dynamics of the density.

Pseudospectral Scheme for FMT-DDFTs in a Slit

We now present the real-space discretisation method for DFT with FMT in a confining slit using a pseudospectral method. Now the vector space of 2D polynomials approximating a function $f(\mathbf{x})$ defined on the unit cell $\mathbf{x} \in [-1, 1] \times [-1, 1]$, which here is the computational domain in 2D, is defined as the tensor product of the 1D polynomial vector spaces $\boldsymbol{P}_{N_1} \otimes \boldsymbol{P}_{N_2}$ where $N_1 = i$ is the number of collocation points in each of the two Cartesian directions.

By including FMT formalism in a DFT or DDFT one has to not only discretise the density n but also the weight functions ω_i^α.We see that for a confining domain with a wall at $\pm L$, for some $L \in (0, \infty)$ then one has, due to the conservation of mass, $n(y_2 = \pm L) = 0$. However, by definition of the ω_i^α (1.6.4a)–(1.6.4c), the support of ω_i^α is $\{(y_1, y_2) : |y_2| < L + \frac{\sigma}{2}\}$ where σ is the particle diameter. Additionally, if the density of a hard-sphere fluid is positive at the wall, then the derivatives of the weighted densities in the direction normal to the wall, $\partial_{y_2} n_\alpha$

possesses a jump at $y_2 = \pm\sigma/2$. This may be seen by the behaviour of w_i^2 in (1.6.4b) for the hard-sphere fluid in contact with the hard wall at $y_2 = \pm y_2$. By (1.6.4b) and (1.6.6)n_2, is non-differentiable at $y_2 = \pm\sigma/2$ since ω_i^2 is a delta function.

Domain Discretisation for FMT-DDFT Equations in a Slit

We define the physical domain by the mapping

$$\mathscr{Y}_{\text{slit}}(x_1, x_2) = (\mathscr{A}(x_1), \mathscr{T}_{0,L}(x_2))$$

where we define the mappings in the individual Cartesian directions for slit of width $2L$

$$\mathscr{A} : [-1, 1] \to [-\infty, \infty] \quad x \to L_1 \frac{x}{\sqrt{1 - x^2}} \tag{6.3.4a}$$

$$\mathscr{T}_{0,L} : [-1, 1] \to [-L, L] \quad x \to Lx \tag{6.3.4b}$$

and L_1 is a geometrical parameter linked to the length scale of the physical domain. It may be seen that the algebraic maps (6.3.4a)–(6.3.4b) retain their optimal properties as $N \to \infty$ for fixed mapping parameters [20]. In order to correctly describe the jump discontinuities in derivatives of the weight functions (1.6.6), we augment the physical slit $\mathscr{Y}_{\text{slit}}$ into

$$\mathscr{Y}_{\text{comp}}(x_1, x_2) = \left(\mathscr{A}(x_1), \mathscr{T}_{-L,\sigma/2} \cup \mathscr{T}_{0,L-\sigma/2} \cup \mathscr{T}_{L,\sigma/2}(x_2)\right).$$

In the computations which we present, the number of collocation points in the shoulder slit, N_{slit}, is chosen empirically to be the next even integer to $N_2/3$. This value was found to provide an accurate representation of the density and the weighted densities in the vicinity of the wall.

6.3.3 Colloids In An Infinite Slit

Domain Splitting

For the HI terms in (2.6.1), as in the FMT formalism, we must divide the slit since the support of the HI tensors restricts a hard sphere from being within one radius of the the hard wall. The methodology for doing this is described by the following algorithm

For a slit of width $2L$ centred on the y_2 axis

1. 'Trim off' the slits of width $\sigma/2$ from $y_2 = \pm L$.

2. Construct convolution matrices for the HI terms by computing the intersection of the support of the HI tensors and the trimmed domain, centred at each collocation point in the trimmed domain.

3. The support of the FMT weight functions is the original domain plus 'wings' of width $\sigma/2$. This may be seen by studying at the geometrical weight functions in Rosenfeld's FMT.

4. The new computational domain is then a slit of width $2L + \sigma$ centred around the y_2 axis.

5. No flux is prescribed on $y_2 = \pm L$ so that the density is zero outside the originally defined slit of width $2L$.

We provide plots of the discretised slit in Figure 6.7 and the support of the convolution operators for both the HI terms and FMT for hard spheres in Figure 6.8. Finally, in Figure 6.9 we present a numerical example demonstrating the difference in the evolution of the density for **GMS** compared to the reference solution with Zero HI in a slit of width $2L$. Additionally, in Figure 6.10 we show the corresponding solution to with $\boldsymbol{Z}_i$ constructed with Jeffrey & Onishi

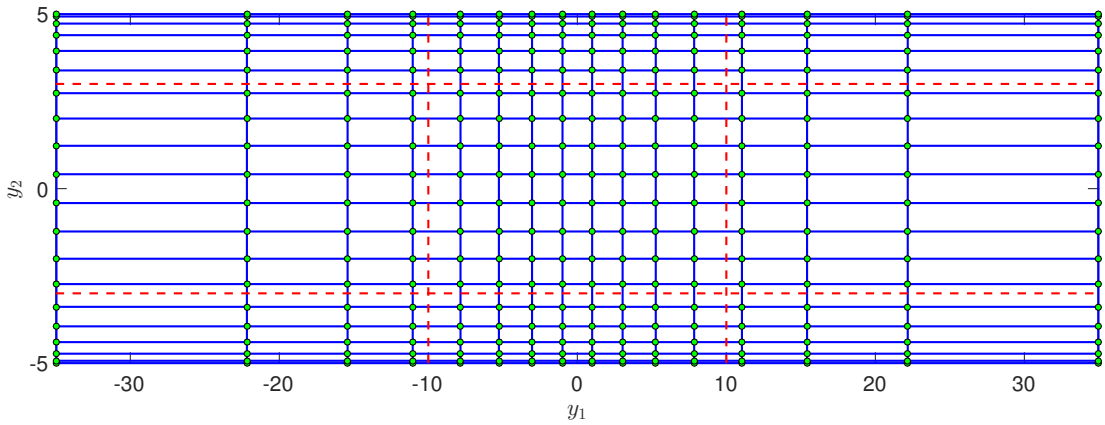

(a) Grid lines used to discretise the density ϱ in the slit. Here $L = 5$.

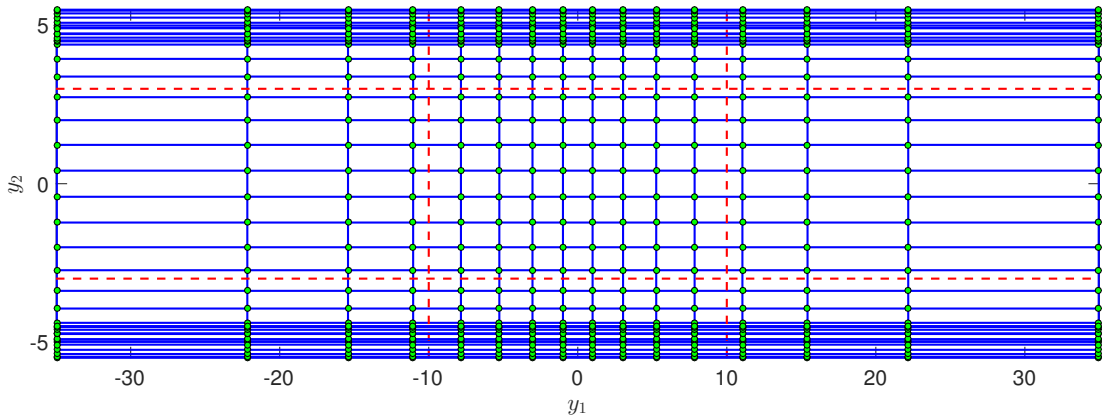

(b) Grid lines used to discretise the slit composed by the physical space $[-\infty, \infty] \times [-L, L]$ and the bounding slits $[-\infty, \infty] \times [-\sigma/2 - L, -L + \sigma/2]$, $[-\infty, \infty] \times [-\sigma/2 + L, L + \sigma/2]$ for the weighted densities n_α. Here $L = 5$ and $\sigma = 1$ so the boundary of the support of the weighted densities n_α are found at $y_2 = \pm 5.5$.

Figure 6.7: Grid lines of the discretisation of density ϱ and weighted densities n_α. In the subplots above, 20 collocation points are employed in each direction with mapping parameter $L_1 = 12$. In both Figures 6.7a, 6.7b 40% of collocation points in the y_1 direction are located between the vertical red dashed lines. In Figure 6.7a, 60% of the collocation points in the y_2 direction are located between the horizontal red dashed lines and the nearest wall $y_2 = \pm L$. In Figure 6.7b, 80% of the collocation points in the y_2 direction are located between the horizontal red dashed lines and the boundary of the n_α support $y_2 = \pm(L + \sigma/2)$.

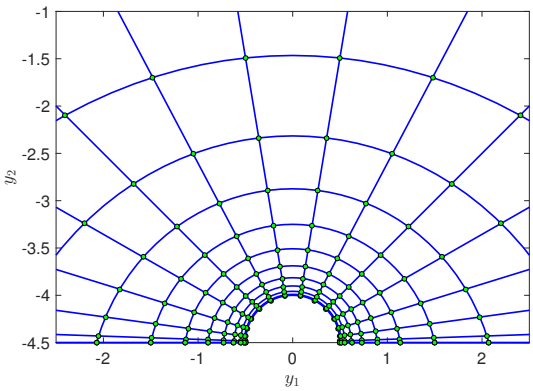

(a) Discretisation of intersection $\mathscr{I}$ between the support of the scalar resistance functions of the HI tensors and the slit-space.

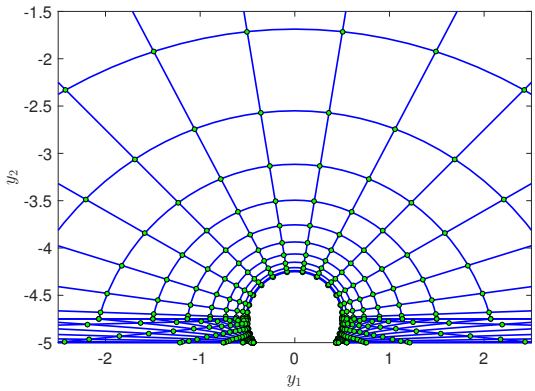

(b) Discretisation of intersection $\mathscr{I}$ between the support of the weighted densities n_α and the slit-space.

Figure 6.8: Example intersection grid lines for the convolution operators of (a) the HI terms and (b) FMT for hard spherical particles at candidate collocation points.

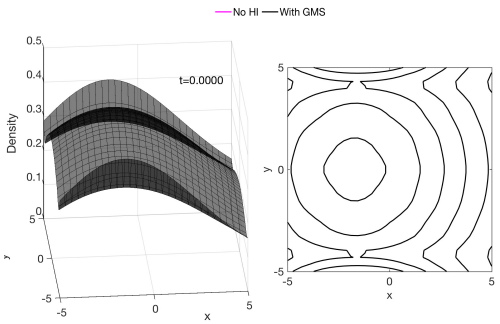

(a) **GMS** $t = 0$

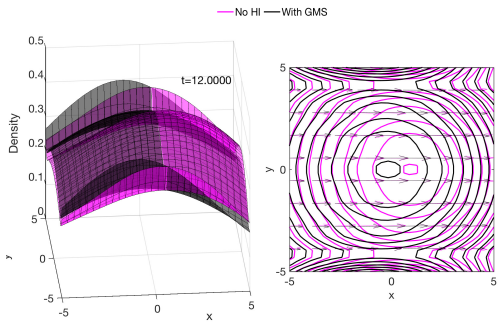

(b) **GMS** $t = 12$

Figure 6.9: $N = 50$ particles evolving with: **GMS** and with Zero HI in a slit of width 10.

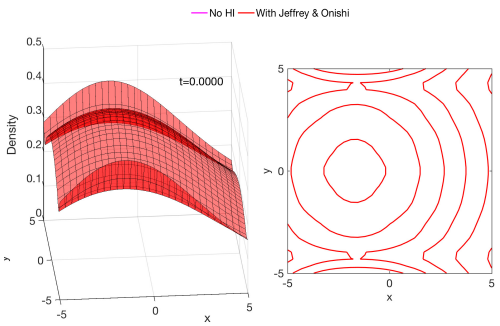

(a) Jeffrey & Onishi $t = 0$

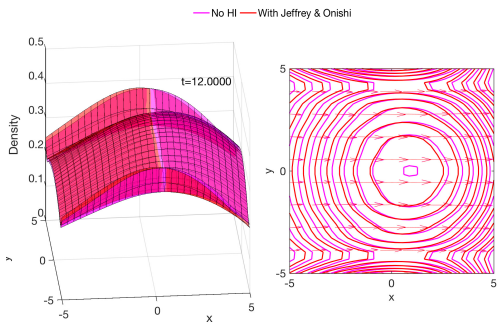

(b) Jeffrey & Onishi $t = 12$

Figure 6.10: $N = 50$ particles evolving with: Jeffrey & Onishi and with Zero HI in a slit of width 10.

compared to the reference solution with Zero HI. Both hard sphere fluids were driven in the slit by the time dependent potential V_{ex} with V_{mov} defined in (6.3.3). The corresponding Kim & Karrila solutions were found to be too stiff in the slit for cut-offs more than one diameter, and the resulting solutions do not differ substantially from the reference solutions Zero HI and are therefore not shown here. The stiffness in the numerical solution of the Kim & Karrila formalism justifies the need for more robust expressions for the short range HI, as presented in this thesis.

Chapter 7

Well-Posedness and Equilibrium Behaviour

In this chapter we establish the global well-posedness of overdamped dynamical density functional theory (DDFT): a nonlinear, nonlocal integro-partial differential equation used in statistical mechanical models of colloidal flow and other applications including nonlinear reaction-diffusion systems and opinion dynamics.

With no-flux boundary conditions, we determine the well-posedness of the full nonlocal equations including two-body hydrodynamic interactions (HI) through the theory of Fredolm operators. Principally, this is done by rewriting the dynamics for the density ϱ as a nonlocal Smoluchowski equation with a non-constant diffusion tensor $\boldsymbol{D}$ dependent on the diagonal part ($\boldsymbol{Z}_1$) of the HI tensor, and an effective drift $\boldsymbol{A}[\mathbf{a}]$ dependent on the off-diagonal part ($\boldsymbol{Z}_2$). We derive a scheme to uniquely construct the mean colloid flux $\mathbf{a}(\mathbf{r}, t)$ in terms of eigenvectors of $\boldsymbol{D}$, show that the stationary density $\varrho(\mathbf{r})$ is independent of the HI tensors, as well as proving exponentially fast convergence to equilibrium.

The stability of the equilibria $\varrho(\mathbf{r})$ is studied by considering the bounded (nonlocal) perturbation of the differential (local) part of the linearised operator. We show that the spectral properties of the full nonlocal operator with no-flux boundary conditions can differ considerably from those with periodic boundary conditions. We showcase our results by using the numerical methods available in the pseudo-spectral collocation scheme 2DChebClass [67].

7.1 Introduction

Existence, uniqueness and global asymptotic stability of the novel Smoluchowski equation in this overdamped limit has, until this work, remained unproven. It is the inclusion of HI that provides richness through additional nonlinearities in both the dissipation and convection terms. The inclusion of HI is interesting from both physical and mathematical standpoints. Physically, as above, the HI give rise to a much more complex evolution in the density. Mathematically, the convergence to equilibrium will depend inherently on the spectral properties of the effective diffusion tensor and effective drift vector arising from the HI. What is more, since the full N-body Fokker-Planck equation is a PDE in a very high dimensional phase space, well-posed nonlinear, nonlocal PDEs governing the evolution of the one-particle distribution function, valid in the mean field limit, describing the flow of nonhomogeneous fluids are desirable for computational reasons.

The equations studied in this paper are related to the McKean-Vlasov equation [32], a nonlinear nonlocal PDE of Fokker–Planck type that arises in the meanfield limit of weakly interacting diffusions. The novelty of the present problem lies in the space dependent diffusion tensor and nonlinear, nonlocal boundary conditions. Additionally, the problem that we study in this paper may in general not be written as a gradient flow, with the exception of the modelling assumption that the off-diagonal elements of the friction tensor $\boldsymbol{\Gamma}$ are zero. This choice is equivalent to setting $\boldsymbol{Z}_2$ to zero, and would be physically relevant for a diffuse system of particles

with a strong hydrodynamic interaction with a wall but weak inter-particle hydrodynamic interactions [66].

7.1.1 Description Of The Model.

In this work we analyse the overdamped partial differential equation (PDE) associated to a system of interacting stochastic differential equations (SDEs) on U an open, bounded subset of $\mathbb{R}^d$ of the following form, governing the positions $\mathbf{r}_i$ and momenta $\mathbf{p}_i$ of $i = 1, \dots, N$ colloidal particles immersed in a bath of many more, much smaller and much lighter particles:

$$\frac{\mathrm{d}\mathbf{r}_i}{\mathrm{d}t} = \frac{1}{m}\mathbf{p}_i, \tag{7.1.1a}$$

$$\frac{\mathrm{d}\mathbf{p}_i}{\mathrm{d}t} = -\nabla_{\mathbf{r}_i} V(\mathbf{r}^N, t) - \sum_{j=1}^{N} \boldsymbol{\Gamma}_{ij}(\mathbf{r}^N)\mathbf{p}_j + \sum_{j=1}^{N} \boldsymbol{B}_{ij}(\mathbf{r}^N)\mathbf{f}_j(t) \tag{7.1.1b}$$

where $\mathbf{r}^N = (\mathbf{r}_1, \cdots, \mathbf{r}_N)$, $\boldsymbol{B} = (mk_B\mathrm{T}\boldsymbol{\Gamma})^{1/2}$, $\boldsymbol{\Gamma} = \gamma(\mathbf{1} + \tilde{\boldsymbol{\Gamma}})$ (where the tilde denotes the nondimensional tensor and $\mathbf{1}$ is the $3N \times 3N$ identity matrix), V is a potential, k_B, T, γ are Boltzmann's constant, temperature and friction, respectively, and $\mathbf{f}_i(t) = (\zeta_i^x(t), \zeta_i^y(t), \zeta_i^z(t))^\top$ is a Gaussian white noise term with mean and correlation given by $\langle \zeta_i^a(t) \rangle = 0$ and $\langle \zeta_i^a(t), \zeta_j^b(t) \rangle = 2\delta_{ij}\delta^{ab}\delta(t - t')$.

In $d = 3$ dimensions, the friction tensor $\boldsymbol{\Gamma}$ comprises N^2 positive definite 3×3 mobility matrices $\boldsymbol{\Gamma}_{ij}$ for the colloidal particles. These couple the momenta of the colloidal particles to HI forces on the same particles, mediated by fluid flows in the bath. Typically, in the underdamped limit with dense suspensions, the HI may be short range lubrication forces, whereas in disperse systems in the overdamped limit, the HI are taken to be the long range forces given by the Rotne-Prager-Yamakawa tensor [154]. However, we do not make any such assumptions on the form of the tensors here.

We have described a general set of coupled Langevin equations with spatially-dependent friction tensor $\boldsymbol{\Gamma}(\mathbf{r}^N)$. As we will see, the dynamics (7.1.1a)–(7.1.1b) tend towards an equilibrium given by the Gibbs probability measure, which we will show to be independent of the friction tensor. Instead of computing the trajectories of individual particles we consider the evolution of the density of particles $\varrho(\mathbf{r}, t)$ given by the Smoluchowski equation in the high friction limit $\gamma \to \infty$,

$$\partial_t \varrho(\mathbf{r}, t) = -\tfrac{k_B\mathrm{T}}{m\gamma}\nabla_{\mathbf{r}} \cdot \mathbf{a}(\mathbf{r}, [\varrho], t) \qquad \text{for } \mathbf{r} \in U,\ t \in [0, T] \tag{7.1.2}$$

where $\mathbf{a}(\mathbf{r}, [\varrho], t)$ is the flux, $[\varrho]$ denotes functional dependence, $U \subseteq \mathbb{R}^d$ and $T < \infty$. Equation (7.1.2) was derived rigorously as a solvability condition of the corresponding Vlasov-Fokker-Planck equation for the one-body density in position and momentum space $f(\mathbf{r}, \mathbf{p}, t)$ by writing f as a Hilbert expansion in a small nondimensional parameter $\epsilon \propto \gamma^{-1}$ [63]. Therein, ϵ has units length, and therefore a problem specific length scale must be introduced to make it truly nondimensional.

We are interested in global existence, uniqueness, positivity and regularity of the weak solution to (7.1.2) when $\mathbf{a}(\mathbf{r}, t)$ is given by the integral equation

$$\mathbf{a}(\mathbf{r}, t) + \boldsymbol{H}[\mathbf{a}, \varrho](\mathbf{r}, t) + \frac{\varrho(\mathbf{r}, t)}{k_B\mathrm{T}}\boldsymbol{D}(\mathbf{r}, [\varrho], t)\nabla_{\mathbf{r}}\frac{\delta\mathscr{F}}{\delta\varrho}[\varrho](\mathbf{r}, t) = 0, \tag{7.1.3a}$$

$$\boldsymbol{H}[\mathbf{a}, \varrho](\mathbf{r}, t) := \varrho(\mathbf{r}, t)\boldsymbol{D}(\mathbf{r}, [\varrho], t)\int_U \mathrm{d}\mathbf{r}'\, g(\mathbf{r}, \mathbf{r}')\boldsymbol{Z}_2(\mathbf{r}, \mathbf{r}')\mathbf{a}(\mathbf{r}', t),$$

$$\frac{\varrho(\mathbf{r}, t)}{k_B\mathrm{T}}\nabla_{\mathbf{r}}\frac{\delta\mathscr{F}}{\delta\varrho}[\varrho](\mathbf{r}, t) := [\nabla_{\mathbf{r}} + \tfrac{1}{k_B\mathrm{T}}\Big(\nabla_{\mathbf{r}}V_1(\mathbf{r}, t) + \int_U \mathrm{d}\mathbf{r}'\varrho(\mathbf{r}', t)g(\mathbf{r}, \mathbf{r}')\nabla_{\mathbf{r}}V_2(\mathbf{r}, \mathbf{r}')\Big)]\varrho(\mathbf{r}, t), \tag{7.1.3b}$$

where to ease notation we have suppressed $[\varrho]$ in the argument of $\mathbf{a}$ and $\mathscr{F}$ is the free energy functional which will be defined in Section 7.1.2. The functions V_1 and V_2 are the external and (two body) interparticle potentials respectively. Additionally, the non-constant diffusion tensor

$$\boldsymbol{D}(\mathbf{r},[\varrho],t) := \frac{k_{\mathrm{B}}\mathrm{T}}{m\gamma}\Big[\mathbf{1} + \int \mathrm{d}\mathbf{r}' g(\mathbf{r},\mathbf{r}')\varrho(\mathbf{r}',t)\boldsymbol{Z}_1(\mathbf{r},\mathbf{r}')\Big]^{-1} \tag{7.1.4}$$

will be considered; this is interesting from a physical point of view. It has been previously shown (see [63]) that for $\boldsymbol{Z}_1$ being positive definite, $\boldsymbol{D}$ is also positive definite and therefore has positive, finite eigenvalues. The term $g(\mathbf{r},\mathbf{r}')$ (regarded as known) is the correlation function defined by the two-body density $\varrho^{(2)}(\mathbf{r},\mathbf{r}',t) = g(\mathbf{r},\mathbf{r}')\varrho(\mathbf{r},t)\varrho(\mathbf{r}',t)$ and the operator $\boldsymbol{H}[\cdot]$ describes terms corresponding to HI.

If $\boldsymbol{D}$ is permitted to be positive semidefinite then $\boldsymbol{D}$ may have a zero eigenvalue, which, physically-speaking, would amount to the colloidal system possessing a zero diffusion rate in some subset of U. Such systems are interesting (for example, in many biological systems the physical domain U could be a substrate including cuts, voids or interior walls) but are not considered in this paper. Throughout this work the largest and smallest eigenvalues of $\boldsymbol{D}$ will be denoted $\mu_{\max}$ and $\mu_{\min}$, respectively.

Furthermore, for two-body HI, $\boldsymbol{Z}_1$, $\boldsymbol{Z}_2$ are the diagonal and off-diagonal blocks respectively of the translational component of the grand resistance matrix originating in the classical theory of low Reynolds number hydrodynamics between suspended particles [75], [92], related to the friction tensor by

$$\tilde{\boldsymbol{\Gamma}}_{ij}(\mathbf{r}^N) = \delta_{ij}\sum_{l\neq i}\boldsymbol{Z}_1(\mathbf{r}_i,\mathbf{r}_l) + (1-\delta_{ij})\boldsymbol{Z}_2(\mathbf{r}_i,\mathbf{r}_j).$$

In $d = 3$ dimensions, and for the particular case $N = 2$ (where N is the number of particles in the system), $\boldsymbol{\Gamma} \in \mathbb{R}^{6\times 6}$ and $\boldsymbol{\Gamma}_{ij}$ may be seen as equivalent to the second-rank tensor of the translational part of the resistance matrix as found in [92] used to model lubrication forces. It should be noted however that the definition of those resistance matrices are formalism dependent, that is, the individual entries are scalar functions arising from the solution of Stokes equations for two-body lubrication interactions using multipole methods. Conversely, $\boldsymbol{\Gamma}_{ij}$ are general tensors, independent of the type of HI under consideration, and are therefore a more general representation of hydrodynamic phenomena of colloidal suspensions. Additionally, $\boldsymbol{\Gamma}_{ij}$ may be used to model not just lubrication forces between particles but also long range forces, wall effects and more. In the case of inter-particle HI, the diagonal blocks $\boldsymbol{\Gamma}_{ii}$ each represent the force exerted on the fluid due to the motion of particle i, which is simply the sum of all the pairwise HI from the perspective of particle i. The off-diagonal blocks $\boldsymbol{\Gamma}_{ij}$ represent the force on particle i due to the motion of particle j.

The stationary equations for the equilibrium density $\varrho(\mathbf{r})$ and equilibrium flux $\mathbf{a}(\mathbf{r})$ are given by

$$\nabla_{\mathbf{r}}\cdot\mathbf{a}(\mathbf{r}) = 0, \tag{7.1.5a}$$

$$\mathbf{a}(\mathbf{r}) + \boldsymbol{H}[\mathbf{a},\varrho](\mathbf{r}) + \frac{\varrho(\mathbf{r},t)}{k_B\mathrm{T}}\boldsymbol{D}(\mathbf{r},[\varrho],t)\nabla_{\mathbf{r}}\frac{\delta\mathscr{F}}{\delta\varrho}[\varrho](\mathbf{r}) = 0. \tag{7.1.5b}$$

Note that given a finite flux vector $\mathbf{a}$ solving (7.1.5a)-(7.1.5b), it is not obvious that ϱ is necessarily a minimiser of the free energy $\mathscr{F} - \int_U \mathrm{d}\mathbf{r}\,\mu_c\varrho$ (where μ_c is the chemical potential of the species). However, for the particular choice $\mathbf{a} \equiv \mathbf{0}$ (which is a natural and physically realistic solution), ϱ is necessarily a minimiser of $\mathscr{F} - \int_U \mathrm{d}\mathbf{r}\,\mu_c\varrho$, and we will show that under reasonable assumptions these are indeed the only fixed points of the system.

Previous well-posedness studies of similar nonlinear, nonlocal PDEs focused on periodic boundary conditions; see, e.g., [29, 33]. In contrast, we are interested in the well-posedness of (7.1.2), (7.1.3a)-(7.1.3b) subject to no-flux boundary conditions. This choice admits the nontrivial effect of the two body forces generated by the potential V_2 interacting with density on the boundary of the physical domain. We also seek to understand the asymptotic stability of stationary states. The motivation for this choice of boundary condition is physical; it cor-

responds to a closed system of particles in which the particle number is conserved over time. It is clear that most applications of such equations will be in confined systems, rather than a periodic domain and, as such, no-flux boundary conditions are natural. We note that the choice of boundary condition is expected to have significant effects on the dynamics, including the form of the bifurcation diagram.

7.1.2 Free Energy Framework.

Related to the system (7.1.3a)-(7.1.3b), we define the free energy functional $\mathscr{F} : P_{\text{ac}}^{+}(U) \to \mathbb{R}$ where P_{ac}^{+} is the set of strictly positive definite absolutely continuous probability measures on U. We define

$$\mathscr{F}[\varrho] := \int_U \mathrm{d}\mathbf{r}\, \varrho(\mathbf{r},t) \log \varrho(\mathbf{r},t) + \int_U \mathrm{d}\mathbf{r}\, \varrho(\mathbf{r},t) \Big[V_1(\mathbf{r},t) + \tfrac{1}{2}(gV_2) \star \varrho \Big], \tag{7.1.6}$$

where $\star$ denotes convolution in space. Here we assume the probability measure ϱ has density with respect to the Lebesgue measure. Additionally we define the probability measure on U

$$\mu(\mathrm{d}\mathbf{r}) = \mathrm{d}\mathbf{r}\, Z^{-1} e^{-\frac{(V_1+(gV_2)\star\varrho)}{k_B \mathrm{T}}} \tag{7.1.7}$$

where $Z = \int_U \mathrm{d}\mathbf{r}\, e^{-\frac{(V_1+(gV_2)\star\varrho)}{k_B \mathrm{T}}}$ and ϱ (when it exists) satisfies the nonlinear equation

$$\varrho = Z^{-1} e^{-\frac{(V_1+(gV_2)\star\varrho)}{k_B \mathrm{T}}}.$$

The existence of a probability density ϱ, and therefore a probability measure μ in (7.1.7), is obtained by Lemma 7.5.1. The functional $\mathscr{F}$ gives rise to the density minimising the free energy associated to the system (7.1.1a)-(7.1.1b) as $\gamma \to \infty$, which will be shown in Theorem 7.4.5.

To make the connection between the free energy functional $\mathscr{F}$ in (7.1.6) and the theory of non-uniform classical fluids, one may consider the Helmholtz free energy functional, which is the central energy functional of DFT [53]

$$\mathscr{F}_H[\varrho] = \int_U \mathrm{d}\mathbf{r}\, \varrho(\mathbf{r},t) V_1(\mathbf{r},t) + k_B \mathrm{T} \int_U \mathrm{d}\mathbf{r}\, \varrho(\mathbf{r},t)[\log(\Lambda^3 \varrho(\mathbf{r},t)) - 1] + \mathscr{F}_{\text{ex}}[\varrho]$$

where $\mathscr{F}_{\text{ex}}$ is the excess over ideal gas term and Λ the de Broglie wavelength, which turns out to be superfluous. The term $\mathscr{F}_{\text{ex}}$ is not in general known, the exception being for one dimensional hard rods [140]. Using the free energy functional $\mathscr{F}_H$, the corresponding Euler-Lagrange equation is

$$\mu_c = V_1(\mathbf{r}) + k_B \mathrm{T}[\log(\Lambda^3 \varrho(\mathbf{r})) - 1] + \tfrac{\delta \mathscr{F}_{\text{ex}}}{\delta \rho}[\varrho] \tag{7.1.8}$$

where μ_c is the chemical potential which is constant at equilibrium. Note that μ_c should not be confused with the measure μ defined in (7.1.7). After taking the gradient of (7.1.8) and multiplying by ϱ we obtain

$$0 = \varrho(\mathbf{r}) \nabla_{\mathbf{r}} \tfrac{\delta \mathscr{F}}{\delta \rho}[\varrho] = k_B \mathrm{T} \nabla_{\mathbf{r}} \varrho + \varrho(\mathbf{r}) \nabla_{\mathbf{r}} \Big(V_1(\mathbf{r}) + \tfrac{\delta \mathscr{F}_{\text{ex}}}{\delta \rho}[\varrho] \Big).$$

At equilibrium, the sum rule holds (see, e.g. [9])

$$\varrho(\mathbf{r}) \nabla_{\mathbf{r}} \tfrac{\delta \mathscr{F}_{\text{ex}}}{\delta \varrho}[\varrho] = \sum_{n=2}^{N} \int \mathrm{d}\mathbf{r}^n \nabla_{\mathbf{r}} V_n(\mathbf{r}^n) \varrho_n(\mathbf{r}^n). \tag{7.1.9}$$

where $\varrho_n(\mathbf{r}^n)$ is the standard $n-$particle configuration distribution function in equilibrium and $V_n(\mathbf{r}^n)$ is the n–body potential contributing to the total potential energy (see (A2)). Limiting the particle interactions to two-body (limiting $n \leq 2$), with the approximation $\varrho_2(\mathbf{r},\mathbf{r}') = \varrho(\mathbf{r})\varrho(\mathbf{r}')g(\mathbf{r},\mathbf{r}',[\varrho])$, we take the first term in the above series to obtain the equality $\nabla_{\mathbf{r}} \mathscr{F}_H[\varrho] = \nabla_{\mathbf{r}} \mathscr{F}[\varrho]$. In this way wee see that the density minimising $\mathscr{F}_H$ will minimise $\mathscr{F}$.

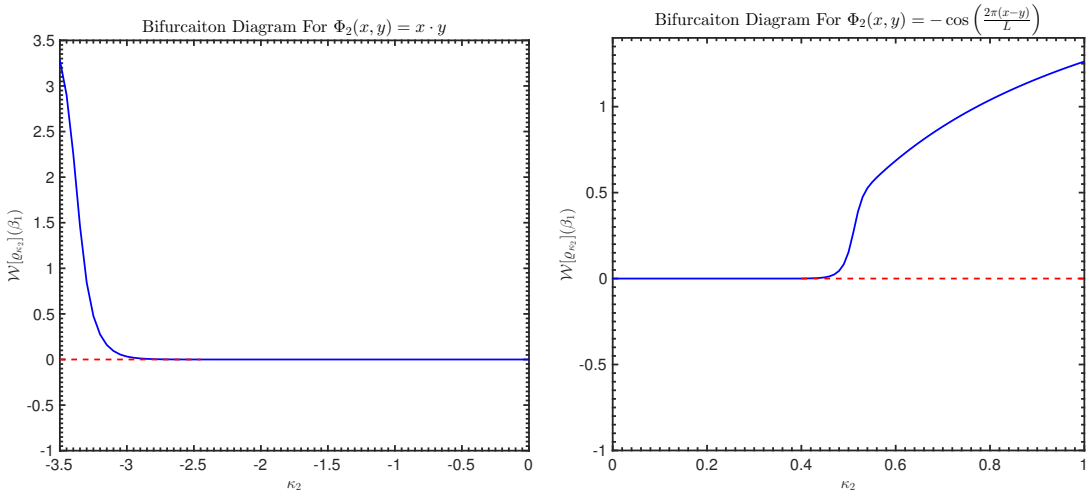

(a) (b)

Figure 7.1: (a). The bifurcation diagram for (a). $V_2(x,y) = x \cdot y$ and (b). $V_2(x,y) = -\cos\left(\frac{2\pi(x-y)}{\mathrm{L}}\right)$ in Section 7.8.1: the solid blue line denotes the stable branch of solutions while the dotted red line denotes the unstable branch of solutions. In (a) the stationary density e^{-x^2}/Z changes stability at the critical interaction energy $\kappa_2 = \kappa_{2\sharp} = -2.4$ and the new stable density is asymmetric adhering to one wall (Figure 7.4a). In (b), in the absence of a confining potential, the uniform density becomes unstable at the critical interaction energy $\kappa_2 = \kappa_{2\sharp} = 0.4$ and the density may become multi-modal (Figure 7.4b).

When $\boldsymbol{Z}_2 \equiv 0$, and after using the adiabatic approximation that (7.1.9) holds out of equilibrium, the PDE (7.1.2) simplifies to (cf. [146])

$$\partial_t \varrho = \nabla_{\mathbf{r}} \cdot \left[\boldsymbol{D}(\mathbf{r},t)\varrho(\mathbf{r},t)\, \nabla_{\mathbf{r}} \tfrac{\delta \mathscr{F}}{\delta \varrho}[\varrho] \right]. \tag{7.1.10}$$

From (7.1.10) we conclude that the dynamics under the choice $\boldsymbol{Z}_2 \equiv 0$ has a gradient flow structure. When $\boldsymbol{Z}_2$ is not zero, despite the fact that ϱ is always a conserved quantity, one cannot in general write the full dynamics (7.1.2) as a closed form gradient flow because ϱ is coupled to an integral equation for the flux $\mathbf{a}$. Hence, the inclusion of HI introduces a novel perturbation away from classical theory with gradient flow structure. Additionally, one sees how the free energy functional gives rise to the concept of a local pressure variation by the term inside the divergence of (7.1.10). In particular, the term $\frac{k_{\mathrm{B}}\mathrm{T}}{m}\varrho(\mathbf{r},t)\,\nabla_{\mathbf{r}}\frac{\delta \mathscr{F}}{\delta \varrho}[\varrho]$ represents the spatial variation of the energy available to change particle configurations per unit volume at fixed particle number, in other words, it is an analogue of a local pressure gradient for the particle density. We will show that $\mathscr{F}[\varrho]$ is associated to the PDE (7.1.2) even when $\boldsymbol{Z}_2 \neq 0$, that is $\partial_t \varrho = 0$ implies ϱ is a critical point of $\mathscr{F}$.

7.1.3 Description Of Main Results And Organisation Of The Chapter.

The main results of this work are threefold.

1. We establish existence and uniqueness of weak solutions to DDFTs including two-body HI governed by equations (7.1.2), (7.1.3a)-(7.1.3b) with no-flux boundary conditions.
2. We derive *a priori* convergence estimates of the density $\varrho(\mathbf{r},t)$ to equilibrium in L^2 and relative entropy.
3. We study the stability of equilibrium states and construct bifurcation diagrams for two numerical applications.

These results are of particular interest for physical applications of colloidal systems where conservation of mass is either a desirable or necessary property of the system. Additionally, the

stability theorem contrasts with simpler linear stability analyses of similar systems of gradient flow structure with periodic boundary conditions [116], [29] which may be tackled by means of Fourier analysis.

The chapter is organised as follows: in Section 7.2 we present the boundary and initial conditions, introduce the main notation, nondimensionalise the main equations, state the stationary equation for the density, define the weak formulation of the Smoluchowski equation including full HI and provide a list of assumptions. In Section 7.3 we state the main results of the present work in a precise manner. In Section 7.4 we provide an existence and uniqueness theorem for the flux $\mathbf{a}$ when full HI are included. In Section 7.5 we characterise solutions of the stationary problem and convergence to equilibrium in L^2 as $t \to \infty$. In Section 7.6 we obtain results on the global asymptotic stability of the stationary densities by showing that the free energy is a continuous functional for all two-body interaction strengths. Additionally we prove an H-theorem for the equilibria, provide *a priori* convergence estimates in relative entropy, derive an asymptotic expansion of the equilibria for small interaction energy and perform a spectral analysis of the linearised nonlocal Smoluchowski operator. In Section 7.7 we provide necessary and sufficient conditions for phase transitions in generalised DDFT-like systems with no-flux boundary conditions. In Section 7.8 we construct the bifurcation diagram for some example problems. In Section 7.9 we obtain an existence and uniqueness theorem for the Smoluchowski equation (7.2.3) with non-constant diffusion tensor and effective drift vector dependent on the two-body HI tensors $\boldsymbol{Z}_1$ and $\boldsymbol{Z}_2$. Finally, in Section 7.10 we provide some technical results that are used in the proof of Theorem 7.3.2.

7.2 Preliminaries

In this section we specify the nonlinear boundary conditions and initial data for the DDFT (7.1.2). We also nondimensionalise the governing equations and provide the assumptions on the regularity of the potentials, correlation function, diffusion tensor and initial data.

7.2.1 Boundary Conditions.

When $U = \mathbb{R}^d$ we take

$$\begin{cases} \varrho(\mathbf{r}, t) \to 0 \\ \mathbf{a}(\mathbf{r}, t) \to \mathbf{0} \end{cases} \quad \text{as} \quad |\mathbf{r}| \to \infty,$$

where we require V_1 to be growing at least quadratically as $\mathbf{r} \to \infty$. Physically-speaking this prevents the density from running out to infinity. When $U \subset \mathbb{R}^d$ is open and bounded we impose that the total mass of the system M remains constant, in particular we have

$$\mathbf{a}(\mathbf{r}, t) \cdot \mathbf{n}\Big|_{\partial U \times [0,T]} = 0. \tag{7.2.1}$$

The boundary condition (7.2.1) may be viewed as a *nonlinear* Robin condition imposing the flux through the boundary ∂U is zero for all time $t \in [0, T]$. If ϱ is a number density then $\int \mathrm{d}\mathbf{r}\, \varrho = N$ for all time, however for the analysis in Section 7.4 and onwards we will assume ϱ is a probability density so that $\int \mathrm{d}\mathbf{r}\, \varrho = 1$. The rescaling between number and probability densities is discussed in the following section.

7.2.2 Initial Conditions.

We will assume that the initial data has finite free energy and is consistent with the imposed boundary conditions. For example, one could prescribe initial data $(\varrho_0, \mathbf{a}_0)^\top$ such that

$$\frac{\delta \mathscr{F}}{\delta \varrho}[\varrho_0](\mathbf{r}) = \mu_c, \qquad \mathbf{a}_0 = \mathbf{0}.$$

where μ_c is the chemical potential, constant at equilibrium. It is straightforward to check that $(\varrho_0, \mathbf{a}_0)^\top$ is an equilibrium point of the system (7.2.2). Commonly, one then drives the system out of equilibrium via a time-dependent external potential. In principle μ_c may be given and the equations (7.1.2), (7.2.3) are well defined. In practice, for complicated particle configurations, μ_c is not known but can be computed by minimising the free energy along with the additional constraint $\int_U \mathrm{d}\mathbf{r}\, \varrho_0(\mathbf{r}) = N$, where N is the (expected) number of particles for a finite system and ϱ_0 is a number density. Note that μ_c is a potential, so by raising it one may force more particles into the system. We will assume that μ_c is constant to fix the number of particles. To ensure ϱ (and ϱ_0) is a probability density one may rescale $\varrho/N = \tilde{\varrho}$, $Ng = \tilde{g}$ and $\mathbf{a}/N^2 = \tilde{\mathbf{a}}$, where the tilde denotes the new variable, so that $\int_U \mathrm{d}\mathbf{r}\, \varrho_0(\mathbf{r}) = 1$ and equations (7.1.3a)-(7.1.3b) become independent of N.

This provides a method of converting back to the number density which is typically used in numerical modelling of finite colloidal systems [66], [62], [61]. Throughout however, since we will frequently use the integral of the density, we will assume ϱ and ϱ_0 are probability densities to ease notation. With this, one has three equations for three unknowns μ_c, ϱ_0, $\mathbf{a}_0$ and the initial density ϱ_0 can be computed. For the rest of paper it is convenient to work in dimensionless units. We now nondimensionalise the governing equations.

7.2.3 Evolution Equations.

We now nondimensionalise our equations. Let L, τ, U be characteristic length, time and velocity scales respectively, then by nondimensionalising

$$\mathbf{r} \sim \mathrm{L}\tilde{\mathbf{r}}, \quad t \sim \tau\tilde{t}, \quad \mathrm{U} = \tfrac{\mathrm{L}}{\tau}, \quad \varrho \sim \tfrac{1}{\mathrm{L}^d}\tilde{\varrho}, \quad \mathscr{F} \sim k_B\mathrm{T}\tilde{\mathscr{F}}, \quad \mathbf{a} \sim \mathrm{A}\tilde{\mathbf{a}}.$$

where d is the physical dimension and A is a characteristic flux scale. The system (7.1.2) becomes (after dropping tildes)

$$\partial_t \varrho(\mathbf{r}, t) = -\tfrac{1}{Fr} \times \tfrac{\tau^{-1}}{\gamma} \times \mathrm{A} \times \mathrm{L}^{d+1} \nabla_{\mathbf{r}} \cdot \mathbf{a}(\mathbf{r}, t),$$

where we have defined the Froude number $Fr = m\mathrm{U}^2/(k_B\mathrm{T})$. By choosing $Fr = 1$, $\tau = \gamma^{-1}$ and $\mathrm{A} = 1/\mathrm{L}^d$ we simplify the system of equations to the following boundary value problem.

Corollary 7.2.1. *The non-dimensional one-body density $\varrho(\mathbf{r}, t)$ and flux $\mathbf{a}(\mathbf{r}, t)$ evolve according the the boundary value problem*

$$\begin{cases} \partial_t \varrho = -\nabla_{\mathbf{r}} \cdot \mathbf{a}(\mathbf{r}, t), \\ \mathbf{a}(\mathbf{r}, t) + \boldsymbol{H}[\mathbf{a}, \varrho] + \varrho(\mathbf{r}, t)\boldsymbol{D}(\mathbf{r}, [\varrho], t)\nabla_{\mathbf{r}} \frac{\delta \mathscr{F}}{\delta \varrho}[\varrho] = 0, \\ \left[\boldsymbol{H}[\mathbf{a}, \varrho] + \varrho(\mathbf{r}, t)\boldsymbol{D}(\mathbf{r}, [\varrho], t)\nabla_{\mathbf{r}} \frac{\delta \mathscr{F}}{\delta \varrho}[\varrho]\right] \cdot \mathbf{n}\big|_{\partial U} = 0. \end{cases} \tag{7.2.2}$$

We note that when the off-diagonal HI tensor $\boldsymbol{Z}_2 = 0$, by using the definitions of $\mathscr{F}$ (7.1.6) and $\boldsymbol{D}$ (7.1.4), the evolution equations in (7.2.2) may be written as a nonlinear Smoluchowski equation (such as (7.1.10)) with non-constant diffusion coefficient. However we observe that even when $\boldsymbol{Z}_2 \neq 0$ the dynamics (7.2.2) may be recast into a Smoluchowski equation for ϱ under an effective drift vector dependent on $\boldsymbol{Z}_2$.

Corollary 7.2.2. *The non-dimensional one-body density $\varrho(\mathbf{r}, t)$ evolves according the the boundary value problem*

$$\begin{cases} \partial_t \varrho = \nabla_{\mathbf{r}} \cdot \left[Pe^{-1} \boldsymbol{D} \nabla_{\mathbf{r}} \varrho + \varrho\, \boldsymbol{D} \left(\nabla_{\mathbf{r}} (\kappa_1 V_1 + \kappa_2 (gV_2) \star \varrho) + \boldsymbol{A}[\boldsymbol{a}] \right) \right], \\ \qquad\qquad \Pi[\varrho] \cdot \mathbf{n}\big|_{\partial U} = 0, \\ \Pi[\varrho] := \boldsymbol{D} \left(\nabla_{\mathbf{r}} \varrho + \varrho\, \nabla_{\mathbf{r}} (\kappa_1 V_1(\mathbf{r}, t) + \kappa_2 (gV_2) \star \varrho) + \boldsymbol{A}[\boldsymbol{a}] \right), \end{cases} \tag{7.2.3}$$

where $\boldsymbol{A}[\boldsymbol{a}]$ is an effective background flow induced by the hydrodynamic interactions defined by

$$\boldsymbol{A}[\mathbf{a}] := \int_U \mathrm{d}\mathbf{r}'\, g(\mathbf{r},\mathbf{r}')\boldsymbol{Z}_2(\mathbf{r},\mathbf{r}')\mathbf{a}(\mathbf{r}',t), \tag{7.2.4}$$

κ_1, κ_2 are non-dimensional constants measuring the strength of confining and interaction potentials respectively, $Pe = \mathrm{LU}/\alpha$ is the Péclet number measuring the ratio of advection rates to diffusive rates and $\alpha = k_B\mathrm{T}/(m\gamma)$.

Corollary 7.2.2 is the general formulation of the nondimensional equations (7.1.3a)-(7.1.3b) when $\boldsymbol{Z}_2 \neq 0$, including a non-constant diffusion coefficient and an effective drift. Throughout this paper, to study the intermediate regime of equally strong advection and diffusion, we set $Pe = 1$. Additionally, to ease notation, we redefine the two-body potential to absorb the correlation function g, $V_2(\mathbf{r},\mathbf{r}') := g(\mathbf{r},\mathbf{r}')V_2(\mathbf{r},\mathbf{r}')$. We note that $g(\mathbf{r},\mathbf{r}')$ is a necessary inclusion in DFT problems, since, in the case of hard spheres, it smooths the singular kernels of the hydrodynamic interaction tensors at long range which diverge at the sphere centres (see, for example [154]). In the context of hard core DFT systems $g(\mathbf{r},\mathbf{r}')V_2(\mathbf{r},\mathbf{r}')$ is the Mayer function, see e.g. [148]. The choice of redefinition is therefore purely in the interest of notational simplicity. In practice, there are many choices for g, for example the hard sphere approximation takes $g(|\mathbf{r}-\mathbf{r}'|) = 0$ for $|\mathbf{r}-\mathbf{r}'| < 1$ and unity otherwise. Alternatively g may be obtained numerically from microscopic dynamics. We consolidate the choices for equations (7.2.2), (7.2.3) in Section 7.2.5.

The effective drift $\boldsymbol{A}[\mathbf{a}]$, dependent on $\boldsymbol{Z}_2$ and $\mathbf{a}$ may be determined once $\mathbf{a}(\mathbf{r},t)$ is solved from the second equation in (7.2.2). Note that the evolution equation in (7.2.3) may be viewed as a generalised McKean-Vlasov equation with a non-constant diffusion tensor and confining potential. In particular the McKean-Vlasov equation may be recovered in the special case $\boldsymbol{Z}_1 = \boldsymbol{Z}_2 = V_1 = 0$, see for example [29], [32]. We will use Corollary 7.2.2, to write the full dynamics including full HI, to obtain our results on weak solutions for $\varrho(\mathbf{r},t)$ (see Theorem 7.4.3, Section 7.4 and Theorem 7.9.10, Section 7.9). We continue to the next section by stating the stationary boundary value problem for equilibrium states $\varrho(\mathbf{r})$.

7.2.4 Stationary Equations.

For general $\boldsymbol{Z}_2$ we will show in Theorem 7.4.5 that the stationary density $\varrho(\mathbf{r})$ satisfies

$$\begin{cases} 0 = \nabla_{\mathbf{r}} \cdot [\boldsymbol{D}\nabla_{\mathbf{r}}\varrho + \varrho\, \boldsymbol{D}\nabla_{\mathbf{r}}(\kappa_1 V_1 + \kappa_2\, V_2 \star \varrho)], \\ \qquad\qquad \Pi[\varrho]\cdot\mathbf{n}\big|_{\partial U} = 0, \\ \Pi[\varrho] := \boldsymbol{D}\,(\nabla_{\mathbf{r}}\varrho + \varrho\,\nabla_{\mathbf{r}}(\kappa_1 V_1(\mathbf{r},t) + \kappa_2\, V_2 \star \varrho)). \end{cases} \tag{7.2.5}$$

We now discuss regularity on the potentials and diffusion tensor.

7.2.5 Assumptions & Definitions.

Typically for long range HI the $\boldsymbol{Z}_i$ exhibit singularities at the origin (particle centres) so the correlation function g is a necessary inclusion and provides a way of smoothing $\boldsymbol{D}$ and we assume $g \in L^\infty(U)$. For $\varrho \geq 0$ the diffusion tensor $\boldsymbol{D}$ as a convolution with the density will then be a weakly differentiable function. For the existence and uniqueness theory in Appendix 7.10 and Section 7.9 we require that first derivatives of $\boldsymbol{D}_{ij}$ to be bounded in $L^\infty(U)$ so that all coeeffiecients of the PDE (7.2.3) are uniformly bounded.

Out of equilibirum, we will suppress the time dependence on $\boldsymbol{D}$, V_1 simply to ease notation. However at equilibrium $\boldsymbol{D}$, V_1 are assumed to be independent of time, indeed in order for equilibrium states of the density and flux to be well defined. We note that is $\boldsymbol{D}$ positive definite and symmetric, as it has been rigorously shown to be [63]. In summary we have the following notational choices and assumptions for the evolution problem (7.2.3).

Notation Throughout we ease notation on the two-body interaction potential.

- The two-body interaction potential is redefined to absorb the correlation function g

$$V_2 \overset{\text{redef}}{:=} gV_2. \tag{N1}$$

For the dynamics we assume:

Assumptions D

- The diffusion tensor $\boldsymbol{D}$ is symmetric, positive definite, and the first derivatives of $\boldsymbol{D}_{ij}$ are bounded in $L^\infty(U)$

$$\boldsymbol{D}_{ij} \in W^{1,\infty}(U). \tag{D1}$$

- The diagonal and off-diagonal blocks of the HI tensors are uniformly bounded in the sense

$$\|gZ_2\|_{L^\infty(U)} < \infty, \quad \|gZ_1\|_{L^\infty(U)} < \infty \tag{D2}$$

- The initial data ϱ_0 is a non-negative, square-integrable, absolutely continuous probability density

$$\varrho_0 \in P_{ac}(U) \cap L^2(U). \tag{D3}$$

- The potentials each have two bounded derivatives

$$V_1, V_2 \in W^{2,\infty}(U). \tag{D4}$$

  The functions V_1 and V_2 are the confining and two-body interaction potentials respectively, the former having explicit time dependence ($V_1 = V_1(\mathbf{r}, t)$) only when we intend to drive (7.1.1a)-(7.1.1b) and (7.1.2) out of equilibrium, and $V_1 = V_1(\mathbf{r})$ when we are concerned with the equilibrium properties of (7.1.1a)-(7.1.1b) and (7.1.2). This distinction will be important for the H Theorem and equilibrium theory in Section 7.6.

For the equilibrium problem (7.2.5) we will assume:

Assumptions E

- The potentials have first order weak derivatives in $L^2(U)$

$$V_1, V_2 \in H^1(U). \tag{E1}$$

In particular, Assumption (E1) will permit us to establish smooth stationary densities. Note that typical inter-particle potentials, such as Morse or Coulomb, are unbounded as the particle separation goes to zero. This is once again mitigated by the choice of g, which we recall has been absorbed into V_2 by assumption (N1). In general we admit non-convex V_1 and V_2, for example multi-well potentials, except for in the convergence result of Theorem 7.6.7 where V_1 must be convex in order to invoke a log-Sobolev inequality on the measure μ given by (7.1.7).

The assumption (D3) that $\varrho_0 \in P_{\text{ac}}(U)$ is included in order to cover a wider set of physically relevant scenarios. In particular we permit initial data such that $\varrho_0|_A = 0$ for some $A \subset U$ where A is non-empty. Physically speaking this system could correspond to, at time $t = 0$, a box partitioned into closed regions with at least one region containing no particles. Then, instantaneously as soon as $t > 0$, the partition is removed allowing the particles to move freely. At the end of Section 7.9 we will show by simple application of Harnack's inequality, that we obtain strictly positive densities $\varrho(\mathbf{r}, t_1) > 0$ after an arbitrarily small time $t_1 > 0$. Principally this is provided by the property (D1), since $\boldsymbol{D}$ is positive definite, the diffusion of density in the system (7.2.3) is everywhere propagating in U.

Additionally, by the positive definite property in (D1) we may uniquely define the square root of $\boldsymbol{D}$ denoted $\boldsymbol{D}^{1/2}$ such that

$$\boldsymbol{D}^{1/2}\boldsymbol{D}^{1/2} = \boldsymbol{D}$$

for every $\mathbf{r} \in U$, $t \in [0,T]$ and each ϱ. We also define the eigenvalues $\mu_i \in \mathbb{R}^+$ of $\boldsymbol{D}$ and eigenvectors $\mathbf{e}_i(\mathbf{r},[\varrho],t) \in L^2(U)$ such that

$$\boldsymbol{D}\mathbf{e}_i = \mu_i \mathbf{e}_i. \tag{7.2.6}$$

Note that $\{\mathbf{e}_i\}_{i=1}^d$ forms an orthonormal basis of $\mathbb{R}^d$ (since $\boldsymbol{D}$ is a bounded, symmetric operator) for $i = 1, \cdots, d$ such that

$$\langle \mathbf{e}_i(\mathbf{r},[\varrho],t), \mathbf{e}_j(\mathbf{r},[\varrho],t)\rangle = \int_U \mathrm{d}\mathbf{r}\, \mathbf{e}_i(\mathbf{r},[\varrho],t)\cdot \mathbf{e}_j(\mathbf{r},[\varrho],t) = \delta_{ij}. \tag{7.2.7}$$

We continue to the next section by defining a weak formulation of the dynamics (7.2.2).

7.2.6 Weak Formulation.

We provide the weak formulation of the full dynamics including HI for $\boldsymbol{Z}_1, \boldsymbol{Z}_2$ not necessarily zero.

Definition 7.2.3 (Weak Solution)**.** *Let $\mathbf{a}(\mathbf{r},t)$ be a given flux. We say $\varrho \in L^2([0,T];H^1(U)) \cap L^\infty([0,T];L^2(U))$ and $\partial_t \varrho \in L^2([0,T];H^{-1}(U))$ is a weak solution to (7.2.2) if for every $\eta \in L^2([0,T];H^1(U))$*

$$\int_0^T \mathrm{d}t\, \langle \partial_t \varrho(t),\, \eta(t)\rangle + \int_0^T \mathrm{d}t \int_U \mathrm{d}\mathbf{r}\, \nabla_{\mathbf{r}}\eta \cdot \boldsymbol{D}\left[\nabla_{\mathbf{r}}\varrho + \varrho\, \nabla_{\mathbf{r}}(\kappa_1 V_1 + \kappa_2\, V_2 \star \varrho + \boldsymbol{A}[\mathbf{a}])\right] = 0 \tag{7.2.8}$$

where $\varrho_0 = \varrho(0)$. Here, $\boldsymbol{A}[\mathbf{a}]$ is the effective drift induced by $\boldsymbol{Z}_2$ and is defined by equation (7.2.4).

It will be shown in the following sections (in particular Corollary 7.4.8) that $\boldsymbol{A}[\mathbf{a}] \to \mathbf{0}$ as $t \to \infty$. We now state our main results in a precise manner.

7.3 Statement Of Main Results

Our main results concern existence, uniqueness and convergence to equilibrium of the density of colloids ϱ and flux $\mathbf{a}$ on U a compact subset of $\mathbb{R}^d$. The first result concerns existence of the flux $\mathbf{a}(\mathbf{r},t)$ with non-zero hydrodynamic interactions, the convergence of $\mathbf{a}(\mathbf{r},t)$ to zero at equilibrium and existence and uniqueness of fixed points of (7.2.2).

Theorem 7.3.1 (Existence & Uniqueness of Flux $\mathbf{a}(\mathbf{r},t)$ with Full HI)**.** *Let $\boldsymbol{Z}_1, \boldsymbol{Z}_2$ be real, symmetric and $\mu_{\max}\|g\boldsymbol{Z}_2\|_{L^\infty(U)} < 1$. Then*

1. *There exists a unique $\mathbf{a}(\mathbf{r},t) \in L^2(U)$ solving the evolution equation (7.2.2) for each $\varrho(\mathbf{r},t)$. In particular*

$$\mathbf{a}(\mathbf{r},t) = \sum_{n=1}^d \delta_n \sum_{i=1}^d \frac{\psi_i}{\phi_n - \mu_i^{-1}} \mathbf{e}_i(\mathbf{r},[\varrho],t)$$

   where $\mathbf{e}_i(\mathbf{r},[\varrho],t)$ are eigenvectors of the diffusion tensor $\boldsymbol{D}(\mathbf{r},[\varrho],t)$ and δ_n, ϕ_n, ψ_i, $\mu_i^{-1} \in \mathbb{R}$.

2. *In addition, every stationary density $\varrho(\mathbf{r})$ and stationary flux $\mathbf{a}(\mathbf{r})$ are independent of the HI tensors and satisfy*

$$\varrho(\mathbf{r})\nabla_{\mathbf{r}} \frac{\delta \mathscr{F}}{\delta \varrho}[\varrho(\mathbf{r})] = \mathbf{0}, \quad \mathbf{a}(\mathbf{r}) = \mathbf{0}$$

and consequently $\varrho(\mathbf{r})$ minimises the free energy $\mathscr{F}[\varrho](r) - \mu_c \int_U \mathrm{d}\mathbf{r}\, \varrho$, where μ_c is the chemical potential.

3. *If, in addition, $|\kappa_2| < \|V_2\|^{-1}_{L^\infty(U)}$ then $(\mathbf{a}_\star(\mathbf{r}), \varrho_\star) = (\mathbf{0}, \varrho_\infty)$ are the unique fixed points of (7.2.2) and $\varrho_\infty(\mathbf{r})$ is given by the self-consistency equation*

$$\varrho_\infty(\mathbf{r}) = \frac{e^{-(\kappa_1 V_1(\mathbf{r}) + \kappa_2 V_2 \star \varrho_\infty)}}{Z(\varrho_\infty)}$$

for $Z(\varrho_\infty) = \int_U \mathrm{d}\mathbf{r}\, e^{-(\kappa_1 V_1(\mathbf{r}) + \kappa_2 V_2 \star \varrho_\infty)}$.

For the evolution system (7.2.2) we present the following second main result of the paper.

Theorem 7.3.2 (Existence, Uniqueness of Weak $\varrho(\mathbf{r}, t)$)**.** *Let $\boldsymbol{Z}_1, \boldsymbol{Z}_2$ be real, symmetric and $\mu_{\max}\|g\boldsymbol{Z}_2\|_{L^\infty(U)} < 1$, where $\mu_{\max}$ is the largest eigenvalue of $\boldsymbol{D}$, with $\varrho_0 \in C^\infty(U)$, $\varrho \geq 0$ and $\int_U \mathrm{d}\mathbf{r}\varrho_0(\mathbf{r}) = 1$. Then there exists a unique weak solution $\varrho \in L^\infty([0,T]; L^2(U)) \cap L^2([0,T]; H^1(U))$, with $\partial_t \varrho \in L^2([0,T]; H^{-1}(U))$ for (7.2.2), in the sense (7.2.8), and the following energy estimate holds*

$$\|\varrho\|_{L^\infty([0,T];L^2(U))} + \|\varrho\|_{L^2([0,T];H^1(U))} + \|\partial_t \varrho\|_{L^2([0,T];H^{-1}(U))} \leq C(T)\|\varrho_0\|_{L^2(U)},$$

where $C(T)$ is a constant dependent on T, U and $\mu_{\max}$.

The existence and uniqueness is proved in Theorem 7.9.10, whilst the bound is shown in Lemma 7.9.7.

Furthermore, we prove existence and uniqueness of the stationary density, and exponentially fast convergence in relative entropy.

Lemma 7.3.3 (Existence and Uniqueness of the Stationary Density)**.** *Let $\boldsymbol{Z}_1, \boldsymbol{Z}_2$ be real, symmetric and ϱ be a solution to the DDFT (7.1.10) with smooth initial data and smooth V_1, V_2. Then there exists stationary density $\varrho(\mathbf{r}, t) = \varrho_0(\mathbf{r})$. If $|\kappa_2| \leq 1/4 \times \|V_2\|^{-1}_{L^\infty}$ then the stationary solution is unique and is denoted by ϱ_∞.*

The proof of this result is standard, see [44].

The third main result of this paper concerns *a priori* estimates for exponential convergence of the density to stationarity.

Theorem 7.3.4 (A Priori Convergence Estimates)**.** *Let $\boldsymbol{Z}_1, \boldsymbol{Z}_2$ be real, symmetric and ϱ be a solution to the DDFT (7.2.2) with smooth initial data and smooth V_1, V_2. If $\kappa_2 \leq 1/4 \times \|V_2\|^{-1}_{L^\infty}$ then*

1. **Convergence in $\boldsymbol{L^2(U)}$:** *For $\kappa_1 = 0$ (in the absence of a confining potential) if*

$$\kappa_2^2 < \frac{\mu_{\min} c_{pw}^{-2} \|\nabla_{\mathbf{r}} V_2\|^{-2}_{L^\infty(U)}}{2(1+e)\mu_{\max}},$$

where $\mu_{\min}$ and $\mu_{\max}$ are the smallest and largest eigenvalues of the diffusion tensor $\boldsymbol{D}$, then $\varrho \to \varrho_\infty$ in $L^2(U)$ exponentially fast as $t \to \infty$. For $\kappa_1 \neq 0$ the convergence criteria is modified to

$$\mu_{\max}(\kappa_1^2 \|\nabla_{\mathbf{r}} V_1\|^2_{L^\infty(U)} + 2\kappa_2^2(1+e)\|\nabla_{\mathbf{r}} V_2\|^2_{L^\infty(U)}) < \frac{\mu_{\min}}{c_{pw}^2}.$$

2. **Convergence in Relative Entropy:** *For any fixed confining potential V_1 such that the measure $\mu'(\mathrm{d}\mathbf{r}) = \mathrm{d}\mathbf{r}\, e^{-\kappa_1 V_1}/Z$ satisfies a log-Sobolev inequality and provided*

$$\kappa_2^2 < \frac{c_{ls}^{-1}}{2\|\nabla V_2\|^2_{L^\infty(U)}}$$

then the measure μ *in* (7.1.7) *satisfies a log-Sobolev inequality and* $\mathscr{H}(\varrho|\varrho_\infty) \to 0$ *exponentially fast as* $t \to \infty$ *where*

$$\mathscr{H}(\varrho|\varrho_\infty) = \int_U \mathrm{d}\mathbf{r}\, \varrho \log\left(\tfrac{\varrho}{\varrho_\infty}\right)$$

denotes the relative entropy.

For part 1, see Theorem 7.5.3 and Proposition 7.5.5. Theorem 7.6.7 gives the result for part 2.

The log-Sobolev inequality for μ is established by the Holley-Stroock perturbation lemma [82]. The constants c_{pw}, c_{ls} are the Poincaré-Wirtinger and log-Sobolev constants respectively. Nowhere do we assume parity on the two-body potential nor V_2 have zero mean. Additionally the optimal c_{pw} is the inverse square root of the smallest eigenvalue of the Laplacian on the domain U with no-flux boundary conditions.

We have the following conditions for the existence of bifurcating branches of steady states $\varrho(\mathbf{r})$.

Theorem 7.3.5 (Stability of Steady States)**.** *Fix* κ_1 *and let* $\kappa_2 \in (-\infty, \infty)$*. Let* $\mathscr{L}_1 = \mathscr{A}_{\kappa_2} + \kappa_2\mathscr{B}$ *denote the linearised operator to the stationary problem with eigenvalues* $\lambda(\kappa_2)$ *and eigenfunctions* $w^{(\kappa_2)}(\mathbf{r})$*. Denote by* $\mathscr{A}_{\kappa_2}$*,* $\mathscr{B}$ *the local and nonlocal parts of* $\mathscr{L}_1$ *respectively. Denote by* $\gamma_k^{(\kappa_2)}$ *the eigenvalues of* $\mathscr{A}_{\kappa_2}$ *with eigenvectors* $v^{(\kappa_2)}$*. If the solution* $\kappa_2^\star(\lambda)$ *of the equation* $\lambda = \lambda_{k^\star}(\kappa_2^\star)$ *exists, then it is unique and is given by the nonlinear equation*

$$\kappa_2^\star(\lambda) = \left(\sum_{i=1}^{\infty} \frac{\theta_i^{(\kappa_2)}\gamma_i^{(\kappa_2)}\beta_i^{(\kappa_2)}}{\lambda - \gamma_i^{(\kappa_2)}}\right)^{-1}.$$

As a corollary we can determine the necessary condition on the interaction strength for a bifurcation of stable equilibrium densities solving (7.2.5).

Corollary 7.3.6 (Necessary Conditions for Bifurcation)**.** *Provided that the spectral gap of* $\mathscr{A}_{\kappa_2}$ *is sufficiently large, that is,*

$$|\kappa_2| < \frac{\min_{i,j\in\mathbb{N}} |\gamma_i^{(\kappa_2)} - \gamma_j^{(\kappa_2)}|}{2\|\mathscr{B}\|}$$

then $\lambda(\kappa_2) \in \mathbb{R}$ *and the point of critical stability* $\kappa_{2_\sharp}$ *occurs at the solution of the nonlinear equation*

$$\kappa_{2_\sharp} = -\left(\sum_{i=1}^{\infty} \theta_i^{(\kappa_2)}\beta_i^{(\kappa_2)}\right)^{-1},$$

where $\theta_i\beta_i$ *are coefficients of the two-body potential expanded in the orthonormal basis of eigenvectors* $\{v_k^{(\kappa_{2_\sharp})}\}_{k=1}^\infty$.

The proofs of these results are given by Theorem 7.6.10 and the discussion immediately following it. We also obtain the following theorem for existence of bifurcations for the stationary equation (7.2.5).

Theorem 7.3.7. *Let* $\kappa_2 \in (-\infty, \infty)$ *and let* $\{\beta_n^{-1}\}_{n=1}^\infty$ *be the eigenvalues of* $\mathscr{R}$ *with eigenfunctions* $\{u_n\}_{n=1}^\infty$ *where*

$$\mathscr{R}[u_n] = -\varrho_{\kappa_2}(\mathbf{r}) \int_U \mathrm{d}\mathbf{r}'\, V_2(\mathbf{r}, \mathbf{r}')u_n(\mathbf{r}')$$

and ϱ_{κ_2} *is a stationary solution to* (7.2.5)*. If* $|\kappa_2| \geq |\beta_1|$ *then* ϱ_{κ_2} *is unstable with respect to* $\{u_n\}_{n=1}^\infty$ *with* (β_1, u_1) *a bifurcation point of* (7.4.21) *where* β_1 *is the smallest eigenvalue*

of $\mathscr{R}^{-1}$ and w_1 is the eigenfunction of $\mathscr{R}$ associated to β_1^{-1}. There exists $\varrho_* > 0$ such that $\mathscr{F}[\varrho_*] < \mathscr{F}[\varrho_{\kappa_2}]$.

We now give our arguments for Theorem 7.3.1.

7.4 Existence & Uniqueness of Flux With Full HI

We return to the full formulation of the overdamped DDFT with HI. The contraction condition $\mu_{\max}\|g\boldsymbol{Z}_2\|_{L^\infty(U)} < 1$ can be seen as a necessary condition on the invertibility of an operator closely related to the positive definite grand friction tensor $\boldsymbol{\Gamma}$. Note that the flux equation in (7.2.2) may be written as

$$(\mathbf{1} + \mathscr{Z}_1^\varrho + \mathscr{Z}_2^\varrho)[\mathbf{a}(\mathbf{r},t)] = -\varrho(\mathbf{r},t)\nabla_{\mathbf{r}}\frac{\delta\mathscr{F}}{\delta\varrho}[\varrho] \tag{7.4.1}$$

where the actions of the integral operators $\mathbf{1} + \mathscr{Z}_1^\varrho$ and $\mathscr{Z}_2^\varrho$ are defined by

$$(\mathbf{1} + \mathscr{Z}_1^\varrho)[\mathbf{a}_1] = \mathbf{a}_1(\mathbf{r},t) + \int_U \mathrm{d}\mathbf{r}' g(\mathbf{r},\mathbf{r}')\varrho(\mathbf{r}',t)\boldsymbol{Z}_1(\mathbf{r},\mathbf{r}') \times \mathbf{a}_1(\mathbf{r},t), \tag{7.4.2a}$$

$$\mathscr{Z}_2^\varrho[\mathbf{a}_2] = \varrho(\mathbf{r},t)\int_U \mathrm{d}\mathbf{r}'\, g(\mathbf{r},\mathbf{r}')\boldsymbol{Z}_2(\mathbf{r},\mathbf{r}')\mathbf{a}_2(\mathbf{r}',t). \tag{7.4.2b}$$

Notice how the integral-matrix operators in (7.4.2a)-(7.4.2b) resemble the operators in the first row of the grand resistance matrix for a two particle system from classical hydrodynamics [75]. The following lemma establishes a solvability condition for the flux equation in equation (7.4.1).

Lemma 7.4.1 (Conditional Convergence of the Fredholm Determinant)**.** *Let $\mathbf{1} + \mathscr{Z}_1^\varrho$ and $\mathscr{Z}_2^\varrho$ be bounded linear operators. Suppose $\mathscr{A}_\varrho := (\mathbf{1} + \mathscr{Z}_1^\varrho)^{-1}\mathscr{Z}_2^\varrho$ is compact in $L^2(U, \varrho^{-1}(\mathbf{r},t))$. If $\mu_{\max}\|g\boldsymbol{Z}_2\|_{L^\infty(U)} < 1$ then the matrix integral operator $\mathbf{1}+\mathscr{Z}_1^\varrho+\mathscr{Z}_2^\varrho$ is invertible and the system (7.4.1) is well-posed.*

Proof. Since $\mathbf{1} + \mathscr{Z}_1^\varrho$ is positive definite it is invertible, therefore (7.4.1) may be rewritten

$$(\mathbf{1} + (\mathbf{1} + \mathscr{Z}_1^\varrho)^{-1}\mathscr{Z}_2^\varrho)[\mathbf{a}(\mathbf{r},t)] = -(\mathbf{1} + \mathscr{Z}_1^\varrho)^{-1}\varrho(\mathbf{r},t)\nabla_{\mathbf{r}}\frac{\delta\mathscr{F}}{\delta\varrho}[\varrho]. \tag{7.4.3}$$

We note that $\mathscr{A}^\varrho$ is a trace-class operator and that the left hand side of (7.4.3) is an operator of the form $\mathbf{1} - \lambda\mathscr{A}_\varrho$. By classical theory [58], [103] we have the identity

$$\det(\mathbf{1} - \lambda\mathscr{A}_\varrho) = \exp\Big\{-\sum_{n=1}^{\infty}\frac{\mathrm{Tr}(\mathscr{A}_\varrho^n)}{n}\lambda^n\Big\}. \tag{7.4.4}$$

When $\lambda = -1$ we recover the determinant for the Fredholm operator on the left hand side of (7.4.3). Particularly, since for our consideration $|\lambda| = 1$, the convergence of the infinite summation inside the argument of the exponential in (7.4.4) will depend on the size of $\mathrm{Tr}\mathscr{A}_\varrho$, and when $\lambda = -1$, the summand is an alternating sequence so we demand absolute convergence for the sum in (7.4.4) to converge. We obtain results in $L^2(U, \varrho^{-1})$.

By definition of the trace we have

$$\mathrm{Tr}\mathscr{A}_\varrho^n = \sum_{k=1}^{d}\langle\mathscr{A}_\varrho^n\mathbf{e}_k(\mathbf{r}), \mathbf{e}_k(\mathbf{r})\rangle_{L^2(U,\varrho^{-1})},$$

where $\{\mathbf{e}_k\}_k$ are vectors such that their components form an orthonormal basis of $L^2(U, \varrho^{-1})$, in particular we choose the eigenvectors of the diffusion tensor $\boldsymbol{D}$. Since $\mathscr{A}$ is an integro-matrix

operator the inner product is given by, for $n = 1$

$$\begin{aligned}\mathrm{Tr}\mathscr{A}_\varrho &= \sum_{k=1}^{d}\langle \mathscr{A}_\varrho \mathbf{e}_k(\mathbf{r}), \mathbf{e}_k(\mathbf{r})\rangle_{L^2(U,\varrho^{-1})} \\ &= \sum_{k=1}^{d}\int_U \mathrm{d}\mathbf{r}\, \mathbf{e}_k(\mathbf{r})\cdot \boldsymbol{D}(\mathbf{r})\int_U \mathrm{d}\mathbf{r}'\, g(\mathbf{r},\mathbf{r}')\boldsymbol{Z}_2(\mathbf{r},\mathbf{r}')\mathbf{e}_k(\mathbf{r}') \\ &\leq \sum_{k=1}^{d}\mu_{\max}\|g\boldsymbol{Z}_2\|_{L^\infty(U)}\int_U \mathrm{d}\mathbf{r}\, \mathbf{e}_k(\mathbf{r})\cdot\int_U \mathrm{d}\mathbf{r}'\, \mathbf{e}_k(\mathbf{r}') \leq d\mu_{\max}\|g\boldsymbol{Z}_2\|_{L^\infty(U)}|U|\end{aligned}$$

where we have used $\int_U \mathrm{d}\mathbf{r}'\, \mathbf{e}_k(\mathbf{r}') \leq \|\mathbf{e}_k\|_{L^1(U)} \leq |U|^{1/2}\|\mathbf{e}_k\|_{L^2(U)} = |U|^{1/2}$ by orthonormality of the basis. Now for $n = 2$ we have

$$\begin{aligned}\mathrm{Tr}\mathscr{A}_\varrho^2 &= \sum_{k=1}^{d}\langle \mathscr{A}_\varrho^2 \mathbf{e}_k(\mathbf{r}), \mathbf{e}_k(\mathbf{r})\rangle_{L^2(U,\varrho^{-1})} \\ &= \sum_{k=1}^{d}\int_U \mathrm{d}\mathbf{r}\, \mathbf{e}_k(\mathbf{r})\cdot \varrho(\mathbf{r})^{-1}\int_U \mathrm{d}\mathbf{r}_1\, \varrho(\mathbf{r})\boldsymbol{D}(\mathbf{r})g(\mathbf{r},\mathbf{r}_1)\boldsymbol{Z}_2(\mathbf{r},\mathbf{r}_1) \\ &\quad\times\int_U \mathrm{d}\mathbf{r}_2\, \varrho(\mathbf{r}_1)\boldsymbol{D}(\mathbf{r}_1)g(\mathbf{r}_1,\mathbf{r}_2)\boldsymbol{Z}_2(\mathbf{r}_1,\mathbf{r}_2)\mathbf{e}_k(\mathbf{r}_2) \\ &\leq \sum_{k=1}^{d}\mu_{\max}^2\|g\boldsymbol{Z}_2\|_{L^\infty(U)}^2\int_U \mathrm{d}\mathbf{r}\, \mathbf{e}_k(\mathbf{r})\cdot\int_U \mathrm{d}\mathbf{r}_2\, \mathbf{e}_k(\mathbf{r}_2) \\ &\leq d\mu_{\max}^2\|g\boldsymbol{Z}_2\|_{L^\infty(U)}^2|U|,\end{aligned}$$

where we have used the fact that $\int_U \mathrm{d}\mathbf{r}_1\, \varrho(\mathbf{r}_1, t) = 1$ for $t \geq 0$ by the no-flux boundary condition (see Section 7.2.1). Iterating this argument one may obtain

$$\begin{aligned}\mathrm{Tr}\mathscr{A}_\varrho^n &= \sum_{k=1}^{d}\langle \mathscr{A}_\varrho^n \mathbf{e}_k(\mathbf{r}), \mathbf{e}_k(\mathbf{r})\rangle_{L^2(U,\varrho^{-1})} \\ &\leq \mu_{\max}^n\|g\boldsymbol{Z}_2\|_{L^\infty(U)}^n\sum_{k=1}^{d}\int_U \mathrm{d}\mathbf{r}\, \mathbf{e}_k(\mathbf{r})\cdot\int_U \mathrm{d}\mathbf{r}_n\, \mathbf{e}_k(\mathbf{r}_n) \\ &= |U|d\times\mu_{\max}^n\|g\boldsymbol{Z}_2\|_{L^\infty(U)}^n.\end{aligned}$$

We observe that absolute convergence of (7.4.4) requires $\mu_{\max}\|g\boldsymbol{Z}_2\| < 1$. In particular, the sum of the absolute values of the terms is given by

$$\sum_{n=1}^{\infty}\left|\tfrac{\mathrm{Tr}(\mathscr{A}_\varrho^n)}{n}\right| \leq d|U|\sum_{n=1}^{\infty}\tfrac{\mu_{\max}^n\|g\boldsymbol{Z}_2\|_{L^\infty(U)}^n}{n} = d|U|\log\left(\frac{1}{1-\mu_{\max}\|g\boldsymbol{Z}_2\|_{L^\infty(U)}}\right).$$

Thus for $\mu_{\max}||g\boldsymbol{Z}_2||_{L^\infty(U)} < 1$ the logarithm is finite and the determinant (7.4.4) is positive, otherwise for the boundary case $\mu_{\max}||g\boldsymbol{Z}_2||_{L^\infty(U)} = 1$ it may vanish, thus making $(\boldsymbol{I}+\mathscr{Z}_1^\varrho+\mathscr{Z}_2^\varrho)$ singular. □

We now provide a scheme for computing solutions of equation (7.4.1) for each time dependent $\varrho(\mathbf{r}, t)$. The existence and uniqueness of $\varrho(\mathbf{r}, t)$ is given in Section 7.9. First we establish that $\mathbf{1} + \mathscr{Z}_1^\varrho - \lambda\mathscr{Z}_2^\varrho$ is a compact self-adjoint operator in $L^2(U, \varrho^{-1})$.

Lemma 7.4.2 ($\mathbf{1} + \mathscr{Z}_1^\varrho - \lambda\mathscr{Z}_2^\varrho$ is compact and self-adjoint)**.** *Let $\lambda \in (-\infty, \infty)$ and assumption* (D2) *hold. Then $\mathbf{1} + \mathscr{Z}_1^\varrho - \lambda\mathscr{Z}_2^\varrho$ is a compact and self-adjoint operator.*

Proof. We let $\mathbf{a} \in L^1(U)$ and calculate $\|(\mathbf{1} + \mathscr{Z}_1^\varrho - \lambda\mathscr{Z}_2^\varrho)[\mathbf{a}]\|_{L^1(U)}$. In particular we have

$$\begin{aligned}\|(\mathbf{1} + \mathscr{Z}_1^\varrho - \lambda\mathscr{Z}_2^\varrho)[\mathbf{a}]\|_{L^1(U)} &= \int \mathrm{d}\mathbf{r} \left|(\mathbf{1} + \mathscr{Z}_1^\varrho - \lambda\mathscr{Z}_2^\varrho)[\mathbf{a}]\right| \\ &\leq \int \mathrm{d}\mathbf{r} \left|(\mathbf{1} + \mathscr{Z}_1^\varrho)\mathbf{a}\right| + |\lambda|\left|\mathscr{Z}_2^\varrho[\mathbf{a}]\right| \\ &\leq (1 + \|g\boldsymbol{Z}_1\|_{L^\infty(U)} + |\lambda|\|g\boldsymbol{Z}_2\|_{L^\infty(U)})\|\mathbf{a}\|_{L^1(U)} < \infty.\end{aligned}$$

Hence $\mathrm{Im}(\mathbf{1} + \mathscr{Z}_1^\varrho - \lambda\mathscr{Z}_2^\varrho)$ is bounded in $\mathbb{R}^3$. Now by Heine–Borel, the closure of $\mathrm{Im}(\mathbf{1} + \mathscr{Z}_1^\varrho - \lambda\mathscr{Z}_2^\varrho)$ is compact and hence $\mathbf{1} + \mathscr{Z}_1^\varrho - \lambda\mathscr{Z}_2^\varrho$ is a compact operator.

We now show that $\mathbf{1} + \mathscr{Z}_1^\varrho - \lambda\mathscr{Z}_2^\varrho$ is self-adjoint. The local part $\mathbf{1} + \mathscr{Z}_1^\varrho$ is a real, symmetric matrix and it is therefore self-adjoint, and in particular self-adjoint in $L^2(U, \varrho^{-1})$. All that remains is to study the nonlocal part $\mathscr{Z}_2^\varrho$. By direct calculation we see that for $\mathbf{b} \in L^2(U)$

$$\begin{aligned}\langle \mathbf{b}, \mathscr{Z}_2^\varrho[\mathbf{a}]\rangle_{L^2(U,\varrho^{-1})} &= \int_U \mathrm{d}\mathbf{r}\, \mathbf{b}(\mathbf{r}) \cdot \int_U \mathrm{d}\mathbf{r}'\, g(\mathbf{r}, \mathbf{r}')\boldsymbol{Z}_2(\mathbf{r}, \mathbf{r}')\mathbf{a}(\mathbf{r}') \\ &= \int_U \mathrm{d}\mathbf{r}'\, \mathbf{b}(\mathbf{r})^\top \int_U \mathrm{d}\mathbf{r}\, g(\mathbf{r}, \mathbf{r}')\boldsymbol{Z}_2(\mathbf{r}, \mathbf{r}')^\top \mathbf{a}(\mathbf{r}') \\ &= \int_U \mathrm{d}\mathbf{r}' \int_U \mathrm{d}\mathbf{r}\, \left(g(\mathbf{r}, \mathbf{r}')\boldsymbol{Z}_2(\mathbf{r}, \mathbf{r}')\mathbf{b}(\mathbf{r})\right)^\top \mathbf{a}(\mathbf{r}') \\ &= \int_U \mathrm{d}\mathbf{r}'\mathbf{a}(\mathbf{r}') \cdot \int_U \mathrm{d}\mathbf{r}\, g(\mathbf{r}, \mathbf{r}')\boldsymbol{Z}_2(\mathbf{r}, \mathbf{r}')\mathbf{b}(\mathbf{r}) \\ &= \langle \mathscr{Z}_2^\varrho[\mathbf{b}], \mathbf{a}\rangle_{L^2(U,\varrho^{-1})}\end{aligned}$$

where we have used the symmetry of $\boldsymbol{Z}_2$, and on the last line used Fubini's theorem to interchange the order of the integration between the $\mathbf{r}'$ and $\mathbf{r}$ variables. Hence the lemma is proved. □

Since we have now established that $\mathbf{1} + \mathscr{Z}_1^\varrho - \lambda\mathscr{Z}_2^\varrho$ is a compact and self-adjoint operator we may use its eigenvectors as a complete basis of $\mathbb{R}^3$ to expand the flux $\mathbf{a}(\mathbf{r}, t)$.

Theorem 7.4.3 (Eigenfunction Expansion of the Flux $\mathbf{a}(\mathbf{r}, t)$)**.** *Let $\boldsymbol{Z}_2$ be symmetric and real and $\mu_{\max}\|g\boldsymbol{Z}_2\|_{L^\infty(U)} < 1$ and let $\mathbf{e}_i(\mathbf{r}, [\varrho], t)$ and μ_i^{-1} be the eigenvectors and eigenvalues of $\boldsymbol{D}^{-1}(\mathbf{r}, [\varrho], t)$ where $[\cdot]$ denotes functional dependence and $i = 1, \cdots, d$. Then there is a unique $\mathbf{a}(\mathbf{r}, t) \in L^2(U)$ solving* (7.4.1) *given by the eigenfunction expansion*

$$\mathbf{a}(\mathbf{r}, t) = \sum_{n=1}^{d} \delta_n \mathbf{w}_n(\mathbf{r}, t). \tag{7.4.5}$$

Here, $\mathbf{w}_n$ are eigenfunctions of $(\mathbf{1} + \mathscr{Z}_1^\varrho - \lambda\mathscr{Z}_2^\varrho)$ obtained by a second expansion in $\mathbf{e}_i(\mathbf{r}, [\varrho], t)$ of the form

$$\mathbf{w}_n(\mathbf{r}, t) = \sum_{i=1}^{d} \frac{\psi_i}{\mu_i^{-1} - \phi_n} \mathbf{e}_i(\mathbf{r}, [\varrho], t). \tag{7.4.6}$$

Additionally, the expansion coefficients δ_n are given by the formula

$$\delta_n = \frac{1}{\phi_n} \sum_{i=1}^{d} \frac{\psi_i}{\phi_n - \mu_i^{-1}} \int_U \mathrm{d}\mathbf{r}\, \varrho(\mathbf{r}, t)\mathbf{e}_i(\mathbf{r}, [\varrho], t) \cdot \nabla_{\mathbf{r}} \frac{\delta \mathscr{F}}{\delta \varrho}[\varrho] \tag{7.4.7}$$

where $\{\phi_n\}_{n=1}^d$ are the discrete set of eigenvalues of $(\mathbf{1} + \mathscr{Z}_1^\varrho - \lambda\mathscr{Z}_2^\varrho)$ given by roots of the

equation $\lambda(\phi_n) = -1$, where the function $\lambda(\cdot)$ is defined by

$$\lambda(\phi_n) := \left[\sum_{l=1}^{d} \frac{\eta_l \, \psi_l}{\mu_l^{-1} - \phi_n}\right]^{-1}.$$

Finally, ψ_k and η_l are the expansion coefficients defined by

$$\varrho(\mathbf{r},t)g(\mathbf{r},\mathbf{r}')\boldsymbol{Z}_2(\mathbf{r},\mathbf{r}') = \sum_{k=1}^{d}\sum_{l=1}^{d} \psi_k \eta_l \mathbf{e}_k(\mathbf{r},[\varrho],t) \otimes \mathbf{e}_l(\mathbf{r}',[\varrho],t) \tag{7.4.8}$$

and each ϱ is obtained from the continuity equation and no-flux condition

$$\begin{aligned} \partial_t \varrho &= -\nabla_{\mathbf{r}} \cdot \mathbf{a}, \\ 0 &= \Pi[\varrho] \cdot \mathbf{n}|_{\partial U}. \end{aligned}$$

Remark 7.4.4. *The scalars μ_i^{-1}, ψ_k, η_l (and by proxy δ_n) each have functional dependence on ϱ since they are obtained by integrals involving $\mathbf{e}_j(\mathbf{r},[\varrho],t)$, for $i,j,k,l = 1,\cdots,d$. The eigenvalues ϕ_n are so called 'moving eigenvalues' of $(\mathbf{1} + \mathscr{Z}_1^{\varrho} - \lambda\mathscr{Z}_2^{\varrho})$ (cf. [39]). If $\boldsymbol{Z}_2 = 0$ then $\phi_i = \mu_i^{-1}$ for each $i = 1,\cdots,d$. In general, for $\boldsymbol{Z}_2 \neq 0$, an eigenvalue of $\boldsymbol{D}^{-1}$ may also be an eigenvalue of $(\mathbf{1} + \mathscr{Z}_1^{\varrho} - \lambda\mathscr{Z}_2^{\varrho})$ and this occurs on the line $\lambda = 0$. Since $\boldsymbol{Z}_2$ is symmetric it can be diagonalised, and therefore the kernel of the operator $\mathscr{Z}_2$ can be decomposed into a finite (of length d) sum of products of continuous functions and has at most d eigenvalues. The equation $\lambda(\phi_n) = -1$ may be rearranged into a characteristic polynomial equation in ϕ_n with coefficients dependent on η_l, ψ_l and μ_l and since $(\mathbf{1} + \mathscr{Z}_1^{\varrho} - \lambda\mathscr{Z}_2^{\varrho})$ is assumed to be real and symmetric, each $\phi_n \in \mathbb{R}$. Finally, the condition $\mu_{max}\|g\boldsymbol{Z}_2\|_{L^\infty(U)} < 1$ ensures $\phi_n \neq 0$ for any $n \in \mathbb{N}$.*

Proof. We consider the more general operator $(\mathbf{1} + \mathscr{Z}_1^{\varrho} - \lambda\mathscr{Z}_2^{\varrho})$ where $\lambda \in \mathbb{R}$. One may think of this operator as a nonlocal matrix operator where $(\mathbf{1} + \mathscr{Z}_1^{\varrho})$ is the local part and $\mathscr{Z}_2^{\varrho}$ is the nonlocal part. Here λ is a perturbation parameter measuring the distance of the full operator $(\mathbf{1}+\mathscr{Z}_1^{\varrho}-\lambda\mathscr{Z}_2^{\varrho})$ from locality. Since $\boldsymbol{Z}_1$ and $\boldsymbol{Z}_2$ are real and symmetric and $\lambda \in \mathbb{R}$, $\mathbf{1}+\mathscr{Z}_1^{\varrho}-\lambda\mathscr{Z}_2^{\varrho}$ coincides with its adjoint in $L^2(U,\varrho^{-1})$. For the homogeneous adjoint equation

$$(\mathbf{1} + \mathscr{Z}_1^{\varrho} - \lambda\mathscr{Z}_2^{\varrho})^{\dagger}\boldsymbol{z} = 0 \tag{7.4.9}$$

we know from Lemma 7.4.1 that when $\mu_{\max}\|g\boldsymbol{Z}_2\|_{L^\infty(U)} < 1$ there is no $\lambda \in \mathbb{R}$ satisfying $\det((\mathbf{1}+\mathscr{Z}_1^{\varrho}-\lambda\mathscr{Z}_2^{\varrho})^{\dagger}) = 0$ and therefore the only solution to the homogeneous adjoint equation (7.4.9) is $\boldsymbol{z} = \mathbf{0}$. Therefore by the Fredholm alternative there is a unique solution to (7.4.1).

Now consider the eigenvalue problem

$$(1 + \mathscr{Z}_1^{\varrho} - \lambda\mathscr{Z}_2^{\varrho})[\mathbf{w}_n(\mathbf{r},t)] = \phi_n \mathbf{w}_n(\mathbf{r},t) \tag{7.4.10}$$

for eigenvalues $\phi_n \in \mathbb{R}$ and eigenvectors $\mathbf{w}_n \in \mathbb{R}^d$. We write

$$\mathbf{w}_n = \sum_{j=1}^{d} \alpha_{j,n}\mathbf{e}_j(\mathbf{r},[\varrho],t). \tag{7.4.11}$$

By inserting (7.4.11) into (7.4.10) we obtain

$$(\mathbf{1} + \mathscr{Z}_1^{\varrho})\sum_{j=1}^{d} \alpha_{j,n}\mathbf{e}_j(\mathbf{r},[\varrho],t) - \lambda\mathscr{Z}_2^{\varrho}\left[\sum_{j=1}^{d} \alpha_{j,n}\mathbf{e}_j(\mathbf{r},[\varrho],t)\right] = \phi_n \sum_{j=1}^{d} \alpha_{j,n}\mathbf{e}_j(\mathbf{r},[\varrho],t). \tag{7.4.12}$$

Now by inserting the expansion (7.4.8) into (7.4.12) we obtain

$$\sum_{j=1}^{d} \alpha_{j,n}(\mu_j^{-1} - \phi_n)\mathbf{e}_j(\mathbf{r},[\varrho],t) - \lambda \sum_{k,l=1}^{d} \psi_k \, \eta_l \int_U \mathrm{d}\mathbf{r}' \mathbf{e}_k(\mathbf{r},[\varrho],t) \otimes \mathbf{e}_l(\mathbf{r}',[\varrho],t)\mathbf{w}_n(\mathbf{r}',t) = 0.$$

Taking the inner product of this equation with $\mathbf{e}_i(\mathbf{r},[\varrho],t)$ and integrating we obtain

$$\alpha_{i,n}(\mu_i^{-1}-\phi_n)-\lambda\,\psi_i\sum_{l=1}^{d}\eta_l\int_U \mathrm{d}\mathbf{r}'\mathbf{e}_l(\mathbf{r},[\varrho],t)\cdot\mathbf{w}_n(\mathbf{r}',t)=0,$$

which may be rearranged to obtain

$$\lambda=\frac{\alpha_{i,n}(\mu_i^{-1}-\phi_n)}{\psi_i\,\sum_{l=1}^{d}\eta_l\int_U \mathrm{d}\mathbf{r}'\mathbf{e}_l(\mathbf{r},[\varrho],t)\cdot\mathbf{w}_n(\mathbf{r}',t)}. \tag{7.4.13}$$

Since both the left hand side of (7.4.13) and $\sum_{l=1}^{d}\eta_l\int_U \mathrm{d}\mathbf{r}'\mathbf{e}_l(\mathbf{r},[\varrho],t)\cdot\mathbf{w}_n(\mathbf{r}',t)$ are independent of the index i it must be that

$$\frac{\alpha_{i,n}(\mu_i^{-1}-\phi_n)}{\psi_i}=K$$

for some constant K for which, without loss of generality, we choose $K=1$. With this we obtain an expression for the coefficients $\alpha_{i,n}$

$$\alpha_{i,n}=\frac{\psi_i}{\mu_i^{-1}-\phi_n}. \tag{7.4.14}$$

We may also obtain a scheme to determine the ϕ_n. In particular by (7.4.13) and (7.4.14) we have

$$\begin{aligned}\lambda&=\left(\sum_{l=1}^{d}\eta_l\int_U \mathrm{d}\mathbf{r}'\mathbf{e}_l(\mathbf{r},[\varrho],t)\cdot\mathbf{w}_n(\mathbf{r}',t)\right)^{-1}\\&=\left(\sum_{l=1}^{d}\eta_l\int_U \mathrm{d}\mathbf{r}'\mathbf{e}_l(\mathbf{r},[\varrho],t)\cdot\sum_{j=1}^{d}\frac{\psi_j}{\mu_j^{-1}-\phi_n}\mathbf{e}_j(\mathbf{r}',[\varrho],t)\right)^{-1}=\left(\sum_{l=1}^{d}\frac{\eta_l\,\psi_l}{\mu_l^{-1}-\phi_n}\right)^{-1}\end{aligned}$$

hence we have that the eigenvalues of $(\mathbf{1}+\mathscr{Z}_1^{\varrho}+\mathscr{Z}_2^{\varrho})$ are given by the roots of the equation $\lambda(\phi_n)=-1$.

We now return to the inhomogeneous problem (7.4.1) and expand $\mathbf{a}(\mathbf{r},t)$ in eigenfunctions $\mathbf{w}_n(\mathbf{r},t)$. We propose an expansion of the form (7.4.5) and insert into (7.4.1) to obtain

$$\sum_{n=1}^{d}\delta_n\phi_n\mathbf{w}_n(\mathbf{r},t)=-\varrho(\mathbf{r},t)\nabla_{\mathbf{r}}\frac{\delta\mathscr{F}}{\delta\varrho}[\varrho].$$

Now by taking the inner product with some $\mathbf{w}_k(\mathbf{r},t)$ and integrating we obtain

$$\delta_k\phi_k=-\int_U \mathrm{d}\mathbf{r}\;\varrho(\mathbf{r},t)\mathbf{w}_k(\mathbf{r},t)\cdot\nabla_{\mathbf{r}}\frac{\delta\mathscr{F}}{\delta\varrho}[\varrho].$$

By inserting the definition of $\mathbf{w}_k$ from (7.4.6) we deduce

$$\delta_k\phi_k=\sum_{i=1}^{d}\frac{\psi_i}{\phi_k-\mu_i^{-1}}\int_U \mathrm{d}\mathbf{r}\,\mathbf{e}_i(\mathbf{r},[\varrho],t)\cdot\varrho(\mathbf{r},t)\nabla_{\mathbf{r}}\frac{\delta\mathscr{F}}{\delta\varrho}[\varrho]. \tag{7.4.15}$$

Now we would like to divide through by ϕ_k but must check that no ϕ_k is zero for each $k=1,\cdots,d$. This is a consequence of the condition $\mu_{\max}\|g\boldsymbol{Z}_2\|<1$. In particular, using properties of the determinant, we have that

$$\det(\mathbf{1}+\mathscr{Z}_1^{\varrho}-\lambda\mathscr{Z}_2^{\varrho})=\det(\mathbf{1}+\mathscr{Z}_1^{\varrho})\times\det(\mathbf{1}-\lambda(\mathbf{1}+\mathscr{Z}_1^{\varrho})^{-1}\mathscr{Z}_2^{\varrho}).$$

Now since $\boldsymbol{D}$ is positive definite, so is $\mathbf{1}+\mathscr{Z}_1^{\varrho}$ and therefore $\det(\mathbf{1}+\mathscr{Z}_1^{\varrho})>0$ because the

determinant is simply the product of its (strictly positive) eigenvalues. Additionally, since $\mu_{\max}\|g\boldsymbol{Z}_2\| < 1$, we have by Lemma 7.4.1 $\det(\mathbf{1} - \lambda(\mathbf{1} + \mathscr{Z}_1^\varrho)^{-1}\mathscr{Z}_2^\varrho) > 0$ therefore $\det(\mathbf{1} + \mathscr{Z}_1^\varrho - \lambda\mathscr{Z}_2^\varrho) > 0$ and $\phi_k \neq 0$ for all $k \in \mathbb{N}$. We may now divide (7.4.15) by ϕ_k to obtain (7.4.7). Finally $\mathbf{a}(\mathbf{r}, t) \in L^2(U)$ may be seen by squaring (7.4.5), integrating over $\mathrm{d}\mathbf{r}$ and using (7.2.7). □

Theorem 7.4.3 provides a scheme for computing the unique flux $\mathbf{a}(\mathbf{r}, t)$, given ϱ satisfying $\partial_t\varrho = -\nabla_{\mathbf{r}} \cdot \mathbf{a}$ over time. We now use this result to show that the free energy functional $\mathscr{F}[\varrho]$ may be associated to the full system (7.2.2) even when $\boldsymbol{Z}_2 \neq 0$. In particular, that $\varrho(\mathbf{r}, t)$ solving (7.2.5) implies ϱ is a critical point of the free energy $\mathscr{F}[\varrho]$.

Theorem 7.4.5 ($\varrho(\mathbf{r})$ is a Critical Point of the Free Energy)**.** *Let $\mu_{\max}\|g\boldsymbol{Z}_2\|_{L^\infty(U)} < 1$ $V_1 = V_1(\mathbf{r})$ be a time independent confining potential so that $\varrho(\mathbf{r})$ is a stationary density to the system (7.2.2) then $\varrho(\mathbf{r})$ is a critical point of $\mathscr{F}[\varrho]$.*

Proof. Let $\varrho(\mathbf{r}, t) = \varrho(\mathbf{r})$ be a stationary density. Then by equation (7.2.2) one has

$$(\mathbf{1} + (\mathbf{1} + \mathscr{Z}_1^\varrho)^{-1}\mathscr{Z}_2^\varrho)[\mathbf{a}(\mathbf{r})] = -\varrho(\mathbf{r})\boldsymbol{D}(\mathbf{r}, [\varrho], t)\nabla_{\mathbf{r}}\frac{\delta\mathscr{F}}{\delta\varrho}[\varrho], \tag{7.4.16}$$

$$\nabla_{\mathbf{r}} \cdot \mathbf{a}(\mathbf{r}) = 0. \tag{7.4.17}$$

We have that for each λ, the operator $\mathbf{1} + \mathscr{Z}_1^\varrho - \lambda\mathscr{Z}_2^\varrho$ is compact self-adjoint in $L^2(U, \varrho^{-1}(\mathbf{r}, t))$ (by Lemma 7.4.2). We also have that $\mathbf{1} + \mathscr{Z}_1^\varrho - \lambda\mathscr{Z}_2^\varrho$ is positive definite for $\mu_{\max}\|gZ_2\|_{L^\infty(U)} < 1$. In particular, $\phi_n \neq 0$ for every $n = 1, \cdots d$ and $\phi_n(\lambda)$ is continuous function of λ such that $\phi_n(0) = \mu_n^{-1} > 0$ for each n. Hence we may invert $\mathbf{1} + \mathscr{Z}_1^\varrho + \mathscr{Z}_2^\varrho$ given $\mu_{\max}\|gZ_2\|_{L^\infty(U)} < 1$. With this, by using equations (7.4.16), (7.4.17) we have

$$0 = \nabla_{\mathbf{r}} \cdot \mathbf{a} = \nabla_{\mathbf{r}} \cdot \left(\varrho(\mathbf{r})(\mathbf{1} + \mathscr{Z}_1^\varrho + \mathscr{Z}_2^\varrho)^{-1}\nabla_{\mathbf{r}}\frac{\delta\mathscr{F}}{\delta\varrho}[\varrho]\right). \tag{7.4.18}$$

Now, assuming ϱ is stationary we see that

$$0 = \left\langle \frac{\delta\mathscr{F}}{\delta\varrho}[\varrho], \partial_t\varrho \right\rangle = -\int_U \mathrm{d}\mathbf{r}\, \frac{\delta\mathscr{F}}{\delta\varrho}[\varrho]\nabla_{\mathbf{r}} \cdot \mathbf{a} = \int_U \mathrm{d}\mathbf{r}\, \nabla_{\mathbf{r}}\frac{\delta\mathscr{F}}{\delta\varrho}[\varrho] \cdot \mathbf{a}$$

where we have used the no-flux boundary condition. Now since $(\mathbf{1} + \mathscr{Z}_1^\varrho + \mathscr{Z}_2^\varrho)^{-1}$ is strictly positive definite and self-adjoint in $L^2(U, \varrho^{-1}(\mathbf{r}, t))$ it possesses a unique strictly positive definite self-adjoint square root in $L^2(U, \varrho^{-1}(\mathbf{r}, t))$ (see [178]). We define $\mathscr{X}_\varrho = (\mathbf{1} + \mathscr{Z}_1^\varrho + \mathscr{Z}_2^\varrho)^{-1}$ and $\mathscr{X}_\varrho^{1/2}\mathscr{X}_\varrho^{1/2} = \mathscr{X}_\varrho$. Then we find

$$\begin{aligned}
0 &= \int_U \mathrm{d}\mathbf{r}\, \nabla_{\mathbf{r}}\frac{\delta\mathscr{F}}{\delta\varrho}[\varrho] \cdot \mathbf{a} = \int_U \mathrm{d}\mathbf{r}\, \nabla_{\mathbf{r}}\frac{\delta\mathscr{F}}{\delta\varrho}[\varrho] \cdot \mathscr{X}_\varrho\left[\varrho\nabla_{\mathbf{r}}\frac{\delta\mathscr{F}}{\delta\varrho}[\varrho]\right] \\
&= \left\langle \varrho\nabla_{\mathbf{r}}\frac{\delta\mathscr{F}}{\delta\varrho}[\varrho], \mathscr{X}_\varrho\left[\varrho\nabla_{\mathbf{r}}\frac{\delta\mathscr{F}}{\delta\varrho}[\varrho]\right] \right\rangle_{L^2(U,\varrho^{-1})} \\
&= \left\langle \mathscr{X}_\varrho^{1/2}\left[\varrho\nabla_{\mathbf{r}}\frac{\delta\mathscr{F}}{\delta\varrho}[\varrho]\right], \mathscr{X}_\varrho^{1/2}\left[\varrho\nabla_{\mathbf{r}}\frac{\delta\mathscr{F}}{\delta\varrho}[\varrho]\right] \right\rangle_{L^2(U,\varrho^{-1})} \\
&= \left\| \mathscr{X}_\varrho^{1/2}\left[\varrho\nabla_{\mathbf{r}}\frac{\delta\mathscr{F}}{\delta\varrho}[\varrho]\right] \right\|^2_{L^2(U,\varrho^{-1})}
\end{aligned} \tag{7.4.19}$$

where we have used the self-adjoint property of $\mathscr{X}_\varrho^{1/2}$. From the above we deduce that, since the integrand in the last line of (7.4.19) is positive, that the stationary density $\varrho(\mathbf{r})$ satisfies

$$\varrho(\mathbf{r})\nabla_{\mathbf{r}}\frac{\delta\mathscr{F}}{\delta\varrho}[\varrho(\mathbf{r})] = \mathbf{0}. \tag{7.4.20}$$

Therefore we obtain that ϱ is a critical point the free energy $\mathscr{F}[\varrho]$. □

Corollary 7.4.6. *Let $\mu_{\max}\|g\boldsymbol{Z}_2\|_{L^\infty(U)} < 1$ $V_1 = V_1(\mathbf{r})$ be a time independent confining potential. If ϱ is a stationary density then it is a critical point of the free energy $\mathscr{F}[\varrho] - \int \mathrm{d}\mathbf{r}\mu_c\varrho$.*

From Theorem 7.4.5 we obtain the following two corollaries. In particular, the proof shows rigorously how the diffusion tenor decouples from the stationary density.

Corollary 7.4.7. *Let $\boldsymbol{Z}_1$, $\boldsymbol{Z}_2$ be real and symmetric. Then the stationary density ϱ is independent of $\boldsymbol{Z}_1$, $\boldsymbol{Z}_2$ and, as a consequence, of $\boldsymbol{D}$.*

Additionally since (7.4.20) holds in equilibrium even when $\boldsymbol{Z}_2 \neq 0$ and the condition $\mu_{\max}\|g\boldsymbol{Z}_2\|_{L^\infty(U)} < 1$ implies that the operator $(\mathbf{1} + (\mathbf{1} + \mathscr{Z}_1^\varrho)^{-1}\mathscr{Z}_2^\varrho)$ has no zero eigenvalue, the homogeneous problem $(\mathbf{1}+(\mathbf{1}+\mathscr{Z}_1^\varrho)^{-1}\mathscr{Z}_2^\varrho) = \mathbf{0}$ (i.e. (7.4.1) at equilibrium) must have only the trivial solution $\mathbf{a}(\mathbf{r}) = \mathbf{0}$. In addition by equation (7.4.18), at equilibrium one has

$$\nabla_{\mathbf{r}} \cdot \left(\varrho(\mathbf{r}) \boldsymbol{D}(\mathbf{r}, [\varrho]) \nabla_{\mathbf{r}} \frac{\delta \mathscr{F}}{\delta \varrho}[\varrho] \right) = 0 \tag{7.4.21}$$

where $\boldsymbol{D}(\mathbf{r}, [\varrho])$ is the time limiting diffusion tensor.

Corollary 7.4.8. *Let $\boldsymbol{Z}_1$, $\boldsymbol{Z}_2$ be real and symmetric. Then $\mathbf{a}(\mathbf{r}) = \mathbf{0}$ is the unique stationary flux. In particular, there do not exist stationary densities which are advected by the existence of some non-zero flux, hence the only stationary states are equilibrium states.*

We remark that Corollary 7.4.7 is related to the well-known result that for finite dimensional reversible diffusions, i.e. Langevin dynamics of the form $dX_t = -(D((X_t))\nabla V((X_t)))\,dt + \nabla \cdot D(X_t)\,dt + \sqrt{2D(X_t)}\,dW_t$ for an arbitrary strictly positive definite mobility matrix D, V a confining potential and Wiener process W_t, the invariant measure $\mu(dx) = \frac{1}{Z}e^{-V(x)}\,dx$ is independent of D. We refer to [134, Sec 4.6]. To our knowledge, this is the first instance where such a result is proved in the context of DDFT.

In the following Sections 7.5, 7.6, 7.7, we consider the global asymptotic stability of the stationary equation (7.4.21) (equivalently (7.2.5)) for which, we have shown by Corollary 7.4.7, that (7.4.21) is the equation determining the equilibrium density the dynamics (7.1.2) driven to equilibrium by the HI tensors $\boldsymbol{Z}_1, \boldsymbol{Z}_2$.

Remark 7.4.9. *Out of equilibrium, the effective drift is augmented by $\boldsymbol{A}[\mathbf{a}]$ (as defined in* (7.2.4)*), the flow induced by the HI. In order to simplify the presentation of the calculations needed for the proofs of several results presented later on, (Theorem 7.5.3, Proposition 7.5.5, all results in Sections 7.9 and 7.10) we suppress $\boldsymbol{A}[\mathbf{a}]$ because it may trivially included as a linear contribution which is bounded in $L^1(U)$:*

$$\|\boldsymbol{A}[\mathbf{a}]\|_{L^1(U)} = \int_U \mathrm{d}\mathbf{r} \left| \int_U \mathrm{d}\mathbf{r}'\, \boldsymbol{Z}_2(\mathbf{r}, \mathbf{r}')\mathbf{a}(\mathbf{r}', t) \right| \leq \|\boldsymbol{Z}_2\|_{L^\infty(U)}\|\mathbf{a}\|_{L^1(U)} < \infty$$

where we have used (D2) *and the fact that, by Theorem 7.4.3, $\|\mathbf{a}\|^2_{L^1(U)} \leq |U|\|\mathbf{a}\|^2_{L^2(U)} < \infty$. Hence all the coefficients of* (7.2.3) *remain uniformly bounded and the existence and uniqueness results of Section 7.9 may be easily obtained with $\boldsymbol{A}[\mathbf{a}]$ included.*

Additionally, since we have shown that at equilibrium $\boldsymbol{A}[\mathbf{a}] = \mathbf{0}$ uniquely, the results of Sections 7.6, 7.7 hold for the dynamics (7.1.2) *tending to equilibrium including the effects of the HI.*

Given this remark, we now discuss the existence of stationary solutions to (7.6.8a).

7.5 Characterisation Of Stationary Solutions

We now define the stationary problem. We seek classical solutions $\varrho \in C^2(\bar{U})$ of

$$\nabla_{\mathbf{r}} \cdot [\boldsymbol{D}\left(\nabla_{\mathbf{r}}\varrho + \varrho\nabla_{\mathbf{r}}[\kappa_1 V_1 + \kappa_2 V_2 \star \varrho]\right)] = 0 \qquad \mathbf{r} \in U, \tag{7.5.1a}$$

$$\Pi[\varrho] \cdot \mathbf{n} = 0 \qquad \mathbf{r} \text{ on } \partial_U. \tag{7.5.1b}$$

where

$$\Pi[\varrho] := \boldsymbol{D}\left(\nabla_{\mathbf{r}}\varrho + \varrho\nabla_{\mathbf{r}}[\kappa_1 V_1 + \kappa_2 V_2 \star \varrho]\right).$$

The existence and uniqueness for the stationary problem is based on a fixed point argument for the nonlinear map, defined by integrating equation (7.5.1a). In particular we find the stationary distribution satisfies the nonlinear map (the self-consistency equation)

$$\varrho(\mathbf{r}) = \frac{e^{-(\kappa_1 V_1(\mathbf{r}) + \kappa_2 V_2 \star \varrho(\mathbf{r}))}}{Z}, \tag{7.5.2}$$

where $Z = \int_U \mathrm{d}\mathbf{r}\, \exp\{-(\kappa_1 V_1(\mathbf{r}) + \kappa_2 V_2 \star \varrho(\mathbf{r}))\}$. Note that the stationary distribution is independent of the diffusion tensor (see Corollary 7.4.7). We now present our first result concerning the existence and uniqueness of the solutions to the self-consistency equation.

Lemma 7.5.1 (Existence and Uniqueness of Stationary Solutions)**.** *The stationary equation* (7.5.1a) *with boundary condition* (7.5.1b) *has a smooth, non-negative solution with* $\|\varrho\|_{L^1(U)} = 1$. *When the interaction energy is sufficiently small,* $|\kappa_2| \leq 1/4 \times \|V_2\|_{L^\infty}^{-1}$, *the solution is unique.*

Proof. The proof follows Dressler et al. [44]. The main idea is to show that the right hand side of equation (7.5.2) is a contraction map on $C^2(U)$, and for sufficiently small interaction energy κ_2, $\varrho_\infty \in L^1(U)$ is the unique invariant measure which is a non-negative function with unit mean. Let $\Upsilon(\mathbf{r}, [\varrho]) = \kappa_1 V_1(\mathbf{r}) + \kappa_2 V_2 \star \varrho(\mathbf{r})$. We show that the map $S : L^1(U) \to L^1(U)$ defined by

$$S\varrho(\mathbf{r}) := \frac{1}{Z(\varrho)} \exp\left\{-\Upsilon(\mathbf{r}, [\varrho])\right\}$$

has a fixed point. Let B be the unit ball in $L^1(U)$ (the subset of normalised functions) we clearly have $S(B) \subset B$ since $\|S\varrho\|_{L_1(U)} = 1$. We must show that S is continuous and $S(B)$ is a compact subset of B. Observe that if V_2 is uniformly continuous then $\{V_2 \star \varrho \,|\, \varrho \in B\}$ is uniformly equicontinuous. Then by Arzela-Ascoli there exists a sequence $V_2 \star \varrho_{n_k}$ converging uniformly to some F,

$$V_2 \star \varrho_{n_k} \to F \quad \text{in } L^\infty(U) \quad \text{as} \quad k \to \infty.$$

Now observe that there exists N such that for every $n_k \geq N$

$$\int \mathrm{d}\mathbf{r}\, |e^{-(\kappa_1 V_1 + \kappa_2 V_2 \star \varrho_{n_k})} - e^{-(\kappa_1 V_1 + F)}| \leq \tfrac{1}{2} \int_U \mathrm{d}\mathbf{r} e^{-\kappa_1 V_1(\mathbf{r})}. \tag{7.5.3}$$

So, by the Lebesgue dominated convergence theorem, since the integral may be dominated by constants times $e^{-\kappa_1 V_1(\mathbf{r})}$ and the limit $k \to \infty$ may be taken inside the left hand side integral of (7.5.3) giving

$$\lim_{k\to\infty} \int \mathrm{d}\mathbf{r}\, |e^{-(\kappa_1 V_1 + \kappa_2 V_2 \star \varrho_{n_k})} - e^{-(\kappa_1 V_1 + F)}| = 0.$$

Similarly the composition of $\exp(\cdot)$ and $V_2 \star \varrho$ is continuous and by the Lebesgue dominated convergence theorem

$$\lim_{n\to\infty} Z(\varrho_n) = Z(\lim_{n\to\infty} \varrho_n) = Z(F).$$

Hence S is continuous.

Now we may write

$$S\varrho_n \to f := \frac{e^{-(F + \kappa_1 V_1)}}{Z(F)} \quad \text{in } L^1 \quad \text{as } n \to \infty.$$

Hence for any sequence in $S(B)$ there is a convergent subsequence whose limit is in $S(B)$ and

$\mathrm{Im}(S)$ is compact. So by Schauder fixed point theorem there exists a fixed point.

Now let $\varrho_1, \varrho_2 \in B$ then

$$\begin{aligned}\|S\varrho_1 - S\varrho_2\|_{L^1} &= \int \mathrm{d}\mathbf{r} \left| \tfrac{e^{-\Upsilon[\varrho_1]}}{Z(\varrho_1)} - \tfrac{e^{-\Upsilon[\varrho_2]}}{Z(\varrho_2)} \right| = \int \mathrm{d}\mathbf{r} \left| \tfrac{e^{-\Upsilon[\varrho_1]}}{Z(\varrho_1)} - \tfrac{e^{-\Upsilon[\varrho_2]}}{Z(\varrho_1)} + \tfrac{e^{-\Upsilon[\varrho_2]}}{Z(\varrho_1)} - \tfrac{e^{-\Upsilon[\varrho_2]}}{Z(\varrho_2)} \right| \\ &\leq \tfrac{1}{Z(\varrho_1)} \int \mathrm{d}\mathbf{r} \left| e^{-\Upsilon[\varrho_1]} - e^{-\Upsilon[\varrho_2]} \right| + \int \mathrm{d}\mathbf{r} \left| \tfrac{e^{-\Upsilon[\varrho_2]}}{Z(\varrho_1)} - \tfrac{e^{-\Upsilon[\varrho_2]}}{Z(\varrho_2)} \right|. \end{aligned} \tag{7.5.4}$$

Considering now the second term of (7.5.4), we have

$$\begin{aligned}\int \mathrm{d}\mathbf{r} \left| \tfrac{e^{-\Upsilon[\varrho_2]}}{Z(\varrho_1)} - \tfrac{e^{-\Upsilon[\varrho_2]}}{Z(\varrho_2)} \right| &= \left| \tfrac{1}{Z(\varrho_1)} - \tfrac{1}{Z(\varrho_2)} \right| \int \mathrm{d}\mathbf{r}\, e^{-\Upsilon[\varrho_2]} = Z(\varrho_2) \left| \tfrac{1}{Z(\varrho_1)} - \tfrac{1}{Z(\varrho_2)} \right| \\ &= \left| \tfrac{Z(\varrho_2) - Z(\varrho_1)}{Z(\varrho_1)} \right| = \tfrac{1}{Z(\varrho_1)} \left| \int \mathrm{d}\mathbf{r}\, e^{-\Upsilon[\varrho_1]} - \int \mathrm{d}\mathbf{r}\, e^{-\Upsilon[\varrho_2]} \right| \\ &\leq \tfrac{1}{Z(\varrho_1)} \int \mathrm{d}\mathbf{r} \left| e^{-\Upsilon[\varrho_1]} - e^{-\Upsilon[\varrho_2]} \right|. \end{aligned}$$

Using this estimate in (7.5.4) then gives

$$\|S\varrho_1 - S\varrho_2\|_{L^1} \leq \tfrac{2}{Z(\varrho_1)} \int \mathrm{d}\mathbf{r} \left| e^{-\Upsilon[\varrho_1]} - e^{-\Upsilon[\varrho_2]} \right|.$$

We will now show that S is a contraction.

We have, by the mean value theorem, $\forall a, b \in \mathbb{R}$, $|e^a - e^b| \leq e^a e^{|a-b|} |a - b|$. Using this inequality with $a = -\Upsilon[\varrho_1]$, $b = -\Upsilon[\varrho_2]$ gives

$$\begin{aligned}\tfrac{2}{Z(\varrho_1)} \int \mathrm{d}\mathbf{r}\, |e^{-\Upsilon[\varrho_1]} - e^{-\Upsilon[\varrho_2]}| &\leq \tfrac{2}{Z(\varrho_1)} \int \mathrm{d}\mathbf{r}\, e^{-\Upsilon[\varrho_1]} e^{|\Upsilon[\varrho_1] - \Upsilon[\varrho_1]|} |\Upsilon[\varrho_1] - \Upsilon[\varrho_1]| \\ &= \tfrac{2}{Z(\varrho_1)} \int \mathrm{d}\mathbf{r}\, e^{-\Upsilon[\varrho_1]} e^{|\kappa_2 V_2 \star (\varrho_1 - \varrho_2)|} |\kappa_2 V_2 \star (\varrho_1 - \varrho_2)|. \end{aligned}$$

Note that

$$|V_2 \star f| = \left| \int \mathrm{d}\mathbf{r}' V_2(\mathbf{r} - \mathbf{r}') f(\mathbf{r}') \right| \leq \|V_2\|_{L^\infty} \left| \int \mathrm{d}\mathbf{r}' f(\mathbf{r}') \right| \leq \|V_2\|_{L^\infty} \|f\|_{L^1},$$

and assuming $|\kappa_2| \leq 1/4 \times \|V_2\|_{L^\infty}^{-1}$, we obtain

$$\begin{aligned}\tfrac{2}{Z(\varrho_1)} \int \mathrm{d}\mathbf{r}\, |e^{-\Upsilon[\varrho_1]} - e^{-\Upsilon[\varrho_2]}| &\leq \tfrac{2}{Z(\varrho_1)} e^{\frac{1}{4}\|\varrho_1 - \varrho_2\|_{L^1}} \tfrac{1}{4} \|\varrho_1 - \varrho_2\|_{L^1} \int \mathrm{d}\mathbf{r}\, e^{-\Upsilon[\varrho_1]} \\ &\leq \frac{e^{1/2}}{2} \|\varrho_1 - \varrho_2\|_{L^1} < \|\varrho_1 - \varrho_2\|_{L^1}, \end{aligned}$$

where we have used that $\|\varrho_1 - \varrho_2\|_{L^1} \leq 2$ and $e^{1/2}/2 < 1$. Hence S is a contraction and by the contraction mapping theorem the fixed point is unique. □

Proposition 7.5.2 (Existence, Regularity, and Strict Positivity of Solutions for the Stationary Problem)**.** *Consider the stationary problem* (7.2.5) *such that Assumption* (E1) *holds. Then we have that*

1. *There exists a weak solution $\varrho \in H^1(U) \cap P_{ac}(U)$ to* (7.2.5) *as a fixed point of the equation* (7.5.2)*.*

2. *Any weak solution $\varrho \in H^1(U) \cap P_{ac}(U)$ is smooth and strictly positive, that is $\varrho \in C^\infty(\bar{U}) \cap P_{ac}^+(U)$.*

Proof. The proof is similar to [29, Theorem 2.3] but one must check the conclusions of the theorem hold with no flux boundary conditions and a confining potential V_1. This result is similar to arguments in [166] but here we consider a compact domain U. The weak formulation

of (7.2.5) is

$$-\int_U \mathrm{d}\mathbf{r}\, \nabla_{\mathbf{r}}\eta \cdot \boldsymbol{D}\nabla_{\mathbf{r}}\varrho - \kappa_1 \int_U \mathrm{d}\mathbf{r}\, \nabla_{\mathbf{r}}\eta \cdot \varrho \boldsymbol{D}\nabla_{\mathbf{r}} V_1 - \kappa_2 \int_U \mathrm{d}\mathbf{r}\, \nabla_{\mathbf{r}}\eta \cdot \varrho \boldsymbol{D}\nabla_{\mathbf{r}} V_2 \star \varrho = 0, \qquad (7.5.5)$$

for $\eta \in H^1(U)$ where we have used the no-flux boundary condition in (7.2.5) on ϱ and we seek solutions $\varrho \in H^1(U) \cap P_{ac}(U)$. Now define $F : P_{ac}(U) \to P_{ac}(U)$ by

$$F\varrho = \frac{1}{Z(\varrho, \kappa_2)} e^{-(\kappa_1 V_1 + \kappa_2 V_2 \star \varrho)}, \quad Z(\varrho, \kappa_2) = \int_U \mathrm{d}\mathbf{r}\, e^{-(\kappa_1 V_1 + \kappa_2 V_2 \star \varrho)}. \qquad (7.5.6)$$

By (7.5.2) we see that

$$\|F\varrho\|^2_{L^2(U)} \leq \frac{1}{|U|} e^{4(|\kappa_1| \|V_1\|_{L^\infty(U)} + |\kappa_2| \|V_2\|_{L^\infty(U)})} =: E_0, \qquad (7.5.7)$$

and therefore we seek solutions to (7.5.2) in the set $E := \{\varrho \in L^2(U) : \|\varrho\|^2_{L^2(U)} \leq E_0\}$. Note that E is a closed, convex subset of $L^2(U)$ and therefore we may redefine F to act on E. Additionally we see that for $\varrho \in E$

$$\begin{aligned} \|F\varrho\|^2_{H^1(U)} &= \|F\varrho\|^2_{L^2(U)} + \|\nabla_{\mathbf{r}} F\varrho\|^2_{L^2(U)} \\ &\leq E_0 \left(1 + 2|\kappa_1|^2 \|\nabla V_1\|^2_{L^2(U)} + |\kappa_2|^2 \|\nabla V_2\|^2_{L^2(U)} E_0\right), \end{aligned} \qquad (7.5.8)$$

where we have used that $\varrho \in L^1(U)$ by Lemma 7.5.1 and $V_1, V_2 \in H^1(U)$. Similarly to [29, Theorem 2.3] we have by (7.5.7) that $F(E) \subset E$ and by (7.5.8) $F(E)$ is uniformly bounded in $H^1(U)$. Therefore by Rellich's compactness theorem, $F(E)$ is relatively compact in $L^2(U)$, and therefore in E, since E is closed.

We may show using similar calculations to [44, Theorem 1] that the non-linear map in (7.5.2) is Lipschitz continuous in E, and by Schauder fixed point theorem there exists $\varrho \in E$ solving (7.5.2) which by (7.5.8) is in $H^1(U)$. By inserting the expression for $F\varrho$ (7.5.6) into (7.5.5) we obtain (1). Also note that solutions $\varrho \in E$ to (7.5.2) are bounded below by $E_0^{-1}/|U|^2$ giving positivity of solutions.

We now show that every weak solution in $\varrho \in H^1(U) \cap P_{ac}(U)$ is a fixed point of the nonlinear map in (7.5.2). Consider the frozen weak formulation

$$-\int_U \mathrm{d}\mathbf{r}\, \nabla_{\mathbf{r}}\eta \cdot \boldsymbol{D}\nabla_{\mathbf{r}}\theta - \kappa_1 \int_U \mathrm{d}\mathbf{r}\, \nabla_{\mathbf{r}}\eta \cdot \boldsymbol{D}\nabla_{\mathbf{r}} V_1 \theta - \kappa_2 \int_U \mathrm{d}\mathbf{r}\, \nabla_{\mathbf{r}}\eta \cdot \boldsymbol{D}\nabla_{\mathbf{r}} V_2 \star \varrho\, \theta = 0. \qquad (7.5.9)$$

This is the weak formulation of the PDE (for the unknown function θ)

$$\nabla_{\mathbf{r}} \cdot (\boldsymbol{D}\nabla_{\mathbf{r}}\theta + \theta \boldsymbol{D}(\nabla_{\mathbf{r}} V_1 + \nabla_{\mathbf{r}} V_2 \star \varrho)) = 0, \quad \text{s.t. } \nabla_{\mathbf{r}} \left((F\varrho)^{-1}\theta\right) \cdot \mathbf{n}|_{\partial U} = 0.$$

We note that we may rewrite the weak formulation (7.5.9) as

$$-\int_U \mathrm{d}\mathbf{r}\, \nabla_{\mathbf{r}}\eta \cdot \boldsymbol{D}\nabla_{\mathbf{r}} h\, F\varrho = 0$$

for every $\eta \in H^1(U)$ and where $h = \theta/(F\varrho)$. This holds true for any η, in particular $\eta = h$ hence we find

$$-\int_U \mathrm{d}\mathbf{r} \left|(F\varrho)^{1/2} \boldsymbol{D}^{1/2} \nabla_{\mathbf{r}} h\right|^2 = 0$$

where we have used that $\boldsymbol{D}$ is positive definite by (D1) and $F\varrho$ is strictly positive. All in all we obtain $\nabla_{\mathbf{r}} h = 0$ a.e. and hence $\theta = F\varrho$ up to normalisation. But if $F\varrho$ is a probability density we must have $\theta \equiv F\varrho$ and we conclude that since $\varrho = F\varrho$, any weak solution $\varrho \in H^1(U) \cap P^+_{ac}(U)$ of (7.5.5) must be such that $\varrho = F\varrho$. The regularity of ϱ follows from the same bootstrapping argument of [29, Theorem 2.3]. □

We can also obtain an estimate on the rate of convergence to the equilibrium density in $L^2(U)$ as $t \to \infty$ with the following theorem. In order to forgo additional assumptions on the initial data ϱ_0 we restrict ourselves to the case where the equilibrium density is unique and given by ϱ_∞.

Theorem 7.5.3 (Trend to Equilibrium in $L^2(U)$)**.** *Let $\varrho \in C^1([0,\infty]; C^2(U))$ be a solution of (7.2.3) with initial data $\varrho_0 \in L^2(U)$ a probability density. For $\kappa_1 = 0$, if*

$$\kappa_2^2 < \min\Big\{\frac{\mu_{\min} c_{pw}^{-2} \|\nabla_{\mathbf{r}} V_2\|_{L^\infty}^{-2}}{2(1+e)\mu_{\max}}, \frac{1}{4\|V_2\|_{L^\infty}}\Big\},$$

where c_{pw} is a Poincaré–Wirtinger constant on the domain U and $\mu_{\max}$ and $\mu_{\min}$ are the largest and smallest eigenvalues of $\boldsymbol{D}$, then $\varrho \to \varrho_\infty$ in $L^2(U)$ exponentially as $t \to \infty$. In particular the convergence in $L^2(U)$ is given by

$$\|\varrho(\cdot,t) - \varrho_\infty(\cdot)\|_{L^2(U)}^2 \le \|\varrho_0(\cdot) - \varrho_\infty(\cdot)\|_{L^2(U)}^2 e^{-r_{\kappa_2} t}$$

as $t \to \infty$ where $r_{\kappa_2} = \mu_{\min} c_{pw}^{-2} - 2\mu_{\max}|\kappa_2|^2(e+1)\|\nabla_{\mathbf{r}} V_2\|_{L^\infty(U)}^2$ is the rate of convergence.

Proof. Let $\psi = \varrho - \varrho_\infty$, then the evolution equation for ψ may be written

$$\partial_t \psi - \nabla_{\mathbf{r}} \cdot [\boldsymbol{D}\, \nabla_{\mathbf{r}} \psi] = \kappa_2 \nabla_{\mathbf{r}} \cdot [\boldsymbol{D}\, (\varrho_\infty \nabla_{\mathbf{r}} V_2 \star \psi + \psi \nabla_{\mathbf{r}} V_2 \star \varrho)]. \tag{7.5.10}$$

Multiplying by ψ, integrating and using the boundary condition $\Pi[\psi] \cdot \mathbf{n} = 0$ on $\partial U \times [0,T]$ we obtain

$$\begin{aligned} &\tfrac{1}{2}\frac{\mathrm{d}}{\mathrm{d}t}\|\psi(t)\|_{L^2(U)}^2 + \|\boldsymbol{D}^{1/2}\nabla_{\mathbf{r}}\psi\|_{L^2(U)}^2 \\ &\quad \le \int_U \mathrm{d}\mathbf{r}\, |\boldsymbol{D}^{1/2}\nabla_{\mathbf{r}}\psi| \times |\kappa_2 \boldsymbol{D}^{1/2}(\varrho_\infty \nabla_{\mathbf{r}} V_2 \star \psi + \psi \nabla_{\mathbf{r}} V_2 \star \varrho)|. \end{aligned}$$

Using Hölder's inequality on the right hand side this becomes

$$\begin{aligned} &\tfrac{1}{2}\frac{\mathrm{d}}{\mathrm{d}t}\|\psi(t)\|_{L^2(U)}^2 + \|\boldsymbol{D}^{1/2}\nabla_{\mathbf{r}}\psi\|_{L^2(U)}^2 \\ &\quad \le \|\boldsymbol{D}^{1/2}\nabla_{\mathbf{r}}\psi\|_{L^2(U)} \times \|\kappa_2 \boldsymbol{D}^{1/2}(\varrho_\infty \nabla_{\mathbf{r}} V_2 \star \psi + \psi \nabla_{\mathbf{r}} V_2 \star \varrho)\|_{L^2(U)}. \end{aligned}$$

Now using Young's inequality twice on the right hand side we obtain

$$\begin{aligned} &\tfrac{1}{2}\frac{\mathrm{d}}{\mathrm{d}t}\|\psi(t)\|_{L^2(U)}^2 + \|\boldsymbol{D}^{1/2}\nabla_{\mathbf{r}}\psi\|_{L^2(U)}^2 \\ &\quad \le \tfrac{1}{2}\|\boldsymbol{D}^{1/2}\nabla_{\mathbf{r}}\psi\|_{L^2(U)}^2 + \tfrac{1}{2}\|\boldsymbol{D}^{1/2}(\varrho_\infty \nabla_{\mathbf{r}} V_2 \star \psi + \psi \nabla_{\mathbf{r}} V_2 \star \varrho)\|_{L^2(U)}^2 \\ &\quad \le \tfrac{1}{2}\|\boldsymbol{D}^{1/2}\nabla_{\mathbf{r}}\psi\|_{L^2(U)}^2 + |\kappa_2|^2\|\varrho_\infty \boldsymbol{D}^{1/2}\nabla_{\mathbf{r}} V_2 \star \psi\|_{L^2(U)}^2 + |\kappa_2|^2\|\psi \boldsymbol{D}^{1/2}\nabla_{\mathbf{r}} V_2 \star \varrho\|_{L^2(U)}^2. \end{aligned} \tag{7.5.11}$$

From the positive definiteness and boundedness of the diffusion tensor, we have

$$\mu_{\min} \le \|\boldsymbol{D}\|_{L^\infty(U)} \le \mu_{\max}$$

, and, we also have the following bounds in terms of $\|\psi\|_{L^2(U)}^2$

$$\|\psi \boldsymbol{D}^{1/2}\nabla_{\mathbf{r}} V_2 \star \varrho\|_{L^2(U)}^2 \le \mu_{\max}\|\nabla_{\mathbf{r}} V_2\|_{L^\infty(U)}^2 \|\psi\|_{L^2(U)}^2 \tag{7.5.12}$$

$$\|\varrho_\infty \boldsymbol{D}^{1/2}\nabla_{\mathbf{r}} V_2 \star \psi\|_{L^2(U)}^2 \le |U|\mu_{\max}\|\varrho_\infty\|_{L^2(U)}^2 \|\nabla_{\mathbf{r}} V_2\|_{L^\infty(U)}^2 \|\psi\|_{L^2(U)}^2 \tag{7.5.13}$$

where $|U|$ denotes the size of U and in (7.5.12) we have used that $\nabla V_2 \star \varrho \le \|\nabla V_2\|_{L^\infty(U)}\|\varrho\|_{L^1(U)}$ and the fact that ϱ is a probability density with $\|\varrho\|_{L^1} = 1$ (see Corollary 7.9.3). To obtain

(7.5.13) we use that

$$\|\varrho_\infty \boldsymbol{D}^{1/2}\nabla_{\mathbf{r}} V_2 \star \psi\|^2_{L^2(U)} \leq \mu_{\max}\|\varrho_\infty\|^2_{L^2(U)}\|\nabla_{\mathbf{r}} V_2\|^2_{L^\infty(U)} \int_U \mathrm{d}\mathbf{r} \left|\rho_\infty(\mathbf{r}) \int \mathrm{d}\mathbf{r}'\, \psi(\mathbf{r}')\right|^2.$$

We then note that, by Hölder's inequality, $\int \mathrm{d}\mathbf{r}'\, \psi(\mathbf{r}') \leq \|\psi\|_{L^2}\|1\|_{L^2(U)} = |U|^{1/2}\|\psi\|_{L^2}$, which gives the result. For (7.5.13) it remains to bound the non explicit stationary distribution ϱ_∞ in $L^2(U)$, to do this we observe that by the self-consistency equation (7.5.2)

$$\|\varrho_\infty\|^2_{L^2(U)} \leq \frac{|U| \times e^{2|\kappa_2|\|V_2\|_{L^\infty}}}{|U|^2 \times e^{-2|\kappa_2|\|V_2\|_{L^\infty}}}. \tag{7.5.14}$$

Using (7.5.12), (7.5.14) and the bounds on $\boldsymbol{D}$, inequality (7.5.11) becomes

$$\begin{aligned}\tfrac{1}{2}\frac{\mathrm{d}}{\mathrm{d}t}\|\psi(t)\|^2_{L^2(U)} \leq &-\tfrac{\mu_{\min}}{2}\|\nabla_{\mathbf{r}}\psi\|^2_{L^2(U)} \\ &+ \mu_{\max}|\kappa_2|^2(e^{4|\kappa_2|\|V_2\|_{L^\infty}}+1)\|\nabla_{\mathbf{r}} V_2\|^2_{L^\infty(U)}\|\psi\|^2_{L^2(U)}.\end{aligned}$$

Now since ψ has mean zero we may use the Poincaré–Wirtinger inequality to write

$$\begin{aligned}\frac{\mathrm{d}}{\mathrm{d}t}\|\psi(t)\|^2_{L^2(U)} \leq &-\mu_{\min}c_{pw}^{-2}\|\psi\|^2_{L^2(U)} \\ &+ 2\mu_{\max}|\kappa_2|^2(e^{4|\kappa_2|\|V_2\|_{L^\infty}}+1)\|\nabla_{\mathbf{r}} V_2\|^2_{L^\infty(U)}\|\psi\|^2_{L^2(U)}.\end{aligned}$$

Finally, by Grönwall's lemma [52], we obtain

$$\begin{aligned}&\|\psi(t)\|^2_{L^2(U)} \\ &\quad\leq \|\psi(0)\|^2_{L^2(U)} \exp\left\{-(\mu_{\min}c_{pw}^{-2} - 2\mu_{\max}|\kappa_2|^2(e^{4|\kappa_2|\|V_2\|_{L^\infty}}+1)\|\nabla_{\mathbf{r}} V_2\|^2_{L^\infty(U)})t\right\}.\end{aligned} \tag{7.5.15}$$

Therefore for any ϱ_* a stationary density the necessary condition for exponential convergence $\varrho \to \varrho_*$ in $L^2(U)$ as $t \to \infty$ is

$$\mu_{\min}c_{pw}^{-2} - 2\mu_{\max}|\kappa_2|^2(e^{4|\kappa_2|\|V_2\|_{L^\infty}}+1)\|\nabla_{\mathbf{r}} V_2\|^2_{L^\infty(U)} > 0.$$

It will now be seen that, under the assumption that ϱ_∞ is the unique stationary density with $\kappa_2 \leq \|V_2\|^{-1}_{L^\infty}/4$, we may obtain an explicit condition for $|\kappa_2|$. In particular (7.5.15) becomes

$$\|\psi(t)\|^2_{L^2(U)} \leq \|\psi(0)\|^2_{L^2(U)} \exp\left\{-(\mu_{\min}c_{pw}^{-2} - 2\mu_{\max}|\kappa_2|^2(e+1)\|\nabla_{\mathbf{r}} V_2\|^2_{L^\infty(U)})t\right\}.$$

Then to ensure the argument in the exponential remains negative, we require

$$|\kappa_2|^2 < \frac{\mu_{\min}c_{pw}^{-2}\|\nabla_{\mathbf{r}} V_2\|^{-2}_{L^\infty}}{2(1+e)\mu_{\max}}.$$

This completes the proof of the theorem. □

Remark 7.5.4. *We remark that $\psi \in \left\{u \in H^1(U) \,|\, \int_U \mathrm{d}\mathbf{r}\, u = 0\right\}$, therefore, we may determine that the sharpest value of c_{pw} conincides with the Poincaré constant as found by Steklov [101], equal to $\nu_1^{-1/2}$ where ν_1 is the smallest eigenvalue of the problem*

$$\begin{aligned}\Delta u &= -\nu u \quad &&\text{in } U,\\ \partial_{\mathbf{n}} u &= 0 &&\text{on } \partial U.\end{aligned}$$

Here $\partial_{\mathbf{n}}$ is the directional derivative along the unit vector $\mathbf{n}$ pointing out of the domain U. Additionally Payne and Weinberger [138] proved that for convex domains in $\mathbb{R}^n$ one has $c_{pw} \leq \frac{\mathrm{diam}(U)}{\pi}$.

One may obtain a similar convergence result including a confining potential as given by the

following corollary.

Proposition 7.5.5 (Convergence with $\kappa_1 \neq 0$)**.** *Let $\kappa_1 \neq 0$ and let $\varrho \in C^1([0,\infty]; C^2(U))$ be a solution of (7.2.3) with initial data $\varrho_0 \in L^2(U)$ a probability density. Then the exponential convergence $\varrho \to \varrho_\infty$ in L^2 criteria is modified to*

$$\mu_{\max}\kappa_1^2 \|\nabla_{\mathbf{r}} V_1\|_{L^\infty(U)}^2 < r_{\kappa_2}$$

along with $|\kappa_2| \leq 1/4 \times \|V_2\|_{L^\infty(U)}^{-1}$. In particular the convergence in L^2 is given by

$$\|\varrho(\cdot,t) - \varrho_\infty(\cdot)\|_{L^2(U)}^2 \leq \|\varrho_0(\cdot) - \varrho_\infty(\cdot)\|_{L^2(U)}^2 e^{-(r_{\kappa_2} - \mu_{\max}\kappa_1^2 \|\nabla_{\mathbf{r}} V_1\|_{L^\infty(U)}^2)t}.$$

Proof. Since the inclusion of an external field is linear in the PDEs (7.2.3), (7.5.1a) the proof is similar to Lemma 7.5.3, the only term to resolve for the evolution equation for ψ first occurring at (7.5.10) being

$$\kappa_1^2 \|\psi \boldsymbol{D}^{1/2} \nabla_{\mathbf{r}} V_1\|_{L^2(U)}^2 \leq \kappa_1^2 \mu_{\max} \|\nabla V_1\|_{L^\infty(U)}^2 \|\psi\|_{L^2(U)}^2.$$

The remainder of the calculations to derive a Grönwall type inequality including this term are similar. □

7.6 Global Asymptotic Stability

In this section we study the stability properties of stationary states. We start by showing the free energy is a strictly convex functional, provided κ_2 is sufficiently small, and that $\mathscr{F}$ is bounded below. Recall the free energy functional $\mathscr{F} : P_{\mathrm{ac}}^+(U) \to \mathbb{R}$ is given by

$$\mathscr{F}[\varrho] := \int_U \mathrm{d}\mathbf{r}\, \varrho(\mathbf{r}) \log \varrho(\mathbf{r}) + \kappa_1 \int_U \mathrm{d}\mathbf{r}\, V_1(\mathbf{r})\varrho(\mathbf{r}) + \frac{\kappa_2}{2} \int_U \mathrm{d}\mathbf{r}\, \varrho(\mathbf{r}) V_2 \star \varrho(\mathbf{r}).$$

Proposition 7.6.1. *For $|\kappa_2| \in [0, \|V_2\|_{L^\infty(U)}^{-1})$ the free energy functional $\mathscr{F}$ is strictly convex. Additionally there exists a positive constant $B_0 < \infty$ for every $\varrho \in P_{ac}^+$ such that $|\mathscr{F}[\varrho]| \geq B_0$.*

Proof. Suppose ϱ_1 and ϱ_2 satisfy (7.1.10) with $\Pi[\varrho_1] \cdot \mathbf{n} = \Pi[\varrho_2] \cdot \mathbf{n} = 0$ on ∂_U for all $t \in [0,\infty)$. Letting $\zeta = \varrho_2 - \varrho_1$ and $\varrho_s = (1-s)\varrho_1 + s\varrho_2$ we compute $\frac{\mathrm{d}^2}{\mathrm{d}s^2}\mathscr{F}_H[\varrho_s]$ by direct calculation

$$\begin{aligned}
\frac{\mathrm{d}^2}{\mathrm{d}s^2}\mathscr{F}_H[\varrho_s] &= \frac{\mathrm{d}}{\mathrm{d}s}\frac{\mathrm{d}}{\mathrm{d}s}\left[\int_U \mathrm{d}\mathbf{r}\, \varrho_s \log \varrho_s + \kappa_1 \int_U \mathrm{d}\mathbf{r}\, \varrho_s V_1 + \frac{\kappa_2}{2}\int_U \mathrm{d}\mathbf{r}\, \varrho_s V_2 \star \varrho_s\right] \\
&= \frac{\mathrm{d}}{\mathrm{d}s}\left[\int_U \mathrm{d}\mathbf{r}\, \zeta \log \varrho_s + \zeta \right. \\
&\qquad \left. + \kappa_1 \int_U \mathrm{d}\mathbf{r}\, \zeta V_1 + \frac{\kappa_2}{2}\int_U \mathrm{d}\mathbf{r}\, \zeta V_2 \star \varrho_s + \frac{\kappa_2}{2}\int_U \mathrm{d}\mathbf{r}\, \varrho_s V_2 \star \zeta\right] \\
&= \int_U \mathrm{d}\mathbf{r}\, \frac{\zeta^2}{\varrho_s} + \kappa_2 \int_U \mathrm{d}\mathbf{r}\, \zeta V_2 \star \zeta.
\end{aligned}$$

Now using the measure $\mathrm{d}\mu = \varrho_s \mathrm{d}\mathbf{r}$ we have, by Jensen's inequality,

$$\int_U \mathrm{d}\mathbf{r}\, \frac{\zeta^2}{\varrho_s} = \int_U \mathrm{d}\mu\, \frac{\zeta^2}{\varrho_s^2} \geq \left(\int_U \mathrm{d}\mathbf{r}\, |\zeta|\right)^2.$$

We also have that V_2 is bounded below by the negative of its its essential supremum from

(7.2.5). Combining these facts we find

$$\frac{\mathrm{d}^2}{\mathrm{d}s^2}\mathscr{F}_H[\varrho_s] \geq (1 - |\kappa_2|\|V_2\|_{L^\infty(U)}\}) \left(\int_U \mathrm{d}\mathbf{r}\, |\zeta|\right)^2 \tag{7.6.1}$$

and we therefore find that, for κ_2 such that $|k_2| \leq \frac{1}{4}\|V_2\|^{-1}_{L^\infty(U)}$, the free energy functional $\mathscr{F}$ is strictly convex.

Now let $\varrho \in P^+_{\mathrm{ac}}$ and observe that

$$\mathscr{F}[\varrho] \geq -\left|\int_U \mathrm{d}\mathbf{r}\, \varrho \log \varrho\right| - |\kappa_1|\|V_1\|_{L^\infty(U)} - \tfrac{|\kappa_2|}{2}\|V_2\|_{L^\infty(U)}.$$

The entropy $\varrho \log \varrho$ is continuous and bounded below on U and therefore we have that

$$\mathscr{F}[\varrho] \geq \int \mathrm{d}\mathbf{r}\, |\varrho \log \varrho| - |\kappa_1|\|V_1\|_{L^\infty(U)} - \tfrac{|\kappa_2|}{2}\|V_2\|_{L^\infty(U)} > -\infty.$$

where we have used the assumptions on the potentials in (7.2.5). Hence $\mathscr{F}[\cdot]$ is bounded below. □

Note that the convexity condition (7.6.1) in Proposition 7.6.1 holds independently of the confining potential V_1. We therefore have the following Corollary for the total free energy $\mathscr{F} - \int_U \mathrm{d}\mathbf{r}\, \mu_c \varrho$.

Corollary 7.6.2. *The total free energy $\mathscr{F} - \int \mathrm{d}\mathbf{r}\, \mu_c \varrho$ is strictly convex for $|\kappa_2| \in [0, \|V_2\|^{-1}_{L^\infty(U)})$ and bounded below.*

We now provide a useful Lemma which will be used eventually to show that $\mathscr{F}$ always has a minimiser, for any κ_2 (see Lemma 7.6.5).

Lemma 7.6.3. *Let V_1, V_2 satisfy the assumptions* (D4) *then there exists a positive constant B_0 such that for every $\varrho \in P_{ac}(U)$ with $\|\varrho\|_{L^\infty(U)} > B_0$ there exists some $\varrho^\dagger \in P_{ac}(U)$ with $\|\varrho^\dagger\|_{L^\infty(U)} \leq B_0$ such that*

$$\mathscr{F}(\varrho^\dagger) < \mathscr{F}(\varrho).$$

Proof. For a proof see [29, Lemma 2.5] or [32, Lemma 2.1], the only modification required is to include V_1 which by assumption is bounded below and the proof follows a similar argument. □

We now show that minimisers of $\mathscr{F}$ exist for all κ_2. First we define the integral operator $\mathscr{R}$ which will be useful for the following calculations.

Definition 7.6.4. *Let $\mathscr{R} : L^1(U) \to L^1(U)$ be given by*

$$\mathscr{R}u = -\varrho V_2 \star u. \tag{7.6.2}$$

We note that $\mathscr{R}$ is a compact (since V_2 is uniformly bounded in $L^\infty(U)$) self-adjoint operator in $L^2(U, \varrho^{-1})$. We label its eigenvalues $\{\beta_n^{-1}\}_{n=1}^\infty$ and eigenfunctions $\{u_n\}_{n=1}^\infty$ satisfying

$$\mathscr{R}u_n = \beta_n^{-1} u_n. \tag{7.6.3}$$

Lemma 7.6.5. *Let $\kappa_2 \in (-\infty, \infty)$ and let V_1, V_2 satisfy the assumptions* (D4). *Then there exists a $\varrho \in P_{ac}(U)$ that minimizes $\mathscr{F}$.*

Proof. Since $\mathscr{F}$ is bounded below there exists a minimising sequence $\{\varrho_j\}_{j=1}^\infty \in P_{ac}(U)$ so that $\mathscr{F}(\varrho_j) < \mathscr{F}(\varrho_{j+1})$. Therefore, by Lemma 7.6.3 $\{\varrho_j\}_{j=1}^\infty$ may be chosen such that $\|\varrho_j\|_{L^2}(U) \leq \|\varrho_j\|^2_{L^\infty(U)}|U|$. Now by the Eberlein-Smuljan theorem, since $\{\varrho_j\}_{j=1}^\infty$ is bounded, there exists a subsequence (which we will denote again by $\{\varrho_j\}_{j=1}^\infty$) such that $\varrho_j \rightharpoonup \varrho_*$ weakly in L^2 to some

ϱ_*. Therefore $\lim_{j\to\infty}\int_U \mathrm{d}\mathbf{r}\,\eta(\varrho_j-\varrho_*)=0$ for every $\eta\in L^2(U)$, so in particular for $\eta=1$ we obtain $\lim_{j\to\infty}\int_U \mathrm{d}\mathbf{r}\,\varrho_j = 1 = \int_U \mathrm{d}\mathbf{r}\,\varrho_*$. Additionally we note that $|\varrho_j|\rightharpoonup|\varrho_*|$ in $L^2(U)$, and therefore $\|\varrho_*\|_{L^1(U)}=1$, which is enough to show that $\varrho_*\geq 0$ a.e. by standard arguments (see, for example, the proof of Corollary 7.9.3).

We define $\Lambda : P_{ac}\to\mathbb{R}$ such that

$$\Lambda(z) := \int_U \mathrm{d}\mathbf{r}\, zV_2\star z.$$

Now let $\varrho_{\beta_n}\in L^1(U)$ be a solution to (7.5.2), which is known to exist by Lemma 7.5.1. Note that ϱ_{β_n} need not be a minimiser of $\mathscr{F}$ and may be an inflection point or local maximum. Additionally since $\varrho_{\beta_n}\in L^1(U)$ solves (7.5.2), we have that $\varrho_{\beta_n} > e^{-(|\kappa_1|\|V_1\|_{L^\infty(U)}+|\beta_n|\|V_2\|_{L^\infty(U)})}/Z>0$ (where Z is a normalisation constant) and therefore there exists $\delta\in\mathbb{R}^+$ such that $\varrho_{\beta_n}>\delta$ for every $\mathbf{r}\in U$.

Now we estimate the interaction energy difference by

$$\begin{aligned}|\Lambda(\varrho_j)-\Lambda(\varrho_*)| &\leq \sum_{n=1}^{N}|\beta_n^{-1}|\Big|\langle\varrho_j,w_n\rangle_{L^2(U,\varrho_{\beta_n}^{-1})}-\langle\varrho_*,w_n\rangle_{L^2(U,\varrho_{\beta_n}^{-1})}\Big|+2|\beta_N^{-1}|\delta^{-1}B_0\\ &\leq 2\delta^{-1}B_0\sum_{n=1}^{N}\langle\varrho_j-\varrho_*,w_n\rangle_{L^2(U)}+2|\beta_N^{-1}|\delta^{-1}B_0\end{aligned}$$

where we have used the fact that the integrand of $\Lambda(z)$ is equal to $\mathscr{R}$ acting on $z\in P_{ac}$. Additionally we have used that $\mathscr{R}$ is self-adjoint in $L^2(U,\varrho_{\beta_n}^{-1})$, to write $\mathscr{R}$ as a projection onto its eigenvectors $\{w_n\}_{n=1}^{\infty}$ and bounded the tail of the infinite sum using Bessel's inequality.

Now since $\mathscr{R}$ is self-adjoint in $L^2(U,\varrho_{\beta_n}^{-1})$ we have that (after reordering) $|\beta_n^{-1}|\to 0$ as $n\to\infty$ so the second term may be made arbitrarily small. The first term may be made arbitrarily small by taking the limit $j\to\infty$ inside the finite sum and using that $\varrho_j\rightharpoonup\varrho_*$ weakly in $L^2(U)$. This shows that $\Lambda(\cdot)$ is continuous in ϱ.

Additionally, for the external energy, we have

$$\begin{aligned}\Big|\int_U \mathrm{d}\mathbf{r}\,V_1(\mathbf{r})\varrho_j(\mathbf{r})-\int_U \mathrm{d}\mathbf{r}\,V_1(\mathbf{r})\varrho_*(\mathbf{r})\Big| &= \Big|\int_U \mathrm{d}\mathbf{r}\,V_1(\mathbf{r})(\varrho_j(\mathbf{r})-\varrho_*(\mathbf{r}))\Big|\\ &\leq \Big|\int_U \mathrm{d}\mathbf{r}\,V_1(\mathbf{r})(\varrho_j(\mathbf{r})-\varrho_*(\mathbf{r}))\Big|\to 0\end{aligned}$$

as $j\to\infty$. The lower semicontinuity of the entropy term in (7.1.6) follows from standard results [94, Lemma 4.3.1]. Therefore the free energy $\mathscr{F}[\varrho]$ has a minimiser ϱ over $P_{ac}(U)$. □

We may refine this result to show that minimisers are attained in $P_{ac}^+(U)$ with the following lemma.

Lemma 7.6.6. *Let $\varrho\in P_{ac}(U)\backslash P_{ac}^+(U)$. Then there exists $\varrho^\dagger\in P_{ac}^+(U)$ such that $\mathscr{F}[\varrho^\dagger]<\mathscr{F}[\varrho]$.*

Proof. The proof is similar to [29, Lemma 2.6]. One must show that the potential energy for a $P_{ac}^+(U)$ density may be bounded by the potential energy of a $P_{ac}(U)$ density. We let $\epsilon>0$ and define the competition state ϱ_ϵ such that

$$\varrho_\epsilon(\mathbf{r}) = \frac{(\varrho(\mathbf{r})+\epsilon\mathbb{I}_{\mathbb{B}_0}(\mathbf{r}))}{1+\epsilon|\mathbb{B}_0|}$$

where $\mathbb{B}_0=\{\mathbf{r}\in U : \varrho(\mathbf{r})=0\}$ and since by assumption $\varrho\notin P_{ac}^+(U)$ one has $|\mathbb{B}_0|>0$ and $\varrho_\epsilon\in P_{ac}^+(U)$. Then we obtain that

$$\int_U \mathrm{d}\mathbf{r}\,V_1\varrho_\epsilon \leq \int_U \mathrm{d}\mathbf{r}\,V_1\varrho+\epsilon|\mathbb{B}_0|.$$

Using this bound, together with the result [29, Lemma 2.6] we obtain the required result. □

7.6.1 Exponential Convergence To Equilibrium In Relative Entropy.

In this section we derive an H-theorem which guarantees that the time evolution of the dynamics converges to the equilibrium distribution given by the self-consistency equation. First consider the time derivative of the integral of the free energy

$$\begin{aligned}\frac{\mathrm{d}}{\mathrm{d}t}\mathscr{F}[\varrho] &= \int_U \mathrm{d}\mathbf{r}\,\partial_t\varrho\,\tfrac{\delta\mathscr{F}[\varrho]}{\delta\varrho} = \int_U \mathrm{d}\mathbf{r}\,\nabla\cdot\left[\boldsymbol{D}(\mathbf{r},t)\varrho(\mathbf{r},t)\nabla_{\mathbf{r}}\tfrac{\delta\mathscr{F}[\varrho]}{\delta\varrho}\right]\tfrac{\delta\mathscr{F}[\varrho]}{\delta\varrho}\\ &= -\int_U \mathrm{d}\mathbf{r}\left|\boldsymbol{D}(\mathbf{r},t)^{1/2}\varrho(\mathbf{r},t)^{1/2}\nabla_{\mathbf{r}}\tfrac{\delta\mathscr{F}[\varrho]}{\delta\varrho}\right|^2,\end{aligned}$$

where we have integrated by parts and used the boundary condition $\Pi\varrho\cdot\mathbf{n}\big|_{\partial_U} = 0$ or $\varrho\to 0$ as $|\mathbf{r}|\to\infty$ for bounded and unbounded domains respectively. Here we see that as long as both $\boldsymbol{D}(\mathbf{r},t)$ and $\varrho(\mathbf{r},t)$ remain positive definite then the free energy is monotonically decreasing in time. Indeed the diffusion tensor $\boldsymbol{D}$ is positive definite as proven in [63] and we will show strict positivity of $\varrho(\mathbf{r},t)$ in Section 7.9.4.

We now introduce the relative entropy functional

$$\mathscr{H}[\varrho|\varrho_\infty] := \int_U \mathrm{d}\mathbf{r}\,\varrho\log\left(\frac{\varrho}{\varrho_\infty}\right), \tag{7.6.4}$$

and obtain the following theorem for convergence to equilibrium in relative entropy. The following result is analogous to the relative entropy convergence result Carrillo et al. [29, Proposition 3.1] and extends to densities in the presence of an external potential V_1. The main differences here are that we must take care with application of the log-Sobolev inequality for non-convex potentials by use of Holley-Stroock perturbation Lemma.

Theorem 7.6.7. *Let V_1 be convex, $|\kappa_2| < \frac{1}{4}\|V_2\|^{-1}_{L^\infty(U)}$ and $\varrho\in C^1([0,\infty];C^2(U))$ be a classical solution to equation (7.2.3). If $\kappa_2^2 < \frac{c_{ls}^{-1}}{2\|\nabla V_2\|^2_{L^\infty(U)}}$ then ϱ is exponentially stable in relative entropy and it holds that*

$$\mathscr{H}[\varrho|\varrho_\infty] \le \mathscr{H}[\varrho_0|\varrho_\infty]e^{-\frac{1}{2}(c_{ls}^{-1}-2|\kappa_2|^2\|\nabla V_2\|^2_{L^\infty(U)})t},$$

where $c_{ls}>0$ is the log-Sobolev constant for the measure μ.

Proof. By direct calculation we find

$$\begin{aligned}\frac{\mathrm{d}\mathscr{H}[\varrho|\varrho_\infty]}{\mathrm{d}t} &= \int_U \mathrm{d}\mathbf{r}\,\partial_t\left(\varrho\log\left(\frac{\varrho}{\varrho_\infty}\right)\right) = \int_U \mathrm{d}\mathbf{r}\,\partial_t\varrho\log\left(\frac{\varrho}{\varrho_\infty}\right) + \int_U \mathrm{d}\mathbf{r}\,\partial_t\varrho\\ &= \int_U \mathrm{d}\mathbf{r}\,\partial_t\varrho\log\left(\frac{\varrho}{\varrho_\infty}\right) + \frac{\mathrm{d}M}{\mathrm{d}t} = -\int_U \mathrm{d}\mathbf{r}\,\varrho\nabla\frac{\delta\mathscr{F}[\varrho]}{\delta\varrho}\cdot\nabla\log\left(\frac{\varrho}{\varrho_\infty}\right)+0\\ &= -\int_U \mathrm{d}\mathbf{r}\,\varrho\left(\nabla\log\varrho+\kappa_1\nabla V_1+\kappa_2\nabla V_2\star\varrho\right)\cdot\nabla\log\left(\frac{\varrho}{\varrho_\infty}\right)\\ &= -\int_U \mathrm{d}\mathbf{r}\,\varrho\left(\nabla\log\varrho+\kappa_2\nabla V_2\star\varrho-(\nabla\log\varrho_\infty+\kappa_2\nabla V_2\star\varrho_\infty)\right)\cdot\nabla\log\left(\frac{\varrho}{\varrho_\infty}\right)\\ &= -\int_U \mathrm{d}\mathbf{r}\,\varrho\left(\nabla\log\left(\frac{\varrho}{\varrho_\infty}\right)+\kappa_2\nabla V_2\star(\varrho-\varrho_\infty)\right)\cdot\nabla\log\left(\frac{\varrho}{\varrho_\infty}\right)\end{aligned}$$

where we have used the no-flux boundary condition and the self-consistency equation $\nabla\log\varrho_\infty+\kappa_1\nabla V_1+\kappa_2\nabla V_2\star\varrho_\infty=0$. Note that the contribution from the V_1 term is constant, independent of ρ, and so cancels after using the self-consistency equation.

Continuing by expanding out the integrand and using Hölder's inequality we obtain

$$\begin{aligned}\frac{\mathrm{d}\mathscr{H}[\varrho|\varrho_\infty]}{\mathrm{d}t} &= -\int_U \mathrm{d}\mathbf{r}\,\varrho\Big|\nabla\log\left(\frac{\varrho}{\varrho_\infty}\right)\Big|^2 + \kappa_2\int_U \mathrm{d}\mathbf{r}\,\varrho\nabla\log\left(\frac{\varrho}{\varrho_\infty}\right)\cdot\nabla V_2\star(\varrho-\varrho_\infty)\\ &\leq -\int_U \mathrm{d}\mathbf{r}\,\varrho\Big|\nabla\log\left(\frac{\varrho}{\varrho_\infty}\right)\Big|^2\\ &\quad + \left[\int_U \mathrm{d}\mathbf{r}\,\varrho\Big|\nabla\log\left(\frac{\varrho}{\varrho_\infty}\right)\Big|^2\right]^{1/2}\times\left(\kappa_2^2\int_U \mathrm{d}\mathbf{r}\,\varrho|\nabla V_2\star(\varrho-\varrho_\infty)|^2\right)^{1/2}.\end{aligned}$$

Now, by Young's inequality,

$$\frac{\mathrm{d}\mathscr{H}[\varrho|\varrho_\infty]}{\mathrm{d}t} \leq -\tfrac{1}{2}\int_U \mathrm{d}\mathbf{r}\,\varrho\Big|\nabla\log\left(\frac{\varrho}{\varrho_\infty}\right)\Big|^2 + \tfrac{\kappa_2^2}{2}\int_U \mathrm{d}\mathbf{r}\,\varrho|\nabla V_2\star(\varrho-\varrho_\infty)|^2$$

and we may estimate the second term on the right hand side (in particular using that $\int_U \rho = 1$ from Corollary 7.9.3), giving

$$\frac{\mathrm{d}\mathscr{H}[\varrho|\varrho_\infty]}{\mathrm{d}t} \leq -\tfrac{1}{2}\int_U \mathrm{d}\mathbf{r}\,\varrho\Big|\nabla\log\left(\frac{\varrho}{\varrho_\infty}\right)\Big|^2 + \tfrac{\kappa_2^2}{2}\|\nabla V_2\|^2_{L^\infty(U)}\|\varrho-\varrho_\infty\|^2_{L^1(U)} \tag{7.6.5}$$

We bound the first term as follows. Since V_1 is convex, we have

$$\nabla^2_{\mathbf{r}} V_1 \geq \theta_1 > 0$$

for some $\theta_1 \in \mathbb{R}^+$. Now by the Bakry–Émery criterion (see [119, Sec 3, Theorem 3.1], and [110]) the measure $\mu'(\mathrm{d}\mathbf{r}) = \mathrm{d}\mathbf{r}\,e^{-\kappa_1 V_1}/Z$ where Z is a normalisation constant satisfies a log-Sobolev inequality (LSI) with constant c'_{ls} such that

$$\frac{1}{c'_{ls}} \geq \theta_1\kappa_1.$$

However since V_2 is not general a convex function, we cannot use the Bakry–Émery criterion for μ as defined in (7.1.7). However we may deduce a LSI using the Holley–Stroock perturbation lemma [119, Sec 3, Theorem 3.2] since $V_1 + V_2\star\varrho_\infty$ is a bounded perturbation of V_1, in particular

$$\Big|V_1 + V_2\star\varrho_\infty\Big| \leq \Big|V_1\Big| + \|V_2\|_{L^\infty}\|\varrho_\infty\|_{L^1(U)} < \infty.$$

Therefore μ as defined in (7.1.7) with $\varrho = \varrho_\infty$ (after appropriate nondimensionalisation) is unique and satisfies a LSI with constant

$$c_{ls}^{-1} \geq \exp\left(-\kappa_1\kappa_2\,\mathrm{Osc}\left[V_2\star\varrho_\infty\right]\right)\frac{1}{c'_{ls}}$$

where

$$\mathrm{Osc}\left[V_2\star\varrho_\infty\right] = \sup V_2\star\varrho_\infty - \inf V_2\star\varrho_\infty.$$

The constant c_{ls} is such that such that for each $f : U \to \mathbb{R}^+$ one has

$$\int_U f^2\log f^2\mathrm{d}\mu - \int_U f^2\log\left(\int_U f^2\mathrm{d}\mu\right)\mathrm{d}\mu \leq c_{ls}\int_U |\nabla f|^2\mathrm{d}\mu = c_{ls}\int_U f^2|\nabla\log f^2|^2\mathrm{d}\mu. \tag{7.6.6}$$

We let $f = \sqrt{\varrho/\varrho_\infty}$ and $\mathrm{d}\mu = \varrho_\infty\mathrm{d}\mathbf{r}$ and the second term on the left hand side of (7.6.5) is zero (since, again $\int_U \rho = 1$). Hence this shows that

$$\mathscr{H}[\varrho|\varrho_\infty] = \int_U f^2\log f^2\mathrm{d}\mu \leq c_{ls}\int_U \mathrm{d}\mathbf{r}\,\varrho\Big|\nabla\log\left(\frac{\varrho}{\varrho_\infty}\right)\Big|^2.$$

We combine the LSI (7.6.6) with Pinsker's inequality [18] to deduce

$$\frac{\mathrm{d}\mathscr{H}[\varrho|\varrho_\infty]}{\mathrm{d}t} \leq -\tfrac{1}{2}(c_{ls}^{-1} - 2\kappa_2^2\|\nabla V_2\|^2_{L^\infty(U)})\mathscr{H}[\varrho|\varrho_\infty].$$

Thus we obtain, by Grönwall's inequality,

$$\mathscr{H}[\varrho|\varrho_\infty] \leq \mathscr{H}[\varrho_0|\varrho_\infty]\exp[-\tfrac{1}{2}(c_{ls}^{-1} - 2\kappa_2^2\|\nabla V_2\|^2_{L^\infty(U)})t]$$

and the theorem is proved. □

The constant c_{ls} is not known explicitly but may be estimated in terms of the convexity of V_1, V_2 and the curvature of U [34]. We now consider asymptotic expansions of the steady states for small interaction energy κ_2.

7.6.2 Asymptotic Expansion Of The Steady States For Weak Interactions.

We begin this section by recalling that steady states satisfy the self-consistency equation

$$\varrho = \frac{e^{-(\kappa_1 V_1 + \kappa_2 V_2 \star \varrho)}}{Z}, \tag{7.6.7}$$

where $Z = \int_U \mathrm{d}\mathbf{r}\, e^{-(\kappa_1 V_1 + \kappa_2 V_2 \star \varrho)}$. We know from Lemma 7.5.1 that for sufficiently weak interactions, i.e. $|\kappa_2| < 1/4\|V_2\|^{-1}_{L^\infty(U)}$, the stationary distribution is unique; equivalently, the nonlinear equation (7.6.7) has a unique fixed point. Let $\kappa_2 \ll 1$, then the stationary solution $\varrho(\mathbf{r}) = \varrho_\infty(\mathbf{r})$ has the form

$$\varrho(\mathbf{r}) = \frac{e^{-\kappa_1 V_1(\mathbf{r})}}{Z(\varrho)}(1 + O(\kappa_2)),$$

where the first order correction may be obtained explicitly as follows.

Recall the stationary equation for ϱ:

$$\begin{aligned} \nabla_{\mathbf{r}} \cdot [\boldsymbol{D}(\nabla_{\mathbf{r}}\varrho + \kappa_1 \varrho\, \nabla_{\mathbf{r}} V_1(\mathbf{r}) + \kappa_2 \varrho\, \nabla_{\mathbf{r}} V_2 \star \varrho)] = 0 \text{ on } U, \\ \boldsymbol{D}(\nabla_{\mathbf{r}}\varrho + \kappa_1 \varrho\, \nabla_{\mathbf{r}} V_1 + \kappa_2 \varrho\, \nabla_{\mathbf{r}} V_2 \star \varrho) \cdot \mathbf{n} = 0 \text{ on } \partial_U. \end{aligned} \tag{7.6.8a}$$

Fix $\kappa_1 = 1$ and insert the perturbation expansion

$$\varrho(\mathbf{r}) = \sum_{k=0}^{\infty} \kappa_2^k \varrho_k(\mathbf{r}).$$

We find at the first order of κ_2

$$\begin{aligned} \mathscr{L}_0\varrho_0 := \nabla_{\mathbf{r}} \cdot (\boldsymbol{D}\nabla_{\mathbf{r}}\varrho_0 + \boldsymbol{D}\,(\varrho_0 \nabla_{\mathbf{r}} V_1)) = 0 \text{ on } U, \\ \boldsymbol{D}(\nabla_{\mathbf{r}}\varrho_0 + \varrho_0 \nabla_{\mathbf{r}} V_1) \cdot \mathbf{n} = 0 \text{ on } \partial_U, \end{aligned}$$

from which we deduce

$$\varrho_0(\mathbf{r}) = \frac{e^{-V_1(\mathbf{r})}}{Z_0}$$

for $Z_0 = \int_U \mathrm{d}\mathbf{r}\, e^{-V_1(\mathbf{r})}$.

Note that $\mathscr{L}_0$ is self-adjoint in the space $L^2(U, \varrho_0^{-1})$. We may also show that the resolvent of $\mathscr{L}_0$ is compact in $L^2(U, \varrho_0^{-1})$.

Lemma 7.6.8. *The operator $\mathscr{L}_0$ has a compact resolvent in $L^2(U, \varrho_0^{-1})$.*

Proof. We let $\phi \in C^2(U)$, by direct calculation we have that

$$\mathscr{L}_0\phi = [\nabla_{\mathbf{r}} \cdot \boldsymbol{D}] \cdot \nabla_{\mathbf{r}}\phi + \mathrm{Tr}\left[\boldsymbol{D}\nabla_{\mathbf{r}}^2\phi\right] + [\boldsymbol{D}\nabla_{\mathbf{r}}V_1] \cdot \nabla_{\mathbf{r}}\phi + \phi\left[[\nabla_{\mathbf{r}} \cdot \boldsymbol{D}] \cdot \nabla_{\mathbf{r}}V_1 + \mathrm{Tr}[\boldsymbol{D}\nabla_{\mathbf{r}}^2 V_1]\right]$$

then we have that

$$\begin{aligned}\|\mathscr{L}_0\phi\|^2_{L^2(U,\varrho_0^{-1})} &= \int_U \mathrm{d}\mathbf{r}\left|\nabla_{\mathbf{r}} \cdot \left(\boldsymbol{D}\nabla_{\mathbf{r}}\phi + \boldsymbol{D}\left(\phi\nabla_{\mathbf{r}}V_1\right)\right)\right|^2 \varrho_0^{-1} \\ &\leq C(U;\boldsymbol{D};V_1)\sum_{n=0}^{2}\sup_{\mathbf{r}\in U}\left|\phi^{(n)}(\mathbf{r})\right| < \infty\end{aligned}$$

where the constant $C(U;\boldsymbol{D};V_1)$ is dependent on U, the diffusion tensor $\boldsymbol{D}$ and the first weak derivatives of its entries (bounded in $L^\infty(U)$ by (D1)), and the confining potential V_1 and its first two weak derivatives (bounded in $L^\infty(U)$ by (D4)).

Therefore there exists $C \in \mathbb{R}^+$ such that $\|\mathscr{L}_0\|_{L^2(U,\varrho_0^{-1})} < C$ and the spectrum of $\mathscr{L}_0$ is bounded. Now let $z \in \rho(\mathscr{L}_0)$ with $|z| > C$, where $\rho(\cdot)$ denotes the resolvent set, then we may write the resolvent $R(z;\mathscr{L}_0)$ of the operator $\mathscr{L}_0$ as

$$R(z;\mathscr{L}_0) = -z^{-1}\sum_{k=0}^{\infty} z^{-k}\mathscr{L}_0^k.$$

We now show that R is compact. First consider the sequence $(R^N)_{N\geq 1}$ defined by

$$R^N(z;\mathscr{L}_0) := -z^{-1}\sum_{k=0}^{N} z^{-k}\mathscr{L}_0^k,$$

then let $(\phi_j)_{j\geq 1}$ be a sequence in $C^2(U)$. We have that $(\phi_j)_{j\geq 1}$ is a bounded sequence in $C^2(U)$ and

$$\begin{aligned}\|R^N(z;\mathscr{L}_0)[\phi_j]\|_{L^2(U,\varrho_0^{-1})} &\leq |z|^{-1}\sum_{k=0}^{N}|z|^{-k}\|\mathscr{L}_0^k[\phi_j]\|_{L^2(U,\varrho_0^{-1})} \\ &\leq |z|^{-1}\sum_{k=0}^{N}|z|^{-k}C^K.\end{aligned}$$

Hence, as long as $|z| > C$ then, $\|R^N(z;\mathscr{L}_0)[\phi_j]\|_{L^2(U,\varrho_0^{-1})}$ converges for all N and $\mathrm{Im}\left(R^N\right)$ is relatively compact in $L^2(U,\varrho_0^{-1})$. It is then a standard result that the limit of a sequence of compact operators is compact, hence R is compact. □

Thus we have a complete set of orthonormal basis functions $\{v_k^{(0)}\}_{k=0}^{\infty}$ and corresponding eigenvalues $\{\gamma_n^{(0)}\}_{n\geq 1}$. Note that $v_0^{(0)} = \varrho_0$ and $\gamma_0^{(0)} = 0$. At the next order of κ_2 we obtain

$$\mathscr{L}_0\varrho_1 + f(\varrho_0) = 0, \tag{7.6.10}$$

where

$$f(\varrho_0) := -\nabla_{\mathbf{r}} \cdot (\boldsymbol{D}\varrho_0\,\nabla_{\mathbf{r}}V_2 \star \varrho_0),$$

subject to

$$\boldsymbol{D}(\nabla_{\mathbf{r}}\varrho_1 + \varrho_1\,\nabla_{\mathbf{r}}V_1 + \varrho_0\,\nabla_{\mathbf{r}}V_2 \star \varrho) \cdot \mathbf{n} = 0 \text{ on } \partial_U.$$

The solvability condition for (7.6.10) then becomes

$$0 = \langle f(\varrho_0), v_0^{(0)}\rangle_{L^2(U,\varrho_0^{-1})} = \int_U \mathrm{d}\mathbf{r}\,\nabla_{\mathbf{r}} \cdot (\varrho_0\,\boldsymbol{D}\nabla_{\mathbf{r}}V_2 \star \varrho_0) = \int_{\partial U}\mathrm{d}S\,\mathbf{n} \cdot \varrho_0\,\boldsymbol{D}\nabla_{\mathbf{r}}V_2 \star \varrho_0. \tag{7.6.11}$$

If the solvability condition (7.6.11) is satisfied then, by the Fredholm alternative, there exists a solution to (7.6.10).

We may then write ϱ_1 in an eigenfunction expansion

$$\varrho_1(\mathbf{r}) = \sum_{j=0}^{\infty} \alpha_j v_j^{(0)} \quad \text{where} \quad \alpha_j = -\frac{1}{\gamma_j \|v_j^{(0)}\|^2_{L^2_{\varrho_0^{-1}}}} \langle f(\varrho_0),\, v_j^{(0)} \rangle_{L^2_{\varrho_0^{-1}}}.$$

This yields that

$$\varrho(\mathbf{r}) = \frac{e^{-V_1(\mathbf{r})}}{Z_0} + \kappa_2 \sum_{j=0}^{\infty} \frac{\langle \nabla_{\mathbf{r}} \cdot (\boldsymbol{D}\varrho_0 \nabla_{\mathbf{r}} V_2 \star \varrho_0),\, v_j^{(0)} \rangle_{L^2_{\varrho_0^{-1}}} v_j^{(0)}(\mathbf{r})}{\gamma_j \|v_j^{(0)}\|^2_{L^2_{\varrho_0^{-1}}}} + O(\kappa_2^2).$$

We now consider a linear stability analysis of the equilibrium density (7.5.2) solving (7.2.5).

7.6.3 Linear Stability Analysis.

We first investigate the spectrum of the linearised operator $\mathscr{L}_1$ in terms of the eigenspace of its local part. We determine a scheme for computing the eigenvalues of $\mathscr{L}_1$ explicitly. Writing $\varrho = \varrho + \epsilon\,\omega + O(\epsilon^2)$ where $\epsilon \ll 1$ is an arbitrary parameter and not equal to κ_2, we obtain

$O(\epsilon^0)$**:**

$$\mathscr{L}\varrho = 0$$

where we have set $\varrho = \varrho_\infty$ (the unique stationary state) to ease notation and

$$\mathscr{L}\varrho = \nabla \cdot (\boldsymbol{D}\,\nabla\varrho) + \kappa_1 \nabla \cdot (\boldsymbol{D}\,\varrho \nabla V_1) + \kappa_2 \nabla \cdot (\varrho \boldsymbol{D}\,\nabla V_2 \star \varrho).$$

$O(\epsilon^1)$**:**

$$\dot{\omega} = \mathscr{L}_1 w \tag{7.6.12}$$

where

$$\mathscr{L}_1\omega := \nabla \cdot (\boldsymbol{D}\,\nabla\omega) + \kappa_1 \nabla \cdot (\boldsymbol{D}\,\omega \nabla V_1) + \kappa_2 \nabla \cdot (\varrho \boldsymbol{D}\,\nabla V_2 \star \omega) + \kappa_2 \nabla \cdot (\omega \boldsymbol{D}\,\nabla V_2 \star \varrho). \tag{7.6.13}$$

We remark that the operator $\mathscr{L}_1$ is different to the one found in the linear stability analysis of [29, Sec 3.3] due to the difference in boundary conditions.

Perturbations must be mean zero, that is $\int_U \mathrm{d}\mathbf{r}\,\omega = 0$, which may be determined by observing that

$$1 = \int \mathrm{d}\mathbf{r}\,\varrho + \epsilon \int \mathrm{d}\mathbf{r}\,w + O(\epsilon^2).$$

Equally, all higher order perturbations must have mean zero. Physically speaking this is a compatibility condition with the no-flux boundary condition in (7.2.5) to ensure that perturbations do not change the mass of the system.

Additionally by linearising the self-consistency equation (7.5.2) we find that mean zero perturbations w satisfy the integral equation

$$w = -\varrho_\infty \kappa_2 V_2 \star w. \tag{7.6.14}$$

We linearise the nonlinear boundary condition to find that

$$\Pi_1[\omega]\cdot\mathbf{n}|_{\partial_U} := 0$$

where

$$\Pi_1[\omega] = \boldsymbol{D}\left(\nabla_{\mathbf{r}}\omega + \omega\nabla_{\mathbf{r}}(\kappa_1 V_1(\mathbf{r},t) + \kappa_2\, V_2\star\varrho) + \kappa_2\varrho\,\nabla_{\mathbf{r}}V_2\star\omega\right). \tag{7.6.15}$$

We note that if any such ω exist for (7.6.14), then (7.6.15) trivially holds, and equation (7.6.12) is underdetermined. In order to properly determine ω we let $\omega\in L^2_c(U,\varrho^{-1})$ where

$$L^2_c(U,\varrho^{-1}) := \left\{u\in L^2(U,\varrho^{-1})\,:\,\nabla_{\mathbf{r}}(\varrho^{-1}u)\cdot\mathbf{n}|_{\partial U}=0\right\}.$$

The choice $\omega\in L^2_c(U,\varrho^{-1})$ preserves the boundary condition $\Pi_1[\varrho]\cdot\mathbf{n}|_{\partial U}=0$ and we will show in Lemma 7.6.9 that it is the most general restriction to ensure that the local part of $\mathscr{L}_1$ is self-adjoint in $L^2(U,\varrho^{-1})$. With this we write

$$\begin{aligned}
\mathscr{L}_1 &= \mathscr{A}_{\kappa_2} + \kappa_2\mathscr{B},\\
\mathscr{A}_{\kappa_2}w &:= \nabla_{\mathbf{r}}\cdot[\boldsymbol{D}(\nabla_{\mathbf{r}}w + w\nabla_{\mathbf{r}}\varphi_{\kappa_2})], &\text{(7.6.16a)}\\
\mathscr{B}w &:= \nabla_{\mathbf{r}}\cdot\left(\varrho\boldsymbol{D}\,\nabla_{\mathbf{r}}V_2\star w\right), &\text{(7.6.16b)}\\
\varphi_{\kappa_2} &:= \kappa_1 V_1 + \kappa_2 V_2\star\rho. &\text{(7.6.16c)}
\end{aligned}$$

Here, $\mathscr{A}_{\kappa_2}$ and $\mathscr{B}$ are the local and nonlocal parts of $\mathscr{L}_1$, respectively. Note however that $\mathscr{A}_{\kappa_2}\neq\mathscr{L}_0$ by definition since κ_2 is no longer small. All operators $\mathscr{A}_{\kappa_2}$, $\mathscr{B}$, $\mathscr{L}_1$ are maps $H^2(U,\varrho_\infty^{-1})\to L^2(U)$. We now show that A_{κ_2} is a self-adjoint operator in the space $L^2_c(U,\varrho^{-1})$.

Lemma 7.6.9. *$\mathscr{A}_{\kappa_2}$ is self-adjoint in $L^2_c(U,\varrho^{-1})$.*

Proof. First note that from (7.6.16c) and (7.5.2) we have that $\nabla_{\mathbf{r}}\varphi_{\kappa_2}=\rho\nabla_{\mathbf{r}}\rho^{-1}$ and so $\mathscr{A}_{\kappa_2}w = \nabla_{\mathbf{r}}\cdot[\rho\boldsymbol{D}\nabla_{\mathbf{r}}(\rho^{-1}w)]$. Let $u\in L^2_c(U,\varrho^{-1})$ then

$$\begin{aligned}
\langle u,\,\mathscr{A}_{\kappa_2}w\rangle_{L^2(U,\varrho^{-1})} &= \int_U \mathrm{d}\mathbf{r}\,\varrho^{-1}u\mathscr{A}_{\kappa_2}w\\
&= \int_U \mathrm{d}\mathbf{r}\,\varrho^{-1}u\nabla_{\mathbf{r}}\cdot[\rho\boldsymbol{D}\nabla_{\mathbf{r}}(\rho^{-1}w)]\\
&= \int_{\partial U}\mathrm{d}S\mathbf{n}\cdot u\boldsymbol{D}\nabla_{\mathbf{r}}(\varrho^{-1}\omega) - \int_U \mathrm{d}\mathbf{r}\,\nabla_{\mathbf{r}}\left[\varrho^{-1}u\right]\cdot\left[\varrho\boldsymbol{D}\nabla_{\mathbf{r}}\left(\varrho^{-1}w\right)\right]\\
&= -\int_{\partial U}\mathrm{d}S\mathbf{n}\cdot w\boldsymbol{D}\nabla_{\mathbf{r}}(\varrho^{-1}u) + \int_U \mathrm{d}\mathbf{r}\,\nabla_{\mathbf{r}}\cdot[\rho\boldsymbol{D}\nabla_{\mathbf{r}}(\rho^{-1}u)]\varrho^{-1}w\\
&= \langle A_{\kappa_2}u,\,w\rangle_{L^2(\mathbb{R},\varrho^{-1})}
\end{aligned}$$

where we have integrated by parts twice and used that $\boldsymbol{D}$ is symmetric and the fact that $u,w\in L^2_c(U,\varrho^{-1})$ to eliminate the boundary terms. □

We have established that $\mathscr{A}_{\kappa_2}$ is self-adjoint in $L^2_c(U,\varrho^{-1})$. Additionally we observe that $\mathscr{A}_{\kappa_2}$ has a compact resolvent in $L^2_c(U,\varrho^{-1})$ by a similar result to Lemma 7.6.8. The spectral theorem therefore provides a complete basis of orthonormal eigenfunctions $v_k^{(\kappa_2)}$ spanning $L^2_c(U,\varrho^{-1})$ with corresponding eigenvalues $\gamma_k^{(\kappa_2)}$ such that

$$A_{\kappa_2}v_k^{(\kappa_2)} = \gamma_k^{(\kappa_2)}v_k^{(\kappa_2)}. \tag{7.6.17}$$

We note that the operator $\mathscr{B}$ as defined in (7.6.16b) is, in general, not self-adjoint. From now on we assume that the set of eigenfunctions $\{v_k^{(\kappa_2)}\}_{k=1}^\infty$ are normalised to form an orthonormal basis. The stability of the equilibrium density will depend on the spectrum of the operator $\mathscr{L}_1$ so that perturbations evolving according to (7.6.12) either grow or decay. We now study the

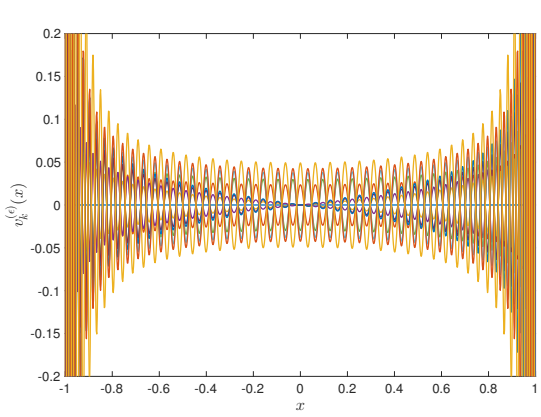

(a) The first ten eigenfunctions $v_k^{(\kappa_2)}$.

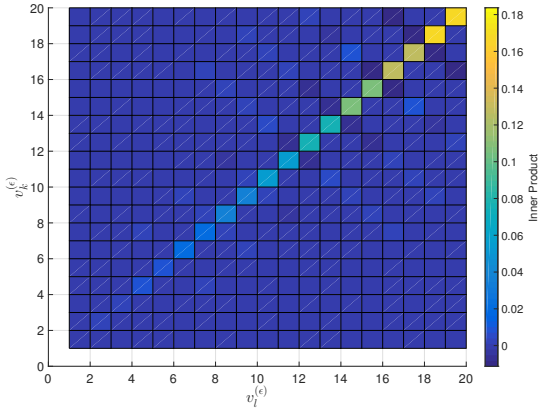

(b) The weighted L^2 inner product of pairs of eigenfunctions $\langle v_k^{(\kappa_2)}, v_l^{(\kappa_2)} \rangle_{L^2([-1,1],\varrho_\infty^{-1})}$.

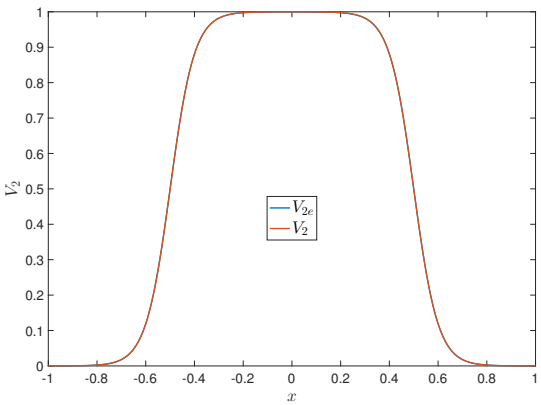

(c) A repulsive potential V_2 and the expansion V_{2e} in the eigenfunctions $\{v_k^{(\kappa_2)}\}_{k=1}^N$.

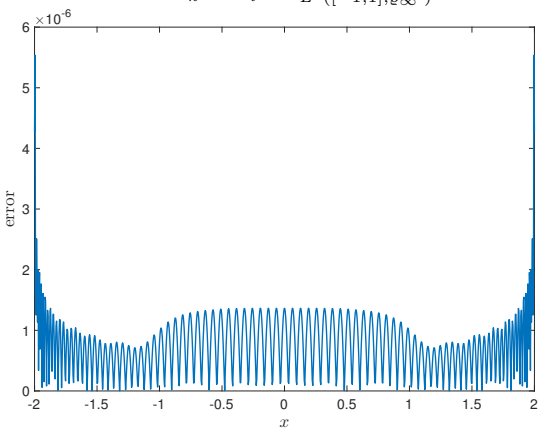

(d) The absolute error between V_2 and the expansion in $\{v_k^{(\kappa_2)}\}_{k=1}^N$.

Figure 7.2: Plots of a) The eigenfunctions of A_{κ_2} in $L^2([-1,1],\varrho_\infty^{-1})$ as computed with pseudospectral methods for $\kappa_2 = 1$ and $N = 100$ spectral points, b) the inner product between pairs of eigenfunctions showing orthogonality of the $\{v_k^{(\kappa_2)}\}$, c) the eigenfunction expansion of $V_2(r) = 1/2(-\tanh((r-1/2)/.05)+\tanh((r+1/2)/.05))$ and d) the absolute error between the expansion V_{2e} and V_e. The L^2 error between V_2 and its expansion in eigenfunctions V_{2e} was found to be 5.761e-9.

spectrum of $\mathscr{L}_1$. We fix κ_1 and consider κ_2, not necessarily small, as a perturbation parameter from the differential part of $\mathscr{L}_1$. The following theorem establishes the parametrisation of the eigenvalues λ by κ_2.

Theorem 7.6.10. *Suppose that $\lambda \neq \gamma_k^{(\kappa_2)}$ for all $k \in \mathbb{N}$. If the solution $\kappa_2^\star(\lambda)$ of the equation $\lambda = \lambda_{k^\star}(\kappa_2^\star)$ exists, then it is given by*

$$\kappa_2^\star(\lambda) = \left(\sum_{i=0}^{\infty} \frac{\theta_i^{(\kappa_2)} \gamma_i^{(\kappa_2)} \beta_i^{(\kappa_2)}}{\lambda - \gamma_i^{(\kappa_2)}} \right)^{-1}, \tag{7.6.18}$$

where $\theta_j^{(\kappa_2)}$ and $\beta_j^{(\kappa_2)}$ are given by

$$\theta_k^{(\kappa_2)} \beta_l^{(\kappa_2)} = \int_U \mathrm{d}\mathbf{r}\, v_l^{(\kappa_2)}(\mathbf{r}) V_2 \star v_k^{(\kappa_2)}(\mathbf{r}). \tag{7.6.19}$$

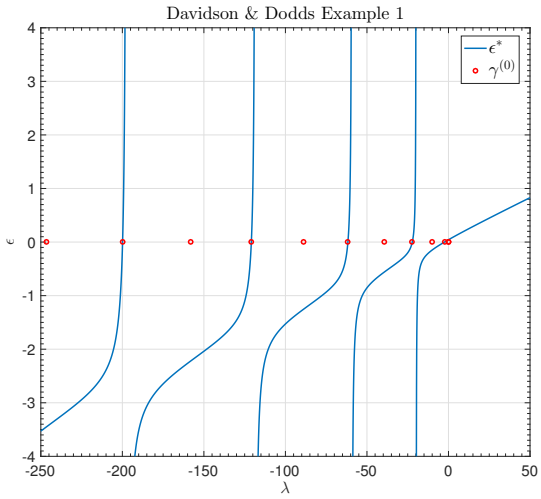

(a) Moving eigenvalues λ_ϵ^* and static eigenvalues $\gamma^{(0)}$ for the functions $c(x) = d(x) = 1$ for $x \in [-1, 1]$ and the operator $\mathscr{L}_\epsilon u = u'' + \epsilon c(x) \int_U \mathrm{d}x'\, d(x')u(x')$.

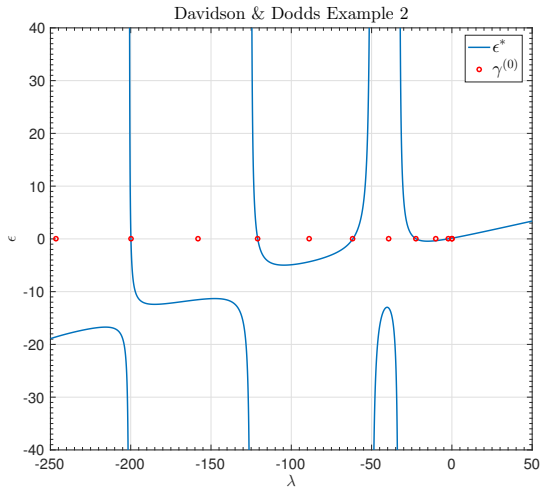

(b) Moving eigenvalues λ_ϵ^* and static eigenvalues $\gamma^{(0)}$ for the functions $c(x) = (1 - 9x^2)\mathbb{I}_{\{|x|<1/3\}}$, $d(x) = 1$ for $x \in [-1, 1]$ and the operator $\mathscr{L}_\epsilon u = u'' + \epsilon c(x) \int_U \mathrm{d}x'\, d(x')u(x')$.

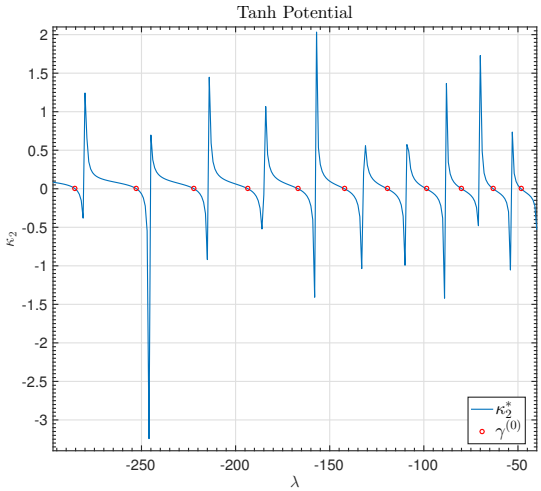

(c) Moving eigenvalues $\lambda_{\kappa_2}^*$ and static eigenvalues $\gamma^{(0)}$ for the differential nonlocal operator $\mathscr{L}_1$ with $V_2(r) = 1/8(-\tanh((r-1/2)/.1) + \tanh((r+1/2)/.1))$.

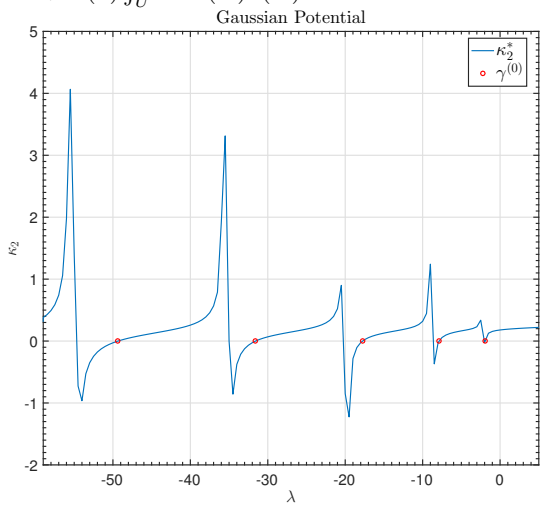

(d) Moving eigenvalues $\lambda_{\kappa_2}^*$ and static eigenvalues $\gamma^{(0)}$ for the differential nonlocal operator $\mathscr{L}_1$ with $V_2(r) = (1/2)\exp(-r^2/.1)$.

Figure 7.3: Moving eigenvalues for various differential nonlocal operators.

Proof. Let

$$V_2(\mathbf{r} - \mathbf{r}') = \varrho^{-1}(\mathbf{r})\varrho^{-1}(\mathbf{r}') \sum_{j,k=0}^{\infty} \beta_j^{(\kappa_2)} v_j^{(\kappa_2)}(\mathbf{r}) \theta_k^{(\kappa_2)} v_k^{(\kappa_2)}(\mathbf{r}'),$$

$$w(\mathbf{r}) = \sum_{i=0}^{\infty} \alpha_i v_i^{(\kappa_2)}(\mathbf{r}).$$

Inserting these expressions into the eigenvalue problem $\mathscr{L}_1 w = \lambda w$ we find

$$\sum_{i=1}^{\infty} \alpha_i (\gamma_i^{(\kappa_2)} - \lambda) v_i^{(\kappa_2)}(\mathbf{r}) + \kappa_2 \nabla_{\mathbf{r}} \cdot (\varrho \boldsymbol{D} \nabla_{\mathbf{r}} V_2 \star w) = 0.$$

Multiplying this equation by $v_n^{(\kappa_2)}$ and integrating against the weight function ϱ^{-1} we obtain

$$\begin{aligned}0 &= \alpha_n(\gamma_n^{(\kappa_2)} - \lambda) + \kappa_2 \int_U \mathrm{d}\mathbf{r}\, \varrho^{-1}(\mathbf{r}) v_n^{(\kappa_2)}(\mathbf{r}) \nabla_{\mathbf{r}} \cdot (\varrho(\mathbf{r}) \boldsymbol{D} \nabla_{\mathbf{r}} V_2 \star w) \\ &= \alpha_n(\gamma_n^{(\kappa_2)} - \lambda) - \kappa_2 \int_U \mathrm{d}\mathbf{r}\, \left[\nabla_{\mathbf{r}} v_n^{(\kappa_2)}(\mathbf{r}) + v_n^{(\kappa_2)}(\mathbf{r}) \nabla_{\mathbf{r}} \varphi_{\kappa_2}\right] \cdot \boldsymbol{D}\, \nabla_{\mathbf{r}} V_2 \star w,\end{aligned}$$

where there is no boundary term since $\nabla_{\mathbf{r}} V_2 \star w = -\kappa_2^{-1} \nabla_{\mathbf{r}}(\varrho^{-1} w)$ is zero on the boundary of U because $w \in L_c^2(U, \varrho^{-1})$.

Continuing by integrating by parts we find

$$\begin{aligned}0 &= \alpha_n(\gamma_n^{(\kappa_2)} - \lambda) + \kappa_2 \int_U \mathrm{d}\mathbf{r}\, \nabla_{\mathbf{r}} \cdot [\boldsymbol{D}(\nabla_{\mathbf{r}} v_n^{(\kappa_2)}(\mathbf{r}) + v_n^{(\kappa_2)}(\mathbf{r}) \nabla_{\mathbf{r}} \varphi_{\kappa_2})] V_2 \star w \\ &= \alpha_n(\gamma_n^{(\kappa_2)} - \lambda) - \kappa_2 \int_U \mathrm{d}\mathbf{r}\, \nabla_{\mathbf{r}} \cdot (\varrho \boldsymbol{D} \nabla_{\mathbf{r}} (\varrho^{-1} v_n^{(\kappa_2)}(\mathbf{r}))) V_2 \star w \\ &= \alpha_n(\gamma_n^{(\kappa_2)} - \lambda) + \kappa_2 \gamma_n^{(\kappa_2)} \int_U \mathrm{d}\mathbf{r}\, v_n^{(\kappa_2)}(\mathbf{r}) V_2 \star w\end{aligned}$$

where we have used $\nabla_{\mathbf{r}}(\varrho^{-1} v_n^{\kappa_2}) = 0$ on ∂_U to eliminate the boundary term, and in the last line used the fact that $v_n^{\kappa_2}$ is an eigenfunction of $\mathscr{A}_{\kappa_2}$. Inserting the expansion for V_2 and using the orthonormality of the $v_i^{(\kappa_2)}$ gives

$$\kappa_2 = \frac{(\lambda - \gamma_n^{(\kappa_2)})\alpha_n}{\gamma_n^{(\kappa_2)} \theta_n^{(\kappa_2)} \sum_{j=0}^{\infty} \int_U \mathrm{d}\mathbf{r}'\, \varrho_\infty^{-1}(\mathbf{r}') \beta_j^{\kappa_2} v_j^{(\kappa_2)}(\mathbf{r}') w(\mathbf{r}')}.$$

This holds for all V_2 and, in particular, for all $\theta_n^{(\kappa_2)} \neq 0$ so it be must be the case that

$$\frac{(\lambda - \gamma_n^{(\kappa_2)})\alpha_n}{\gamma_n^{(\kappa_2)} \theta_n^{(\kappa_2)}} = K,$$

for some constant K, independent of n. Without loss of generality we can take $K = 1$. Hence we have

$$w(x) = \sum_{i=0}^{\infty} \frac{\gamma_n^{(\kappa_2)} \theta_n^{(\kappa_2)}}{\lambda - \gamma_n^{(\kappa_2)}} v_n^{(\kappa_2)}(x)$$

and it follows that

$$\kappa_2 = \left(\sum_{j=0}^{\infty} \int_U \mathrm{d}\mathbf{r}'\, \varrho^{-1}(\mathbf{r}') \beta_j^{(\kappa_2)} v_j^{(\kappa_2)}(\mathbf{r}') w(\mathbf{r}') \right)^{-1} = \left(\sum_{i=0}^{\infty} \frac{\theta_i^{(\kappa_2)} \gamma_i^{(\kappa_2)} \beta_i^{(\kappa_2)}}{\lambda - \gamma_i^{(\kappa_2)}} \right)^{-1}. \tag{7.6.20}$$

Hence the theorem is proved. □

The expression (7.6.18) for κ_2 allows the paths of the eigenvalues $\lambda_k(\kappa_2)$ to be computed. For practical purposes, it may be sufficient to use a truncation of the series or, if $w(\mathbf{r})$ can be computed explicitly, the first expression in (7.6.20) can be used. As shown in [96, Section II-5.1], the eigenvalues of $\mathscr{L}_1$ will remain real as long as

$$|\kappa_2| < \frac{\min_{i,j \in \mathbb{N}} |\gamma_i^{(\kappa_2)} - \gamma_j^{(\kappa_2)}|}{2\|\mathscr{B}\|}. \tag{7.6.21}$$

We see from (7.6.20) that the point of critical stability (if it exists) $\kappa_{2\sharp}$ occurs at

$$\kappa_{2\sharp} = -\left(\sum_{i=0}^{\infty} \theta_i^{(\kappa_2)} \beta_i^{(\kappa_2)} \right)^{-1} \tag{7.6.22}$$

Table 7.1: The first 10 eigenvalues $-\gamma_k^{(\kappa_2)} \cdot 10^3$ and boundary condition values of the corresponding eigenvectors $v_{k(\kappa_2)}$ for $\kappa_2 = .05$.

k	$-\gamma_k^{(\epsilon)} \cdot 10^3$	$\nabla_{\mathbf{r}}(\varrho^{-1} v_k^{(\kappa_2)}) \cdot \mathbf{n}\big\|_{x=-1}$	$\nabla_{\mathbf{r}}(\varrho^{-1} v_k^{(\kappa_2)}) \cdot \mathbf{n}\big\|_{x=1}$
1	0.042470931917315	-0.326629834290770e-10	-0.049430114879555e-10
2	0.161343622578368	0.177791115163473e-11	-0.638172005587933e-11
3	0.359053918066979	-0.532729416136135e-11	-0.705155659306588e-11
4	0.635777464488092	0.040225600628219e-10	-0.10593000196636e-10
5	0.991543834922971	-0.143929312912405e-11	-0.982251087217608e-11
6	1.426361079097481	-0.421040979858844e-11	0.332564751050043e-11
7	1.940232081076136	0.130651045537888e-11	0.966037681231493e-11
8	2.533158075256826	-0.417399448338074e-11	-0.401360089043934e-11
9	3.205139660109592	-0.019828583219805e-11	-0.919929559744713e-11
10	3.956177153938488	-0.687472301308389e-11	0.423840601914807e-11

and is independent of $\gamma_n^{(\kappa_2)}$ (the eigenvalues of the local operator A_{κ_2}). The critical point of stability will have implicit dependence on $\boldsymbol{D}$, V_1 and V_2 through (7.6.19). As long as κ_2 remains sufficiently small, Lemma 7.6.10 provides a nonlinear map to compute κ_2 parametrised by λ therefore permitting the paths of the moving eigenvalues to be calculated. In particular by fixing $\lambda \in \mathbb{R}$ we have the iterative problem

$$\begin{cases} \frac{1}{\kappa_2^{l+1}} = \sum_{i=1}^{\infty} \frac{\theta_i^{(\kappa_2^l)} \gamma_i^{(\kappa_2^l)} \beta_i^{(\kappa_2^l)}}{\lambda - \gamma_i^{(\kappa_2^l)}}, \\ \gamma_n^{(\kappa_2^0)} = \gamma_n^{(0)}. \end{cases} \tag{7.6.23}$$

We note that the eigenvalues $\lambda_k^{(\kappa_2)}$ are implicitly dependent on the diffusion tensor $\boldsymbol{D}$ and confining potential V_1.

Figure 7.2a shows typical eigenfunctions $v_k^{(\kappa_2)}$ of the local part of the linearised operator $\mathscr{L}$. Figure 7.2b shows the pairwise $L_c^2(U, \varrho^{-1})$ inner product of the $v_k^{(\kappa_2)}$ demonstrating orthogonality of the basis functions. Figure 7.2c shows the expansion of the two-body function V_2 (here a Morse like potential) in terms of the eigenfunctions v_k meanwhile Figure 7.2d shows the error between the expansion and V_2. We also demonstrate the accuracy of the collocation scheme in computing eigenvalues and eigenfunctions of $\mathscr{A}_{\kappa_2}$ in Table 7.1. In particular, $\mathscr{A}_{\kappa_2}$ is composed of dense first and second order differentiation matrices and the value $\nabla_{\mathbf{r}}(\varrho^{-1} v_k^{(\kappa_2)}) \cdot \mathbf{n}$ is very small on the boundary using only 100 collocation points.

In Figures 7.3c, 7.3d, we plot various paths $\kappa_2^\star(\lambda)$ as solutions to the equation $\lambda = \lambda_{k^\star}(\kappa_2^*)$ for k the wave number by numerically solving (7.6.23) for different two-body potentials. We also reproduce figures from Davidson & Dodds [39] in Figures 7.3a, 7.3b, verifying our numerical procedure for computing the spectra of similar nonlocal differential operators. Note however that operators in [39] do not contain convolution type integral operators, and, with Dirichlet boundary conditions, their spectra differ substantially from those considered here (for example Figures 7.3c, 7.3d). The intersection through the λ axis in each Figure 7.3a–7.3d gives the local eigenvalues $\gamma_k^{(0)}$ for the corresponding nonlocal differential operator. Note that it is not necessary for $\gamma_k^{(0)}$ to lie on the moving path for every k.

The numerical solution of (7.6.23) involves both a truncation of the infinite series and a numerical tolerance for the zeros of the nonlinear function $f(\kappa_2) = \kappa_2 - \kappa_2(\lambda_k)$. Note that $\mathscr{L}$ is self-adjoint in $L_c^2(U, \varrho^{-1})$ (with real eigenvalues) only for $\kappa_2 = 0$. The λ's are otherwise complex and the curves plotted show when the paths drop to the real plane. When $|\kappa_2|$ is sufficiently large, that is when (7.6.21) is violated, the λ's have non-zero imaginary part.

We now investigate the spectrum of the linearised operator $\mathscr{L}$ in terms of the eigenspace of its nonlocal part. We determine necessary conditions for bifurcations.

7.7 Bifurcation Theory

We now provide our first result of the section which relates the stability of equilibrium density to the two-body interaction potential.

Theorem 7.7.1. *Let $\kappa_2 \in (-\infty, \infty)$ and suppose ϱ is a solution to the self-consistency equation (7.5.2). Let $\mathscr{R}$ be given by*

$$\mathscr{R}w = -\varrho V_2 \star w,$$

where $w \in L^2(U, \varrho^{-1})$ is mean zero. If $\mathscr{R}$ is positive definite and $\kappa_2 < \beta_1$ where β_1 is the smallest eigenvalue of $\mathscr{R}^{-1}$, then equilibrium densities formed from repulsive two–body kernels V_2 are stable. Conversely if $\mathscr{R}$ is negative definite and $\kappa_2 > \beta_1$ where β_1 is the largest eigenvalue of $\mathscr{R}^{-1}$, then equilibrium densities formed from attractive two–body kernels V_2 are stable.

Proof. We observe that $\mathscr{L}_1$ is self-adjoint in $L^2(U, \varrho^{-1})$ only when there is no interaction ($\kappa_2 = 0$). We may however expand the eigenfunctions of $\mathscr{L}_1$ in the eigenfunctions of $\mathscr{R}$, $\{u_n\}_{n=1}^{\infty}$ which form an orthonormal basis of $L^2(U, \varrho^{-1})$ (see Definition 7.6.4). We write $w_n = \sum_{i=1} \alpha_{n_i} u_i$. By the definition of the eigenvalue problem for $\mathscr{L}_1$

$$\mathscr{L}_1 w_n = \lambda_n w_n.$$

Now inserting the expansion in u_i's we obtain

$$\begin{aligned}
\lambda_n \sum_{i=1} \alpha_{n_i} u_i &= \mathscr{L}_1 \sum_{i=1} \alpha_{n_i} u_i \\
&= [\mathscr{A}_{\kappa_2} + \kappa_2 \mathscr{B}] \sum_{i=1} \alpha_{n_i} u_i \\
&= \sum_{i=1} \alpha_{n_i} \left\{ \mathscr{A}_{\kappa_2} u_i + \kappa_2 \mathscr{B} u_i \right\} \\
&= \sum_{i=1} \alpha_{n_i} \left\{ \nabla_{\mathbf{r}} \cdot \left(\boldsymbol{D} \varrho \left(\nabla_{\mathbf{r}} (\varrho^{-1} u_i) \right) \right) - \kappa_2 \nabla_{\mathbf{r}} \cdot \left(\boldsymbol{D} \varrho \left(\nabla_{\mathbf{r}} (\varrho^{-1} (\varrho \mathscr{R} u_i)) \right) \right) \right\} \\
&= \sum_{i=1} \alpha_{n_i} \left\{ \nabla_{\mathbf{r}} \cdot \left(\boldsymbol{D} \varrho \left(\nabla_{\mathbf{r}} (\varrho^{-1} u_i) \right) \right) - \kappa_2 \nabla_{\mathbf{r}} \cdot \left(\boldsymbol{D} \varrho \left(\nabla_{\mathbf{r}} (\varrho^{-1} (\varrho \mathscr{R} u_i)) \right) \right) \right\} \\
&= \sum_{i=1} \alpha_{n_i} \left\{ 1 - \frac{\kappa_2}{\beta_i} \right\} \nabla_{\mathbf{r}} \cdot \left(\boldsymbol{D} \varrho \left(\nabla_{\mathbf{r}} (\varrho^{-1} u_i) \right) \right),
\end{aligned}$$

where we have used the definitions (7.6.16a), (7.6.16b) and (7.6.2) and that each u_i is an eigenfunction of $\mathscr{R}$. Now by multiplying my $\varrho^{-1} u_j$ and integrating we obtain

$$\lambda_n \alpha_{n_j} \|u_j\|^2_{L^2(U, \varrho^{-1})} = \sum_{i=1} \alpha_{n_i} \left\{ 1 - \frac{\kappa_2}{\beta_i} \right\} \int_U \mathrm{d}\mathbf{r}\, u_j \nabla_{\mathbf{r}} \cdot \left(\boldsymbol{D} \varrho \left(\nabla_{\mathbf{r}} (\varrho^{-1} u_i) \right) \right)$$

Now by integrating by parts, using Gauss's theorem and the condition that $\nabla_{\mathbf{r}}(\varrho^{-1} u_i)$ is zero on the boundary of U, we obtain

$$\lambda_n = \alpha_{n_j}^{-1} \sum_{i=1} \alpha_{n_i} \left(\frac{\kappa_2}{\beta_i} - 1 \right) \int_U \mathrm{d}\mathbf{r} \left| \varrho^{1/2} \boldsymbol{D}^{1/2} \nabla_{\mathbf{r}} \left(\varrho^{-1} u_i \right) \right|^2$$

for every $j = 1, \cdots$. Hence, a bifurcation from the equilibrium density ϱ may occur when κ_2 coincides with β_j, for some $j = 1, \cdots$ and perturbations w_n are linear combinations of u_j. To ensure ϱ is stable one must have, for every $j \in \mathbb{N}$

$$\begin{cases} \kappa_2 < \beta_j & \text{if } \mathscr{R} \text{ is positive definite,} \\ \beta_j < \kappa_2 & \text{if } \mathscr{R} \text{ is negative definite.} \end{cases}$$

Now by the spectral theorem, the $\{\beta_n^{-1}\}_{n\geq 1}$ are discrete, countable and may be ordered such that $|\beta_n^{-1}| \to 0$. Therefore to ensure the stability of ϱ we require $\kappa_2 < \beta_1$ if $\mathscr{R}$ is positive definite and $\beta_1 < \kappa_2$ if $\mathscr{R}$ is negative definite. This completes the proof of the theorem. □

We now relate theorem 7.7.1 to the H-stability result in [29].

Remark 7.7.2. *We remark on the consistency with the H-stability condition of [29] with periodic boundary conditions, the equilibrium density may bifurcate if the interaction kernel has a negative Fourier mode. In the present work, the distribution of the eigenvalues of the operator $\mathscr{R}$ determines whether the equilibrium density is stable with respect to $\{u_j\}_{j=1}^{\infty}$. In particular, if $\mathscr{R}$ has a negative eigenvalue then equilibrium densities formed from repulsive V_2 may become unstable.*

We may obtain an estimate for the eigenvalues β_n^{-1} in terms of V_2 and ϱ in the following way, by the eigenvalue problem (7.6.3) *we have*

$$\begin{aligned}|\beta_n^{-1}| &= |\beta_n^{-1}|\langle u_n, u_n\rangle_{L^2(U,\varrho^{-1})} = |-\langle u_n, V_2 \star u_n\rangle_{L^2(U)}| \\ &\leq \|V_2\|_{L^\infty(U)}\|u_n\|_{L^1(U)}^2 = \|V_2\|_{L^\infty(U)}\|\varrho^{1/2}(\varrho^{-1/2})u_n\|_{L^1}^2 \\ &\leq \|V_2\|_{L^\infty(U)}\|\varrho\|_{L^1(U)}^2\|(\varrho^{-1/2})u_n\|_{L^2(U)}^2 = \|V_2\|_{L^\infty(U)},\end{aligned}$$

where we have used the Cauchy-Schwarz inequality and the fact that the $\{u_n\}_{n=1}^{\infty}$ are orthonormal in $L^2(U,\varrho^{-1})$. From this we obtain the lower bound $\|V_2\|_{L^\infty(U)}^{-1} \leq |\beta_n|$, this lower bound shows that the bifurcation point coincides with the boundary of the interval in which free energy $\mathscr{F}$ is convex (c.f. Proposition 7.6.1).

Theorem 7.7.3. *Let $\{\beta_n^{-1}\}_{n=1}^{\infty}$ be the ordered eigenvalues of $\mathscr{R}$. If $|\kappa_2| \geq |\beta_1|$ then (β_1, w_1) is a bifurcation point of* (7.4.21) *where w_1 is the eigenfunction of $\mathscr{R}$ associated to β_1^{-1} and there exists $0 < \varrho_* \neq \varrho_\infty$ solving* (7.5.2).

Proof. Let ϱ_{κ_2} denote the solution to (7.5.2) for a given κ_2 which is known to exist by Theorem 7.5.1. Since ϱ_{κ_2} is continuous in κ_2 and $\mathscr{F}[\varrho]$ is continuous in ϱ, then $\mathscr{F}$ is continuous in κ_2. By Lemma 7.6.5 we know that a minimiser of $\mathscr{F}$ exists for each κ_2 and by Lemma 7.6.6 the minimiser is strictly positive. Given $|\kappa_2| \geq \|V_2\|_{L^\infty(U)}^{-1}$ then by Proposition 7.6.1, $\mathscr{F}$ is no longer convex and ϱ_{κ_2} is either an inflection point or a local maximum of $\mathscr{F}$. Hence ϱ_{κ_2} is unstable and by Lemma 7.6.5 there exists ϱ_* such that $\mathscr{F}[\varrho_*] < \mathscr{F}[\varrho_{\kappa_2}]$. Additionally by the self-adjointness and compactness of $\mathscr{R}$, one has that $\beta_n^{-1} \to 0$ as $n \to \infty$ and hence $\beta_n \to \infty$ as $n \to \infty$ and β_1 is the smallest of the $\{\beta_n\}_{n=1}^{\infty}$.

If $\mathscr{R}$ is positive definite, there are no negative β_n and the only solution to (7.6.3) is $u_n \equiv 0$ and ϱ_{κ_2} will be stable for all $\kappa_2 < \beta_1$. Similarly, if $\mathscr{R}$ is negative definite, there are no positive β_n and the only solution to (7.6.3) is $u_n \equiv 0$ and ϱ_{κ_2} will be stable for all $\kappa_2 > \beta_1$. If $\mathscr{R}$ is indefinite, by Remark 7.7.2, for $|\beta_n| < \|V_2\|_{L^\infty(U)}^{-1}$ there are no solutions (other than $w_n \equiv 0$) to $\mathscr{R}[w_n] = \beta_n^{-1}w_n$, and once again for $|\kappa_2| < |\beta_1|$, $\varrho_{\kappa_2} = \varrho_\infty$ is stable. For $\kappa_2 \geq \|V_2\|_{L^\infty(U)}^{-1}$ there are infinitely many non-trivial solutions to $\mathscr{R}[w_n] = \beta_n^{-1}w_n$ and $\kappa_2 = \beta_1$ is the first.

Hence if $|\kappa_2| \geq |\beta_1|$ then the unique stationary density ϱ_∞ is unstable and by Lemma 7.6.5 there must exist ϱ_* such that $\mathscr{F}[\varrho_*] < \mathscr{F}[\varrho_{\kappa_2}]$. □

We define the $\mathscr{W} : L^2(U) \to \mathbb{R}$ transform such that

$$\mathscr{W}[f](n) = \int_U \mathrm{d}\mathbf{r}\varrho_{\beta_n}^{-1}w_n(\mathbf{r})f(\mathbf{r})$$

where ϱ_{β_n} solves (7.5.2) with $\kappa_2 = \beta_n$. With this we may plot the bifurcation diagram for the stability of the unique equilibrium state $\varrho = \varrho_\infty$, see for example Figure 7.1.

7.8 Application To Nonlinear Diffusion Equations

In this section we consider sufficient conditions for bifurcations under particular forms of nonlocal operators. We will show that, by use of numerical examples, there may be more than one

stationary solution under additional assumptions on the two-body potential by making use of the bifurcation theory developed in Section 7.7. We fix κ_1 and consider boundary value problems where the nonlocal term is not of convolution type. Let $V_2(\mathbf{r},\mathbf{r}')$ be a two-body function and consider

$$\begin{cases} \mathscr{P}[\varrho] := \nabla\cdot\Big[\boldsymbol{D}\Big(\nabla\varrho + \varrho\kappa_1\nabla V_1 + \kappa_2\varrho\nabla\int_U \mathrm{d}\mathbf{r}' V_2(\mathbf{r},\mathbf{r}')\varrho(\mathbf{r}')\Big)\Big] = 0 & \text{in } U,\\ \Omega[\varrho]\cdot\mathbf{n} := \boldsymbol{D}\Big(\nabla\varrho + \varrho\kappa_1\nabla V_1 + \kappa_2\varrho\nabla\int_U \mathrm{d}\mathbf{r}' V_2(\mathbf{r},\mathbf{r}')\varrho(\mathbf{r}')\Big)\cdot\mathbf{n} = 0 & \text{on } \partial U. \end{cases} \tag{7.8.1}$$

Solutions of $\mathscr{P}\varrho = 0$ with $\Omega[\varrho]\cdot\mathbf{n} = 0$ on the boundary are denoted by $\varrho = \varrho_{\kappa_2}$ and satisfy the self-consistency equation

$$\varrho_{\kappa_2} = \frac{e^{-(\kappa_1 V_1 + \kappa_2\int_U \mathrm{d}\mathbf{r}'\, V_2(\mathbf{r},\mathbf{r}')\varrho_{\kappa_2}(\mathbf{r}'))}}{Z}. \tag{7.8.2}$$

The linear stability of the steady state may be studied implicitly by examining the properties of the linearised self-consistency map. By linearising equation (7.8.2), by writing $\varrho_{\kappa_2} = \phi_0 + \epsilon\phi_1$, for some small ϵ, we obtain the original nonlinear problem

$$\phi_0 = \frac{e^{-(\kappa_1 V_1 + \kappa_2\int_U \mathrm{d}\mathbf{r}'\, V_2(\mathbf{r},\mathbf{r}')\phi_0(\mathbf{r}'))}}{Z_0} \quad \text{s.t} \quad \Omega[\phi_0]\cdot\mathbf{n} = 0$$

where $Z_0 = \int_U \mathrm{d}\mathbf{r}\, e^{-(\kappa_1 V_1 + \kappa_2\int_U \mathrm{d}\mathbf{r}'\, V_2(\mathbf{r},\mathbf{r}')\phi_0(\mathbf{r}'))}$, along with the linearised equation

$$\phi_1 = -\kappa_2\,\phi_0\int_U \mathrm{d}\mathbf{r}'\, V_2(\mathbf{r},\mathbf{r}')\phi_1(\mathbf{r}') \quad \text{s.t} \quad \int_U \mathrm{d}\mathbf{r}\,\phi_1(\mathbf{r}) = 0. \tag{7.8.3}$$

The integral condition in (7.8.3) comes from the fact that higher order perturbations to ϕ_0 must possess zero mean to preserve the mass in the system. We define the linear operator $\mathscr{T}$ in $L_1(U)$ by

$$\mathscr{T}\phi(\mathbf{r}) := \phi_0(\mathbf{r})\int_U \mathrm{d}\mathbf{r}'\, V_2(\mathbf{r},\mathbf{r}')\phi(\mathbf{r}'). \tag{7.8.4}$$

We also define the mapping from $\mathscr{G} : (L_1(U),\mathbb{R}) \to L_1(U)$ by

$$\mathscr{G}(\phi,\kappa) := \phi - f(\phi,\kappa)$$

where $f(\phi,\kappa) := \frac{e^{-(\kappa_1 V_1 + \kappa\mathrm{d}\mathbf{r}'\, V_2(\mathbf{r},\mathbf{r}')\phi(\mathbf{r}'))}}{\int_U \mathrm{d}\mathbf{r} e^{-(\kappa_1 V_1 + \kappa\mathrm{d}\mathbf{r}'\, V_2(\mathbf{r},\mathbf{r}')\phi(\mathbf{r}'))}}$. To construct the bifurcation diagram, we will use the following result from [166, Tamura (1984)], or [29, Carrillo et al. 2019], which is a direct consequence of the Crandall-Rabinowitz theorem, see, e.g. [38].

Theorem 7.8.1 (Tamura (1984), Carrillo et al. (2019))**.** *Let $V_2(x,y) = V_2(y,x)$. Also let (ψ_0,ν_0) be a fixed point in $L^1(U)\times\mathbb{R}$ such that:*

1. $\mathscr{G}(\psi_0,\nu_0) = 0$,
2. ν_0^{-1} *is an eigenvalue of* $\mathscr{T}$,
3. $\int_U \mathrm{d}\mathbf{r}\, V_2(\mathbf{r},\mathbf{r}')\psi_0(\mathbf{r}) = 0$,
4. $\dim\{\psi\in L^1(U) \,:\, \psi = \nu_0\mathscr{T}\psi\} = 1$.

Then (ψ_0,ν_0) is a bifurcation point of $\mathscr{G} = 0$. That is, for any neighbourhood B of (ψ_0,ν_0) in $L^1(U)\times\mathbb{R}$ there exists $(\psi_1,\nu_1)\in B$ such that $\psi_1\neq\psi_0$ and $\mathscr{G}(\psi_1,\nu_1) = 0$.

Proof. The proof relies on checking the conditions of the Crandall-Rabinowitz Theorem and is equivalent to Tamura's proof [166]. We will need the first few Frechét derivatives of f in

variations w with zero mean. We have that

$$\begin{aligned}
D_\phi f(\phi,\kappa)[w](\mathbf{r}) &= \kappa f(\phi,\kappa)(\mathbf{r}) \int_U \mathrm{d}\mathbf{r}'\, V_2(\mathbf{r},\mathbf{r}')w(\mathbf{r}') \\
&\quad - \kappa f(\phi,\kappa)(\mathbf{r}) \int_U \mathrm{d}\mathbf{s}\, f(\phi,\kappa)(\mathbf{s}) \int_U \mathrm{d}\mathbf{r}'\, V_2(\mathbf{s},\mathbf{r}')w(\mathbf{r}'), \\
D_\kappa f(\phi,\kappa)(\mathbf{r}) &= f(\phi,\kappa)(\mathbf{r}) \int_U \mathrm{d}\mathbf{r}'\, V_2(\mathbf{r},\mathbf{r}')\phi(\mathbf{r}') \\
&\quad - f(\phi,\kappa)(\mathbf{r}) \int_U \mathrm{d}\mathbf{s}\, f(\phi,\kappa)(\mathbf{s}) \int_U \mathrm{d}\mathbf{r}'\, V_2(\mathbf{s},\mathbf{r}')\phi(\mathbf{r}'), \\
D_\kappa D_\phi f(\phi,\kappa)[w](\mathbf{r}) &= f(\phi,\kappa)(\mathbf{r}) \int_U \mathrm{d}\mathbf{r}'\, V_2(\mathbf{r},\mathbf{r}')w(\mathbf{r}') \\
&\quad - f(\phi,\kappa)(\mathbf{r}) \int_U \mathrm{d}\mathbf{s}\, f(\phi,\kappa)(\mathbf{s}) \int_U \mathrm{d}\mathbf{r}'\, V_2(\mathbf{s},\mathbf{r}')w(\mathbf{r}') \\
&\quad + D_\phi f(\phi,\kappa)[w](\mathbf{r}) \int_U \mathrm{d}\mathbf{r}'\, V_2(\mathbf{r},\mathbf{r}')\phi(\mathbf{r}') \\
&\quad - D_\phi f(\phi,\kappa)[w](\mathbf{r}) \int_U \mathrm{d}\mathbf{s}\, f(\phi,\kappa)(\mathbf{s}) \int_U \mathrm{d}\mathbf{r}'\, V_2(\mathbf{s},\mathbf{r}')\phi(\mathbf{r}') \\
&\quad - f(\phi,\kappa)(\mathbf{r}) \int_U \mathrm{d}\mathbf{s}\, D_\phi f(\phi,\kappa)[w](\mathbf{s}) \int_U \mathrm{d}\mathbf{r}'\, V_2(\mathbf{s},\mathbf{r}')\phi(\mathbf{r}'). \qquad (7.8.5)
\end{aligned}$$

Firstly we have from Theorem 7.5.1 that there exists ψ_0 such that $\mathscr{G}(\psi_0,\kappa)=0$ for any $\kappa\in\mathbb{R}$ so certainly ψ_0 exists such that $\mathscr{G}(\psi_0,\nu_0)=0$ with ν_0 is a eigenvalue of $\mathscr{T}$ and so Condition 1 holds. Secondly we have that

$$\begin{aligned}
D_\kappa \mathscr{G}(\phi,\kappa)(\mathbf{r})|_{(\psi_0,\nu_0)} &= D_\kappa[\phi - f(\phi,\kappa)]|_{(\psi_0,\nu_0)} \\
&= [-\kappa f(\phi,\kappa)(\mathbf{r}) \int_U \mathrm{d}\mathbf{r}'\, V_2(\mathbf{r},\mathbf{r}')\phi(\mathbf{r}') \\
&\quad + \kappa f(\phi,\kappa)(\mathbf{r}) \int_U \mathrm{d}\mathbf{s}\, f(\phi,\kappa)(\mathbf{s}) \int_U \mathrm{d}\mathbf{r}'\, V_2(\mathbf{s},\mathbf{r}')\phi(\mathbf{r}')]|_{(\psi_0,\nu_0)} \\
&= 0
\end{aligned}$$

where we have used assumption 3 (similarly $\mathscr{G}(\psi_0,\kappa)=0$ so $D_\kappa\mathscr{G}(\phi,\kappa)(\mathbf{r})|_{(\psi_0,\nu_0)}=0$). Thirdly, by direct calculation

$$D_\phi \mathscr{G}(\phi,\kappa)(\mathbf{r})|_{(\psi_0,\nu_0)} = I - \nu_0 \mathscr{T}.$$

Also, by Fredholm theory, $\mathrm{Im}(D_\phi\mathscr{G}(\psi_0,\nu_0))^\perp = \ker(I-\nu_0\mathscr{T}^*)$ and $\mathscr{T}$ is normal as seen by the definition of its adjoint

$$\mathscr{T}^* w = \int_U \mathrm{d}\mathbf{r}' V_2(\mathbf{r},\mathbf{r}')\psi_0(\mathbf{r}')w(\mathbf{r}').$$

Now since $\mathscr{T}$ is normal $I-\mathscr{T}$ is normal and hence $\dim\ker(I-\nu\mathscr{T}) = \dim\ker(I-\nu\mathscr{T}^*)$ and $\mathrm{Im}(D_\phi\mathscr{G}(\psi_0,\nu_0))$ is closed and $\mathrm{codim}(D_\phi\mathscr{G}(\psi_0,\nu_0))=1$ by assumption 4. Fourthly, since $D_\kappa D_\kappa\mathscr{G}(\psi_0,\nu_0)=0$ we have $D_\kappa D_\kappa\mathscr{G}(\psi_0,\nu_0)\in \mathrm{Im}\, D_\phi\mathscr{G}(\psi_0,\nu_0)$ as there is one eigenvector of $I-\nu_0\mathscr{T}$ for each ν_0.

Finally we must show that $D_\phi D_\kappa\mathscr{G}(\psi_0,\nu_0)[\psi_2]\notin \mathrm{Im}\, D_\phi\mathscr{G}(\psi_0,\nu_0)$ for some eigenvector ψ_2 of $I-\nu_0\mathscr{T}$. For this it will be sufficient to show that a projection of $D_\phi D_\kappa\mathscr{G}(\psi_0,\nu_0)[\psi_2]$ into the orthogonal complement of $\mathrm{Im}\, D_\phi\mathscr{G}(\psi_0,\nu_0)$ is nonzero. Note that if ψ_2 is an eigenvector of $I-\nu_0\mathscr{T}$ then $\psi_2/\psi_0\in\ker(I-\nu_0\mathscr{T}^*)\perp \mathrm{Im}\, D_\phi\mathscr{G}(\psi_0,\nu_0)$. Now, by (7.8.5) $D_\phi D_\kappa\mathscr{G}(\psi_0,\nu_0)[\psi_2] = -\nu_0^{-1}\psi_2$ and with $\mathrm{d}\mu = \mathrm{d}\mathbf{r}\psi_0(\mathbf{r})$ we have

$$\int_U \mathrm{d}\mu\, D_\phi D_\kappa\mathscr{G}(\psi_0,\nu_0)[\psi_2](\mathbf{r})\tfrac{\psi_2}{\psi_0}(\mathbf{r}) = \nu_0^{-1}\int_U \mathrm{d}\mathbf{r}\,|\psi_2(\mathbf{r})|^2 > 0.$$

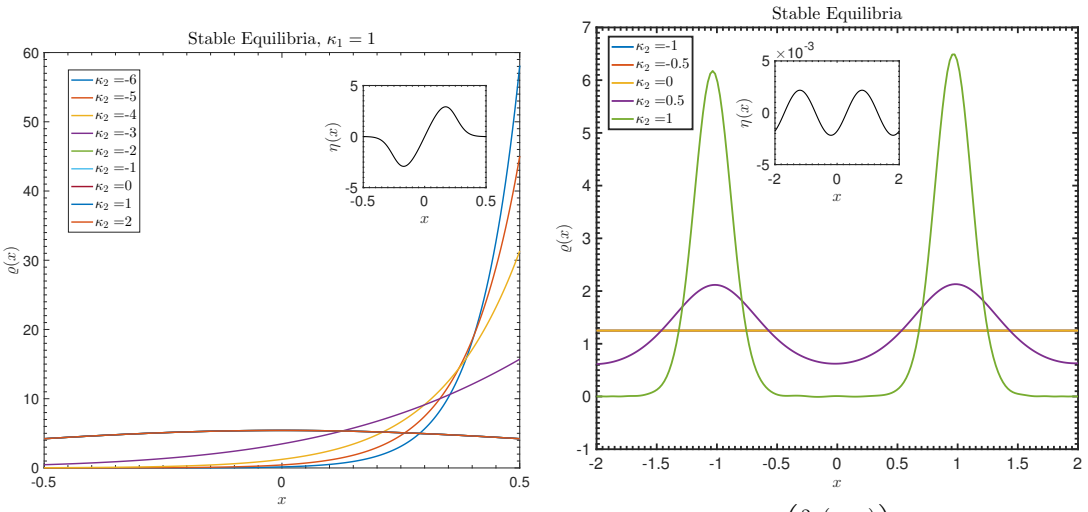

(a) $V_2(x,y) = xy$ with $\eta(x,\theta) = -\frac{1}{2}\sin x(-\tanh((x-1/2)/\theta)+\tanh((x+1/2)/\theta))$

(b) $V_2(x,y) = -\cos\left(\frac{2\pi(x-y)}{L}\right)$ with $\eta(x)$ eigenvectors of the operator $\mathscr{T}$ and $\psi_0 = \frac{N}{L}$.

Figure 7.4: Stable densities bifurcating from (a). $\psi_0 = \exp\{-\kappa_1 V_1(x)\}/Z$ and (b). $\psi_0 = \frac{N}{2L}$ where $2L$ is the length of the interval, which solve (7.8.2) for different two-body functions (a). $V_2(x,y) = xy$ and (b). $V_2(x,y) = -\cos\left(\frac{2\pi(x-y)}{L}\right)$. Insets show the shape of perturbation function.

Therefore $D_\phi D_\kappa \mathscr{G}(\psi_0,\nu_0)[\psi_2] \notin \operatorname{Im} D_\phi \mathscr{G}(\psi_0,\nu_0)$. Thus the theorem is proved. □

Remark 7.8.2. *Note that ψ_0 is, by construction, the background density given by $\psi_0 = \frac{e^{-V_1(\mathbf{r})}}{\int_U \mathrm{d}\mathbf{r} e^{-V_1(\mathbf{r})}}$. Theorem 7.8.1 presents sufficient conditions to permit bifurcations from ψ_0 with stationary equations of the form* (7.8.1)*. In particular it will be sufficient that the two-body potential satisfies the normality condition (condition 3. of Theorem 7.8.1). Then bifurcations occur at discrete eigenvalues of the nonlocal operator $\mathscr{T}$ as defined in* (7.8.4)*. We remark that these conditions are consistent with Theorem 7.7.3.*

7.8.1 Numerical Experiments.

In this section we compute the branches of solutions that may evolve in the DDFT-like example considered in Section 7.8 with nonlinear, nonlocal boundary conditions. Given simple interaction kernels we show that symmetry-breaking systems may be constructed quite easily given sufficiently high interaction strength. For the numerical examples presented here, ϱ is a number density and hence $\int_U \mathrm{d}\mathbf{r}\, \varrho = N$. We consider numerical solutions to

$$\begin{cases} \partial_t \varrho = \nabla \cdot \left[\boldsymbol{D}\left(\nabla\varrho + \varrho\kappa_1 \nabla V_1 + \kappa_2 \varrho \nabla \int_U \mathrm{d}\mathbf{r}' V_2(\mathbf{r},\mathbf{r}')\varrho(\mathbf{r}') \right) \right] & \text{in } U, \\ \Omega[\varrho]\cdot\mathbf{n} := \boldsymbol{D}\left(\nabla\varrho + \varrho\kappa_1 \nabla V_1 + \kappa_2 \varrho \nabla \int_U \mathrm{d}\mathbf{r}' V_2(\mathbf{r},\mathbf{r}')\varrho(\mathbf{r}') \right)\cdot\mathbf{n} = 0 & \text{on } \partial U, \\ \varrho(\mathbf{r},0) = \frac{e^{-\kappa_1 V_1(\mathbf{r}) + \kappa_2 \int_U \mathrm{d}\mathbf{r}' V_2(\mathbf{r},\mathbf{r}')\varrho(\mathbf{r}',0)}}{Z} & \text{at } t = 0. \end{cases} \tag{7.8.6}$$

The nonlocal terms in (7.8.6), both in the evolution equation and the boundary condition, mean that numerical implementations require efficient and accurate quadrature. We demonstrate the power with which the pseudo-spectral collocation scheme 2DChebClass [67] may compute solutions with such efficiency and accuracy. For a more detailed explanation of pseudospectral methods for DDFT problems, particularly the efficient computation of convolution integrals, see [127].

Some numerical experiments were performed by solving (7.8.1) in 1D with the choice $V_2 = xy$ and $V_1 = x^2$ on $U = [-1/2, 1/2]$. Under this choice of confining and two-body potentials the normality condition (3) of Theorem 7.8.1 holds. Additionally, for $|\kappa_2|$ sufficiently small, the

unique stationary density is $\psi_0 = e^{-\kappa_1 V_1}/Z$. Upon increasing κ_2 and perturbing with a mean zero function $\eta(x,\theta)$ the stability of ψ_0 breaks and transitions may be observed to non symmetric equilibria. The asymmetry of the equilibria depends on the sign of η as seen in Figure 7.4.

Figure 7.4 shows long time numerical solutions to the IBVP (7.8.6) subject to a mean zero perturbation for different interaction strengths κ_2, with V_2 fixed. In Figure 7.4a, the symmetric solution $\psi_0 = \exp(-\kappa_1 V_1)/Z$ was shown to be unstable as interaction strength κ_2 was made ever negative. In particular by perturbing with a sinusoidal function with positive or negative sign, the stationary density can be shown to adhere to one boundary, thereby bifurcating from the previously symmetric solution ψ_0. The skewness of the density is controlled by the sign of the perturbation function η and $\eta \in \text{Span}\mathscr{T}$, hence densities which adhere to the left boundary may be obtained by changing the sign of η. We predict the stable and symmetric branch to bifurcate at the critical interaction energy $\kappa_2 = -2.4$ (to 1 decimal place) which is the negative inverse of smallest eigenvalue of $\psi_0^{-1}\mathscr{T}$ in $U = [-1/2, 1/2]$. This is verified in Figure 7.1 and the transition between a stable symmetric density and a stable nonsymmetric one is observed in Figure 7.4a for the curves labelled $\kappa_2 = -2$ and $\kappa_2 = -3$.

In Figure 7.4b, we see how the uniform density may become unstable. Here $\psi_0 = N/(2L)$ where $2L$ is the length of the interval. We perturb with eigenvectors of $\mathscr{T}$ at increasing interaction strengths. The critical strength was $\kappa_{2\sharp} = 0.4$ (to 1 decimal place), the negative inverse of smallest eigenvalue of $\psi_0^{-1}\mathscr{T}$. This is verified in Figure 7.1 and the transition between a stable uniform density and a stable multi-modal one is observed in Figure 7.4b for the curves labelled $\kappa_2 = 0$ and $\kappa_2 = 0.5$.

7.9 Existence & Uniqueness Of Weak Solutions Of The Density With Full HI

In this section we determine the existence and uniqueness of the weak density $\varrho(\mathbf{r}, t)$ solving (7.2.3) in the sense (7.2.8). To ease notation we suppress $\boldsymbol{A}[\mathbf{a}]$ as it may be trivially added (see Remark 7.4.9). We begin by determining some useful results: first, that $\varrho(\mathbf{r}, t)$ is bounded above in $L^1(U)$ for all time by initial data ϱ_0 and second, the $L^1(U)$ norm of ϱ is unity for all time and $\varrho(\mathbf{r}, t)$ is non-negative. We will strengthen the non-negativity to strict positivity of $\varrho(\mathbf{r}, t)$ in Section 7.9.4. The results in this section are analogous to those in [33], [29] with the difference that the boundary conditions we consider are no-flux the diffusion tensor is non-constant.

7.9.1 Useful Results.

We identify the expansion of the absolute value function.

Definition 7.9.1. *Let $\epsilon > 0$ and define the convex C^2 approximation of $|\cdot|$ by*

$$\chi_\epsilon(\psi) = \begin{cases} |\psi| & \text{for} \quad \psi > \epsilon, \\ -\frac{\psi^4}{8\epsilon^3} + \frac{3\psi^2}{4\epsilon} + \frac{3\epsilon}{8} & \text{for} \quad \psi \leq \epsilon. \end{cases}$$

We now present our first result concerning the boundedness of the the L^1 norm of ϱ in terms of the initial data ϱ_0.

Lemma 7.9.2. *If $\varrho \in C^1([0,\infty); C^2(U))$ is a solution of (7.2.3) with $\varrho_0 \in L^1(U)$ then $\|\varrho(t)\|_{L^1(U)} \leq \|\varrho_0\|_{L^1(U)}$ for all time $t \geq 0$.*

Proof. Multiplying (7.2.3) by $\chi'_\epsilon(\varrho)$, integrating and using the divergence theorem and chain rule, we have

$$\begin{aligned} &\frac{\mathrm{d}}{\mathrm{d}t}\int_U \mathrm{d}\mathbf{r}\, \chi_\epsilon(\varrho) + \|\boldsymbol{D}^{1/2}\nabla_{\mathbf{r}}\varrho\,[\chi''_\epsilon(\varrho)]^{1/2}\|^2_{L^2(U)} \\ &\quad = -\int \mathrm{d}\mathbf{r}\, \nabla_{\mathbf{r}}\varrho\, \chi''_\epsilon(\varrho)\cdot[\varrho\, \boldsymbol{D}(\mathbf{r})\nabla_{\mathbf{r}}(\kappa_1 V_1(\mathbf{r}) + \kappa_2[V_2 \star \varrho](\mathbf{r}))]. \end{aligned}$$

Now by Hölder's inequality and then Young's inequality

$$\begin{aligned}
&\frac{\mathrm{d}}{\mathrm{d}t}\int_U \mathrm{d}\mathbf{r}\,\chi_\epsilon(\varrho) + \|\boldsymbol{D}^{1/2}\nabla_{\mathbf{r}}\varrho\,[\chi_\epsilon''(\varrho)]^{1/2}\|_{L^2(U)}^2 \\
&\quad\le \|\boldsymbol{D}^{1/2}\nabla_{\mathbf{r}}\varrho[\chi_\epsilon''(\varrho)]^{1/2}\|_{L^2(U)} \times \|[\chi_\epsilon''(\varrho)]^{1/2}\varrho\,\boldsymbol{D}^{1/2}\nabla_{\mathbf{r}}(\kappa_1 V_1 + \kappa_2[V_2\star\varrho])\|_{L^2(U)} \\
&\quad\le \tfrac{1}{2}\|\boldsymbol{D}^{1/2}\nabla_{\mathbf{r}}\varrho[\chi_\epsilon''(\varrho)]^{1/2}\|_{L^2(U)}^2 + \tfrac{1}{2}\|[\chi_\epsilon''(\varrho)]^{1/2}\varrho\,\boldsymbol{D}^{1/2}\nabla_{\mathbf{r}}(\kappa_1 V_1 + \kappa_2[V_2\star\varrho])\|_{L^2(U)}^2.
\end{aligned}$$

Note there are no boundary terms due to the condition $\Pi[\varrho]\cdot\mathbf{n} = 0$ on ∂U. All together this implies the inequality

$$\begin{aligned}
&\frac{\mathrm{d}}{\mathrm{d}t}\int_U \mathrm{d}\mathbf{r}\,\chi_\epsilon(\varrho) + \tfrac{1}{2}\|\boldsymbol{D}^{1/2}\nabla_{\mathbf{r}}\varrho\,\chi_\epsilon''(\varrho)^{1/2}\|_{L^2(U)}^2 \\
&\quad\le \tfrac{1}{2}\|[\chi_\epsilon''(\varrho)]^{1/2}\varrho\,\boldsymbol{D}^{1/2}\nabla_{\mathbf{r}}(\kappa_1 V_1 + \kappa_2[V_2\star\varrho])\|_{L^2(U)}^2 \\
&\quad\le \tfrac{1}{2}\|\boldsymbol{D}^{1/2}\nabla_{\mathbf{r}}(\kappa_1 V_1 + \kappa_2[V_2\star\varrho])\|_{L^\infty}^2\|[\chi_\epsilon''(\varrho)]^{1/2}\varrho\|_{L^2}^2 \\
&\quad\le c_0\|[\chi_\epsilon''(\varrho)]^{1/2}\varrho\|_{L^2}^2(1+\|\varrho\|_{L^1(U)}^2)
\end{aligned}$$

for the constant $c_0 = 2\mu_{\max}\max\{|\kappa_1|^2\|\nabla_{\mathbf{r}}V_1\|_{L^\infty}^2, |\kappa_2|^2\|V_2\|_{L^\infty}^2\}$. It is an elementary calculation to show that

$$\varrho^2\chi_\epsilon''(\varrho) = \tfrac{3\varrho^2}{2\epsilon} - \tfrac{3\varrho^4}{2\epsilon^3}$$

for $\varrho\le\epsilon$. With this, and the fact that $\chi''(\varrho) = 0$ for $\varrho > \epsilon$, we have

$$\begin{aligned}
\|[\chi_\epsilon''(\varrho)]^{1/2}\varrho\|_{L^2}^2 &= \int_U \mathrm{d}\mathbf{r}\,\varrho^2\chi_\epsilon''(\varrho)\mathbb{I}_{\varrho\le\epsilon} + \int_U \mathrm{d}\mathbf{r}\,\varrho^2\chi_\epsilon''(\varrho)\mathbb{I}_{\varrho>\epsilon} \\
&= \int_U \mathrm{d}\mathbf{r}\,\frac{3\varrho^2(\epsilon^2-\varrho^2)}{2\epsilon^2}\mathbb{I}_{\varrho\le\epsilon} \le \int_U \mathrm{d}\mathbf{r}\,\frac{3\epsilon}{2}\mathbb{I}_{\varrho\le\epsilon} \le c_1\epsilon
\end{aligned} \tag{7.9.1}$$

for some constant c_1 dependent on U. Applying Grönwall's lemma to $\eta(\cdot)$ a nonnegative, absolutely continuous function on $[0,T]$ which satisfies for a.e. t

$$\eta'(t) \le \phi(t)\eta(t) + \psi(t)$$

where ϕ, ψ nonnegative and integrable functions on $[0,T]$ gives

$$\eta(t) \le e^{\int \mathrm{d}s_0^t\,\phi(s)}\eta(t)\Big[\eta(0) + \int_0^t \mathrm{d}s\,\psi(s)\Big]. \tag{7.9.2}$$

Observe that $\|\varrho\|_{L^1(U)} \le \int_U \mathrm{d}\mathbf{r}\,\chi_\epsilon(\varrho)$. Using this with (7.9.1), (7.9.1) and (7.9.2) with $\eta(t) = \phi(t) = c_1\epsilon\int_U \mathrm{d}\mathbf{r}\,\chi_\epsilon(\varrho)$ and $\psi(t) = c_1\epsilon$ we obtain

$$\int_U \mathrm{d}\mathbf{r}\,\chi_\epsilon(\varrho) \le \left(\int_U \mathrm{d}\mathbf{r}\,\chi_\epsilon(\varrho_0) + c_1\epsilon\,t\right) e^{c_1\epsilon\int_0^t \mathrm{d}s\,\int_U \mathrm{d}\mathbf{r}\,\chi_\epsilon(\varrho(\mathbf{r},s))}.$$

Now since ϱ is assumed to be continuous in time on $[0,\infty)$ the integral in the exponential is finite. Therefore taking $\epsilon\to 0$ one obtains

$$\|\varrho\|_{L^1} \le \|\varrho_0\|_{L^1}$$

for every $t > 0$. □

Corollary 7.9.3. *If $\varrho\in C^1([0,\infty);C^2(U))$ is a solution of (7.2.3) with ϱ_0 a probability density, that is $\varrho_0\ge 0$ and $\int_U \mathrm{d}\mathbf{r}\,\varrho_0(\mathbf{r}) = 1$, then $\|\varrho(t)\|_{L^1(U)} = 1$ and $\varrho(t)\ge 0$ in U for all time $t\ge 0$.*

Proof. The argument is a standard one. Since, due to no-flux boundary conditions, one has

that $\frac{\mathrm{d}}{\mathrm{d}t}\int \mathrm{d}\mathbf{r}\,\rho(\mathbf{r},t)=0$, we have

$$1=\int_U \mathrm{d}\mathbf{r}\,\varrho_0(\mathbf{r})=\int_U \mathrm{d}\mathbf{r}\,\varrho(\mathbf{r},t)\leq\|\varrho(t)\|_{L^1(U)}\leq\|\varrho(0)\|_{L^1(U)}=\int_U \mathrm{d}\mathbf{r}\,\varrho_0(\mathbf{r})=1,$$

so $\|\varrho(t)\|_{L^1(U)}=1$. Also observe the two equalities

$$\begin{aligned}1&=\int_U \mathrm{d}\mathbf{r}\,\varrho(\mathbf{r},t)=\int_U \mathrm{d}\mathbf{r}\,\varrho(\mathbf{r},t)\mathbb{I}_{\varrho\geq 0}+\int_U \mathrm{d}\mathbf{r}\,\varrho(\mathbf{r},t)\mathbb{I}_{\varrho<0},\\ 1&=\int_U \mathrm{d}\mathbf{r}\,|\varrho(\mathbf{r},t)|=\int_U \mathrm{d}\mathbf{r}\,\varrho(\mathbf{r},t)\mathbb{I}_{\varrho\geq 0}-\int_U \mathrm{d}\mathbf{r}\,\varrho(\mathbf{r},t)\mathbb{I}_{\varrho<0},\end{aligned}$$

where in the second line we have used the definition of the absolute value function. Subtracting these equalities we obtain

$$2\int_U \mathrm{d}\mathbf{r}\,\varrho(\mathbf{r},t)\mathbb{I}_{\varrho<0}=0$$

which implies $\varrho(\mathbf{r},t)\geq 0$ almost everywhere in U. Non-negativity of ϱ on all of U follows from continuity. □

With these results we may continue to determine the existence and uniqueness of weak densities solving (7.2.3) in the sense (7.2.8). The method we use follows [33] but here we must include calculations for the confining potential V_1^{eff} (which for ease of notation is written V_1 for each $\mathbf{a}(\mathbf{r},t)$) and a much wider class of two-body potentials V_2 which are not necessarily step functions. To start we introduce (7.9.3), the frozen version of (7.2.3), indexed by $n\in\mathbb{N}$, by substituting $\varrho=u_n$ everywhere except in the convolution term where we substitute $\varrho=u_{n-1}$. Each equation is parametrised by n, a linear parabolic PDE for the unknown u_n in terms of the solution u_{n-1} at the previous index, for which we have existence and uniqueness of weak solutions for each n. The remainder of the argument is to show $\lim_{n\to\infty}u_n$ exists and is a limit point solving the weak problem (7.2.8). In this section we will make references to Appendix 7.10 for results and definitions required for $u_n\in H^1(U)$, which differ slightly from the standard arguments found in textbooks for classical linear PDE theory (e.g. [52]).

7.9.2 Energy Estimates.

The results of Section 7.10 are that the initial boundary value problem

$$\begin{cases}\partial_t u_n-\nabla_{\mathbf{r}}\cdot[\boldsymbol{D}\nabla_{\mathbf{r}}u_n]=\nabla_{\mathbf{r}}\cdot[u_n\,\boldsymbol{D}\nabla_{\mathbf{r}}(\kappa_1V_1+\kappa_2V_2\star u_{n-1})],\\ \Xi[u_n]\cdot\mathbf{n}=0\quad\text{ on }\partial U\times[0,T],\\ \Xi[u_n]:=\boldsymbol{D}\left(\nabla_{\mathbf{r}}u_n+u_n\,\nabla_{\mathbf{r}}(\kappa_1V_1(\mathbf{r},t)+\kappa_2V_2\star u_{n-1})\right),\\ u_n=\varrho_0\quad\text{ on }U\times\{t=0\}\end{cases}\tag{7.9.3}$$

is well posed, and there exists weak solutions u_n for each $n\in\mathbb{N}$ in the sense (7.10.2). All that remains is to take the limit $n\to\infty$ to recover the original Smoluchowski equation (7.2.3). We start by deriving our first estimate on energy of u_n. To ease notation we derive all results with the time dependence on $\boldsymbol{D}$ suppressed since time may be trivially added to the exposition. Additionally, for a stationary density one has

$$\lim_{t\to\infty}\boldsymbol{D}(\mathbf{r},t)=\left(\mathbf{1}+\int \mathrm{d}\mathbf{r}'g(\mathbf{r},\mathbf{r}')\boldsymbol{Z}_1(\mathbf{r},\mathbf{r}')\varrho(\mathbf{r}')\right)^{-1}$$

which is a positive definite tensor and hence diagonalisable, and may be bounded by its smallest and largest eigenvalues which are positive and finite for $t\to\infty$. Hence energy estimates remain valid for $0<t\leq T$ when provided in terms of $\mu_{\min}$ and $\mu_{\max}$, both eigenvalues which depend on time but always remain positive and finite. It will be seen that a natural dual space to $H^1(U)$ is provided by the no-flux condition. In particular we denote by $H^{-1}(U)$ the dual space of $H^1(U)$, this is due to the divergence theorem and the boundary condition $\Xi[u_n]\cdot\mathbf{n}=0$ on

$\partial U \times [0,T]$, there is no boundary term, and the normal characterisation of $H^{-1} = (H_0^1)^*$ carries over to $H^1(U)$.

We now obtain uniform estimates on u_n in terms of the initial data ϱ_0 in all the required energy norms. The detailed calculations follow [33] but take into account the confining potential and non-constant diffusion tensor $\boldsymbol{D}$. The explicit calculations can be found in Section 7.10. The first estimate is in $L^\infty([0,T];L^2(U))$ and $L^2([0,T];H^1(U))$ norms.

Proposition 7.9.4. *Let $T > 0$ and suppose $\{u_n\}_{n\geq 1}$ satisfies (7.9.3) with $\varrho_0 \in C^\infty(U)$ a probability density. Then there exists a constant $C(T)$, dependent on time and $\mu_{\max}$, such that*

$$\|u_n\|_{L^\infty([0,T];L^2(U))} + \|u_n\|_{L^2([0,T];H^1(U))} \leq C(T,\mu_{\max})\|\varrho_0\|_{L^2(U)}. \tag{7.9.4}$$

Proof. Multiplying (7.9.3) by u_n and using the divergence theorem with $\Xi[u_n]\cdot\mathbf{n} = 0$ on $\partial U \times [0,T]$ one obtains

$$\begin{aligned}&\tfrac{1}{2}\frac{\mathrm{d}}{\mathrm{d}t}\|u_n(t)\|^2_{L^2(U)} + \int \mathrm{d}\mathbf{r}\,\nabla_{\mathbf{r}}u_n\cdot\boldsymbol{D}\nabla_{\mathbf{r}}u_n\\ &\qquad\leq \int \mathrm{d}\mathbf{r}\,|\nabla_{\mathbf{r}}u_n\cdot[u_n\,\boldsymbol{D}\nabla_{\mathbf{r}}(\kappa_1 V_1 + \kappa_2\, V_2\star u_{n-1})]|.\end{aligned}$$

Now since $\boldsymbol{D}$ is positive definite, we may write

$$\begin{aligned}&\int \mathrm{d}\mathbf{r}\,|\nabla_{\mathbf{r}}u_n\cdot[u_n\,\boldsymbol{D}\nabla_{\mathbf{r}}(\kappa_1 V_1 + \kappa_2\, V_2\star u_{n-1}])|\\ &\quad= \int \mathrm{d}\mathbf{r}\,|\boldsymbol{D}^{1/2}\nabla_{\mathbf{r}}u_n\cdot[u_n\,\boldsymbol{D}^{1/2}\nabla_{\mathbf{r}}(\kappa_1 V_1 + \kappa_2\, V_2\star u_{n-1})]|\\ &\quad\leq \|\boldsymbol{D}^{1/2}\nabla_{\mathbf{r}}u_n\|_{L^2(U)}\|u_n[\boldsymbol{D}^{1/2}\nabla_{\mathbf{r}}(\kappa_1 V_1 + \kappa_2\, V_2\star u_{n-1}])\|_{L^2(U)}\end{aligned}$$

where we have used Hölder's inequality. Now by Young's inequality

$$\begin{aligned}&\|\boldsymbol{D}^{1/2}\nabla_{\mathbf{r}}u_n\|_{L^2(U)}\|u_n\boldsymbol{D}^{1/2}\nabla_{\mathbf{r}}(\kappa_1 V_1 + \kappa_2 V_2\star\varrho_{n-1})\|_{L^2(U)}\\ &\quad\leq \tfrac{1}{2}\|\boldsymbol{D}^{1/2}\nabla_{\mathbf{r}}u_n\|^2_{L^2(U)} + \tfrac{1}{2}\|u_n\boldsymbol{D}^{1/2}\nabla_{\mathbf{r}}(\kappa_1 V_1 + \kappa_2\, V_2\star u_{n-1})\|^2_{L^2(U)}\\ &\quad\leq \tfrac{1}{2}\|\boldsymbol{D}^{1/2}\nabla_{\mathbf{r}}u_n\|^2_{L^2(U)} + \tfrac{1}{2}\|u_n\|^2_{L^2(U)}\|\boldsymbol{D}^{1/2}\nabla_{\mathbf{r}}(\kappa_1 V_1 + \kappa_2\, V_2\star u_{n-1})\|^2_{L^\infty(U)}.\end{aligned}$$

Using that $u_{n-1}\in H^1(U)$, $\nabla V_2 \in L^\infty$ and Hölder's inequality, we have

$$\begin{aligned}\int \mathrm{d}\mathbf{r}\Big|\int \mathrm{d}\mathbf{r}'\nabla_{\mathbf{r}}V_2(\mathbf{r},\mathbf{r}')u_{n-1}(\mathbf{r}')\Big|^2 &\leq \int \mathrm{d}\mathbf{r}\int \mathrm{d}\mathbf{r}'\,|\nabla_{\mathbf{r}}V_2(\mathbf{r},\mathbf{r}')|^2\int \mathrm{d}\mathbf{r}'|u_{n-1}(\mathbf{r}')|^2\\ &= |U|\|u_{n-1}\|^2_{L^2(U)}\|\nabla_{\mathbf{r}}V_2\|^2_{L^\infty(U)} < \infty.\end{aligned}$$

A similar bound exists for the term multiplying $\nabla_{\mathbf{r}}V_1$. Therefore (along with boundedness of $\boldsymbol{D}^{1/2}$) we have

$$\begin{aligned}\tfrac{1}{2}\frac{\mathrm{d}}{\mathrm{d}t}\|u_n(t)\|_2^2 + \tfrac{1}{2}\|\boldsymbol{D}^{1/2}\nabla_{\mathbf{r}}u_n(t)\|^2_{L^2(U)} &\leq C\|u_n(t)\|^2_{L^2(U)},\\ \tfrac{1}{2}\frac{\mathrm{d}}{\mathrm{d}t}\|u_n(t)\|_2^2 &\leq C\|u_n(t)\|^2_{L^2(U)}.\end{aligned} \tag{7.9.5}$$

Applying Grönwall to the second inequality gives

$$\|u_n(t)\|^2_{L^2(U)} \leq C(T)\|\varrho_0\|^2_{L^2(U)} \tag{7.9.6}$$

and integrating the first estimate in (7.9.5) gives

$$\int_0^T \mathrm{d}t\,\|\boldsymbol{D}^{1/2}\nabla_{\mathbf{r}}u_n\|^2_{L^2(U)} \leq C(T)\|\varrho_0\|^2_{L^2(U)}. \tag{7.9.7}$$

Finally by positive definiteness of $\boldsymbol{D}$ and by adding together (7.9.6) and (7.9.7) one obtains the result. □

The second estimate is for $L^\infty([0,T];H^1(U))$ and $L^2([0,T];L^2(U))$ norms.

Proposition 7.9.5. *Let $T > 0$ and suppose $\{u_n\}_{n\geq 1}$ satisfies (7.9.3) with $\varrho_0 \in C^\infty(U)$ a probability density. Then there exists some constant dependent on time $C(T)$ such that*

$$\begin{aligned}&\|u_n\|_{L^\infty([0,T];H^1(U))} + \|\nabla_{\mathbf{r}} \cdot [\boldsymbol{D}\,\nabla_{\mathbf{r}} u_n]\|^2_{L^2([0,T];L^2(U))}\\ &\quad\leq C(T)(\|\varrho_0\|^2_{H^1(U)} + (1+\|\varrho_0\|_{L^2(U)})\|\varrho_0\|_{L^2(U)})^{1/2}.\end{aligned}$$

Proof. Multiplying (7.9.3) by $-\nabla_{\mathbf{r}} \cdot [\boldsymbol{D}\,\nabla_{\mathbf{r}} u_n]$, integrating over U and using the divergence theorem and the boundary condition $\Xi[\varrho]\cdot\mathbf{n} = 0$ on $\partial_U \times [0,T]$ one obtains

$$\begin{aligned}&\tfrac{1}{2}\frac{\mathrm{d}}{\mathrm{d}t}\|\boldsymbol{D}^{1/2}\nabla_{\mathbf{r}} u_n(t)\|^2_{L^2(U)} + \|\nabla_{\mathbf{r}} \cdot [\boldsymbol{D}\,\nabla_{\mathbf{r}} u_n(t)]\|^2_{L^2(U)}\\ &\quad\leq \int \mathrm{d}\mathbf{r}\,|\nabla_{\mathbf{r}} \cdot [\boldsymbol{D}\,\nabla_{\mathbf{r}} u_n]\nabla_{\mathbf{r}} \cdot [u_n\,\boldsymbol{D}\,\nabla_{\mathbf{r}}(\kappa_1 V_1 + \kappa_2 V_2 \star u_{n-1})]|.\end{aligned} \tag{7.9.8}$$

Now by using the product rule and Young's inequality twice, we have

$$\begin{aligned}&\int \mathrm{d}\mathbf{r}\,|\nabla_{\mathbf{r}} \cdot [\boldsymbol{D}\,\nabla_{\mathbf{r}} u_n]\nabla_{\mathbf{r}} \cdot [u_n\,\boldsymbol{D}\,\nabla_{\mathbf{r}}(\kappa_1 V_1 + \kappa_2 V_2 \star u_{n-1})]|\\ &\leq \tfrac{1}{2}\|\nabla_{\mathbf{r}} \cdot [\boldsymbol{D}\,\nabla_{\mathbf{r}} u_n]\|^2_{L^2(U)} + \|\nabla_{\mathbf{r}} u_n \cdot \boldsymbol{D}\,(\kappa_1 \nabla_{\mathbf{r}} V_1 + \kappa_2 \nabla_{\mathbf{r}} V_2 \star u_{n-1})\|^2_{L^2(U)}\\ &\quad + \|u_n \nabla_{\mathbf{r}} \cdot (\boldsymbol{D}\,(\kappa_1 \nabla_{\mathbf{r}} V_1(\mathbf{r}) + \kappa_2 \nabla_{\mathbf{r}} V_2 \star u_{n-1}))\|^2_{L^2(U)}\end{aligned}$$

From the Sobolev inequality, for any $u \in H^1(U)$ with $2 < d$

$$\|u\|_{L^\infty(U)} \leq C\|u\|_{H^1(U)}$$

for some constant C depending only on d and U. Assuming $d \geq 3$ we may bound the terms on the right hand side by

$$\begin{aligned}&\|\nabla_{\mathbf{r}} u_n \cdot \boldsymbol{D}\,(\kappa_1 \nabla_{\mathbf{r}} V_1(\mathbf{r}) + \kappa_2 \nabla_{\mathbf{r}} V_2 \star u_{n-1})\|^2_{L^2(U)}\\ &\quad + \|u_n \nabla_{\mathbf{r}} \cdot (\boldsymbol{D}\,(\kappa_1 \nabla_{\mathbf{r}} V_1 + \kappa_2 \nabla_{\mathbf{r}} V_2 \star u_{n-1}))\|^2_{L^2(U)}\\ &\qquad\leq C_1\|\nabla_{\mathbf{r}} u_n(t)\|^2_{L^2(U)} + C_2\|u_n\|^2_{L^\infty(U)}(1 + \|u_{n-1}\|^2_{L^2(U)}\|\nabla_{\mathbf{r}} V_2\|^2_{L^\infty(U)})\\ &\qquad\leq C_1\|\nabla_{\mathbf{r}} u_n(t)\|^2_{L^2(U)} + C_2\|u_n\|^2_{H^1(U)}(1 + \|u_{n-1}\|^2_{L^2(U)})\\ &\qquad\leq C_1\|\nabla_{\mathbf{r}} u_n(t)\|^2_{L^2(U)} + C_2\|u_n\|^2_{H^1(U)}(1 + \|\varrho_0\|^2_{L^2(U)})\end{aligned}$$

for some appropriately redefined constants C_1, C_2. Note that and we have bounded $\|u_{n-1}\|^2_{L^2(U)}$ by the initial data ϱ_0, for example using (7.9.6) at the $n-1$ level.

Now by combining with (7.9.8) we have

$$\begin{aligned}&\tfrac{1}{2}\frac{\mathrm{d}}{\mathrm{d}t}\|\boldsymbol{D}^{1/2}\nabla_{\mathbf{r}} u_n(t)\|^2_{L^2(U)} + \tfrac{1}{2}\|\nabla_{\mathbf{r}} \cdot [\boldsymbol{D}\,\nabla_{\mathbf{r}} u_n]\|^2_{L^2(U)}\\ &\quad\leq C_1\|\nabla_{\mathbf{r}} u_n(t)\|^2_{L^2(U)} + C_2\|u_n\|^2_{H^1(U)}(1 + \|\varrho_0\|^2_{L^2(U)}).\end{aligned}$$

Integrating over $t \in [0,T]$ we obtain

$$\begin{aligned}&\tfrac{1}{2}\sup_{0\leq t\leq T}\|\boldsymbol{D}^{1/2}\nabla_{\mathbf{r}} u_n(t)\|^2_{L^2(U)} + \tfrac{1}{2}\|\nabla_{\mathbf{r}} \cdot [\boldsymbol{D}\,\nabla_{\mathbf{r}} u_n]\|^2_{L^2([0,T];L^2(U))}\\ &\quad\leq \|\boldsymbol{D}^{1/2}\|^2_{L^\infty}\|\nabla_{\mathbf{r}} u_n(0)\|^2_{L^2(U)}\\ &\qquad + C(T)\left(\|u_n(t)\|^2_{L^2([0,T];H^1(U))} + (1 + \|\varrho_0\|^2_{L^2(U)})\|u_n\|^2_{L^2([0,T];H^1(U))}\right)\end{aligned}$$

where the first term on the right hand side is the constant of integration and the constant $C(T)$

depends on U and T. By applying the estimates of Proposition 7.9.4 we obtain

$$\begin{aligned}&\tfrac{1}{2}\sup_{0\leq t\leq T}\|\boldsymbol{D}^{1/2}\nabla_{\mathbf{r}}u_n(t)\|^2_{L^2(U)}+\tfrac{1}{2}\|\nabla_{\mathbf{r}}\cdot[\boldsymbol{D}\,\nabla_{\mathbf{r}}u_n]\|^2_{L^2([0,T];L^2(U))}\\&\quad\leq C(T)(\|\varrho_0\|^2_{H^1(U)}+(1+\|\varrho_0\|_{L^2(U)})\|\varrho_0\|_{L^2(U)})\end{aligned}$$

and the lemma is proved. □

We now have strong convergence of $(u_n)_{n=1}^{\infty}$, by showing it is a Cauchy sequence in a complete metric space.

Lemma 7.9.6 ($\{u_n\}_{n=1}^{\infty}$ is a Cauchy sequence)**.** *Let $T>0$ and suppose $\{u_n\}_{n\geq 1}$ satisfies* (7.9.3) *with $\varrho_0\in C^{\infty}(U)$. Then there exists $\varrho\in L^1([0,T];L^1(U))$ such that $u_n\to\varrho$ in $L^1([0,T];L^1(U))$.*

Proof. Let $\phi_n:=u_n-u_{n-1}$ for $n\geq 2$ then ϕ_n satisfies

$$\begin{aligned}\partial_t\phi_n-\nabla_{\mathbf{r}}\cdot[\boldsymbol{D}\,\nabla_{\mathbf{r}}\phi_n]&=\kappa_1\nabla_{\mathbf{r}}\cdot[\phi_n\boldsymbol{D}\,\nabla_{\mathbf{r}}V_1]\\&\quad+\kappa_2\nabla_{\mathbf{r}}\cdot[\phi_n\boldsymbol{D}\,\nabla_{\mathbf{r}}(V_2\star u_{n-1})]+\kappa_2\nabla_{\mathbf{r}}\cdot[u_{n-1}\boldsymbol{D}\,\nabla_{\mathbf{r}}(V_2\star\phi_{n-1})]\end{aligned}\tag{7.9.9}$$

subject to $\Xi[\phi_n]\cdot\mathbf{n}=0$ on $\partial_U\times[0,T]$. By multiplying (7.9.9) by $\chi_\epsilon'(\phi_n)$ and integrating, using the divergence theorem and the boundary condition for ϕ_n one obtains

$$\begin{aligned}&\frac{\mathrm{d}}{\mathrm{d}t}\int\mathrm{d}\mathbf{r}\,\chi_\epsilon(\phi_n)+\|\,[\chi_\epsilon''(\phi_n)]^{1/2}\,\boldsymbol{D}^{1/2}\nabla_{\mathbf{r}}\phi_n\|^2_{L^2(U)}\\&\quad\leq\kappa_1\int\mathrm{d}\mathbf{r}\,|\chi_\epsilon''(\phi_n)\phi_n\,\nabla_{\mathbf{r}}\phi_n\cdot\boldsymbol{D}\,\nabla_{\mathbf{r}}V_1|\\&\qquad+\kappa_2\int\mathrm{d}\mathbf{r}\,|\chi_\epsilon''(\phi_n)\nabla_{\mathbf{r}}\phi_n\cdot[\phi_n\boldsymbol{D}\,\nabla_{\mathbf{r}}(V_2\star u_{n-1})]|\\&\qquad+\kappa_2\int\mathrm{d}\mathbf{r}\,|\chi_\epsilon'(\phi_n)\nabla_{\mathbf{r}}\cdot[u_{n-1}\boldsymbol{D}\,\nabla_{\mathbf{r}}(V_2\star\phi_{n-1})]|.\end{aligned}\tag{7.9.10}$$

Now we may bound each of the terms on the right hand side, firstly, using Young's inequality,

$$\begin{aligned}&\kappa_1\int\mathrm{d}\mathbf{r}\,|\chi_\epsilon''(\phi_n)\phi_n\,\nabla_{\mathbf{r}}\phi_n\cdot\boldsymbol{D}\,\nabla_{\mathbf{r}}V_1|\\&\quad=\kappa_1\int\mathrm{d}\mathbf{r}\,|[\chi_\epsilon''(\phi_n)]^{1/2}\boldsymbol{D}^{1/2}\nabla_{\mathbf{r}}\phi_n\cdot\phi_n\,[\chi_\epsilon''(\phi_n)]^{1/2}\boldsymbol{D}^{1/2}\,\nabla_{\mathbf{r}}V_1|\\&\quad\leq\tfrac{1}{2}\|\,[\chi_\epsilon''(\phi_n)]^{1/2}\,\boldsymbol{D}^{1/2}\nabla_{\mathbf{r}}\phi_n\|^2_{L^2(U)}+\tfrac{\kappa_1^2}{2}\int\mathrm{d}\mathbf{r}\,|\phi_n\,[\chi_\epsilon''(\phi_n)]^{1/2}\boldsymbol{D}^{1/2}\,\nabla_{\mathbf{r}}V_1|^2.\end{aligned}\tag{7.9.11}$$

Now note that, by definition of χ, one has the estimate

$$\begin{aligned}&\tfrac{\kappa_1^2}{2}\int\mathrm{d}\mathbf{r}\,|\phi_n\,[\chi_\epsilon''(\phi_n)]^{1/2}\boldsymbol{D}^{1/2}\,\nabla_{\mathbf{r}}V_1|^2\leq\|\\&\quad\leq\mu_{\max}\tfrac{\kappa_1^2}{2}\|\nabla_{\mathbf{r}}V_1\|^2_{L^\infty(U)}\Big(\int\mathrm{d}\mathbf{r}\,\phi_n^2\chi_\epsilon''(\phi_n)\mathbb{I}_{\{|\phi_n|>\epsilon\}}+\int\mathrm{d}\mathbf{r}\,\phi_n^2\chi_\epsilon''(\phi_n)\mathbb{I}_{\{|\phi_n|\leq\epsilon\}}\Big)\leq C_3\epsilon\end{aligned}\tag{7.9.12}$$

where C_3 depends U, κ_1 and $\|\nabla_{\mathbf{r}}V_1\|^2_{L^\infty(U)}$.

Secondly, again using Young's inequality,

$$\begin{aligned}&\kappa_2\int\mathrm{d}\mathbf{r}\,|\chi_\epsilon''(\phi_n)\phi_n\,\nabla_{\mathbf{r}}\phi_n\cdot\boldsymbol{D}\,\nabla_{\mathbf{r}}V_2\star u_{n-1}|\\&\quad=\kappa_2\int\mathrm{d}\mathbf{r}\,|[\chi_\epsilon''(\phi_n)]^{1/2}\boldsymbol{D}^{1/2}\nabla_{\mathbf{r}}\phi_n\cdot\phi_n\,[\chi_\epsilon''(\phi_n)]^{1/2}\boldsymbol{D}^{1/2}\,\nabla_{\mathbf{r}}V_2\star u_{n-1}|\\&\quad\leq\tfrac{1}{2}\|[\chi_\epsilon''(\phi_n)]^{1/2}\boldsymbol{D}^{1/2}\nabla_{\mathbf{r}}\phi_n\|^2_{L^2(U)}+\tfrac{\kappa_2^2}{2}\int\mathrm{d}\mathbf{r}\,|\phi_n\,[\chi_\epsilon''(\phi_n)]^{1/2}\boldsymbol{D}^{1/2}\,\nabla_{\mathbf{r}}V_2\star u_{n-1}|^2\end{aligned}\tag{7.9.13}$$

where the second term on the final line is $O(\epsilon)$ by similar argument to (7.9.12).

Thirdly

$$\kappa_2 \int \mathrm{d}\mathbf{r}\, |\chi_\epsilon'(\phi_n)\nabla_{\mathbf{r}} \cdot [u_{n-1}\boldsymbol{D}\,\nabla_{\mathbf{r}}(V_2 \star \phi_{n-1})]| \\ \leq \kappa_2 \|\chi_\epsilon'(\phi_n)\|_{L^\infty(U)} \int \mathrm{d}\mathbf{r}\, |\nabla_{\mathbf{r}} \cdot [u_{n-1}\boldsymbol{D}\,\nabla_{\mathbf{r}}(V_2 \star \phi_{n-1})]|.$$

By elementary differentiation and the definition of $\chi_\epsilon$we have that $|\chi_\epsilon'(\cdot)| \leq C_4$ for some constant dependent on U. All that remains is to bound $\int \mathrm{d}\mathbf{r}\, |\nabla_{\mathbf{r}} \cdot [u_{n-1}\boldsymbol{D}\,\nabla_{\mathbf{r}}(V_2 \star \phi_{n-1})]|$ in terms of $\|\phi_{n-1}\|_{L^1(U)}$ and the initial data ϱ_0. To do this we expand the gradient inside the integral and split up the absolute value as follows

$$\int \mathrm{d}\mathbf{r}\, |\nabla_{\mathbf{r}} \cdot [u_{n-1}\boldsymbol{D}\,\nabla_{\mathbf{r}}(V_2 \star \phi_{n-1})]| \\ \leq \int \mathrm{d}\mathbf{r}\, |\nabla_{\mathbf{r}} u_{n-1} \cdot \boldsymbol{D}\nabla_{\mathbf{r}} V_2 \star \phi_n| + \int \mathrm{d}\mathbf{r}\, |u_{n-1}\nabla_{\mathbf{r}} \cdot (\boldsymbol{D}\nabla_{\mathbf{r}} V_2 \star \phi_n)|.$$

Continuing using Hölder's inequality and that $\|f\|_{L^2(U)} \leq \|f\|_{L^\infty(U)}|U|^{1/2}$, we obtain

$$\int \mathrm{d}\mathbf{r}\, |\nabla_{\mathbf{r}} u_{n-1} \cdot \boldsymbol{D}\nabla_{\mathbf{r}} V_2 \star \phi_n| + \int \mathrm{d}\mathbf{r}\, |u_{n-1}\nabla_{\mathbf{r}} \cdot (\boldsymbol{D}\nabla_{\mathbf{r}} V_2 \star \phi_n)| \\ \leq \|\boldsymbol{D}\nabla_{\mathbf{r}} V_2 \star \phi_{n-1}\|_{L^\infty(U)} \times |U|^{1/2} \times \|\nabla_{\mathbf{r}} u_{n-1}\|_{L^2(U)} \\ + \|\nabla_{\mathbf{r}} \cdot (\boldsymbol{D}\nabla_{\mathbf{r}} V_2 \star \phi_{n-1})\|_{L^\infty(U)} \times |U|^{1/2} \times \|u_{n-1}\|_{L^2(U)}.$$

The primary coefficients may be bounded as follows

$$\|\boldsymbol{D}\nabla_{\mathbf{r}} V_2 \star \phi_{n-1}\|_{L^\infty(U)} \leq \mu_{\max} \|\nabla_{\mathbf{r}} V_2\|_{L^\infty(U)} \|\phi_{n-1}\|_{L^1(U)},$$

$$\|\nabla_{\mathbf{r}} \cdot (\boldsymbol{D}\nabla_{\mathbf{r}} V_2 \star \phi_{n-1})\|_{L^\infty(U)} \\ \leq (\|\nabla_{\mathbf{r}} \cdot \boldsymbol{D}\|_{L^\infty(U)} \|\nabla_{\mathbf{r}} V_2\|_{L^\infty(U)} + \|\boldsymbol{D} : \nabla_{\mathbf{r}}\nabla_{\mathbf{r}} V_2\|_{L^\infty(U)}) \|\phi_{n-1}\|_{L^1(U)}$$

Since $\boldsymbol{D} \in W^{1,\infty}$ and $V_2 \in W^{2,\infty}$ the right hand side is finite. All in all we may write

$$\kappa_2 \int \mathrm{d}\mathbf{r}\, |\chi_\epsilon'(\phi_n)\nabla_{\mathbf{r}} \cdot [u_{n-1}\boldsymbol{D}\,\nabla_{\mathbf{r}}(V_2 \star \phi_{n-1})]| \\ \leq 2C_5(\|u_{n-1}\|_{L^2(U)} + \|\nabla_{\mathbf{r}} u_{n-1}\|_{L^2(U)}) \|\phi_{n-1}\|_{L^1(U)}$$

for a constant

$$C_5 := |U|^{1/2} \max\left\{\mu_{\max}\|\nabla_{\mathbf{r}} V_2\|_{L^\infty(U)}, \|\nabla_{\mathbf{r}} \cdot \boldsymbol{D}\|_{L^\infty(U)} \|\nabla_{\mathbf{r}} V_2\|_{L^\infty(U)} + \|\boldsymbol{D} : \nabla_{\mathbf{r}}\nabla_{\mathbf{r}} V_2\|_{L^\infty(U)}\right\}.$$

Additionally one has, from the definition of the H^1 norm and Young's inequality,

$$\|u_{n-1}\|_{L^2(U)} + \|\nabla_{\mathbf{r}} u_{n-1}\|_{L^2(U)} \leq \sqrt{2}\|u_{n-1}\|_{H^1(U)}$$

giving

$$\kappa_2 \int \mathrm{d}\mathbf{r}\, |\chi_\epsilon'(\phi_n)\nabla_{\mathbf{r}} \cdot [u_{n-1}\boldsymbol{D}\,\nabla_{\mathbf{r}}(V_2 \star \phi_{n-1})]| \leq 2\sqrt{2}C_5|U|\|u_{n-1}\|_{H^1(U)}\|\phi_{n-1}\|_{L^1(U)}. \quad (7.9.14)$$

All together from (7.9.10), (7.9.11), (7.9.12), (7.9.13), (7.9.14), Proposition 7.9.5, and by letting $\epsilon \to 0$, we obtain

$$\frac{\mathrm{d}}{\mathrm{d}t}\|\phi_n\|_{L^1(U)} \leq \alpha(\varrho_0; 2, T)\|\phi_{n-1}\|_{L^1(U)}$$

where $\alpha(\varrho_0;2,T) := C_6(T)(\|\varrho_0\|^2_{H^1(U)} + (1+\|\varrho_0\|_{L^2(U)})\|\varrho_0\|_{L^2(U)})^{1/2}$ for a constant C_6 depending on C_5 and U.

By the usual argument we now show the sequence $\{\|\phi_n(t)\|_{L^1(U)}\}_{n\geq 1}$ tends to zero in appropriate norm. Define the partial sum

$$\Phi^N(t) := \sum_{n=2}^{N} \|\phi_n(t)\|_{L^1(U)}$$

Then applying Corollary 7.9.3 we obtain

$$\begin{aligned}\frac{\mathrm{d}}{\mathrm{d}t}\Phi(t) &\leq \alpha(\varrho_0;2,T)(\|\Phi_N(t)\|_{L^1(U)} + \|\phi_1(t)\|_{L^1(U)} - \|\phi_N(t)\|_{L^1(U)}) \\ &\leq \alpha(\varrho_0;2,T)(\|\Phi_N(t)\|_{L^1(U)} + 4)\end{aligned}$$

Applying Grönwall's lemma we obtain (noting that $\Phi_N(0) \equiv 0$)

$$\Phi_N(t) \leq 4T\alpha(\varrho_0;2,T)e^{\alpha(\varrho_0;1,T)T}.$$

Thus we have determined a uniform over N bound on the monotone increasing sequence $\{\Phi_N(t)\}_{N\geq 2}$ and therefore the limit $\Phi_N(t) \nearrow \Phi_\infty(t)$ must exist pointwise for $t \in [0,T]$. By elementary application of the monotone convergence theorem

$$\int_0^T \mathrm{d}t\, \Phi_N(t) \to \int_0^T \mathrm{d}t\, \Phi_\infty(t)$$

so that $\Phi_N(t) \to \Phi_\infty(t)$ in $L^1([0,T];L^1(U))$, thus $\phi_n(t) \to 0$ in $L^1([0,T];L^1(U))$ and therefore u_n is a Cauchy sequence in $L^1([0,T];L^1(U))$ (which is complete) hence there exists $u \in L^1([0,T];L^1(U))$ such that $u_n \to u$ strongly. □

Lastly we have the uniform estimate on the limit point $\varrho(\mathbf{r},t)$ in terms of the initial data ϱ_0.

Lemma 7.9.7. *One has $\varrho \in L^2([0,T];H^1(U)) \cap L^\infty([0,T];L^2(U))$ and that $\partial_t\varrho \in L^2([0,T];H^{-1}(U))$ with the uniform bound*

$$\|\varrho\|_{L^\infty([0,T];L^2(U))} + \|\varrho\|_{L^2([0,T];H^1(U))} + \|\partial_t\varrho\|_{L^2([0,T];H^{-1}(U))} \leq C(T)\|\varrho_0\|_{L^2(U)}. \tag{7.9.15}$$

Additionally there exists a subsequence $\{u_{n_k}\}_{k\geq 1}$ such that

$$u_{n_k} \rightharpoonup \varrho \quad \text{in } L^2([0,T];H^1(U)), \tag{7.9.16}$$

$$\partial_t u_{n_k} \rightharpoonup \partial_t\varrho \quad \text{in } L^2([0,T];H^{-1}(U)). \tag{7.9.17}$$

where $\rightharpoonup$ denotes weak convergence.

Proof. From Proposition 7.9.4 we have the uniform bound

$$\|u_n\|_{L^\infty([0,T];L^2(U))} + \|u_n\|_{L^2([0,T];H^1(U))} \leq C\|\varrho_0\|_{L^2(U)}.$$

Now observe that we may rewrite the parabolic equation for u_n as

$$\partial_t u_n = \nabla_{\mathbf{r}} \cdot [\boldsymbol{D}\nabla_{\mathbf{r}} u_n + u_n\, \boldsymbol{D}\, \nabla_{\mathbf{r}}(\kappa_1 V_1 + \kappa_2 V_2 \star u_{n-1})]\,.$$

Now by taking the inner product with $v \in H^1(U)$, using the divergence theorem and the boundary condition $\Xi[u_n]\cdot\mathbf{n}$ on $\partial U \times [0,T]$, and Hölder's inequality

$$\int \mathrm{d}\mathbf{r}\, \partial_t u_n\, v \leq \left\{\int \mathrm{d}\mathbf{r}\, |\boldsymbol{D}\,\nabla_{\mathbf{r}} u_n + u_n\, \boldsymbol{D}\,\nabla_{\mathbf{r}}(\kappa_1 V_1 + \kappa_2\, V_2 \star u_{n-1})|^2\right\}^{1/2} \times \left\{\int \mathrm{d}\mathbf{r}|\nabla_{\mathbf{r}} v|^2\right\}^{1/2}.$$

Now taking the supremum over $v \in H^1(U)$ with $\|v\|_{H^1(U)} \leq 1$ we obtain on the left hand side the definition of the $H^{-1}(U)$ norm (see [52]) and by integrating over $[0,T]$ we find

$$\sup_{\substack{v\in H^1(U),\\ \|v\|_{H^1(U)}\leq 1}} \Big| \int \mathrm{d}\mathbf{r}\, \partial_t u_n\, v(\mathbf{r})\Big| \equiv \|\partial_t u_n\|^2_{L^2([0,T];H^{-1}(U))}$$
$$\leq \int_0^T \mathrm{d}t\, \|\boldsymbol{D}\nabla_{\mathbf{r}} u_n + u_n \boldsymbol{D}\,\nabla_{\mathbf{r}}(\kappa_1 V_1 + \kappa_2\, V_2 \star u_{n-1})\|^2_{L^2(U)}.$$

By Young's inequality, it follows that

$$\|\partial_t u_n\|^2_{L^2([0,T];H^{-1}(U))} \leq 2\int_0^T \mathrm{d}t\, \|\boldsymbol{D}\,\nabla_{\mathbf{r}}(\kappa_1 V_1 + \kappa_2\, V_2 \star u_{n-1})\|^2_{L^\infty(U)} \|u_n(t)\|^2_{L^2(U)}$$
$$+ 2\int_0^T \mathrm{d}t\, \|\boldsymbol{D}\,\nabla_{\mathbf{r}} u_n\|^2_{L^2(U)} \leq C(T)\|\varrho_0\|^2_{L^2(U)} \tag{7.9.18}$$

for some constant $C(T)$ and where we have used the bounds (7.9.6), (7.9.7). Together (7.9.4) and (7.9.18) give

$$\|u_n\|_{L^\infty([0,T];L^2(U))} + \|u_n\|_{L^2([0,T];H^1(U))} + \|\partial_t u_n\|_{L^2([0,T];H^{-1}(U))} \leq C(T)\|\varrho_0\|_{L^2(U)}.$$

and since each term on the left hand side of this inequality is positive for all n each must be independently finite in the limit $n \to \infty$. Combining this with Eberlein-Smuljan theorem we may extract a weakly convergent subsequence $\varrho_{n_k} \rightharpoonup \varrho$ in the senses (7.9.16), (7.9.17). Thus the lemma is proved. □

The nature of convergence of the sequence $\{\varrho_n\}_{n\geq 1}$ as $n \to \infty$ are consolidated into the following result.

Corollary 7.9.8. *There exists a subsequence $\{u_{n_k}\}_{k\geq 1} \subset \{u_n\}_{n\geq 1}$ and a function $\varrho \in L^2([0,T];H^1(U))$ with $\partial_t \varrho \in L^2([0,T];H^{-1}(U))$ such that*

$$u_n \to \varrho \quad \text{in } L^1([0,T];L^1(U)),$$
$$u_{n_k} \rightharpoonup \varrho \quad \text{(weakly) in } L^2([0,T];H^1(U)),$$
$$\partial_t u_{n_k} \rightharpoonup \partial_t \varrho \quad \text{(weakly) in } L^2([0,T];H^{-1}(U)).$$

We are now in the position to obtain the existence and uniqueness of weak solutions $\varrho(\mathbf{r},t)$. First we state a calculus result which will be useful when working with the weak formulation (7.2.8).

Lemma 7.9.9. *Suppose $\varrho \in L^2([0,T];H^1(U))$ and $\partial_t \varrho \in L^2([0,T];H^{-1}(U))$ then the mapping*

$$t \to \|\varrho(t)\|^2_{L^2(U)}$$

is absolutely continuous with

$$\frac{\mathrm{d}}{\mathrm{d}t}\|\varrho(t)\|^2_{L^2(U)} = 2\langle \partial_t \varrho(t),\, \varrho(t)\rangle$$

for a.e. $t \in [0,T]$.

Proof. Since the condition $\Pi[\varrho]\cdot\mathbf{n} = 0$ on $\partial U \times [0,T]$ guarantees integration by parts without extra terms the proof is identical to the textbook one [52]. □

We are now in the position to prove existence of the weak solution to (7.2.3).

7.9.3 Existence And Uniqueness.

By using Propositions 7.9.4, 7.9.5 and Lemmas 7.9.6, 7.9.7, 7.9.9 we may obtain the following theorem.

Theorem 7.9.10. *(Existence and Uniqueness of Weak Density)*
Let $\varrho_0 \in C^\infty(U)$, $\varrho \geq 0$ and $\int_U \mathrm{d}\mathbf{r}\varrho_0(\mathbf{r}) = 1$. Then there exists a unique weak solution $\varrho \in L^\infty([0,T];L^2(U)) \cap L^2([0,T];H^1(U))$, with $\partial_t \varrho \in L^2([0,T];H^{-1}(U))$, to equation (7.2.3) in the sense (7.2.8) with the estimate (7.9.15).

Proof. Multiply (7.9.3) by $\eta \in L^2([0,T];H^1(U))$ after setting $n = n_k \in \mathbb{N}$ and integrate over U_T to obtain

$$\int_0^T \mathrm{d}t\,\langle \partial_t u_{n_k},\, \eta(t)\rangle + \int_0^T \mathrm{d}t\,\int_U \mathrm{d}\mathbf{r}\,\nabla_{\mathbf{r}}\eta \cdot \boldsymbol{D}\,[\nabla_{\mathbf{r}} u_{n_k} + u_{n_k}\nabla_{\mathbf{r}}(\kappa_1 V_1 + \kappa_2\, V_2 \star u_{n_k-1})] = 0.$$

For the transport term we write

$$\begin{aligned}
&\int_0^T \mathrm{d}t\,\nabla_{\mathbf{r}}\eta \cdot u_{n_k}\boldsymbol{D}\,\nabla_{\mathbf{r}}[\kappa_1 V_1 + \kappa_2\, V_2 \star u_{n_k-1}]\\
&= \int_0^T \mathrm{d}t\,\nabla_{\mathbf{r}}\eta \cdot\, (u_{n_k} - \varrho)\boldsymbol{D}\,\nabla_{\mathbf{r}}[\kappa_1 V_1 + \kappa_2\, V_2 \star u_{n_k-1}]\\
&\quad + \int_0^T \mathrm{d}t\,\nabla_{\mathbf{r}}\eta \cdot\, \varrho\boldsymbol{D}\,\nabla_{\mathbf{r}}[\kappa_1 V_1 + \kappa_2\, V_2 \star (u_{n_k-1} - \varrho)] + \int_0^T \mathrm{d}t\,\nabla_{\mathbf{r}}\eta \cdot\, \varrho\boldsymbol{D}\,\nabla_{\mathbf{r}}\kappa_2\, V_2 \star \varrho.
\end{aligned}$$

Note that $u_{n_k} \rightharpoonup \varrho$ in $L^2([0,T];H^1(U)) \subset L^2([0,T];L^2(U))$ and $(\nabla_{\mathbf{r}} \cdot \boldsymbol{D}) \cdot \nabla_{\mathbf{r}}[\kappa_1 V_1(\mathbf{r}) + \kappa_2\, V_2 \star (\varrho_{n_k-1})]$ is uniformly bounded and so

$$\int_0^T \mathrm{d}t\,\int_U \mathrm{d}\mathbf{r}\,\nabla_{\mathbf{r}}^T\eta\,(\varrho_{n_k} - \varrho)\boldsymbol{D}\,\nabla_{\mathbf{r}}[\kappa_1 V_1 + \kappa_2\, V_2 \star \varrho_{n_k-1}] \to 0$$

as $k \to \infty$.

Now by Hölder's inequality one has

$$\begin{aligned}
&\int_0^T \mathrm{d}t\,\nabla_{\mathbf{r}}\eta \cdot\, \varrho\,\boldsymbol{D}\,\nabla_{\mathbf{r}}\kappa_2(V_2 \star (u_{n_k-1} - \varrho)) \leq \mu_{\max}\|\nabla_{\mathbf{r}}\eta\|_{L^2([0,T];L^2(U))}\|\nabla_{\mathbf{r}} V_2\|_{L^\infty(U)}\\
&\quad \times \left(\int_0^T \mathrm{d}t\,\|u_{n_k-1}(t) - \varrho(t)\|_{L^1(U)}^2\right)^{1/2} \to 0.
\end{aligned}$$

Now note that by Lemma 7.9.6, $\|\phi_n\|_{L^1(U)}$ is bounded and therefore

$$\int_0^T \mathrm{d}t\|u_{n_k-1}(t) - \varrho(t)\|_{L^1(U)}^2 \leq C\int_0^T \mathrm{d}t\|u_{n_k-1}(t) - \varrho(t)\|_{L^1([0,T];L^1(U))} \to 0.$$

Therefore we have

$$\int_0^T \mathrm{d}t\,\nabla_{\mathbf{r}}\eta\,\cdot\, u_{n_k}\boldsymbol{D}\,\nabla_{\mathbf{r}}[\kappa_1 V_1 + \kappa_2\, V_2 \star u_{n_k-1}] \to \int_0^T \mathrm{d}t\,\nabla_{\mathbf{r}}\eta \cdot \varrho\boldsymbol{D}\,\nabla_{\mathbf{r}}[\kappa_1 V_1 + \kappa_2\, V_2 \star \varrho]$$

as $k \to \infty$. By the weak convergence results of Lemma 7.9.7 we have

$$\begin{aligned}
\int_0^T \mathrm{d}t\,\langle \partial_t u_{n_k},\, u_{n_k}\rangle &\to \int_0^T \mathrm{d}t\,\langle \partial_t \varrho,\, \varrho\rangle,\\
\int_0^T \mathrm{d}t\,\int_U \mathrm{d}\mathbf{r}\,\nabla_{\mathbf{r}}\eta \cdot \boldsymbol{D}\,\nabla_{\mathbf{r}} u_{n_k} &\to \int_0^T \mathrm{d}t\,\int_U \mathrm{d}\mathbf{r}\,\nabla_{\mathbf{r}}\eta \cdot \boldsymbol{D}\,\nabla_{\mathbf{r}}\varrho
\end{aligned}$$

as $k \to \infty$. This establishes existence of weak solution to (7.2.2) in the sense (7.2.8). Estab-

lishing $\varrho(0) = \varrho_0$ is a routine argument (see [52]).

To prove uniqueness we set $\xi = \varrho_1 - \varrho_2$ where ϱ_1, ϱ_2 are weak solutions then we have

$$\int_0^T \mathrm{d}t\, \langle \partial_t \xi(t),\, \eta(t)\rangle + \int_0^T \mathrm{d}t \int_U \mathrm{d}\mathbf{r}\, \nabla_{\mathbf{r}}\eta \cdot \boldsymbol{D}\left[\nabla_{\mathbf{r}}\xi + \xi\, \nabla_{\mathbf{r}}\kappa_1 V_1 + \kappa_2 \varrho_1 \nabla_{\mathbf{r}} V_2 \star \varrho_1 - \kappa_2 \varrho_1 \nabla_{\mathbf{r}} V_2 \star \varrho_2\right] = 0$$

Adding and subtracting $\int_0^T \mathrm{d}t \int_U \mathrm{d}\mathbf{r}'\, \nabla_{\mathbf{r}}\eta \cdot \kappa_1 \varrho_2 \nabla_{\mathbf{r}} V_2 \star \varrho_1$ we find

$$\begin{aligned}
&\int_0^T \mathrm{d}t\, \langle \partial_t \xi(t),\, \eta(t)\rangle + \int_0^T \mathrm{d}t \int_U \mathrm{d}\mathbf{r}\, \nabla_{\mathbf{r}}\eta \cdot \boldsymbol{D}\, \nabla_{\mathbf{r}}\xi \\
&\quad = -\int_0^T \mathrm{d}t \int_U \mathrm{d}\mathbf{r}\, \nabla_{\mathbf{r}}\eta \cdot \boldsymbol{D}\left[\xi\, \nabla_{\mathbf{r}}\kappa_1 V_1 + \kappa_2 \xi \nabla_{\mathbf{r}} V_2 \star \varrho_1 - \kappa_2 \varrho_2 \nabla_{\mathbf{r}} V_2 \star \xi\right] \\
&\quad \le \int_0^T \mathrm{d}t \int_U \mathrm{d}\mathbf{r}\, |\nabla_{\mathbf{r}}\eta \cdot \boldsymbol{D}^{1/2}\boldsymbol{D}^{1/2}\left[\xi\, \nabla_{\mathbf{r}}\kappa_1 V_1 + \kappa_2 \xi \nabla_{\mathbf{r}} V_2 \star \varrho_1 - \kappa_2 \varrho_2 \nabla_{\mathbf{r}} V_2 \star \xi\right]|.
\end{aligned}$$

By Young's inequality we have

$$\begin{aligned}
&\int_0^T \mathrm{d}t \int_U \mathrm{d}\mathbf{r}\, |\nabla_{\mathbf{r}}\eta \cdot \boldsymbol{D}^{1/2}\boldsymbol{D}^{1/2}\left[\xi\, \nabla_{\mathbf{r}}\kappa_1 V_1 + \kappa_2 \xi \nabla_{\mathbf{r}} V_2 \star \varrho_1 - \kappa_2 \varrho_2 \nabla_{\mathbf{r}} V_2 \star \xi\right]| \\
&\quad \le \int_0^T \mathrm{d}t \int_U \mathrm{d}\mathbf{r}\, |\boldsymbol{D}^{1/2}\nabla_{\mathbf{r}}\eta|^2 \\
&\qquad + \tfrac{1}{4}\int_0^T \mathrm{d}t \int_U \mathrm{d}\mathbf{r}\, |\boldsymbol{D}^{1/2}[\xi\, \nabla_{\mathbf{r}}\kappa_1 V_1 + \kappa_2 \xi \nabla_{\mathbf{r}} V_2 \star \varrho_1 - \kappa_2 \varrho_2 \nabla_{\mathbf{r}} V_2 \star \xi]|^2.
\end{aligned}$$

Using the triangle inequality and Young's inequality we expand the absolute value inside the integral

$$\begin{aligned}
&\tfrac{1}{4}\int_0^T \mathrm{d}t \int_U \mathrm{d}\mathbf{r}\, |\boldsymbol{D}^{1/2}[\xi\, \nabla_{\mathbf{r}}\kappa_1 V_1 + \kappa_2 \xi \nabla_{\mathbf{r}} V_2 \star \varrho_1 - \kappa_2 \varrho_2 \nabla_{\mathbf{r}} V_2 \star \xi]|^2 \\
&\quad \le \tfrac{1}{4}\int_0^T \mathrm{d}t \int_U \mathrm{d}\mathbf{r}\, |\boldsymbol{D}^{1/2}\xi\, \nabla_{\mathbf{r}}\kappa_1 V_1|^2 + \kappa_2^2 |\boldsymbol{D}^{1/2}[\xi \nabla_{\mathbf{r}} V_2 \star \varrho_1 - \varrho_2 \nabla_{\mathbf{r}} V_2 \star \xi]|^2 \\
&\quad \le \tfrac{1}{4}\int_0^T \mathrm{d}t \int_U \mathrm{d}\mathbf{r}\, \Big(|\boldsymbol{D}^{1/2}\xi\, \nabla_{\mathbf{r}}\kappa_1 V_1|^2 + 2\kappa_2^2 |\boldsymbol{D}^{1/2}\xi \nabla_{\mathbf{r}} V_2 \star \varrho_1|^2 + 2\kappa_2^2 |\boldsymbol{D}^{1/2}\varrho_2 \nabla_{\mathbf{r}} V_2 \star \xi|^2\Big) \\
&\quad \le \tfrac{\mu_{\max}}{4}\int_0^T \mathrm{d}t \int_U \mathrm{d}\mathbf{r}\, |\xi\, \nabla_{\mathbf{r}}\kappa_1 V_1|^2 + 2\kappa_2^2 |\xi \nabla_{\mathbf{r}} V_2 \star \varrho_1|^2 + 2\kappa_2^2 |\varrho_2 \nabla_{\mathbf{r}} V_2 \star \xi|^2. \qquad (7.9.19)
\end{aligned}$$

Estimating each of these terms, first

$$\int_0^T \mathrm{d}t \int_U \mathrm{d}\mathbf{r}\, |\xi\, \nabla_{\mathbf{r}}\kappa_1 V_1|^2 \le \kappa_1^2 \|\nabla_{\mathbf{r}} V_1\|^2_{L^\infty(U)} \|\xi\|_{L^2([0,T];L^2(U))}. \qquad (7.9.20)$$

Second,

$$2\kappa_2^2 \int_0^T \mathrm{d}t \int_U \mathrm{d}\mathbf{r}\, |\xi \nabla_{\mathbf{r}} V_2 \star \varrho_1|^2 \le 2\kappa_2^2 |U| \|\nabla_{\mathbf{r}} V_2\|^2_{L^\infty(U)} \|\xi\|_{L^2([0,T];L^2(U))}, \qquad (7.9.21)$$

and third

$$2\kappa_2^2 \int_0^T \mathrm{d}t \int_U \mathrm{d}\mathbf{r}\, |\varrho_2 \nabla_{\mathbf{r}} V_2 \star \xi|^2 \le 2\kappa_2^2 |U| \|\varrho_2\|_{L^\infty([0,T];L^2(U))} \|\nabla_{\mathbf{r}} V_2\|^2_{L^\infty(U)} \|\xi\|_{L^2([0,T];L^2(U))}.$$

Combining (7.9.3), (7.9.19), (7.9.20), (7.9.21), (7.9.3) we obtain, after setting $\eta = \xi$, and

using boundedness of ϱ_2 in terms of its initial data

$$\int_0^T \mathrm{d}t\, \langle \partial_t \xi(t),\, \xi(t) \rangle \leq (C_1(T) + C_2(T) \|\varrho_0\|^2_{L^2(U)}) \|\xi\|^2_{L^2([0,T];L^2(U))}$$

for some constants $C_1(T)$, $C_2(T)$ dependent on U. This holds for all T so it must be the case that

$$\frac{\mathrm{d}}{\mathrm{d}t} \|\xi(t)\|^2_{L^2(U)} \leq (C_1(T) + C_2(T) \|\varrho_0\|^2_{L^2(U)}) \|\xi(t)\|^2_{L^2(U)}$$

implying by Grönwall's lemma that

$$\|\xi(t)\|_{L^2(U)} \leq (C_1(T) + C_2(T) \|\varrho_0\|^2_{L^2(U)}) \|\xi(0)\|_{L^2(U)}$$

a.e. $t \in [0, T]$. However, $\xi(0) \equiv 0$ hence $\|\varrho_1(t) - \varrho_2(t)\|^2_L(U) = 0$ for all $t \in [0, T]$. □

7.9.4 Strict Positivity Of ϱ.

With the existence of weak solutions we may establish positivity of ϱ solving (7.2.3) with reference to [17]. In particular since $\boldsymbol{D}$ is positive definite and $\mathbf{b}$ is uniformly bounded and

$$\sup_{\mathbf{r} \in U} \varrho(\mathbf{r}, t_1) < C \inf_{\mathbf{r} \in U} \varrho(\mathbf{r}, t_2)$$

for $0 < t_1 < t_2 < \infty$ and C is a constant depending on d (the dimension) and $\mu_{\max}$. Since ϱ is nonnegative for all time we must have $\inf_{\mathbf{r} \in U} \varrho(\mathbf{r}, t)$ is positive and hence ϱ is positive.

7.10 Classical Linear Parabolic PDE

The first goal is to derive a similar set of estimates as [33, Lemma 3.5, Lemma 3.7]. The standard argument is to set up a sequence of linear parabolic PDEs. Let U be a bounded and open subset of $\mathbb{R}^d$ and set $U_T = U \times (0, T]$ for some time $T > 0$. Now consider the linear parabolic equation

$$\partial_t u_n - \nabla_{\mathbf{r}} \cdot [\boldsymbol{D} \nabla_{\mathbf{r}} u_n] = \nabla_{\mathbf{r}} \cdot [u_n \, \boldsymbol{D} \nabla_{\mathbf{r}} (\kappa_1 V_1 + \kappa_2 V_2 \star u_{n-1})]. \tag{7.10.1}$$

In general d dimensions we are in the divergence form of the parabolic PDE

$$\begin{cases} \partial_t u_n + L u_n = 0 & \text{in } U_T, \\ \Xi[u_n] \cdot \mathbf{n} = 0 & \text{on } \partial U \times [0, T], \\ u_n = \varrho_0 & \text{on } U \times \{t = 0\} \end{cases}$$

where ∂U is a C^1 boundary with unit normal $\mathbf{n}$. We define L to be the linear differential operator given by

$$\begin{aligned} L u_n &:= -\sum_{ij=1}^{d} \partial_{r_j} (\boldsymbol{D}_{ij}(\mathbf{r}, t) \partial_{r_i} u_n) + \sum_{i=1}^{d} b_i(\mathbf{r}) \partial_{r_i} u_n + c(\mathbf{r}) u_n, \\ \mathbf{b}(\mathbf{r}) &:= -\boldsymbol{D}(\mathbf{r}, t) \nabla_{\mathbf{r}} (\kappa_1 V_1(\mathbf{r}) + \kappa_2 [V_2 \star u_{n-1}]), \\ c(\mathbf{r}) &:= -\nabla_{\mathbf{r}} \cdot (\boldsymbol{D}(\mathbf{r}, t) \nabla_{\mathbf{r}} (\kappa_1 V_1(\mathbf{r}) + \kappa_2 [V_2 \star u_{n-1}]), \\ \Xi[u_n] &:= \boldsymbol{D}(\mathbf{r}, t) \left(\nabla_{\mathbf{r}} u_n + u_n \, \nabla_{\mathbf{r}} (\kappa_1 V_1(\mathbf{r}, t) + \kappa_2 \, V_2 \star u_{n-1}) \right). \end{aligned}$$

Since $\boldsymbol{D}(\mathbf{r}, t)$ is assumed to positive definite, there exists θ for every $\mathbf{r}$, ξ such that $\xi^T D(\mathbf{r}, t) \xi \geq \theta |\xi|^2$, therefore the operator $\partial_t + L$ is uniformly parabolic. The Sobolev space of functions that permit the no-flux condition $\Xi[u_n] \cdot \mathbf{n}$ on $\partial U \times [0, T]$ is $H^1(U)$ which is reflexive, so that $\partial_t u$ interpreted as a bounded linear functional can be paired to an element in $H^1(U)$, and further

by the Riez-Representation theorem there exists a unique element from $H^1(U)$ for the pairing. Additionally $H^1(U)$ is separable so that the (unique) weak solution may be approximated by a sequence of smooth functions coming from a countably dense subset.

7.10.1 Weak Formulation.

Equation (7.10.1) may be recast into weak form. We first introduce the bilinear operator, defined by

$$B[u,v;t] := \int_U \mathrm{d}\mathbf{r}\, \nabla_{\mathbf{r}} v \cdot \boldsymbol{D}\, \nabla_{\mathbf{r}} u + \int_U \mathrm{d}\mathbf{r}\, \mathbf{b}(\mathbf{r}) \cdot \nabla_{\mathbf{r}} u\, v + \int_U \mathrm{d}\mathbf{r}\, c(\mathbf{r}) u\, v$$

for $u, v \in H^1(U)$ and a.e. $0 \le t \le T$. We regard u as a mapping $[\mathfrak{u}(t)](\mathbf{r}) := u(\mathbf{r},t)$ from the time interval $[0,T]$ to the function space $H^1(U)$. Now fixing $v \in H^1(U)$ we multiply by v and integrate by parts to obtain the weak formulation

$$(\partial_t \mathfrak{u},\, v) + B[\mathfrak{u},\, v; t] = 0 \tag{7.10.2}$$

for each $0 \le t \le T$ with $(\ ,\ )$ denoting inner product in $L^2(U)$.

We introduce the notation

$$\partial_t u = g^0 + \sum_{j=1}^{d} \partial_{r_j} g^j, \quad g^0 := -\mathbf{b}(\cdot)\cdot\nabla_{\mathbf{r}} u - c(\cdot)u, \quad g^j := \sum_{i=1}^{d} \boldsymbol{D}_{ij}(\mathbf{r})\partial_{r_i} u. \tag{7.10.3}$$

Observe that the right hand side of (7.10.3) lies in the dual space $H^{-1}(U)$. The usual characterisation of H^{-1} as a dual to H_0^1 (see for example [52]) carries over to the present analysis, since multiplying (7.10.1) by a test function v and using the divergence theorem with the condition $\Xi[u]\cdot\mathbf{n} = 0$ on $\partial U \times [0,T]$ produces no boundary terms. By definition of the H^{-1} norm we have

$$\begin{aligned}\|\partial_t u\|_{H^{-1}} &= \Big\| g^0 + \sum_{j=1}^{d} \partial_{r_j} g^j \Big\|_{H^{-1}} \le \Big[\int_U \sum_{j=0}^{d} |g^j|^2 \Big]^{1/2} \\ &= \Big[\sum_{j=0}^{d} \|g^j\|^2_{L^2(U)} \Big]^{1/2} \le \|g^0\|_{L^2(U)} + \sum_{j=1}^{d} \|g^j\|_{L^2(U)}\end{aligned}$$

where we have used, on the last line, $\sum_{j=0}^{d} a_j^2 \le (\sum_{j=0}^{d} a_j)^2$ for all $a_j > 0$, $j = 1, \cdots, d$. Now by Cauchy-Schwartz inequality on g^j, assumptions on $\boldsymbol{D}$, and the regularity of the coefficients $\mathbf{b}(\cdot)$ and $c(\cdot)$ we have

$$\|\partial_t u\|_{H^{-1}} \le c_2 \|u\|_{H^1(U)}$$

for some appropriately defined constant c_2. Since the left hand side is bounded in terms of u in the chosen Sobolev space $(H^1(U))$ it is reasonable to seek solutions $\partial_t \mathfrak{u} \in H^{-1}(U)$ for a.e. $0 \le t \le T$ and we identify the pairing $(\partial_t \mathfrak{u},\, \phi) = \langle \partial_t \mathfrak{u},\, \phi \rangle$. We now define what it will mean for a solution to (7.10.1) to be a weak solution.

Definition 7.10.1 (Weak Solution)**.** *We say a function* $\mathfrak{u} \in L^2\big([0,T]; H^1(U)\big)$ *with* $\partial_t \mathfrak{u} \in L^2\big([0,T]; H^{-1}(U)\big)$ *is a weak solution of the initial-boundary value problem* (7.10.1) *provided*

$$\langle \mathfrak{u}',\, v\rangle + B[\mathfrak{u},\, v; t] = 0 \tag{7.10.4}$$

for each $v \in H^1(U)$*, a.e.* $0 \le t \le T$ *and* $u(\mathbf{r}, 0) = u_0$*.*

7.10.2 Galerkin Approximation

Now in the usual way we build weak solutions by constructing a solution as a finite dimensional approximation to u before passing to the limit. Assuming $\boldsymbol{D}_{ij}(\cdot)$ is a compact and symmetric

operator then the eigenfunctions satisfying

$$-\nabla_{\mathbf{r}} \cdot (\boldsymbol{D}(\mathbf{r})\nabla_{\mathbf{r}} w_k) = \alpha_k w_k$$

for some $\alpha_k \in \mathbb{R}$ form an orthonormal basis of $L^2(U)$ with $w_k \in H^1(U)$. Fixing m we look for a function $\mathfrak{u}^m : [0,T] \to H^1(U)$ of the form

$$\mathfrak{u}^m(t) := \sum_{k=1}^{m} d_m^k(t) w_k$$

where $d_m^k(0) = (u_0, w_k)$ for $k = 1, ..., m$ and

$$(\partial_t \mathfrak{u}^m,\, w_k) + B[\mathfrak{u}^m,\, w_k; t] = 0. \tag{7.10.5}$$

Thus (7.10.5) represents the projection of (7.10.4) onto the finite dimensional subspace spanned by $\{w_k\}_{k=1}^m$. The standard existence theory of ODEs gives existence of weak solutions in the sense (7.10.5). In particular by differentiating with respect to t we have $(\partial_t \mathfrak{u}_n^m, w_k) = \frac{\mathrm{d}}{\mathrm{d}t} d_m^k(t)$, and by orthogonality of the w_k one obtains

$$\frac{\mathrm{d}}{\mathrm{d}t} d_m^k(t) + \sum_{l=1}^{m} B[w_l, w_k; t] d_m^l(t) = 0. \tag{7.10.6}$$

Assuming the Carathéodory conditions with the Cauchy–Picard theorem there exists a unique absolutely continuous function $\mathbf{d}_m(t) = [d_m^1(t), ..., d_m^m(t)]^\top$ satisfying the ODE (7.10.6) for a.e. $0 \le t \le T$. Thus $\mathfrak{u}^m(t)$ solves (7.10.5) uniquely in the same sense.

7.10.3 Energy Estimates

The finite dimensional approximation, or Galerkin method, implies by construction (by writing $\mathfrak{u}^m$ expanded in the basis w_k with coefficients d_m^k)

$$(\partial_t \mathfrak{u}^m,\, \mathfrak{u}^m) + B[\mathfrak{u}^m,\, \mathfrak{u}^m; t] = 0 \tag{7.10.7}$$

for a.e. $0 \le t \le T$. We now require uniform energy estimates on $\mathfrak{u}^m$ given by the following lemma.

Lemma 7.10.2. *With the assumptions on $\boldsymbol{D}_{ij}(\cdot)$, $\mathbf{b}(\cdot)$ and $c(\cdot)$ there is the uniform energy estimate*

$$\begin{aligned} &\max_{0\le t\le T} \|\mathfrak{u}^m(t)\|_{L^2(U)} + \|\mathfrak{u}^m\|_{L^2([0,T];H^1(U))} \\ &+ \|\frac{\partial}{\partial t}\mathfrak{u}^m\|_{L^2([0,T];H^{-1}(U))} \le c_6 \|u_0\|_{L^2(U)} + c. \end{aligned}$$

where c_6, c are constants dependent on T and U.

Proof. Using u, v as arbitrary functions for a moment, it is readily seen that

$$\begin{aligned} |B[u,v]| &\le c_3 \int_U \mathrm{d}\mathbf{r} \left[|\nabla_{\mathbf{r}} u \| \nabla_{\mathbf{r}} v| + |\nabla_{\mathbf{r}} u \| v| + |u\| v| \right] \\ &\le c_3 (\|\nabla_{\mathbf{r}} u\|_{L^2(U)} + \|u\|_{L^2(U)})(\|\nabla_{\mathbf{r}} v\|_{L^2(U)} + \|v\|_{L^2(U)}) \\ &\le 2c_3 \|u\|_{H^1(U)} \|v\|_{H^1(U)}. \end{aligned}$$

To see this, first use the Cauchy-Schwarz inequality to bound the inner product terms within B. Then note that choosing

$$c_3 = \max\{\mu_{max}, \|\boldsymbol{b}\|_{L^\infty(U)}, \|c \\ |_{L^\infty(U)}\}$$

allows us to remove the explicit dependence on $\boldsymbol{D}$, $\boldsymbol{b}$ and c. The second inequality follows by using Hölder's inequality on each of the terms and adding a non-negative term. For the last line we us the generalised Young's inequality $(a+b)(c+d) \leq 2(a^2+b^2)^{1/2}(c^2+d^2)^{1/2}$ with $a = \|\nabla_{\mathbf{r}} u\|_{L^2(U)}$, $b = \|u\|_{L^2(U)}$, $c = \|\nabla_{\mathbf{r}} v\|_{L^2(U)}$ and $d = \|v\|_{L^2(U)}$. Secondly, using positive definiteness of $\boldsymbol{D}(\cdot)$ with $\mu_{min}\|\mathbf{v}\|_{L^2}^2 \leq \|\boldsymbol{D}^{1/2}\mathbf{v}\|_{L^2(U)}^2$ for every $\mathbf{v} \in L^2(U)$, we have

$$\begin{aligned}\mu_{min}\int_U \mathrm{d}\mathbf{r}\,|\nabla_{\mathbf{r}} u|^2 &\leq \int_U \mathrm{d}\mathbf{r}\,\sum_{ij=1}^{d} \boldsymbol{D}_{ij}(\mathbf{r})\partial_{r_i} u\,\partial_{r_j} u \\ &= B[u,u] - \int_U \mathrm{d}\mathbf{r}\,[\boldsymbol{b}(\mathbf{r})\cdot\nabla u\, u - c(\mathbf{r})|u|^2] \\ &\leq B[u,u] + \|\boldsymbol{b}\|_{L^\infty(U)}\int_U \mathrm{d}\mathbf{r}\,|\nabla_{\mathbf{r}} u\|u| + \|c\|_{L^\infty(U)}\int_U \mathrm{d}\mathbf{r}\,|u|^2.\end{aligned}$$

Then by Hölder's and Young's inequality with $\epsilon = \frac{\mu_{min}}{2}\|\boldsymbol{b}\|_{L^\infty(U)}^{-1} > 0$ we have

$$\int_U \mathrm{d}\mathbf{r}\,|\nabla_{\mathbf{r}} u\|u| \leq \epsilon\int_U \mathrm{d}\mathbf{r}\,|\nabla_{\mathbf{r}} u|^2 + \tfrac{1}{4\epsilon}\int_U \mathrm{d}\mathbf{r}\,|u|^2$$

so that (7.10.3) becomes

$$\tfrac{\mu_{min}}{2}\int_U \mathrm{d}\mathbf{r}\,|\nabla_{\mathbf{r}} u|^2 \leq B[u,u] + c_4\|u\|_{L^2(U)}^2 \tag{7.10.8}$$

for some constant c_4.

Now since $u \in H^1(U)$ and $\Xi[u]\cdot\mathbf{n} = 0$ on $\partial U \times [0,T]$, the mass of the system is conserved so that

$$(u)_{U_T} = \tfrac{1}{|U_T|}\int \mathrm{d}\mathbf{r}\,u(\mathbf{r},t) = c$$

where $U_T = U \times [0,T]$ for some $c \in \mathbb{R}$ independent of time. Therefore by Poincaré's inequality and (7.10.8) we have the estimate $c_5\|u-c\|_{L^2(U)}^2 \leq B[u,u] + c_6\|u\|_{L^2(U)}^2$ for some appropriate constants c_5 and c_6. Applied to the finite dimensional approximation we have Calculus gives $(\partial_t \mathfrak{u}^m,\, \mathfrak{u}^m) = \frac{1}{2}\frac{\mathrm{d}}{\mathrm{d}t}(\|\mathfrak{u}^m\|_{L^2(U)}^2)$ and so with (7.10.7) and (7.10.13) one obtains the differential inequality (after redefining constants)

$$\frac{\mathrm{d}}{\mathrm{d}t}(\|\mathfrak{u}^m\|_{L^2(U)}^2) + 2c_5\|\mathfrak{u}^m - c\|_{H^1(U)}^2 \leq c_6\|\mathfrak{u}^m\|_{L^2(U)}^2 \tag{7.10.9}$$

implying

$$\frac{\mathrm{d}}{\mathrm{d}t}(\|\mathfrak{u}^m\|_{L^2(U)}^2) \leq c_6\|\mathfrak{u}^m\|_{L^2(U)}^2.$$

Now one is in the form to apply Grönwall's lemma on the nonnegative absolutely continuous function $\|\mathfrak{u}^m(t)\|_{L^2(U)}^2$ giving the bound

$$\|\mathfrak{u}^m(t)\|_{L^2(U)}^2 \leq e^{c_6 t}\|\mathfrak{u}^m(0)\|_{L^2(U)}^2.$$

Note that $\|\mathfrak{u}^m(0)\|_{L^2(U)}^2 \leq \|\mathfrak{u}_0\|_{L^2(U)}^2$ by definition of $d_m^k(0)$. Taking the maximum over $0 \leq t \leq T$ of this inequality we obtain

$$\max_{0\leq t\leq T}\|\mathfrak{u}^m(t)\|_{L^2(U)}^2 \leq e^{c_6 T}\|\mathfrak{u}(0)\|_{L^2(U)}^2. \tag{7.10.10}$$

Integrating (7.10.9) from 0 to T and using (7.10.10) one finds (with the triangle inequality)

$$\|\mathfrak{u}^m\|_{L^2([0,T];H^1(U))}^2 - \|c\|_{L^2([0,T];H^1(U))}^2 \leq c_7\|u_0\|_{L^2(U)}^2$$

where c_7 depends on T. Rearranging this inequality we find

$$\|\mathfrak{u}^m\|^2_{L^2([0,T];H^1(U))} \leq c_7\|u_0\|^2_{L^2(U)} + c \tag{7.10.11}$$

for a positive constant c now depending on U and T. This inequality establishes how $\mathfrak{u}^m$, not necessarily zero on the boundary of U, nor periodic, may be bounded in $L^2([0,T];H^1(U))$.

All that remains is to estimate the time derivative $\dot{\mathfrak{u}}^m$. Since $\dot{\mathfrak{u}}^m$ is written as a finite linear combination of basis functions in the subspace spanned by w_k, the characterisation as supremum over $\langle\,,\,\rangle$ may be used. In particular take an arbitrary $v \in H^1(U)$ such that $\|v\|_{H^1(U)} \leq 1$ and $v = v_1 + v_2$ for $v_1 \in \text{span}\{w_k\}_{k=1}^m$ and $(v_2, w_k) = 0$ for every $k = 1, ..., m$. Then trivially $\|v_1\|_{H^1(U)} \leq 1$ by the way that v was chosen and one has the equation

$$(\partial_t\mathfrak{u}^m,\, v_1) + B[\mathfrak{u}^m,\, v_1; t] = 0$$

by (7.10.7) for a.e. $0 \leq t \leq T$. Therefore the H^{-1} inner product gives the relation $\langle\partial_t\mathfrak{u}^m, v\rangle = (\partial_t\mathfrak{u}^m, v) = (\partial_t\mathfrak{u}^m, v_1) = -B[\mathfrak{u}^m,\, v_1; t]$ and by the triangle inequality, taking the supremum over all v (to use the definition of $\|\cdot\|_{H^{-1}}$ [52]) and using (7.10.3) one obtains

$$\|\partial_t\mathfrak{u}^m(t)\|_{H^{-1}} \leq c_7\|\mathfrak{u}^m\|_{H^1(U)} \tag{7.10.12}$$

for a redefined constant c_7. Using this, and (7.10.11), (7.10.12) becomes

$$\|\partial_t\mathfrak{u}^m\|_{L^2([0,T];H^{-1}(U))} \leq \|u_0\|^2_{L^2(U)} + c.$$

for a new constant c depending on U and T. Therefore upon redefining appropriate constants we obtain the uniform estimate. □

$$\int_0^T \mathrm{d}t \int \mathrm{d}\mathbf{r}\, \partial_t\varrho\, \eta + \int_0^T \mathrm{d}t \int \mathrm{d}\mathbf{r}\, \nabla_{\mathbf{r}}\eta \cdot D(\mathbf{r})\nabla_{\mathbf{r}}\varrho$$
$$+\kappa\int_0^T \mathrm{d}t \int \mathrm{d}\mathbf{r}\, \nabla_{\mathbf{r}}(D(\mathbf{r})\,\nabla_{\mathbf{r}}\eta) \cdot [\varrho\,\nabla_{\mathbf{r}}(V_1(\mathbf{r}) + [V_2 \star (\varrho \times g)](\mathbf{r}))] = 0$$

7.10.4 Existence.

The method to establish weak solution for the indexed problem is a textbook one. The method is described as follows. Fix n then the evolution equation (7.10.1) is a uniformly parabolic PDE for the unknown $u_n = u$. One now expands $\mathfrak{u} = \mathfrak{u}^m$ in a linear combination of m eigenvectors of the operator $-\nabla_{\mathbf{r}} \cdot (\boldsymbol{D}(\mathbf{r})\nabla_{\mathbf{r}}w_k)$ for finite dimensional approximation to u. Since $\boldsymbol{D}_{ij}(\cdot)$ is a compact and symmetric operator then the eigenfunctions w_k form an orthonormal basis of $L^2(U)$ with $w_k \in H^1(U)$. Thus $\mathfrak{u}^m$ is projected onto the finite dimensional subspace spanned by $\{w_k\}_{k=1}^m$. The standard existence theory of ODEs (the Carathéodory conditions with the Cauchy–Picard theorem) gives existence of weak solutions $\mathfrak{u}^m$ as expanded in the functions $\{w_k\}_{k=1}^m$ on a finite dimensional subspace of $H^1(U)$. All that remains is to pass to the limit $m \to \infty$ to realise the result in $H^1(U)$. To do this energy estimates are required on $\mathfrak{u}^m$, these are routine calculations except in the textbooks they are done for simpler boundary condition choices (homogeneous Dirichlet or periodic) and make use of Poincare's inequality (holding only for H^1_0 functions). The calculations are similar and for the present boundary condition choice, however a weaker result is used throughout, namely the Poincaré–Wirtinger inequality, to obtain

$$\max_{0\leq t\leq T}\|\mathfrak{u}^m(t)\|_{L^2(U)} + \|\mathfrak{u}^m\|_{L^2([0,T];H^1(U))}$$
$$+ \|\frac{\partial}{\partial t}\mathfrak{u}^m\|_{L^2([0,T];H^{-1}(U))} \leq c_1\|u_0\|_{L^2(U)} + c_2.$$

where c_1, c_2 are constants dependent on T and U and $\mu_{\min}, \mu_{\max}$. Note that the left hand side of (7.10.2) forms a bounded sequence in $\mathbb{R}$ and by the Bolzano–Weierstrass theorem there exists

a convergent subsequence $\{\mathfrak{u}^{m_l}\}_{l\geq 1} \subset \{\mathfrak{u}^m\}_{m\geq 1}$. In particular there exists $\mathfrak{u}$ such that

$$\begin{aligned} \mathfrak{u}^{m_l} &\rightharpoonup \mathfrak{u} \quad \text{weakly in } L^2([0,T];H^1(U)), \\ \partial_t \mathfrak{u}^{m_l} &\rightharpoonup \mathfrak{u}' \quad \text{weakly in } L^2([0,T];H^{-1}(U)). \end{aligned}$$

Note of course that $\mathfrak{u} = \mathfrak{u}_n$, but we have not yet established existence of weak solution to the full nonlinear Smoluchowski equation (7.2.3). This result establishes existence of weak solution for the parabolic equation (7.9.3) for every index n. Now since $L^2([0,T];H^1(U))$ is separable, and weak solutions currently only exist in a finite dimensional subspace of $H^1(U)$, it makes sense to choose a test function $\boldsymbol{\phi} \in C^1([0,T];H^1(U)) \subset L^2([0,T];H^1(U))$. We may therefore write

$$\int_0^T \mathrm{d}t\, \langle \partial_t \mathfrak{u}^m,\, \boldsymbol{\phi}^N \rangle + B[\mathfrak{u}^m,\, \boldsymbol{\phi}^N; t] = 0$$

for $\boldsymbol{\phi}^N = \sum_{k=1}^N d^k(t) w_k$. Making the choice $N \leq m$ and letting $N \to \infty$ one obtains

$$\int_0^T \mathrm{d}t\, \langle \partial_t \mathfrak{u},\, \boldsymbol{\phi}^\infty \rangle + B[\mathfrak{u},\, \boldsymbol{\phi}^\infty; t] = 0$$

for any function $\boldsymbol{\phi}^\infty \in L^2([0,T];H^1(U))$ since ϕ^N are dense in $L^2([0,T];H^1(U))$. Now since $\boldsymbol{\phi}^\infty$ is arbitrary we obtain

$$\langle \partial_t \mathfrak{u},\, \phi \rangle + B[\mathfrak{u},\, \phi; t] = 0$$

for an arbitrary $\phi \in H^1(U)$. Hence the criteria of weak solution is satisfied.

7.10.5 Uniqueness.

To show uniqueness we argue by contradiction that there exists two weak solutions solutions. By linearity, their difference $\boldsymbol{\chi}$ is a weak solution of (7.10.1) with $\chi_0 \equiv 0$, for χ_0 initial data. Then as it is a weak solution, we may test $\boldsymbol{\chi}$ against itself

$$\langle \partial_t \boldsymbol{\chi},\, \boldsymbol{\chi} \rangle + B[\boldsymbol{\chi},\, \boldsymbol{\chi}; t] \equiv 0$$

giving

$$\tfrac{1}{2} \frac{\mathrm{d}}{\mathrm{d}t} (\|\boldsymbol{\chi}(t)\|^2_{L^2(U)}) + B[\boldsymbol{\chi},\, \boldsymbol{\chi}; t] = 0$$

but $B[\boldsymbol{\chi},\, \boldsymbol{\chi}; t] \geq -c_7 \|\boldsymbol{\chi}(t)\|^2_{L^2(U)}$ which may be obtained by the following estimate

$$c_5 \|\mathfrak{u}^m - c\|^2_{H^1(U)} \leq B[\mathfrak{u}^m, \mathfrak{u}^m] + c_6 \|\mathfrak{u}^m\|^2_{L^2(U)}. \tag{7.10.13}$$

and hence by Grönwall

$$\|\boldsymbol{\chi}(t)\|^2_{L^2(U)} \leq c_7(t) \|\chi_0\|^2_{L^2(U)} = 0$$

and $\boldsymbol{\chi} = 0$ for a.e. $\mathbf{r} \in U$ for every $0 \leq t \leq T$. We have established the existence and uniqueness of the weak solution to the linear parabolic equation (7.10.1) and may apply this to an iteration problem on (7.2.3).

Chapter 8

Conclusion

8.1 Dynamic Density Functional Theory

We have derived, from first principles, a general DDFT (2.6.1),(2.6.2) for systems of colloidal particles including inertial effects, inter-particle HI and externally driven solvents. This derivation required the usual assumptions, firstly that the adiabatic approximation that the higher order densities are equal to those of an steady system with the same one-body distribution, and we thus employ a newly derived sum rule for the steady flow, holding exactly at steady state. The second assumption that was made, was that the contributions from the part of the one-body distribution which are not captured by the local-steady approximation are neglected. Thirdly that the n–body distributions governing the HI terms are well approximated by functionals of ϱ and $\mathbf{v}$, by assuming the existence of the correlation function $g(\mathbf{r}_1, \mathbf{r}_2, [\varrho])$.

We have also shown our equations agree to previously considered DDFTs in various heuristic limits (see Section 2.7). For example, in the overdamped limit we recover the DDFTs [21], [145], [144]. We have also derived a novel Bernoulli principle for steadily driven systems.

There are many promising numerical applications for the theory formulated here, including the HI derived in Chapters 3, 4 in confining geometries, for which we have presented some preliminary experiments in Chapter 6. Such extensions would allow the study of many systems of physical interest including microfluidics such as in drug delivery models of nanoparticles in the circulatory system as well as comparison to direct numerical simulation techniques of rheological phenomena.

8.2 Microhydrodynamics

The formula obtained in spherical bipolar coordinates is uniformly accurate for all separations, up to the particle contact point where the governing equations break down. In Figure 3.4a, the **GMS**, Kim & Karrila and Jeffrey & Onishi curves differ substantially at surface separations equal to roughly 1 sphere radius; we therefore claim the spherical bipolar formalism would be particularly useful for simulations of colloidal flow with HI in the moderately-dense volume fraction regime. Additionally we expect our method to perform better for different particle radii as evidenced by Figure 3.4b, so the contributions of the present work go well into polydisperse particle systems.

We therefore expect that the derived formulae can be implemented in all numerical methods that incorporate the existing lubrication models and improve the simulation accuracy. We discuss, as examples, the potential application to and impact on a few different types of numerical methods.

For methods solving particle dynamics using Newtonian equations, e.g., the discrete element method (DEM), the new formulae can be used to directly compute the hydrodynamic forces. Instead of using the existing formulae ($F_{z,l}$) with an arbitrary outer cut off [124], implementing either the exact F_z^1 or the asymptotic F_z^e formulae could better capture the hydrodynamic interaction between $10^{-1}r_1$ and $10^0 r_1$, as seen in Figure 3.2a. This is expected to improve suspension viscosity predictions, compared to using F_z, which underestimates the viscosity

especially at moderate concentrations [124]. Note however that by using F_z^* for DEM, one requires accurate knowledge of the position of a hard cutoff of the asymptotic expressions for the force, if such a cutoff exists at all.

Computational formalisms which use the closed asymptotic formula F_z in-line can be trivially updated with the new asymptotic formulae F_z^e, meaning the applications of the presented results may also extend more generally to, e.g., lattice Boltzmann method Nguyen and Ladd [125] and Stokesian dynamics (SD) Brady and Bossis [22]. SD takes into account singular lubrication interactions by making use of the explicit formulae F_z between pairs of close particles without considering the lubrication many-body effects, thus forgoing the large number of degrees of freedom required to resolve the lubrication flow of the interstitial fluid between particles. The missing many-body effects are considered in a more recent work [104] by decomposing the velocity field into a singular flow containing the short-range lubrication interactions and a remainder field which is regular and dealt with using a chosen fluid solver. Such methods may seek to use the present stream function ψ for the decomposition. Meanwhile new approaches [170] have been proposed to overcome unphysical results in pairwise lubrication models due the lost screening effects provided by neglected long-range HI. The present work can determine the deficit in lubrication beyond the critical interaction radius used in these methods.

Lastly, for continuum approaches such as dynamical density functional theory [61], the inclusion of long range HI has been shown to produce qualitatively different colloidal fluid flows compared to systems without HI. So far the physical phenomena included in the governing fluid equations has extended to: inertial colloids with long range HI (including models of $\boldsymbol{R}^{-1}$) [62] and without HI [7], systems of multiple-species [65] and particles with angular dependence [45]. Thus we expect natural numerical implementations of the present formulae to include lubrication interactions in the DDFT modelling formalism. In particular, for DDFT, since the terms corresponding to HI take the form of convolution integrals it is desirable to have explicit continuous integrands (and decay estimates) for the hydrodynamic interaction valid at all separations in order to ensure the convergence of these terms, which is what the current formalism provides.

Finally we remark that the rate of convergence of the force asymptoting to unity at infinity will depend on r_2/r_1, as seen in Figure 3.2b, and therefore we anticipate the novel study of bulk flow properties using the F_z^1, F_z^2 in the modelling of suspensions involving multiple species.

In this paper we have presented a new formula for the hydrodynamic force exerted on two converging spheres in viscous fluid in a functional form, as well as asymptotic formulae as the spheres are close, showing good agreement with the exact value even at centre to centre distances of $d = O(\sigma^0)$. By construction, the derivation of this functional form provides the way for consideration of alternative boundary conditions. For the asymptotic results, the small argument limit newly derived shows better agreement with the exact solution compared to that from existing lubrication theory. The sphere plane limit may also be recovered more accurately. Additionally, in Chapter 5, we have provided an analysis of the spectral properties of $\boldsymbol{R}$, demonstrating *numerically* that the scalar resistance functions as determined by spherical bipolar coordinates **GMS** preserves positivity in simple *regular* sphere systems, with $N = 2, 3$ and larger sphere numbers. Positivity is destroyed when using the perturbative functions of Kim & Karrila without an arbitrary cut-off, meanwhile cut-offs may drastically underestimate the lubrication effect, as demonstrated by a numerical application in DDFT. It would be an interesting topic of future work to investigate the generality of this positive definiteness.

Furthermore we have shown that the scalar resistance functions obtained by Jeffrey & Onishi, while preserving positivity in the examined systems, are inaccurate compared to **GMS** in inner regimes of flow (close particle surfaces) principally because they are based on multipole expansions which, intrinsic to the method, requires arbitrarily many terms as $h \to 0$, which for each $h > 0$, become more computationally expensive to obtain. This property is an important consideration for dense particle systems. It would be an interesting topic of future work to investigate the generality of the positive definiteness obtained in this paper.

There are many promising extensions which may naturally be made to the theory presented here such as: alternative boundary conditions to model slippery particles and the shearing motion of two spheres converging perpendicular to their line of centres akin to Goldman et al. [70]. The former is generally important in liquid spreading problems [36], in particular, molecular dynamics simulations of Newtonian liquids have shown that there exists a nonlinear relationship

between the amount of slip and the local shear rate of fluid at a solid surface[168].

8.3 Global Well Posedness & Equilibrium Behaviour

In this thesis, the global asymptotic stability and well-posedness of overdamped DDFT with two-body HI was studied. It was shown that bifurcations occur in DDFT systems with no-flux boundary conditions at an infinite and discrete set of critical energies equal to eigenvalues of the two-body interaction integral operator $\mathscr{R}$. Additionally we have shown that a weak solution to the density with no-flux boundary conditions and strong solution to the flux equation exist and are unique under sensible assumptions on the confining and interaction potentials and initial data V_1, V_2 and $\varrho(\mathbf{r}, 0)$ respectively. Assuming a classical solution to the DDFT we also derived *a priori* convergence estimates in L^2 and relative entropy.

Well-posedness and global asymptotic stability of the phase space equation for the time evolution of $f(\mathbf{r}, \mathbf{p}, t)$ remains open (see [63, Proposition 2.1] for the evolution equation for $f(\mathbf{r}, \mathbf{p}, t)$). It is of similar form to the Vlasov equation considered by [41] but with Hermite dissipative term and modified nonlocal term in the momentum variable $\mathbf{p}$ dependent on the HI tensors. To progress further some maximum principles on f solving the linearised version of the phase space equation must be found. Additionally, the existence results on the overdamped equations considered here may be made more regular by routine arguments.

We also note that the present analysis is based on the Smoluchowski equation rigorously derived from the phase space Fokker-Planck equation using homogenisation methods [63]. As an alternative to this, assuming inertia is small altogether, or if one is interested only in very short times to begin with, the system of interacting particles maybe considered solely in configuration space. Only the positions (and not the momenta) of a system of interacting Brownian particles are then taken into account with Smoluchowski equation as in [146], and, the underlying Langevin dynamics contain only velocity equations for each particle which are usually written down *a posteriori*. The justification for this is that the momentum distribution is assumed to have a minor role in the dynamical description of the fluid density, and indeed is taken to be irrelevant at the microscopic level. This Brownian approximation may also hold for highly dense suspensions, since in dense Newtonian systems there is a fast transfer of momentum and kinetic energy from the particle collisions, and this effect may be accounted for most efficiently by the bath in the Brownian dynamics with a non constant diffusion tensor.

It is known however that the one-body Smoluchowski equation in [146] does not equate to equations (7.1.2)-(7.1.3b) which are obtained in the rigorous overdamped limit starting from the Newtonian dynamics. Intuitively this is because the two-body assumption for the HI ($\boldsymbol{\Gamma}$) and mobility ($\boldsymbol{D}$) tensors and the matrix inversion $\boldsymbol{D} = \boldsymbol{\Gamma}^{-1}$ are not commutable operations; even if $\boldsymbol{D}$ is two body then $\det(\boldsymbol{D})$ is not. A flow chart demonstrating the permitted commutations between various formalisms is included in [63]. The nonequivalence of the two Smoluchowski equations is not considered here, and therefore a natural extension for future work would be to determine the existence, uniqueness and regularity of of the density starting from [146] as well as the corresponding conditions for linear stability.

Finally we remark that a bifurcation analysis of DDFT equations of the form (7.1.10) to include a hard-sphere contribution to the free energy by fundamental measure theory (FMT) e.g. Rosenfeld [148] or Roth [151] would be very interesting.

Appendices

Appendix A

Asymptotic Theory For Normal Interaction

A.1 Small & Large Argument Approximations

We divide this section into two cases: nondimensional separation going to zero and to infinity. First we identify a small parameter.

A.1.1 Small Parameter

Taking care that $\eta_2 < 0$, we have by the geometric properties of the bipolar coordinate system

$$r_1 \sinh\eta_1 + r_2 \sinh\eta_2 = 0, \qquad d = r_1 \cosh\eta_1 + r_2 \cosh\eta_2, \tag{A.1.1}$$

where d is the centre to centre distance of the spheres. The equations (A.1.1) constitute a coupled pair of transcendental equations in η_1, η_2. The determinant of the Jacobian associated to the system (A.1.1) is always positive because $\sinh(\eta_1 - \eta_2) > 0$ and, given d, r_1, and r_2, it may be solved using a Newton iteration scheme. In the case $r_1 = r_2$ we may find η_1 (and η_2) explicitly. As d approaches $r_1 + r_2$ one obtains

$$r_1\eta_1 + r_2\eta_2 \sim 0, \qquad d \sim r_1(1 + \tfrac{\eta_1^2}{2}) + r_2(1 + \tfrac{\eta_2^2}{2}).$$

Noting that $r_1 + h + r_2 = d$, the system may be solved with $\epsilon = \frac{\eta_1^2}{2}\frac{\beta+1}{\beta}$ where $\epsilon = h/r_1$ and $\beta = r_2/r_1$. Thus we see, with an abuse of notation, by setting $a = r_1$ and $b = r_2$ that the gap distance may be written in terms of the average of the radii: $a\epsilon = \eta_1^2(a+b)/2$. This illuminates the relationship between the present small parameter η_1 and the lubrication theory small parameter ϵ [90].

A.1.2 Small Argument Behaviour

We would like to examine the singular behaviour as spheres of unequal radii become arbitrarily close and we approach this limit from first principles. Firstly it will be seen that the limit $-\eta_2 \searrow 0 \swarrow \eta_1$ may not be commuted with the infinite series in (3.7.5),(3.7.6) because a divergent series is obtained. The infinite series does not possess sufficient dominated convergence in the small η_1 limit despite for physical reasons the limit being well posed (at least from the right $\eta_1 \searrow 0$). The singular limit of the infinite series is treated as a perturbation problem of Van Dyke type, whereby two series overlap in a shared regime of validity. We consider sphere 1 (a similar method may be applied to sphere 2) and nondimensionalise F_z^1 in (3.7.5) by the Stokes unit $[6\pi\mu U r_1]$. Let N be a large positive integer, then we write

$$F_z = F_s + F_r$$

with

$$\begin{aligned} F_s :=& \tfrac{\sinh\eta_1}{3\sqrt{2}} \sum_{n=1}^{N} (2n+1)(a_n+b_n+c_n+d_n), \\ F_r :=& \tfrac{\sinh\eta_1}{3\sqrt{2}} \sum_{n=N+1}^{\infty} (2n+1)(a_n+b_n+c_n+d_n). \end{aligned} \tag{A.1.2}$$

With this decomposition the difficulties arising in the limit $\eta_1 \to 0$ of F_z may be circumvented with proper control of the asymptotic parameter η_1, a summation index n and the introduction of an intermediate variable in a shared regime of validity for F_s and F_r. For the remaining calculations we set $\alpha = \eta_1$ which is small, and $\eta_2 = -\beta^{-1}\alpha$. We proceed to the rigorous limit $\alpha \to 0$ by proving the following two lemmas.

Lemma A.1.1. *The singular part F_s may be written in the form*

$$F_s = \tfrac{4\beta^3}{(1+\beta^2)}\alpha^{-2} + a(\beta)\log N + O(\alpha^{-2}N^{-2}) + O(\alpha^0)$$

for a known function $a(\beta)$.

Proof. Starting with F_s we expand for small α using expressions

$$\begin{aligned} \cosh x &= 1 + \tfrac{x^2}{2} + \tfrac{x^4}{24} + O(x^6), \\ \sinh x &= x + \tfrac{x^3}{6} + \tfrac{x^5}{120} + O(x^7) \end{aligned}$$

obtaining

$$F_s = \alpha^{-2}\mathfrak{f}_1 + \mathfrak{f}_2 + \alpha\mathfrak{f}_3 + O(\alpha^2) \tag{A.1.3}$$

where

$$\mathfrak{f}_1 = \frac{128\,\beta^3}{(1+\beta)^3} \sum_{n=1}^{N} \frac{n(n+1)}{(2n-1)^2(2n+1)(2n+3)^2},$$

$$\begin{aligned} \mathfrak{f}_2 = &\frac{32\,\beta}{15(1+\beta)^3} \sum_{n=1}^{N} \frac{n(n+1)(15+12n+12n^2)}{(2n-1)^2(2n+1)(2n+3)^2} + \frac{32\,\beta^2}{15(1+\beta)^3} \sum_{n=1}^{N} \frac{n(n+1)(-15+84n+84n^2)}{(2n-1)^2(2n+1)(2n+3)^2} \\ &+ \frac{32\,\beta^3}{15(1+\beta)^3} \sum_{n=1}^{N} \frac{n(n+1)(25+12n+12n^2)}{(2n-1)^2(2n+1)(2n+3)^2}, \end{aligned}$$

and

$$\mathfrak{f}_3 = -\frac{8(1+3\beta)}{3(1+\beta)^3} \sum_{n=1}^{N} \frac{n(n+1)}{(2n-1)(2n+3)}.$$

Consider $\mathfrak{f}_1$. We may explicitly sum $\mathfrak{f}_1$ by expressing its summand in partial fractions and telescoping resulting expression. In particular we have

$$\begin{aligned} &\sum_{n=1}^{N} \frac{n(n+1)}{(2n-1)^2(2n+1)(2n+3)^2} \\ &\quad= \sum_{n=1}^{N} \tfrac{1}{64}\left[\tfrac{1}{(2n-1)(2n+1)} - \tfrac{1}{(2n+1)(2n+3)}\right] + \tfrac{3}{128}\left[\tfrac{1}{(2n-1)^2} - \tfrac{1}{(2n+3)^3}\right] \\ &\quad= \tfrac{1}{64}\left[\tfrac{1}{3} - \tfrac{1}{(2N+1)(2N+3)}\right] + \tfrac{3}{128}\left[\tfrac{10}{9} - \tfrac{1}{(2N+1)^2} - \tfrac{1}{(2N+3)^2}\right]. \end{aligned}$$

Therefore we have

$$\mathfrak{f}_1 = \left[4 - \tfrac{2}{(2N+1)(2N+3)} - 3\left[\tfrac{1}{(2N+1)^2} + \tfrac{1}{(2N+3)^2}\right]\right]\tfrac{\beta^3}{(1+\beta)^3}$$

and $\mathfrak{f}_1 = \frac{4\beta^3}{(1+\beta)^3} - 2\frac{\beta^3}{(1+\beta)^3}N^{-2}$ as $N \to \infty$. Now consider f_2. Notice that $\mathfrak{f}_2$ may be rewritten into the form

$$\begin{aligned}\mathfrak{f}_2 = &\frac{32\,\beta}{15(1+\beta)^3}\sum_{n=1}^{N}\frac{n(n+1)(3(2n-1)(2n+3)+24)}{(2n-1)^2(2n+1)(2n+3)^2}\\ &+\frac{32\,\beta^2}{15(1+\beta)^3}\sum_{n=1}^{N}\frac{n(n+1)(21(2n-1)(2n+3)+48)}{(2n-1)^2(2n+1)(2n+3)^2}\\ &+\frac{32\,\beta^3}{15(1+\beta)^3}\sum_{n=1}^{N}\frac{n(n+1)(3(2n-1)(2n+3)+34)}{(2n-1)^2(2n+1)(2n+3)^2}.\end{aligned}$$

or further than this

$$\begin{aligned}\mathfrak{f}_2 = &\frac{3\cdot 32\,\beta}{15(1+\beta)^3}\sum_{n=1}^{N}\frac{n(n+1)((2n-1)(2n+3)+8)}{(2n-1)^2(2n+1)(2n+3)^2}\\ &+\frac{21\cdot 32\,\beta^2}{15(1+\beta)^3}\sum_{n=1}^{N}\frac{n(n+1)((2n-1)(2n+3)+8-\frac{120}{21})}{(2n-1)^2(2n+1)(2n+3)^2}\\ &+\frac{3\cdot 32\,\beta^3}{15(1+\beta)^3}\sum_{n=1}^{N}\frac{n(n+1)((2n-1)(2n+3)+8+\frac{10}{3})}{(2n-1)^2(2n+1)(2n+3)^2}.\end{aligned} \tag{A.1.4}$$

By use of the identity

$$\begin{aligned}&\frac{n(n+1)\left[(2n-1)(2n+3)+8\right]}{(2n-1)^2(2n+1)(2n+3)^2}\\ &\quad=\frac{3}{32(2n-1)}+\frac{1}{16(2n+1)}+\frac{3}{32(2n+3)}+\frac{8\,n(n+1)}{(2n-1)^2(2n+1)(2n+3)^2}\end{aligned} \tag{A.1.5}$$

we may sum (A.1.4) explicitly. Notice that the last term on the right hand side of (A.1.5) is repeated from contributions to $\mathfrak{f}_1$. Notice too that

$$\begin{aligned}\sum_{n=1}^{N}\frac{1}{2n+1} &= \sum_{n=1}^{N}\frac{1}{2n-1} - 1 + \frac{1}{2N+1},\\ \sum_{n=1}^{N}\frac{1}{2n+3} &= \sum_{n=1}^{N}\frac{1}{2n-1} - \frac{4}{3} + \frac{1}{2N+1} + \frac{1}{2N+3}.\end{aligned}$$

Thus all contributions to $\mathfrak{f}_2$ may be written in terms of $\sum_{n=1}^{N}(2n-1)^{-1}$ and $\mathfrak{f}_1$, the former of which may be dealt with by asymptotics of partial summation expressions of the natural logarithm.

Summing the identity (A.1.5) from $n=1$ to $n=N$ one obtains, by $\mathfrak{f}_1$

$$\begin{aligned}&\sum_{n=1}^{N}\frac{n(n+1)\left[(2n-1)(2n+3)+8\right]}{(2n-1)^2(2n+1)(2n+3)^2}\\ &\quad=\frac{1}{4}\sum_{n=1}^{N}\frac{1}{2n-1}-\frac{3}{16}+\frac{5}{32(2N+1)}+\frac{3}{32(2N+3)}+8\sum_{n=1}^{N}\frac{n(n+1)}{(2n-1)^2(2n+1)(2n+3)^2}.\end{aligned}$$

So that $\mathfrak{f}_2$ may be summed by use of $\mathfrak{f}_1$

$$\begin{aligned}\mathfrak{f}_2 = \tfrac{32}{15(1+\beta)^3}\left[3\beta + 21\beta^2 + 3\beta^3\right]\left[\frac{1}{4}\sum_{n=1}^{N}\tfrac{1}{2n-1} + \tfrac{1}{16} + O(N^{-1})\right] \\ + \tfrac{1}{15(1+\beta)^3}\left[-120\beta^2 + 10\beta^3 + O(N^{-2})\right]\end{aligned}$$

Now from asymptotic expansions for large argument of the polygamma function, for example [43]

$$\sum_{n=1}^{N}\frac{1}{2n-1} \sim \tfrac{1}{2}(\gamma + \log N) + \log 2 + \frac{1}{48\,N^2} + O(N^{-4})$$

as $N \to \infty$ where γ is the Euler-Masheroni constant. Thus we have

$$\mathfrak{f}_2 = \tfrac{4}{5(1+\beta)^3}\left[\beta + 7\beta^2 + \beta^3\right]\left[\gamma + \log N + 2\log 2 + \frac{1}{2}\right] + \tfrac{1}{15(1+\beta)^3}\left[-120\beta^2 + 10\beta^3\right] + O(N^{-1})$$

as $N \to \infty$.

Now consider $\mathfrak{f}_3$. By the identity

$$\frac{n(n+1)}{(2n-1)(2n+3)} = \frac{1}{4} + \frac{3}{16}\left[\frac{1}{2n-1} - \frac{1}{2n+3}\right]$$

summing between $n = 1$ and N and telescoping we obtain

$$\mathfrak{f}_3 = -\tfrac{8\beta^2(\beta+3)}{3(1+\beta)^3}\left[\tfrac{N}{4} + \tfrac{1}{16} + O(N^{-1})\right]$$

as $N \to \infty$. Now returning to (A.1.3) we have

$$\begin{aligned}F_s \sim \tfrac{4\beta^3}{(1+\beta)^3}\alpha^{-2} + a(\beta)\,\log N + b(\beta)\left[\gamma + \log 2 + c(\beta)\right] \\ + O(\alpha\,N) + O(N^{-1}) + O(\alpha^{-2}N^{-2}) + O(\alpha)\end{aligned}$$

for some rational functions of β $a(\cdot)$, $b(\cdot)$, $c(\cdot)$. For the singular part then all that remains is to order the error estimates. Returning to the decomposition (A.1.2) we observe that N is large and chosen such that in the shared regime of validity $N = O(\alpha^{-1})$ for the singular part and $N = O(\alpha^0)$ for the regular part, reminiscent of typical matching problems found in [78]. Since the former estimate holds for all $n \leq N$ we must have $N \to \infty$ as $\alpha \to 0$. We stress here that the integer N is arbitrary and must not appear in the final expression of F, but it is permissible that F_s and F_r may depend on N individually. Typical of matched asymptotic problems the index N is implicitly a function of α the natural choice being $N = \delta\alpha^{-(1-\theta)}$ for some $0 < \theta < 1$ and both δ, θ are independent of α, so certainly N may lie in the overlap regime and $N \to \infty$ as $\alpha \to 0$.

With N in terms of α in this way we have

$$N^{-1} = O(\alpha^{1-\theta}) = o(1)$$

since $0 < \theta < 1$. One also has

$$\alpha N = O(\alpha^{\theta}) = o(1).$$

Finally note that $O(\alpha)$ is higher than $o(1)$ with respect to α and may be neglected. Thus

$$F_s \sim \tfrac{4\beta^3}{(1+\beta)^3}\alpha^{-2} + \tfrac{4\beta(1+7\beta+\beta^2)}{5(1+\beta)^3}\left[\log N + \gamma + 2\log 2 + \tfrac{1}{2}\right] + \tfrac{-120\beta^2+10\beta^3}{15(1+\beta)^3} - \tfrac{2\beta^3}{(1+\beta)^3}(\alpha N)^{-2} + o(1)$$

and the lemma is proved. □

Lemma A.1.2. *The regular part F_r can be transformed into the Riemann sum and explicitly*

integrated to obtain the form

$$F_r \sim C + d(\beta)\log X + O(X^{-2}) + O(\alpha X^{-3}) + O(\alpha X^{-1}) + O(\alpha)$$

where C is a constant depending on β, d is a rational function of β and $X = N\alpha$ is a fixed intermediate variable as $\alpha \to 0$.

Proof. Now consider F_r. Here the summation index is getting larger while α is going to zero so it is natural to introduce the intermediate variable $x = n\alpha$ where $\alpha \to 0$ with x fixed making $n \to \infty$. With this F_r takes the form

$$F_r = \tfrac{2\sqrt{2}\sinh\alpha}{6\pi\,\mu\,U\,r_1} \sum_{\substack{x=n\alpha \\ n=N+1}}^{\infty} (2n+1)(a_n + b_n + c_n + d_n).$$

and expanding the summand for x fixed and α small one obtains

$$F_r = \tfrac{2}{3}(1+O(\alpha)) \sum_{\substack{x=n\alpha \\ n=N+1}}^{\infty} \alpha \tfrac{f(x)}{g(x)}$$

where

$$\begin{aligned} f(x) := &-\beta^2 + \beta^2\left(2x^2+2x+1\right)e^{\frac{2(\beta+2)x}{\beta}} - e^{\frac{2x}{\beta}}\left(\beta^2+2x^2-2\beta x\right) \\ &+e^{\frac{2(\beta+1)x}{\beta}}\left(\beta^2+4(\beta+1)x^3+2(\beta+1)^2x^2+2\beta(\beta+1)x\right) \end{aligned}$$

and

$$g(x) := \beta^2 - 2e^{\frac{2(\beta+1)x}{\beta}}\left(\beta^2+2(\beta+1)^2x^2\right) + \beta^2 e^{\frac{4(\beta+1)x}{\beta}}.$$

Note that the summand is implicitly indexed by n through the variable x. Note also that $\alpha = (n+1)\alpha - n\,\alpha = x_{n+1} - x_n =: \Delta x$. Thus

$$F_r = \tfrac{2}{3}(1+O(\alpha)) \sum_{x=X}^{\infty} \tfrac{f(x)}{g(x)}\Delta x \tag{A.1.6}$$

where X is the intermediate variable defined such that N is the positive integer first less than X/α, thus $\alpha \to 0$ implies $X \to 0$. Referring to Euler-Maclaurin [95] one has

$$\sum_{x=X}^{\infty} \tfrac{f(x)}{g(x)}\Delta x = \int_X^{\infty} \tfrac{f(x)}{g(x)}\,\mathrm{d}x + \tfrac{\alpha}{2}\left[\tfrac{f(\infty)}{g(\infty)} + \tfrac{f(X)}{g(X)}\right] + \alpha\sum_{k=1}^{\infty} \tfrac{B_{2k}}{2k!}\left[\left(\tfrac{f}{g}\right)^{(2k-1)}(\infty) - \left(\tfrac{f}{g}\right)^{(2k-1)}(X)\right]$$

where B_m is the m^{th} Bernoulli number. It is now of importance to know the behaviour of the the function $l(x) := \frac{f}{g}(x)$ at $x = 0$ and $x = \infty$. It is not hard to see that $l(x) \to 0$ as $x \to \infty$ due to the presence of the fourth exponential power $\exp(4x)$ in $g(x)$. Now as $x \to 0$ one has

$$l(X) = \tfrac{6\beta^3}{(1+\beta)^3X^3} + \tfrac{6\beta(1+7\beta+\beta^2)}{5(1+\beta)^3X} - \tfrac{3\beta^2+\beta^3}{(1+\beta)^3} + O(X).$$

Therefore limiting the summation (A.1.6) to the integral via Euler-Maclaurin one has

$$\sum_{x=X}^{\infty} \tfrac{f(x)}{g(x)}\Delta x \sim \int_X^{\infty} l(x)\,\mathrm{d}x + \alpha\tfrac{6\beta^3}{(1+\beta)^3X^3} + \alpha\tfrac{6\beta(1+7\beta+\beta^2)}{5(1+\beta)^3X} - \alpha\tfrac{3\beta^2+\beta^3}{(1+\beta)^3} + O(\alpha\,X) \tag{A.1.7}$$

where we have deemed the boundary term at infinity and terms of high order derivatives of $l(x)$ at infinity negligible, the latter which may be justified by the persistence of the term $\exp(4kx)$ in the denominator at the k^{th} derivative of $l(x)$. Additional terms in the regular expansion F_r may be obtained by considering the terms $l^{(k)}(X)$. Since $X \to 0$ as $\alpha \to 0$ it is natural to

decompose the integrand in (A.1.7) its small arguments. In particular the equation

$$\int_X^\infty l(x)\,\mathrm{d}x = \int_1^\infty k(x)\,\mathrm{d}x + \int_X^1 j(x)\,\mathrm{d}x + \int_X^1 \tfrac{6\beta(1+7\beta+\beta^2)}{5(1+\beta)^3 x}\,\mathrm{d}x + \int_X^\infty \tfrac{6\beta^3}{(1+\beta)^3x^3}\,\mathrm{d}x \qquad \text{(A.1.8)}$$

is exact where $j(x) := l(x) - \frac{6\beta^3}{(1+\beta)^3x^3} - \frac{6\beta(1+7\beta+\beta^2)}{5(1+\beta)^3x}$ and $k(x) := l(x) - \frac{6\beta^3}{(1+\beta)^3x^3}$. The latter integrals in (A.1.8) are evaluated as

$$\int_X^1 \tfrac{6\beta(1+7\beta+\beta^2)}{5(1+\beta)^3x}\,\mathrm{d}x = -\tfrac{6\beta(1+7\beta+\beta^2)}{5(1+\beta)^3}\log X,$$
$$\int_X^\infty \tfrac{6\beta^3}{(1+\beta)^3x^3}\,\mathrm{d}x = \tfrac{3\beta^3}{(1+\beta)^3}X^{-2}.$$

The former integrals are dealt with thus. Note that

$$\int_X^1 j(x)\,\mathrm{d}x = \int_0^1 j(x)\,\mathrm{d}x - \int_0^X j(x)\,\mathrm{d}x$$

and that $j(x) = O(x)$ as $x \to 0$ so that $\int_0^X j(x)\,\mathrm{d}x = O(X)$ as $\alpha \to 0$. Thus upon defining the constants (depending on β)

$$C_1 = \int_1^\infty k(x)\,\mathrm{d}x,$$
$$C_2 = \int_0^1 j(x)\,\mathrm{d}x$$

all the expanded leading terms of F_r have been integrated. It is elementary to show that both C_1 and C_2 are finite. For C_1, the contribution proportional to x^{-3} converges on $[1,\infty]$ and $l(x)$ decays exponentially as $x \to \infty$. Consider C_2, we have the power series expansion as $x \to 0$

$$j(x) = -\tfrac{3\beta^2(3+\beta)}{(1+\beta)^3} + \tfrac{4(8-19\beta+8\beta^2)x}{175\beta(1+\beta)} + O(x).$$

Therefore $j(x)$ is a continuous function at zero, moreover continuous a closed interval and there must exist a finite bound $M > |j(x)|$ so that $C_1 < M$. Therefore taking all the contributions together and with $X = N\alpha$ fixed

$$F_r \sim \tfrac{2}{3}(C_1+C_2) - \tfrac{4\beta(1+7\beta+\beta^2)}{5(1+\beta)^3}\log X + \tfrac{2\beta^3}{(1+\beta)^3}X^{-2} + O(\alpha X^{-3}) + O(\alpha X^{-1}) + O(\alpha)$$

as $\alpha \to 0$. □

With these two Lemmas in hand we may formulate the following theorem.

Theorem A.1.3. *As $\alpha \to 0$ from above the force on sphere 1 is given by*

$$F_z^* = \tfrac{4\beta^3}{(1+\beta)^3}\alpha^{-2} + \tfrac{4\beta(1+7\beta+\beta^2)}{5(1+\beta)^3}\log\alpha^{-1} + K_1 + o(1) \qquad \text{(A.1.9)}$$

where $K_1 = \frac{4\beta(1+7\beta+\beta^2)}{5(1+\beta)^3}\left(\gamma + 2\log 2 + \frac{1}{2}\right) + \frac{2}{3}(C_1+C_2) + \frac{-120\beta^2+10\beta^3}{15(1+\beta)^3}$.

Proof. By combining the results of Lemmas A.1.1 and A.1.2 one sees that by writing $\log N = \log X - \log\alpha$ the $\log X$ terms cancel. Similarly with $X = N\alpha$ the $O(N^{-2}\alpha^{-2})$ terms cancel leaving the final expression for F_z^* as $\alpha \to 0$ independent of X as it should be. □

Corollary A.1.4. *In Eulcidean units the force on sphere 1 reads*

$$F_z^e = \tfrac{2\beta^2}{(1+\beta)^2}\epsilon^{-1} + \tfrac{2\beta(1+7\beta+\beta^2)}{5(1+\beta)^3}\log\epsilon^{-1} + K_2 + o(1) \qquad \text{(A.1.10)}$$

where where $K_2 = \frac{4\beta(1+7\beta+\beta^2)}{5(1+\beta)^3}(\gamma + \frac{1}{2} + 2\log 2 + \frac{1}{2}\log\frac{2\beta}{1+\beta}) + \frac{2}{3}(C_1+C_2) + \frac{(10\beta^2-120\beta)}{15(1+\beta)^3}$.

A.1.3 Large Argument Behaviour

We note that for large separations it is sufficient to consider the symmetric case $\eta_1 = -\eta_2$, since by the inner analysis the force quickly decays for surface separations ϵ not small. To this end we consider the asymptotic behaviour of the series

$$\frac{F_z^1(\eta_1, -\eta_1)}{6\pi\mu U r_1} = \frac{\sqrt{2}\sinh\eta_1}{6}\sum_{n=1}^{\infty}(2n+1)(b_n + c_n)$$

as $\eta_1 \to \infty$ since η_1 is a proxy for sphere distance. The following lemma shows that when the spheres are sufficiently separated they experience isolated drag.

Theorem A.1.5. *In the large separation regime Stokes' law is recovered, that is*

$$\lim_{\eta_1\to\infty}\frac{F_z^1}{6\pi\mu U r_1} = 1.$$

Proof. Expanding F in an infinite series of exponential functions we have

$$\frac{F_z^1(\eta_1, -\eta_1)}{6\pi\mu U r_1} = \frac{\sinh\eta_1}{3}\sum_{n=1}^{\infty}\frac{n(n+1)}{(2n+3)(2n-1)}\frac{\mathscr{C}_n(\eta_1)}{\mathscr{D}_n(\eta_1)}$$

where

$$\begin{aligned}\mathscr{C}_n(\eta_1) &= 8e^{\eta_1} - 2(2n-1)(2n+3)e^{2\eta_1(n+1)} + (2n+1)(2n-1)e^{2\eta_1 n}\\ &\quad + (2n+3)(2n+1)e^{2\eta_1(2+n)},\\ \mathscr{D}_n(\eta_1) &= 2\left(e^{\eta_1} - e^{\eta_1(4n+3)}\right) + (2n+1)\left(e^{2\eta_1(n+1)} - e^{2\eta_1 n}\right).\end{aligned}$$

We observe that the limit of the summand as $\eta_1 \to \infty$ exists for each n and the resulting series can be dominated by a second convergent series, thus the limit and the sum may be commuted

$$\frac{\sinh\eta_1}{3}\sum_{n=1}^{\infty}\frac{n(n+1)}{(2n+3)(2n-1)}\frac{\mathscr{C}_n(\eta_1)}{\mathscr{D}_n(\eta_1)} \sim \frac{1}{6}\sum_{n=1}^{\infty}\frac{n(n+1)(2n+1)}{2n-1}e^{-2\eta_1(n-1)}. \tag{A.1.11}$$

Expanding the summation in (A.1.11) we have

$$\frac{e^{-2\eta_1}F_z^1(\eta_1, -\eta_1)}{6\pi\mu U r_1} \sim \sum_{n=1}^{\infty}\frac{n^3 e^{-2\eta_1 n}}{3(2n-1)} + \sum_{n=1}^{\infty}\frac{n^2 e^{-2\eta_1 n}}{2(2n-1)} + \sum_{n=1}^{\infty}\frac{n e^{-2\eta_1 n}}{6(2n-1)}.$$

We may bound this series in terms of known geometric and logarithmic summations as follows

$$\begin{aligned}&\sum_{n=1}^{\infty}\frac{n e^{-2\eta_1 n}}{3} + \sum_{n=1}^{\infty}\frac{e^{-2\eta_1 n}}{2} + \sum_{n=1}^{\infty}\frac{e^{-2\eta_1 n}}{6n}\\ &\quad\le \frac{e^{-2\eta_1}F_z^1(\eta_1, -\eta_1)}{6\pi\mu U r_1} < \sum_{n=1}^{\infty}\frac{n^2 e^{-2\eta_1 n}}{3} + \sum_{n=1}^{\infty}\frac{n e^{-2\eta_1 n}}{2} + \sum_{n=1}^{\infty}\frac{e^{-2\eta_1 n}}{6}.\end{aligned}$$

Summing these lower and upper bounds we find

$$\begin{aligned}&\frac{e^{4\eta_1}}{3(e^{2\eta_1}-1)^2} + \frac{e^{2\eta_1}}{2(e^{2\eta_1}-1)} - e^{2\eta_1}\log\left(e^{-2\eta_1}(e^{2\eta_1}-1)\right)^{1/6}\\ &\quad\le \frac{F_z^1(\eta_1, -\eta_1)}{6\pi\mu U r_1} < \frac{e^{4\eta_1}\left(1+e^{2\eta_1}\right)}{3(e^{2\eta_1}-1)^3} + \frac{e^{4\eta_1}}{2(e^{2\eta_1}-1)^2} + \frac{e^{2\eta_1}}{6(e^{2\eta_1}-1)}\end{aligned}$$

and upon taking the limit $\eta_1 \to \infty$ with the sandwich theorem we yield the required result. □

A.2 Reduction To A Sphere And Plane

The limit of the second sphere radius tending to infinity $\beta = r_2/r_1 \to \infty$ corresponds to a plane wall. It is of interest how the present theory compares to existing formulae for the slow motion of a sphere perpendicular to a plane wall. Consider the formula (A.1.9). Assuming the limit exists one obtains

$$\lim_{\beta\to+\infty} F_z^*(\alpha,\beta) = 4\alpha^{-2} + \tfrac{4}{5}\log\alpha^{-1} + K_3 + o(1) \tag{A.2.1}$$

where $K_3 := \frac{4}{5}(\gamma + \log 2) + \frac{16}{5} + \frac{2}{3}\lim_{\beta\to+\infty}(C_1 + C_2) + \frac{4}{5}\log 2$. The five two terms in the expansion (A.2.1) differ from [2.45] of [37] by a total factor of two, originating from the motion of the plane in our analysis. All that remains is to study $C_1 + C_2$ under the limit $\beta \to +\infty$. Observe that

$$\lim_{\beta\to+\infty} l(x,\beta) = \tfrac{4e^{2x}x^2+4e^{2x}x+2e^{2x}-2}{-2e^{2x}(2x^2+1)+e^{4x}+1} = \tfrac{\sinh 2x+2x}{\cosh 2x-1-2x^2} - 1$$

which is precisely the integrand for the numerical constants [2.43] of [37]. Therefore, up to errors of order $\frac{4}{5}\log 2 = O(10^{-1})$ uniformly in the separation, the sphere-plane limit is recovered $\beta \to +\infty$.

Appendix B

Tangential Interaction

B.1 Recurrence Relations For Unequal Spheres

We now obtain the unknown constants for the case of equal spheres. In spherical bipolar coordinates this is equivalent to imposing

$$z^{(1)} = \frac{c\sinh\eta_1}{\cosh\eta_1-\cos\xi}, \qquad z^{(2)} = \frac{c\sinh\eta_2}{\cosh\eta_2-\cos\xi}$$
$$r^{(1)} = \frac{c\sin\xi}{\cosh\eta_1-\cos\xi}, \qquad r^{(2)} = \frac{c\sin\xi}{\cosh\eta_2-\cos\xi}.$$

We introduce the notation

$$c_\alpha^k = \cosh k\alpha, \qquad s_\alpha^k = \sinh k\alpha.$$

and the generating function for the Legendre polynomials

$$(\cosh\eta-\mathfrak{x})^{-1/2} = \sum_{n=0}^{\infty} s_n(\eta)P_n(\mathfrak{x}) \tag{B.1.1}$$

where $s_n(\eta) = \sqrt{2}e^{\pm(n+\frac{1}{2})\eta}$ where the sign is chosen so that the exponential decays on each sphere.

To obtain a recurrence relation for A_n, B_n and C_n we integrate equation (B.1.8) over $\mathfrak{x}\in[-1,1]$. We consolidate the recurrence relations into the following proposition.

Proposition B.1.1. *For unequal spheres, the equations establishing all the expansion coefficients are*

$$\begin{aligned}0 =& s_{\eta_1}^1\sum_{n=1}^{\infty}[B_nc_{\eta_1}^{n+1/2}+C_ns_{\eta_1}^{n+1/2}]\mathfrak{t}_n(\eta_1)+\sum_{n=1}^{\infty}A_nc_{\eta_1}^{n+1/2}(c_{\eta_1}^1\mathfrak{t}_n(\eta_1)-\mathfrak{u}_n(\eta_1)-\mathfrak{v}_n(\eta_1))\\ &-s_{\eta_2}^1\sum_{n=1}^{\infty}[B_nc_{\eta_2}^{n+1/2}+C_ns_{\eta_2}^{n+1/2}]\mathfrak{t}_n(\eta_2)-\sum_{n=1}^{\infty}A_nc_{\eta_2}^{n+1/2}(c_{\eta_2}^1\mathfrak{t}_n(\eta_2)-\mathfrak{u}_n(\eta_2)-\mathfrak{v}_n(\eta_2)),\end{aligned}$$

$$\begin{aligned}0 =& \sum_{n=1}^{\infty}[B_nc_{\eta_1}^{n+1/2}+C_ns_{\eta_1}^{n+1/2}]\mathfrak{w}_n(\eta_1)+\sum_{n=1}^{\infty}[B_nc_{\eta_2}^{n+1/2}+C_ns_{\eta_2}^{n+1/2}]\mathfrak{w}_n(\eta_2)\\ &+\sum_{n=2}^{\infty}[F_nc_{\eta_1}^{n+1/2}+G_ns_{\eta_1}^{n+1/2}]\mathfrak{x}_n(\eta_1)+\sum_{n=2}^{\infty}[F_nc_{\eta_2}^{n+1/2}+G_ns_{\eta_2}^{n+1/2}]\mathfrak{x}_n(\eta_2)\\ &+\sum_{n=0}^{\infty}[D_nc_{\eta_1}^{n+1/2}+E_ns_{\eta_1}^{n+1/2}]\mathfrak{y}_n(\eta_1)+\sum_{n=0}^{\infty}[D_nc_{\eta_2}^{n+1/2}+E_ns_{\eta_2}^{n+1/2}]\mathfrak{y}_n(\eta_2),\end{aligned}$$

$$0 = \sum_{n=2}^{\infty}[F_n c_{\eta_1}^{n+1/2} + G_n s_{\eta_1}^{n+1/2}]\mathfrak{x}_n(\eta_1) + \sum_{n=2}^{\infty}[F_n c_{\eta_2}^{n+1/2} + G_n s_{\eta_2}^{n+1/2}]\mathfrak{x}_n(\eta_1)$$
$$- \sum_{n=0}^{\infty}[D_n c_{\eta_1}^{n+1/2} + E_n s_{\eta_1}^{n+1/2}]\mathfrak{y}_n(\eta_1) - \sum_{n=0}^{\infty}[D_n c_{\eta_2}^{n+1/2} + E_n s_{\eta_2}^{n+1/2}]\mathfrak{y}_n(\eta_2),$$

$$0 = s_{\eta_1}^1 \sum_{n=1}^{\infty}[B_n c_{\eta_1}^{n+1/2} + C_n s_{\eta_1}^{n+1/2}]\mathfrak{t}_n(\eta_1) + 2\sum_{n=1}^{\infty} A_n c_{\eta_1}^{n+1/2}[c_{\eta_1}^1 \mathfrak{t}_n(\eta_1) - \mathfrak{u}_n(\eta_1) - \mathfrak{v}_n(\eta_1)]$$
$$+ s_{\eta_2}^1 \sum_{n=1}^{\infty}[B_n c_{\eta_2}^{n+1/2} + C_n s_{\eta_2}^{n+1/2}]\mathfrak{t}_n(\eta_2) + 2\sum_{n=1}^{\infty} A_n c_{\eta_2}^{n+1/2}[c_{\eta_1}^1 \mathfrak{t}_n(\eta_1) - \mathfrak{u}_n(\eta_1) - \mathfrak{v}_n(\eta_1)],$$

$$0 = \sum_{n=1}^{\infty}[B_n c_{\eta_1}^{n+1/2} + C_n s_{\eta_1}^{n+1/2}]\mathfrak{t}_n(\eta_1) - \sum_{n=1}^{\infty}[B_n c_{\eta_2}^{n+1/2} + C_n s_{\eta_2}^{n+1/2}]\mathfrak{t}_n(\eta_1)$$
$$+ 4\sum_{n=2}^{\infty}[F_n c_{\eta_1}^{n+1/2} + G_n s_{\eta_1}^{n+1/2}]\mathfrak{z}_n(\eta_1) - 4\sum_{n=2}^{\infty}[F_n c_{\eta_2}^{n+1/2} + G_n s_{\eta_2}^{n+1/2}]\mathfrak{z}_n(\eta_2),$$

$$2 = \sum_{n=1}^{\infty}[B_n c_{\eta_1}^{n+1/2} + C_n s_{\eta_1}^{n+1/2}]\mathfrak{w}_n(\eta_1) - \sum_{n=1}^{\infty}[B_n c_{\eta_2}^{n+1/2} + C_n s_{\eta_2}^{n+1/2}]\mathfrak{w}_n(\eta_2)$$
$$+ 2\sum_{n=0}^{\infty}[D_n c_{\eta_1}^{n+1/2} + E_n s_{\eta_1}^{n+1/2}]\mathfrak{y}_n(\eta_1) - 2(c_{\eta_2}^1 - \mathfrak{x})^{1/2}\sum_{n=0}^{\infty}[D_n c_{\eta_2}^{n+1/2} + E_n s_{\eta_2}^{n+1/2}]\mathfrak{y}_n(\eta_2),$$

where

$$\begin{aligned}
\mathfrak{t}_n(\eta_1) &:= s_{n-1}(\eta_1) + s_{n-3}(\eta_1)\cdots, \\
\mathfrak{u}_n(\eta_1) &:= \tfrac{n-1}{2n-3}s_{n-2}(\eta_1) + \tfrac{n-3}{2n-7}s_{n-4}(\eta_1) + \cdots, \\
\mathfrak{v}_n(\eta_1) &:= \tfrac{n}{2n+1}s_n(\eta_1) + \tfrac{n-2}{2n-3}s_{n-3}(\eta_1) + \cdots, \\
\mathfrak{w}_n(\eta_1) &:= \tfrac{n(n+1)}{2n+1}\left[\tfrac{s_{n-1}(\eta_1)}{2n-1} - \tfrac{s_{n+1}(\eta_1)}{2n+3}\right], \\
\mathfrak{x}_n(\eta_1) &:= -n(n+1)\left[\tfrac{c_{\eta_1}^1 s_n(\eta_1)}{2n+1} - \tfrac{n+1}{2n+1}\tfrac{s_{n+1}(\eta_1)}{2n+3} - \tfrac{n}{2n+1}\tfrac{s_{n-1}(\eta_1)}{2n-1}\right] \\
&\quad + \tfrac{2}{2n+1}\Big[(n+1)(c_{\eta_1}^1 \mathfrak{t}_{n-1}(\eta_1) - \mathfrak{u}_{n-1}(\eta_1) - \mathfrak{v}_{n-1}(\eta_1)) \\
&\quad + n(c_{\eta_1}^1 \mathfrak{t}_{n+1}(\eta_1) - \mathfrak{u}_{n+1}(\eta_1) - \mathfrak{v}_{n+1}(\eta_1))\Big], \\
\mathfrak{y}_n(\eta_1) &:= \frac{c_{\eta_1}^1 s_n(\eta_1)}{2n+1} - \frac{n+1}{2n+1}\frac{s_{n+1}(\eta_1)}{2n+3} - \frac{n}{2n+1}\tfrac{s_{n-1}(\eta_1)}{2n-1}, \\
\mathfrak{z}_n(\eta_1) &:= (c_{\eta_1}^1 \mathfrak{t}_n(\eta_1) - \mathfrak{u}_n(\eta_1) - \mathfrak{v}_n(\eta_1)) + (c_{\eta_1}^1 \mathfrak{t}_{n-2}(\eta_1) - \mathfrak{u}_{n-2}(\eta_1) - \mathfrak{v}_{n-2}(\eta_1)) + \cdots.
\end{aligned}$$

and $s_n(\eta) = \sqrt{2}e^{\pm(n+\frac{1}{2})\eta}$ *and the sign is chosen so that the exponential decays on each sphere.*

Proof. By subtracting (4.4.6) from (4.4.3) we find

$$\tfrac{s_{\eta_1}^1}{(c_{\eta_1}^1 - \mathfrak{x})^{1/2}}\sum_{n=1}^{\infty}[B_n c_{\eta_1}^{n+1/2} + C_n s_{\eta_1}^{n+1/2}]P_n'(\mathfrak{x}) + 2(c_{\eta_1}^1 - \mathfrak{x})^{1/2}\sum_{n=1}^{\infty} A_n c_{\eta_1}^{n+1/2}P_n'(\mathfrak{x})$$
$$- \tfrac{s_{\eta_2}^1}{(c_{\eta_2}^1 - \mathfrak{x})^{1/2}}\sum_{n=1}^{\infty}[B_n c_{\eta_2}^{n+1/2} + C_n s_{\eta_2}^{n+1/2}]P_n'(\mathfrak{x}) - 2(c_{\eta_2}^1 - \mathfrak{x})^{1/2}\sum_{n=1}^{\infty} A_n c_{\eta_2}^{n+1/2}P_n'(\mathfrak{x}) = 0. \quad \text{(B.1.2)}$$

We now integrate this equation. By interchanging the order of summation and integration and

using (B.1.1), we obtain the following identity

$$\int_{-1}^{1} \mathrm{d}\mathfrak{x}\, \tfrac{P_n'(\mathfrak{x})}{(c_{\eta_1}^1-\mathfrak{x})^{1/2}} = \int_{-1}^{1} \mathrm{d}\mathfrak{x} \sum_{j=0}^{\infty} s_j(\eta_1) P_j(\mathfrak{x}) P_n'(\mathfrak{x})$$

We now use the descending summation expression for P_n'

$$P_{n+1}'(\mathfrak{x}) = 2\left[\frac{P_n(\mathfrak{x})}{\|P_n\|^2} + \frac{P_{n-2}(\mathfrak{x})}{\|P_{n-2}\|^2} + \cdots\right] \tag{B.1.3}$$

to obtain

$$\begin{aligned}
&\int_{-1}^{1} \mathrm{d}\mathfrak{x}\, \tfrac{P_n'(\mathfrak{x})}{(c_{\eta_1}^1-\mathfrak{x})^{1/2}} \\
&= 2\sum_{j=0}^{\infty} s_j(\eta_1) \int_{-1}^{1} \mathrm{d}\mathfrak{x}\, P_j(\mathfrak{x}) \left[\tfrac{P_{n-1}(\mathfrak{x})}{\|P_{n-1}\|^2} + \tfrac{P_{n-3}(\mathfrak{x})}{\|P_{n-3}\|^2} + \cdots\right] \\
&= 2\sum_{j=0}^{n-1} s_j(\eta_1) \int_{-1}^{1} \mathrm{d}\mathfrak{x}\, P_j(\mathfrak{x}) \left[\tfrac{P_{n-1}(\mathfrak{x})}{\|P_{n-1}\|^2} + \tfrac{P_{n-3}(\mathfrak{x})}{\|P_{n-3}\|^2} + \cdots\right] \\
&\quad + 2\sum_{j=n}^{\infty} s_j(\eta_1) \int_{-1}^{1} \mathrm{d}\mathfrak{x}\, P_j(\mathfrak{x}) \left[\tfrac{P_{n-1}(\mathfrak{x})}{\|P_{n-1}\|^2} + \tfrac{P_{n-3}(\mathfrak{x})}{\|P_{n-3}\|^2} + \cdots\right] \\
&= 2\left[s_{n-1}(\eta_1) + s_{n-3}(\eta_1)\cdots\right] =: 2\mathfrak{t}_n(\eta_1)
\end{aligned} \tag{B.1.4}$$

where the finite sum for t_n is $\lceil \frac{n}{2} \rceil$ long. Additionally we obtain the following integral expression

$$\int_{-1}^{1} \mathrm{d}\mathfrak{x}\, (c_{\eta_1}^1-\mathfrak{x})^{1/2} P_n'(\mathfrak{x}) = \int_{-1}^{1} \mathrm{d}\mathfrak{x}\, \frac{(c_{\eta_1}^1-\mathfrak{x})P_n'(\mathfrak{x})}{(c_{\eta_1}^1-\mathfrak{x})^{1/2}} = 2c_{\eta_1}^1 t_n(\eta_1) - \int_{-1}^{1} \mathrm{d}\mathfrak{x}\, \frac{xP_n'(\mathfrak{x})}{(c_{\eta_1}^1-\mathfrak{x})^{1/2}}. \tag{B.1.5}$$

By using the descending summation expression (B.1.3) we may continue evaluating the integral on the last line with

$$\begin{aligned}
&\int_{-1}^{1} \mathrm{d}\mathfrak{x}\, (c_{\eta_1}^1-\mathfrak{x})^{1/2} P_n'(\mathfrak{x}) \\
&= 2c_{\eta_1}^1 \mathfrak{t}_n(\eta_1) - 2\sum_{j=0}^{\infty} s_j(\eta_1) \int_{-1}^{1} \mathrm{d}\mathfrak{x}\, \mathfrak{x} P_j(\mathfrak{x}) \left[\tfrac{P_{n-1}(\mathfrak{x})}{\|P_{n-1}\|^2} + \cdots\right] \\
&= 2c_{\eta_1}^1 \mathfrak{t}_n(\eta_1) - 2\sum_{j=0}^{\infty} s_j(\eta_1) \int_{-1}^{1} \mathrm{d}\mathfrak{x}\, \tfrac{(j+1)P_{j+1}(\mathfrak{x})+jP_{j-1}(\mathfrak{x})}{2j+1} \left[\tfrac{P_{n-1}(\mathfrak{x})}{\|P_{n-1}\|^2} + \cdots\right] \\
&= 2c_{\eta_1}^1 \mathfrak{t}_n(\eta_1) - 2\sum_{j=0}^{\infty} s_j(\eta_1) \int_{-1}^{1} \mathrm{d}\mathfrak{x}\, \tfrac{(j+1)P_{j+1}(\mathfrak{x})}{2j+1} \left[\tfrac{P_{n-1}(\mathfrak{x})}{\|P_{n-1}\|^2} + \cdots\right] \\
&\quad - 2\sum_{j=0}^{\infty} s_j(\eta_1) \int_{-1}^{1} \mathrm{d}\mathfrak{x}\, \tfrac{jP_{j-1}(\mathfrak{x})}{2j+1} \left[\tfrac{P_{n-1}(\mathfrak{x})}{\|P_{n-1}\|^2} + \cdots\right] \\
&= 2c_{\eta_1}^1 \mathfrak{t}_n(\eta_1) - 2\left(\sum_{j=0}^{n-2} + \sum_{j=n-1}^{\infty}\right) s_j(\eta_1) \int_{-1}^{1} \mathrm{d}\mathfrak{x}\, \tfrac{(j+1)P_{j+1}(\mathfrak{x})}{2j+1} \left[\tfrac{P_{n-1}(\mathfrak{x})}{\|P_{n-1}\|^2} + \cdots\right] \\
&\quad - 2\left(\sum_{j=0}^{n} + \sum_{j=n+1}^{\infty}\right) s_j(\eta_1) \int_{-1}^{1} \mathrm{d}\mathfrak{x}\, \tfrac{jP_{j-1}(\mathfrak{x})}{2j+1} \left[\tfrac{P_{n-1}(\mathfrak{x})}{\|P_{n-1}\|^2} + \cdots\right] \\
&= 2c_{\eta_1}^1 \mathfrak{t}_n(\eta_1) - 2\mathfrak{u}_n(\eta_1) - 2\mathfrak{v}_n(\eta_1)
\end{aligned} \tag{B.1.6}$$

where we have use the definitions of $\mathfrak{u}_n(\eta_1)$ and $\mathfrak{v}_n(\eta_1)$. By using the formulas in (B.1.4) and

(B.1.5), equation becomes (B.1.2) becomes

$$\begin{aligned}0 =&2s^1_{\eta_1}\sum_{n=1}^{\infty}[B_n c^{n+1/2}_{\eta_1}+C_n s^{n+1/2}_{\eta_1}]\mathfrak{t}_n(\eta_1)+2\sum_{n=1}^{\infty}A_n c^{n+1/2}_{\eta_1}(c^1_{\eta_1}\mathfrak{t}_n(\eta_1)-\mathfrak{u}_n(\eta_1)-\mathfrak{v}_n(\eta_1))\\ &-2s^1_{\eta_2}\sum_{n=1}^{\infty}[B_n c^{n+1/2}_{\eta_2}+C_n s^{n+1/2}_{\eta_2}]\mathfrak{t}_n(\eta_2)-2\sum_{n=1}^{\infty}A_n c^{n+1/2}_{\eta_2}(c^1_{\eta_2}\mathfrak{t}_n(\eta_2)-\mathfrak{u}_n(\eta_2)-\mathfrak{v}_n(\eta_2))\end{aligned} \tag{B.1.7}$$

Note that in the equal sphere case, $\eta_2=-\eta_1$ (B.1.7) implies $B_n=0$ for every $n\in\mathbb{N}$.

We now combine the boundary conditions to produce another independent set of equations for the unknown coefficients. By adding (4.4.1) to (4.4.4) one obtains

$$\begin{aligned}&\tfrac{(1-\mathfrak{x}^2)}{(c^1_{\eta_1}-\mathfrak{x})^{1/2}}\sum_{n=1}^{\infty}[B_n c^{n+1/2}_{\eta_1}+C_n s^{n+1/2}_{\eta_1}]P'_n(\mathfrak{x})+\tfrac{(1-\mathfrak{x}^2)}{(c^1_{\eta_2}-\mathfrak{x})^{1/2}}\sum_{n=1}^{\infty}[B_n c^{n+1/2}_{\eta_2}+C_n s^{n+1/2}_{\eta_2}]P'_n(\mathfrak{x})\\ &+(c^1_{\eta_1}-\mathfrak{x})^{1/2}(1-\mathfrak{x}^2)\sum_{n=2}^{\infty}[F_n c^{n+1/2}_{\eta_1}+G_n s^{n+1/2}_{\eta_1}]P''_n(\mathfrak{x})\\ &+(c^1_{\eta_2}-\mathfrak{x})^{1/2}(1-\mathfrak{x}^2)\sum_{n=2}^{\infty}[F_n c^{n+1/2}_{\eta_2}+G_n s^{n+1/2}_{\eta_2}]P''_n(\mathfrak{x})\\ &+(c^1_{\eta_1}-\mathfrak{x})^{1/2}\sum_{n=0}^{\infty}[D_n c^{n+1/2}_{\eta_1}+E_n s^{n+1/2}_{\eta_1}]P_n(\mathfrak{x})\\ &+(c^1_{\eta_2}-\mathfrak{x})^{1/2}\sum_{n=0}^{\infty}[D_n c^{n+1/2}_{\eta_2}+E_n s^{n+1/2}_{\eta_2}]P_n(\mathfrak{x})\\ &=0.\end{aligned} \tag{B.1.8}$$

To obtain an recurrence relation for the equation (B.1.8) we consider various integrals of the P_n. Firstly we have that

$$\begin{aligned}&\int_{-1}^{1}\mathrm{d}\mathfrak{x}\,(c^1_{\eta_1}-\mathfrak{x})^{1/2}P_n(\mathfrak{x})=\int_{-1}^{1}\frac{\mathrm{d}\mathfrak{x}\,(c^1_{\eta_1}-\mathfrak{x})P_n(\mathfrak{x})}{(c^1_{\eta_1}-\mathfrak{x})^{1/2}}=c^1_{\eta_1}\int_{-1}^{1}\frac{\mathrm{d}\mathfrak{x}\,P_n(\mathfrak{x})}{(c^1_{\eta_1}-\mathfrak{x})^{1/2}}-\int_{-1}^{1}\frac{\mathrm{d}\mathfrak{x}\,\mathfrak{x}P_n(\mathfrak{x})}{(c^1_{\eta_1}-\mathfrak{x})^{1/2}}\\ &=2\frac{c^1_{\eta_1}s_n(\eta_1)}{2n+1}-2\frac{n+1}{2n+1}\frac{s_{n+1}(\eta_1)}{2n+3}-2\frac{n}{2n+1}\tfrac{s_{n-1}(\eta_1)}{2n-1}=:2\mathfrak{y}_n(\eta_1)\end{aligned} \tag{B.1.9}$$

Additional recurrence relations for P_n are needed to integrate the remaining terms in equation (B.1.8). In particular we note that

$$(1-\mathfrak{x}^2)P'_n(\mathfrak{x})=\tfrac{n(n+1)}{2n+1}(P_{n-1}-P_{n+1}), \tag{B.1.10}$$

$$(1-\mathfrak{x}^2)P''_n(\mathfrak{x})=-n(n+1)P_n(\mathfrak{x})+\tfrac{2}{2n+1}\left[(n+1)P'_{n-1}(\mathfrak{x})+nP'_{n+1}(\mathfrak{x})\right], \tag{B.1.11}$$

the former being the standard integration identity of the Legendre polynomials and the latter may be established from Legendre's equation and Bonnet's recursion formula

$$(n+1)P_{n+1}(\mathfrak{x})=(2n+1)\mathfrak{x}P_n(\mathfrak{x})-nP_{n-1}(\mathfrak{x}).$$

By equation (B.1.10) and (B.1.1) we obtain

$$\int_{-1}^{1}\mathrm{d}\mathfrak{x}\,\tfrac{(1-\mathfrak{x}^2)P'_n(\mathfrak{x})}{(c^1_{\eta_1}-\mathfrak{x})^{1/2}}=2\tfrac{n(n+1)}{2n+1}\left[\tfrac{s_{n-1}(\eta_1)}{2n-1}-\tfrac{s_{n+1}(\eta_1)}{2n+3}\right]=:2\mathfrak{w}_n(\eta_1)$$

and by equation (B.1.11), (B.1.6) and (B.1.9) we have

$$\begin{aligned}\int_{-1}^{1} \mathrm{d}\mathfrak{x}\,(c_{\eta_1}^1-\mathfrak{x})^{1/2}(1-\mathfrak{x}^2)P_n''(\mathfrak{x}) &= -2n(n+1)\left[\tfrac{c_{\eta_1}^1 s_n(\eta_1)}{2n+1}-\tfrac{n+1}{2n+1}\tfrac{s_{n+1}(\eta_1)}{2n+3}-\tfrac{n}{2n+1}\tfrac{s_{n-1}(\eta_1)}{2n-1}\right]\\ &\quad+\tfrac{4}{2n+1}\Big[(n+1)(c_{\eta_1}^1\mathfrak{t}_{n-1}(\eta_1)-\mathfrak{u}_{n-1}(\eta_1)-\mathfrak{v}_{n-1}(\eta_1))\\ &\quad+n(c_{\eta_1}^1\mathfrak{t}_{n+1}(\eta_1)-\mathfrak{u}_{n+1}(\eta_1)-\mathfrak{v}_{n+1}(\eta_1))\Big]=:2\mathfrak{x}_n(\eta_1).\end{aligned}$$

We may therefore rewrite (B.1.8) as

$$\begin{aligned}&2\sum_{n=1}^{\infty}[B_n c_{\eta_1}^{n+1/2}+C_n s_{\eta_1}^{n+1/2}]\mathfrak{w}_n(\eta_1)+2\sum_{n=1}^{\infty}[B_n c_{\eta_2}^{n+1/2}+C_n s_{\eta_2}^{n+1/2}]\mathfrak{w}_n(\eta_2)\\ &+2\sum_{n=2}^{\infty}[F_n c_{\eta_1}^{n+1/2}+G_n s_{\eta_1}^{n+1/2}]\mathfrak{x}_n(\eta_1)+2\sum_{n=2}^{\infty}[F_n c_{\eta_2}^{n+1/2}+G_n s_{\eta_2}^{n+1/2}]\mathfrak{x}_n(\eta_2)\\ &+2\sum_{n=0}^{\infty}[D_n c_{\eta_1}^{n+1/2}+E_n s_{\eta_1}^{n+1/2}]2\mathfrak{y}_n(\eta_1)+2\sum_{n=0}^{\infty}[D_n c_{\eta_2}^{n+1/2}+E_n s_{\eta_2}^{n+1/2}]\mathfrak{y}_n(\eta_2)=0.\end{aligned}$$

Note that in the equal sphere case, when $\eta_2=-\eta_1$, we have that $B_n=0$ for every $n=\in\mathbb{N}$ and all terms with a factor of $s_{\eta_1}^{n+1/2}$ will cancel, eliminating E_n and G_n. This then implies that $D_n=F_n\equiv 0$ for every $n\in\mathbb{N}\cup\{0\}$ in the equal sphere case.

By adding (4.4.2) to (4.4.5) we have the recurrence relation

$$\begin{aligned}&(1-\mathfrak{x}^2)(c_{\eta_1}^1-\mathfrak{x})^{1/2}\sum_{n=2}^{\infty}[F_n c_{\eta_1}^{n+1/2}+G_n s_{\eta_1}^{n+1/2}]P_n''(\mathfrak{x})\\ &+(1-\mathfrak{x}^2)(c_{\eta_2}^1-\mathfrak{x})^{1/2}\sum_{n=2}^{\infty}[F_n c_{\eta_2}^{n+1/2}+G_n s_{\eta_2}^{n+1/2}]P_n''(\mathfrak{x})\\ &-(c_{\eta_1}^1-\mathfrak{x})^{1/2}\sum_{n=0}^{\infty}[D_n c_{\eta_1}^{n+1/2}+E_n s_{\eta_1}^{n+1/2}]P_n(\mathfrak{x})\\ &-(c_{\eta_2}^1-\mathfrak{x})^{1/2}\sum_{n=0}^{\infty}[D_n c_{\eta_2}^{n+1/2}+E_n s_{\eta_2}^{n+1/2}]P_n(\mathfrak{x})=0\end{aligned}$$

which may be integrated to obtain

$$\begin{aligned}&2\sum_{n=2}^{\infty}[F_n c_{\eta_1}^{n+1/2}+G_n s_{\eta_1}^{n+1/2}]\mathfrak{x}_n(\eta_1)+2\sum_{n=2}^{\infty}[F_n c_{\eta_2}^{n+1/2}+G_n s_{\eta_2}^{n+1/2}]\mathfrak{x}_n(\eta_1)\\ &-2\sum_{n=0}^{\infty}[D_n c_{\eta_1}^{n+1/2}+E_n s_{\eta_1}^{n+1/2}]\mathfrak{y}_n(\eta_1)-2\sum_{n=0}^{\infty}[D_n c_{\eta_2}^{n+1/2}+E_n s_{\eta_2}^{n+1/2}]\mathfrak{y}_n(\eta_2)=0\end{aligned}$$

By adding (4.4.6) to (4.4.3) we find the summation

$$\begin{aligned}&\tfrac{s_{\eta_1}^1}{(c_{\eta_1}^1-\mathfrak{x})^{1/2}}\sum_{n=1}^{\infty}[B_n c_{\eta_1}^{n+1/2}+C_n s_{\eta_1}^{n+1/2}]P_n'(\mathfrak{x})+2(c_{\eta_1}^1-\mathfrak{x})^{1/2}\sum_{n=1}^{\infty}A_n c_{\eta_1}^{n+1/2}P_n'(\mathfrak{x})\\ &+\tfrac{s_{\eta_2}^1}{(c_{\eta_2}^1-\mathfrak{x})^{1/2}}\sum_{n=1}^{\infty}[B_n c_{\eta_2}^{n+1/2}+C_n s_{\eta_2}^{n+1/2}]P_n'(\mathfrak{x})+2(c_{\eta_2}^1-\mathfrak{x})^{1/2}\sum_{n=1}^{\infty}A_n c_{\eta_2}^{n+1/2}P_n'(\mathfrak{x})=0\end{aligned}$$

which may be integrated to find

$$2s^1_{\eta_1}\sum_{n=1}^{\infty}[B_nc^{n+1/2}_{\eta_1}+C_ns^{n+1/2}_{\eta_1}]\mathfrak{t}_n(\eta_1)+4\sum_{n=1}^{\infty}A_nc^{n+1/2}_{\eta_1}[c^1_{\eta_1}\mathfrak{t}_n(\eta_1)-\mathfrak{u}_n(\eta_1)-\mathfrak{v}_n(\eta_1)]$$
$$+2s^1_{\eta_2}\sum_{n=1}^{\infty}[B_nc^{n+1/2}_{\eta_2}+C_ns^{n+1/2}_{\eta_2}]\mathfrak{t}_n(\eta_2)+4\sum_{n=1}^{\infty}A_nc^{n+1/2}_{\eta_2}[c^1_{\eta_1}\mathfrak{t}_n(\eta_1)-\mathfrak{u}_n(\eta_1)-\mathfrak{v}_n(\eta_1)]=0.$$

Subtracting (4.4.4) from (4.4.1), subtracting (4.4.5) from (4.4.2) and adding (4.4.3) to (4.4.6) yields

$$\tfrac{r^{(1)}}{c}W_1-\tfrac{r^{(2)}}{c}W_2+X_1-X_2+Y_1-Y_2=2, \tag{B.1.12}$$
$$X_1-X_2-Y_1+Y_2=-2, \tag{B.1.13}$$
$$z_1W_1+z_2W_2+2c(Z_1+Z_2)=0.$$

Now adding together (B.1.12) and (B.1.13) one obtains

$$\tfrac{1}{(c^1_{\eta_1}-\mathfrak{x})^{1/2}}\sum_{n=1}^{\infty}[B_nc^{n+1/2}_{\eta_1}+C_ns^{n+1/2}_{\eta_1}]P_n'(\mathfrak{x})$$
$$-\tfrac{1}{(c^1_{\eta_2}-\mathfrak{x})^{1/2}}\sum_{n=1}^{\infty}[B_nc^{n+1/2}_{\eta_2}+C_ns^{n+1/2}_{\eta_2}]P_n'(\mathfrak{x})$$
$$+2(c^1_{\eta_1}-\mathfrak{x})^{1/2}\sum_{n=2}^{\infty}[F_nc^{n+1/2}_{\eta_1}+G_ns^{n+1/2}_{\eta_1}]P_n''(\mathfrak{x})$$
$$-2(c^1_{\eta_2}-\mathfrak{x})^{1/2}\sum_{n=2}^{\infty}[F_nc^{n+1/2}_{\eta_2}+G_ns^{n+1/2}_{\eta_2}]P_n''(\mathfrak{x})=0.$$

We need an additional integration identity, namely

$$\int_{-1}^{1}\mathrm{d}\mathfrak{x}\,(c^1_{\eta_1}-\mathfrak{x})^{1/2}P_n''(\mathfrak{x})=2\int_{-1}^{1}\mathrm{d}\mathfrak{x}\,(c^1_{\eta_1}-\mathfrak{x})^{1/2}\left[\tfrac{P_{n-1}'(\mathfrak{x})}{\|P_{n-1}\|^2}+\tfrac{P_{n-3}'(\mathfrak{x})}{\|P_{n-3}\|^2}+\cdots\right]$$
$$=2\left[(c^1_{\eta_1}\mathfrak{t}_n(\eta_1)-\mathfrak{u}_n(\eta_1)-\mathfrak{v}_n(\eta_1))+(c^1_{\eta_1}\mathfrak{t}_{n-2}(\eta_1)-\mathfrak{u}_{n-2}(\eta_1)-\mathfrak{v}_{n-2}(\eta_1))+\cdots\right]$$
$$=:2\mathfrak{z}_n(\eta_1).$$

Integrating this equation we obtain

$$\sum_{n=1}^{\infty}[B_nc^{n+1/2}_{\eta_1}+C_ns^{n+1/2}_{\eta_1}]\mathfrak{t}_n(\eta_1)-\sum_{n=1}^{\infty}[B_nc^{n+1/2}_{\eta_2}+C_ns^{n+1/2}_{\eta_2}]\mathfrak{t}_n(\eta_1)$$
$$+4\sum_{n=2}^{\infty}[F_nc^{n+1/2}_{\eta_1}+G_ns^{n+1/2}_{\eta_1}]\mathfrak{z}_n(\eta_1)-4\sum_{n=2}^{\infty}[F_nc^{n+1/2}_{\eta_2}+G_ns^{n+1/2}_{\eta_2}]\mathfrak{z}_n(\eta_2)=0.$$

Now subtracting (B.1.13) from (B.1.12) one obtains

$$\tfrac{(1-\mathfrak{x}^2)}{(c^1_{\eta_1}-\mathfrak{x})^{1/2}}\sum_{n=1}^{\infty}[B_nc^{n+1/2}_{\eta_1}+C_ns^{n+1/2}_{\eta_1}]P_n'(\mathfrak{x})$$
$$-\tfrac{(1-\mathfrak{x}^2)}{(c^1_{\eta_2}-\mathfrak{x})^{1/2}}\sum_{n=1}^{\infty}[B_nc^{n+1/2}_{\eta_2}+C_ns^{n+1/2}_{\eta_2}]P_n'(\mathfrak{x})$$
$$+2(c^1_{\eta_1}-\mathfrak{x})^{1/2}\sum_{n=0}^{\infty}[D_nc^{n+1/2}_{\eta_1}+E_ns^{n+1/2}_{\eta_1}]P_n(\mathfrak{x})$$
$$-2(c^1_{\eta_2}-\mathfrak{x})^{1/2}\sum_{n=0}^{\infty}[D_nc^{n+1/2}_{\eta_2}+E_ns^{n+1/2}_{\eta_2}]P_n(\mathfrak{x})=2.$$

Integrating this equation we obtain

$$2\sum_{n=1}^{\infty}[B_n c_{\eta_1}^{n+1/2}+C_n s_{\eta_1}^{n+1/2}]\mathfrak{w}_n(\eta_1)-2\sum_{n=1}^{\infty}[B_n c_{\eta_2}^{n+1/2}+C_n s_{\eta_2}^{n+1/2}]\mathfrak{w}_n(\eta_2)$$
$$+4\sum_{n=0}^{\infty}[D_n c_{\eta_1}^{n+1/2}+E_n s_{\eta_1}^{n+1/2}]\mathfrak{y}_n(\eta_1)-4(c_{\eta_2}^1-\mathfrak{x})^{1/2}\sum_{n=0}^{\infty}[D_n c_{\eta_2}^{n+1/2}+E_n s_{\eta_2}^{n+1/2}]\mathfrak{y}_n(\eta_2)=2.$$

This completes the proof of the proposition. □

Appendix C

Pseudospectral Methods

Monte Carlo methods are popular ways to solve the underlying Fokker–Planck equation, essentially by sampling the Langevin dynamics, to obtain particle trajectories and phase diagrams. However they quickly become too computationally expensive for reasonably sized systems and longer observation times. Conversely, on the macro/mesoscopic level, DFT and DDFT problems, which may include complicated convolution terms, can be efficiently tackled with pseudospectral methods. This is because of the highly accurate Gauss quadrature offered by such methods. In particular, for the convolution terms, Gauss quadrature offers exponential accuracy, with collocation points located near interfaces, meaning a reduction in the number of grid points needed to reach a desired accuracy compared to finite element and difference methods. What is more the pseudospectral methods can be shown to satisfy the statistical mechanical sum rules intrinsic to DFT and DDFT [127].

Fundamental Measure Theory as introduced by Rosenfeld [148] is a highly accurate free energy functional for hard sphere fluids which uses a functional of weighted densities, as convolutions of the fluid density with weight functions (See Section 1.6). This provides the particle-particle exclusion contribution to the free energy of the hard sphere fluid. The attractive intermolecular interactions are usually provided in a perturbative manner via a meanfield approximation, as a convolution of the fluid density with the attractive part of the total intermolecular potential energy. The upshot is the DFT and DDFT equations involving highly stiff and non-linear integral terms therefore posing significant numerical challenges.

Common techniques are to compute the convolutions in Fourier space by application of the convolution theorem [150]

$$n \star \chi = F^{-1}\left\{F\left\{n\right\} \times F\left\{\chi\right\}\right\} \tag{C.0.1}$$

where F is the Fourier transform, n is the number density and χ is a arbitrary weight function from the FMT formalism (Section 1.6). As stated in [126] a Fast Fourier Transform (FFT) has $O(N \log N)$ complexity for N Fourier modes. FFTs require a uniform Cartesian grid, and accurate computations typically use dense 20 to 50 discretisation points per hard sphere diameter to produce good resolutions of the number density n near interfaces. Improvements can be obtained if the Fourier transform of χ performed analytically. However, since χ generally possesses discontinuities, and given the fact that n possesses a discontinuity at a wall interface (since there is no flux at the wall), special treatment of the Gibbs phenomenon in interpolating n at the wall is required. Additionally any Fourier method will require a truncation of the physical domain and a non-physical assumption of periodicity. The use of a highly dense uniform grids is also wasteful far from the wall where n is near-constant.

In this chapter we outline a real-space quadrature based on the non-uniform pseudospectral discretisation, applicable to both bounded and unbounded physical domains. In particular we outline how to implement the FMT and HI computations in a confining slit. This develops the suite of numerical methods contained in 2DChebClass, using an accurate discretisation of the fluid density profile with a small number of collocation points. By positioning collocation points close to fluid interfaces, avoiding regions of near-constant fluid density, the convolutions are performed in real space by using a quadrature scheme with spectral accuracy.

Chebyshev Pseudospectral Method

We let $f(x)$ take values from $x \in [-1,1]$ with known data at some finite collocation points $x_n \in [-1,1]$. Then $f(x)$ for all values in $[-1,1]$ may be represented by a linear combination of Lagrange polynomials, agreeing with f at x_n where

$$x_n = \cos\left(\frac{\pi n}{N}\right) \qquad \text{for } n = 0, \cdots N.$$

The $\{x_n\}_{n=1}^{N}$ are the Gauss–Lobatto–Chebyshev collocation points and are clustered at either end of the interval $[-1,1]$. It may be shown that the average spacing between the points is $O(N^{-2})$ for x near the endpoints of $[-1,1]$ and $O(N^{-1})$ for x in the interior of $[-1,1]$, as $N \to \infty$ (see [171]). The Lagrange interpolant of $f(x)$ is defined as

$$p_N(x) = \sum_{n=0}^{N} f(x_n) P_n(x)$$

where $P_n(x)$ is a Lagrange polynomial of degree N given by

$$P_n(x) = \prod_{\substack{m=0,\\ m\neq n}}^{N} \frac{x - x_m}{x_n - x_m}. \tag{C.0.2}$$

Note the identity for the Lagrange polynomial

$$P_n(x_k) = \begin{cases} 1 & \text{for } k = n, \\ 0 & \text{for } k \neq n, \end{cases}$$

where x_k is a Gauss–Lobatto–Chebyshev collocation point. The Runge phenomenon, that is oscillation at the edges of the interval when using N is large for a set of equispaced collocation points, is avoided with the clustered Gauss–Lobatto–Chebyshev collocation points. It is unwise in practice to use the interpolant (C.0.2), primarily because: each evaluation of $p_N(x)$ requires $O(N^2)$ additions and multiplications, and the addition of a new data point $(x_{n+1},\ f(x_{n+1}))$ requires computing $P_{n+1}(x)$, not obtainable from $P_n(x)$. This difficulty may be overcome by using the Barycentric Lagrange Interpolant

$$p_N(x) = \frac{\sum_{k=0}^{N} \frac{\bar{w}_k}{x - x_k} f(x_k)}{\sum_{k=0}^{N} \frac{\bar{w}_k}{x - x_k}} \tag{C.0.3}$$

where $\bar{w}_k$ are the Barycentric weights given by

$$\bar{w}_j = (-1)^j d_j \quad \text{for} \quad d_j = \begin{cases} \frac{1}{2} & \text{for } j \in \{0, \cdots, N\} \\ 1 & \text{otherwise} \end{cases}.$$

Note that the quantities in (C.0.3) that have to be computed in $O(N^2)$ floating point operations do not depend on the data $f(x_j)$. Integration may be performed by Clenshaw—Curtis quadrature

$$\int_{-1}^{1} \mathrm{d}x\, f(x) = \sum_{k=0}^{N} w_k f(x_k)$$

where w_k are the Clenshaw–Curtis weights

$$w_j = \frac{2 d_j}{N} \begin{cases} 1 - \sum_{k=1}^{\frac{N-2}{2}} \frac{2\cos(2k\frac{\pi n}{N})}{4k^2-1} - \frac{\cos(\pi j)}{N^2-1} & \text{for } N \text{ even} \\ 1 - \sum_{k=1}^{\frac{N-1}{2}} \frac{2\cos(2k\frac{\pi n}{N})}{4k^2-1} & \text{for } N \text{ odd} \end{cases}.$$

The formulas have been obtained from Boyd [20].

Bibliography

[1] H. M. Al-Saedi, A. J. Archer, and J. Ward. Dynamical density-functional-theory-based modeling of tissue dynamics: Application to tumor growth. *Phys. Rev. E*, 98(2):022407, 2018.

[2] D. M. Anderson, M. G. Worster, and S. H. Davis. The case for a dynamic contact angle in containerless solidification. *J. Cryst. Growth*, 163(3):329–338, 1996.

[3] J. D. Anderson. A history of aerodynamics, cambridge aerospace series 8, 1997.

[4] J. G. Anero, P. Español, and P. Tarazona. Functional thermo-dynamics: A generalization of dynamic density functional theory to non-isothermal situations. *J. Chem. Phys.*, 139 (3):034106, 2013.

[5] A. J. Archer. Dynamical density functional theory: binary phase-separating colloidal fluid in a cavity. *J. Phys.: Condens. Matter*, 17(10):1405, 2005.

[6] A. J. Archer. Dynamical density functional theory for dense atomic liquids. *J. Phys.: Condens Matter*, 18(24):5617, 2006.

[7] A. J. Archer. Dynamical density functional theory for molecular and colloidal fluids: A microscopic approach to fluid mechanics. *J. Chem. Phys.*, 130(1):014509, 2009.

[8] A. J. Archer and R. Evans. Binary Gaussian core model: Fluid-fluid phase separation and interfacial properties. *Phys. Rev. E*, 64(4):041501, 2001.

[9] A. J. Archer and R. Evans. Dynamical density functional theory and its application to spinodal decomposition. *J. Chem. Phys.*, 121(9):4246–4254, 2004.

[10] A. J. Archer, M. J. Robbins, and U. Thiele. Dynamical density functional theory for the dewetting of evaporating thin films of nanoparticle suspensions exhibiting pattern formation. *Phys. Rev. E*, 81:021602, Feb 2010. doi: 10.1103/PhysRevE.81.021602. URL `http://link.aps.org/doi/10.1103/PhysRevE.81.021602`.

[11] R. E. A. Arndt. Cavitation in fluid machinery and hydraulic structures. *Annu. Rev. Fluid Mech.*, 13(1):273–326, 1981.

[12] R. A. Bagnold. Auto-suspension of transported sediment; turbidity currents. *Proc. R. Soc. Lond. A.*, 265(1322):315–319, 1962.

[13] R. C. Ball and J. R. Melrose. A simulation technique for many spheres in quasi-static motion under frame-invariant pair drag and Brownian forces. *Physica A.*, 247(1-4):444–472, 1997.

[14] E. N. Bart. *Interaction of two spheres falling slowly in a viscous medium.* PhD thesis, 1959.

[15] G. O. Berim and E. Ruckenstein. Simple expression for the dependence of the nanodrop contact angle on liquid-solid interactions and temperature. *J. Chem. Phys.*, 130(4):044709, 2009.

[16] F. Bickelhaupt and E. J. Baerends. Kohn-Sham density functional theory: predicting and understanding chemistry. *Rev. Comp. Ch.*, 15:1–86, 2000.

[17] V. I. Bogachev, N. V. Krylov, M. Röckner, and S. V. Shaposhnikov. *Fokker–Planck–Kolmogorov Equations*, volume 207. American Mathematical Society, 2015.

[18] F. Bolley and C. Villani. Weighted Csiszár-Kullback-Pinsker inequalities and applications to transportation inequalities. In *Ann. Fac. Sci. Toulouse Math.*, volume 14, pages 331–352, 2005.

[19] G. Bossis and J. F. Brady. Dynamic simulation of sheared suspensions. I. General method. *J. Chem. Phys.*, 80(10):5141–5154, 1984.

[20] J. P. Boyd. *Chebyshev and Fourier spectral methods*. Courier Corporation, 2001.

[21] J. M. Brader and M. Krüger. Density profiles of a colloidal liquid at a wall under shear flow. *Mol. Phys.*, 109(7-10):1029–1041, 2011.

[22] J. F. Brady and G. Bossis. Stokesian dynamics. *Annu. Rev. Fluid. Mech.*, 20:111–157, 1988.

[23] H. Brenner. The slow motion of a sphere through a viscous fluid towards a plane surface. *Chem. Eng. Sci.*, 16(3-4):242–251, 1961.

[24] R. W. Burgess. The uniform motion of a sphere through a viscous liquid. *Am. J. Math.*, 38(1):81–96, 1916.

[25] J. W. Cahn and J. E. Hilliard. Free energy of a nonuniform system. i. interfacial free energy. *J. Chem. Phys.*, 28(2):258–267, 1958.

[26] S. Camazine, J. Deneubourg, N. R. Franks, J. Sneyd, E. Bonabeau, and G. Theraula. *Self-organization in biological systems*, volume 7. Princeton University Press, 2003.

[27] J. A. Canizo, J. A. Carrillo, and J. Rosado. Collective behavior of animals: Swarming and complex patterns. *Arbor*, 186:1035–1049, 2010.

[28] J. A. Carrillo, M. R. D'orsogna, and V. Panferov. Double milling in self-propelled swarms from kinetic theory. *Kinet. Relat. Mod.*, 2(2):363–378, 2009.

[29] J. A. Carrillo, R. S. Gvalani, G. A. Pavliotis, and A. Schlichting. Long-time behaviour and phase transitions for the McKean–Vlasov equation on the torus. *Arch. Ration. Mech. An.*, Jul 2019. ISSN 1432-0673. doi: 10.1007/s00205-019-01430-4. URL `https://doi.org/10.1007/s00205-019-01430-4`.

[30] G. K. L. Chan and R. Finken. Time-dependent density functional theory of classical fluids. *Phys. Rev. Lett.*, 94(18):183001, 2005.

[31] D. Chandler, J. D. McCoy, and S. J. Singer. Density functional theory of nonuniform polyatomic systems. I. general formulation. *J. Chem. Phys.*, 85(10):5971–5976, 1986.

[32] L. Chayes and V. Panferov. The McKean–Vlasov equation in finite volume. *J. Stat. Phys.*, 138(1-3):351–380, 2010.

[33] B. Chazelle, Q. Jiu, Q. Li, and C. Wang. Well-posedness of the limiting equation of a noisy consensus model in opinion dynamics. *J. Differ. Equations.*, 263(1):365–397, 2017.

[34] M. Chen and F. Wang. Estimates of logarithmic Sobolev constant: An improvement of Bakry–Emery criterion. *J. Funct. Anal.*, 144(2):287–300, 1997.

[35] D. Coppersmith and S. Winograd. Matrix multiplication via arithmetic progressions. *J. Symb. Comput.*, 9(3):251–280, 1990.

[36] R. G. Cox. The dynamics of the spreading of liquids on a solid surface. part 1. viscous flow. *J. Fluid Mech.*, 168:169–194, 1986.

[37] R. G. Cox and H. Brenner. The slow motion of a sphere through a viscous fluid towards a plane surface ii small gap widths, including inertial effects. *Chem. Eng. Sci.*, 22(12): 1753–1777, 1967.

[38] M. G. Crandall and P. H. Rabinowitz. Bifurcation from simple eigenvalues. *J. Funct. Anal.*, 8(2):321–340, 1971.

[39] F. A. Davidson and N. Dodds. Spectral properties of non-local differential operators. *Appl. Anal.*, 85(6-7):717–734, 2006.

[40] P. de Gennes. Dynamics of fluctuations and spinodal decomposition in polymer blends. *J. Chem. Phys.*, 72(9):4756–4763, 1980.

[41] P. Degond. Global existence of smooth solutions for the Vlasov-Fokker-Planck equation in 1 and 2 space dimensions. In *Ann. Sci. Ecole. Norm. S.*, volume 19, pages 519–542. Elsevier, 1986.

[42] J. K. G. Dhont. *An introduction to dynamics of colloids*, volume 2. Elsevier, 1996.

[43] DLMF. *NIST Digital Library of Mathematical Functions*. http://dlmf.nist.gov/, Release 1.0.18 of 2018-03-27. URL `http://dlmf.nist.gov/`. F. W. J. Olver, A. B. Olde Daalhuis, D. W. Lozier, B. I. Schneider, R. F. Boisvert, C. W. Clark, B. R. Miller and B. V. Saunders, eds.

[44] K. Dressler and H. Neunzert. Stationary solutions of the Vlasov-Fokker-Planck equation. *Math. Method. Appl. Sci.*, 9(1):169–176, 1987.

[45] M. A. Durán-Olivencia, B. D. Goddard, and S. Kalliadasis. Dynamical density functional theory for orientable colloids including inertia and hydrodynamic interactions. *J. Stat. Phys.*, 164(4):785–809, 2016.

[46] C. Ebner and W. F. Saam. New phase-transition phenomena in thin argon films. *Phys. Rev. Lett.*, 38(25):1486, 1977.

[47] A. Einstein. *Eine neue bestimmung der moleküldimensionen*. PhD thesis, ETH Zurich, 1905.

[48] A. Einstein. Eine neue bestimmung der moleküldimensionen. *Ann. Phys.*, 324(2):289–306, 1906.

[49] E. W. Errill. Rheology of blood. *Physiol. Rev.*, 49(4):863–888, 1969.

[50] L. P. Euler. General principles concerning the motion of fluids. originalmente publicado en. *Mém. Acad. Sc. Berlin*, 11(1757):274–315, 1757.

[51] D. J. Evans and G. P. Morriss. Shear thickening and turbulence in simple fluids. *Phys. Rev. Lett.*, 56(20):2172, 1986.

[52] L. C. Evans. Partial differential equations, ams, providence, ri, 1998. *Grad. Stud. Math.*, 19, 2002.

[53] R. Evans. The nature of the liquid-vapour interface and other topics in the statistical mechanics of non-uniform, classical fluids. *Adv. Phys.*, 28(2):143–200, 1979.

[54] A. Fall, N. Huang, F. Bertrand, G. Ovarlez, and D. Bonn. Shear thickening of cornstarch suspensions as a reentrant jamming transition. *Phys. Rev. Lett.*, 100(1):018301, 2008.

[55] H. Faxén. Die geschwindigkeit zweier kugeln, die unter einwirkung der schwere in einer zähen flüssigkeit fallen. *Zamm-Z. Angew. Math. Me.*, 7(1):79–81, 1927.

[56] R. C. Fetecau, J. E. Marsden, M. Ortiz, and M. West. Nonsmooth Lagrangian mechanics and variational collision integrators. *SIAM. J. Appl. Dyn. Syst.*, 2(3):381–416, 2003.

[57] G. W. Ford, M. Kac, and P. Mazur. Statistical mechanics of assemblies of coupled oscillators. *J. Math. Phys.*, 6(4):504–515, 1965.

[58] I. Fredholm. *Sur une nouvelle méthode pour la résolution du problème de Dirichlet.* 1900.

[59] P. H. Gilbert and A. J. Giacomin. Transport phenomena in bispherical coordinates. *Phys. Fluids*, 31(2):021208, 2019.

[60] B. D. Goddard. Mathematical analysis of quantum chemical models for small atoms. 2007.

[61] B. D. Goddard, A. Nold, N. Savva, G. A. Pavliotis, and S. Kalliadasis. General dynamical density functional theory for classical fluids. *Phys. Rev. Lett.*, 109(12):120603, 2012.

[62] B. D. Goddard, A. Nold, N. Savva, P. Yatsyshin, and S. Kalliadasis. Unification of dynamic density functional theory for colloidal fluids to include inertia and hydrodynamic interactions: derivation and numerical experiments. *J. Phys.: Condens. Matter*, 25(3): 035101, 2012.

[63] B. D. Goddard, G. A. Pavliotis, and S. Kalliadasis. The overdamped limit of dynamic density functional theory: Rigorous results. *Multiscale Model. Sim.*, 10(2):633–663, 2012.

[64] B. D. Goddard, A Nold, and S Kalliadasis. Multi-species dynamical density functional theory. *J. Chem. Phys.*, 138:144904, 2013.

[65] B. D. Goddard, A. Nold, and S. Kalliadasis. Multi-species dynamical density functional theory. *J. Chem. Phys.*, 138(14):144904, 2013.

[66] B. D. Goddard, A. Nold, and S. Kalliadasis. Dynamical density functional theory with hydrodynamic interactions in confined geometries. *J. Chem. Phys.*, 145(21):214106, 2016.

[67] B. D. Goddard, A. Nold, and S. Kalliadasis. 2DChebClass [Software]. http://dx.doi.org/10.7488/ds/1991, 2017.

[68] B. D. Goddard, R. D. Mills-Williams, and G. A. Pavliotis. Well-posedness and equilibrium behaviour of overdamped dynamic density functional theory. *arXiv preprint arXiv:2002.11663*, 2020..

[69] B. D. Goddard, R. D. Mills-Williams, and J. Sun. The singular hydrodynamic interactions between two spheres in Stokes flow. *arXiv preprint arXiv:1809.05459*, 2020..

[70] A. J. Goldman, R. G. Cox, and H. Brenner. The slow motion of two identical arbitrarily oriented spheres through a viscous fluid. *Chem. Eng. Sci.*, 21(12):1151–1170, 1966.

[71] Golse. F. The Boltzmann equation and its hydrodynamic limits. *Evolutionary Equations*, 2:159–301, 2005.

[72] A. Gorban and I. Karlin. Hilbert's 6th problem: exact and approximate hydrodynamic manifolds for kinetic equations. *B. Am. Math. Soc.*, 51(2):187–246, 2014.

[73] S. Haber, G. Hetsroni, and A. Solan. On the low Reynolds number motion of two droplets. *Int. J. Multiphas. Flow*, 1(1):57–71, 1973.

[74] R. E. Hansford. On converging solid spheres in a highly viscous fluid. *Mathematika*, 17 (2):250–254, 1970.

[75] J. Happel and H. Brenner. *Low Reynolds number hydrodynamics: with special applications to particulate media*, volume 1. Springer Science & Business Media, 2012.

[76] L. Harnau and S. Dietrich. Inhomogeneous platelet and rod fluids. *Soft Matter*, 3:159–160, 2007.

[77] E. J. Hinch. Application of the Langevin equation to fluid suspensions. *J. Fluid Mech.*, 72(3):499–511, 1975.

[78] E. J. Hinch. *Perturbation methods*. Cambridge University Press, 1991.

[79] N. Hoda and S. Kumar. Brownian dynamics simulations of polyelectrolyte adsorption in shear flow with hydrodynamic interaction. *J. Chem. Phys.*, 127(23):234902, 2007.

[80] C. Hoell, H. Löwen, and A. M. Menzel. Dynamical density functional theory for circle swimmers. *New J. Phys.*, 19(12):125004, 2017.

[81] P. Hohenberg and W. Kohn. Inhomogeneous electron gas. *Phys. Rev.*, 136(3B):B864, 1964.

[82] R. Holley and D. W. Stroock. Logarithmic Sobolev inequalities and stochastic Ising models. *J. Stat. Phys.*, 46:1159–1194, 1987.

[83] T. Y. Hou, J. S. Lowengrub, and M. J. Shelley. Boundary integral methods for multicomponent fluids and multiphase materials. *J. Comput. Phys.*, 169(2):302–362, 2001.

[84] Y. A. Houndonougbo, B. B. Laird, and B. J. Leimkuhler. A molecular dynamics algorithm for mixed hard-core/continuous potentials. *Mol. Phys.*, 98(5):309–316, 2000.

[85] G. Huber, S. A. Koehler, and J. Yang. Micro-swimmers with hydrodynamic interactions. *Math. Comput. Model.*, 53(7):1518–1526, 2011.

[86] C. Huh and L. E. Scriven. Hydrodynamic model of steady movement of a solid/liquid/fluid contact line. *J. Colloid. Interf. Sci.*, 35(1):85–101, 1971.

[87] G. B. Jeffery. On a form of the solution of Laplace's equation suitable for problems relating to two spheres. *Proc. R. Soc. Lond. A.*, 87(593):109–120, 1912.

[88] D. J. Jeffrey. Programs for Stokes Resistance Functions. `https://www.uwo.ca/apmaths/faculty/jeffrey/research/Resistance.html`, . [Accessed 01-March-2019].

[89] D. J. Jeffrey. Programs for Stokes Resistance Functions, first 300 terms of X_{11}^A eq (3.13). `https://www.uwo.ca/apmaths/faculty/jeffrey/research/resistancefunctions/xa/rxa300.dat.txt`, . [Accessed 01-March-2019].

[90] D. J. Jeffrey. Low-Reynolds-number flow between converging spheres. 1982.

[91] D. J. Jeffrey. The calculation of the low Reynolds number resistance functions for two unequal spheres. *Phys. Fluids A.: Fluid.*, 4(1):16–29, 1992.

[92] D. J. Jeffrey and Y. Onishi. Calculation of the resistance and mobility functions for two unequal rigid spheres in low-Reynolds-number flow. *J. Fluid Mech.*, 139:261–290, 1984.

[93] W. Jianzhong. Density functional theory for chemical engineering: From capillarity to soft materials. *AIChE journal*, 52(3):1169–1193, 2006.

[94] J. Jost and X. Li-Jost. *Calculus of variations*, volume 64. Cambridge University Press, 1998.

[95] V. Kac and P. Cheung. *Quantum calculus*. Springer Science & Business Media, 2001.

[96] T. Kato. *Perturbation theory for linear operators*, volume 132. Springer Science & Business Media, 2013.

[97] E. Kierlik and M. L. Rosinberg. Free-energy density functional for the inhomogeneous hard-sphere fluid: Application to interfacial adsorption. *Phys. Rev. A*, 42(6):3382, 1990.

[98] S. Kim and S. J. Karrila. *Microhydrodynamics: principles and selected applications*. Courier Corporation, 2013.

[99] R. T. Knapp, J. W. Daily, and F. G. Hammitt. *Cavitation, (1970)*. Institute of Hydraulic Research, University of Iowa, 1970.

[100] R. Kubo. The fluctuation-dissipation theorem. *Rep. Prog. Phys.*, 29(1):255, 1966.

[101] N. Kuznetsov and A. Nazarov. Sharp constants in the Poincaré, Steklov and related inequalities (a survey). *Mathematika*, 61(2):328–344, 2015.

[102] E. Lauga and T. M. Squires. Brownian motion near a partial-slip boundary: A local probe of the no-slip condition. *Phys. Fluids*, 17(10):103102, 2005.

[103] P. D. Lax. *Functional Analysis*. Pure and Applied Mathematics: A Wiley Series of Texts, Monographs and Tracts. Wiley, 2014. ISBN 9781118626740. URL `https://books.google.co.uk/books?id=e_BjBAAAQBAJ`.

[104] A. Lefebvre-Lepot, B. Merlet, and T. N. Nguyen. An accurate method to include lubrication forces in numerical simulations of dense Stokesian suspensions. *J. Fluid Mech.*, 769: 369–386, 2015.

[105] B. Leimkuhler and C. Matthews. *Molecular Dynamics*. Springer, 2016.

[106] K. Lichtner, A. J. Archer, and S. H. L. Klapp. Phase separation dynamics in a two-dimensional magnetic mixture. *J. Chem. Phys.*, 136:024502, 2012.

[107] N. Y. C. Lin, M. Guy, B, M. Hermes, C. Ness, J. Sun, W. C. K. Poon, and I. Cohen. Hydrodynamic and Contact Contributions to Continuous Shear Thickening in Colloidal Suspensions. *Phys. Rev. Lett.*, 115(22):228304, November 2015.

[108] J. F. Lutsko. Recent developments in classical density functional theory. *Adv. Chem. Phys.*, 144:1, 2010.

[109] J. F. Lutsko. A dynamical theory of nucleation for colloids and macromolecules. *J. Chem. Phys.*, 136(3):034509, 2012.

[110] F. Malrieu. Logarithmic Sobolev inequalities for some nonlinear pde's. *Stoc. Proc. Appl.*, 95(1):109–132, 2001.

[111] U. M. B. Marconi and S. Melchionna. Phase-space approach to dynamical density functional theory. *J. Chem. Phys.*, 126:184109, 2007.

[112] U. M. B. Marconi and P. Tarazona. Dynamic density functional theory of fluids. *J. Chem. Phys.*, 110(16):8032–8044, 1999.

[113] U. M. B. Marconi, P. Tarazona, and F. Cecconi. Theory of thermostatted inhomogeneous granular fluids: A self-consistent density functional description. *J. Chem. Phys.*, 126: 164904, 2007.

[114] U. M. B. Marconi, P. Tarazona, F. Cecconi, and S. Melchionna. Beyond dynamic density functional theory: the role of inertia. *J. Phys.: Condens. Matter*, 20:494233, 2008.

[115] M. A. L. Marques and E. K. U. Gross. Time-dependent density functional theory. *Annu. Rev. Phys. Chem.*, 55:427–455, 2004.

[116] N. Martzel and C. Aslangul. Mean-field treatment of the many-body Fokker–Planck equation. *J. Phys. A.: Math. Gen.*, 34(50):11225, 2001.

[117] A. D. Maude. End effects in a falling-sphere viscometer. *Brit. J. Appl. Phys.*, 12(6):293, 1961.

[118] W. J. McNeil and W. G. Madden. A new method for the molecular dynamics simulation of hard core molecules. *J. Chem. Phys.*, 76(12):6221–6226, 1982.

[119] G. Menz and A. et al. Schlichting. Poincaré and logarithmic Sobolev inequalities by decomposition of the energy landscape. *Ann. Probab.*, 42(5):1809–1884, 2014.

[120] A. M. Menzel, A. Saha, C. Hoell, and H. Löwen. Dynamical density functional theory for microswimmers. *J. Chem. Phys.*, 144(2):024115, 2016.

[121] N. D. Mermin. Thermal properties of the inhomogeneous electron gas. *Phys. Rev.*, 137: A1441, 1965.

[122] P. Moon and D. E. Spencer. Eleven coordinate systems. In *Field Theory Handbook*, pages 1–48. Springer, 1961.

[123] C. L. M. H. Navier. Sur les lois des mouvement des fluides, en ayant egard a l'adhesion des molecules. *Ann. Chim. Paris*, 19:244–260, 1821.

[124] C. Ness and J. Sun. Shear thickening regimes of dense non-Brownian suspensions. *Soft Matter*, 12(3):914–924, 2016.

[125] N. Q. Nguyen and A. J. C. Ladd. Lubrication corrections for lattice-Boltzmann simulations of particle suspensions. *Phys. Rev. E*, 66(4):046708–046708, October 2002.

[126] A. Nold. *From the Nano-to the Macroscale: Bridging Scales for the Moving Contact Line Problem*. PhD thesis, Imperial College London, 2016.

[127] A. Nold, B. D. Goddard, P. Yatsyshin, N. Savva, and S. Kalliadasis. Pseudospectral methods for density functional theory in bounded and unbounded domains. *J. Comput. Phys.*, 334:639–664, 2017.

[128] M. E. O'Neill. A slow motion of viscous liquid caused by a slowly moving solid sphere. *Mathematika*, 11(1):67–74, 1964.

[129] M. E. O'Neill and R. Majumdar. Asymmetrical slow viscous fluid motions caused by the translation or rotation of two spheres. part i: The determination of exact solutions for any values of the ratio of radii and separation parameters. *Z. Angew. Math. Phys.*, 21(2): 164–179, 1970.

[130] L. Onsager. The effects of shape on the interaction of colloidal particles. *Ann. NY. Acad. Sci.*, 51(4):627–659, 1949.

[131] D. W. Oxtoby. Density functional methods in the statistical mechanics of materials. *Ann. Rev. Mater. Res.*, 32(1):39–52, 2002.

[132] D. Papavassiliou and G. P. Alexander. Exact solutions for hydrodynamic interactions of two squirming spheres. *J. Fluid Mech.*, 813:618–646, 2017.

[133] A. O. Parry, A. Malijevskỳ, and C. Rascón. Capillary contact angle in a completely wet groove. *Phys. Rev. Lett.*, 113(14):146101, 2014.

[134] G. A. Pavliotis. *Stochastic processes and applications: diffusion processes, the Fokker-Planck and Langevin equations*, volume 60. Springer, 2014.

[135] G. A. Pavliotis and A. Stuart. *Multiscale methods: averaging and homogenization.* Springer Science & Business Media, 2008.

[136] L. E. Payne. Representation formulas for solutions of a class of partial differential equations. *J. Math. Phys. Camb.*, 38(1):145–149, 1959.

[137] L. E. Payne and W. H. Pell. The Stokes flow problem for a class of axially symmetric bodies. *J. Fluid Mech.*, 7(4):529–549, 1960.

[138] L. E. Payne and H. F. Weinberger. An optimal Poincaré inequality for convex domains. *Arch. Ration. Mech. An.*, 5(1):286–292, 1960.

[139] F. Penna, J. Dzubiella, and P. Tarazona. Dynamic density functional study of a driven colloidal particle in polymer solutions. *Phys. Rev. E*, 68(6):061407, 2003.

[140] J. K. Percus. Equilibrium state of a classical fluid of hard rods in an external field. *J. Stat. Phys.*, 15(6):505–511, 1976.

[141] A. Pereira and S. Kalliadasis. Equilibrium gas–liquid–solid contact angle from density-functional theory. *J. Fluid Mech.*, 692:53–77, 2012.

[142] M. Plischke and B. Bergersen. *Equilibrium statistical physics*. World Scientific Publishing Company, 1994.

[143] T. V. Ramakrishnan and M. Yussouff. First-principles order-parameter theory of freezing. *Phys. Rev. B*, 19(5):2775, 1979.

[144] M. Rauscher. Ddft for Brownian particles and hydrodynamics. *J. Phys.: Condens. Matter*, 22(36):364109, 2010.

[145] M. Rauscher, A. Domínguez, M. Krüger, and F. Penna. A dynamic density functional theory for particles in a flowing solvent. *J. Chem. Phys.*, 127(24):244906, 2007.

[146] M. Rex and H. Löwen. Dynamical density functional theory for colloidal dispersions including hydrodynamic interactions. *Eur. Phys. J. E.*, 28(2):139–146, 2009.

[147] Y. Rosenfeld. Free-energy model for the inhomogeneous hard-sphere fluid mixture and density-functional theory of freezing. *Phys. Rev. Lett.*, 63(9):980–983, 1989.

[148] Y. Rosenfeld. Free-energy model for the inhomogeneous hard-sphere fluid mixture and density-functional theory of freezing. *Phys. Rev. Lett.*, 63(9):980, 1989.

[149] Y. Rosenfeld. Free-energy model for the inhomogeneous hard-sphere fluid in D dimensions: Structure factors for the hard-disk (d= 2) mixtures in simple explicit form. *Phys. Rev. A*, 42(10):5978, 1990.

[150] R. Roth. Fundamental measure theory for hard-sphere mixtures: a review. *J. Phys.: Condens. Matter*, 22:063102, 2010.

[151] R. Roth. Fundamental measure theory for hard-sphere mixtures: a review. *J. Phys.: Condens. Matter*, 22(6):063102, 2010.

[152] R. Roth, R. Evans, A. Lang, and G. Kahl. Fundamental measure theory for hard-sphere mixtures revisited: the White Bear version. *J. Phys.: Condens. Matter*, 14:12063, 2002.

[153] R. Roth, M. Rauscher, and A. J. Archer. Selectivity in binary fluid mixtures: Static and dynamical properties. *Phys. Rev. E*, 80(2):021409, 2009.

[154] J. Rotne and S. Prager. Variational treatment of hydrodynamic interaction in polymers. *J. Chem. Phys.*, 50(11):4831–4837, 1969.

[155] J. S. Rowlinson. Translation of JD van der Waals' "the thermodynamik theory of capillarity under the hypothesis of a continuous variation of density". *J. Stat. Phys.*, 20(2): 197–200, 1979.

[156] E. Runge and E. K. U. Gross. Density-functional theory for time-dependent systems. *Phys. Rev. Lett.*, 52(12):997, 1984.

[157] D. N. Sibley, A. Nold, N. Savva, and S. Kalliadasis. The contact line behaviour of solid-liquid-gas diffuse-interface models. *Phys. Fluids*, 25(9):092111, 2013.

[158] D. N. Sibley, A. Nold, N. Savva, and S. Kalliadasis. A comparison of slip, disjoining pressure, and interface formation models for contact line motion through asymptotic analysis of thin two-dimensional droplet spreading. *J. Eng. Math.*, 94(1):19–41, 2015.

[159] Y. Singh. Density-functional theory of freezing and properties of the ordered phase. *Phys. Rep.*, 207(6):351–444, 1991.

[160] M. Slemrod. Hilbert's sixth problem and the failure of the Boltzmann to Euler limit. *Philos. T. R. Soc. A*, 376(2118):20170222, 2018.

[161] J. H. Snoeijer and P. Brunet. Pointy ice-drops: How water freezes into a singular shape. *Am. J. Phys.*, 80(9):764–771, 2012.

[162] M. Stimson and G. B. Jeffery. The motion of two spheres in a viscous fluid. *P. R. Soc. Lond. A-Conta.*, 111(757):110–116, 1926.

[163] G. G. Stokes. *On the effect of the internal friction of fluids on the motion of pendulums*, volume 9. Pitt Press Cambridge, 1851.

[164] D. Stopper, K. Marolt, R. Roth, and H. Hansen-Goos. Modeling diffusion in colloidal suspensions by dynamical density functional theory using fundamental measure theory of hard spheres. *Phys. Rev. E*, 92:022151, Aug 2015. doi: 10.1103/PhysRevE.92.022151. URL `http://link.aps.org/doi/10.1103/PhysRevE.92.022151`.

[165] G. T. Symm. Integral equation methods in potential theory. ii. *Proc. R. Soc. Lon. Ser.: A*, 275(1360):33–46, 1963.

[166] Y. Tamura. On asymptotic behaviors of the solution of a nonlinear diffusion equation. *J. Fac. Sci. U. Tokyo 1.*, 31(1):195–221, 1984.

[167] Y. Tang and J. Wu. A density-functional theory for bulk and inhomogeneous Lennard-Jones fluids from the energy route. *J. Chem. Phys.*, 119(14):7388–7397, 2003.

[168] P. A. Thompson and S. M. Troian. A general boundary condition for liquid flow at solid surfaces. *Nature*, 389(6649):360, 1997.

[169] A. K. Townsend. Generating, from scratch, the near-field asymptotic forms of scalar resistance functions for two unequal rigid spheres in low-Reynolds-number flow. *arXiv preprint arXiv:1802.08226*, 2018.

[170] A. K. Townsend and H. J. Wilson. Anomalous effect of turning off long-range mobility interactions in Stokesian dynamics. *Phys. Fluids*, 30(7):077103, 2018.

[171] L. N. Trefethen. *Spectral methods in MATLAB*, volume 10. SIAM, 2000.

[172] S. van Teeffelen, C. N. Likos, and H. Löwen. Colloidal crystal growth at externally imposed nucleation clusters. *Phys. Rev. Lett.*, 100:108302, Mar 2008. doi: 10.1103/PhysRevLett.100.108302. URL `http://link.aps.org/doi/10.1103/PhysRevLett.100.108302`.

[173] E. Wacholder and D. Weihs. Slow motion of a fluid sphere in the vicinity of another sphere or a plane boundary. *Chem. Eng. Sci.*, 27(10):1817–1828, 1972.

[174] A. Weinstein. Discontinuous integrals and generalized potential theory. *T. Am. Math. Soc.*, 63(2):342–354, 1948.

[175] R. Wittkowski and H. Löwen. Dynamical density functional theory for colloidal particles with arbitrary shape. *Mol. Phys.*, 109:2935–2943, 2011.

[176] R. Wittkowski, H. Löwen, and H. R. Brand. Derivation of a three-dimensional phase-field-crystal model for liquid crystals from density functional theory. *Phys. Rev. E*, 82: 031708, Sep 2010. doi: 10.1103/PhysRevE.82.031708. URL `http://link.aps.org/doi/10.1103/PhysRevE.82.031708`.

[177] R. Wittkowski, H. Löwen, and H. R. Brand. Extended dynamical density functional theory for colloidal mixtures with temperature gradients. *J. Chem. Phys.*, 137(22):224904, 2012.

[178] A. Wouk. A note on square roots of positive operators. *SIAM Rev.*, 8(1):100–102, 1966.

[179] J. Wu and Z. Li. Density-functional theory for complex fluids. *Annu. Rev. Phys. Chem.*, 58:85–112, 2007.

[180] A. Wysocki and H. Löwen. Effects of hydrodynamic interactions in binary colloidal mixtures driven oppositely by oscillatory external fields. *J. Phys.: Condens. Matter*, 23 (28):284117, 2011.

[181] U. Zimmermann, F. Smallenburg, and H. Löwen. Flow of colloidal solids and fluids through constrictions: dynamical density functional theory versus simulation. *J. Phys.: Condens. Matter*, 28(24):244019, 2016.

[182] R. W. Zwanzig. High-temperature equation of state by a perturbation method. I. Nonpolar gases. *J. Chem. Phys.*, 22(8):1420–1426, 1954.